1991

Modelling Catalytic Cracking In A Novel Riser Simulator (volumes I And Ii)

Daniel William Kraemer

MODELLING CATALYTIC CRACKING IN A NOVEL RISER SIMULATOR

Volume I

by

Daniel W. Kraemer

Faculty of Engineering Science

Submitted in partial fulfilment
of the requirements for the degree of
Doctor of Philosophy

Faculty of Graduate Studies
The University of Western Ontario
London, Ontario
December 1990

ISBN 0-315-64240-8

ABSTRACT

A 45 mL bench-scale internal recycle reactor, named a 'Riser Simulator' was used to study the kinetics of catalytic cracking. This reaction system is well suited for riser cracking reactions since it can be operated at reaction times as low as 3 seconds and can simulate the reaction regime of a riser. The reactor operates in a batch mode with a gas recirculation in the upward direction through the central catalyst zone to maintain a well fluidized bed. The fluid-solid dynamics in the reactor were verified using a fibre optic probe technique.

Experimental runs performed in the unit included the cracking of two commercial feedstocks and three mixtures of pure light oil compounds with two commercial catalysts (Octacat and GX-30). The reactor conditions were varied with temperatures of 500, 525 and 550°C; reaction times of 3 to 10 seconds and catalyst to oil ratios of 3 to 7. The products were analyzed using gas chromatography and mass spectrometry with automatic data storage for further computer analysis of yields, conversions and octane numbers.

The kinetic parameters associated with the three lump model were evaluated based on a reactor model which intrinsically includes the effect of molar expansion during cracking. The kinetic values obtained fell in the range of values reported in other works using pilot scale riser units.

Three different catalyst decay functions were used and it was found that first order decay was sufficient to describe the data for short contact times. The use of a power law decay function and a decay function based on the mass of coke on the catalyst gave no advantage in terms of model prediction.

An eight lump model was also developed which takes into account feedstock composition. The gas oil feed is lumped into paraffins, naphthenes and aromatics in both heavy and light fractions. The model predicted gasoline yields to within ± 2.3 wt% and light gases plus coke yields to within ± 3.9 wt%. The fit of the model to the six oil lumps was found to be adequate for the two different gas oils used and the cracking constants for the paraffin groups were comparable to literature values.

The information presented in this work should help furnish the existing gap of kinetic data for short contact time riser cracking. In fact no such data has appeared in the literature for an eight-lump model evaluated at reaction times of less than 10 seconds. This makes the Riser Simulator a valuable tool for determination of relevant kinetic data. The device could also be used for purposes of catalyst screening since it achieves a reaction regime which is more realistic for riser cracking than that achieved by the industry standard MAT unit.

ACKNOWLEDGEMENTS

I would like to express my sincere thanks to Professor Hugo de Lasa for his superb support and assistance in the supervision of this work.

I am very grateful as well for the support and friendships of fellow colleagues Donald Huskey, Miguel Larocca, Arnaud Mahay, Paul Lee, François Simard, Julie Chabot, Ulises Sedran, Hany Farag, Alberto Blasetti, Ahmet Pekediz, Ethel Nakano, Ron Hankewich, Lina Cloutier, Anh Vo-Nugyen, Todd Anderson, Thuy Pham, Laki Vogiatzis and many others.

Special acknowledgement is given to the University of Western Ontario Mechanical Shop for their expertise in building the reaction system; to Professors M. A. Bergougnou and K. A. Shelstad, members of the Advisory Committee, for their support and guidance and to Souheil Afara for his excellent drawings.

I would also like to thank my parents to whom I am greatly indebted to for their support and understanding.

TABLE OF CONTENTS

Volume I

LIST OF TABLES

LIST OF FIGURES

VOLUME II

Appendices

NOMENCLATURE

a_i	Total area count from the integrator for the sample loop injection
a_{cal}	Total area count from the integrator for the calibration gas injection
A	Symbol for gas oil in the three lump model, aromatic compounds in the 8-lump model
B	Symbol for gasoline lump in the three lump model
C	Symbol for light gases plus coke lump
C_A	Concentration of gas oil ($gmol/cm^3$)
C_B	Concentration of gasoline ($gmol/cm^3$)
C_c	Coke concentration ($g_{coke}/g_{catalyst}$)
C_i	Concentration of component i (gmol/mL)
C_t	Total active sites (gmol sites/g catalyst).
d	Diameter of the catalyst chamber (cm)
D	Constant involved in power law decay = $[(n-1)k_d]^{-N}$ (s^N)
D_p	Average particle size diameter (m)
E_A	Energy of activation (kcal/gmol)
G	Symbol for gasoline lump in the 8-lump model
h	Height of the catalyst chamber (cm)
k_o	Overall gas oil cracking rate constant in the 3-lump model ($cm^6/g_{cat}.s.gmol_{oil}$)
k_o'	Overall gas oil cracking rate constant in the 3-lump model using power law decay ($cm^6/g_{cat}.s^{1-N}.gmol_{oil}$)
k_1	Gasoline formation rate constant in the 3-lump model ($cm^6/g_{cat}.s.gmol_{oil}$)
k_2	Gasoline cracking rate constant in the 3-lump model ($cm^3/g_{cat}.s$)
k_3	C-lump formation rate constant from gas oil in the

	3-lump model ($cm^6/g_{cat}.s.gmol_{oil}$)
k_d	Deactivation rate constant (1/s)
k_d'	Deactivation rate constant ($cm^6/gmol^2.s$)
k_{OC}	Rate constant for gasoline cracking to C-lump ($cm^3/g_{cat}.s$)
k_h	Overall rate constant for the cracking of heavy lumps ($cm^3/g_{cat}.s$)
k_{hC}	Rate constant for heavy lump cracking to C-lump ($cm^3/g_{cat}.s$)
k_{hO}	Rate constant for heavy lump cracking to gasoline ($cm^3/g_{cat}.s$)
k_{hl}	Rate constant for heavy lump cracking to light lump ($cm^3/g_{cat}.s$)
k_l	Overall rate constant for the cracking of light lumps ($cm^3/g_{cat}.s$)
k_{lC}	Rate constant for light lump cracking to C-lump ($cm^3/g_{cat}.s$)
k_{lO}	Rate constant for light lump cracking to gasoline ($cm^3/g_{cat}.s$)
m	Constant related to coke formation (equation 1.3)
m_c	Mass of catalyst (g)
M_{avg}	Average molecular weight of vapours in the reactor
M_i	Molecular weight of component i (g/gmol)
M_{HC}	Final molecular weight of hydrocarbons (g/gmol)
m_{cal}	Mass of calibration gas (g)
m_{HC}	Total mass of hydrocarbons (g)
$m_{HC,l}$	Mass of hydrocarbons in the sample loop (g)
$m_{HC,p}$	Mass of hydrocarbons purged from the reactor (g)
$m_{HC,r}$	Mass of hydrocarbons remaining in the reactor (g)
m_p	Total mass purged from the reactor (g)

n	Order of catalyst activity decay
n_{AR}	Mole fraction of argon
n_{HC}	Mole fraction of hydrocarbons
N	Function of the order of decay (= 1/(n-1))
N_i	Moles of component i (gmol)
P_i	Partial pressure of component i (atm)
P_{Re}	Reactor pressure just before purging (atm)
P_{Ri}	Initial reactor pressure (= 1 atm always)
P_{Vf}, P_{Vi}	Final and initial vacuum pressures (atm)
r_A	Rate of gas oil cracking ($gmol_{oil}/g_{cat}.s$)
r_B	Rate of gasoline formation ($gmol/g_{cat}.s$)
REO	Rare earth oxide
Q	Volumetric flow rate (mL/s)
R	Universal gas constant ($atm.cm^3/gmol/K$)
S	Symbol for aromatic substituent groups
t	Reaction time (s)
T_l	Sample loop temperature (°K)
T_V, T_R	Vacuum system and reactor temperatures (°K)
u_{mf}	Minimum fluidization velocity (cm/s)
u_t	Terminal particle velocity (m/s)
v	Velocity vector throught the catalyst bed (cm/s)
v_1	Stoichiometric coefficient for gasoline formation from gas oil (~ M_A/M_B)
V_l	Volume of the sample loop (mL)
V_T	Total internal gas volume in the reactor (mL)
V_V, V_R	Vacuum system and reactor volumes (mL)

w_i	Mass of component i (g)
w_o	Mass of oil injected minus coke (g)
w_T	Total mass of gases in the reactor (g)
W	Oil refractoriness
X_{HC}	Mass fraction of hydrocarbons (g_{HC}/g_{total})
y_i	Mole fraction of component i ($gmol_i/gmol_{total}$)
Y_i	Weight fraction of component i (g_i/g_{total})
Y_{io}	Initial weight fraction of component i

Greek Symbols

α	Alternate symbol for k_d (1/s)
δ	Constant related to coke formation (equation 1.4)
ϕ	Deactivation function
ϵ	Constant related to coke formation (equation 1.3)
σ	Proportionality factor (gmol sites/gmol coke)
ρ	Gas density (g/mL)
μ_i	Gas viscosity of component i (cp)
Ψ	Parameter for equation (B6) = $P_{Ri}\ V_R\ /\ (R\ T_R\ w_o)$ (gmol/g)

Subscripts

A	Refers to aromatic compounds in the 8-lump model, gas oil in the 3-lump model
B	Refers to gasoline in the 3-lump model
G	Refers to gasoline lump in the 8-lump model
h	Refers to heavy lumps
i	P, N, or A
l	Refers to light lumps

N	Refers to naphthenic compounds
P	Refers to paraffinic compounds

CHAPTER 1

INTRODUCTION

The catalytic cracking of gas oil is considered the most important and most profitable unit operation of the petroleum-refining industry. The basic operation involves the breakdown of large hydrocarbon molecules found in the heavier oil streams from crude distillation into smaller ones by means of contacting the oil for a short time with hot catalyst. It serves as a major refinery tool to produce high quality motor fuel, heating fuel and raw petrochemical feedstocks.

According to Occelli (1988), in the United States approximately one-third of all processed crude oil is converted by fluid catalytic cracking (FCC) requiring the use of over 500 tons of catalyst daily. This process is the work horse of the modern refinery for gasoline production and research and development efforts over the last 50 years have been very profitable (Venuto and Habib, 1978). From the time of its inception in 1939, FCC has grown significantly and has revolutionized the oil industry (Jahnig et al., 1984). It represents the largest single stride in the development of refining processes that the petroleum industry has ever made.

1.1 HISTORICAL DEVELOPMENT OF CATALYTIC CRACKING

Several reviews on the historical development of catalytic cracking and the technological changes in equipment design have appeared in the literature (Avidan et al., 1990a; Jahnig et al., 1980, 1984; McKetta, 1981; Squires, 1986; Reichele, 1988; Wrench et al, 1986; Nieskens et al, 1990; de Lasa, 1982). The excellent review by Avidan et al. (1990a), who cover the adoption of FCC at Mobil Oil Corp., lists important dates of the many innovative developments in the cracking process.

1.1.1 The Fixed Bed Process

With the large demand for automotive fuel at the beginning of the 20th century efforts were made to upgrade less valuable petroleum products to gasoline whose demand could not be furnished solely by naturally occurring gasoline. In 1913 W.M. Burton of Standard Oil Company of Indiana was awarded a patent for the Burton thermal cracking process. This spurred the development of 5 major batch cracking processes which supplied the world's gasoline requirements during the years 1913 to 1936 (Avidan et al., 1990a). These processes consisted of crude distillation followed by heating of the heaviest fraction of the barrel and soaking in a coking vessel. Typical severities achieved 1000°F and 1000 psig in commercial units. Thermally derived gasolines were superior

to natural gasolines but suffered in quality from high olefin and di-olefin contents giving it a yellowish appearance and poor response to lead additives.

The discovery of aluminum chloride by A.M. McAfee of Gulf Refining Co. (now Chevron) to catalytically crack heavy oils with improved yields and gasoline quality led to the first commercial trial of cat-cracking in 1915 (Jahnig et al, 1980). However, the process fell into discard due to batch operation and high cost of recovering catalyst. Later, in the 1920's Eugene Houdry identified acid-treated clays as giving improved performance in racing cars and invented a process using air regeneration to burn coke off the catalyst (Houdry, 1956). Most major oil companies were sceptical of Houdry's experiments but in 1931 the Houdry Process Company was formed by Eugene Houdry and Vacuum Oil Company (Avidan et al. 1990a). In 1931 Socony-Vacuum Oil Company was formed (now Mobil) and with the effort of Sun Oil Company in 1933, to help in the development of a catalytic cracking process, the first commercial cracking unit was started in 1936 in Paulsboro, New Jersey, operating at 2,000 barrels per day (Avidan et al., 1990). As well, Sun operated a 15,000 barrel per day unit in March 1937 and by 1941 fourteen Houdry units were in operation in the U.S. (Squires, 1986).

The Houdry process involved the use of three reactors with fixed beds of silica-alumina catalyst in pellet form. Cyclic operation was used where oil was charged to one reactor while the other two were undergoing purge and carbon burning cycles.

A 30 minute cycle was used with 10 minutes for reaction. An elaborate design (see Figure 1.1) allowed molten salts to pass through tubes in the catalyst bed to remove heat during regeneration of the catalyst and supplying this heat to the bed undergoing cracking reactions (McKetta, 1981). Automatic valves and control algorithms were used to accomplish this feat. The drawbacks to the process were expensive alloy heat exchanger in the reactor, lack of operation flexibility due to fixed bed operation and poor heat utilization. The reaction bed temperature varied widely during reaction and regeneration periods, and the temperature differential within the bed during each cycle was considerable.

It became apparent that the Houdry process was inadequate and that advantages could be gained from making the process continuous with flow of catalyst back and forth between a cracking zone and a regeneration zone (Jahnig et al., 1984). The catalyst in the form of a powder could accomplish this and at the same time the smaller catalyst size would increase the rate of the diffusion-limited reactions (cracking and combustion). A method to circulate the catalyst between reaction and regeneration zones led to the moving bed process and the combination of this with fine powders led to the fluid-bed reactor and hence a new unit operation called fluidization (Avidan et al., 1990a).

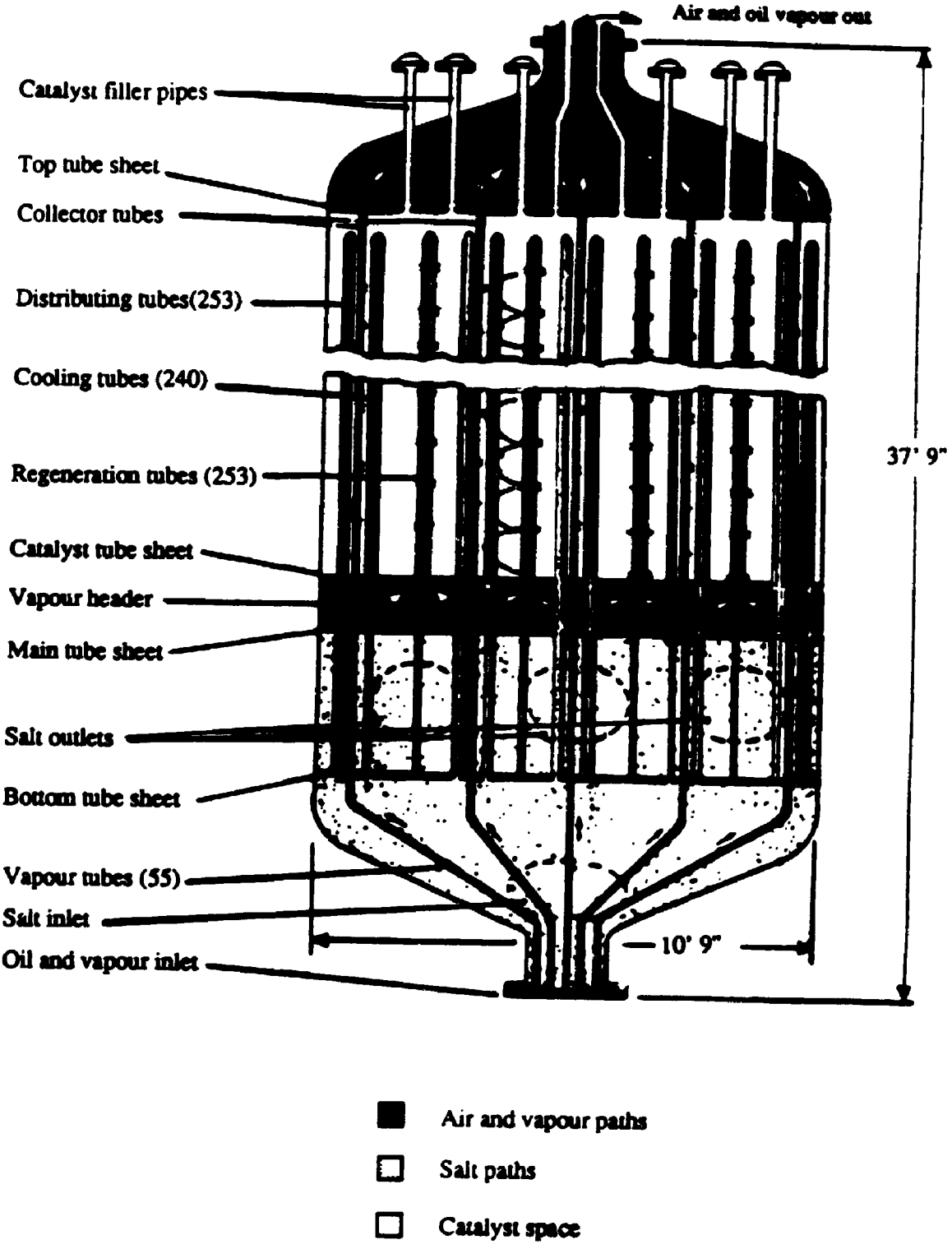

Figure 1.1 Schematic of the Houdry fixed bed catalytic cracking reactor (Avidan et al., 1990).

1.1.2 The Moving Bed Process

The moving bed process was based on a bucket elevator Thermofor Catalytic Cracking (TCC) unit developed by Socony-Vacuum and the Houdry Process Company. Catalyst was transferred by bucket between the reactor and regeneration zones. At the same time, Socony-Vacuum developed the air-lift TCC process. In this operation the reactor vessel is suspended above one or more regenerators with the regenerated catalyst flowing out to an air lift where it is pneumatically conveyed back to the reactor zone. In the period of 1948 to 1950 the new air-lift TCC was designed and during 1950 to 1952 Socony-Vacuum established success in licensing these units. However, competition from the fluid bed process was great and eventually the advantages of this powdered type operation led to the obsolescence of the moving bed process. The TCC catalyst was always diffusion limited (diffusion is proportional to the square of particle diameter) and the TCC bead catalyst was 50 times larger than FCC catalyst and more difficult to circulate (Avidan et al., 1990a). The last air-lift TCC unit was built in 1960 and a study showed that even with royalty costs a 1960 FCC design was cheaper than the TCC design by 20% (Avidan et al., 1990a).

1.1.3 The Fluid Bed Process

The parallel development of the fluid-bed catalytic cracking process was a result of increased demand for high-octane aviation gasoline during the Second World War and the high licensing fee for the Houdry units. Standard Oil Co. of New Jersey (now Exxon) had applied for a license but found it to be too costly and thus decided to develop its own process. The use of fine powders was based on a discovery by R. K. Stratford at Exxon's Canadian affiliate, Imperial Oil, that fine clay discarded from lube oil treating had catalytic effects (Reichele, 1989). This pioneering work using a suspensoid process established the feasibility of using powdered catalyst in pipe coil reactors to accelerate liquid phase cracking. In 1938, the Catalytic Research Associates (CRA) was formed which consisted of a consortium of eight companies; Exxon, M.W. Kellogg Co., Standard Oil Co. of Indiana, Anglo-Iranian Oil Co., UOP, Texaco, Royal Dutch Shell and I.G. Farben (Avidan et al., 1990a). The objective of the CRA was to develop a catalytic cracking process that would not infringe on the Houdry patents. Over four hundred men at Exxon and six hundred in the other companies resulted in one of the greatest scientific efforts directed at a single project (Squires, 1986).

CRA chose Exxon's powdered catalyst approach and converted the 100 barrel per day fixed-bed cracker at Baton Rouge to powder operation. This pilot unit was named PECLa (Powdered

Experimental Catalyst Louisiana) and consisted of a folded reactor riser with standpipes and slide valves for control of solids circulation (Squires, 1986). The switch in process basis from fixed bed operation with pelleted or extruded catalyst to a powdered catalyst reactor was based on several factors. The catalyst rapidly lost activity due to carbon deposition and it was envisioned that better utilization of catalyst activity could be achieved with shorter contact times in flowing solids systems.

Later, the PECLa design was modified with diameter expansions in the reactor and regenerator to increase solids hold-up without the folded risers. This modification was implemented as a result of the work by W.K. Lewis and co-workers at M.I.T. who found that fine powders exhibit a terminal settling velocity far in excess of what Stokes law would predict based on single particles. It was found that a dense bed of fluidized solids would form at low gas velocity if the solids feed rate exceeded the entrainment rate. Small particles in fluidized solids seemed to behave as agglomerates rather than as discrete particles (Vanderwals forces dominate for small particles). Thus, it was realized that the concentration of catalyst would be greater in up-flow compared to down-flow pipes as a result of slippage (Jahnig et al., 1980).

The standpipe concept to build up a pressure differential was a breakthrough and in combination with a low density riser and a dense phase fluid-bed reactor allowed high circulation

rates of the catalyst to transfer heat from the regenerator to the reactor without mechanical pumps or moving parts in contact with the abrasive solids. This led to the construction of the first commercial FCC unit called "Model I" at the Baton Rouge refinery in May 1942 (Decroocq, 1984). This model was referred to as up-flow design since catalyst and feed moved upwards together in both the reactor and the regenerator. A combination of external cyclones and hoppers that operated between 20 and 30 psig were used to recover the catalyst. The collected catalyst was then allowed to fall into a standpipe which had a slide valve at the base to control catalyst flow (McKetta, 1981; Montogomery, 1980).

Shortly after this and at the same time other Model I units were being installed, it was realized that a dense phase fluid bed of fine powder would form at gas velocities lower than 1 m/sec. This led to the basis for the turbulent fluid bed concept (currently used today in many other applications) and resulted in the Model II FCC unit (see Figure 1.2). In this new unit, introduced in 1944 and still used today, the catalyst is separated from the hydrocarbon vapours in the fluidized catalyst bed of the reactor vessel and is continuously removed down-flow from the bed (McKetta, 1981). The Model II allowed for higher catalyst to oil ratios thus increasing conversions of oil and a lower gas velocity was obtained because of larger vessel diameter to allow cyclones inside the regenerator unit. Other advantages of this down-flow design included simplified catalyst recovery, simplified

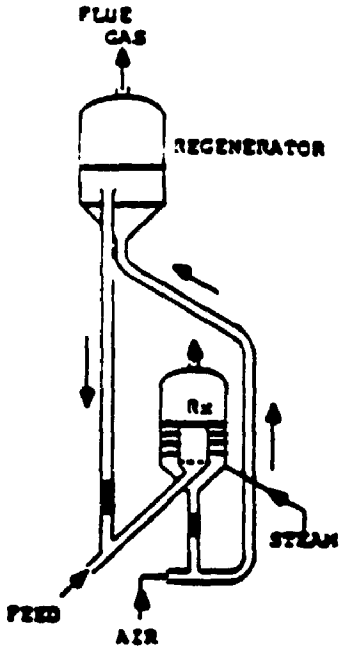

MODEL II

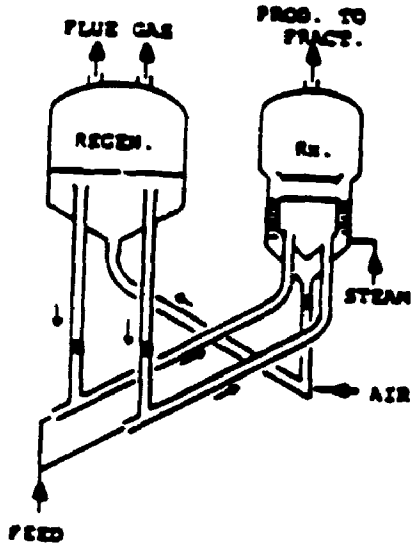

MODEL III

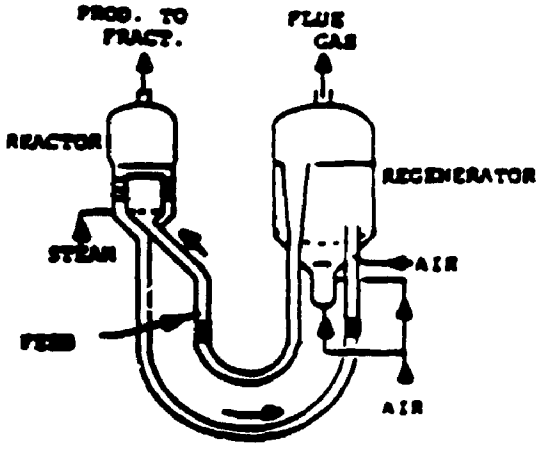

MODEL IV

Figure 1.2 Model II, III and IV FCC designs.

support structure and plant layout and improved operating flexibility (Decroocq, 1984).

After the Second World War the CRA agreement ended and the various companies pursued independent development of FCC processes. In 1947 M.W. Kellogg introduced the Model III unit as shown in Figure 1.2 which was based on an improved pressure balance design (Avidan et al., 1990a). The design scheme had the reactor and regenerator mounted at the same level thereby reducing significantly the overall height of the cracking unit. Advantages were lower capital investment, lower pressure, improved yields, ease of maintenance and lowered utility costs (Montgomery, 1980; McKetta, 1981; Decroocq, 1984).

Furthermore, in 1951 Exxon perfected the Model IV unit which had a reduced height and diameter of the vessels for the same throughput. The catalyst circulated between the reactor and regenerator which were at the same level by means of U-bends. The U-bend slide valves were left in the wide open position and were used only for start-up and shut down. The catalyst circulation was controlled by pressure balance and a variable dense phase riser. The density in this control riser could vary between 160 and 320 Kg/m^3 by changing the gas velocity between 2 and 5 m/s (McKetta, 1981). The reactor and regenerator bed zones were designed to run at 1 to 2 m/s resulting in lower bed densities and more efficient reactions in both vessels. With newer highly active catalysts many of the Model IV units are now run with no reactor bed where the

catalyst level is held below the reactor grid in the stripper zone. This results in a dilute phase environment for the oil and catalyst reducing excessive cracking.

The other members of CRA continued development of FCC technology. Universal Oil Products (UOP) introduced its highly popular stacked unit in 1947 and thirty such units were sold in the 1950s with capacities in the 4,000 to 10,000 barrel per day range (Avidan et al., 1990a). In this design, the reactor is placed just above the regenerator thus eliminating the need of an air riser and expansion joints. Also, a simple support structure can be used and a reduced regenerator size is made possible by increased pressure. UOP later built large side-by-side riser FCC units and together with Mobil developed the high-efficiency riser regenerator.

M.W. Kellogg designed 47 side-by-side FCC units during the period 1944 to 1955 (Avidan et al., 1990a). Then in 1951, Kellogg put on stream the first Orthoflow A design where vertical catalyst standpipes with internal plug valves were used for catalyst circulation and the reaction and regeneration zones were within a single vessel. In 1958 the Orthoflow B design was introduced with the reactor and regenerator switched in position from the A configuration (reactor below regenerator). Other designs were introduced including the C and F Orthoflow models. Orthoflow F is shown in Figure 1.3 and was the result of evolutionary FCC development at Kellogg (Wrench et al., 1986). It employs all riser cracking to take advantage of high-activity, coke

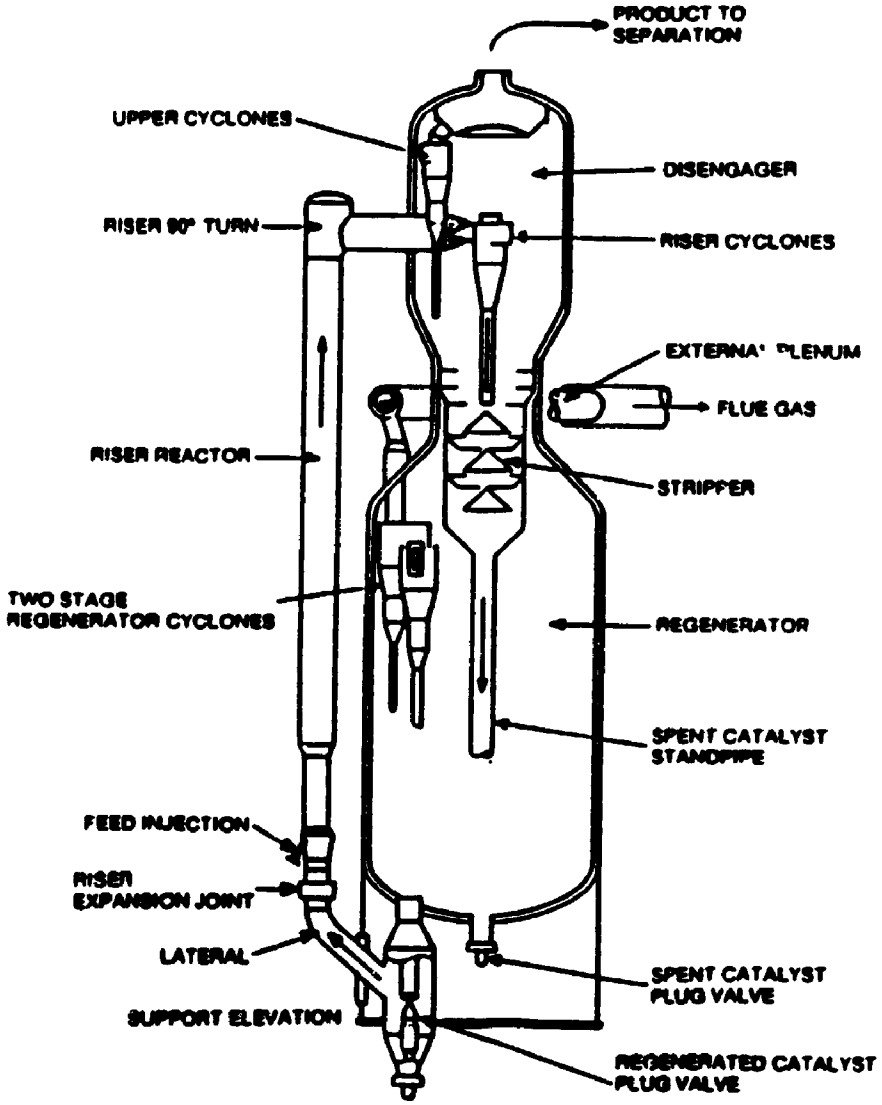

Figure 1.3 Kellogs Orthoflow F FCC unit (Avidan et al., 1990).

selective zeolite catalysts.

1.1.4 FCC Riser Reactors

The introduction of high activity zeolite catalysts in the 1960s resulted in a revolution in FCC designs (de Lasa, 1982). The work by Plank et al. (1964) showed that by incorporating zeolite into a silica-alumina matrix, 100-1000 times improved activity could be achieved as compared to the amorphous silica-alumina and improved hydrogen transfer capability was also possible which would increase gasoline yields significantly. Plank (1984) reviews the invention of zeolite cracking catalysts and the developments that took place at Mobil.

The advent of these new zeolite catalysts into the market (Gussov et al., 1972; Montgomery, 1972) resulted in a shift to shorter contact time cracking. The requirement for long residence times in dense fluidized beds was no longer valid since the high activity catalysts became excessively coked and overcracking resulted in large amounts of light gases. Efforts were made to modify existing units to take advantage of the activity and selectivity of the new catalysts generating a new FCC concept. In fact, reaction began in the transport line conveying the catalyst to the reactor hence these lines were lengthened to provide a 3-4 second reaction time followed by a shallow dense bed in the reactor (Blazek, 1973; Strother et al., 1972; Whittington et al., 1972; Bunn et

al., 1969).

New FCC designs were then patented in the late 1960's and early 1970's based on all 'riser' cracking where reaction occurred only in the transfer line such as Exxon's Flexicracker, the Texaco FCC process, the UOP straight riser, Gulf's riser unit and the Orthoflow F unit from M.W. Kellogg (Murcia et al., 1979; Murphy and Soudek, 1977; Finnerman et al., 1974; Pierce et al., 1972; Bryson and Huling, 1972). Shell had invented a short-residence time FCC riser reactor almost a decade before the use of zeolite cracking catalysts (Avidan et al., 1990a). The up-flow reactor with short contact times, high temperature and other concepts was ahead of its time.

Since the switch to riser cracking other improvements and advances in FCC technology emerged due in part to catalyst development, advances in metallurgy, need to process heavier feeds and environmental concerns. The legislated reduction of CO emissions led to the use of combustion promoters such as platinum deposited in small concentrations on the cracking catalyst to ensure complete combustion of CO to CO_2 within the regenerator (Hartzell and Chester, 1979; Chester et al., 1979). With increased oil prices and a new demand pattern for oil products (high octane gasoline without lead additives) it was necessary to crack heavier feeds which contained high levels of nickel and vanadium metals leading to excess coke and light gases as well as catalyst deactivation (vanadium degrades zeolite structure) (Hemler et al., 1985; Elvin, 1983;

Otterstadt et al., 1986). The use of metal passivators such as antimony (patented by Phillips Petroleum to reduce nickel dehydrogenation by 50%), and bismuth have been used as well as vanadium traps and new families of zeolitic catalysts (Redsicat, GRZ) to overcome these problems (Davies, 1977; Dale and McKay, 1977; Magee et al., 1979; Edelman et al., 1979).

Furthermore, FCC units were modified to process heavy oil and Heavy Oil Cracking process (HOC) was developed by M.W. Kellogg and Phillips Petroleum. Later in the mid 1970's Ashland Oil and UOP Inc. patented the RCC process (resid catalytic cracking) and Total Petroleum developed the R2R process which used two regenerator stages (Johnson et al., 1985; Hemler et al., 1984; Mauleon and Sigaud, 1987). Also, Shell has developed resid FCC technology as reviewed by Nieskens et al. (1990) which includes a more compact reactor with a few seconds residence time, a high-efficiency riser-end-separator, an integral swirl-tube separator inside the regenerator vessel, single stage regenerator cyclones, complete or partial CO combustion, larger capacity catalyst coolers, and reduced unit catalyst inventory. Huskey (1990) reviews in more detail the various resid processes.

Features of these designs include better mix temperature control in the riser through advanced multiple nozzle feed injection systems (Murphy, 1984; Galtier and Pontier, 1989), catalyst coolers in the regenerator to handle larger energy inventory as a result of higher coke make from the heavier feeds (Mauleon and Courcelle, 1985) and dual stage

regeneration as in the R2R process. The first stage regenerator operates at approximately 700°C with insufficient oxygen to burn most of the hydrogen present in the coke. In the second stage high temperature combustion (900°C) takes place in the absence of water vapour obtaining near to complete combustion and minimizing deactivation of the zeolite.

In general hardware advancements have been made over the years to obtain improvements in catalyst-oil contact, higher reaction temperatures, quick quench and product/catalyst separation, more efficient catalyst stripping, increased catalyst recovery and less catalyst inventory. The design of feed nozzles is crucial to ensure rapid feed vapourization and uniform mixing with the regenerated catalyst. Atomizing devices are used with the aid of injected steam to generate droplets smaller than 100 μm (Avidan et al., 1990a). Multiple nozzles which extend into the region of catalyst entry and angled upward have been effective in more uniform distribution of the feed and faster vapourization (Saxton and Worley, 1970). Figure 1.4 shows solids density contours in a riser reactor as obtained by gamma radiation techniques using different numbers of nozzles. Local densities near the wall can be as high as 60 lb/ft^3 and less than 3 lb/ft^3 near the riser center for a poor injection system (Saxton and Worley, 1970). At the wall catalyst 'rains' downward due to frictional forces resulting in the higher density levels.

Contacting improves as the number of nozzles increases and

	Test 2	Test 3	Test 4A	Test 5	Test 6
No. oil nozzles	1	1	1	3	2
Cat/oil ratio	6.42	6.54	6.81	6.64	6.58
Cat rate T/min	17.6	17.9	19.0	19.0	18.8
Total feed rate, b/d	23566	23233	24038	24313	24336
Total injector steam lb/hr	4276	4276	4276	4199	4199
Steam to oil nozzle, lb/hr	1173	2107	1173	1173	1173

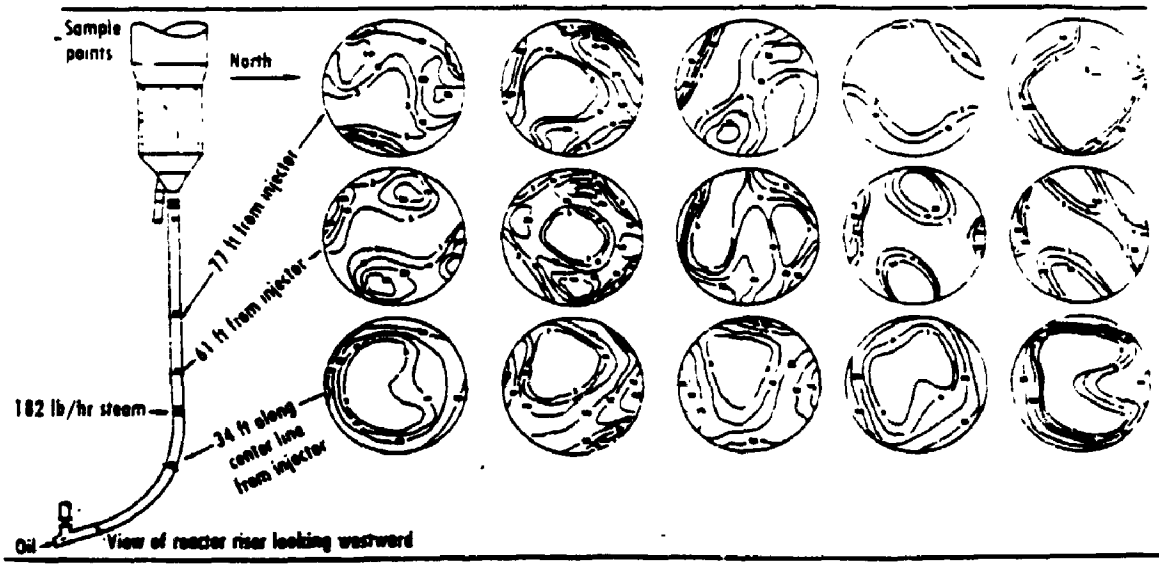

Figure 1.4 Density contours in a riser reactor at different locations as a function of the number of injector nozzles (Saxton and Worley, 1970).

also as the catalyst-gas mixture proceeds up the riser. Figure 1.5 shows the catalyst density profile as a function of riser height. With the initial solids/oil contact, pneumatic transport occurs and the rapid molar expansion of cracking causes a sharp increase in vapour velocity. The catalyst accelerates over a few seconds from a low initial velocity to one close to the vapour velocity (Hemler et al., 1985). The difference in catalyst-vapour velocity is the slip velocity and is normally assessed using the ratio of catalyst residence time to vapour residence time (Pohlenz, 1963). This ratio can be as high as 1.5 over the entire reactor length. However, high exit gas velocities of above 25 m/s can significantly reduce this ratio close to unity which is desirable to avoid backmixing and hence overcracking (Venuto and Habib, 1978). Shell has done work in developing a model to describe the two-phase gas-dispersed solid flow occurring in a riser (Berker and Tulig, 1986).

Another important development in FCC designs has been the improvement of separation technology. The use of closed cyclones has eliminated post-riser, nonselective thermal cracking which occurs as the result of using higher temperatures (Avidan et al., 1990b). In this design the top of the riser is directly connected to the cyclones where the catalyst is quickly separated and the product sent to the fractionator. In retrofitting some earlier FCC models (Models II to IV) for riser cracking, the product was separated first in a rough cut low-efficiency cyclone. It then passed to the

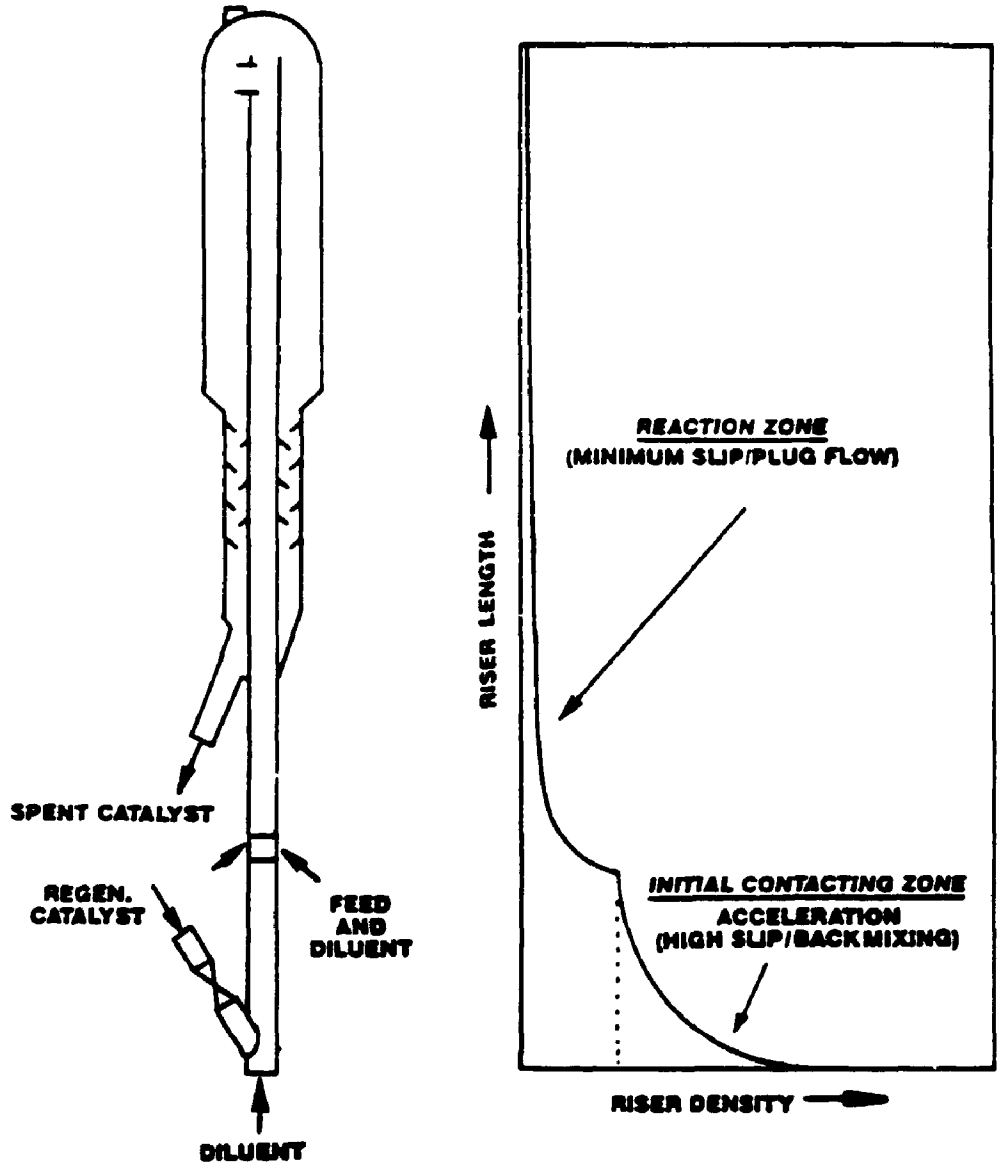

Figure 1.5 Density profile along the height of a riser reactor (Hemler et al., 1985).

primary cyclones housed in the larger diameter vessel before going to the fractionator resulting in additional residence times of up to one minute during which period post riser cracking could occur. The closed cyclone system eliminates this extra residence time. Stripper cyclones and other techniques such as high length/diameter ratio, unbaffled staged stripping have been patented (Parker et al., 1984; Krug and Schmidt, 1988).

1.1.5 Recent Trends and Future Challenges

The main direction of research in the FCC process is in the catalyst development and manufacturing area (Occelli, 1988; Desai, 1989). Environmental concerns are in the spot light for the 1990s and depending on government legislations, the oil industry will be challenged to meet stringent levels set for acceptable products and emissions.

Public awareness of global warming and the greenhouse effect has resulted in regulations on CO, CO_2, SO_x, NO_x and hydrocarbon emissions. Governments are now proposing reformulated gasoline and diesel fuels to improve air quality and reduce human exposure to critical hydrocarbons (Unzelman, 1990). The reformulations include lower aromatics and olefins, lower sulphur, reduced vapour pressure and lower poly-nuclear aromatics. Some of these have been legislated in critical areas in the United States and Canada.

The reduction of aromatics (due to their carcinogenicity)

and lowered olefins (due to their high atmospheric reactivity) in gasoline is a formidable challenge for refiners since these classes of hydrocarbons are a major contributor to gasoline octane (Piel, 1989). Now that lead additives have been completely eliminated from gasoline, alternate high octane components will be required to replace aromatics and olefins. Refiners will be forced to increase alkylation and isomerization facilities to produce more highly branched paraffins which have high octane and are acceptable components.

Ethers such as methyl tertiary butyl ether (MTBE), ethyl tertiary butyl ether (ETBE) and tertiary amyl methyl ether (TAME) produced from the addition reaction of either methanol or ethanol and an iso-olefin (i-butylene, and the 2-methyl butenes) have high octane value, low RVP characteristics and are clean burning, gasoline compatible components. They are and will continue to be the most significant component in reformulated gasolines since they convert highly reactive and volatile i-olefins into high octane, low emission components (Unzelman, 1989). MTBE is the only fuel ether currently being produced on a large commercial basis, the other is TAME. A limiting factor in ether production is i-olefin feedstock source which for MTBE is obtained from FCC C_4 streams, steam cracked C_4s or by the n-butane isomerization-dehydrogenation route. ARCO, the largest producer of MTBE uses tert-butyl alcohol (a by-product from their propylene oxide process) which is dehydrated to i-butene as a feed source. MTBE

production is forecasted to grow significantly through the 1990s and beyond.

The FCC process is a major source of light olefins for alkylate and ether production. Thus, according to Stokes et al. (1990), its future primary role may be as a light olefin generator. Modification of process operation and development of new catalysts (such as ZSM-5 addition) will be required for this scenario.

On top of environmental concerns, the oil price structure will cause a shift towards processing heavier and more contaminated oils in the FCC unit. The development of dual function cracking catalysts containing scavenging agents to deal with high metal levels is expected to be at the forefront of FCC catalyst research and development.

In terms of process development, Avidan et al. (1990) discuss two possible breakthrough areas which are high-activity, high temperature, once-through cracking and very short contact time cracking. Chen and Lucki (1986) showed that when high temperature cracking (above 550°C) is employed at very short contact times (less than 1 second) the contribution of thermal cracking can be minimized and at the same time olefinic and aromatic hydrocarbon yields are increased which increases gasoline octane. Furthermore, coke yield drops and conversion increases. Chen and Lucki (1986) proposed a new FCC unit operating without continuous catalyst regeneration under high temperature and short residence time. One drawback of such a scheme is a practical means of

supplying heat to the unit for the high temperatures involved.

In general, the FCC process is expected to continue in developing just as it has over the past 50 years. Catalysis research and process improvements will likely be the major contributors to the advancement of FCC technology.

1.2 CATALYTIC CRACKING CHEMISTRY

The reactions taking place during the cracking of hydrocarbons over acidic catalysts have been studied extensively by several researchers (Greensfelder and Voge, 1945a; 1945b; 1945c; Greensfelder et al., 1945; Plank et al, 1964; John and Wojciechowski, 1975a; 1975b; Thomas and Barmby, 1968; Nace, 1969a; 1969b; Moscou and Moné, 1973; Jacob et al., 1976; Corma et al., 1986; Abbot and Wojciechowski, 1985a). Several reviews concerning the reactions and chemistry of catalytic cracking are also available in the literature (Gates et al., 1979; Venuto and Habib, 1978; McKetta, 1981; Decroocq, 1984; Scherzer, 1989; Magee and Blazek, 1976; Wojciechowski and Corma, 1986).

The transformations that occur when gas oil is catalytically cracked are complex with many of the primary products undergoing secondary reactions. Cracking reactions involve the rupture of carbon-carbon bonds and are thermodynamically favoured by high temperatures due to the endothermic nature of the reaction. A summary of the main

reactions according to Gates et al. (1979) is given below showing how cracking can occur:

1. Paraffins are cracked to give olefins and smaller paraffins;

   eg. $C_{16}H_{34}$ ---> C_9H_{18} + C_7H_{16}

2. Olefins are cracked to give smaller olefins;

   eg. $C_{12}H_{24}$ ---> C_7H_{14} + C_5H_{10}

3. Alkyl aromatics undergo de-alkylation;

   eg. $C_6H_5-C_nH_{2n+1}$ ---> C_6H_6 + C_nH_{2n}

4. Aromatics also undergo side-chain scission;

   eg. $C_6H_5-C_{12}H_{25}$ ---> $C_6H_5-C_8H_{15}$ + C_4H_{10}

5. Naphthenes are cracked to give olefins;

   eg. $C_{20}H_{40}$ ---> $C_{12}H_{24}$ + C_8H_{16}

Secondary reactions occurring after the initial cracking steps include hydrogen transfer (eg. naphthene + olefin gives aromatic + paraffin), isomerization, alkyl-group transfer, condensation reactions and disproportionation of low molecular weight olefins (Gates et al., 1979). These reactions are important in determining the final product compositions. Side reactions such as isomerization, alkyl-group rearrangement and dealkylation of aromatics occur only to a moderate extent at equilibrium under cracking conditions. Reactions such as paraffin-olefin alkylation, aromatic hydrogenation and olefin polymerization (except for ethylene polymerization) cannot proceed to any appreciable extent.

The endothermic reactions always predominate in cracking processes with the heat effect depending on the feedstock,

catalyst and reaction conditions. Hydrogen transfer reactions are exothermic such as the case of cyclohexane combining with c-2-butene to yield benzene and n-butane with a heat of reaction equal to -259 BTU/lb whereas the cracking of n-decane to yield n-pentane and 1-pentene has a heat of reaction equivalent to +249 BTU/lb (Leuenberger and Wilbert, 1987). Thus, using a rare earth exchanged zeolite catalyst, which promotes hydrogen transfer reactions, can raise the overall heat of cracking.

The reactions occurring in catalytic cracking are distinctly different from those of thermal cracking (McKetta, 1981). The differences are quite noticeable in the distribution of light gases. Major products of catalytic cracking are C3's and C4's whereas C1's and C2's are found in thermal cracking. The extensive work done by Greensfelder et al. (1949) on the cracking of the various molecular types of hydrocarbons over amorphous catalysts revealed the differences in thermal (or non-selective) and catalytic cracking as summarized in Table 1.1. For example, with alkyl aromatics carbon bond scission in the side-chain group occurs during thermal cracking to leave one or two carbon atoms attached to the ring. When alkyl aromatics are catalytically cracked the entire alkyl group next to the ring is readily severed to form an olefin (Greensfelder et al., 1949). Also, the olefins crack at a much higher rate than the corresponding paraffins during catalytic cracking as compared to thermal cracking. Another important difference is that hydrogen transfer occurs

Table 1.1 Catalytic versus thermal cracking reactions for the various hydrocarbons molecular types (Greensfelder et al., 1945a).

HYDROCARBON	CATALYTIC CRACKING	THERMAL CRACKING
n-Paraffins	Extensive breakdown to C2 and larger fragments. Product largely in C2 to C6 range and contains many branched aliphatics. Few normal alpha olefins above C6	Extensive breakdown to C2 fragments with much C1 and C2. Prominent amounts of C4 to Cn-1 normal alpha olefins. Aliphatics largely unbranched
Isoparaffins	Cracking rate relative to n-paraffins increased by t-carbonium atoms	Cracking rate increased to a relatively small degree by presence of t-carbon atoms
Naphthenes	Crack at about same rate as those paraffins with similar numbers of tertiary carbon atoms. Aromatics produced, with much hydrogen transfer to unsaturates	Crack at lower rate than normal paraffins. Aromatics produced with little hydrogen transfer to unsaturates
Unsubstituted aromatics	Little reaction: some condensation to biaryls	Little reaction: some condensation to biaryls
Alkyl aromatics (substituents C3 or larger)	Entire alkyl group cracked next to ring and removed as olefin. Crack at much higher rate than paraffins	Alkyl group cracked to leave one or two carbon atoms attached to ring. Crack at lower rate than paraffins
n-Olefins	Product similar to that from n-paraffins but more olefinic	Product similar to that from n-paraffins but more olefinic
All olefins	Hydrogen transfer is an important reaction, especially with tertiary olefins. Crack at much higher rate than corresponding paraffins	Hydrogen transfer is a minor reaction, with little preference for tertiary olefins. Crack at about same rate as corresponding paraffins

to a minimal extent in thermal cracking but is much more evident in the catalytic reactions yielding increased C2 to C6 compounds.

1.2.1 Reaction Mechanism

The differences in product distributions between thermally cracked and catalytically cracked hydrocarbons can be explained in terms of the reaction mechanism. Free radical mechanisms are postulated for thermal cracking whereas the intermediate formation of positively charged organic species, called carbocations is generally accepted for catalytic cracking (Decroocq, 1984; Gates et al., 1979; Scherzer, 1989). Carbocations include both carbenium ions (the charge-carrying carbon atom can be di- or tricoordinated) and carbonium ions (charge-carrying can be tetra- or pentacoordinated). Carbocations are most stable in the tertiary form followed by secondary then primary ones. Thus, primary carbocations tend to isomerize to the more stable tertiary and secondary forms.

The mechanism was first proposed by Whitemore (1948) who suggested a carbonium ion as the intermediate in the low-temperature acid-catalyzed reactions such as alkylation and polymerization. The concept was applied to catalytic cracking and many previous experimental observations could easily be correlated, resulting in the general acceptance of the mechanism (Davis and Hettinger, 1983).

It has been postulated that the active sites on the

the introduction of zeolites as cracking catalysts (Plank, 1984). These molecular sieves whose active sites are located in controlled pores gave more selective cracking and hence less coke formation (Davis and Hettinger, 1983). Zeolites were found to be more active than amorphous silica-alumina due to greater concentration of active sites and greater effective concentration of hydrocarbons in the vicinity of a site resulting from the strong adsorption in the fine micropore structure. The zeolite material was embedded in a silica-alumina matrix to form the cracking catalyst which revolutionized FCC operation.

The first zeolite used in catalytic cracking was the rare earth exchanged form of X-type zeolite. This was soon replaced by Y-type zeolite which had improved thermal and hydrothermal stability because of a higher silica/alumina ratio. The basic Y zeolite structure has since been chemically modified to produce HY (a hydrogen form of Y zeolite) and ultra-stable Y (USY) which is a stabilized form of HY (Yanik et al., 1985).

With the switch from amorphous silica-alumina to zeolite catalysts a significant advantage in addition to the higher activity was the better selectivity obtained. Yields of products increased in the C5 to C10 range and decreased in the C3 to C4 range when using the zeolite catalyst. The reason for this is attributed to the zeolites greater hydrogen-transfer activity as compared to chain-scission reactions. Hydride-ion transfer to the carbenium ion and hydrogen

terminated when the carbenium ion loses a proton to the catalyst and is converted to an olefin. The intermolecular hydride transfer between the carbenium ion and a paraffin propagates the reaction and is the rate-determining step of the cracking reaction (Scherzer, 1989). In competition with the scission mechanism there are other steps such as the tendency of the carbenium ion to find a more stable configuration and carbenium ion interaction with a double bond which provides a route for cyclization.

The mechanism concerning pentacoordinated carbonium ion intermediates (eg. $R_1-CH_3^+-CH_2-R_2$, $R_1-CH_2^+=CH-R_2$, $C_6H_7^+$) occurs at temperatures above 500°C with the intermediates undergoing ß-scission to smaller paraffins and carbenium ions. As well, the carbonium ions are converted to carbenium ions through the loss of hydrogen, present as molecular hydrogen in the cracking products. This mechanism is also favoured by low conversion, low hydrocarbon partial pressure and high constraint indexed zeolites (Scherzer, 1989).

1.2.2 Catalytic Cracking of Gas Oil

Primary Reactions - The primary products of catalytically cracked gas oils are gasoline range (C5 to C12) paraffins and olefins, n-butane, butenes and propylene. The gasoline range paraffins reach a maximum yield with conversion and then undergo further cracking usually referred to as 'over-cracking'. The gasoline range olefins also reach a maximum

yield but at a lower conversion before they over-crack (John and Wojciechowski, 1975a). Butenes are considered unstable primary products which undergo further secondary reactions. Propylene and n-butane are stable primary products which are not significantly converted to other products after their initial formation.

Hydrogen Transfer - Hydrogen transfer plays a key role in the gas oil cracking process (de Jong, 1986). Many of the acid catalyzed secondary reactions involve intra- or intermolecular hydrogen transfer and the final composition of the cracked products depends on the relative rates of these reactions. Hydrogen transfer is important because it reduces the amount of olefins in the product, influences product molecular weight distribution, increases gasoline selectivity, influences gasoline quality and contributes to coke formation and hence catalyst deactivation (Gates et al., 1979).

Hydrogen transfer occurs through the transfer of bimolecular hydrogen from a naphthene to highly reactive olefins to form a stable paraffin and aromatic which are less prone to secondary cracking:

$$3\ C_nH_{2n} + C_mH_{2m} \longrightarrow 3\ C_nH_{2n+2} + C_mH_{2m-6}$$

Olefin Naphthene Paraffin Aromatic

In terms of gasoline quality, as determined by the octane number method, the formation of aromatics is beneficial since they show the highest octane of the various hydrocarbon groups (next are olefins and naphthenes with n-paraffins possessing

low octane values). However, the loss of olefins and naphthenes from the hydrogen transfer reaction results in a net loss of octane and some of the aromatics formed end up in the light oil fraction and also contribute to coke formation. The benefit of increased gasoline yields from hydrogen transfer reactions comes at the cost of lowered gasoline octane.

Hydrogen transfer can also occur by olefins abstracting hydrogen from aromatics or other hydrogen-deficient products to form more paraffins and coke (Schezer, 1989). Zeolites such as REY and REHY readily catalyze hydrogen transfer between olefins and naphthenes because of the high density of acidic sites. In such catalysts the concentration of hydrocarbon reactants in the pore structure is presumably high which also enhances bimolecular hydrogen transfer.

Coke Formation - Coke formation reactions are probably the least well understood of those involved in catalytic cracking. Coke is formed in almost all catalytic hydrocarbon conversion reactions and typically consists of hydrogen deficient mono- and polycyclic aromatic rings connected by aliphatic and alicyclic fragments with characteristics similar to graphite. A chemical and physical characterization of coke deposited on a catalyst indicates the presence of carbon, hydrogen, sulphur oxygen and nitrogen giving a molecular weight ranging from 940 to 1010 (Wolf and Alfani, 1982; Fetting et al., 1984). Rapid decay in the activity of the catalyst occurs when these highly

unsaturated, high molecular weight compounds become adsorbed to the catalyst surface. Catalyst activity is renewed by combustion of the coke deposits.

Some results suggest that the rate of coke formation may be related to olefin formation rates and to an overall hydrogen balance (Nace, 1969). In general, the rate of coke formation increases with increasing acid strength and acid-site density on the catalyst. Usually coke formation requires a source of hydrogen (coke precursor) and a sink for hydrogen (olefin) showing that hydrogen transfer plays an important role.

Appleby et al. (1962) showed that in catalytic cracking coke formation proceeds through intermediate aromatic structures of increasing size and complexity. They also found that the coke forming tendency of many aromatics and their alkyl derivatives correlates well with their basicity and the mechanism of coke formation is that of intermediate carbenium ions. Overall, the mechanism of coke formation is complex involving a multistep reaction sequence comprising: adsorption, dehydrogenation, condensation-polymerization, and cyclization of hydrogen-deficient fragments to form polynuclear residues.

In the FCC process coke yields are classified into four categories:

i) Catalytic coke - from the acid catalyzed cracking reactions shown to be residence time dependent

ii) Contaminant coke - from the catalytic action of metal

poisons such as nickel and vanadium

iii) Conradson coke - hydrogen deficient, high coking tendency feed components which correlates directly with the basic nitrogen and average molecular weight of the feedstock, as well as the Conradson carbon analysis

iv) Cat-to-oil coke - hydrocarbons which are not stripped by steam in the stripper and are left adsorbed to the catalysts surface and thus burned in the regenerator.

In general, the deactivation caused by carbon-containing molecules are structure sensitive to the precursor-catalyst system and the reaction-reactor environment (Wolf and Alfani, 1982).

1.2.3 Effects of Some Operating Variables

Several operating variables play an important role in determining overall conversions, selectivities and product quality in the FCC process. Optimization of these variables is essential to obtain good unit performance.

The effect of increasing reactor temperature at constant conversion is to decrease the C5+ gasoline yield and coke yield while increasing dry gas and total butanes yields (McKetta, 1981). In addition, olefin yields increase; C1 and C2 yields increase; C3 and C4 paraffin yields change only slightly; C5+ paraffin yields decrease; and Motor and Research octane numbers of the gasoline fraction increase (Motor Octane Number or MON is measured at an engine speed of 900 RPM,

whereas Research Octane Number or RON is measured at 600 RPM).

The increase in octane numbers with increasing temperature (RON enhanced more than MON) can be explained by the lower hydrogen transfer rates occurring at the higher temperature levels in comparison with cracking rates (Gates et al., 1979). This results in more olefins and aromatics present as compared to paraffins especially in the heavy gasoline fraction. The increased role of thermal cracking at higher temperatures does not favour the formation of branched hydrocarbons but does favour olefin formation resulting in increased gasoline sensitivity (Scherzer, 1989). The refiner must optimize the trade-off between lowered gasoline yields (but increased conversion) and more attractive octane numbers at higher temperatures.

The mass of catalyst fed to the reactor per unit mass of gas oil injected is normally referred to as the catalyst to oil ratio (c/o). This variable can be increased, at constant space velocity and temperature, to increase conversion (McKetta, 1981). As well, pilot plant and commercial unit studies show that at constant conversion, reactor temperature and catalyst activity, an increase in the c/o ratio gives increased coke yields, decreases hydrogen and C1 to C4 yields and has little effect of C5+ gasoline yield or octane number (Moorman, 1954).

The residence time of the catalyst and oil mixture within the riser is one of the most important parameters. With high activity catalysts the contact between oil and catalyst is

kept at a few seconds in order to minimize excess coke formation and secondary reactions. In this way gasoline selectivity is optimized and more olefins are formed thus increasing the RON. A unit operating at high contact times will give somewhat higher MON of the gasoline due to increased selectivity for aromatics and branched hydrocarbons (Corma and Orchillés, 1989).

The effect of operating pressure in the FCC process does not play a significant role since most units operate close to atmospheric pressure (typically 1-3 atm) (Pohlenz, 1963). Lowering the partial pressure of the reacting gases with steam is used mainly to aid the feed injection system in atomizing the feed to small droplets which vapourize quickly. Increasing the amount of inert steam in the process lowers the partial pressure of hydrocarbons and thus lowers conversion. Also, lower oil partial pressures result in increased gasoline RON due to an increase in gasoline olefinicity (Schezer, 1989). Working at higher pressures is not feasible because of the condensation of unsaturated compounds to form coke, difficulty in feed vapourization and increased polymerization reactions which leave a solid residue deposited on the catalyst (Vermillion, 1974).

1.3 CRACKING CATALYSTS

The basic requirements of a cracking catalyst include the ability of the material to increase conversion of the feedstock, improve selectivity towards the desired product, resist poisons, have good thermal, chemical and mechanical stability and have a capacity for regeneration (Satterfield, 1980). Natural clays were used as the earlier cracking catalysts with their activity generated by an acid treatment. However, they exhibited poor mechanical strength, thermal instability and fast deactivation by poisons. Subsequently, they were replaced by synthetic catalysts consisting mainly of amorphous silica and alumina.

These amorphous catalysts were used extensively in the early development of the FCC process from 1940 to 1960 (Avidan et al., 1990). A cogelled mixture of silica and alumina containing mainly silica is highly active (Gates et al., 1979). The incorporation of alumina into silica forms surface sites (Bronsted and/or Lewis) which catalyze cracking reactions. Typically these catalysts contain 10 to 12 percent alumina and have surface areas varying from 200 to about 600 m^2/g (Gates et al., 1979). The pellets or particles of silica-alumina available commercially consist of 30 to 50 Å primary particles packed loosely together to form irregularly shaped aggregates (0.05 to 3 μm in diameter) which are then pressed together.

The catalyst development at Mobil in the 1950s resulted in

the introduction of zeolites as cracking catalysts (Plank, 1984). These molecular sieves whose active sites are located in controlled pores gave more selective cracking and hence less coke formation (Davis and Hettinger, 1983). Zeolites were found to be more active than amorphous silica-alumina due to greater concentration of active sites and greater effective concentration of hydrocarbons in the vicinity of a site resulting from the strong adsorption in the fine micropore structure. The zeolite material was embedded in a silica-alumina matrix to form the cracking catalyst which revolutionized FCC operation.

The first zeolite used in catalytic cracking was the rare earth exchanged form of X-type zeolite. This was soon replaced by Y-type zeolite which had improved thermal and hydrothermal stability because of a higher silica/alumina ratio. The basic Y zeolite structure has since been chemically modified to produce HY (a hydrogen form of Y zeolite) and ultra-stable Y (USY) which is a stabilized form of HY (Yanik et al., 1985).

With the switch from amorphous silica-alumina to zeolite catalysts a significant advantage in addition to the higher activity was the better selectivity obtained. Yields of products increased in the C5 to C10 range and decreased in the C3 to C4 range when using the zeolite catalyst. The reason for this is attributed to the zeolites greater hydrogen-transfer activity as compared to chain-scission reactions. Hydride-ion transfer to the carbenium ion and hydrogen

transfer to olefins stops the cracking of carbon chains in zeolites and gives products with higher molecular weights (Gates et al., 1979).

The higher gasoline yields obtained with zeolite catalysts came at the expense of lowered gasoline octane numbers (Desai and Haseltine, 1989). Subsequently, octanes were increased by the use of lead additives in the 1970s to maintain these increased gasoline yields. Then, with the legislated elimination of lead in gasoline (Weiszmann et al., 1986; Pierce and Logwinuk, 1985; Culberson et al., 1985) octane catalysts based on USY and modified USY type zeolites were implemented to overcome the octane debit. The FCC catalyst based on USY was actually introduced to the market in 1964 but refineries chose to use the rare earth ion-exchanged Y zeolite catalyst (REY) because of its lower cost (Tsai et al., 1989). The USY catalysts increase octane by attaining lower silica/alumina ratios hence decreasing acid site density. This effectively reduces hydrogen transfer reactions giving a more olefinic gasoline.

Another change which stimulated FCC catalyst development was the shift in feedstock from conventional gas oils to heavier feedstocks (bottom of the barrel). Residual feeds contain high levels of vanadium and nickel which result in higher coke and dry gas yields and faster deactivation of the catalyst. Also, the presence of increased basic nitrogen containing molecules in resid feed can result in loss of catalyst activity from poisoning of the acid sites by the

basic compounds (Corma et al., 1987; Fu and Schaffer, 1985).

The larger molecules present in heavy feedstocks exhibit diffusional problems in the zeolite pores (Rajagopalan et al., 1986; Tauster et al., 1987; Maselli and Peters, 1984) and thus new catalysts were explored and developed to include active matrices which could crack the heavier oil compounds (Sterte and Otterstedt, 1988, Tsai et al., 1989; Ritter et al., 1981; Upson et al., 1990). Including an active amorphous component as the matrix is beneficial for bottoms conversion where heavier compounds are cracked on the matrix and then the lighter compounds diffuse through the matrix to the active zeolite sites. However, too much matrix activity may be an unfavourable option because it results in a degradation of product selectivity (Young and Rajagopalan, 1985).

To handle the increased metal levels found in residual oils, elements such as boron, bismuth, tin and antimony can be impregnated on the metal contaminated catalyst through injection of an organic complex with the cat-cracker feedstock (Ritter et al, 1981; Heite et al., 1990). These elements react with the nickel to form an inert residue on the catalyst surface which is less effective for dehydrogenation reactions. Vanadium passivation has not been as successful, although tin has been shown to reduce the detrimental effects of vanadium contaminants (Occelli, 1988; Barlow, 1986). The use of a large pore, low surface area matrix also improves metals tolerance by providing a poor base for dispersion of the metals. W.R. Grace is set to produce a new XP series of FCC

catalyst which cracks more bottom-of-the-barrel oil and improves gasoline yield and octane rating, while reducing coke production (Parkinson and Johnson, 1989). The use of such dual function cracking catalyst systems containing metal scavengers capable of retaining useful activity under severe metals loading is an approach of particular promise (Occelli, 1988; Pasek and Morgan, 1990).

FCC catalysis continues to develop especially in the area of increased bottoms cracking with better gasoline yields and at the same time octane boosts. The number and choice of catalysts available for FCC processing is quite extensive and new commercial catalysts are coming on stream each year (Corbett, 1986, 1990; Parkinson and Johnson, 1989; Alkemade et al., 1990). The manufacture of zeolite catalysts for petroleum refining is a $700 million per year business worldwide and is growing at approximately 5% per year (Chen and Degnan, 1988).

1.3.1 Zeolite Characteristics

Zeolites, also called molecular sieves, are crystalline microporous solids containing cavities and channels of molecular dimensions. These inorganic polymers comprise a negatively charged three dimensional framework of AlO_4 and SiO_4 tetrahedra linked by shared oxygen (Magee and Blazek, 1976). The primary building block of the zeolite structure is a tetrahedron of four oxygen atoms surrounding a central silicon

atom. These are connected through their corners of shared oxygen atoms to form small secondary building units which become interconnected to form polyhedra (Vaughan, 1988). In turn, the polyhedra connect to form infinitely extended frameworks of crystal structure. This type of stacking creates large cavities, called supercages with a diameter of about 13 Å and forms the large pore system of the zeolite. Four tetrahedrally distributed openings (12-membered rings) allows access to the supercages. A small pore system is also present, comprising sodalite cages (truncated octahedra) and the connecting hexagonal prisms (Scherzer, 1989).

In the order of 60 different zeolite structures have been found but only 11 are in commercial use (Vaughan, 1988). Also, approximately 1,000 different zeolite patents are issued each year indicating the widespread research and development going on in this area (Vaughan, 1988). For the cracking of oil the largest-pore size zeolites (zeolite Y) are used whereas selective petrochemical reactions use smaller pore ZSM-5 (pore size of 5.8 Å) (Yanik et al., 1985).

An industrial cracking catalyst is composed of 3 to 25 weight percent of 1-7 micron crystallites of a zeolite embedded in a matrix of amorphous silica-alumina (Gates et al., 1979). These catalyst particles are manufactured to be about 60 micron average size spheroids suitable for fluidization. Synthetic faujasite (zeolite Y) is preferred for cracking due to its somewhat larger internal cavity of 8-9 Å. A silica-alumina matrix is used as support for the

zeolites because pure zeolites are expensive and too active to be used in an industrial unit. The use of pure zeolites (1-7 micron size) may also involve problems resulting from complex separation in cyclones and conventional particle separation equipment.

The major function of the matrix is to bind the zeolite particles together in spray-dried microspheroidal catalyst particles which are highly attrition resistant. The matrix also serves as a diffusion medium for the feedstock molecules, as a diluting medium for the active zeolite, as a sink for sodium ions to increase thermal and hydrothermal stability, and as a heat carrier to facilitate heat transfer during cracking and regeneration (Scherzer, 1989). As stated above, an active matrix can also be used to contributes to the cracking of big molecules which cannot enter into the zeolite structure (Dean and Dadyburjor, 1989).

The structure of faujasite, as shown in Figure 1.6, reveals two separate 3-dimensional inter-connecting channels. The active sites I and II indicate the location of the sodium ions in the structure which can be replaced at high temperature by rare earth ions, like cerium or lanthanum (Chen and Garwood, 1986). The hexagonal prisms have a minimum opening of 2.5 Å and the 'super-cage windows' have openings of 7.4 Å (Satterfield, 1980). Pure faujasite has a surface area of 500 to 800 m^2/g which results in high activity. Incorporation into a matrix gives a more workable commercial FCC catalyst with a typical average surface area in the order

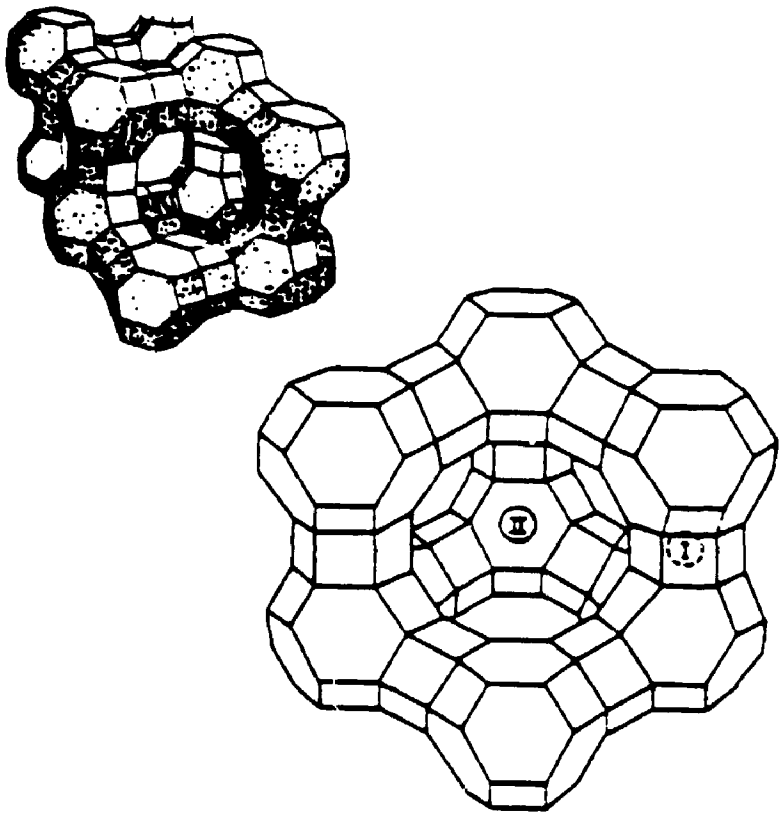

Figure 1.6 Perspective view of faujasite structure (Gates et al., 1979).

of 220 m^2/g.

The synthesis of zeolites is done using hydrothermal methods usually under mild conditions (90-100°C, 1-5 atm and pH less than 10) (Vaughan, 1988). The reactants can be silica from sodium silicate or an aqueous colloidal silica, aluminum from sodium aluminate and sodium or potassium hydroxides. These components are mixed to form a homogeneous slurry for 12-24 hours to produce sodium zeolite. This zeolite must be removed from the initial liquor at the proper time and then is thoroughly washed to remove sodium silicate from the pore structure. Properly washed zeolite has a sodium/alumina ratio of one (Gates et al., 1979).

The zeolite may be ion-exchanged in a rare earth ion solution where about 80-97% of the sodium is replaced by a mixture of lanthanum, cerium and neodymium which stabilizes the structure of the zeolite with their strong interaction with the sodalite cage. The zeolite is then added to a silica-alumina gel under high homogenization and spray dried to form the particles. Particle size distribution is controlled in this step by changing feed viscosity, pressure and temperature. A final washing step reduces the sodium content and drying is done in a rotary drier to remove water.

The diffusion of molecules in zeolites is unique due to the very small size of the channels and is also not well understood (Palekar and Rajadhyaksha, 1986). Numerous investigations have been made on the subject including attempts to extend the theory of diffusion of reactions in

other porous catalysts to zeolites (Gelbin and Fiedler, 1980; Hsu and Haynes, 1981; McLaughlin and Anthony, 1985; Ruthven, 1983; Pachovsky and Wojciechowski, 1973; Best et al., 1971). Palekar and Rajadhyaksha (1986) state that it is difficult to visualize the existence of a free gas phase in intracrystalline cavities. The diffusion regime in zeolites is different from the Knudsen diffusion observed in other porous catalysts and is referred to as 'configurational diffusion'. Diffusivities for this regime are lower by a few orders of magnitude than Knudsen diffusivities.

Methods of evaluating intraparticle diffusional inhibition usually involve testing different particle sizes of the catalyst. However, with FCC catalysts a change in particle size does not change the size of the zeolite crystal which is embedded into the matrix and represents in fact the controlling step for diffusion. This presents a challenge to determine diffusional limitations since one would have to obtain at least two catalysts with different zeolite sizes dispersed throughout the matrix.

Coke formation can cause diffusional limitations as well, indicated by a decrease in activation energy and a decrease in product selectivity (Gates et al., 1979). Pore-mouth plugging of the zeolite crystallite by coke prevents hydrocarbon molecules from entering the fine channels.

1.3.2 Octane Catalysts

The octane rating of FCC gasoline is affected by feedstock type, operating conditions of the unit and type of catalyst used to process the oil. Catalysts can be specially manufactured to enhance the octane rating of the gasoline by approximately 3 RON and 1-1.5 MON (Magee et al., 1985). Octane catalysts in general consist of a zeolite component, which has the most significant effect and a matrix component. Additives included as part of the catalyst matrix or as separate particles are also used to boost octane. Octane FCC catalysts can consist of an octane-boosting Y zeolite in an inert matrix or in an active matrix or can contain REY and an additive such as ZSM-5 (Scherzer, 1989; Ritter et al., 1986).

An octane-boosting Y zeolite is the ultra-stable Y form and is synthesized by careful thermal and hydrothermal treatment of ammonium Y zeolite. Ultra-stabilization results from the removal of aluminum ions from the zeolite framework and decomposition of the ammonia ions thus giving a highly siliceous hydrogen form of faujasite. Essentially the Si-O-Al bonds are hydrolyzed at high temperature forming nonframework aluminum species and increasing the framework silica/alumina ratio, therefore decreasing the unit cell size. The unit cell size is the smallest 3-dimensional repeating unit and is proportional to the number of aluminum atoms (potential acid sites). The empty sites left by this de-alumination phenomena are filled mostly by silica leading to the highly stable

framework. USY zeolites are more thermally and hydrothermally stable than conventional Y zeolites, maintaining their structure up to 1000°C and have a smaller number of Bronsted acid sites (Scherzer, 1989). Attempts to increase the silica/alumina ratio of Y zeolites by direct synthesis have not been very successful.

Some of the common properties of high-silica Y zeolites are listed below according to Scherzer (1989):

1. Framework Si/Al ratio increases.
2. Thermal and hydrothermal stability increases.
3. Unit cell size decreases.
4. Total acidity of the zeolite decreases.
5. Acid strength of the zeolite increases.
6. Catalytic site density decreases.

With the reduction in the concentration of acid sites by partial dealumination, the ratio between the rate of hydrogen transfer and that of cracking is reduced. The lower density of acid sites in USY zeolites reduces the rate of conversion of olefins into paraffins and of aromatics into condensed polycycles (Scherzer and Ritter, 1978). Thus, using dealuminated zeolites results in higher olefinic and aromatic molecules in the gasoline fraction (higher octane) as well as lower coke levels (hence the term coke selective catalysts) (Blazek, 1987; Montgomery, 1985; Ritter, 1985).

Hydrogen transfer reactions are bimolecular and assumed to occur between molecules co-adsorbed on adjacent acid sites located at aluminum atoms bonded to the same silicon atom

(Pine et al., 1984). These aluminum atoms are called next-nearest neighbours. The probability of hydrogen transfer can be lowered then by decreasing the acid site density which results in acid sites becoming more isolated from other acid sites. As well, with fewer acid sites per unit cell the total acidity of the zeolite decreases and the strength of the acid sites associated with the remaining aluminum atoms increases (Scherzer, 1989).

The concept of unit cell size can be used to correlate silica/alumina ratio, acid site density and acid site distribution (Pine et al., 1984). A low unit cell size corresponds to a high silica-alumina ratio (see Figure 1.7) and hence lower acid site density and lower total acidity. In general, using a catalyst with a lower unit cell size will result in higher RON and MON values for the gasoline (see Figure 1.8) since hydrogen transfer reactions are reduced allowing the formation of more olefins. At the same time, the lower unit cell size means lower overall acidity which results in decreased gasoline selectivity due to secondary cracking of olefins in the gasoline boiling range to form light gases. The strongest octane increase is observed at very low unit cell size values (less than 24.30 Å) at which a significant drop in gasoline selectivity occurs (Scherzer, 1989). It should be mentioned that, according to Corma et al. (1988), acid strength and site density are not the only parameters controlling activity and selectivity for dealuminated Y zeolites. They claim a non-uniform chemical composition along

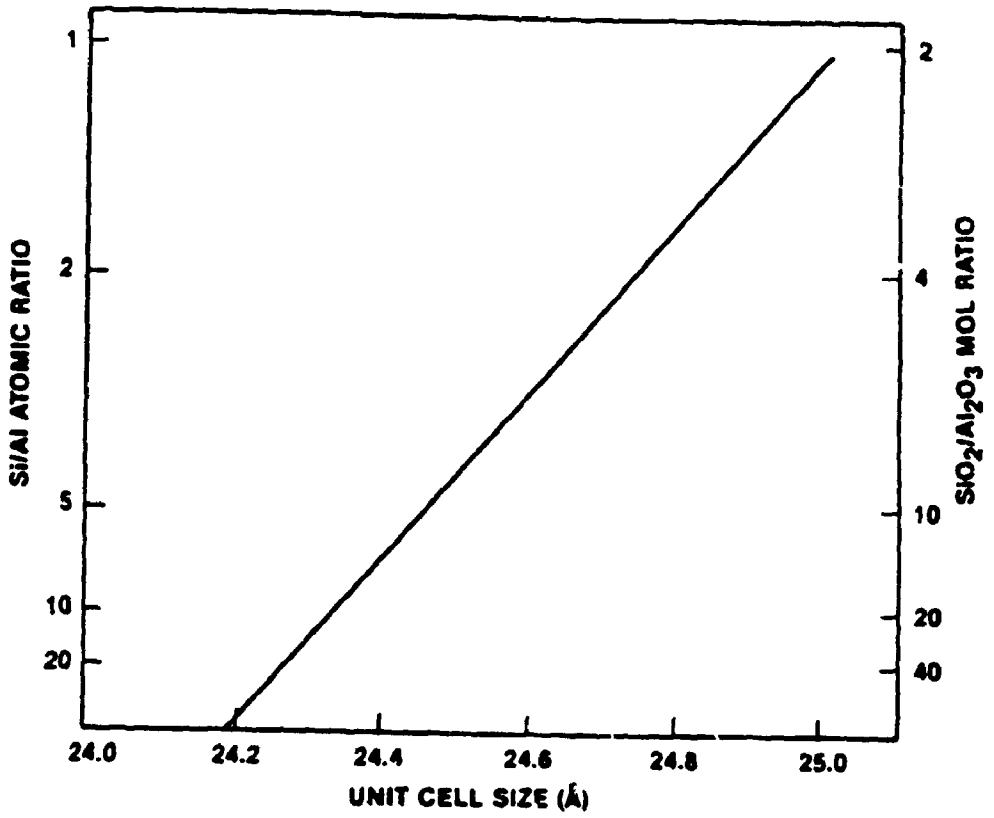

Figure 1.7 Correlation between zeolite unit cell size and the silica/alumina ratio (Scherzer, 1989).

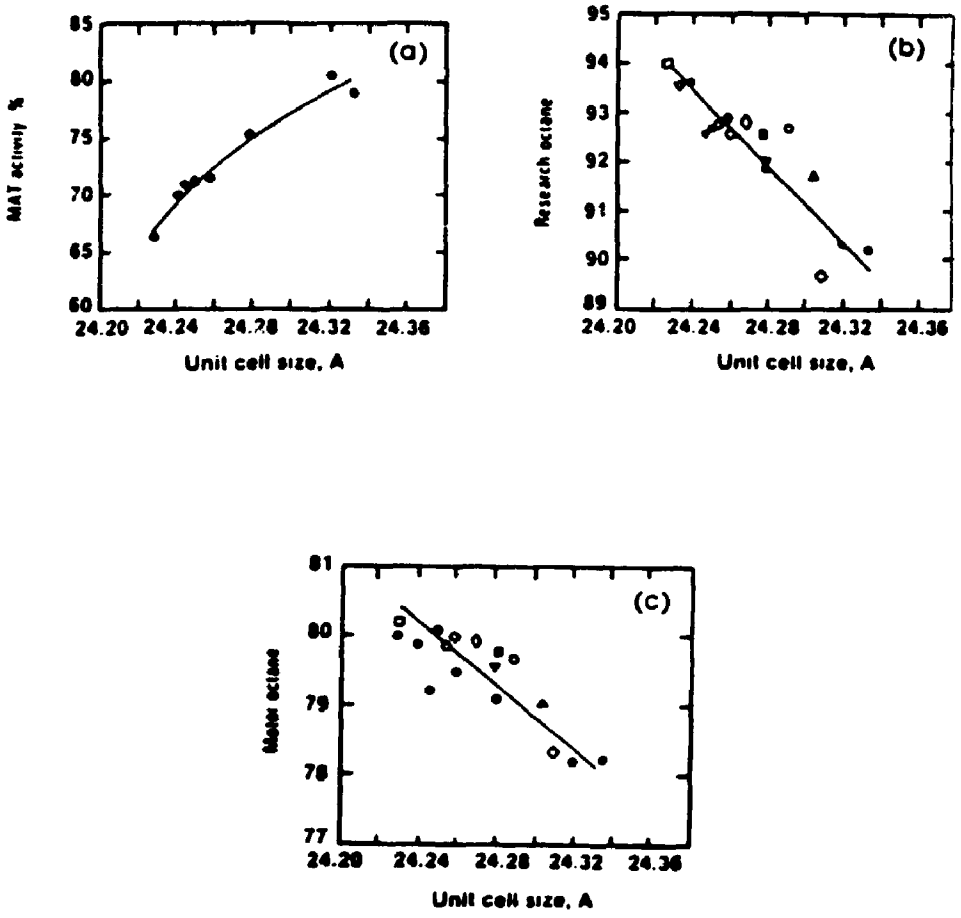

Figure 1.8 Correlation between unit cell size and a) catalytic activity; b) gasoline RON; c) gasoline MON (Scherzer, 1989).

the crystal and the presence of more than one type of active site where cracking takes place via carbocations and also radical-cation type species.

To compensate for lower activity found in USY zeolite catalysts as compared to REY catalysts, the zeolite content of the catalyst is increased. As well, RE-USY catalysts can be used since they are more acidic to give higher activity and gasoline selectivity but with more coke production. By exchanging small amounts of rare earth into USY zeolites, their activity and gasoline selectivity can be improved without any significant octane loss. The presence of the rare earth causes less shrinkage of the unit cell under the high temperature conditions of the regenerator in the presence of steam. Thus, the rare earth content in the high-silica zeolite can be used to obtain a unit cell size that optimizes between gasoline quantity and quality.

Gasoline octanes have also been shown to increase by using ZSM-5 additive to the USY catalyst (Magee et al., 1985; Biswas and Maxwell, 1990; Anderson and Dwyer, 1984; Santilli, 1990; Donnely, 1990). Other zeolites such as the erionite-type and silicon-enriched ZSM 20 have also been used (Marcilly et al., 1989; Huss and Schwartz, 1990). The smaller pore size of ZSM-5 restricts the access of branched and cyclic hydrocarbons but allows straight chains to enter. These straight chain molecules, which have lower octane, are then cracked to form lighter compounds. Typically linear C7 to C13 molecules in the heavier end of the gasoline are cracked forming C3 to C5

compounds. The result is a net loss in gasoline yield since light gases were formed, but an increase in octane since the linear paraffins have been converted.

It has been postulated that the ZSM-5 provides some isomerization activity resulting in the conversion of n-paraffins to branched paraffins which would increase the octane number (Magee et al., 1985; Anderson and Dwyer, 1984; Abbot and Wojciechowski, 1985b, 1985c). However, Biswas and Maxwell (1990) obtained results indicating no increase in gasoline component branching with the use of ZSM-5. They found significant losses in gasoline yield and suggest that the higher octane is due to a concentration effect. They argue that cracking of linear compounds (especially the paraffins) leaves a greater concentration of aromatics and naphthenes which gives the higher octane number.

1.3.3 Catalyst Steaming Methods

Catalytic cracking catalysts can deactivate by the extended exposure to water vapour at very high temperatures. In a commercial cracking unit such conditions can occur in the regenerator vessel where the burning of coke produces water vapour and heat. After burning of CO in the dilute phase and cyclone regions can cause high enough temperatures for irreversibly deactivating the catalyst. This hydrothermal deactivation involves the loss of active sites in the zeolite through crystal destruction as well as changes in the surface

area and pore size distribution in the matrix (Chen et al., 1977a; 1977b).

As mentioned in the previous section, the zeolite undergoes dealumination where high temperature hydrolysis of the silica-oxygen-alumina bonds causes the expulsion of aluminum ions into nonframework positions. Subsequently, the gaps in the framework structure are filled by silica resulting in a higher silica/alumina zeolite and thus a lowered unit cell size. This deactivation process in combination with other causes of activity loss (metals loading) and attrition, amounts to a zeolite catalyst life in a commercial unit between 40 and 200 days (Chen et al., 1977a). The unit is maintained at a constant catalyst activity by continuous addition of fresh catalyst and withdrawal of spent catalyst from the regenerator (low inventory, 1-2%).

The dealuminated state of the catalyst represents the so-called 'equilibrium' condition of the catalyst which is achieved after several cycles of reaction and regeneration. For studies done on a laboratory scale this type of equilibrated condition must be closely simulated in order to obtain meaningful results. Using fresh catalyst would certainly give different results in terms of conversion and selectivity than an aged catalyst because of the differences in unit cell size, surface area and porosity. It has been suggested that the only way to obtain an aged catalyst is to run a laboratory unit under commercial operating conditions (Letzsch et al., 1976) but this is practically impossible

because of the cost and time involved for such a procedure. Thus, the generally accepted method involves a severe steaming treatment of the fresh catalyst (Chen et al., 1977a; 1977b; Chester and Stover, 1977; Larocca, 1988; Berak and Manik, 1982; Mauge and Courcelle, 1986; Hettinger et al., 1983; Campagna et al., 1986). Chen et al. (1977) point out that such a method likely does not duplicate the true composition of a catalyst aged by commercial operation and will also not be representative of the heterogeneous inventory in the unit.

Steaming of fresh catalyst samples for laboratory performance studies has been done in fixed or fluidized bed units. Several factors such as temperature, steam partial pressure and total time of the treatment can influence the final results. The catalyst can be steamed in the presence of 100% steam or as low as 10%. Temperature can vary from 500°C to 850°C, pressures from 1 t0 3 atm and steaming times from 2 to 36 hours. There seems to be no consistent agreement on the optimum conditions to be used with most researchers finding appropriate conditions based on equipment available and the catalyst used.

Chen et al. (1977) found that accelerated deactivation occurred with temperatures above the normally accepted maximum dense bed regenerator temperatures of 700°C. Their results showed no significant catalyst deactivation under normal regenerator conditions (700°C and 190 mmHg water partial pressure). At temperatures of 760°C, which can be obtained in the dilute phase of the regenerator or during upsets, the

catalyst was deactivated (as determined by X-ray analysis). In general, steaming at 1 atm with 100% steam for 4 hours at temperatures 50 to 80°C higher than regenerator bed temperatures is adequate to simulate an aged condition similar to a commercial equilibrated catalyst (Speronello and Reagan, 1984).

Steam treatment severity has been varied to match commercial equilibrium catalyst activities and other properties. One measure of a suitably steam-aged catalyst is the surface area which should be in the range of 51 to 200 m^2/g (Ritter, 1985). Perhaps a more meaningful measure is to use a bulk property of the zeolite, the unit cell size, which is measured by X-ray diffraction. Typically, the unit cell size of USY zeolites are reduced to below 24.26 Å whereas RE-USY zeolites equilibrate to 24.26-24.32 Å and REY zeolites to 24.5 Å in the FCC unit (Scherzer, 1989). These shrinkages are dependent upon initial unit cell size, type of cations present and on steaming severity.

1.4 KINETIC MODELLING OF CATALYTIC CRACKING

In developing a kinetic model for the catalytic cracking of petroleum oils the usual approach has been to use lumping techniques (Wei and Kuo, 1969; Kuo and Wei, 1969; Weekman, 1979). This is because of the large number of individual species present in gas oil feedstocks. Normally FCC feeds have boiling points ranging from about 220°C to higher than 530°C in which tens of thousands of individual molecular species may be present (Sachanen, 1945). Such a diversity of molecules makes it necessary to group or lump species together into a smaller number of pseudospecies to obtain a feasible and manageable system of kinetic equations.

The basic theory in lumping strategy is that species should be lumped together only if the dynamic behaviour of the resulting pseudospecies is independent of the composition of species (Coxson and Bischoff, 1987). The first proposed and most widely used reaction scheme for catalytic cracking was the three lump model based on the feedstock, gasoline and light gases plus coke (Weekman and Nace, 1970). Later, with the development of lumping theory higher lumping models were used where the feedstock was further lumped to account for molecular type (Jacob et al., 1976). A discussion of the various models will be given below.

A further complication in modelling catalytic cracking is due to coking reactions which cause the catalyst to quickly lose activity with time as well as to change its selectivity

(Yates, 1983). Despite these complications kinetic models have been developed and incorporated into reactor-regenerator models used to predict the performance of commercial units.

1.4.1 The Three Lump Model

The early work of Blanding (1953), Andrews (1959) and Weekman (1968) describe the kinetic behaviour of catalytic cracking in terms of conversion behaviour only. Weekman (1969) and Weekman and Nace (1970) then developed a model which also accounted for the product selectivity resulting in a triangular reaction scheme. This three lump model consists of a feedstock lump, a gasoline lump (boiling fraction of C5 to 220°C) and a dry gas lump (C4 and less plus coke). The gasoline fraction is the most profitable component of the cracked products and thus this scheme allowed for an understanding of the interaction between process variables and the kinetic parameters. The three lump model is shown below where A represents the gas oil, B the gasoline, and C the light gases and coke:

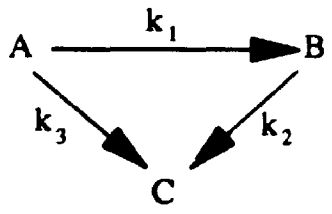

In this triangular scheme, the gas oil can crack either to

form gasoline as given by the rate constant k_1 or to form C-lump components as given by rate constant k_3. The overall gas oil cracking rate is described by k_o which is the summation of k_1 and k_3. The gasoline formed may also undergo further cracking to C-lump as described by rate constant k_2.

The reaction kinetics for the cracking of the gas oil lump has been found experimentally to follow a reaction order close to two (Weekman, 1968; Pachovsky and Wojciechowski, 1971; Blanding, 1953; Kraemer, 1987). Pure hydrocarbons are known to crack according to a first order rate law (Nace, 1969a). Since gasoline is a mixture of hydrocarbons having a limited range of boiling points then it is assumed to behave as a pseudo-pure component exhibiting a cracking order of one (Weekman and Nace, 1970). On the other hand, gas oil has a broad boiling range of compounds with a large number of first order reactions (from individual species) acting in parallel. The first gas oil molecules to crack show a much higher reaction velocity than subsequent molecules which are more refractory. This depth of cracking effect due to the distribution in crackability of components within the feed results in a decrease in gas oil reactivity as the conversion increases.

Pryor and Young (1984) showed that a large variation in cracking rate exists from the low boiling end to the high boiling end of a gas oil. It is well accepted that the feedstock crackability seems to correlate well with boiling point where within many hydrocarbon classes crackability

increases with molecular weight and the relative concentration of the more crackable groups is greater in the high boiling fraction.

Furthermore, during the cracking process there is an increase in the number of moles of products being formed from the gas oil. In a riser, which is normally modeled as a plug flow reactor, this results in a decrease in the vapour density. If the concentration of the reactants is defined at a constant volumetric flow, the apparent order also increases because the actual concentration decreases much faster than expected as the conversion increases. A pseudo-second-order reaction has been normally used to account for these non-linear effects (Weekman, 1968). However, the reaction order should be independent of the reaction system used and an additional term to account for the increased vapour velocity in a flow unit should be used to define the formal kinetics (Shaikh and Carberry, 1984).

According to the three lump model, the rates of gas oil cracking and gasoline cracking may be written as:

$$r_A = - k_0 \Phi_1 C_A^2 \qquad (1.1)$$

$$r_B = k_1 \Phi_1 C_A^2 - k_2 \Phi_2 C_B \qquad (1.2).$$

Pachovsky et al. (1973) used a more fundamental approach by assuming a gas oil reaction order of (1+W) where W represents the oil refractoriness accounting for feedstock crackability and catalyst characteristics. Essentially, the

depth of cracking effect is left as an additional parameter to be solved for which is feedstock dependent.

The deposition of coke on the catalyst results in rapid activity decay and hence a catalyst decay function is multiplied by the intrinsic rate to give the actual rate. It is normally assumed that the same active sites will crack both gas oil and gasoline molecules, therefore the activity decay functions Φ_1 and Φ_2 are assumed equal (Weekman, 1968). In general, the catalyst activity is dependent on the carbon laid down and is thus related to the time the catalyst is exposed to hydrocarbons. Then, to completely describe the kinetics of cracking according to the three lump model involves the determination of the parameters k_0, k_1, k_2 and the deactivation function Φ.

The three lump model has been successful in adequately describing gasoline selectivity behaviour from laboratory experimental data from studies done for one specific feedstock with one particular catalyst (Pachovsky and Wojciechowski, 1971, 1975a, 1975b 1975c; John and Wojciechowski, 1975; Campbell and Wojciechowski, 1969, 1971; Gross et al., 1974; Corella et al., 1985). As well, the model as been used in commercial and pilot transfer line units with reasonable success (Shah et al., 1977; Paraskos et al., 1976; Corella et al., 1986).

The work of Nace (1970, Nace et al. (1971) and Voltz et al. (1971) showed that the rate constants of this model changed with gas oil composition and that they could be

correlated to the paraffinic, naphthenic and aromatic compositions of the feed. Gross et al. (1974) verified that feedstocks with the highest content of paraffins and/or naphthenes showed the highest rate constants for cracking and gasoline formation and the lowest rate of catalyst deactivation. Therefore, rate constants obtained using the three lump model are adequate for the range of feedstocks used and extrapolation to unknown feedstocks can be done with little confidence. It became evident that the chemistry of the feedstock would have to be accounted for by the use of higher lumping models to be able to obtain rate constants independent of feedstock composition.

1.4.2 The Ten-Lump Model

A ten-lump model developed by Mobil researchers (Jacob et al., 1976) identifies lumps whose rate constants are independent of initial gas oil composition. The reaction scheme they developed, as shown in Figure 1.9, is an extension of their earlier 3-lump model (Weekman and Nace, 1970). The ten lumps are based on groups of paraffins, naphthenes, aromatic rings, and aromatic substituent groups in light (220°C to 345°C) and heavy oil (345°C +) fractions. The gasoline (G) and light gases plus coke (C) lumps remain the same as in the 3-lump model. The kinetic scheme shows that a heavy paraffinic molecule (P_h) can crack to form a light oil paraffinic molecule (P_l) and molecules in G lump and C lump.

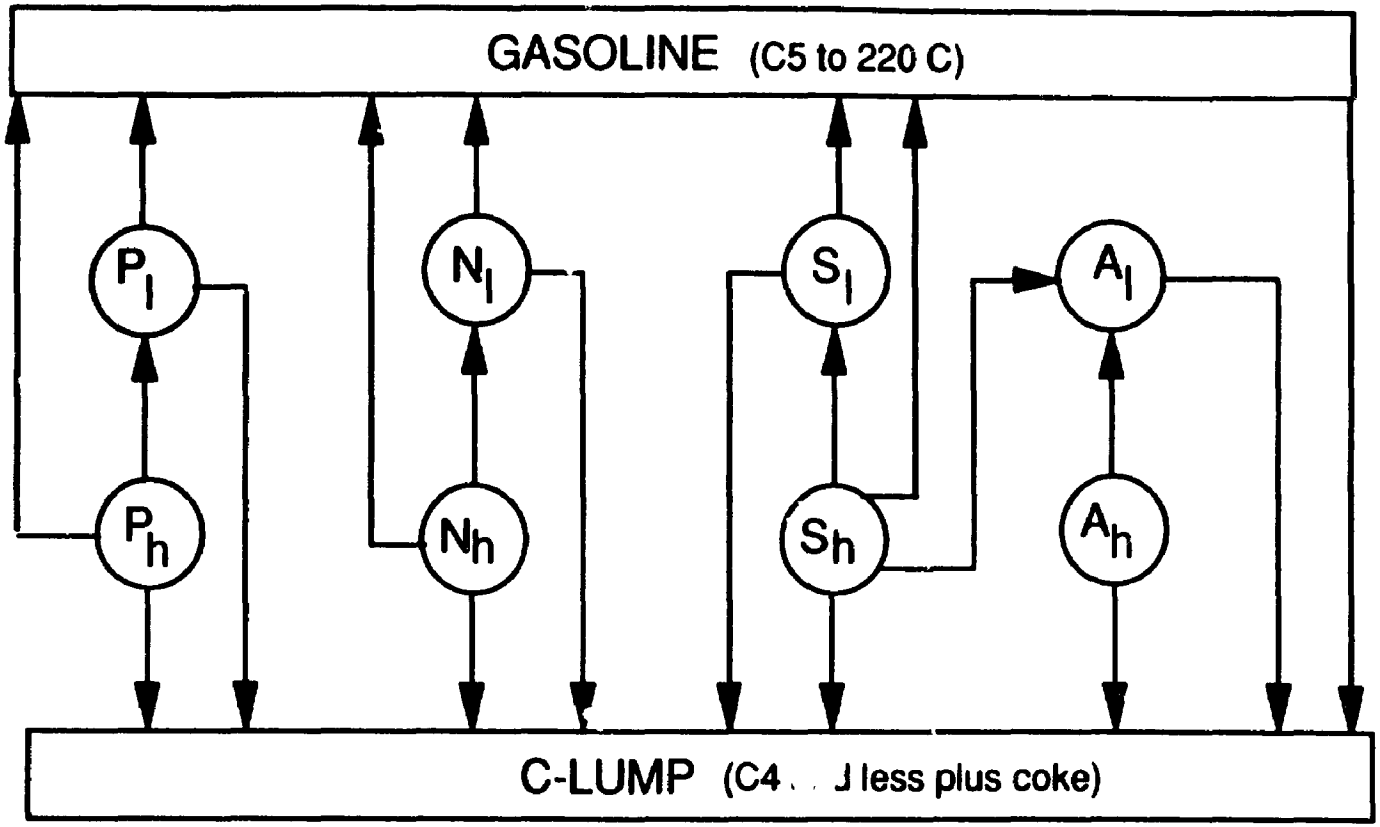

l = light oil fraction (220 to 345 C)

h = heavy oil fraction (345 C+)

S = aromatic substituent groups

A = aromatic rings

Fig. 1.9 Kinetic scheme for the 10-lump model
(Jacob et al., 1976)

P_l molecules can crack to form G and C lump components. The same network is given for the naphthenic compounds. No interaction terms are included between the paraffinic, naphthenic and aromatic groups. It was determined that such interaction terms did not significantly improve the model (Jacob et al., 1976).

The aromatic hydrocarbons are further subdivided into two categories one representing substituent groups attached to the rings in both heavy and light oil fractions (S_h and S_l) and the other representing aromatic rings in heavy and light oil fractions (A_h and A_l) as determined by the n-d-M method. The aromatic rings are shown to form coke species and not gasoline due to their refractoriness and coke precursor characteristics. The fact that aromatic rings with side chains can form gasoline when a side chain is cleaved and the ring drops into the gasoline fraction is accounted for in the rate constant for the substituent group. As well, an interaction term is used to include the reaction where S_h molecules crack to form A_l molecules (such as a three-ringed aromatic with a side-chain cracking to form a bare three-ringed molecule in the light oil fraction).

The gasoline fraction is maintained as a single lump to avoid further complexity involved with such a model that would distinguish between P, N and A molecules in this group. Such a scheme would however allow the prediction of gasoline composition and quality (Jacob et al., 1976).

The overall reaction network results in ten-simultaneous

equations which can be solved in a step-wise fashion due to the irreversible reactions. The matrix of rate constants is lower triangular involving 20 kinetic constants (plus deactivation function parameters).

The ten-lump model has shown success in adequately describing selectivity and conversion behaviour in pilot plant and commercial risers for a wide variety of feeds without modification of the rate constants. However, the simplicity of kinetic representations such as the ones for the three-lump model are partially lost. In using higher lumping models where the number of parameters is significantly increased means that greater amounts of experimental data are also required.

Coxson and Bischoff (1987) have shown that the ten lump model can be represented by a six lump model based on statistical methods. They used cluster analysis which determines the error (additional sum of squares error) associated with using successively smaller numbers of lumps. Starting with the 8 oil lumps (Figure 1.9) the number of lumps were reduced by fusing lumps together that statistically fell into similarity classes. In reducing the number of oil lumps to 4 it was found that the error increase went from 0.019 to 0.537 whereas a further reduction to 3 clusters gave an error of 1.44. Thus it was concluded that without a significant increase in error, the 4 clusters could be adequate. The resulting lumps consisted of P_h, N_h and N_l as one lump; S_h, S_l and P_l as a second lump with the A_l and A_h lumps remaining the

same. The reaction paths included the first lump forming compounds in the second lump which may be questionable since it does not make sense chemically that light naphthene molecules would form heavy aromatic substituent groups during cracking.

Coxson and Bischoff (1987) also comment on the inherent tradeoff in lumping systems which are not exactly lumpable. Using higher lumps will lead to successive model improvement but at the expense of the advantage of having a small number of lumps. They suggest a criterion for choice of the number of lumps based on comparing the clustering error with the actual experimental errors. The use of more lumps involves an increased number of experiments which leads to increased experimental error. However, with the improvement of analytical techniques and rapid advances in computing technology and capacity, higher lumped models will be favoured. One must also weigh the benefits of the additional information obtained from the more complex model against the additional time and cost involved in obtaining the extra experimental data.

1.4.3 Other Models

Some other models have been used in evaluating the kinetics of catalytic cracking. Yen et al. (1988) expanded the three lump model into a four-lump model by separating the coke and the C4 and lighter gases in the original C-lump. The

kinetic model is shown in Figure 1.10a where instead of three kinetic constants there is six since both the gas oil and gasoline can crack to form coke as well as light gases.

This model is more of a process model and provides information on coke yield and selectivity. The amount of coke formed is important for the heat balance in the FCC process as well as in determining the extent of reaction and primary product yield. Although the model is claimed to predict better coke yields it suffers the same weakness as the three-lump model in that the chemistry of the feed is not accounted for.

Another approach has been to subdivide the oil from the four-lump model into boiling fractions. Takatsuka et al. (1987) presented a six-lump model for residual oil cracking where the oil lump was divided into a residual oil fraction, a vacuum gas oil/heavy cycle oil fraction and a light oil fraction as shown in Figure 1.10b. The cracking of the resid fraction and the VGO fraction was taken as second order and the light oil was assumed to crack with first order kinetics. Each of the oil lumps can crack into the subsequent lighter fractions as well as to gasoline, gas and coke.

The reactor was modelled as a multistage CSTR and the proposed model satisfactorily predicted product quantity and quality. Again the oil lumps in this model do not account for the chemistry of the oil molecules, however it does prove useful from an correlative view point. With further subdivision of the oil lumps into narrower boiling ranges

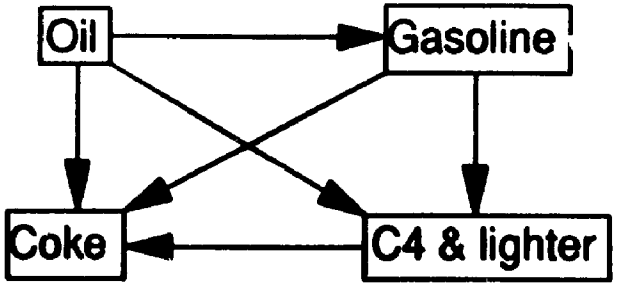

a) 4 LUMP MODEL

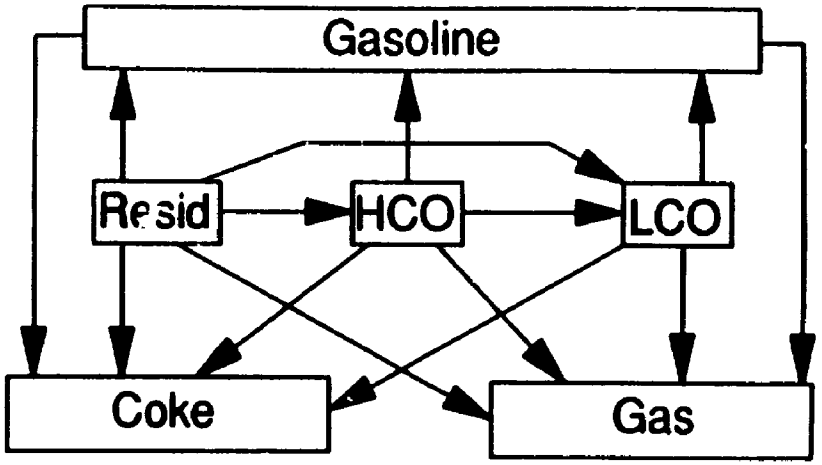

b) 6 LUMP MODEL

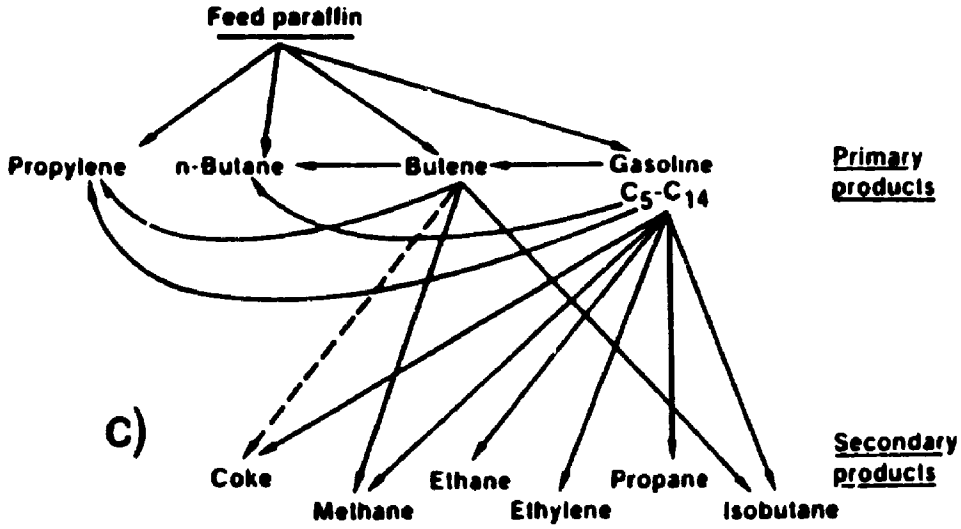

Fig. 1.10 Various lumping models: a) A 4 lump model (Yen et al., 1988), b) A 6 lump model (Takatsuka et al., 1987), c) model for paraffin cracking from John and Wojciechowski (1975)

could improve the predictive capabilities of the model.

The work of John and Wojciechowski (1975b) involved identifying primary and secondary reaction products from the cracking of a mainly paraffinic feed. They proposed a complex reaction network as shown in Figure 1.10c based on observed selectivity patterns where propylene, n-butane, and butenes were considered primary and secondary products formed from gas oil as well from gasoline. The secondary products were identified as coke, methane, ethane, ethylene, propane and iso-butane formed by gasoline cracking. Oliveira and Biscaia (1989) studied the cracking of gasoline based on a general 4-lump model which includes gasoline, primary gas products, primary plus secondary gas products and coke. These types of models allow prediction of individual light gases yields and coke yields separately. Combining this with a feedstock lumping scheme would result in an overall detailed yet complex kinetic model for catalytic cracking.

1.4.4 Catalyst Activity Decay Functions

One of the earliest and most important studies on the kinetics of coking was published by Voorhies (1945). The simple rate law developed from his work has played a vital role in the design of most commercial FCC units. The amount of coke deposited on both natural and synthetic clay catalysts at various temperatures and with a wide variety of charge stocks was studied by Voorhies. He showed that coke formation

was primarily a function of catalyst to oil contact time, t:

$$C_c = \epsilon\ t^m \qquad (1.3)$$

where C_c is the mass fraction of coke on the catalyst and ϵ and m are constants (m being about 0.5). Later, studies by Rudershausen and Watson (1954) on cyclohexane cracking and by Prater and Lago (1956) on cumene cracking verified Voorhies formulation. A difficulty with the Voorhies equation, as pointed out by Yates (1983), is its implication that the coking rate is independent of reactant composition, extent of conversion and space velocity. A partial confirmation of equation (1.3) is the work of Eberly et al. (1966) who used a much greater range of space velocities and observed an independent space velocity effect on coke formation. Further work done by Voltz et al. (1971) showed that, for a wide variety of charge stocks with a zeolite catalyst, Voorhies law was quite adequate. However, Ozawa and Bischoff (1968) reported higher initial coking rates than the Voorhies rate law would predict.

Froment and Bischoff (1961, 1962) examined the effect of catalyst decay and reactor performance when coke is produced from both products and reactants. They showed a Voorhies type law holds over certain operating ranges and defined a deactivation function as the fraction of active sites remaining active on the catalyst. They related this function, Φ, to the coke content, C_c, by the following two empirical relationships which are equivalent at low coke concentrations:

$$\Phi = \exp(-\delta C_c) \quad \text{and} \quad \Phi = 1/(1 + \delta C_c) \qquad (1.4)$$

where δ is a constant.

Levenspiel (1972) and Wojciechowski (1968) developed similar expressions but based on the catalyst time-on-stream as the main variable. This approach also used by Gustafson (1972) and Weekman (1969) includes a decreasing exponential decay function. This so-called exponential law is a particular case of a more general power law function which has been used in various forms by various researchers to fit their particular experimental data (Wojciechowski, 1974; Pachovsky et al., 1973; Newson, 1975; Mann et al., 1985; Mann and Thomson, 1987; Tan and Fuller, 1970; Forzatti et al., 1984; Fuentes, 1985; El-Kady and Mann, 1982a, 1982b).

It is evident that there are two general approaches used in modelling catalyst activity decay due to coking. One relates activity to the time-on-stream (Wojciechowski, 1974) and the other relates activity to the amount of coke deposited on the catalyst (Froment and Bischoff, 1979; Hatcher, 1985; Nam and Kittrell, 1984). From a mechanistic point of view the catalytic activity should be related to coke concentration on the catalyst. However, the time-on-stream theory which ignores the relation of hydrocarbon concentration with the fraction of active catalyst sites, has been used for plant simulation (Paraskos et al., 1976; Shah et al., 1977; Jacob et al., 1976) because of simplicity and the fact that the residence time of the catalyst in a riser is an important

parameter.

Szepe and Levenspiel (1971) showed that many of the rate laws proposed can be readily derived by assuming that the rate of decay is a function of the number of active sites. The general equation for aging by coke deposition on a catalyst of homogeneous surface can be written as a function of the fraction of active sites or as a combined function of the fraction of active sites and the concentration of gas oil to the power two:

$$- d\Phi/dt = k_d \Phi^n \qquad (1.5a)$$

$$- d\Phi/dt = k_d' C_A^2 \Phi \qquad (1.5b)$$

where Φ is the fraction of active sites remaining, t is the catalyst time on stream, k_d and k_d' are deactivation kinetic constants, n is the order of decay and C_A is the gas oil concentration. Equation (1.5b) assumes that the relationship between the fraction of active sites, Φ, and the fraction of active sites covered by coke, Φ_c, is $\Phi = (1-\Phi_c)$.

The two popular forms of Equation (1.5a) used to describe decaying catalysts during catalytic cracking are the exponential law and the power law given by the following equations:

Exponential: $$\Phi = \exp(-k_d t) \qquad (1.6)$$

Power Law: $$\Phi = Dt^{-N} \qquad (1.7)$$

where $D = [(n-1)k_d]^{-N}$ and $N = 1/(n-1)$.
The exponential decay form is derived from assuming first

order decay (ie. n=1) and integrating equation (1.5a) with Φ=1 at t=0. The power law given by equation (1.7) is the integrated form of equation (1.5a) with the unrealistic limits of Φ equal to infinity at zero contact time. A more adequate form of the general power law is given by Wojciechowski (1974) which is the integrated expression of equation (1.5a) with Φ=1 at t=0:

$$\Phi = [\ 1 + k_d t(n-1)\ ]^{-N} \qquad (1.8)$$

From equation (1.8) it is apparent that two parameters, k_d and n, are required to describe the decay kinetics. Thus, authors such as Nace et al.(1971) and Corella et al.(1985) who used the decay function of the form $\Phi = Dt^{-N}$ did not evaluate k_d but instead included it in their overall kinetic constant, a combined cracking and decay constant. This is certainly sufficient from an empirical stand point but to adequately describe the deactivation kinetics the value of k_d must be assessed. As well, the activation energy from these studies represents the combination of the energy of activation of gas oil cracking and the activation energy for the loss of active sites.

Another approach taken in describing the kinetics of catalyst deactivation in the FCC process has been to consider the catalyst as having a non-homogeneous surface that is, with active sites of different strength or acidity (Corella et al. 1985; Corella and Menendez, 1986). At least three types of

acid sites are considered being strong, medium and weak in acid strength. Corella et al. (1985) showed, that with first order kinetics the decay function results in a summation of at least three different exponential decay functions. The relative contribution of each exponential function varies with time-on-stream similar to the decreasing order of deactivation with increasing time-on-stream using the power law function. The work done by Weekman (1968), Nace (1970), Nace et al. (1971), Gross et al. (1974), Paraskos et al. (1976) and Shah et al. (1977) using the same decay function based on the time-on-stream theory obtained different values for the deactivation parameters. Corella et al. (1985) showed that the discrepancy in values obtained by Nace et al. (1971) and Weekman (1968), who used relatively high contact times (from 1.2 to 40 min.), and the values reported by Paraskos et al. (1976) and Shah et al. (1977), who used shorter contact times (from 0.1 to 10 s), was due to the variation in mechanism and observable order of the catalyst decay with time.

This type of modelling, taking into account the distribution of acid strengths in the catalyst and using a summation of exponential functions, describes the deactivation kinetics using a sound mechanistic approach. This may become important for developing a way to predict the kinetic behaviour of cracking from a change in catalyst properties. However, there is still uncertainty as to which parameters in addition to reaction testing, should also be incorporated in the model. As well, it suggests that in the first seconds of

cracking, which are the most important ones in an industrial riser, one could use a simple first order decay model to describe the catalyst deactivation adequately. Of course, the value of k_d obtained would be valid only for the short contact time periods covered and for the particular catalyst and gas oil used.

1.5 REACTORS USED FOR FCC STUDIES

Many different types of laboratory catalytic reactors are available for assessing kinetic rate parameters including fixed bed, fluidized bed, stirred batch, continuous stirred tank, re-circulating transport, differential, recycle, straight-through transport and pulse reactors (Doraiswamy and Tajbl, 1974; Weekman, 1974; Sunderland, 1976). In the case of studying catalytic cracking reactions on a bench scale, fixed bed and fluidized bed reactors have been traditional choices (Weekman, 1968; Gross et al., 1974; Campbell and Wojciechowski, 1970; Weekman and Nace, 1970). However, most of the kinetic data from these studies were obtained using reaction times greater than 2 minutes which are not representative of commercial riser contact times.

Tubular fixed bed reactors for studying FCC reactions are also somewhat limited by large temperature gradients due to the highly endothermic nature of cracking and pressure drops across extremely fine fluid catalyst beds. These deficiencies

can be eased to some degree by using a micro-reactor with catalyst dilution (Nace, 1969; Collyer, 1987; Larocca, 1988).

Fluidized bed reactors are quite suitable for handling fast, complex reactions with good temperature and mixing control. These systems are also very appropriate for fast aging catalysts because the possibility of removing them easily from the reactor as in the case of FCC units. Some disadvantages are that residence time distribution of reactants in the reactor are uncertain and attrition is a problem. As well, these reactors are very complex to model and operate. However, differential aging within the catalyst bed is possible for integral gas phase reactant conversions across the reactor giving a reaction rate directly. For the case of dense bed FCC operation, to obtain reliable and consistent data from the lab scale, a fluid-bed reactor would be more suitable than a conventional fixed bed unit.

For moving bed reactors, Sunderland (1976) suggests that the disadvantages (catalyst attrition, separation of catalyst and reactants, high ratio of gas to catalyst volume) usually outweigh the advantages.

In general, for obtaining reliable kinetic data that is representative of riser cracking, equipment must be used that allows for short contact times and under conditions that closely simulate those in a riser.

1.5.1 The Micro Activity Test (MAT) Reactor

A great need exists for reliable FCC performance tests which can be used for the evaluation of feedstocks and catalysts (O'Connor and Hartkamp, 1988; Mitchell and Moore, 1988). With the hundreds of catalyst variations available the choice of a suitable catalyst becomes complex and the ability to predict unit performance rests on the evaluation test used. This catalyst choice is crucial since small changes in yield structure will have a large impact on FCC economics. Most laboratories have unique testing programs with wide differences in both catalyst steaming methods and catalysts activity test procedures (Moorehead et al., 1988).

The traditional Micro Activity Test (MAT) remains the main tool for basic FCC research and catalyst and feedstock evaluation (O'Connor and Hartkamp, 1988; Campagna et al., 1986). This test was developed because of its simplicity, reproducibility and quickness of evaluation in comparison to pilot units.

The MAT method is an ASTM procedure (ASTM D-3907-80) which comprises a fixed bed of 4 grams of catalyst, operated with continuous oil vapour feed for 75 seconds at a temperature of 482°C under a cumulative catalyst to oil ratio of 3. This specific form of the MAT procedure has not been successful in predicting commercial unit performance and provides only very limited information on selectivity (Carter and McElhiney, 1989; Mauleon and Courcelle, 1985; O'Connor and Hartkamp,

1988). In general, catalyst choice based solely on MAT data is questionable and rarely done and it is not suited for simulating commercial operation. Its main use is in the relative comparison of activity of FCC catalysts (Humphries and Wilcox, 1990).

Mott (1987) outlines the shortcomings of the original MAT test which seriously question the reliability of the results. He suggests that the MAT activity is commonly misinterpreted because of the indirect interactions of the catalyst with the dynamics of the heat balance. In some cases catalysts with very high MAT activity were observed to perform poorly in FCC units. For example, an ultrastable zeolite catalyst with low coke selectivity introduced into a unit that had been running on a rare earth zeolite catalyst with high coke selectivity, gave good performance despite having a low MAT activity (Davison, 1984). The basic problem lies in the fact that in the MAT unit the catalyst remains fixed while in a FCC riser reactor the catalyst moves along with the hydrocarbon vapours. Mott (1987) describes this in terms of the number of active sites. In the MAT unit the number of active sites is fixed while in real operation the number of active sites delivered to the riser per unit of feed is dynamic and will change according to the heat requirements and the combined coke-making tendencies of the feed and catalyst. Thus, the most effective FCC catalyst should be determined by the number of active sites it can bring to the reactor per mass of feed which may not necessarily be the catalyst with the highest MAT

activity (Mott, 1987).

In general, the MAT procedure has the following four drawbacks:

1. Long contact times (75 seconds) which are not representative of commercial units (less than 10 seconds).
2. The partial pressure of reactant hydrocarbons is much lower than in commercial units (0.05 atm instead of 1 atm).
3. Coke profiles exist in the 150 mm long catalyst bed, making coke a function of the axial position inside the reactor and creating the possibility of channelling.
4. There is no standard test for the steam deactivation procedure thus making the observed activity value a function of steaming conditions.
5. The method is unable to predict commercial performance because it reports an average specific activity per mass of catalyst rather than on its coke-making tendency.

As a result of the above describe inadequacies of the MAT method, modifications have been made to provide a more reliable method which has been called the 'micro-selectivity test' (Carter and McElhiney, 1989) and the 'microscale simulation test' (O'Connor and Hartkamp, 1988). These modified tests provide detailed yield structure information and an economical and quick means of comparing catalysts which is very valuable to the refiner (McElhiney, 1988; Montgomery and Letzsch, 1971; Mott, 1987; Yatsu and Keyworth, 1990; Mauleon and Courcelle, 1985); Tsai et al., 1989). The modifications include higher reactor temperatures, shorter oil

feed durations and better reactor design. A usual criterion is to use the catalyst mix temperature as the operating temperature of the test which is 25 to 45°C higher than the riser outlet temperature (Mauleon and Courcelle, 1985). Run times of 15 seconds with 2 to 4 seconds of vapour contact time have been reported giving yield breakdowns and trends which correspond very well with actual FCC data (O'Conner and Hartkamp, 1988).

The modified MAT has also been used in combination with improved gas chromatographic analysis of the product to give gasoline properties (GC-RON, GC-MON, front end olefinicity, mid-cut branching, aromaticity and GC-bromine number) that can predict quite well actual refinery results (Yatsu and Keyworth, 1990).

Despite the improvements to the MAT test it still has the shortcomings of developing coke profiles in the catalyst bed, due to the nature of the fixed bed operation and also in achieving non-isothermal conditions. These two facts are very undesirable in terms of performing catalytic studies to determine kinetic parameters for riser cracking. Kinetic modelling of catalytic cracking reactions using the MAT test then becomes difficult and certain approximations are necessary (Forissier and Bernard, 1989). This can lead to inaccurate and unreliable data to be used for modelling commercial units.

1.5.2 The Pulse-Microcatalytic Reactor

A pulse reactor used for kinetic studies usually involves cumbersome mathematical equations due to the unsteady state condition of the reacting system. However, the pulse technique has been demonstrated to be successful (Bett and Hall, 1968; Matsen et al., 1965; Desay and Anthony, 1987; Kalthod, 1985) and has been used for kinetic FCC studies (Nace, 1969a, 1969b; Collyer, 1987; Morely, 1987; Larocca, 1988).

The pulse-microcatalytic technique applied for catalytic cracking studies involves the passage of a small pulse of vapourized oil (in the order of 0.5 mL) through a small bed of catalyst diluted with inert solids. The effluents from the reactor can be sent directly to a gas chromatograph for on-line analysis. The system can be kept under isothermal conditions because of the small amount of catalyst in a large heat sink. Other advantages include simple design and construction with low cost. Also, the results from each pulse injection give directly the instantaneous values for kinetic parameter evaluation.

The technique is particularly suited for deactivation studies since the catalyst activity is assumed constant during every single pulse (hence instantaneous rate measurements). In one particular unit, the time-on-stream is defined on a cumulative basis over several injections of 5 μL of gas oil and a reverse flow of gas between injections fluidizes the bed

of solids (0.1 grams of catalyst diluted with 2.3 grams of inerts) and therefore prevents the development of coke profiles because of the uniform mixing of the particles (Larocca, 1988). In terms of simulating riser cracking, this type of approach is somewhat equivalent to riser operation with multiple feed injection points along its height, a possible valuable alternative for riser cracking. This is a result of the several pulse injections with fresh oil which are summed to give a cumulative catalyst to oil ratio and coke make.

1.5.3 Pilot Plant Units

For the advancement in FCC technology it is necessary to have a successful scale-up procedure. The ability to bridge lab-scale performance results to commercial units is crucial. Circulating riser pilot units potentially provide the best small-scale simulation of commercial FCC yields (Carter and McElhiney, 1989). Different types of pilot units have been used including once through or 'sling-shot' reactor systems, fixed fluid bed, moving fluid bed and folded riser systems (Young and Weatherbee, 1989; Leuenberger et al., 1988; Humes, 1983; Corella et al., 1986). The types of pilot plants most favoured are those which have riser reactors and include continuous regeneration of the coked catalyst (Young and Weatherbee, 1989).

The once through pilot unit offers simple design and

operation but does not include continuous regeneration. Large inventories of catalyst are required and thus these systems are limited to the type of studies that can be done. Some of the large pilot plants process 1-5 barrels per day requiring in the order of 40 feet height which is fairly capital intensive (Young and Weatherbee, 1989). ARCO licenses technology for their smaller circulating pilot plant with continuous regeneration (LABFCC). Early configurations included a moving fluid bed reactor used to mimic bed type FCC operation and then a five stage reactor was used to decrease backmixing to try for better simulation of riser cracking. Folded riser reactors were later employed along with pressurized cperation and computer control (Humes, 1983). Young and Weatherbee (1989) state the major deficiencies of this technology:

1. Limited ability to process heavier resid feeds

2. Inability to closely simulate commercial riser with high temperature regeneration

3. Folded riser design has operating uncertainties at commercial pressures

4. Inability to simulate the interrelation of process variables

5. Isothermal temperature instead of adiabatic as in the commercial process.

Technology offered by Davison in their Davison Circulating Riser (DCR) unit overcomes these limitations. The DCR involves an adiabatic riser reactor where the reactor temperature is maintained by controlling the circulation rate of hot catalyst from the regenerator to the reactor, identical

to commercial operation. In this way the temperature profile in the reactor is determined automatically as the natural result of the unit operating conditions (reactor exit temperature, catalyst temperature and feed preheat temperature). A schematic of the DCR unit is shown in Figure 1.11 which is a small scale unit of approximately 12 feet in height where the catalyst residence time in the riser is about 6 seconds and the vapour residence time is about 3 seconds (Young and Weatherbee, 1989). Other operating conditions of the DCR are indicated in Table 1.2.

Davison claims that the DCR can effectively match commercial yields and can be applied to resid processing and can be used for process or catalyst studies. As well, the riser reactor can be operated in an isothermal mode to perform kinetic studies.

Although pilot units can provide the best simulation of commercial yields, these units are expensive to purchase and operate and are usually not suited for testing large numbers of samples. Small continuous pilot plant units (2-3 m height; 1-2 cm diameter) could show other limitations concerning the combinations of catalyst/oil ratios and residence times allowed to be explored (Corella et al., 1986). For example, the increase in space time in a tube reactor is limited by the height of the tube, as determined by the choking velocity for the unit. As well, small pilot units always have close to 1.0 slip velocity, whereas commercial risers have 3-4 slip near the feed nozzles and 1.5 slip at the exit. Furthermore, to

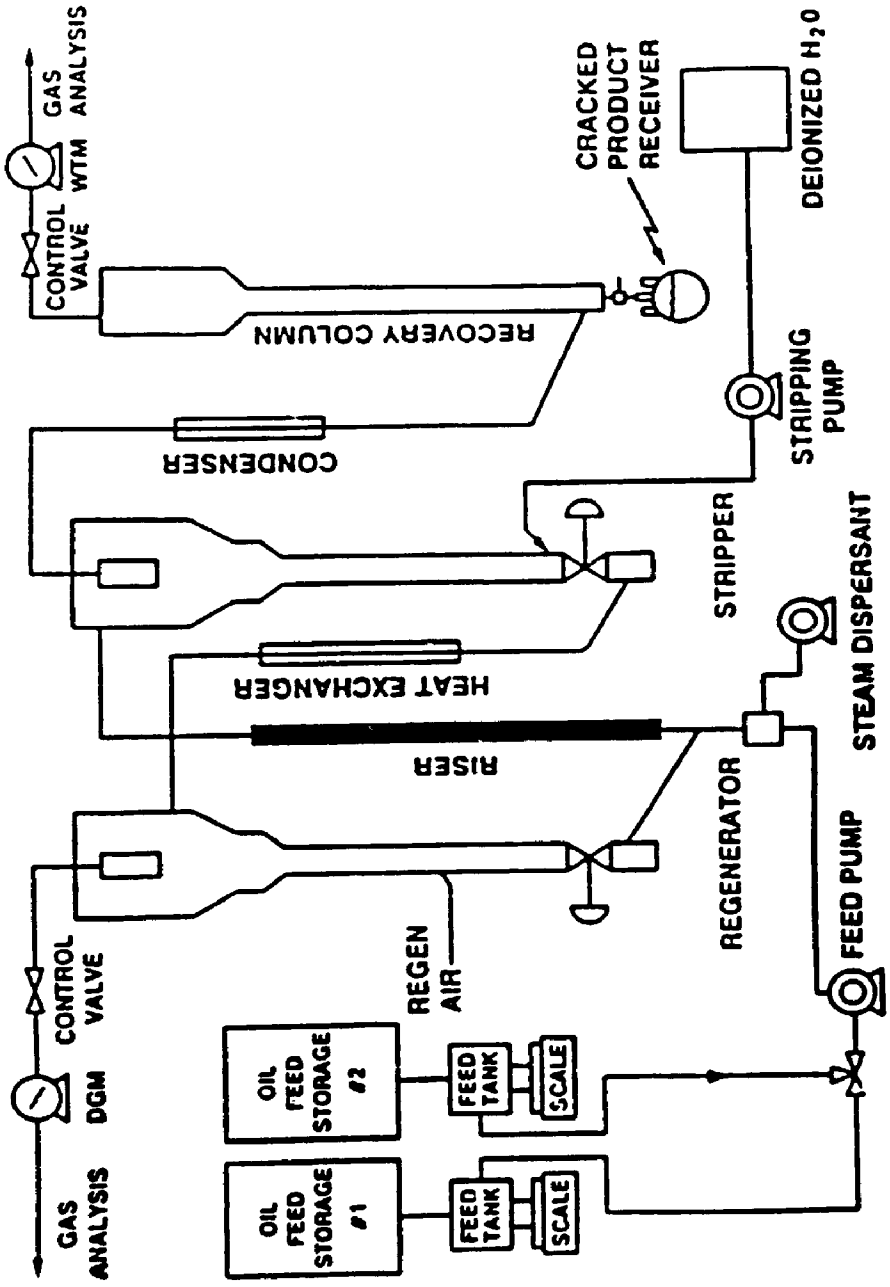

Figure 1.11 Schematic diagram of the Davison Circulating Riser unit (Young and Weatherbee, 1989).

Table 1.2 Operating ranges for the Davison Circulating Riser unit (Young and Weatherbee, 1989).

	Normal Range
System Pressure, psig	15 - 25
Riser Temperature, °F	950 - 1000
Regenerator Temperature, °F	1275 - 1350
Stripper Temperature, °F	900 - 1000
Stabilizer Temperature, °F	-30
Feed Preheat Temperature, °F	250 - 750
Feedrate, g/h	400 - 1500
Catalyst Charge, g	3000
Catalyst Circulation Rate, g/h	4500 - 7500
Feed Types	VGO, CGO, Resid, ATB (up to 5.3 conradson carbon)

perform kinetic studies, isothermal conditions are much preferred which may be somewhat more difficult to achieve in pilot units.

1.5.4 Recycle Reactors

Internal recycle reactors have evolved into a useful device for catalyst testing and kinetic studies since they can be run at very close to large-scale reactor operating conditions including mass velocities. They are particularly suited for obtaining kinetic data on heterogeneous vapour-phase fixed bed reactions where mass and heat transfer effects are minimal (Berty, 1974, 1979, 1984; Mahoney, 1974; Kuchciniski and Squires, 1976; Caldwell, 1983; Carberry, 1969; Hannoun and Regalbuto, 1988). Kinetic data from laboratory and pilot plant reactors can be obscured by these physical processes occurring simultaneously with the catalytic reaction especially for gas-solid systems.

The concept of internal recycle reactors as discussed by Berty (1974) is to sacrifice geometric similarity completely in order to maintain similarity for the flow, thermal and kinetic regimes of the catalyst pellet. It must be realized that in scale-up or scale-down, the catalyst pellet size remains the same.

The reactor itself, with appropriate design and high recycle ratio, approximates the performance of a CSTR. Two designs are commonly employed: The spinning basket type in

which the catalyst moves through the reactants (Carberry, 1969); and the Berty type in which the reactant mixture moves through a stationary catalyst bed (Berty, 1974). Both are referred to as gradientless because they are designed to suppress all gas-phase internal gradients. With regards to the spinning basket type, there is some doubt as to how fast the gas actually moves past the catalyst particles and temperature measurement in the vicinity of the catalyst is difficult due to the movement of the basket (Mahoney, 1974).

The Berty type reactor has mainly been used for modelling fixed bed reactions by using a stationary bed of catalyst in a bench scale internal recycle reactor under continuous flow conditions. For simulating catalytic cracking reactions similar to those taking place in riser reactor, a fluidized bed of catalyst (to avoid coke profiles and possible channelling of gas flow when using fine FCC particles in a fixed bed) and a short reaction time batch type operation would be more appropriate. This was the design basis for the Riser Simulator developed in the initial research phase of the present work (de Lasa, 1987; Kraemer, 1987). It was envisioned that tne use of an internal recycle reactor with an impeller located above the catalyst basket could provide a fluidized bed of solids as well as appropriate recycle rates to provide an environment to simulate the reaction regime in a riser. This system, which can be classified as an internal recycle fluidized batch reactor, is a novel approach for studying catalytic cracking reactions on a bench-scale level

that appropriately simulate the reaction regime in a riser reactor.

CHAPTER 2

SCOPE AND OBJECTIVES OF THE RESEARCH

The research carried out in the present study was the second phase of an experimental program to evaluate the kinetics of catalytic cracking under conditions similar to the reaction regime found in modern day commercial risers. The first phase, completed in an M.E.Sc. program (Kraemer, 1987), involved the design and testing of a bench scale Riser Simulator to be used for the kinetic studies.

Most of the kinetic data for cat-cracking reported in the literature has been obtained using moving and fluidized bed reactors under long catalyst times-on-stream ranging from 1 to 15 minutes (Weekman, 1969; Weekman and Nace, 1970; Nace et al., 1971; Voltz et al., 1971; Pachovsky et al., 1973; Jacob et al. 1976). This data was useful at the time since a lot of commercial FCC units were operating under reaction times in the range of minutes. However, as mentioned in chapter 1, the ever changing technology of the FCC process has led to extensive commercial application of the riser reactor where more advanced units operate below 10 seconds of reaction time, some in the 2 to 3 second range.

Furthermore, the majority of kinetic information has been reported based on the three-lump model, or slight modifications of it to include coke selectivity. Although

this model is simple and can adequately describe unit performance for a particular feedstock and catalyst, the ability to extrapolate it to other feedstocks with different molecular compositions is questionable. The different cracking rates of the various molecular types has led to higher lumping models, such as the ten-lump model, to obtain kinetic constants that are independent of feed composition. The evaluation of this model performed by Mobil workers (Jacob et al., 1976; Gross et al., 1976) was done using data obtained from a dense phase fluidized-bed reactor unit under reaction times of 1.25 to 5 minutes.

Other data have been reported from studies using model compounds, as reviewed by Gates et al. (1979), Corma and Wojciechowski (1982) and Wojciechowski and Corma (1986). While this information is important for a fundamental understanding of the catalytic transformations taking place, it cannot be applied to industrial units where real feedstocks contain complex mixtures of hydrocarbon compounds.

More recent data obtained in a small FCC pilot plant (2.75 meter height) (Corella et al., 1986) and in a commercial size pilot unit (30 meters) (Paraskos et al., 1976; Shah et al., 1977) report kinetic parameters associated with the three lump model for short contact times. A comparison of kinetic constants for the three lump model obtained in the M.E.Sc. study was made with the above mentioned parameters and were shown to be of comparable magnitude. For example, the overall gas oil cracking constant obtained from Paraskos et al. (1976)

was in the range of 0.36 to 0.7 (1/s) and the values determined in the bench-scale Riser Simulator (under 10 seconds reaction time) were in the range of 0.4 to 0.5 (1/s). It should be mentioned that this type of comparison is very general since identical feedstocks and catalysts were not used in the two studies and the units are reported as 1/s. For heterogeneous kinetic studies, the dimensions of the kinetic constants should include the weight of the catalyst (i.e. $cm^3/g_{cat}.s$ for first order reactions, $cm^6/gmol_{oil}.g_{cat}.s$ for second order reactions etc.).

The conclusion that the Riser Simulator could effectively represent riser cracking conditions and the fact that kinetic data is lacking in the literature, for kinetic parameters independent of feed composition and applicable to short contact times, led to the primary focus of this study. The main objective was to evaluate catalytic cracking kinetics under conditions that resemble as close as possible the reaction regime in a riser. The development of an effective kinetic model with an appropriate catalyst activity decay function (Kraemer et al., 1990) was seen as a key research area for the advancement of FCC technology.

It was hoped that the experimental technique developed would be useful for presenting more valuable and reliable data for catalyst comparison and selection. This remains an important practice for refiners involved in FCC operations where crucial decisions such as possible changes in operating conditions of cat-crackers, scaling-up, processing of heavy

feedstocks with high levels of nickel and vanadium compounds depend on this data.

Another objective of this work was tc further advance the understanding of the fluid-solid dynamics taking place in the Riser Simulator unit (bench scale fluidized recycle reactor) built for the kinetic analysis. The use of a fibre optic probe was implemented for this purpose.

CHAPTER 3

EXPERIMENTAL SYSTEM DESIGN AND MODELLING EQUATIONS

The first phase of this research was devoted mainly to the design and set-up of the reactor and experimental system (Kraemer, 1987; Kraemer and de Lasa, 1987; Kraemer and de Lasa, 1988a). A discussion of the main reactor design considerations used and modifications to the experimental system made for the present work will be described here. The development of the reactor kinetic modelling equations and the mass balance equations will also be discussed.

3.1 REACTOR DESIGN

3.1.1 Simulation of the reaction regime in a riser

A bench scale internal recycle batch reactor was chosen to achieve the objective of simulating, as close as possible, the same reaction regime that occurs in a commercial riser. This objective is not easy nor straight forward considering the complex fluid-dynamic interactions that take place in riser reactors. These include phenomena such as solids 'raining' down at the wall, slip velocities and differences in solids density from top to bottom. However, if one considers an ideal riser (approached in a down flow riser) where a given mass of vapour and a given mass of catalyst travel through the transport line in nearly plug flow, then the simulation of the

reaction regime becomes more manageable. Therefore, on a bench scale level the approach taken was to simulate the case of an ideal riser with plug flow of both the gas and solids.

The advantage of using an internal recycle reactor for this application is that gas phase mixing can approach ideality thus minimizing concentration gradients. In general, recycle reactors on a small scale approach conditions close to ideally stirred tank reactors (Berty, 1984). With a high degree of volumetric re-circulation, this well mixed gas phase can continuously contact the catalyst so that these particles see a changing hydrocarbon environment with time similar to solids flowing in a riser.

A schematic diagram of the Riser Simulator is shown in Figure 3.1 indicating the essential design features. The unit differs from conventional Berty reactors (Berty, 1974, 1979) by the important fact that the catalyst bed is fluidized. This condition is achieved by locating the impeller in the upper region of the reactor, above the catalyst basket. Upon rotation of the shaft, gas is forced outward from the center of the impeller towards the walls. This creates a lower pressure in the center region of the impeller thus inducing flow of gas upwards through the catalyst chamber from the bottom of the reactor annular region where the pressure is slightly higher. The small clearance between the impeller and the top of the catalyst basket avoids gas from re-entering the impeller region through this pathway. The overall direction of gas flow is indicated by the arrows in Figure 3.1, where

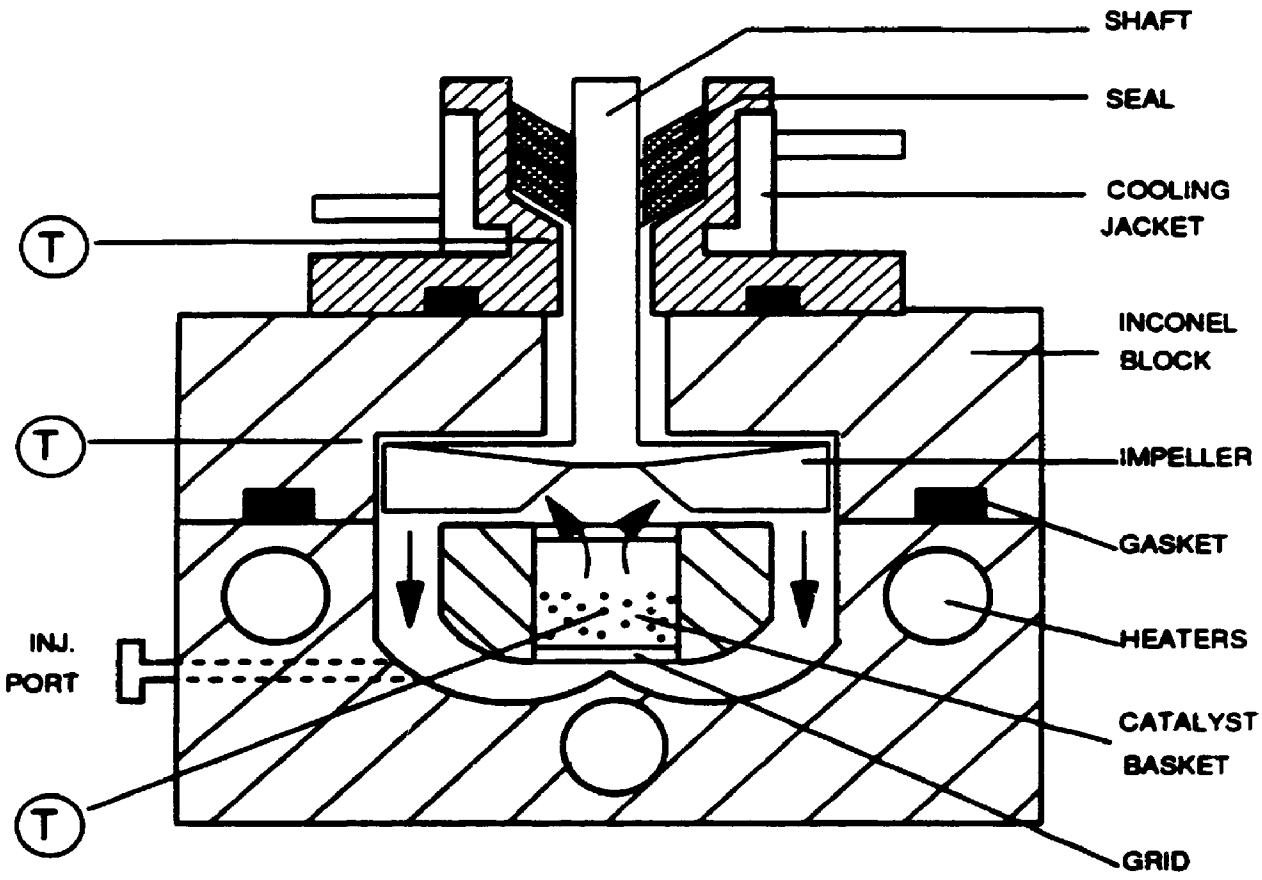

Fig. 3.1 Schematic diagram of the Riser Simulator

gas if forced to swirl downward in the annular region and then upward through the catalyst bed generating a re-circulating pattern.

The incentive for this novel fluidized internal recycle design (de Lasa, 1987) was to provide intense mixing of gas and solids, preventing the formation of coke profiles that could develop during cracking and possible channelling of gas that could exist in a fixed bed of fine solids such as FCC catalyst (60 μm average particle size). The catalyst sample can then be considered, at a specific contact time, homogeneous from the point of view of its activity. This represents one important advantage over an MAT unit in which the first layer of catalyst particles see the highest concentration of gas oil resulting in higher coke deposits in this layer. Subsequent kinetic interpretation becomes difficult and not representative of riser cracking.

A further design aspect of the reactor that differentiated it from other internal recycle units was the condition of batch operation. In fact this is essential when trying to simulate riser-type cracking since the catalyst moves along with the reaction vapours as it passes up the conduit. Therefore catalyst particles undergo a batch cracking operation where they 'see' a changing hydrocarbon concentration as they move up the riser with a declining activity due to coke formation.

The simulation of the reaction regime occurring in an ideal riser reactor can be done in this bench scale unit as

summarized in Figure 3.2. The approach is to cut a thin slice from the riser which contains a defined mass of catalyst and gas in a certain volume. This slice essentially moves from bottom to top (defined time period) where hydrocarbons contact the catalyst undergoing cracking reactions and forming coke on the catalyst. Using the same mass of catalyst per unit volume (solids hold-up) this slice of the riser can be represented on a bench scale by confining the catalyst in a bed and circulating the gases at a high rate through this chamber for a defined time. The reaction time for the Riser Simulator is then defined as the time period in which the hydrocarbons spend in the reactor (time of injection until time of purge). This is equivalent to the contact time in the ideal riser as defined by the volumetric flow of gas, diameter and height of the transport line.

It is therefore important to reproduce in the Riser Simulator unit the same loading of catalyst (grams of catalyst per unit volume) and achieve a high re-circulation rate of fluid. It should be noted that in commercial risers catalyst loadings may vary from 0.16 g/mL at the bottom to 0.02 g/mL at the top where plug flow is approached. In the Riser Simulator the catalyst loading remains constant during a run mimicking the conditions of a plug flow riser. Although it is important to simulate the varying catalyst hold-up that is found in commercial risers, it is easier to separate out fluid-dynamic effects when evaluating kinetics. As well, using similar oil partial pressures (0.8 to 2 atm), catalyst to oil ratios (3 to

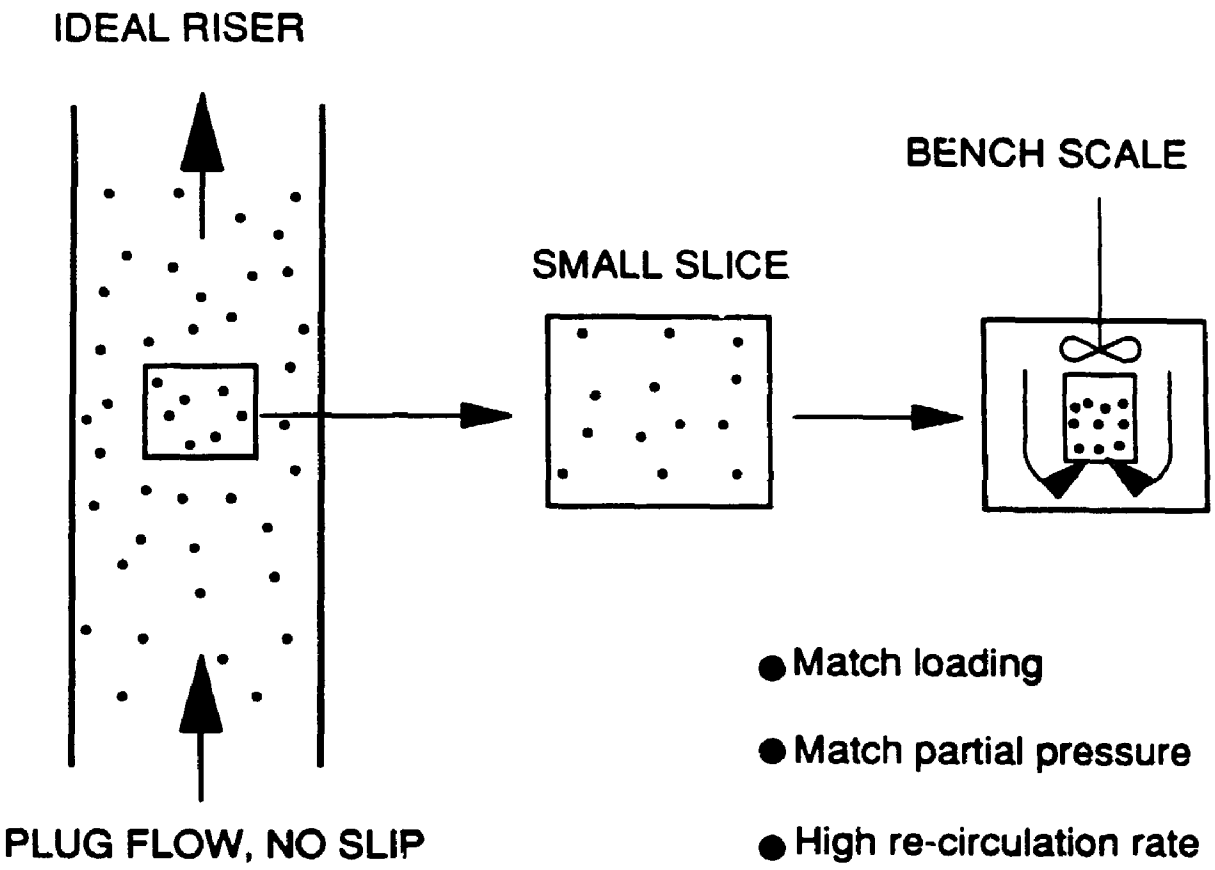

Fig. 3.2 Simulating the reaction regime of an ideal riser on a bench scale

10), temperatures (500 to 550°C) and reaction times (less than 10 seconds) as those used in commercial operation then a similar reaction regime can be achieved. For a desired set of conditions the cracking reactions are then carried out by having the reactor loaded with a defined mass of catalyst then injecting a gas oil sample through the injection port where it vapourizes instantly and contacts the catalyst. At the end of the desired reaction time a sample of the reaction vapours is quickly trapped and subsequently analyzed to give the product distribution.

In commercial risers steam is used as an inert gas to help atomize the feed injected through nozzles at the bottom of the riser and also to fluidize the catalyst in the standpipe section between the regenerator and the riser line. The actual reaction mixture thus contains steam as well as the hydrocarbons. For the Riser Simulator an inert gas such as nitrogen or argon can be used to represent the partial pressure of steam and is initially present in the reactor at 1 atm before injection. The initial partial pressure of oil resulting from the injected sample is then defined from this basis. It is noted that an inert gas was chosen instead of steam since it was more practical to use in a laboratory setting and there was no reason to suspect differences in terms of kinetics since steam only affects the catalyst properties during combustion in the regenerator.

Another important aspect of FCC operation is the stripper where separated catalyst from the riser outlet vapours is

passed into a baffled fluidized zone. Steam flowing upward through this dense fluidized bed (typically 15 cm/s) is used to remove residual hydrocarbons trapped in the pores of the catalyst which are included in the product stream. The reaction products thus obtained in the present bench scale unit represent what one would expect at the exit of the riser reactor. However, it is also possible that in the Riser Simulator constant stripping of the catalyst occurs due to the fluidized condition achieved. Subsequently, residual heavy oil trapped in the catalyst pores is likely a minimal amount and the product distribution obtained from the bulk gas phase is representative of the one formed at the outlet of a riser.

3.1.2 Details of the reactor

The schematic diagram shown in Figure 3.1 shows the main features of the reactor unit. Two reactors of identical internal dimensions were constructed, one being made of Plexiglas for cold model experiments and the other machined from Inconel 600 for the actual cracking runs. The hot model reactor as a unit consists of 4 main components: the reactor shell consisting of two blocks, the catalyst basket, the impeller and the impeller drive-housing unit. All parts are removable and the shell was constructed in two halves for easy access to the catalyst chamber. The bottom half contains three cartridge heater cavities and houses the catalyst basket. Two additional cartridge heaters were inserted in the

upper shell which were not present in the initial design (Kraemer, 1987). As well, a thermocouple cavity was added in the upper block to measure temperature in this region. This modification was made in order to see the temperature gradient between the bottom and top block of the reactor. The impeller drive unit was kept cool by a water cooling jacket which results in net upward flux of heat. The addition of the two cartridge heaters in the upper block eliminated the temperature gradient from the catalyst basket to the top of the impeller region (500°C and 450°C respectively).

Detailed drawings of the reactor shell are shown in Figures 3.3 and 3.4 showing the modifications made from the initial design. Figure 3.3 shows a side view of the 6 inch diameter reactor. The top half is 1 inch thick while the bottom half is 2 inches thick. The two halves are sealed using a spiral wound gasket consisting of Inconel metal spirals alternating with graphite filler. These particular gaskets were obtained from Parker Seals (2.125" I.D. by 2.25" O.D. by 1/8" thick) and were seated in the grooves provided. Eight 3/8 inch bolts are used to tighten the two halves together.

Figure 3.4 shows a top view of the reactor. The front face of the reactor was machined flat to house the equal length cylindrical cartridge heaters. The cavities shown for the inlet and outlet lines, pressure line and thermocouple well are 1/4 inch in diameter and contain inserts with a 1/16 inch internal diameter. These inserts contain Gyrolok

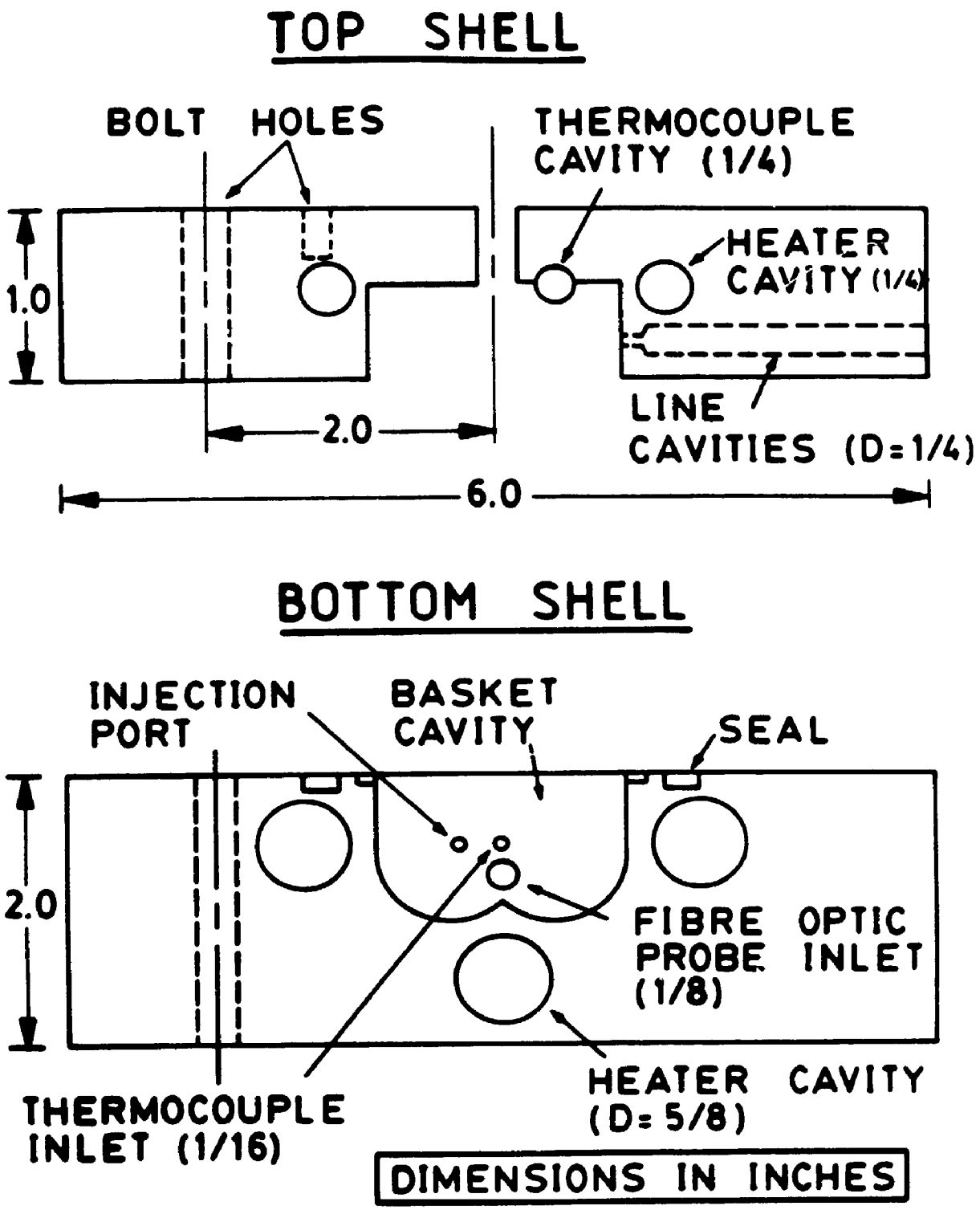

Figure 3.3 Side view detailed drawing of the reactor.

TOP VIEW
(Dimensions in inches)

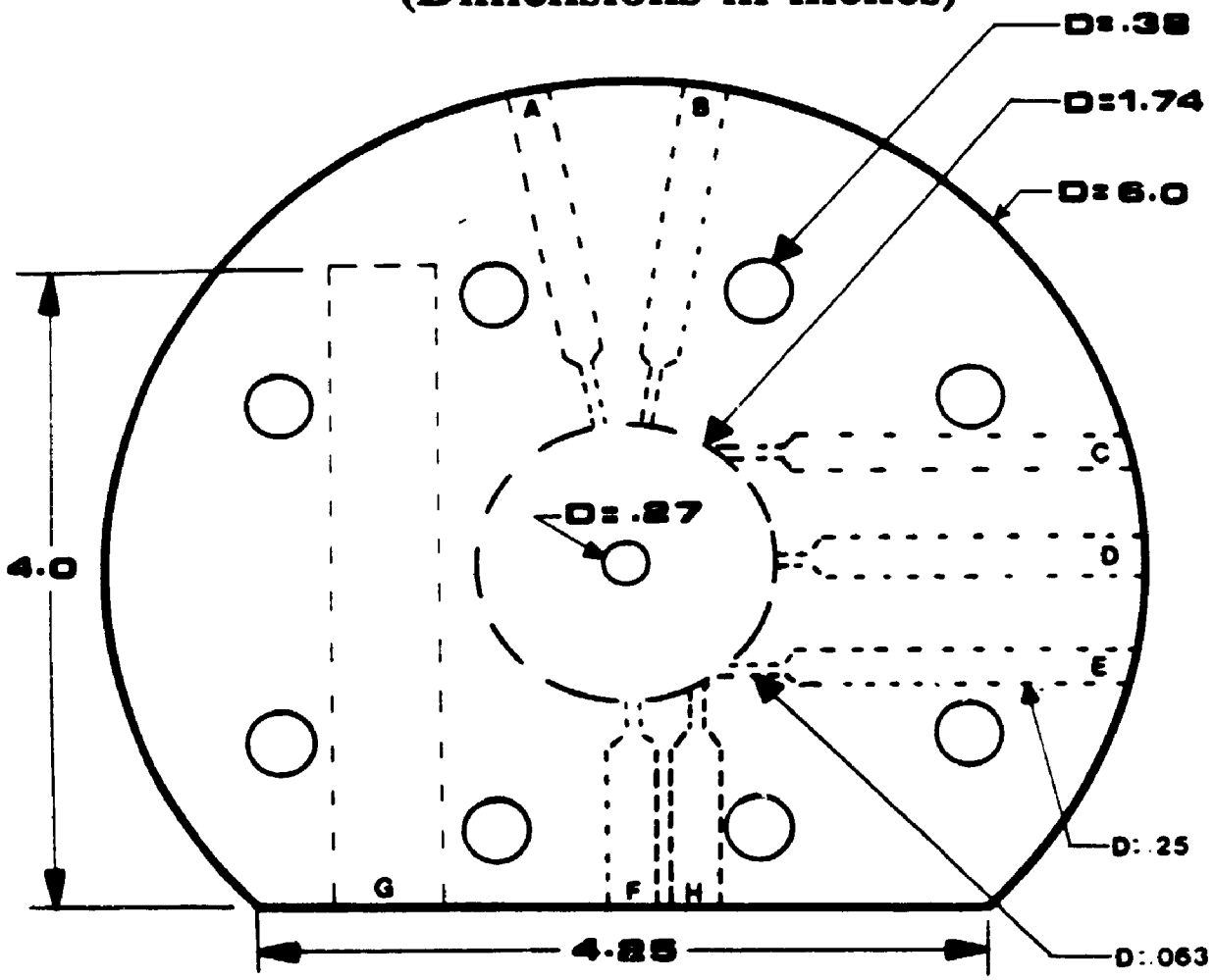

A - Injection Port
B, H - Thermocouple Ports
C - Outlet
D - Pressure Tap
E - Inlet
F - Fibre Optic Probe Inlet
G - Heater Cavity

Note: **All ports have inserts to reduce dead volume (1/4 O.D., 1/16 I.D.)**

Figure 3.4 Top view detailed drawing of the reactor.

fittings on the ends to connect the various lines and were welded to the reactor block. This was done to keep the fittings at a lower temperature away from the reactor. From operational experience, fittings that were welded directly onto the block eventually broke after several cycles of connecting and disconnecting of the lines and thermocouple due to the severe service temperature and dissimilar metals (i.e. fittings were stainless steel). The inserts also reduced the dead volume of the cavities which had to be drilled 1/4 inch in diameter due to the hardness of the metal. At the end of these cavities, close to the internal reactor chamber a smaller diameter hole (1/16 inch) was possible to be drilled. It should be mentioned that the pressure ports located in the bottom block were plugged with solid rods and welded closed at the external end of the block for the actual cracking runs to eliminate unnecessary dead volume.

The insert for the injection port was a 5/16 inch diameter cylindrical metal piece with a 0.04 inch internal diameter designed to guide the needle of the syringe into the reactor chamber. The end of the insert was machined to allow a cap with a high temperature septum, rated for 350°C, to be attached for syringe injections. For the heavier gas oils used a metal syringe was constructed as well as a heating block for the syringe. The block had a hole into which the metal syringe was set, was heated by a cartridge heater and controlled by a thermocouple inserted into the block.

A detailed drawing of the catalyst basket is shown in

Figure 3.5. The basket is supported in the bottom block by a ring structure in order to suspend it creating an annular space between the outer portion of the basket and inner part of the reactor shell. Catalyst is held in the central basket cavity using 20 micron Inconel porous discs placed at the bottom and top and held in place using snap rings. The baffles located on the sides of the basket are used to help direct gas flow downward through the annular region. The bottom pressure port was enlarged to a 1/8 inch diameter to allow a fibre optic probe to reach the inner catalyst chamber.

Figure 3.6 shows the dimensions of the 6 blade impeller. The blades and hub were machined from a solid piece of Inconel 600 and this piece was then welded to a 3/8 inch diameter shaft. The shaft drive-housing unit is shown in Figure 3.7. This flanged unit attaches to the top of the reactor and sealing is provided by a spiral wound gasket. The impeller is held suspended in place by a nut at the top of the drive unit (not shown). This drive unit obtained from Parr Instruments screws into the flanged housing piece and uses roller bearings as the rotating mechanism. A pulley was attached to the drive unit allowing the use of a timing belt to deliver rotation from a 1/4 hp motor. This motor was located adjacent to the reactor with a large pulley that was parallel with the pulley on the impeller drive unit. The top speed of the motor is 1750 RPM and the pulley ratio of 6 allows for a top impeller speed of 10,500 RPM. Motor speed was varied using a Ratiopax controller.

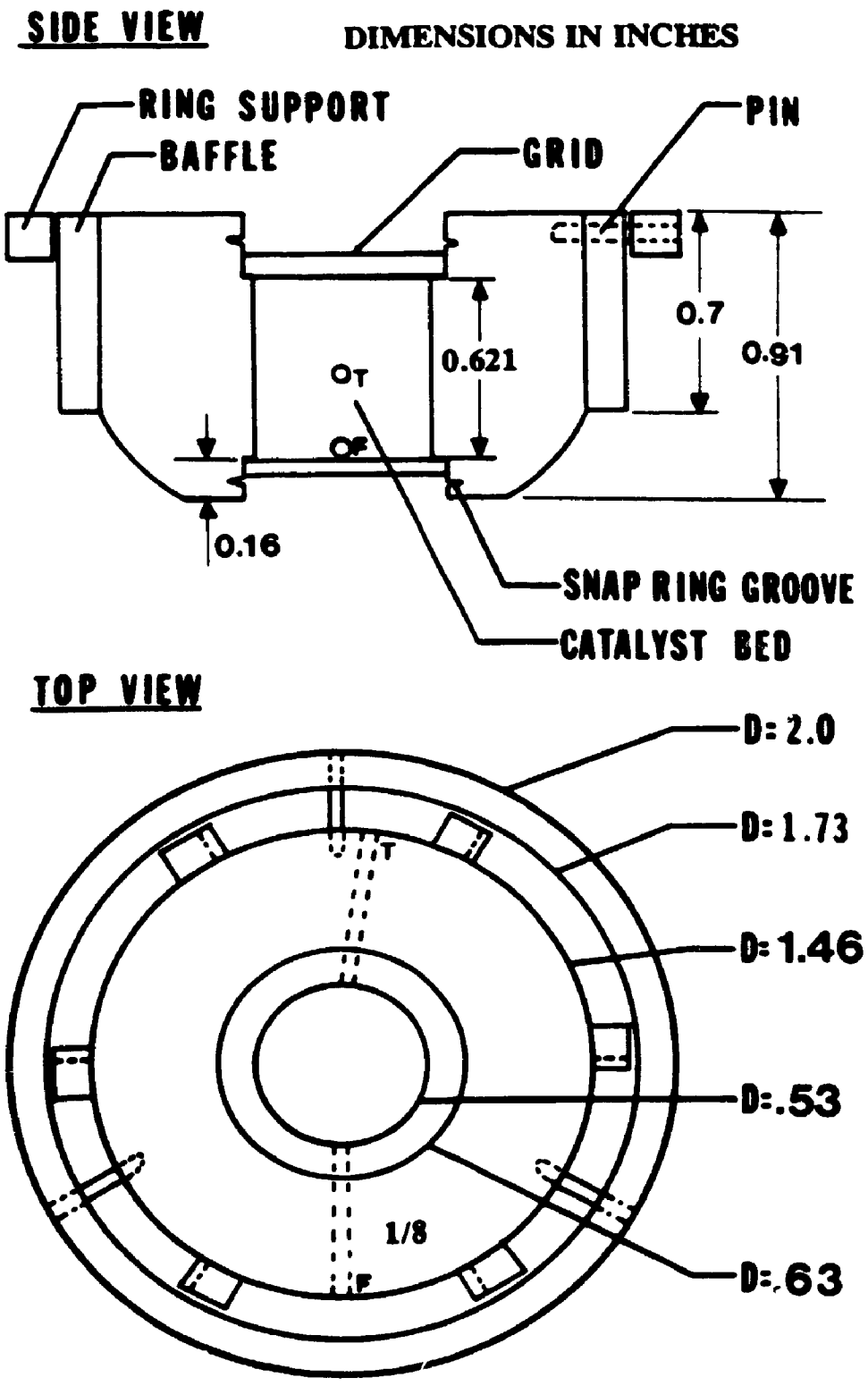

Figure 3.5 Detailed drawing of the catalyst basket.

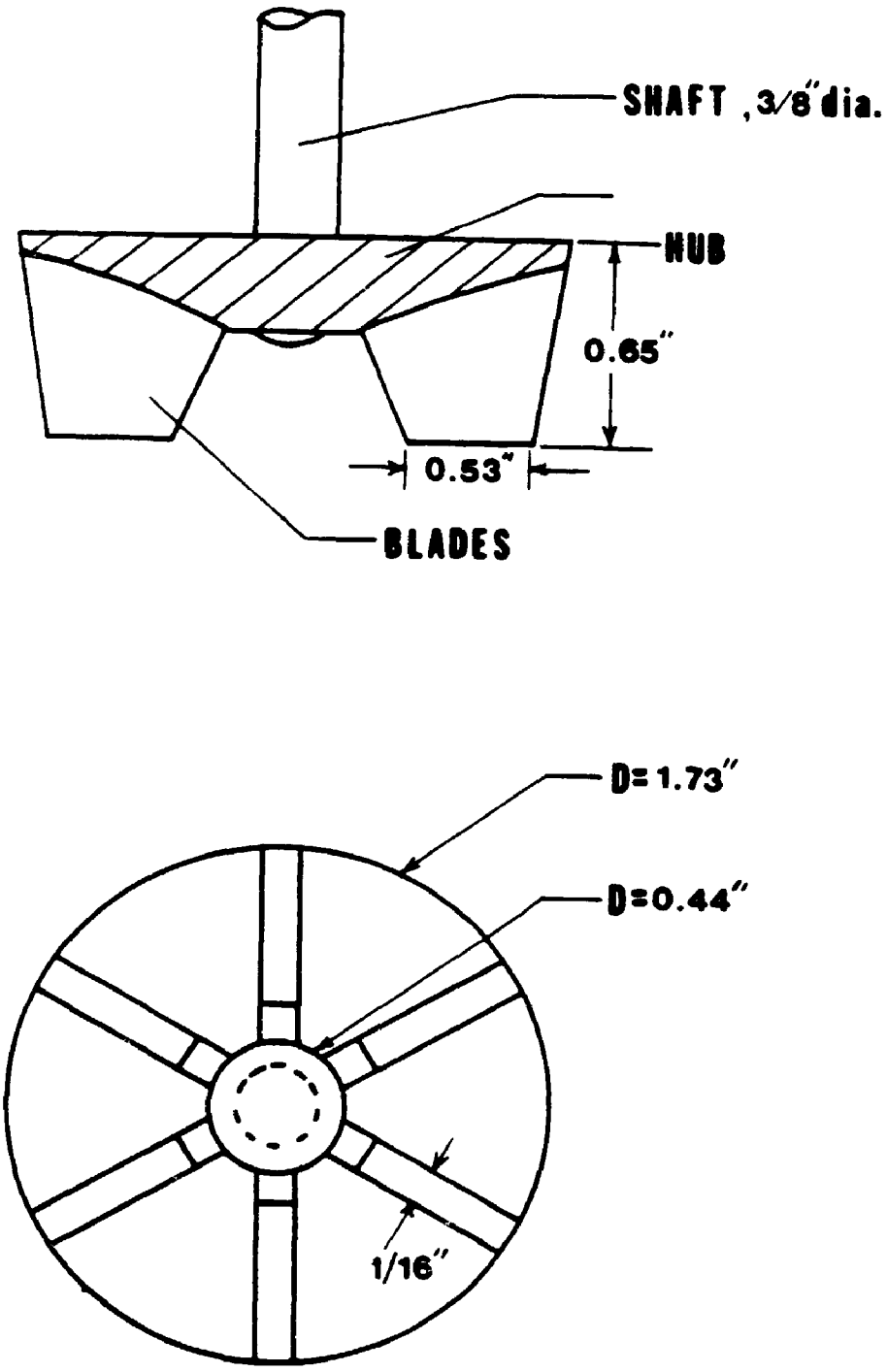

Figure 3.6 Detailed drawing of the impeller.

To seal the reactor through the shaft area a Parr packing gland was used which is located at the bottom region of the housing unit (Figure 3.7). This compact gland uses alternating self lubricating reinforced Teflon cones and Viton O-rings in conjunction with pressure from within the vessel to develop a positive dynamic seal on the rotating shaft. This packing also provides support and alignment of the shaft. To protect the cones and rings from excess temperature a water cooling jacket was fitted around the housing unit and a thermocouple located near the bottom of the unit was used to monitor temperature.

The assembled reactor can be suspended from the top by the use of four stud bolts extending upwards from the top reactor block. A reactor stand was constructed to support the reactor and hold it firmly in place. Sufficient room below the reactor allows the bottom block to be lowered for easy access to the catalyst basket. As well, an insulating jacket was constructed using layers of Fiberfrax insulation to cover the entire reactor.

3.2 VACUUM-PURGE-SAMPLING SYSTEM

To effectively remove the reaction vapours from the reactor a vacuum-purge method was used. Since the unit behaves as an ideally stirred vessel with concentration of hydrocarbons being constant in all points of the reactor at

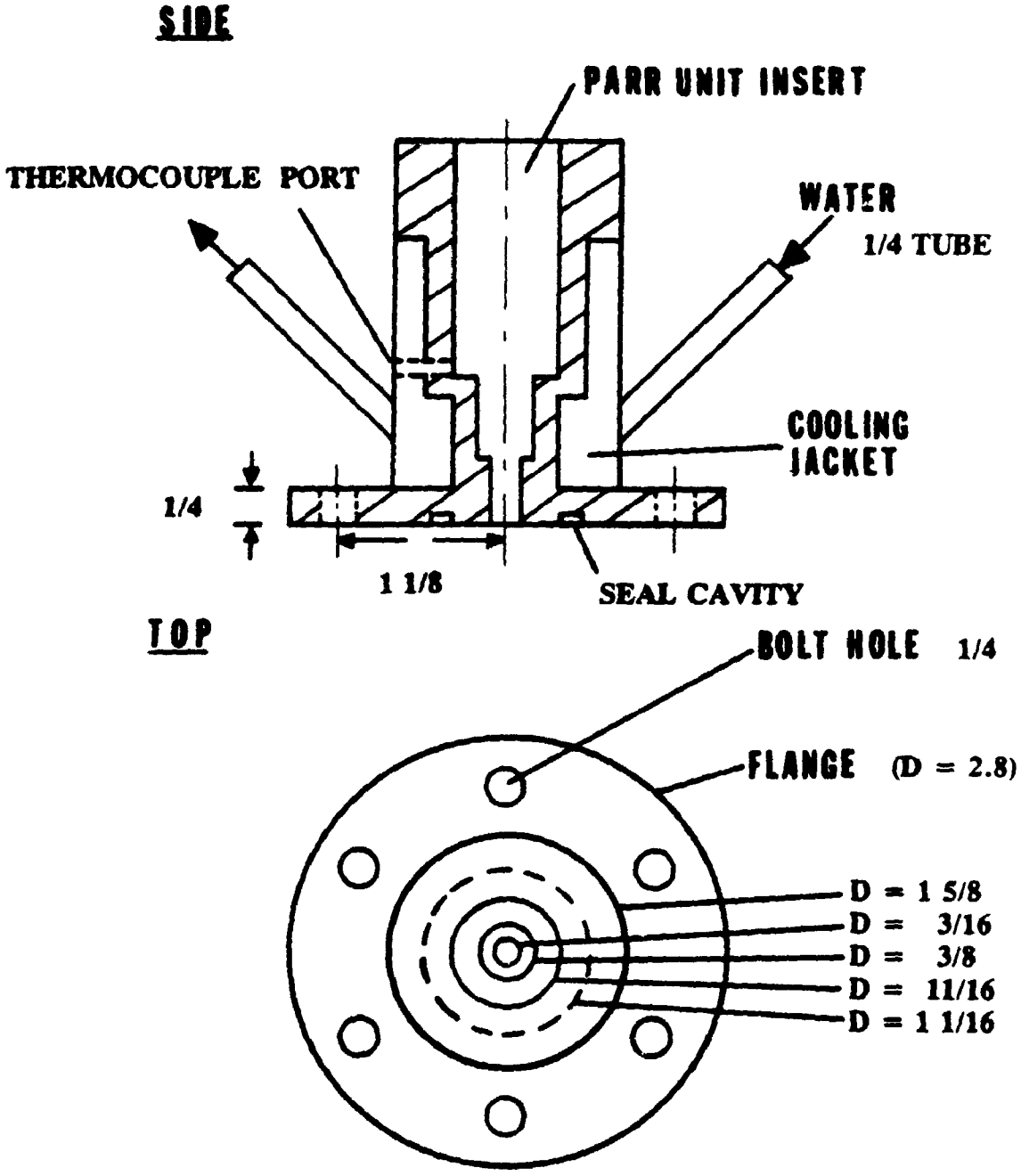

Figure 3.7 Detailed drawing of the shaft housing-drive unit.

any given time and considering that batch conditions were used, then the necessary information required to satisfy the kinetic equations is the distribution of hydrocarbons at the end of the desired reaction time. Therefore, trapping a small sample of these gases at the end of the reaction period and sampling to a GC provides this information.

The various components of the vacuum-purge-sampling system and the experimental set-up are shown in Figure 3.8. The use of two high temperature chromatographic valves and a vacuum chamber are the essential features. The 4-port valve (4PV) is a low dead volume switching valve which has two positions. In the 'reactor open' position line 1 is connected to line 2 and at the same time line 3 connects to line 4. In the other position (reactor closed) line 1 connects to line 4 and line 2 joins line 3. As well, lines 2 and 3 are low dead volume 1/16 inch stainless steel tubing (I.D. = 0.03 inches).

The 6-port valve is also a 2 position valve and is used to sample reaction vapours to the gas chromatograph. In the load position line 4 connects with the sample loop (line 5), which has a volume of 2 mL, and line 6 also connects to line 5 while line 7 joins line 8. This position allows gases to pass from the reactor via line 3, through line 4 and into the sample loop. The sampling position of the 6PV connects line 4 to line 6 and joins lines 7 and 8 to the sample loop allowing helium carrier gas to take the vapours contained in the loop to the GC.

The maximum operating temperature for the two

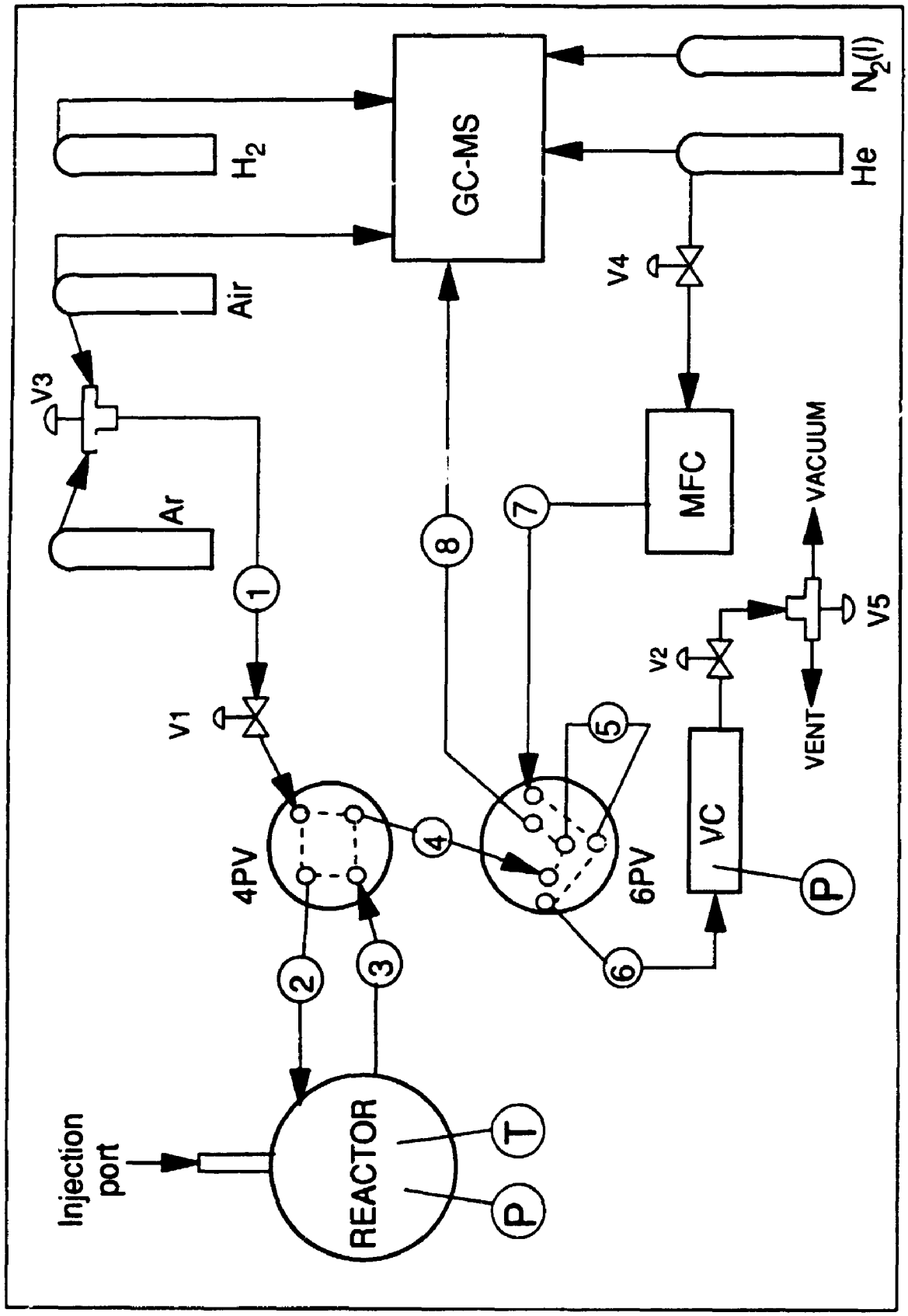

Fig. 3.8 Flow diagram for the experimental set-up

chromatographic valves is 300°C. To ensure proper temperature control for these expensive valves, an aluminum block with a cartridge heater inserted was used. The cylindrical valve bodies were bolted to the block and wrapped with insulation. A thermocouple placed on the valve body was used to control the temperature. Temperature was maintained at close to 300°C when an injection was made and lowered between runs. The valve handles were extended away from the heated zone to allow for manual manipulation.

The vacuum chamber, denoted as VC in Figure 3.8, is a cylindrical steel vessel with a nominal 2 inch diameter and a volume of 550 mL. This gives a volume ten times that of the reactor which results in a rapid equilibration when the two vessels are connected. The vacuum chamber is brought to low pressure by the use of valves V2 and V5. With V5 connected to the vacuum pump (assuming 4PV in the reactor closed position with V1 closed) then V2 is opened and the vacuum-purge system is brought to vacuum pressure. A pressure gauge connected to the vacuum chamber monitors this pressure which typically reaches 0.1 atm. After reaching this pressure V2 is closed resulting in vacuum pressure for lines 4, 5, 6 and the vacuum chamber.

The vacuum chamber was placed in a heated box with temperature maintained at 350°C. As well, all lines were wrapped with heating tapes and temperature was monitored in each line. Typically all lines were kept at approximately 350°C. At this temperature and the vacuum pressures used, the

hydrocarbons are maintained in the vapour state. More specific details of the heating and temperature control for the system are described in the M.E.Sc. report (Kraemer, 1987).

The set-up of the experimental system as indicated in Figure 3.8 allows the reactor to be operated in a continuous or a discontinuous mode. Valve V3 is used to switch flow from argon (used as an inert gas in the reactor) to air which is used for regeneration of the catalyst between injections of oil. The steps involved for a cracking run can be divided into five parts:

1. Initial purge
2. Setting of vacuum pressure
3. Reaction period
4. Purging and sampling
5. Regeneration

In step 1 argon flows via line 1 into the reactor (4PV in reactor open position) and out through line 3 then through the sample loop (6PV in load position), line 6, the vacuum chamber and finally to a vent. Valve V1 is a metering valve and can be used to control the flow of argon. The reactor is set to 1 atm argon by closing V1 and allowing for pressure equilibration. This leads to step 2 where the 4PV is switched to the reactor closed position and then V5 is switched to vacuum for setting the vacuum pressure as previously mentioned.

Step 3 involves the injection of the gas oil sample which denotes time zero. At the end of the desired reaction time the 4PV is turned to the reactor open position allowing the

vacuum chamber to be connected with the reactor for rapid equalization of pressure. In this step vapours under pressure in the reactor quickly flow into lines 4, 5 and 6 as well as the vacuum chamber because of the lower pressure. The final equilibrium pressure is reached rapidly (1 second) and is measured using the pressure gauge connected to the vacuum chamber.

Step 5 involves switching the 6PV to the sampling position which allows line 7 to flush vapours from the sample loop to the GC facility via line 8. The entire system can then be purged by opening valves V1 and V2 with V6 switched to vent. This allows argon to flow through the reactor and vacuum system flushing remaining hydrocarbon vapours. Step 5 is accomplished by turning V3 to allow air to pass through the reactor which has been heated to the regeneration temperature to burn off the coke. Step 1 is then repeated to complete the cycle. Further details of the cracking run procedure will be given again in Chapter 5.

3.3 ANALYTICAL EQUIPMENT

The major analytical device used in the study was a Hewlett Packard 5890A gas chromatograph which gave quantitative analysis of the reaction vapours. This unit is equipped with an alphanumeric display keyboard to permit convenient definition of instrument setpoints. The inlet

system is capable of split or splitless capillary column mode, as well as packed column mode, all connected to a back-pressure regulated flow. Temperature programming of the oven was possible with three temperature ramps available with the smallest increment being 0.1 degrees per minute. In the cryogenic mode liquid nitrogen is used to lower oven temperature to -30°C which was the initial temperature used in all runs. The upper temperature limit for the oven depends on the type of column used and was set for a maximum of 350°C.

The detection systems used was a flame ionization detector (FID). The FID responds to compounds which produce ions when burned in a hydrogen-air flame. All organic compounds were then suitable for use with this detector. Linear response is obtainable for most organic compounds from the minimum detectable limit through concentrations greater than 10^7 times the minimum detectable limit.

The split mode with capillary column was used in the cracking runs performed. The vapours injected to the GC from the helium carrier gas line are split into two portions by a glass capillary inlet splitter. The smaller portion is sent to the capillary column thus reducing the amount of sample in the column to avoid flooding of the FID and column overloading. Split ratios can range from 10:1 to 500:1 with high values used for high resolution columns. One problem with the split injection technique is that there exists the possibility of sample discrimination.

The capillary column used for separation of the various

components in the reaction mixture was an Hewlett Packard HP-1 column. This column was 25 meters long, 0.2 mm in diameter, with a 0.33 micrometer thick crosslinked methyl silicone film and is most suitable for petroleum components ranging from gases up to heavy gas oil molecules. It was not practical in the present application to separate the various fractions of the products by distillation because of the small amounts involved. The combination of temperature programming and the adsorption-desorption capacity of the column allowed for effective separation and detection of the hydrocarbon compounds ranging from lignt gases, gasoline and gas oil groups.

The chromatograms generated for each injection were produced using an HP 3393A integrator. The integrator accepted voltage outputs from the GC instrument, detecting and integrating peaks and plotting the chromatogram. As well, this information was stored on the integrator and was later transferred to an HP 1000 computer through a compatible interface for further analysis.

A mass selective detector was also used for identification of several compounds present in the cracked products and initial gas oil. The capillary column was disconnected from the GC and re-connected to an HP 5970A mass selective detector to form the GC-MS system. Typically, the injected hydrocarbons were separated by the GC and the eluting compounds were ionized by an electron beam in the MS inlet which operates under very low pressure. The ions were

filtered by a hyperbolic quadropole mass analyzer and were detected by an electron multiplier. The detector can monitor total ion abundance from the GC effluents and the mass spectra of these compounds were automatically recorded. The mass spectrometer is capable of giving qualitative information such as characteristic mass spectra, as well as quantitative information about selected ion peak areas.

The data obtained from the mass selective detector was analyzed using an HP 9828B desktop computer with an HP 2671G graphics printer to plot the mass spectrums. As well, software was supplied containing mass spectral libraries which allowed for an automatic search and comparison of recorded spectra for reliable compound identification.

3.4 REACTOR MODELLING AND KINETIC EQUATIONS

The rate equations in the case of the Riser Simulator can be formulated on a weight basis, which is equivalent to using the mechanistically more correct partial pressures because in this unit the gas volume is constant. In contrast, rate equations based on weight fractions for a flow reactor must be corrected for volume expansion due to the increase in the number of moles generated during the cracking reactions. Usually the velocity term in the plug flow riser reactor model must account for the change in fluid density along the height of the reactor thus an additional equation is required. The

fluid density may be written in terms of the molecular weights of the lumped components which adds extra complexity.

Since the Riser Simulator operates as a batch reactor, then the change in the number of moles of gas oil with time is equal to the cracking rate of the oil. This can be expressed in terms of molar concentrations (or equivalently as partial pressures) as follows:

$$dC_A/dt = r_A\, m_c\, /V_T \qquad (3.1)$$

where r_A is the rate of gas oil cracking expressed in moles of oil per gram of catalyst per second, C_A is the concentration of gas oil expressed in moles of oil per reactor gas volume, m_c is the mass of catalyst and V_T is the total reactor gas volume.

3.4.1 Equations For The Three Lump Model

The three lump model as described in Chapter 1 involves three simultaneous equations describing the cracking of the gas oil lump (A), the gasoline lump (B) and the light gases plus coke lump (C). Considering first the gas oil lump then the rate of cracking, r_A, in equation (3.1) can be expressed as:

$$r_A = - \Phi\, k_o\, C_A^2 \qquad (3.2).$$

A deactivation function Φ is needed to account for the catalyst activity decay due to coke deposition on the

catalyst. The various forms of this function were discussed in Chapter 1 where Φ can be a function of catalyst time-on-stream or more appropriately as a function of coke content on the catalyst. The kinetic constant, k_o, is the overall gas oil cracking rate constant which is the sum of k_1 and k_3 from the 3-lump scheme. Substituting this value for r_A in equation (3.1) results in:

$$-dC_A/dt = \Phi\, k_o\, C_A^2\, m_c\, /V_T \qquad (3.3).$$

From the ideal gas law the concentration of gas oil in the reactor can be represented as follows:

$$C_A = Y_A\, w_T\, /\, (M_A\, V_T) \qquad (3.4)$$

where Y_A is the weight fraction of gas oil in the reactor, w_T is the total weight of vapours in the reactor (inert gas plus hydrocarbons) and M_A is the molecular weight of the gas oil. This value of C_A can be substituted into equation (3.3) to obtain the gas oil mass balance equation in terms of weight fractions:

$$-dY_A/dt = \Phi\, k_o\, Y_A^2\, w_T\, m_c\, /(M_A\, V_T^2) \qquad (3.5).$$

With an appropriate expression for $\Phi(t)$ this equation may be directly integrated since all other parameters are constant with time. The initial gas oil weight fraction is defined from the known mass of injected oil and the initial mass of inert gas present in the reactor.

The mass balance for the gasoline lump can be obtained in

a similar fashion with the rate of gasoline formation containing two terms, one for the formation from the gas oil cracking and the other for the disappearance due to gasoline cracking. The change in gasoline concentration (C_B) can then be written as:

$$dC_B/dt = \Phi \left[v_1 k_1 C_A^2 - k_2 C_B \right] m_c / V_T \qquad (3.6)$$

where v_1 is the stoichiometric coefficient for gasoline formation from gas oil usually estimated as the ratio of molecular weights (M_A/M_B). By using the relationship to express concentrations in terms of weight fractions, as given in equation (3.4), then the following equation results for the gasoline mass balance equation:

$$dY_B/dt = \Phi \left[(w_T/M_A V_T) k_1 Y_A^2 - k_2 Y_B \right] m_c / V_T \qquad (3.7).$$

It should be mentioned that the stoichiometric coefficient cancels out in this transformation to weight fractions. This equation, with the appropriate decay function can be solved numerically where the value of Y_A is obtained from equation (3.5). Similarly the mass balance equation for the light gases plus coke lump can be written as:

$$dY_C/dt = \Phi \left[(w_T/M_A V_T) k_3 Y_A^2 + k_2 Y_B \right] m_c / V_T \qquad (3.8).$$

In general the gas oil and gasoline mass balance equations (equations (3.5) and (3.7)) can be used to solve for the kinetic parameters k_o, k_1, and k_2 where k_3 is calculated by difference from the known values of k_o and k_1. A Marquardt

regression technique for parameter estimation combined with a Runge-Kutta method for solution of the differential equations can be used.

The various deactivation functions described in Chapter 1 can be substituted for Φ in equation (3.5). These three decay functions were used in the present study to evaluate kinetic and decay parameters and the validity of each model was assessed. Substituting for Φ, as given by the exponential decay function of equation (1.6), into equation (3.5) and integrating gives the following for gas oil weight fraction:

$$Y_A = [1/Y_{Ao} - \{(e^{-\alpha t} - 1)\ w_T\ m_c\ k_o\ /\ (\alpha\ M_A\ V_T^2)\}]^{-1} \qquad (3.9)$$

where Y_{Ao} is the initial weight fraction of oil. It should be noted that in equation (3.9) the parameter α is used instead of k_d because it is most commonly used throughout the literature when describing the exponential decay function (i.e. $\alpha = k_d$).

Similarly, substituting into equation (3.5) for Φ from the power law decay function as given by equation (1.7) and integrating gives the following for gas oil weight fraction:

$$Y_A = \{1/Y_{Ao} - t^{1-N}\ w_T\ m_c\ k_o'\ /\ [M_A\ V_T^2(1-N)]\}^{-1} \qquad (3.10)$$

where $k_o' = Dk_o$. It is now evident that the deactivation constant, k_d, which is included in the parameter D, becomes combined with the cracking kinetic constant, k_o, when using the power-law decay function. Thus, the unknown parameters in equation (3.10) are N, related to the deactivation order, and

k_o' which is a combined cracking and decay kinetic rate constant.

It can also be shown (see Appendix A) that the third catalyst activity decay function described in Chapter 1, which relates the catalyst activity to the amount of coke on the catalyst, has the following form:

$$\Phi = 1 + [(Y_A - 1)\ w_T\ k_d' / (k_o\ m_c\ M_A)] \qquad (3.11)$$

where k_d' is the deactivation rate constant.
This expression for Φ can be substituted into equation (3.5) and the resulting differential equation can be solved using numerical methods as described in Appendix A.

3.4.2 Equations for an Eight Lump Model

To keep in line with the objectives of the study an 8-lump model (Kraemer and de Lasa, 1988b; 1989; 1990) will be used to further breakdown the gas oil lump of the 3-lump model into six groups to account for the chemistry of the feedstock. This model is similar to the 10-lump model but does not distinguish between bare aromatic rings and aromatic rings with substituent groups. It was not possible to make this distinction with the analytical methods available in this study.

The 8-lump kinetic scheme, as depicted in Figure 3.9, divides the oil into paraffins, naphthenes and aromatics in both a light fuel oil (LFO) and a heavy fuel oil (HFO)

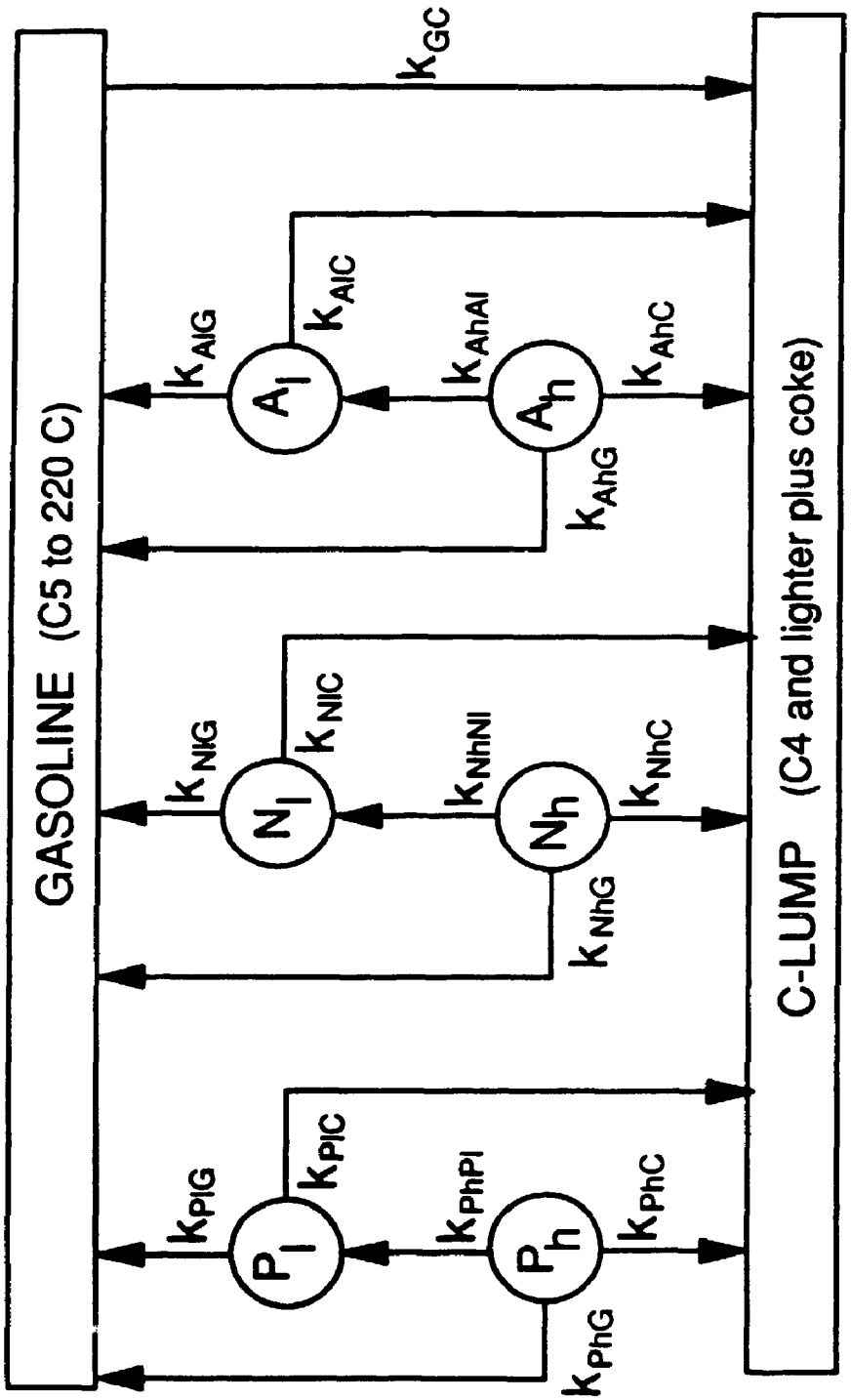

l = light oil fraction (220 to 345 C)

h = heavy oil fraction (345 C +)

Fig. 3.9 Kinetic scheme for the 8-lump model

fraction. The LFO is defined by the boiling range of 220°C to 345°C and the HFO fraction refers to compounds boiling above 345°C. The gasoline lump (C_{12} to 220°C) and the C-lump (C_4 and less plus coke) from the triangular model remain the same. This model involves 16 kinetic constants where the HFO lumps (P_h, N_h, A_h) can crack to light oil fractions, to gasoline and to light gases plus coke (C-lump). The LFO lumps (P_l, N_l, and A_l) crack to form gasoline and light gases plus coke. The gasoline lump formed from the oil lumps can further crack to C-lump.

The six oil lumps each represent a reasonably narrow boiling range of compounds and thus the cracking order is assumed to be one (Jacob et al., 1976; Weekman, 1979). The equations for the Riser Simulator model can then be expressed as follows for the weight fractions of the three heavy oil lumps:

$$dY_{ih}/dt = - \Phi\, k_{ih}\, Y_{ih}\, m_c \,/\, V_T \qquad (3.12)$$

where i = P, N, or A.

In these three equations the kinetic constant k_{ih} is the overall heavy lump cracking constant and is the sum of k_{ihG}, k_{ihG}, and k_{ihC}. A simplifying assumption is that the cracking sites are the same for each lump (i.e. the same active sites will crack P, N or A molecules) and thus the deactivation function, Φ, is the same for each lump.

For the three light oil lumps, the change in the weight fraction of the light oil lump with reaction time can be

written as:

$$dY_{il}/dt = \Phi \left[k_{ihil} Y_{ih} - k_{il} Y_{il} \right] m_c / V_T \qquad (3.13)$$

where $k_{il} = k_{ilG} + k_{ilC}$.

Furthermore, for the mass balance on the gasoline fraction, the change in weight fraction can be expressed as:

$$dY_G/dt = \Phi \left[k_{PhG} Y_{Ph} + k_{NhG} Y_{Nh} + k_{AhG} Y_{Ah} + k_{PlG} Y_{Pl} + k_{NlG} Y_{Nl} + k_{AlG} Y_{Al} - k_{GC} Y_G \right] m_c / V_T \qquad (3.14)$$

A similar expression can be written for the C-lump formation but is not need in solving for the coke formation kinetic constants. These values of k_{ilC} and k_{ihC} can be found by difference knowing the values of k_{ih} and k_{il} obtained from equations (3.12) and (3.13). The matrix of rate constants is lower triangular thus the three equations for the heavy lumps described in equation (3.12) can be solved independently from each other as well as independently from the light oil equations and the gasoline equation. Similarly, the three light oil equations can be solved, in conjunction with the known values from the corresponding heavy oil equations, independently of the gasoline equation. This result is due to the irreversible nature of the cracking network leading to a stepwise solution (Jacob et al., 1976).

The solution of the gasoline equation requires the input from the six oil lump equations resulting in seven simultaneous differential equations which can be solved using

a Runge-Kutta algorithm. The solution strategy for the eight lump model is presented in Appendix A.

3.5 MASS BALANCE CONSIDERATIONS

To perform a mass balance on the reaction system the mass of hydrocarbons purged from the reactor at the end of the reaction time period must be known. Also, the mass of hydrocarbons left in the reactor must be assessed. The sum of these two masses should then equal the injected mass of oil (minus coke) known from the syringe volume used and the density of the oil. These calculations can be done by measuring the pressure in the vacuum system before and after purging, measuring the system temperatures (reactor, sample loop, vacuum chamber) and knowing the volume of the system (reactor and vacuum lines). As well, the molecular weight of the hydrocarbon mixture resulting from the cracking reactions must be assessed.

The moles of vapour purged from the reactor can be calculated using the ideal gas law relationship and knowing the difference in the vacuum system pressure before and after the purge procedure. The total mass purged is then found by multiplying by the average molecular weight of the gas mixture (hydrocarbons and argon). As well, the ratio of the weight of hydrocarbons (excluding coke) to weight of argon in the reactor can be considered constant since it operates as a

closed system. This holds true for the purged vapours since they come from the reactor. This relationship allows for the calculation of the mass fraction of hydrocarbons in the purged gases. Thus, the mass of hydrocarbons purged from the reactor can be expressed as:

$$m_{HC,p} = [M_{HC} / (1 + ¥ M_{HC})] [(P_{Vf} - P_{Vi}) V_V / (RT_V)] \quad (3.15)$$

where $¥ = P_{Ri} V_R / (R T_R w_o)$.

The detailed derivation of equation (3.15) is shown in Appendix B. The factor ¥ accounts for the presence of argon initially present in the reactor and the molecular weight of hydrocarbons can be assessed from the GC analysis of the sampled vapours. It is important to note that the vacuum system volume, V_V, includes the total volume contained between valve V1 and valve V2 with the 4PV in the reactor closed position as seen in Figure 3.8. This includes the volumes of lines 4, 5 and 6, the vacuum chamber volume and volume in the lines between the 4PV and V1 and between VC and V2. This total volume, consisting mainly of the volume of VC, was measured experimentally (approximately 575 mL) and is discussed in Chapter 4. Also, the vacuum system temperature was taken to be that of the vacuum chamber and the purged gases were assumed to be at this temperature.

To calculate the mass of hydrocarbons left in the reactor it is assumed that the reactor and vacuum system reach pressure equilibrium during the purging process. This

condition is achieved rapidly considering the large difference in volumes between the reactor and vacuum chamber and because the final reactor pressure is much higher than the vacuum system pressure. Therefore, the final pressure in the reactor is set equal to the vacuum system pressure (measured value). Knowing this pressure as well as the reactor volume, temperature and the weight fraction of hydrocarbons to argon (which is constant) then the mass of hydrocarbons remaining in the reactor is given by:

$$m_{HC,r} = [M_{HC} / (1 + ¥ M_{HC})] [P_{Vf} V_R / (R T_R)] \qquad (3.16).$$

The summation of equations (3.15) and (3.16) then gives the total mass of hydrocarbons in the system:

$$(m_{HC} = m_{HC,p} + m_{HC,r}) \qquad (3.17).$$

The resulting total mass of hydrocarbons can then be added to the amount of coke produced and this number compared to the initial amount of oil injected. The mass balance is closed by assuming that any missing mass is due to unconverted oil not detected by the GC. The mass balance correction procedure is further discussed in Chapter 5. Furthermore, the adequacy of the mass balance equation was tested using injections of propane at both room temperature and operating temperatures and is presented in Chapter 4.

CHAPTER 4

TESTING OF THE REACTOR SYSTEM

4.1 INTRODUCTION

The initial part of this research concerning design and testing of the experimental system is documented in a M.E.Sc. thesis (Kraemer, 1987). The tests performed in this work included measurements of pressure drops across the catalyst bed and catalyst grid at varying impeller speeds. Several experiments were performed and a plot of bed pressure drop versus impeller speed is shown in Figure 4.1. This relationship was developed for the case a nitrogen gas at a temperature of 25°C and a pressure of 1 atm and defines the range of RPM's in which the bed is in a fluidized state. As can be seen the pressure drop across the bed increases at a linear rate with impeller speed until the condition of fluidization is reached where the bed pressure drop becomes constant. This is typical behaviour for a fluidized bed where the pressure drop across the bed becomes equivalent to the weight of the bed. In the case of Figure 4.1 the fluidized bed pressure drop was 0.35 inches of water which corresponds well to the expected pressure drop at minimum fluidization for the 1.2 g of catalyst used (0.33 in. H_2O).

One of the disadvantages of the differential pressure system used was that the bed pressure drop could not be measured under actual cracking conditions. Condensation of

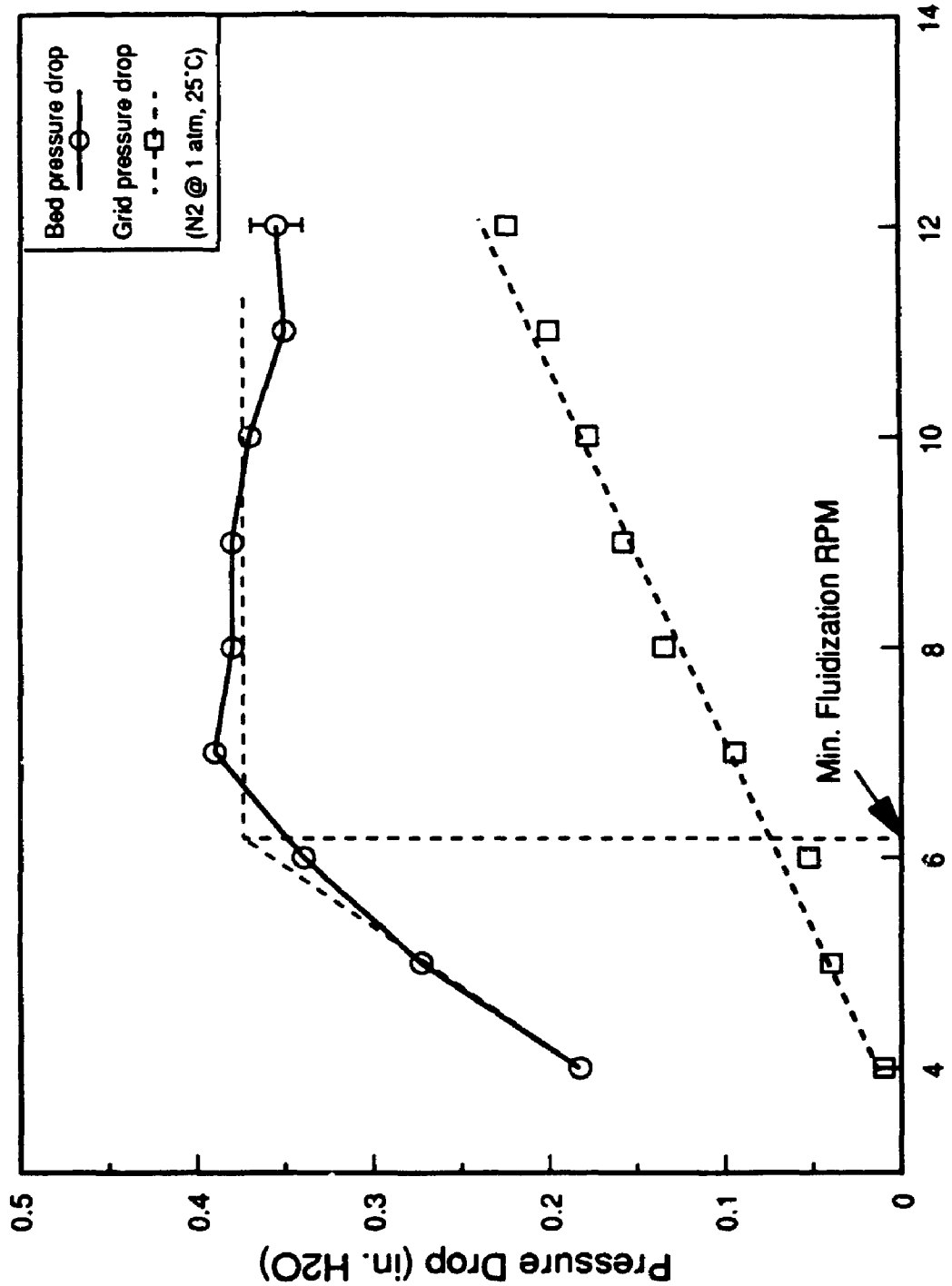

Fig. 4.1 Pressure drop versus impeller speed

oil in the lines leading to the pressure gauges and in the gauges themselves could not permit this assessment. Also, with the reactor under pressure problems resulted such as catalyst being transported out the pressure tap lines and difficulty was also experienced with equilibration of the Magnahelic differential pressure gauges. This led to the use of a fibre optic probe technique, which will be discussed in the next section, to further evaluate the bed dynamics.

Gas mixing in the reactor was assessed using tracer tests with the reactor operated as a CSTR. Pulsed injections of nitrogen at room temperature and pulsed injections of hexadecane at 500°C into a continuous helium stream were used. The residence time distribution function was recorded and showed an exponential decay with time as in an ideally stirred tank. The ideal reactor volume was calculated using this distribution and was very close to the measured reactor volume (43.8 versus 45 mL). From this result it was apparent that the gas mixing in the reactor was close to ideal.

Further tests included a check for thermal cracking in the reactor which was minimal (gas oil injection with no catalyst) and a check for isothermicity during reaction. Maximum temperature drop during reaction was observed to be 5°C which when operating at 500°C results in a 7.3% deviation of the kinetic constant (assuming E_A = 18 kcal/gmol). This maximum temperature drop was observed only at the higher conversion levels and on average a 2 degree drop was common which results in only a 3% average deviation (see Appendix D for

calculations). Therefore the assumption of isothermal conditions in the reactor for the purpose of solving the kinetic equations was assumed valid.

The adequacy and reproducibility of the vacuum-purge sampling system was checked using a calibration mixture of hexane, toluene and hexadecane. Injections to the reactor were made with no reaction (no catalyst present) and repeated sampling of the purged products was made to the GC. These results were compared with direct injections of the known mixture to the GC. Good agreement was obtained with an average error of ± 4.0% between the compositions of the original mixt .e and those from the vacuum-purge system. Also the standard error for repeated GC analysis of the purged products was ±0.94 wt% indicating that the sampling method was reliable and accurate.

The effect of external mass transfer in the reactor was also assessed. To confirm that mass transfer from the bulk phase to the surface of the catalyst particle was not limiting an estimation was made considering an extreme case of stagnant flow (impeller at rest). For the case of stagnant flow the mass transfer coefficient can be estimated form the Sherwood number which has a value of 2 under these conditions (i.e. Reynolds number equals zero). The results showed that the maximum difference in the bulk phase concentration and concentration at the interface is only 0.2% for this extreme cases. Thus with the impeller rotating at operational speed external mass transfer limitation is certainly not a factor

for this unit.

4.2 FIBRE OPTIC PROBE MEASUREMENTS

To further evaluate the fluid-solid mixing characteristics taking place in the catalyst bed a fibre optic probe technique was used. The advantage of using such a method over pressure drop measurements was that the reactor could be pressurized avoiding the difficulties of catalyst blow-out and off-scale readings experienced with the differential pressure gauges. As well, a fibre optic probe system, complete with laser signal, data acquisition and data analysis facilities was available in the laboratory. This set-up was developed during three other research projects for measuring fluid-dynamic parameters in a gas-solid fluidized bed (Huskey, 1990) and in three-phase fluidized beds (Lee, 1986; Chabot, 1989). In the present work the approach was to measure light signals reflected by the particles as the impeller speed was varied under differing conditions of pressure and inert gases. In this way a simulated reaction condition could be achieved by using a mixture of gases in the reactor at room temperature and under a certain pressure that had the same density and viscosity as a typical reaction mixture (hydrocarbons plus inert gas) at high temperature.

4.2.1 Description of the Fibre Optic Probe

Details of the fibre optic probe system used can be found in the works by Lee (1986) and Chabot (1989) thus a brief description will be given here. The main components of the photometric measuring system are shown in Figure 4.2 and include a light source, light guides and photodetectors. The light source used was a Spectra Physics helium-neon laser (35 mW) model no. 124B-255 which provided a stable red light (wavelength of 632.8 nm). To carry the laser signal, pure silica single core 400 μm optical fibres were used. The reflected light intensity was measured by two EG&G photodetectors model no. 460-1A. Signals were recorded via adapters attached to the back of these detectors with sensitivity adjustment made by selection of the proper resistor attached to the adapter. The analog signals were digitized using an HP-1000 model A600+ computer system and stored on magnetic tape cartridges.

To construct the fibre optic probe measuring device two 400 μm optical fibres were inserted inside a 1/8" O.D. tube which was approximately 30 cm in length. One fibre was for transmitting the light signal to the bed, the other to catch the reflected signal. The fibres consisted of 3 layers (see Figure 4.3): an inner silica core, a cladding layer (to maintain light in central silica core) and an external coating for protection and flexibility. The ends of the fibres were polished using micro sand paper to ensure good light

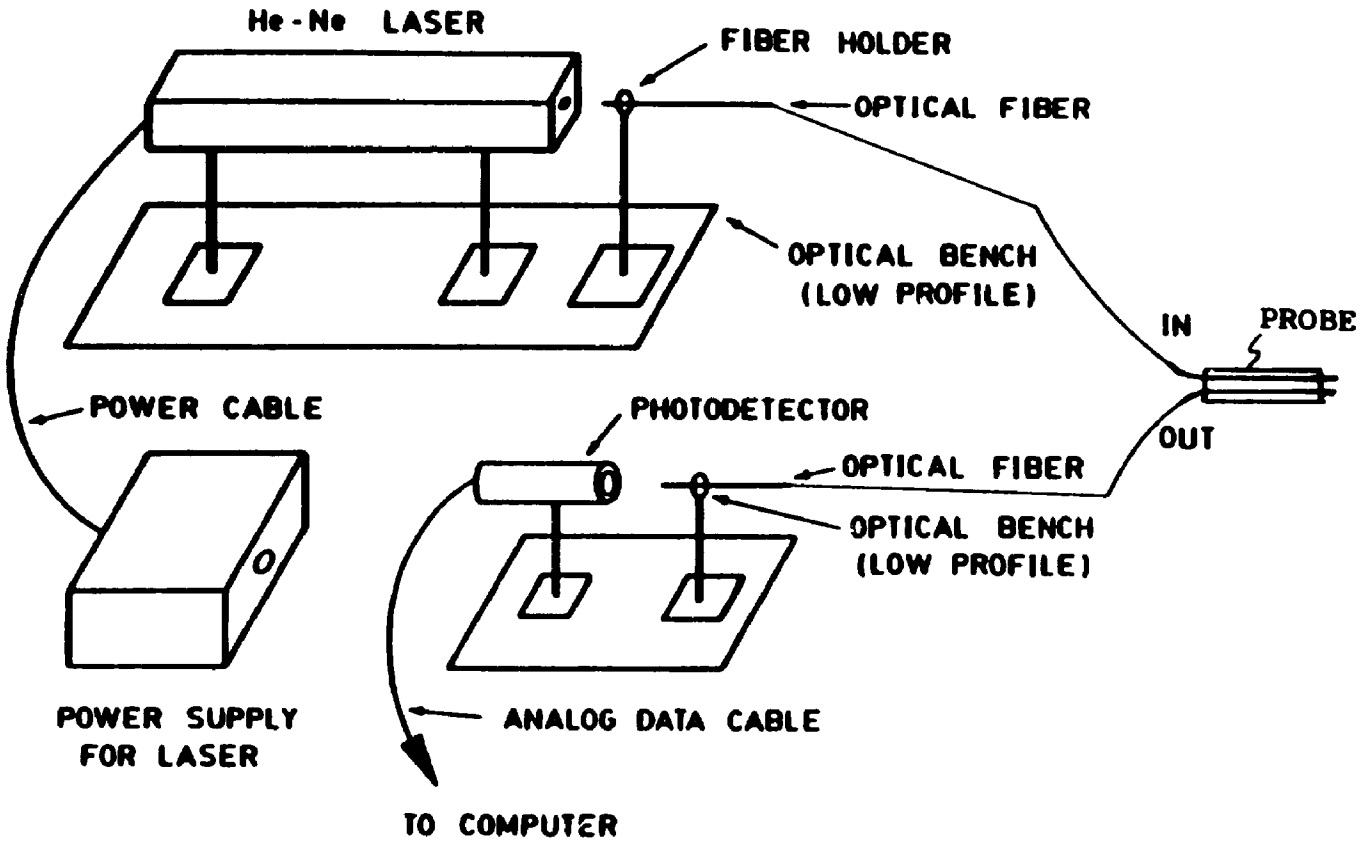

Figure 4.2 Schematic diagram of the photometric measuring system (Chabot, 1989).

transmittance. The tips of the two fibres were extended 2mm past the end of the tube sheath. A high temperature cement was used to fix the fibres in this position. The cement was applied at both ends of the sheath to provide support and sealing. A period of 24 hours was required for drying of the cement.

The probe was then inserted through an existing pressure tap that had been re-drilled to fit a 1/8" tube. Figure 4.3 shows the placement of the probe which was just above the bottom grid with the fibres protruding into the bed approximately 2 mm. A Swagelok fitting was used to hold the probe in place and to seal the device from gas leakage between the tube and probe cavity. An identical location for the fibre optic probe was also adapted in the cold model unit.

4.2.2 Experimental Conditions Used

A set of experiments were first conducted in the Plexiglas unit to measure signals from the reflected light as well as to visually observe the particle movement. In this way it was possible to qualitatively verify that a certain spectrum obtained from the recorded signal corresponded to a fluidized bed of catalyst. A typical run procedure with the probe in place involved the following:

1. Allow gas flow to purge reactor for approximately 5 minutes, then close valve.
2. Start computer program which measures reflected light signal as captured on the photodetectors.

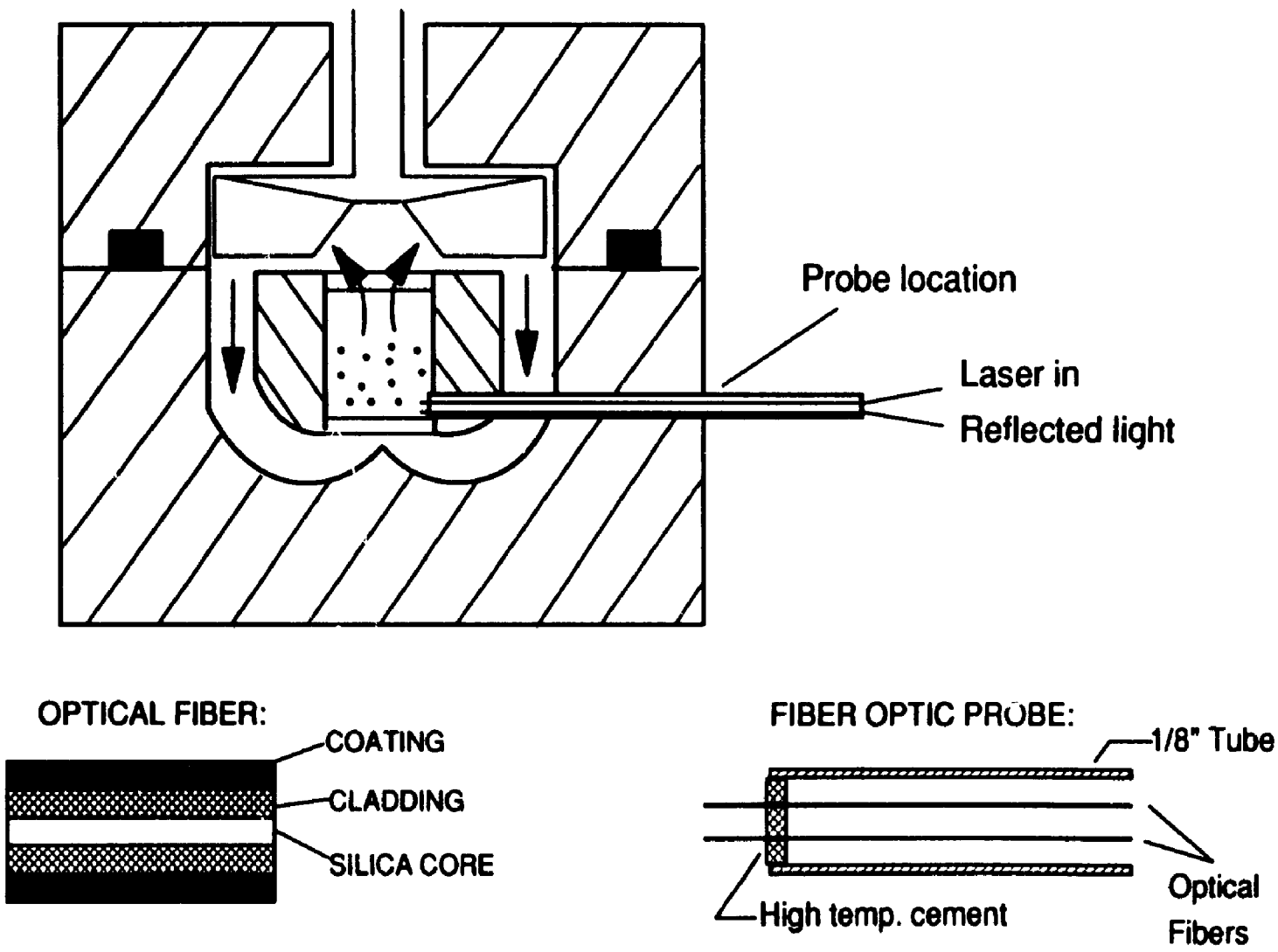

Fig. 4.3 Location and details of the fiber optic probe

3. Increase impeller RPM's to desired speed using motor speed controller.

4. Let motor run for approximately 30 seconds, then shut off.

5. Data is recorded for 90 seconds then processed to produce a spectrum (signal intensity versus time).

The original design of the cold model unit did not facilitate for an inlet or outlet gas flow and was not sealed through the shaft area (high speed, double bearing unit). An existing pressure tap line was used to allow gas to be introduced to the reactor and the outlet was through the shaft cavity (unsealed). It was not possible then to pressurize this vessel, however different gases could be used in the Plexiglas unit at room pressure and temperature. The range of gases and experimental conditions used for the cold model experiments are shown in Table 4.1. A second set of experiments were performed in the hot model reactor which could be pressurized to see the effect of density on the re-circulation rate. The range of experimental conditions performed in the hot model with the fibre optic probe are also listed in Table 4.1. Spectrums obtained from these experiments are shown in Appendix D. The weight of catalyst used in all experiments was constant to maintain a constant bed height. Also, some repeat experiments were performed to check the reproducibility of the optical measurements which were found to be consistent.

Table 4.1 Range of experimental conditions used for the fiber optic probe measurements in the hot and cold reactors.

Cold Model (1 atm, 25°C)

Gas	RPM	Catalyst (0.8 g)
air	0 - 12,000	Octacat, coked catalyst
nitrogen	0 - 10,080	Octacat, none
argon	7875	Octacat, GX-30
methane	7875	Octacat
helium	7875	Octacat

Hot Model (25°C)

Gas	P(atm)	RPM	Catalyst
nitrogen	1 - 3	0 - 8000	Octacat, none
argon	1 - 3	7875	Octacat, GX-30
methane	1	7875	Octacat
helium	1 - 3	7875	Octacat
N_2/air	1 - 2	7875	Octacat
He/N_2	1 - 2	7875	Octacat
He/air/Ar	1 - 3	7875	Octacat

4.2.3 Relationship Between the Optical Signal and Bed Dynamics

In contemplating the possible scenarios for the state of the catalyst bed during operation of the reactor, two extreme conditions could exist. The first would be a fixed bed of catalyst corresponding to a low gas velocity through the bed (i.e. low re-circulation rate) which would be detrimental to the objective of this unit (low degree of mixing, insufficient gas-solid contacting). The second extreme would be the case of over-revving of the impeller causing a high velocity through the bed (pneumatic transport range) resulting in a fixed bed of catalyst stuck at the top grid. This case would also be undesirable since the idea is to mix the catalyst particles for uniform coking. Therefore it was necessary to test the type of signal spectrum that would be obtained using the fibre optic probe if these two situations were to exist.

The spectrum for the first case (fixed bed) was obtained by simply leaving the impeller at zero RPM so that no flow was sent through the catalyst chamber. The resulting spectrum indicated no peaks because the catalyst was covering the emitting fibre thus no light could be reflected. The spectrum for the second case was obtained by using no catalyst in the bed (i.e. probe located at bottom of bed) and running the impeller at operational speed. Again no peaks were recorded since there were no catalyst particles to reflect the emitted

light. Thus, if over-revving were to occur during operation, the recorded spectrum would be blank. It is noted that no such condition was observed when simulating the reaction conditions as will be discussed later.

The experiments done in the cold model allowed visual observation of the phenomena taking place. Observing the bed with the laser signal on and the impeller at rest only a small amount of red light was visible. As the RPM was increased the light became more intense. When the bed was fluidized the light from the laser was clearly visible and appeared to be glowing resembling a flickering flame. This behaviour is the result of catalyst particles or groups of particles that pass through the path of the emitted light and reflect it in different directions.

As the bed agitation was increased by using higher impeller speeds the flickering light became more intense. This relationship was quantified by recording the reflected light spectrum at various impeller RPM's. Figure 4.4 shows two signal spectrums using N_2 at room conditions in the cold model with catalyst present. Spectrum 1 was obtained using an impeller speed of 6300 RPM and spectrum 2 was measured at an RPM of 7875. It can be seen that there is an obvious correlation between impeller speed and signal intensity. In the initial part of each spectrum (less than 10 seconds) the impeller is at 0 RPM showing that no light is reflected. When the impeller is brought to 6300 RPM (spectrum 1) reflected light peaks are observed with intensity levels less than 0.1

Spectrum 1: RPM = 6300, 1 atm N_2, 25°C

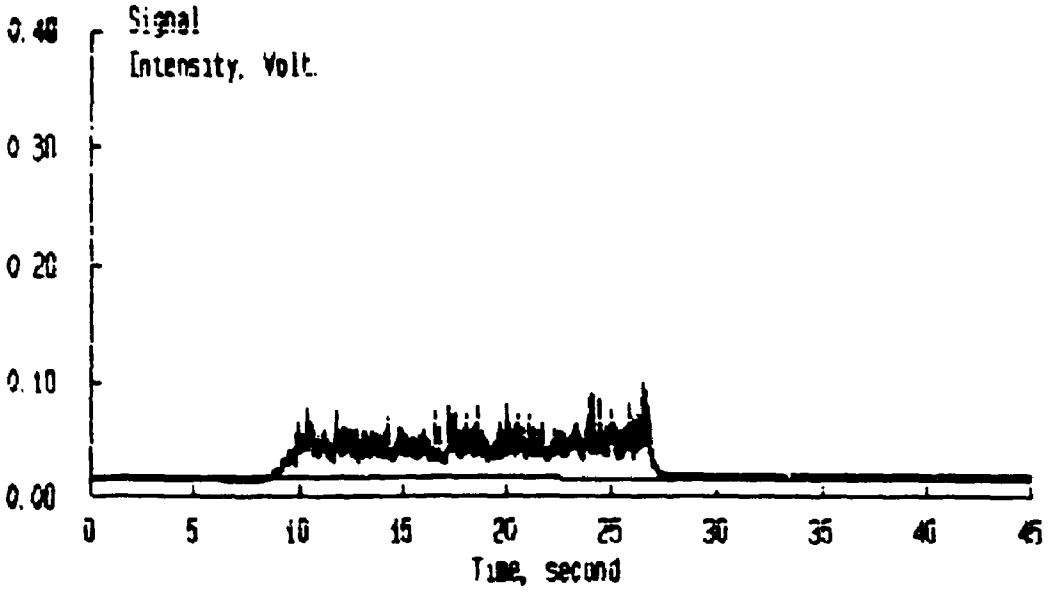

Spectrum 2: RPM = 7875, 1 atm N_2, 25°C

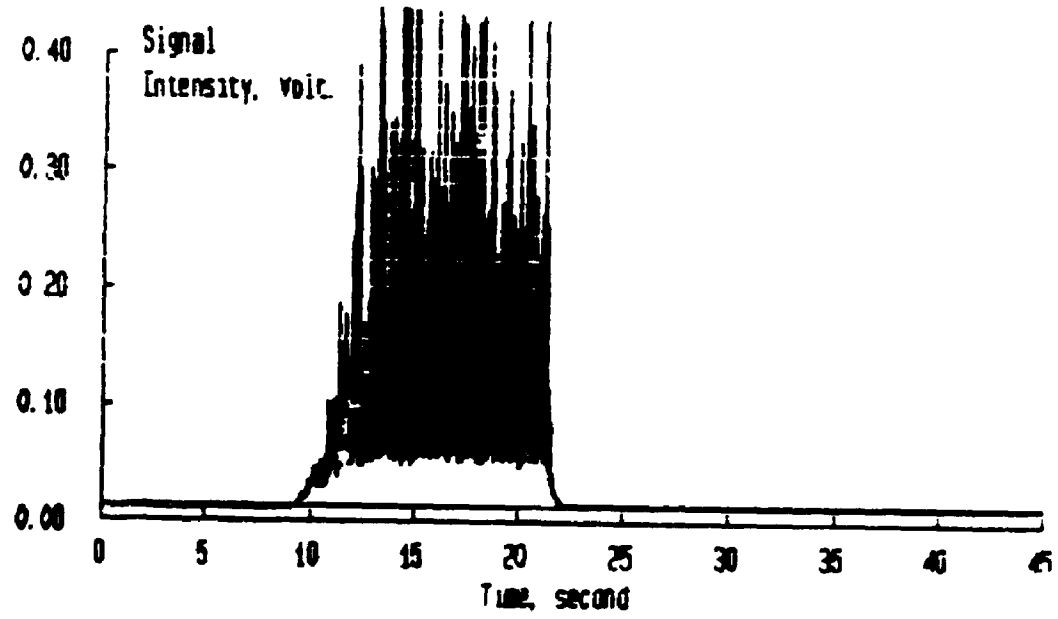

Figure 4.4 Signal spectrums obtained from the optical probe at two different impeller speeds.

volts. At the higher RPM indicated by spectrum 2 the intensity of reflected peaks is much higher with values reaching above 0.4 volts. The interpretation of this behaviour is that as the impeller rotational speed is increased more fluid passes through the bed resulting in additional bed expansion. With this expansion more light is able to pass into the bed from the emitting fibre and subsequently more light may be reflected back to the receiving fibre. Furthermore, with higher re-circulation rates the bed becomes increasingly agitated resulting in an increase in the number of reflections of light (signal frequency). This suggests the possibility of correlating average signal intensity and/or average signal frequency with bed pressure drop through the corresponding RPM value, since both can be measured under the same conditions (nitrogen at room conditions).

Figure 4.5 is a zoom in of a portion of spectrum 2 from Figure 4.4 for the case of nitrogen at room conditions and 7875 RPM. The signal peaks are shown for the time interval of 13 to 14 seconds. This gives a closer look at the actual data being recorded. Each spike represents a pulse of light reflected from the catalyst bed. Individual peaks show varying intensities because of the complexity of the reflections involved. For example a catalyst particle or group of particles crossing the beam of light from the emitting fibre scatters light in several directions, some going directly to the collector fibre and some reflecting off

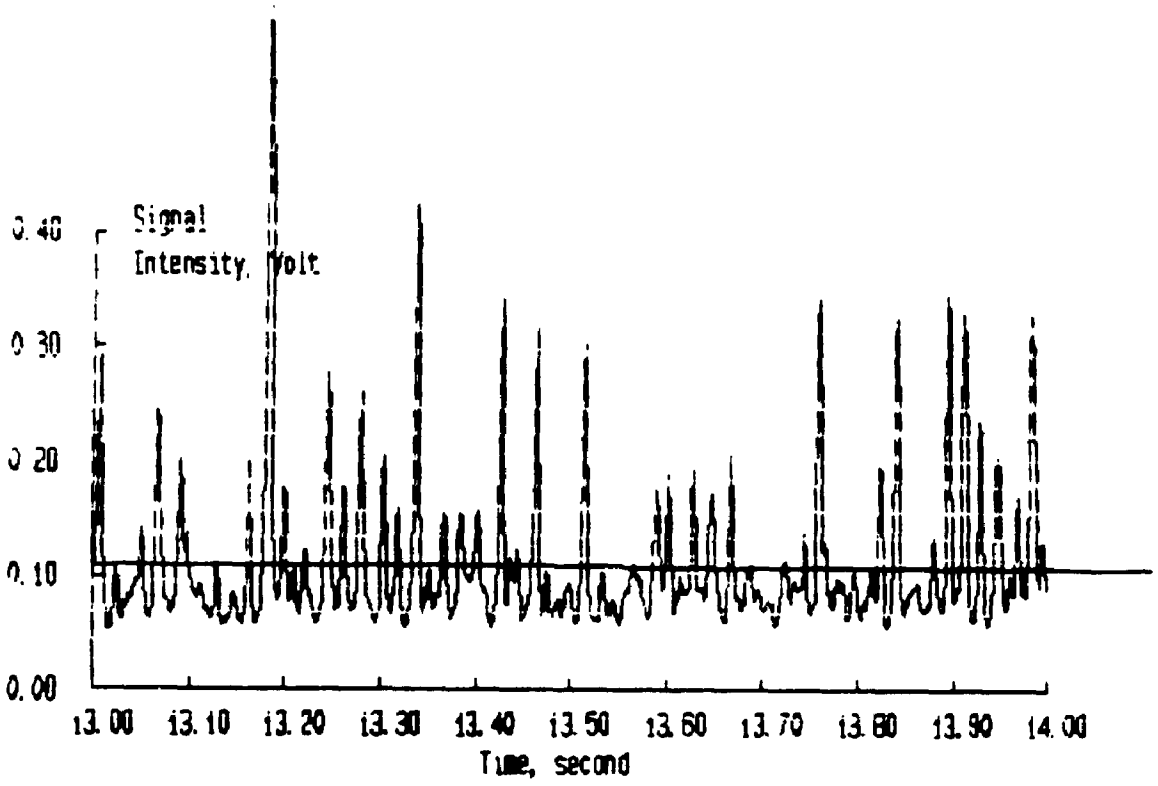

Figure 4.5 A zoom-in of spectrum 2 in Figure 4.4.

other particles before reaching the collector fibre. The intensity of reflected light depends then on the angle of reflection and the number of particles involved in the scattering/reflecting pathway before being detected. As well, with higher agitation more particles pass back and forth between the fibres increasing the number of reflections. Thus, an average signal intensity was calculated for each spectrum by summing the total intensity of peaks and dividing by the number of peaks obtained during the measuring time interval. Also, the average signal frequency (peaks/second) could be calculated by counting the number of peaks in a certain time interval. Program FRQSM.FTN from Chabot (1989) was used for these calculations.

Knowing the average signal frequency versus RPM curve and the pressure drop versus RPM curve for the same fluid could provide information on the bed density and consequently on the state of the bed (fluidized/not fluidized) for a certain reactor environment. Thus runs were performed in both the hot and cold units where fibre optic probe signals were recorded under several different impeller speeds. The results for the average signal frequency and average signal intensity measured at the various RPM's are plotted in Figures 4.6 and 4.7 respectively. These results were obtained using nitrogen gas in both reactors at room conditions. Referring to Figure 4.6 it can be observed that at low RPM's (less than 6000) there is very little motion in the bed with average signal frequencies being close to zero. As the RPM's are increased

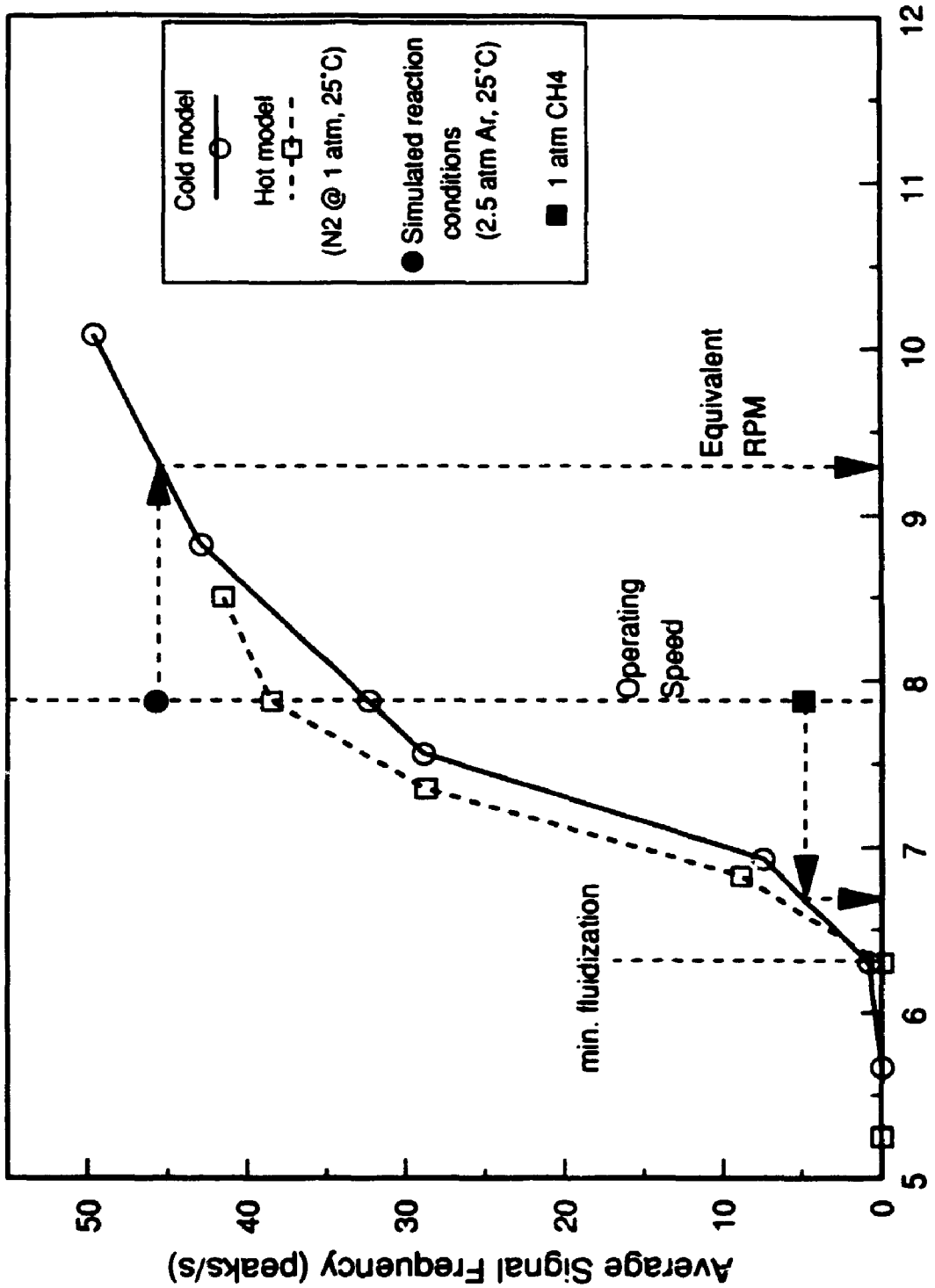

Fig. 4.6 Average Signal Frequency versus Impeller Speed

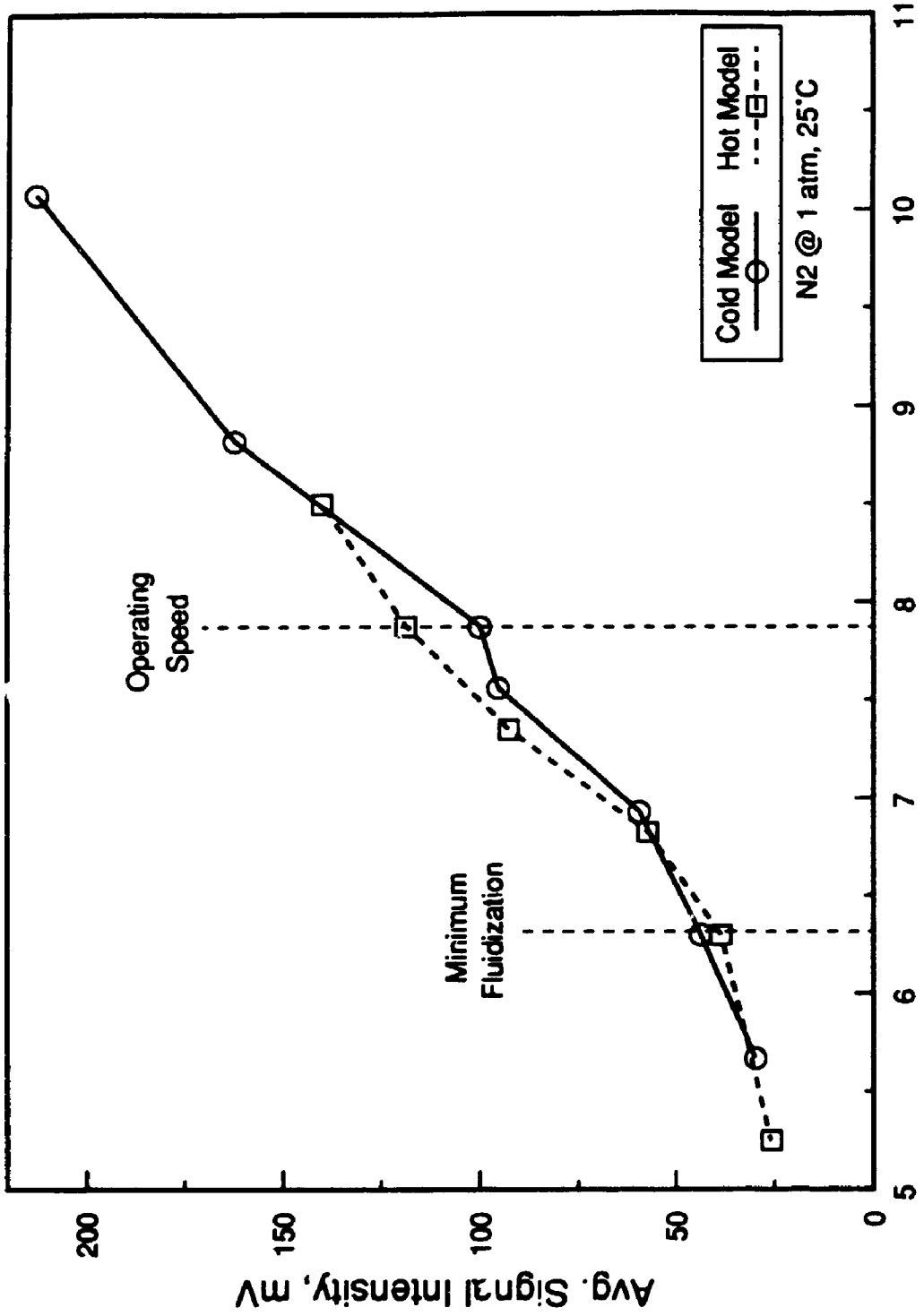

Fig. 4.7 Average Signal Intensity versus Impeller Speed

to about 6300, minimum fluidization occurs and the average frequency significantly increases. The value of the impeller speed for minimum fluidization was determined by visual observation and by the pressure drop versus RPM curve (Figure 4.1) and are quite close in agreement. Beyond minimum fluidization the number of signal reflections increases rapidly with further increases in RPM and then starts to level off. Presumably if the curve were extended to higher RPM's a drop in the average signal intensity would eventually occur as the regime of fluidization changed from aggregative to pneumatic transport. In this extreme case one would expect solids to be stuck at the top grid and no light would be reflected back to the probe as mentioned previously.

The signal frequency versus RPM curve obtained from the hot model runs (dotted line in Figure 4.6) follows the same path as that for the cold model with nearly similar shape. This is not too surprising since both reactors are of identical internal dimensions. It is noted that the curve for the hot model shows slightly higher frequency values than that for the cold model. This is likely due to the fact that the hot model is a sealed unit thus the velocity head generated by the impeller is somewhat more effective than in the cold model where there may be some pressure loss through the shaft area.

The plot of average signal intensity versus RPM as shown in Figure 4.7 follows a similar trend as the frequency curve which was expected since both increase with increasing bed

agitation. At low RPM, below minimum fluidization the signal intensity is relatively low and increases slowly with RPM. After minimum fluidization is reached the average signal intensity increases more rapidly with increasing RPM and then starts to level off. The operating RPM is well into the intensively fluidized regime of the bed for the conditions used.

In general the information obtained in Figures 4.1, 4.6 and 4.7 provides a guideline for the operational speeds of the impeller indicating when the bed is in a fluidized condition. Below 6300 RPM the bed will not be fluidized and somewhere above 10,000 RPM pneumatic transport will occur. It has to be mentioned that a run was done in the cold model using an air driven impeller which had a maximum speed of 20,000 RPM. Using ambient air it was observed that at speeds in excess of 12,000 RPM bed agitation was violent with solids hitting the top grid and falling back down. Eventually at higher speeds catalyst became stuck at the upper grid. The exact value of impeller speed at this condition was difficult to assess because of the instability of the motor at this speed. Thus it was concluded that the impeller speed should not exceed 12,000 RPM to achieve satisfactory operation.

The operating impeller speed used in the actual experiments was chosen based on a combination of the fluidization regimes attainable according to Figures 4.1, 4.6 and 4.7 and on the physical constraints of the mechanical system. Above 8000 RPM the shaft-sealing system in the hot

model became unstable causing mechanical failure of the seal which also aided in shaft alignment. In some instances grinding of the impeller blades against the inner reactor walls and top catalyst basket surface occurred. This was certainly an unpleasant noise and more importantly caused the shaft to go out of alignment. Therefore 8000 RPM was taken as the maximum value for the impeller speed and falls in the well fluidized regime. The actual value used was 7875 RPM which corresponds to 75% of the motor speed on the speed controller (maximum motor speed is 1750 RPM with a 6:1 pulley gear ratio). Markings on the controller were made for every 5% thus the value of 75% was the closest to 8000 RPM without exceeding it. Another important factor namely the re-circulation rate at this impeller speed will be discussed in a subsequent section.

4.2.4 Gas Density and Viscosity Effects

The above mentioned guidelines for the impeller speed only apply for the case of nitrogen at 1 atm and 25°C. The effect of changes in the reactor fluid was studied by using different gases and different pressures in the hot model as listed in Table 4.1. The relevant properties that change with using a different fluid in the reactor are viscosity and density. A change in pressure only affects the density of the mixture (small effect on viscosity). As well, these changes affect the pumping rate of the impeller which is the main concern in

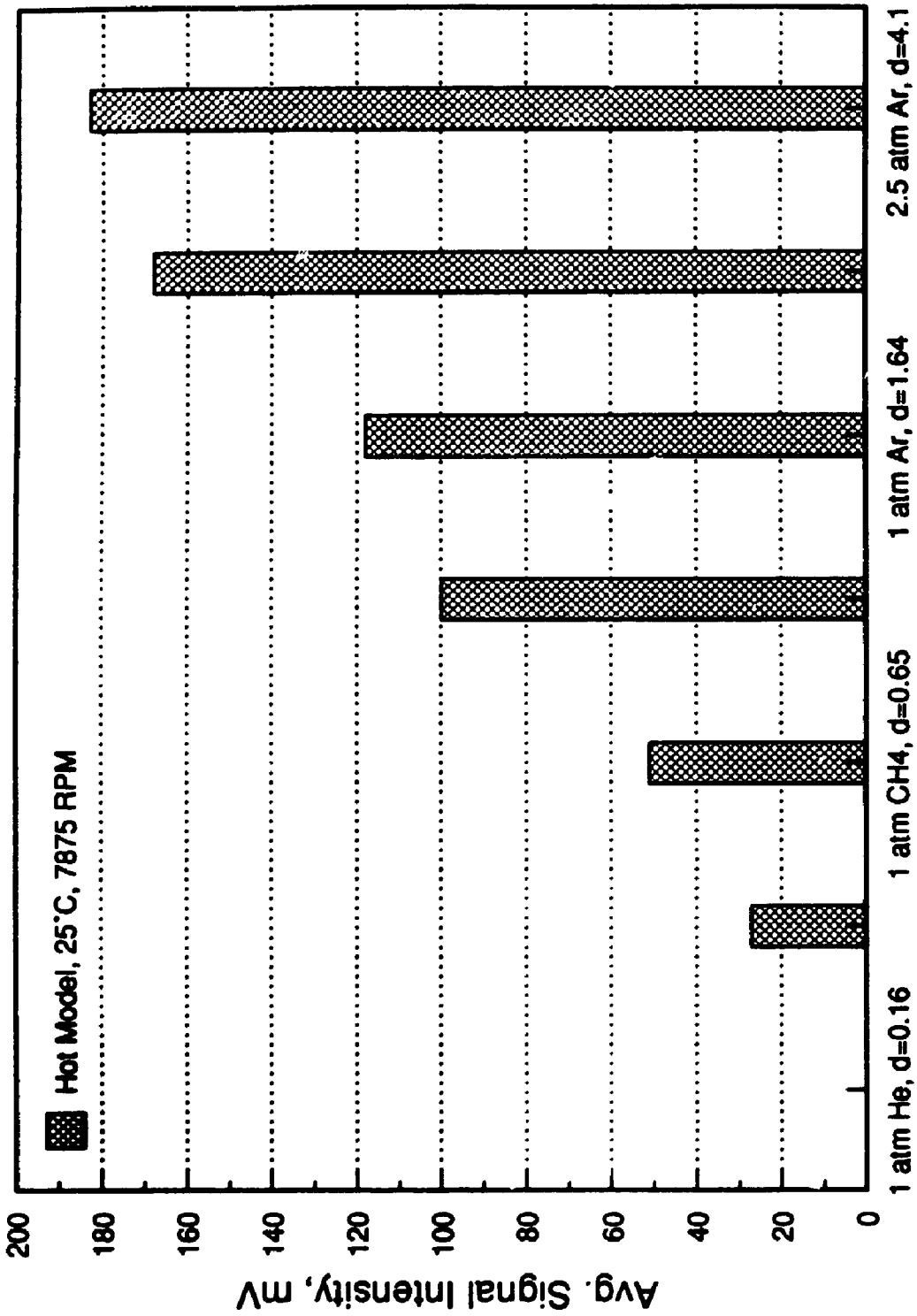

Fig. 4.8 Effect of gas density on average signal intensity

an internal recycle reactor. From correlations on impeller discharge rates in liquids it is known that the volumetric flow rate generated is proportional to the square root of the liquid density and inversely proportional to the square root of the liquid viscosity (McCabe and Smith, 1976). However, for a gas the main effect is that of changing density. This was observed in the present work as well as in another study using a micro-Berty reactor (Hannoun and Regalbuto, 1988). With greater densities in the reactor the re-circulation rate is improved. The gas viscosity may play a small role in the fluidizibility of the particles (i.e. u_{mf} increases as viscosity decreases) but the pumping rate of the impeller is the driving force for the fluidization of the catalyst.

The effect of gas density on the impeller pumping capacity can be seen in Figure 4.8 where the average signal intensity is shown for different gas densities in the reactor. The gas density was varied by using different fluids as well as by using different reactor pressures. The bar chart of Figure 4.8 clearly shows that at higher gas densities the signal intensity increases due to the higher gas velocities through the bed, a direct result of higher impeller volumetric discharge.

To be able to predict the bed behaviour under actual reaction conditions the signal frequency or bed pressure drop data was needed. It was not possible to use the pressure drop measuring system under reaction conditions as mentioned previously and attempts to use the fibre optic probe at high

temperature failed due to melting of the cladding layer which resulted in loss of the light signal. Furthermore, experiments done with the fibre optic probe using coked catalyst showed very weak signals due to light absorption by the black particles suggesting difficulties in using this technique under actual gas oil cracking experiments. However, this point remains to be defined and certainly the use of a more adequate probe to withstand high temperature (metal cladding) for future work could provide useful information.

Due to the above mentioned difficulties the next best approach was to simulate the actual reaction conditions in the hot model at room temperature. This could be accomplished by using a gas or gas mixture at room temperature and a defined pressure that resulted in the same density and viscosity a the reaction fluid. Under actual reaction conditions the mixture in the reactor consisted of an inert gas which was initially present and injected oil which was vapourized virtually instantaneously. Argon was chosen as the inert gas because of its high molecular weight (hence higher density) as compared to other inert gases available (helium, nitrogen). The actual density of the reaction mixture could be assessed from the initial amount of argon present and the mass of injected oil. The mass of argon initially present was calculated from the ideal gas law knowing the temperature of the reactor, the volume and the initial pressure (always 1 atm before injection). The total mass of vapour in the reactor was thus known and dividing by the reactor volume (volume

occupied by the gas) gave the gas density. It is noted that the gas density remains constant in the reactor even with the generation of more moles due to cracking because the system is closed thus mass and volume are constant. A slight drop in gas density actually occurs because of coke deposition on the catalyst but this is small.

To reproduce the reaction mixture density at room temperature an appropriate gas was chosen and the pressure needed to give the correct density was calculated using the ideal gas law:

$$P = f\ R\ T\ /\ M \qquad (4.1)$$

where f is the density of the reaction fluid, M is the molecular weight of the chosen gas and T is room temperature. Argon was chosen as the simulation gas because it also had a viscosity at 25°C similar to that of the reaction mixture at 500°C. Details of the calculation of the reaction mixture viscosity and density are shown in appendix D. It is also mentioned that during cracking the viscosity of the mixture changes only slightly. The reaction temperature of 500°C was the lowest temperature to be used in the experimental runs which gives the largest density thus it was chosen for the simulation.

The calculations indicated that argon in the reactor at 25°C and a pressure of 2.5 atm would have the same density (4.1×10^{-3} g/cm^3) and similar viscosity (0.022 cp for Ar versus

0.021 cp for reaction condition) as the reaction vapours. Measurements using the fibre optic probe in the hot model under these simulated conditions were taken and the average signal frequency obtained is indicated in Figure 4.6 by the darkened circle. This value of 47.7 peaks/second can be used to find an equivalent RPM on the frequency versus RPM curve for nitrogen (1 atm, 25°C). A horizontal line is extended to the curve as shown in the figure giving an equivalent RPM of 9250. This value is in the well fluidized regime as seen in Figure 4.1 and indicates that under reaction conditions the bed is in fact intensely fluidized and the condition of over-revving does not occur.

4.2.5 Reaction Procedure Effect on Bed Dynamics

Concerns about what type of dynamics were taking place in the bed during actual reaction procedure were addressed by using simulated conditions. The reaction operating sequence involved three steps: initial condition with argon at 1 atm (impeller at operating speed), injection and vapourization of gas oil with subsequent reaction, and vacuum purging of the products (impeller stopped). The first condition was analyzed using the fibre optic probe with methane in the reactor at 1 atm and room temperature (impeller at operational speed). This gives a density equivalent to that of argon at 500°C and 1 atm (6.3×10^{-4} g/cm^3). The details of this calculation are shown in Appendix D. The average signal frequency obtained

is plotted in Figure 4.6 indicated by the darkened square. Using the equivalent RPM method it can be seen that this condition results in a fluidized bed just above minimum fluidization.

The effect of injection and purging on the bed dynamics can be seen in Figure 4.9 which is the spectrum obtained for an injection of 50 mL of air into an initial mixture of N_2 and air at 1 atm and 25°C. The procedure for this experiment involved initially filling the reactor under vacuum with nitrogen and then adding air to bring the reactor to 1 atm pressure. The impeller was brought to operational speed (7875 RPM) and then the laser signal was turned on (data acquisition simultaneously started). Approximately 15 seconds later 50 mL of air was injected. Then, roughly 10 seconds after this the 4 port valve was opened to purge the gases (impeller motor shut-off in situ).

It is interesting to see from Figure 4.9 that the signal intensity jumps almost instantaneously to a higher value upon injection of the air due to the increased fluid mixture density. This indicates bed expansion with increased agitation of the catalyst and takes place at approximately the 15 second mark which was the time of injection from the start of the signal (time scale in Figure 4.9 is real time divided by 2). Also, when purging takes place, 10 seconds later, the signal intensity drops sharply to the baseline value indicating bed collapse due to the loss in pressure. This result shows that purging of the reactor effectively

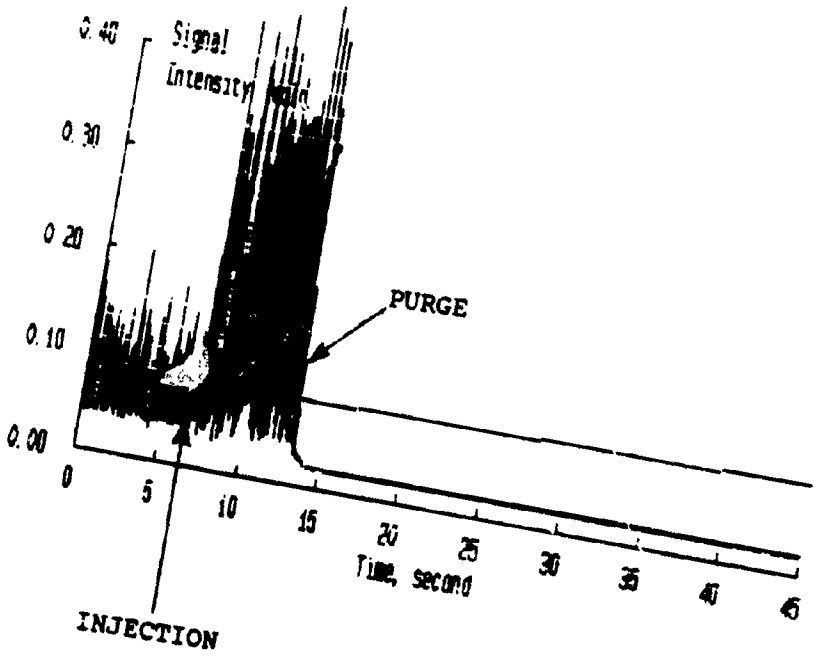

Figure 4.9 Spectrum showing effect of reaction procedure on the bed dynamics.

stops flow going through the bed and only the fluid occupying the catalyst volume can undergo further reaction (about 2% of the total volume).

In summary, the above analysis shows that under initial conditions before oil injection the bed is in a state of fluidization somewhat above minimum fluidization. Upon injection the resulting gas pressure increase (or gas density increase) causes an increase in the impeller pumping rate vaulting the bed into a state of intense fluidization, with a smaller catalyst bed density (or increased solids hold-up). The overall effect is a high degree of agitation. Since the gas density remains constant and the viscosity of the reaction mixture changes only slightly during cracking then this bed condition is maintained until purging. The rapid decrease in pressure causes quick bed collapse with gas flow being diverted to the outlet line.

One aspect of this sequence of events that could not be simulated using the probe at room conditions was the vapourization effect of the gas oil. However, from operational experience with the unit it was noticed that upon injection of the heated oil, rapid vapourization took place as evidenced by the very quick needle movement in the reactor pressure gauge. Thus, it was assumed that vapourization was instantaneous validating the simulation of the bed dynamics using air injection.

4.3 GAS RE-CIRCULATION RATE IN THE REACTOR

To estimate the volumetric re-circulation rate within the reactor a 'rough' calculation was performed based on observed flow patterns in the bed and certain simplifying assumptions. The action of the impeller causes the fluid to spin and the pressure drop created between the centre of the impeller region and the bottom of the reactor forces flow through the catalyst bed. Thus, the actual direction of gas flow through the bed is not linear but follows a cyclonic path. This behaviour was visually observed in the cold model where some particles placed in the annular region between the wall of the reactor and the catalyst basket were seen to travel in a circular motion. Also, particles being ejected from the top of the catalyst bed exhibited a swirling motion. It must be mentioned that catalyst particles in the bed were not observed to circulate in cyclonic fashion with particles forced against the wall of the basket.

As a result of the above observations it can be seen that the measurement of gas flow going through the inner chamber is not obvious. The method used by Berty (1974) to estimate the superficial velocity through the bed does not apply since it pertains to the case of a down-flow fixed bed internal recycle reactor.

To estimate the gas re-circulation rate in the case of the Riser Simulator, the velocity can be separated into tangential

and vertical component vectors according to curvilinear motion. The overall velocity vector can then be calculated from the magnitude of the component vectors. The tangential gas velocity component is proportional to the impeller speed and the usual approach is to define the fluid velocity as a fraction of the impeller blade tip velocity. This fraction is found by correlations relating impeller geometry, fluid density and fluid viscosity for agitation of liquids (McCabe and Smith, 1976) which are not valid in the present case for vapours.

In order to obtain an estimate of the superficial velocity through the bed it was assumed that the vertical velocity component was equal to the terminal particle velocity. This was based on observations of single particles at the bed surface being transported upwards. It was assumed that 3 complete spirals of gas flow are achieved through the bed chamber which then allows calculation of the angle between the vertical and tangential velocity vectors based on the bed geometry. The overall velocity vector was then assessed based on these assumptions. The detailed calculations are shown in Appendix D. The volumetric flow through the bed was then estimated assuming the area normal to the velocity vector was that of an equivalent 'tunnel' through which the gas passes in a spiral direction. From this calculation, the volumetric flow of gas through the bed was found to be approximately 48 mL/s which indicates that in one second, approximately 5 lower region reactor volumes pass through the catalyst bed.

4.4 TESTING OF THE MASS BALANCE PROCEDURE

To assess the adequacy of the mass balance procedure as described by equation (3.17) in Chapter 3, three different tests were performed. First, at room temperature conditions, injections of known amounts of propane were made into the reactor and the amount of hydrocarbons purged and the amount remaining in the reactor were calculated based on the measured pressures and known volumes. The second test included repeats of test one but at 500°C. The third test involved the injection of a standard calibration mixture (commercially available from Supelco, D-3710) consisting of pure compounds ranging from C_5 to C_{15} hydrocarbons under non-cracking conditions (inert catalyst, 350°C).

Table 4.2 summarizes the results of the above described tests on the mass balance procedure. The propane injections at room temperature showed an average mass balance closure of close to 99%. In this case the temperature is constant and the hydrocarbon injected (single compound) is already in the vapour state and the mass injected is calculated from the known gas volume from the syringe reading. Test number 2 done at a reactor temperature of 500°C shows the effect of including the temperature as a measured variable in the mass balance equation (equation (3.17)). The mass balance closure is still very good being in the range of 97 to 98%. The

Table 4.2 Summary of test results for the mass balance procedure.

Test 1: Propane injections at room temperature

m_{inj} (g)	P_{vi} (in. Hg vac)	P_{vf}	m_{HC} (g)	difference
0.09151	19.0	15.0	0.09131	0.22%
0.09151	17.8	13.8	0.09217	-0.72%
0.09151	17.3	13.5	0.08980	1.87% (avg. 1%)

Test 2: Propane injections at high temperature (T_R = 500°C, T_v = 367°C)

- mass inj. = 0.0372 g
- P_{vi}, P_{vf} = 26.0, 22.0 (in. Hg vac.)
- mass calculated = 0.0366 g
- difference = 2.58%

Test 3: Injection of C_5-C_{15} calibration mixture (T_R = 304°C, T_v = 284°C)

- mass inj. = 0.0807 g
- P_{vi}, P_{vf} = 19.5, 16.5 (in. Hg vac)
- mass calculated = 0.0774 g
- difference = 4.1%
- Molecular weight from known composition = 100.61
- Molecular weight from sampled GC analysis = 101.32

note: m_{HC} was obtained from equation (3.17)

increased error is due to the additive effect of the uncertainty of the additional measured variable.

Test number 3 shows that extra error is incurred by the effect of vapourization for the multi-component liquid mixture. In this test the mass of material injected was calculated from the known liquid injection amount and the given density. The mass balance closure obtained was in the range of 95% showing the adequacy of the mass balance procedure. As well, the measured molecular weight obtained from the analysis of the purged vapours was very close to the value quoted by the supplier verifying the appropriateness of the sampling method.

CHAPTER 5

EXPERIMENTAL PROCEDURE AND METHODS

5.1 RANGE OF EXPERIMENTAL CONDITIONS

In the initial series of experiments performed during the M.E.Sc. work, a paraffinic gas oil was cracked using Octacat catalyst for reaction times of 5 and 10 seconds, catalyst to oil ratios of 3, 5 and 7 and temperature levels of 500 and 550°C. The data from these 12 experimental conditions were used to assess the kinetic constants associated with the 3-lump model. For the present work several more runs were required to assess the kinetic parameters of the 8-lump model which has 16 kinetic constants plus a deactivation parameter. Since each of these constants has an energy of activation associated with it then the total number of unknown parameters is 34. Thus the minimum requirement needed to solve the 8 simultaneous equations is 26 experimental data points.

5.1.1 Hydrocarbon Feedstocks

It was decided then to use in addition to two commercial feedstocks available in the lab, three pure mixtures of light oil compounds. Three synthetic light oils were made by using pure compounds obtained from Aldrich Chemicals. These three pure oil mixtures were made to simulate average compositions of the light paraffins (P_l), light naphthenes (N_l), and light

aromatics (A_t) associated with the 8-lump model. The cracking of these feedstocks provided additional data points for evaluating the 34 kinetic parameters. The compositions and properties of these pure oil mixtures are shown in Table 5.1. The measured weight percents were calculated using the known volume and density of each individual compound. A GC analysis was performed on each oil to verify this composition as is indicated in Table 5.1. Average molecular weights and average densities were calculated based on the known composition of each mixture.

The choice of compounds to make up these light oils was based on typical classifications (ASTM, 1977) and analysis of gas oils (Liguras and Allen, 1989) as well as availability. For the P_t pure mixture five compounds ranging from C_{13} to C_{18} were used. The classification of the light paraffins includes alkanes or alkenes, branched or straight chains, with boiling ranges of 220°C to 345°C. Equal volumes (approximately 3 mL) of each paraffin were blended to make the P_t mixture. It was necessary to heat the octadecane in order to add this volume to the mixture since it was solid at room temperature.

For naphthenic oils the classification of compounds includes cyclic alkanes or alkenes, saturated rings, bridged, spiro and polycyclic hydrocarbons. The rings can include side chains of paraffinic molecules. The availability of pure compounds in this light oil fraction was limited. Four compounds were obtained as listed in Table 5.1 with the cyclododecane and tricyclodecane being solids at room

Table 5.1. Composition and Properties of the three pure oil mixtures.

Compound	MW*	mp(°C)	bp(°C)	f(g/cc)	wt%	wt%(GC)
P_1 Oil Mixture:						
Tridecane	184	-5	234	0.756	19.55	9.92
Pentadecane	212	9.9	270	0.769	19.88	19.97
Hexadecane	226	18	287	0.773	19.98	20.27
Heptamethylnonane	226	<18	240	0.793	20.50	20.93
Octadecane	254	30	317	0.777	20.09	18.90
N_1 Oil Mixture:						
Tricyclodecane	136	78	-	-	9.71	9.42
Dicyclohexyl	166	3.4	227	0.864	38.53	37.87
Cyclododecane	168	60	>231	-	13.07	12.87
Cyclododecatriene	162	-18	231	0.890	38.69	39.84
A_1 Oil Mixture:						
Phenylhexane	162	-61	226	0.861	17.73	17.16
Cyclohexylbenzene	160	5	240	0.950	23.01	22.78
dimethyl naphth.	156	<20	266	1 010	12.23	13.41
Dodecylbenzene	246	-3	320	0.856	22.81	22.72
Fluorene	166	115	298	-	12.11	11.33
Phenanthrene	178	100	340	-	12.11	12.60

Oil Mixture	Avg. MW	Avg. Density(g/cc)
P_1	217.8	0.774
N_1	161.6	0.988
A_1	176.9	0.948

* Physical properties from Aldrich (1990)

cracking, which are the most important ones in an industrial riser, one could use a simple first order decay model to describe the catalyst deactivation adequately. Of course, the value of k_d obtained would be valid only for the short contact time periods covered and for the particular catalyst and gas oil used.

1.5 REACTORS USED FOR FCC STUDIES

Many different types of laboratory catalytic reactors are available for assessing kinetic rate parameters including fixed bed, fluidized bed, stirred batch, continuous stirred tank, re-circulating transport, differential, recycle, straight-through transport and pulse reactors (Doraiswamy and Tajbl, 1974; Weekman, 1974; Sunderland, 1976). In the case of studying catalytic cracking reactions on a bench scale, fixed bed and fluidized bed reactors have been traditional choices (Weekman, 1968; Gross et al., 1974; Campbell and Wojciechowski, 1970; Weekman and Nace, 1970). However, most of the kinetic data from these studies were obtained using reaction times greater than 2 minutes which are not representative of commercial riser contact times.

Tubular fixed bed reactors for studying FCC reactions are also somewhat limited by large temperature gradients due to the highly endothermic nature of cracking and pressure drops across extremely fine fluid catalyst beds. These deficiencies

temperature. The dicyclohexyl and 1,5,9-cyclododecatriene were added in excess amounts to help dissolve the other two solids. In this way 10 mL each of dicyclohexyl and cyclododecatriene were added to approximately 2.5 g each of tricyclodecane and cyclododecane to make up the N_l mixture.

The classification of light aromatic compounds in the 220°C to 345°C range includes completely unsaturated ring compounds or in general any compound containing a benzene ring. This includes rings with long paraffin chains and/or cyclic alkanes attached. For single ring compounds side chains with C_6 up to C_{14} alkanes are possible as well as cyclic side groups. For two ringed compounds side chains with up to 7 carbons atoms are possible. Also present in this boiling range are 3-ringed aromatics with no side groups. Thus a representative sample from each of these possibilities was chosen resulting in six compounds as shown in Table 5.1 for the composition of the A_l oil. The mixture was made by adding 10 mL of each of the liquid compounds (phenylhexane, cyclohexyl-benzene, dimethyl naphthalene isomers and dodecylbenzene) and 10 grams of fluorene and phenanthrene.

The properties of the two commercial feedstocks used are shown in Table 5.2. Feedstock A consists mainly of paraffinic molecules and feedstock B is mainly aromatic. These two gas oils thus gave a different range of oil lump distributions which were used in calculating the kinetic constants for the 8-lump model.

Table 5.2 Properties of the gas oil feedstocks

Property	Feedstock A	Feedstock B
Specific Gravity	0.9117	0.9389
Aniline Point (°C)	79.4	59
Sulfur, wt%	1.19	0.24
Nitrogen, wt%	0.0012	0.102
Volumetric Average Boiling Point (°C)	377.2	393
Molecular weight	344.8	331
Composition (220 to 345°C):		
Light paraffins, wt%	17.35	3.27
Light naphthenes, wt%	6.40	12.43
Light aromatics, wt%	6.25	10.88
(345°C +) Heavy paraffins, wt%	43.03	5.52
Heavy naphthenes, wt%	20.08	25.13
Heavy aromatics, wt%	6.89	42.77

5.1.2 Catalysts Used

In combination with the five oils described above, two commercial FCC catalysts available from Davison and Grace Co. were used for the cracking runs. These two catalysts (Octacat and GX-30) are octane enhancing catalysts and the properties of each are shown in Table 5.3. It is noted that GX-30 has a much higher unit cell size (24.40 Å) than Octacat (24.24 Å) and is designed for increased bottoms cracking.

5.1.3 Range of operating parameters used

The operating conditions used in this work included reaction times of 3, 5, 7 and 10 seconds, and temperatures of 500, 525 and 550°C. The selection of reaction times of 10 seconds or less was made considering the fact that most kinetic data available in the literature were obtained using long catalyst times-on-stream and because the more advanced industrial sized risers operate at contact times below the 10 second range. The choice of temperatures covers the range of normal operation for commercial FCC units. Three temperature levels were studied in order to provide sufficient data points to calculate the activation energies involved in the 8-lump model.

The amount of catalyst used for all runs was kept constant in order to maintain a constant bed height of catalyst without the addition of inerts. This meant that the catalyst to oil

Table 5.3. Catalyst Properties

	Octacat	GX-30
Al_2O_3 (wt%)	26	34
Na (wt%)	.22	0.37
REO (wt%)	>2	4.5
Unit cell size (Å) (steamed)	24.24	24.40
Surface area (m^2/g) (steamed)	145	126

ratio was kept constant for the series of runs done with each oil. The effect of catalyst/oil (c/o) ratio in the Riser Simulator was examined in the earlier work (Kraemer, 1987) and for the purposes of this study a wide enough range of conversions and yields was possible by varying the reaction time and temperature. The weight of catalyst used was 0.8 grams which gave a bed height of approximately 50% of the total height of the internal chamber (1.6 cm). The resulting hold-up of solids is in the range of 0.02 grams of catalyst per reactor gas volume. This is in the lower range of solids density found in commercial risers (Gates et al., 1979; Saxton and Worley, 1970).

The amount of oil used for the liquid injections to the reactor was chosen based on partial pressures of hydrocarbons used in FCC units as well as establishing a reasonable c/o ratio. It is important to use a similar partial pressure of hydrocarbons as found in commercial units to ensure the attainment of relevant kinetic data. According to Wollaston et al. (1975) the range of hydrocarbon partial pressures used in riser pilot plants is 0.8 to 2.0 atm. These values depend on several factors including the type of feedstock being processed and the severity of the unit (temperature, c/o, contact time, amount of inert steam) (Mcketta, 1981). Since the amount of catalyst was fixed a value of 0.2 mL of oil injection volume was chosen because it resulted in reasonable oil partial pressures in the Riser Simulator ranging from 0.75 to 1.47 atm depending on the feedstock used. It has to be

mentioned that these values refer to the initial partial pressure of oil upon injection into the unit. The total initial pressure is then the initial oil pressure plus the initial pressure of the inert Argon always present in the reactor at 1 atm before injection. Since the reactor is a closed system (fixed volume) the pressure will increase as the cracking reaction proceeds with the generation of more moles of cracked products.

Table 5.4 shows the range of experimental conditions used for the cracking runs of both the commercial gas oil feedstocks and the pure light oil mixtures. A further breakdown of the experimental sequence is given in Appendix E in the master table for run number identifications. The resulting matrix of runs totals 96 experimental conditions (48 for each catalyst). Considering that for most experimental points 3 repeat runs were made then the total number of data points becomes more than 250. The repeat runs allowed assessment of pure error and improved the confidence intervals for the parameter estimates.

5.2 CATALYST PREPARATION

The fresh catalyst obtained from Davison and Grace was steamed at 766°C for 18 hours in the presence of 100% steam. As discussed in Chapter 1 steaming of the catalyst is necessary to simulate an aged condition of the catalyst with an activity level similar to that of a catalyst after many

Table 5.4. Range of experimental conditions used for the cracking runs

For both Octacat and GX-30:

Feedstock	t_R(s)	T(°C)	c/o	P_{oil}(atm)
A	3, 5, 7, 10	500, 525, 550	4.4	0.75 - 0.80
B	3, 5, 7, 10	500, 525, 550	4.3	0.85 - 0.91
P_l	3, 5, 7, 10	500, 550	5.2	0.95 - 1.01
N_l	3, 5, 7, 10	500, 550	4.5	1.47 - 1.57
A_l	3, 5, 7, 10	500, 550	4.2	1.38 - 1.47

notes:

mass of catalyst = 0.8 g
volume of oil injection = 0.2 mL
$P_{oil} = m_{oil} R T / M_{oil} V$, where V = 45 mL

No. of runs = 2 oils x 2 catalysts x 4 t_R x 3 T
+ 3 oils x 2 catalysts x 4 t_R x 2 T = 96

cycles of cracking/regeneration. The above conditions were found to be satisfactory to achieve this objective (Kraemer, 1987 and Larocca, 1988). A fluidized bed reactor (2.5 cm dia. steel tube, 20 cm height) was used for this procedure. Full details of the catalyst steaming system are given by Larocca (1988). The reactor had a bottom porous disc to support the catalyst and distribute the steam which entered the bottom of the unit. A Gilson pump, Model 302, was used to send water to a vaporizer which provided the steam to the reactor. The pump was capable of delivering liquids at low volumetric flows in the range of 0.01 to 10 mL /min.

Typically 5 to 6 grams of catalyst were steamed at one time. From the canister containing fresh catalyst approximately 5 g of catalyst were weighed. The canister was shaken well before extracting the catalyst to obtain a representative sample. The catalyst sample was then transferred into the reactor which was then capped using a metal lid with a porous grid on top. The reactor was then set in the furnace and a 25 cm long Chromel-Alumel thermocouple was inserted vertically from the top reaching the catalyst bed. A 1/8" stainless steel line attached to the conical reactor bottom was connected to a vaporizer which is a 1.5 m long soft copper coil with a nominal 1.6 mm diameter wrapped with heating tape. Next, the reactor and evaporator heaters were turned on. The vaporizer was set to 200°C and the reactor to 766°C. When the reactor temperature was above 400°C the water pump was started with a liquid flowrate set

at 0.1 mL/min using de-ionized water. This gave a velocity of steam in the reactor of approximately 1.6 cm/s which was above the minimum fluidization velocity for FCC catalysts (0.2 cm/s). When the reactor temperature reached 766°C the start time was recorded.

After 18 hours the water pump was shut-off then, 15 minutes later the reactor heating was shut down. When the reactor temperature was close to 200°C the evaporator heat was shut-off. This procedure was done to ensure any excess water vapour would pass through the reactor in the vapour state. When the reactor was cool the catalyst was recovered by disconnecting the reactor, removing the top cover and pouring the catalyst out.

For each catalyst (Octacat and GX-30) a 50 g batch of steamed catalyst was made. Both separate batches were obtained from approximately 10 steaming runs for each catalyst. This was to be the source of catalyst samples used in the experimental runs. The two final batches were then dried in an oven at 200°C to remove any adsorbed water vapour and then placed in a decanter where they remained for the series of runs performed. The final batch of each was shaken and stirred each time before catalyst was withdrawn to be used in a particular run.

The surface area of the steamed catalyst was evaluated using a Perkin-Elmer Shell Model 212C Sorptometer. The instrument is equipped with a sample tube, a TCD detector, gas flow lines, and various gas flow controllers. A

potentiometric recorder is connected to the detector. In this procedure a stream of gas is passed over a cooled solid sample and the surface area of the sample is determined by measuring the amount of adsorbed gas. The mobile gas phase is a known mixture of a suitable adsorbate and an inert gas carrier. Nitrogen was used as the adsorbate and helium as the inert carrier gas. Detailed calculations can be found in the thesis of Larocca (1989).

5.3 CRACKING RUN PROCEDURE

To perform an experimental cracking run in the reactor unit a consistent procedural method was used. First, 0.8 g of catalyst was weighed from the steamed catalyst sample and placed on wax paper. This was then loaded into the catalyst basket of the reactor using the wax paper as the transfer medium. The top grid was then placed in its position and secured in place using the snap ring. As well, the reactor gasket was inserted in its grooved seat. The bottom reactor half, which houses the catalyst basket, was then bolted to the upper reactor block. To do this the bolt holes in the bottom piece were aligned with bolts protruding from the upper block and then the bottom block was lifted into place. The 8 nuts and washers required were then put in place (finger tight) to support the bottom block. The nuts were then tightened using a torque wrench and in the conventional alternating diagonal fashion used for any compression type flange.

The spiral wound inconel-graphite gaskets used to seal the two reactor halves do not have the same feel as other metallic gaskets during the bolting-up procedure. It was thus necessary to tighten the bolts in small steps and in proper sequence. The impact wrench was set at about 1/2 final torque for first go around and care was taken to make sure the two blocks were parallel to avoid uneven contact and eventual leaking. The final tightening was uniform for each bolt such that each pulled the same load. For 1/8" thick gaskets the compression to a thickness of 0.100 ±0.005 inches was recommended (0.130 ±0.005 in. for 3/16" gaskets). This was checked using metal measuring shims inserted between the reactor blocks to determine when the desired compression thickness was reached. The reactor was then pressurized to 60 psig and checked for leaks. A soap solution was applied to various areas to identify any leaks. In general if the reactor pressure remained constant for 1 minute then the unit was considered adequately sealed. The gaskets lasted for approximately 3 or 4 runs (tightening-untightening) at high temperature after which they were replaced since they became permanently compressed and were no longer able to seal the reactor. The reactor was also checked at high temperature for leaking by monitoring the pressure gauge with the reactor at 60 psig. In the event that there was substantial leaking, the bolts were hot-tightened. This usually was not necessary except for cases where the gaskets were used beyond their lifetime.

With the reactor sealed, the insulating jacket was then put in place and the reactor was ready for heating. The circuit breakers for the heaters were turned on and the reactor temperature was set to the desired value using a temperature controller (Omega KC-4002). As well, the cooling water for the shaft packing/sealing gland was turned on. Flow of cooling water was adjusted to maintain a temperature of 50 to 75°C in this region. A flow of argon was allowed to pass through the reactor during the heating period. This was accomplished by opening V1 as seen in Figure 3.8 with V3 switched to Ar and with the 4PV in the reactor open mode. Typically valve V1 was adjusted to maintain a pressure in the reactor of approximately 5 psig. This flow was allowed to pass through the reactor and the purge lines before being vented. The rest of the experimental system was also heated at this time with all lines and the vacuum box set to 350°C and the valve block set to 300°C. As well the GC was turned on and the desired conditions set. The mass flow controller was set to 120 mL/min of helium. The temperature program was set for -30°C for 3 minutes then increasing at 15°C/min to 320°C for 10 minutes for the majority of runs.

After desired temperatures were reached for the entire system (approximately 2 hours) the oil to be injected was loaded into the liquid syringe. For the gas oil samples the heated injection system was used where the metal syringe was placed in the heated block set at 150°C. For the pure oil mixtures a glass syringe was used. Care was taken to avoid

air bubbles being trapped in the syringe. This was accomplished by removing the needle and then filling the syringe past the 0.2 mL mark. The needle was then re-attached (a simple hub system) and the excess oil was discarded by moving the plunger to the desired mark. When the liquid oil sample is injected into the reactor the resulting spray of oil hits the outer wall of the catalyst basket and vapourizes almost instantaneously. The heat required for vapourization has a negligible effect on the reactor temperature.

The following steps outline the procedure used to perform the injection - reaction - purging - sampling - regeneration sequence:

1. Replace nut on injection port with the septum seal. Set the reactor pressure to 1 atm by closing V1 and allowing reactor pressure gauge to fall to zero, then switch the 4PV to the reactor closed position.

2. Ensuring that the 6PV is in the load position open V2, switch V5 to the vacuum position and turn on the vacuum pump.

3. Allow the vacuum chamber to reach the maximum vacuum pressure (usually 26" Hg vac.) and then close V2 and switch V5 back to vent.

4. Record the vacuum pressure and all temperatures.

5. Set the GC to -30°C.

6. Turn on impeller motor and slowly bring to speed (75% = 7875 RPM).

7. Insert the needle of the syringe through the septum of the injection port. Simultaneously depress plunger (sharp, rapid motion) and observe time zero.

8. Continuously watching the time (seconds) turn the 4PV to the reactor open position when the desired reaction time is reached (simultaneous action).

9. Pull syringe out from injection port rapidly and turn off the impeller motor.

10. When the vacuum pressure gauge has reached equilibrium (i.e. needle stops moving) switch the 4PV back to the reactor closed position. Equilibrium is reached very quickly.

11. Record the final vacuum pressure.

12. Press start on the GC (with pre-programmed temperature ramps) and then turn the 6PV to the sample position. This allows the helium carrier gas of line 7 to pass through sample loop 5 and take the vapour products to the GC.

13. Remove septum fitting on injection port and replace with nut. Switch the 4PV to reactor open position and open V1 allowing argon to fill vacuum chamber until pressure reaches 1 atm. Then open V5 to allow purging of the system. In this mode the flow of Ar is such that the reactor pressure gauge reads 10 psig.

14. Set reactor temperature to 650°C. When this temperature is reached switch V3 to the air position and increase flow by adjusting V1 to give a reactor pressure of 15 - 20 psig.

15. Allow the regeneration period to last for 10 minutes then switch V3 back to argon flow and adjust reactor pressure to 5 psig. Set reactor temperature to desired cracking level.

16. After reaching the desired reactor temperature a repeat run can be made (go to step 1).

The usual procedure for one experimental condition was to perform 3 repeat injections with regeneration in between and then a final injection was made where the products were vented rapidly. This was designated as the coke run since after this run the reactor was cooled and the catalyst recovered to measure the amount of coke formed.

In the coke run the steps involved are the same up to step 9. After this step for a coke run, V1 and V5 are opened allowing a high flow of argon (reactor pressure of 30 psig)

to rapidly vent hydrocarbon vapours from the reactor. The reactor temperature controller is then shut-off. After approximately 4 hours, the reactor is cool enough to be disassembled. During a typical catalyst recovery procedure the insulation from the reactor is removed, the bottom block lowered by removing the nuts from the 8 bolts in sequential order and the top grid of the catalyst basket removed. A crucible is then placed upside down on top of the basket and the reactor block is then turned over to allow the coked catalyst to pass into the crucible. The catalyst basket, grids and internal reactor chamber were then cleaned by using compressed air to remove any left over coked catalyst. The reactor is then ready for a new batch of catalyst.

The amount of time required for 1 run was approximately 1 hour. This included the GC analysis which was the time limiting factor (45 to 60 minutes per analysis), and the regeneration between repeat injections (main consumption of time due to cooling reactor from regeneration temperature to cracking temperature). Usually the regeneration could be accomplished as the GC analysis was taking place. For one complete experimental point consisting of three repeat GC analysis and a final injection for the coke run the time required was close to 3.5 hours. The cooling of the reactor to recover the coked catalyst, re-loading with new catalyst and heating back to reaction temperature took from 3 to 4 hours. Thus it was possible to complete 2 experimental points in a period of 12 hours with the cooling of the reactor from

the coke run of the second set of runs being done overnight.

5.4 DATA ANALYSIS

For each injection performed a data sheet was used to record all temperatures, pressures, total area calibrations and GC conditions used for the run. An example of a raw data sheet is shown in Appendix E. The peaks generated from the GC chromatogram were stored on the GC integrator and were then transferred to an HP 1000 computer. The transferred signals were converted to reproduce the chromatographic report giving the retention times, area counts and area percents for each peak generated by the FID. For hydrocarbons the relative sensitivity values for the flame ionization detector are all approximately 1.0 (Dietz, 1967). This means that the area percents obtained are equivalent to weight percents and thus the distribution of products from the reactor is given by these values. The raw GC values were processed and were adjusted to account for the amount of coke produced and corrected to satisfy mass balance considerations.

5.4.1 Calculation of Conversions and Yields

To assess the conversion of gas oil, yield of gasoline and light gases it was necessary to know the retention times (or order of appearance) of the first and last gasoline peaks. The gasoline fraction was defined using the normal convention

as consisting of hydrocarbon molecules ranging from C_5 up to and including n-C_{12}. The first C_5 molecule to appear was 3-methyl-1-butene and was used to define the start of the gasoline lump. This was confirmed by running a mass spectrum analysis on the cracked products where this peak was easily identified. Also, it is well known that c-2-butene is the last molecule to appear from a capillary column analysis of C_4 gases. The appearance of c-2-butene followed by 3-methyl-1-butene was consistent for all runs done. In fact the first 11 peaks were identified as light gases (C_4 and less) which are shown in the product distribution tables of Appendix E. This order of appearance was consistent for all runs and is typical for cracked gases (HP Analytical Supplies Catalog, 1990). Depending on the temperature program used to perform the GC analysis the retention times of these light gas peaks changed but the relative order of appearance remained constant.

To identify the last gasoline peak injections of n-C_{12} were made for each temperature program used. This gave the retention time as well as the relative order for the appearance of n-C_{12}.

For each chromatogram the retention times for 3-methyl-1-butene and n-C_{12} were identified and entered into a computer program which summed the area percents for the light gas fraction and gasoline fraction. This program called SUM.FTN is found in Appendix G. The unconverted oil fraction was calculated by difference (equal to 100 minus the sum of light

gases and gasoline weight percents. In this way the raw yield (no coke included) of light gases, gasoline and unconverted oil was calculated. It is noted that for feedstock A a small fraction of the gas oil was found to be less than C_{12} in carbon number. These compounds were included as gasoline yield. The conversion of gas oil was then calculated as the sum of the light gases and gasoline yield and the selectivity to gasoline was assessed by dividing the gasoline yield by the conversion.

These values of conversion and yield do not include the amount of coke produced. Therefore it was necessary to correct these values to account for the weight percent of coke produced. The yield of light gases and gasoline were normalized by multiplying by the factor $(1 - y_c)$ where y_c is the weight fraction of coke. The sum of these new yields plus the coke yield gave the adjusted conversion and the adjusted yield of oil was then 100 minus this corrected conversion.

5.4.2 Mass Balance Corrections

The final values for conversion and yields were then corrected to satisfy the mass balance constraints. As described in Chapter 3, the mass of hydrocarbons purged and the mass of hydrocarbons remaining in the reactor was measured for each run. A computer program (MASSBAL.FTN) was written to perform these calculations and is shown in Appendix G. For all experimental conditions used the mass balance results are shown in Tables E.6 to E.10 of Appendix E. These values are

averaged values for the repeat injections performed for each experimental condition.

As a general observation, the mass of hydrocarbons calculated from the mass balance procedure was close to 95% of the injected mass. As well, the calculated total mass of hydrocarbons was always less than the injected amount and this missing mass was considered to be the oil fraction. This is a result of heavy hydrocarbons not being detected by the GC either through splitter discrimination or condensation. In general the elution of peaks for the oil fraction resulted in a baseline shift where some peaks became distorted and in some cases tailed badly. This caused error in the assessment of the relative area of these peaks. The light gas and gasoline peaks were considered to be valid since they were sharp, distinct peaks. As a result of this the mass balance correction was performed by adjusting these values by multiplying by the factor w_{cal}/w_{inj} where w_{cal} is the calculated weight of total hydrocarbons and w_{inj} is the initial injected weight of oil. The corrected conversion is then the sum of the corrected light gas and gasoline yield and the oil yield is 100 minus the corrected conversion.

5.4.3 Analysis of the Oil Lumps

To assess the kinetic parameters for the 8-lump model it was necessary to know the yield of the six oil lump groups (P_h, N_h, A_h, P_l, N_l and A_l) from the cracked products. To do this it was necessary to use GC-MS methods. Both feedstocks were first analyzed by direct injection to the GC connected to the mass spectral unit. Each peak separated by the capillary column was sent to the mass spec where the compounds mass spectrum was obtained. A search to compare spectrums using a mass spectral library from HP allowed classification of the compound as a paraffin, naphthene or aromatic. As well, GC-MS analysis of the cracked products from runs using both feedstocks with both catalysts established the identity these classes of oil components.

A reference chromatogram for each feedstock was obtained knowing the retention times and order of appearance of the three classes of hydrocarbons. As well, the cut point between the heavy and light oil fractions was identified on each reference chromatogram. This cut point was taken as n-C_{20} which was included in the light oil fraction. This corresponds to the 220°C to 345°C boiling range for the light oil fraction as defined by the 8-lump model. Any peaks after n-C_{12} were considered heavy oil compounds. The chromatograms from each run were then compared to the appropriate reference file and oil peaks were grouped as paraffins, naphthenes or aromatics. A computer program (see Appendix G) was used to

sum the area percents of these identified three groups for both the light and heavy oil fractions. The final six oil lump yields were adjusted to account for coke and mass balances by normalizing with the correct oil yield discussed above.

5.4.4 Calculation of the GC-Research Octane Number

To asses the research octane number (RON) of the gasoline fraction the method used by Anderson et al. (1972) was employed. This method, based on GC analysis, can be used here for comparative purposes. Other correlations based on the Anderson method claim improved agreement with engine octane number results (Yatsu and Keyworth, 1990). However, for true RON and MON (motor octane number) measurements an engine test must be performed. This was not possible in the present work due to the small size of product samples involved and therefore a GC method was chosen. The research octane number calculated here is then distinguished from actual RON by using the term GC-RON and shows the effects of operating variables, feedstock and catalyst on the octane value of the gasoline produced.

Anderson et al. (1972) used a multiple regression to estimate the effective octane numbers for groups of hydrocarbons. The 29 groups of hydrocarbons in the gasoline range along with the effective octane number are shown in Table 5.5. It is noted that 19 of the groups are individual compounds. To assess the octane number the summation of the

Table 5.5 List of hydrocarbon groups and effective octane values for assessment of the GC-RON (Anderson et al., 1972).

No.	Components	b_r
1.	Components eluting between n-butane and i-pentane	144.3
2.	Iso-pentane	84.0
3.	Components eluting between i-pentane and n-pentane	198.2
4.	n-pentane	67.9
5.	Components eluting between n-pentane 2-methylpentane	95.2
6.	2- and 3- methyl pentane and components inbetween	86.6
7.	Components between 3-methyl pentane and n-hexane	95.9
8.	n-hexane	20.9
9.	Components between n-hexane and benzene	94.9
10.	Benzene	105.2
11.	Components between benzene and 2-methylhexane	113.6
12.	2- and 3-methylhexane and components in between	80.0
13.	Components between 3-methylhexane and n-heptane	97.8
14.	n-Heptane	-47.8
15.	Components between n-heptane and toluene	62.3
16.	Toluene	113.9
17.	Componetns between toluene and 2-methylheptane	115.1
18.	2- and 3-methylheptane and components in between	81.7
19.	Components between 3-methylheptane and n-octane	109.7
20.	n-Octane	10.5
21.	Components between n-octane and ethylbenzene	96.1
22.	Ethylbenzene	122.6
23.	Components between ethylbenzene and p-xylene	45.4
24.	p-Xylene and m-xylene	102.0
25.	Componetns between m-xylene and o-xylene	73.3
26.	o-Xylene	123.6
27.	Components between o-xylene and up to and including n-nonane	35.0
28.	Components between n-nonane and n-decane	112.0
29.	n-Decane and components after n-decane	85.6

weight percent of each group (calculated as the weight of that group divided by the total weight of gasoline) multiplied by its effective octane value (b_r in Table 5.5) is made. Thus to perform this calculation the various groups of hydrocarbons had to be identified for each chromatogram. To do this a reference chromatogram was made based on mass spectral analysis of cracked gasoline and the GC analysis of a calibration mixture (see Chapter 4). This allowed identification of the 19 peaks necessary to establish the 29 hydrocarbon groups. Thus each chromatogram was edited to match the 29 peaks in the reference file, the normalized weight percents calculated and the GC-RON assessed. Computer programs were written to perform these tasks (CLEAN.FTN and RON.FTN found in Appendix G).

The product distribution tables shown in Appendix E were made corresponding to this format of 29 peaks in the gasoline range.

5.5 COKE DETERMINATION

The method used to determine the amount of coke on the catalyst was based on weight difference. The coked catalyst recovered from the reactor was placed in a special 'U' shaped glass tube sampler which was connected to a gas flow line. The bottom of the tube where the catalyst was located was immersed in an electrical heater filled with glass beads which allowed the catalyst to be heated. A thermocouple measured

the temperature of the glass tube. A flow of 5 ml/min of helium (ultra pure) was allowed to pass through a drierite filter and a liquid nitrogen trap before being passed over the catalyst. This ensured the removal of any trace water vapour or other impurities.

The catalyst sample was heated to 200°C for 2 hours under this flow of helium. At the end of this time period the heater was removed and the sampler allowed to cool to room temperature, under a steady flow of helium. This drying procedure eliminated traces of humidity from the catalyst. Next, the sampler was weighed and then re-connected to the gas flow lines and immersed in the heater.

The heating was again applied and the temperature set to 500°C. Air was allowed to pass over the catalyst (5 mL/min) for a period of approximately 8 hours to burn off the coke. This amount of time was more than sufficient to remove all the coke and was checked by repeating the procedure using the same sample. No addition weight difference was noticed. After the 8 hour period gas flow was switched back to helium, the heating was removed and the sampler was cooled to room temperature. The sampler was then removed from the drying unit and weighed again. From the known weight of the sampler and the first weight measurement the total mass of catalyst plus coke was determined. The final weight gave the amount of catalyst. Thus the difference in these two weights gave the mass of coke that was contained on the sampled mass of catalyst.

Knowing the original mass of catalyst used for the cracking run and the grams of coke per gram of sampled catalyst from the above weight difference method allowed determination of the overall mass of coke produced. The actual amount of coked catalyst used for the regeneration procedure was close to the original amount inserted into the reactor, but was always less due to losses in recovering coked catalyst from the reactor. Therefore the above correction was necessary.

The adequacy of the coke determination method was checked by running a non-coked catalyst sample through the entire procedure. The difference in weight was found to be 0.00058g. The actual values for the mass of coke produced ranged from 0.0018 g (approximately 1% coke) to 0.01 g (approximately 6% coke) indicating that the lower coke levels contain some uncertainty.

It should also be mentioned that the validity of the regeneration method used between gas oil injections was checked by running a sample of this regenerated catalyst through the coke determination method. No noticeable weight difference was detected indicating that the conditions used in the reactor for removing coke from the catalyst between injections were effective.

CHAPTER 6

RESULTS AND DISCUSSION

6.1 INTRODUCTION

This chapter presents a detailed description and analysis of the results obtained from the catalytic cracking runs done in the Riser Simulator. First, the trends in conversion of gas oils, yields of products and gasoline research octane numbers will be discussed for both the commercial feedstocks and for the pure light oil mixtures used. Then the kinetic parameters obtained from the 3-lump model and an 8-lump model using various decay functions are presented.

The product distributions obtained from the GC chromatograms for each experimental condition can be found in the tables of Appendix E which show individual components of the light gas fraction and major components of the gasoline cut (in accordance with the GC octane method used). In these tables averaged values from repeat runs are indicated which were corrected to satisfy mass balances and normalized to account for coke yields (see Chapter 5). Further tabulated data pertaining to statistical analysis and model predictions are found in Appendix C. Derivation and solution strategies for the kinetic models used are shown in Appendix A. In general a Marquardt non-linear regression algorithm combined with a 4th order Runge-Kutta method was used to obtained the kinetic parameter estimates. The various computer programs used are contained in Appendix G.

6.2 CRACKING OF COMMERCIAL FEEDSTOCKS

The definition of the conversion of gas oil was chosen to be consistent with the kinetic models used. On this basis the unconverted gas oil was taken as the fraction of products boiling above 220°C which in turn corresponds to compounds eluting from the chromatographic column after n-C_{12}. Then, the GC-conversion of gas oil was defined as one hundred minus the weight percent of unconverted gas oil. This value was then corrected to account for the yield of coke to define the overall conversion.

A summary of product yields and conversions for the two feedstocks and two catalysts used is given in Tables 6.1 to 6.4 for the range of experimental conditions used in the study. These values reported for each lump are averaged values based on three repeat injections for the majority of runs.

6.2.1 Conversion of gas oil

The conversions of feedstocks A and B cracked with both Octacat and GX-30 catalysts for different reaction times (3, 5, 7 and 10 seconds) and temperatures (500, 525 and 550°C) are shown in Figures 6.1 to 6.4. In these figures the symbols refer to experimental results while the lines show model predictions (using the three lump model with exponential decay). The model predictions will be discussed in a later

Table 6.1 Summary of average yields and conversions for the cracking of Feedstock A with Octacat catalyst (c/o = 5)

		wt%				
T(°C)	t_R(s)	coke	Gases	Gasoline	Conversion	Sel.*
500	3	2.03	12.48	20.08	34.59 ±3.3	58.1%
	5	1.68	15.17	23.59	40.44 ±2.8	58.3%
	7	1.73	17.22	28.35	47.30 ±3.5	59.9%
	10	2.30	21.67	31.29	55.26 ±3.3	56.6%
525	3	0.37	19.87	23.24	43.48 ±3.1	53.5%
	5	1.09	22.58	24.93	48.60 ±2.9	51.3%
	7	1.49	25.01	29.97	56.47 ±4.2	53.1%
	10	2.80	29.30	30.46	62.56 ±2.5	48.7%
550	3	2.0	23.25	24.16	49.41 ±2.2	48.9%
	5	2.43	25.63	26.32	54.38 ±2.4	48.4%
	7	3.50	26.59	30.69	60.78 ±3.6	50.5%
	10	3.8	30.0	33.39	67.19 ±3.2	49.7%

* Selectivity to gasoline = wt% gasoline / wt% conversion

Table 6.2 Summary of average yields and conversions for the cracking of Feedstock A with GX-30 catalyst (c/o = 5)

		wt%				
T(°C)	t_R(s)	coke	Gases	Gasoline	Conversion	Sel.*
500	3	2.26	14.36	24.92	41.54 ± 1.4	60.0%
	5	2.50	15.93	28.58	47.01 ± 1.0	60.8%
	7	2.72	19.28	35.90	57.90 ± 2.3	62.0%
	10	3.30	22.48	37.64	63.42 ± 1.6	60.0%
525	3	1.93	21.65	26.69	50.27 ± 3.8	53.1%
	5	2.94	23.53	32.61	59.08 ± 4.1	55.2%
	7	3.14	27.51	33.75	64.40 ± 3.1	52.4%
	10	3.50	30.60	36.92	71.02 ± 3.7	53.4%
550	3	1.92	25.86	26.27	54.05 ± 2.1	48.6%
	5	2.58	30.35	29.20	62.13 ± 4.0	47.0%
	7	4.61	35.24	27.69	67.54 ± 3.4	41.0%
	10	4.92	39.05	30.81	74.78 ± 3.8	41.2%

* Selectivity to gasoline = wt% gasoline / wt% conversion

Table 6.3 Summary of average yields and conversions for the cracking of Feedstock B with Octacat catalyst (c/o = 5)

		wt%				
T(°C)	t_R(s)	coke	Gases	Gasoline	Conversion	Sel.*
500	3	1.47	8.66	15.62	25.75 ±3.2	60.7%
	5	2.13	11.56	20.42	34.11 ±1.7	60.0%
	7	2.24	14.96	24.94	42.14 ±1.9	59.2%
	10	2.8	20.49	26.88	50.17 ±2.6	53.6%
525	3	1.65	12.09	20.69	34.43 ±2.1	60.1%
	5	1.90	15.50	24.52	41.92 ±3.3	58.5%
	7	2.09	19.16	28.64	49.89 ±4.0	57.4%
	10	2.03	24.32	29.84	56.19 ±3.2	53.1%
550	3	1.76	15.44	24.67	41.87 ±2.8	58.9%
	5	2.42	22.43	27.08	51.93 ±2.9	52.1%
	7	3.25	26.06	27.64	56.95 ±3.0	48.5%
	10	3.81	29.19	28.42	61.42 ±2.7	46 3%

* Selectivity to gasoline = wt% gasoline / wt% conversion

Table 6.4 Summary of average yields and conversions for the cracking of Feedstock B with GX-30 catalyst (c/o = 5)

		wt%				
T(°C)	t_R(s)	coke	Gases	Gasoline	Conversion	Sel.*
500	3	2.15	11.02	16.88	30.05 ± 1.6	56.2%
	5	3.58	13.25	21.18	38.01 ± 1.1	55.7%
	7	4.12	16.65	23.99	44.76 ± 2.0	53.6%
	10	4.98	21.36	28.54	54.88 ± 2.1	52.0%
525	3	2.10	15.55	19.98	37.63 ± 0.5	53.1%
	5	3.01	17.89	27.59	48.49 ± 1.0	56.9%
	7	3.80	20.89	33.41	58.10 ± 0.8	57.5%
	10	4.91	26.44	33.69	65.04 ± 1.3	51.8%
550	3	2.27	19.62	22.51	44.40 ± 4.4	50.7%
	5	2.74	23.57	30.70	57.01 ± 3.7	53.9%
	7	3.88	28.31	32.44	64.63 ± 2.8	50.2%
	10	5.10	33.37	32.70	71.17 ± 2.9	45.9%

* Selectivity to gasoline = wt% gasoline / wt% conversion

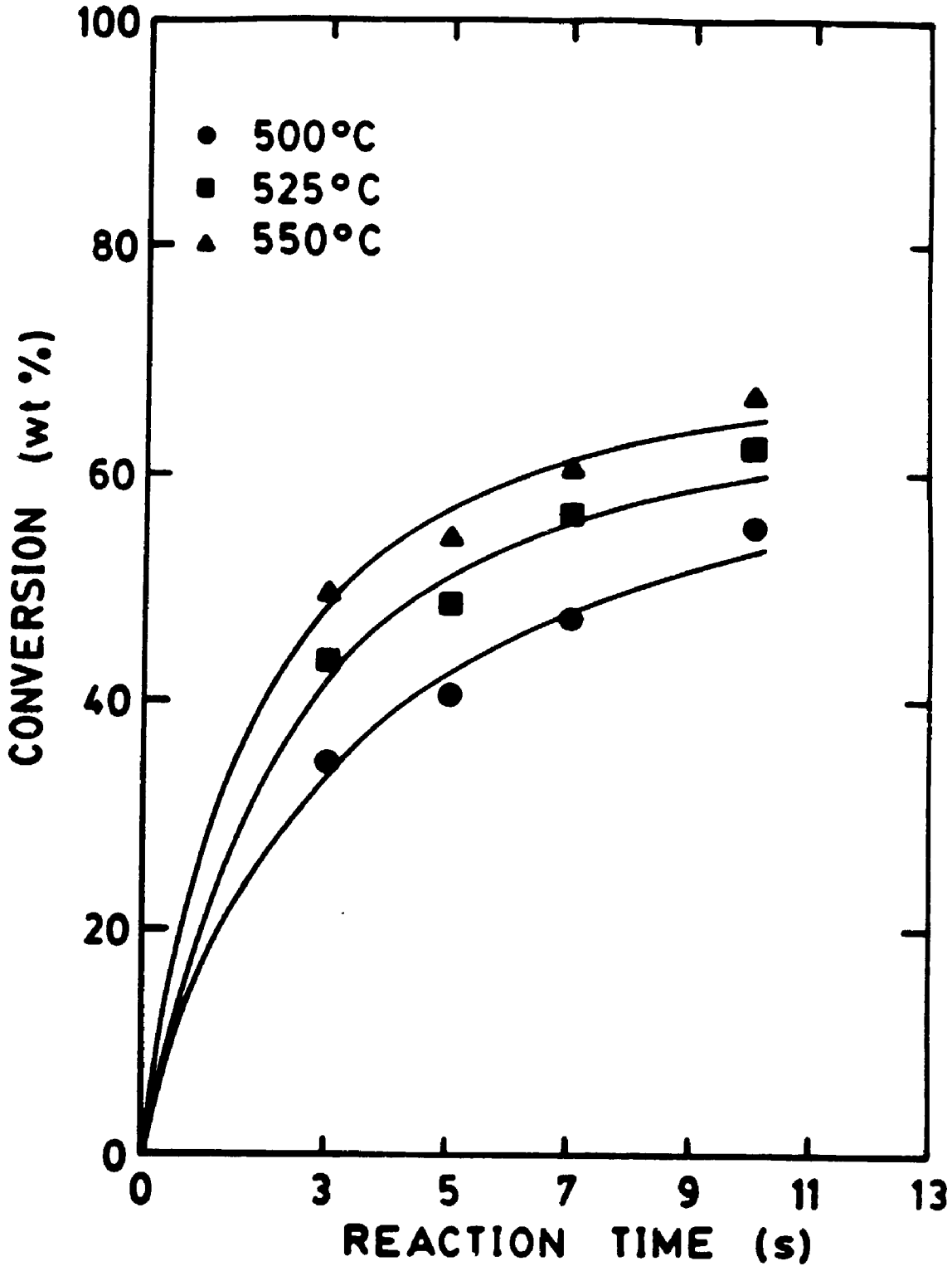

Figure 6.1 Conversion of feedstock A on Octacat catalyst as a function of reaction time and temperature.

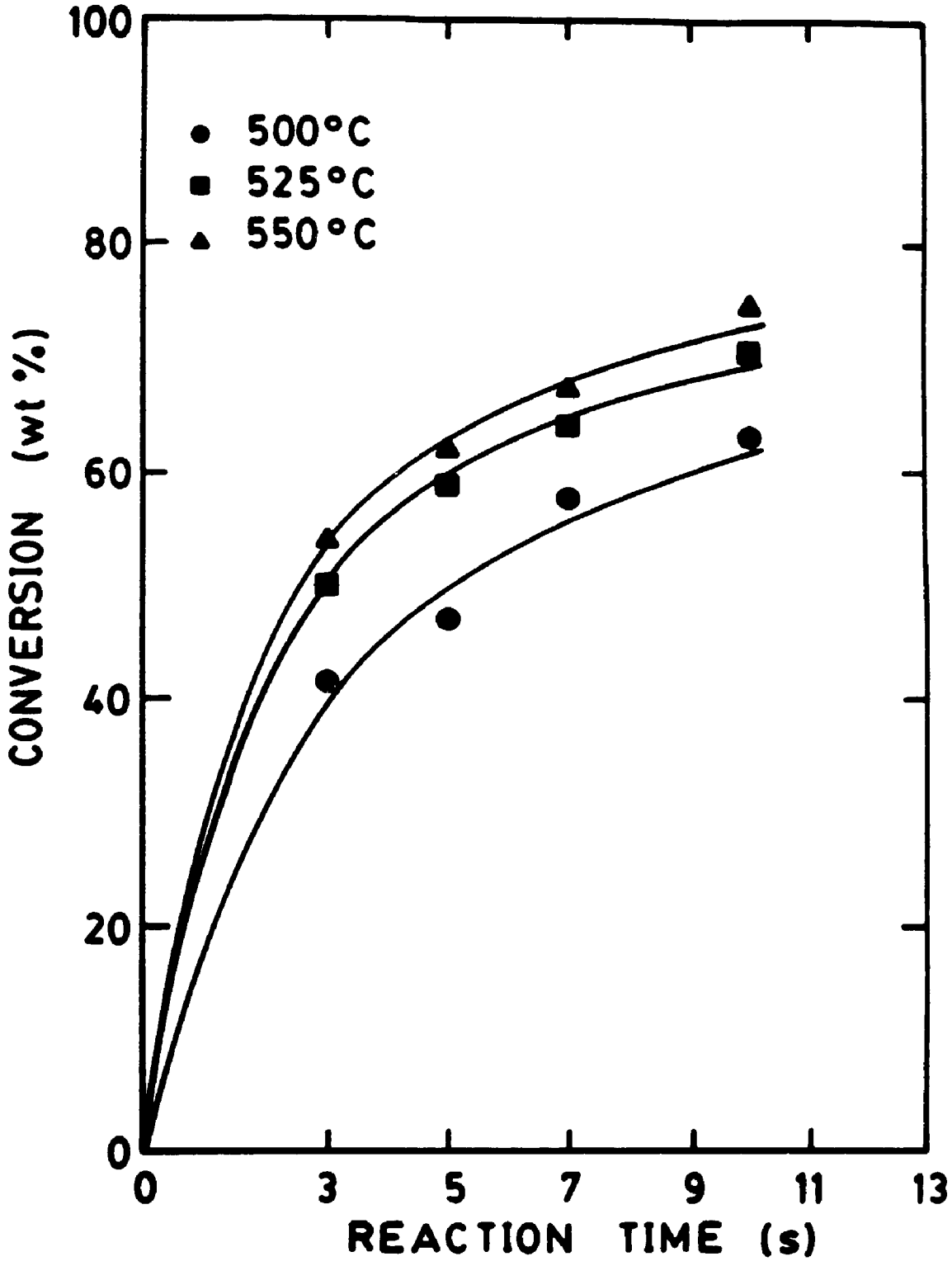

Figure 6.2 Conversion of feedstock A on GX-30 catalyst as a function of reaction time and temperature.

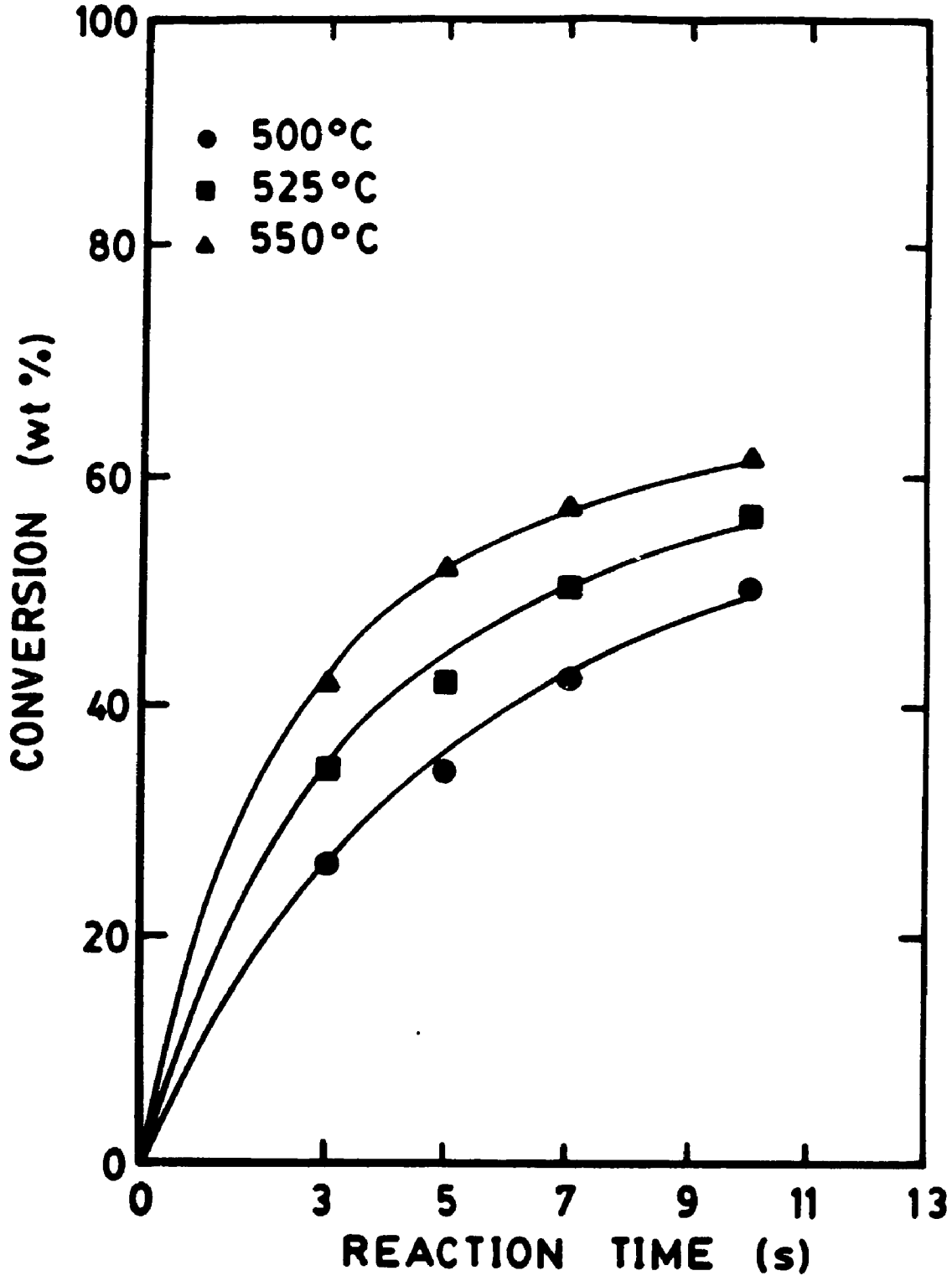

Figure 6.3 Conversion of feedstock B on Octacat catalyst as a function of reaction time and temperature.

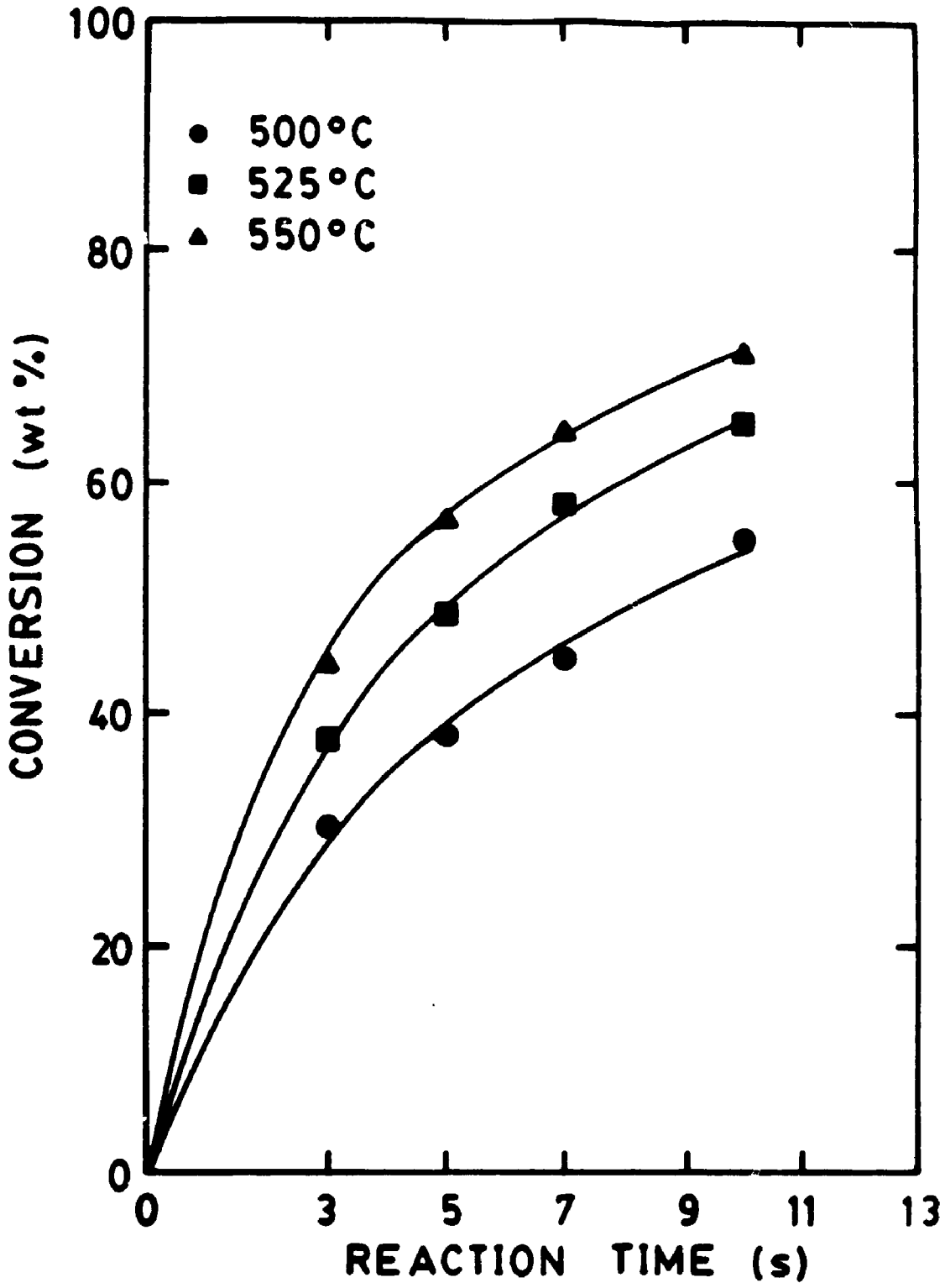

Figure 6.4 Conversion of feedstock B on GX-30 catalyst as a function of reaction time and temperature.

section of this chapter. For now reference is made to the experimental values. The trends in conversion show that with increasing reaction time conversion increases which is an expected result due to the nature of the catalytic cracking reaction. As well, conversion levels were seen to increase with increasing temperature which agrees with the fact that at higher temperatures the kinetic rate constants are higher which results in faster reaction rates. Furthermore the levelling off of conversion at the higher reaction times, as evidenced in Figures 6.1 to 6.4, is indicative of the reaction conditions where the partial pressure of oil decreases because of the transformation of oil into products. This is also enhanced by the effect of declining catalyst activity with increasing reaction time due to the deposition of coke on the catalyst.

Another clear trend can be observed by comparing the conversion levels for the same feedstock using different catalysts. For example, comparing Figures 6.1 and 6.2 it can be seen that GX-30 gives a higher conversion of feedstock A than that obtained using Octacat for all experimental conditions studied. The same is true for feedstock B (Figures 6.3 and 6.4). This result may be explained because of the basic differences between these two catalysts. While both catalysts are designed for octane enhancing purposes, GX-30 has been shown to give increased bottoms cracking (Montgomery, 1985). Moreover, GX-30 has a much larger unit cell size (24.4 Å) as compared to Octacat (24.24 Å) thus one would expect

greater cracking activity for GX-30 because of the postulation that increased unit cell size is proportional to increased acid site density (Pine et al., 1984). Another comparison can be made between conversion levels for the two different feedstocks cracked with the same catalyst. In both cases it was observed that a higher conversion level was achieved with feedstock A than with feedstock B. This result is attributed to the compositional differences between the two gas oils where feedstock B is highly aromatic and thus more refractory to cracking.

6.2.2 Gasoline yields and selectivity

The gasoline fraction was defined as those compounds leaving the reactor with carbon numbers ranging from C_5 to C_{12}. This corresponds to a C_5+ to 220°C boiling range fraction normally used to define gasoline according to the kinetic models used (Jacob et al., 1976). To illustrate the effect of the operating variables on the gasoline yields for the two commercial feedstocks cracked with both catalysts, plots of gasoline yield versus reaction time and temperature were prepared (Figures 6.5 to 6.8). In these figures, the lines correspond to model predictions (which will be discussed later) and the points refer to experimental values. The following general trends can be observed:

- gasoline yield increases initially with reaction time (or conversion) then starts to level off at the longer reaction

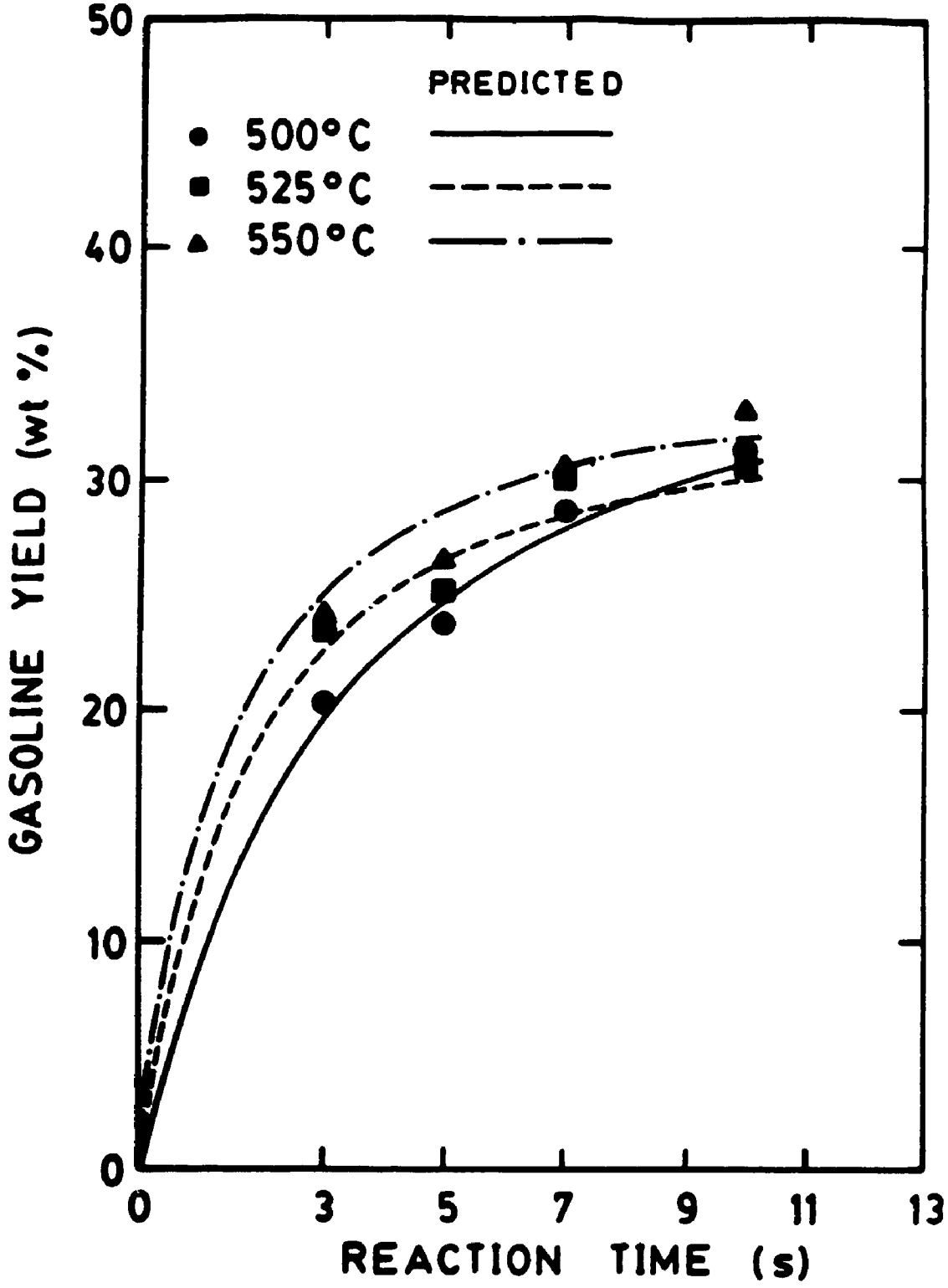

Figure 6.5 Gasoline yields for the cracking of feedstock A on Octacat as a function of reaction time and temperature.

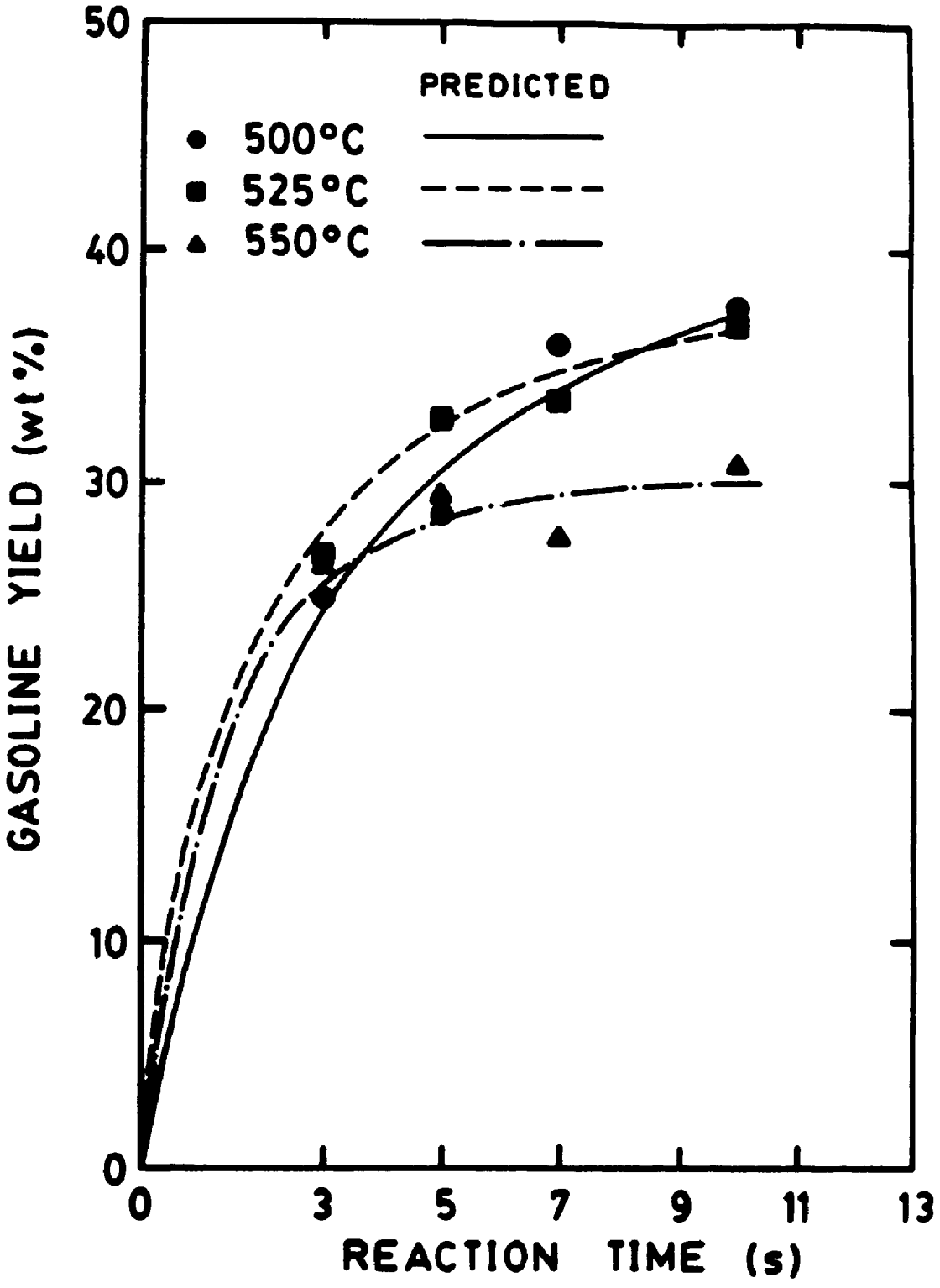

Figure 6.6 Gasoline yields for the cracking of feedstock A on GX-30 as a function of reaction time and temperature.

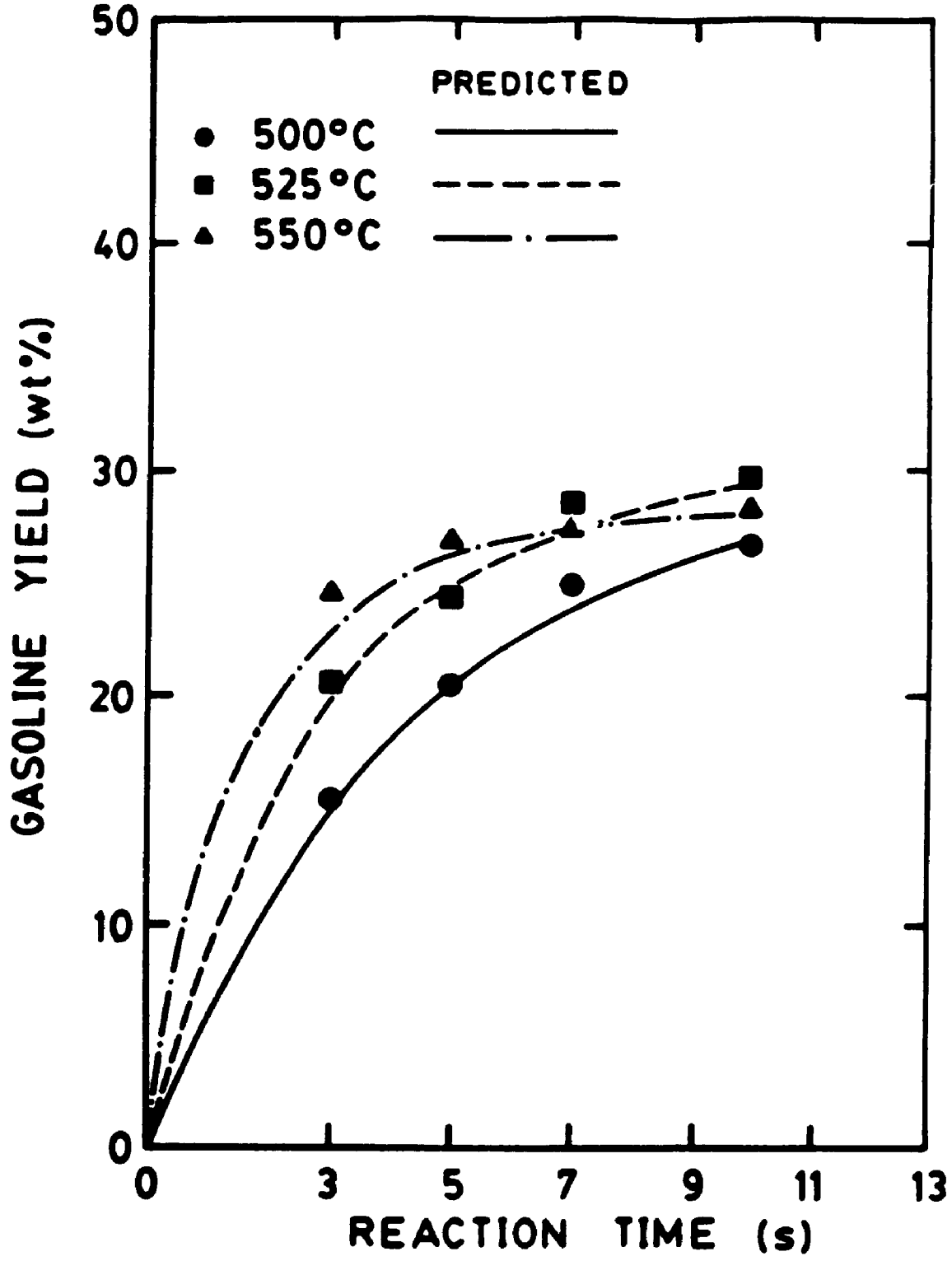

Figure 6.7 Gasoline yields for the cracking of feedstock B on Octacat as a function of reaction time and temperature.

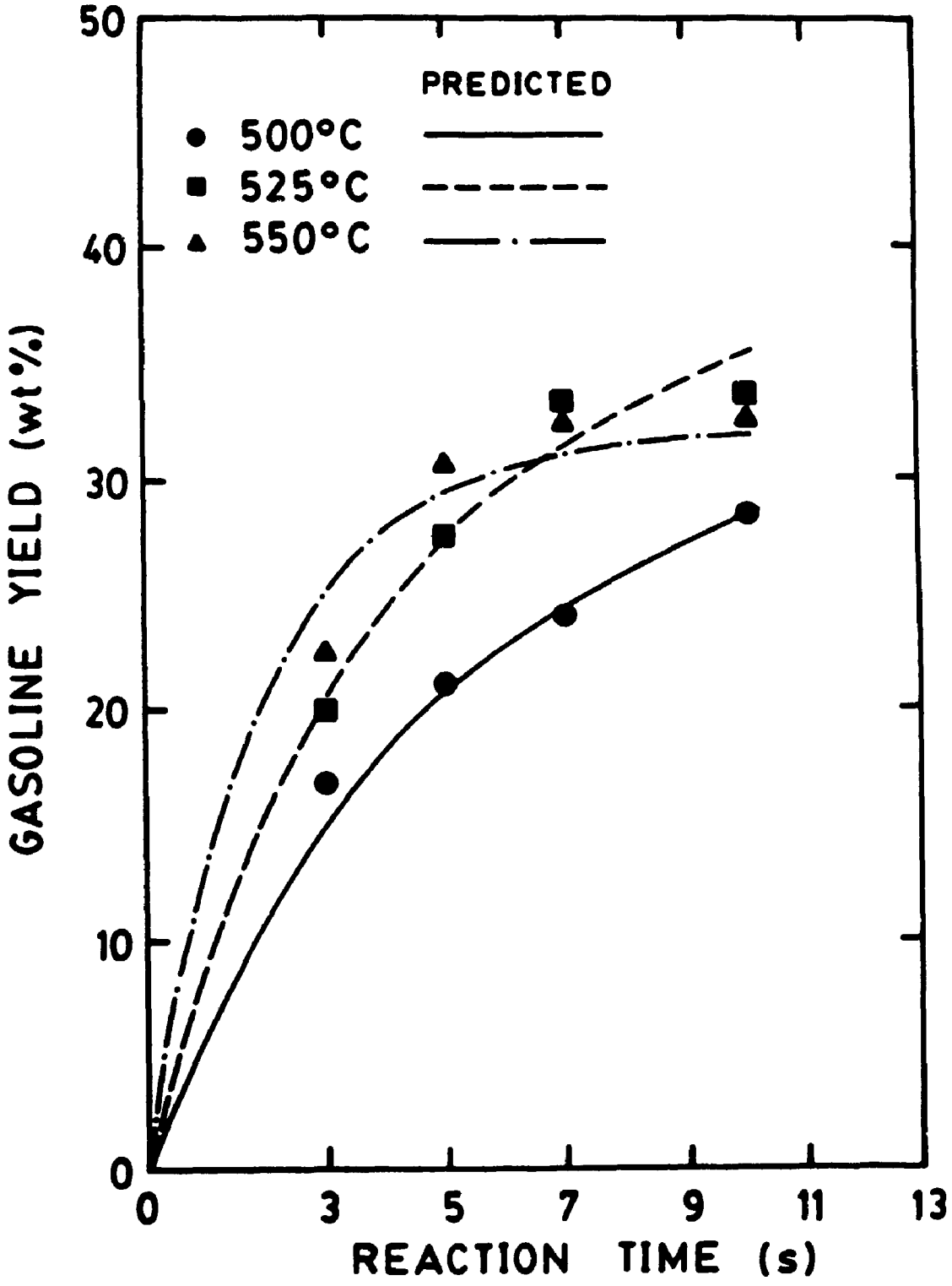

Figure 6.8 Gasoline yields for the cracking of feedstock B on GX-30 as a function of reaction time and temperature.

time (10 s)

- the slope of the gasoline versus time curve decreases at the higher temperature levels.

The first point confirms the fact that secondary reactions, namely gasoline cracking, become significant after a certain conversion level as discussed in Chapter 1. The second point, describing the temperature effect on gasoline yield is better revealed by considering the selectivity to gasoline.

Tables 6.1 to 6.4 contain tabulated values of gasoline selectivity which is defined in the usual way as gasoline yield divided by conversion. It can be seen that, in general, smaller gasoline yields per unit conversion level, reported in the last column of these tables, were obtained as temperature was increased. Reduced gasoline selectivity with higher temperature can be expected due to a higher energy of activation for gasoline cracking as compared to gas oil cracking (Jacob et al., 1976; Larocca, 1988: Kraemer et al., 1990).

It is also possible to observe the differences in gasoline yields for the same oil cracked on a different catalysts. Considering Figures 6.5 and 6.6 for feedstock A cracked with Octacat and GX-30 respectively, the gasoline yields were higher for GX-30 at the temperatures of 500 and 525°C. However, at 550°C the gasoline yield with GX-30 catalyst was significantly reduced and fell below the yields for Octacat at all three temperature levels for reaction times greater than 3 seconds. This indicates that under these conditions

there is undesirable over-cracking of gasoline combined with preferential transformation of gas oil to light gases. The comparison of gasoline yields for feedstock B cracked with Octacat and GX-30 catalysts (Figures 6.7 and 6.8) showed a higher gasoline yield for GX-30 except at 500°C where the yields were quite similar. This suggests that a higher boiling feed containing more bulky and refractory molecules will give better yields when cracked at higher temperatures using a catalyst with a larger unit cell size.

6.2.3 Yield of light gases

The yields of light gases which were considered to be the C_4 and lighter fraction of the products, are shown in Figures 6.9 to 6.12. In these figures lines were drawn to help illustrate experimental trends and do not represent model predictions (i.e. model predicts C-lump which combines light gases and coke). Tabulated data can also be found in Tables 6.1 to 6.4 for feedstocks A and B cracked with both Octacat and GX-30 catalysts. Expected trends were obtained when observing the effect of the operating variables on light gases yield. For the two feedstocks and two catalysts used, the light gases yield increased with both increasing reaction time and temperature. The slope of the yield curve was somewhat larger for higher temperatures reflecting the increase in product selectivity towards light gas formation. This is explained by increased gasoline cracking and more beta-

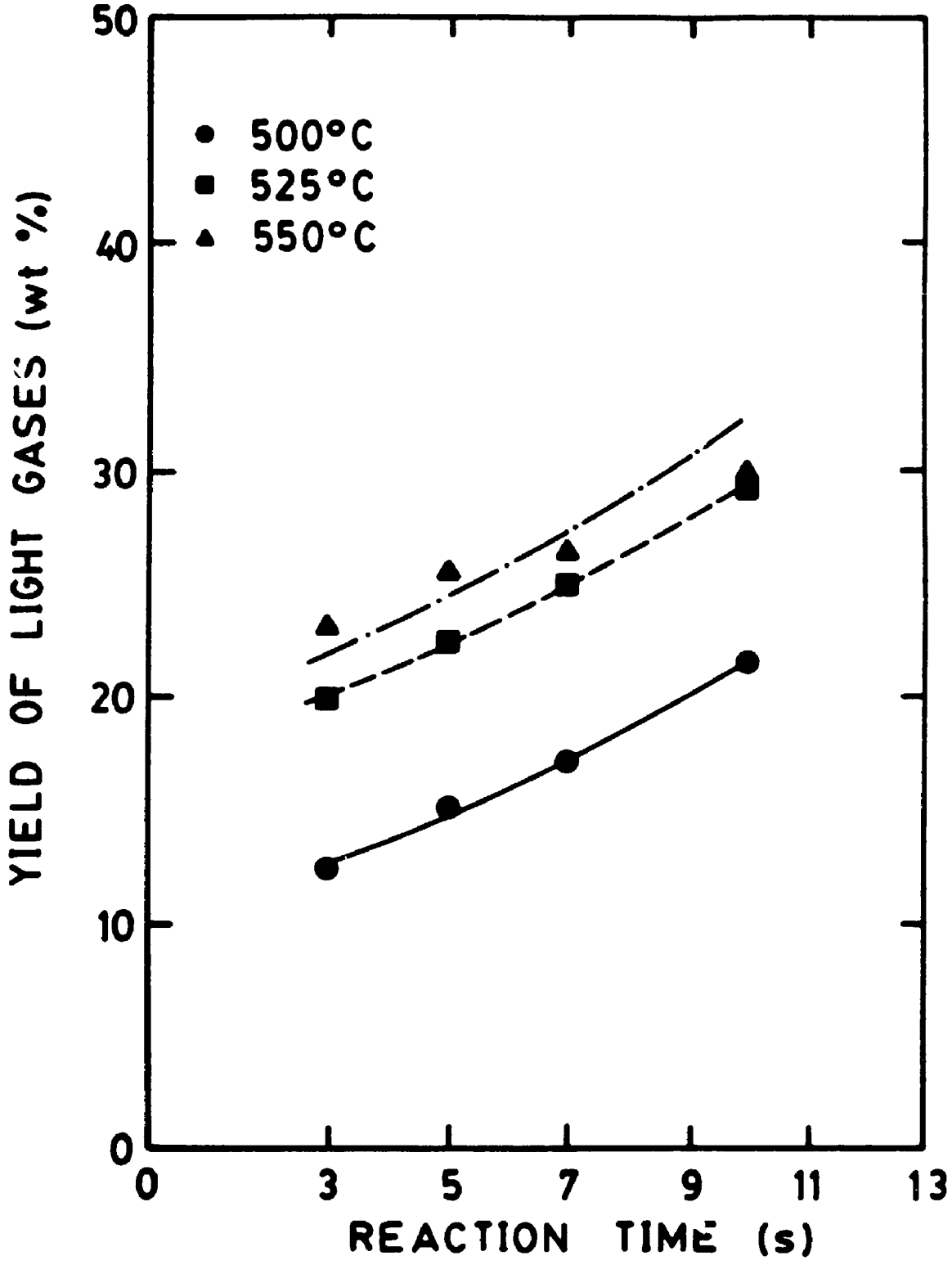

Figure 6.9 Yield of light gases for the cracking of feedstock A on Octacat catalyst as a function of reaction time and temperature.

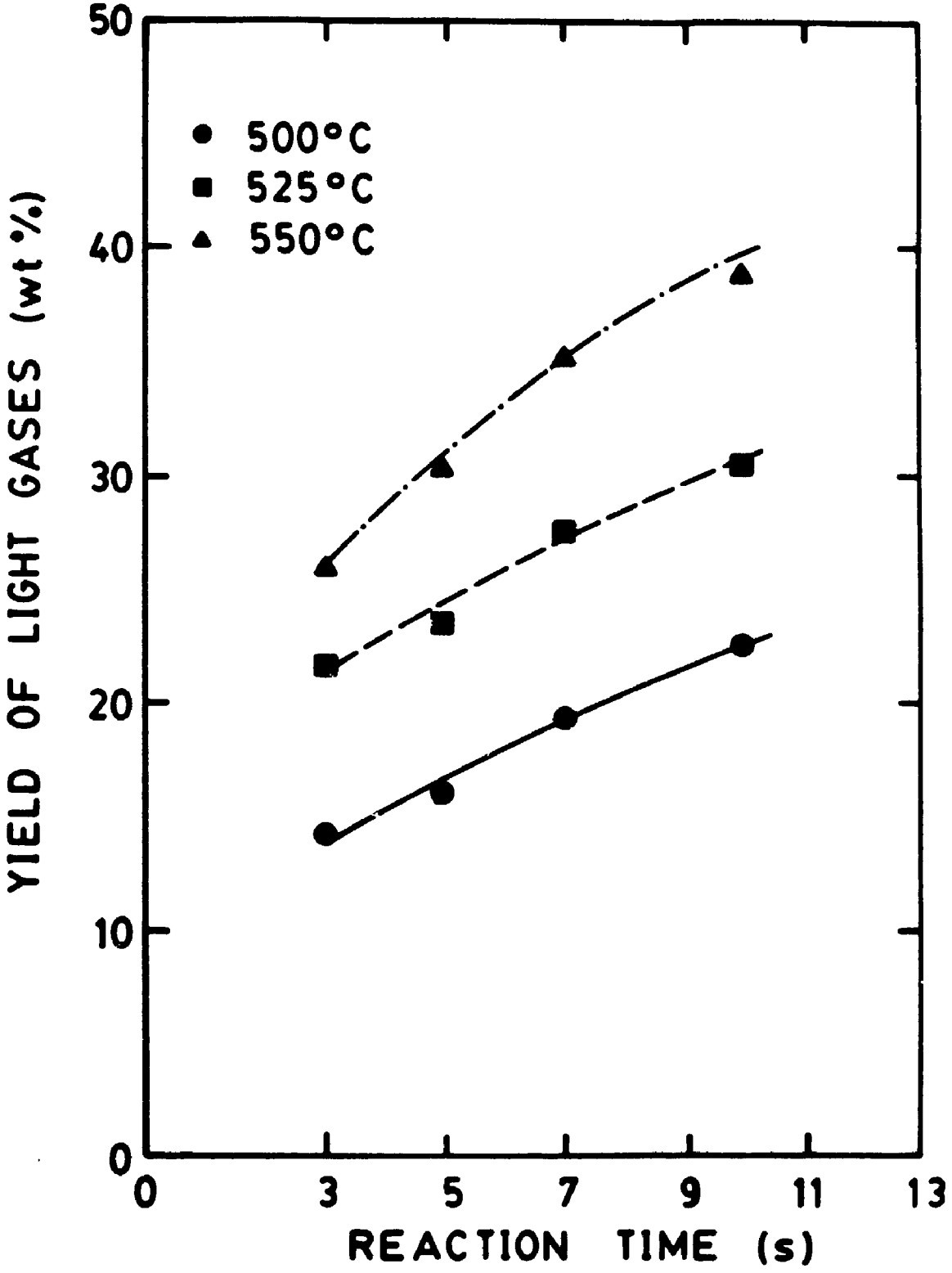

Figure 6.10 Yield of light gases for the cracking of feedstock A on GX-30 catalyst as a function of reaction time and temperature.

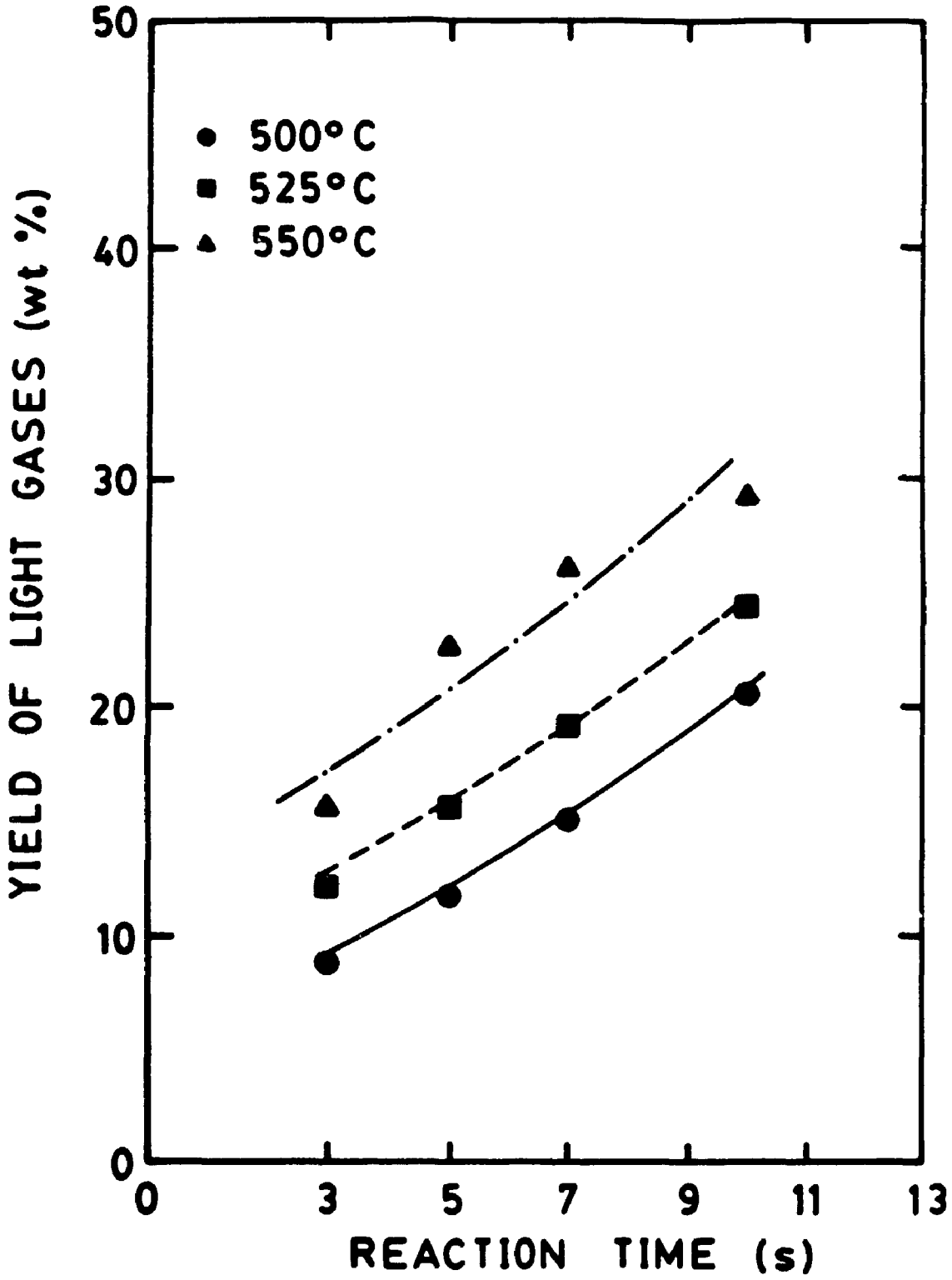

Figure 6.11 Yield of light gases for the cracking of feedstock B on Octacat catalyst as a function of reaction time and temperature.

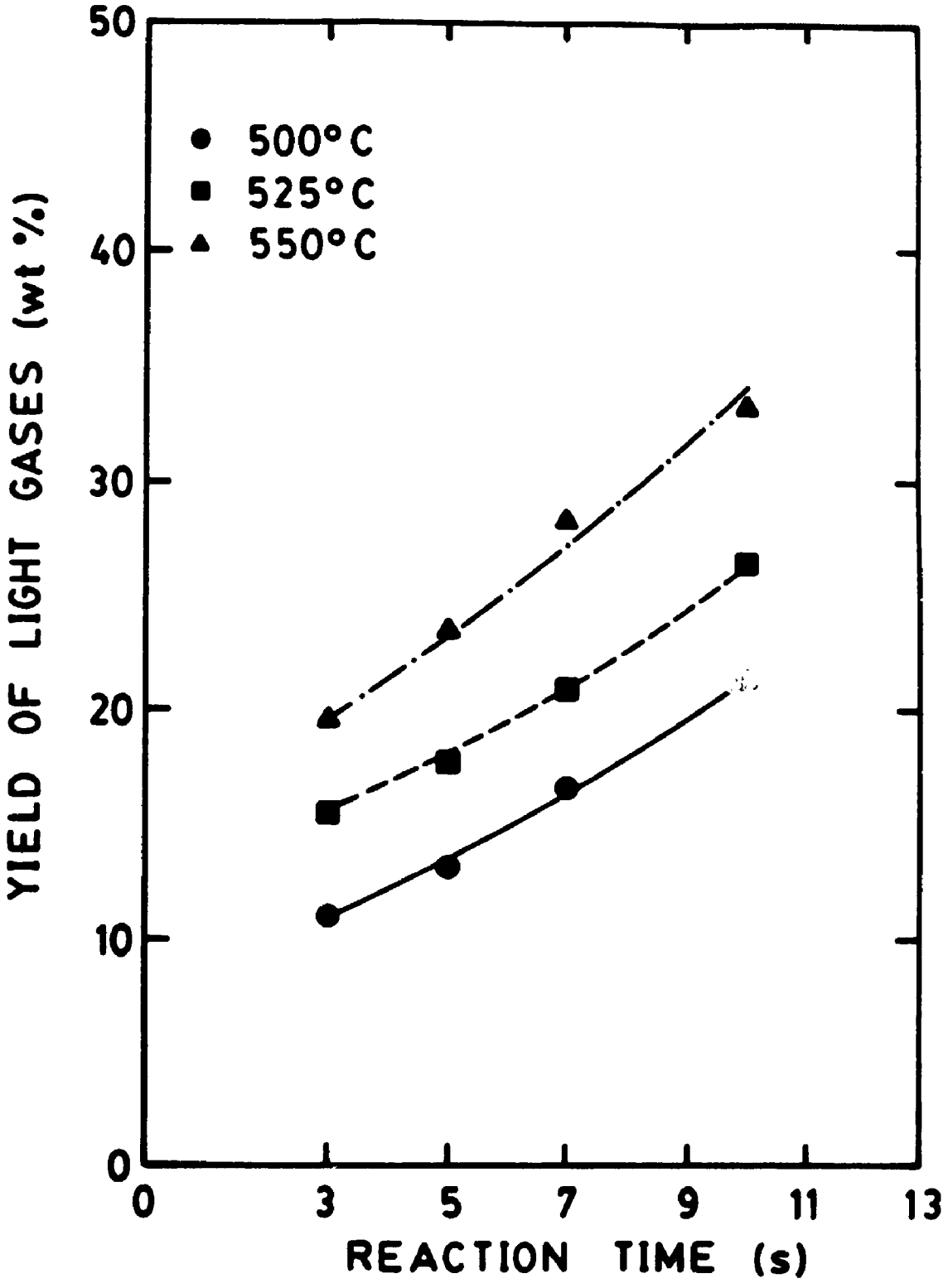

Figure 6.12 Yield of light gases for the cracking of feedstock B on GX-30 catalyst as a function of reaction time and temperature.

scission type cracking at higher temperatures, which both produce larger amounts of lighter molecules.

Comparing the effect of catalyst on gas yields it is seen that yields are higher at the same reaction time and temperature for the GX-30 catalyst, consistent with the fact that conversion is also greater. As well, gas yields are higher for feedstock A than for feedstock B when compared for the same catalyst, temperature and reaction time. Again this result is not surprising since the same is true for conversion.

6.2.4 Coke yields

The coke formation results are shown in Figures 6.13 to 6.16 where coke yield was plotted versus reaction time for the three temperatures considered. Lines were drawn in these figures to aid in visualizing the trends of coke yield with the operating variables. In general, coke formation increased with increasing reaction time due to greater conversion of gas oil.

The effect of increasing temperature was not the same for each catalyst-feedstock combination. For example, feedstock A and B cracked with Octacat (Figures 6.13 and 6.15) showed lower coke make at 525°C compared to 500°C. Feedstock A with GX-30 (Figure 6.14) showed roughly equal amounts of coke yield at the reaction times below 5 seconds for all three temperatures. For the longer reaction times, as temperature

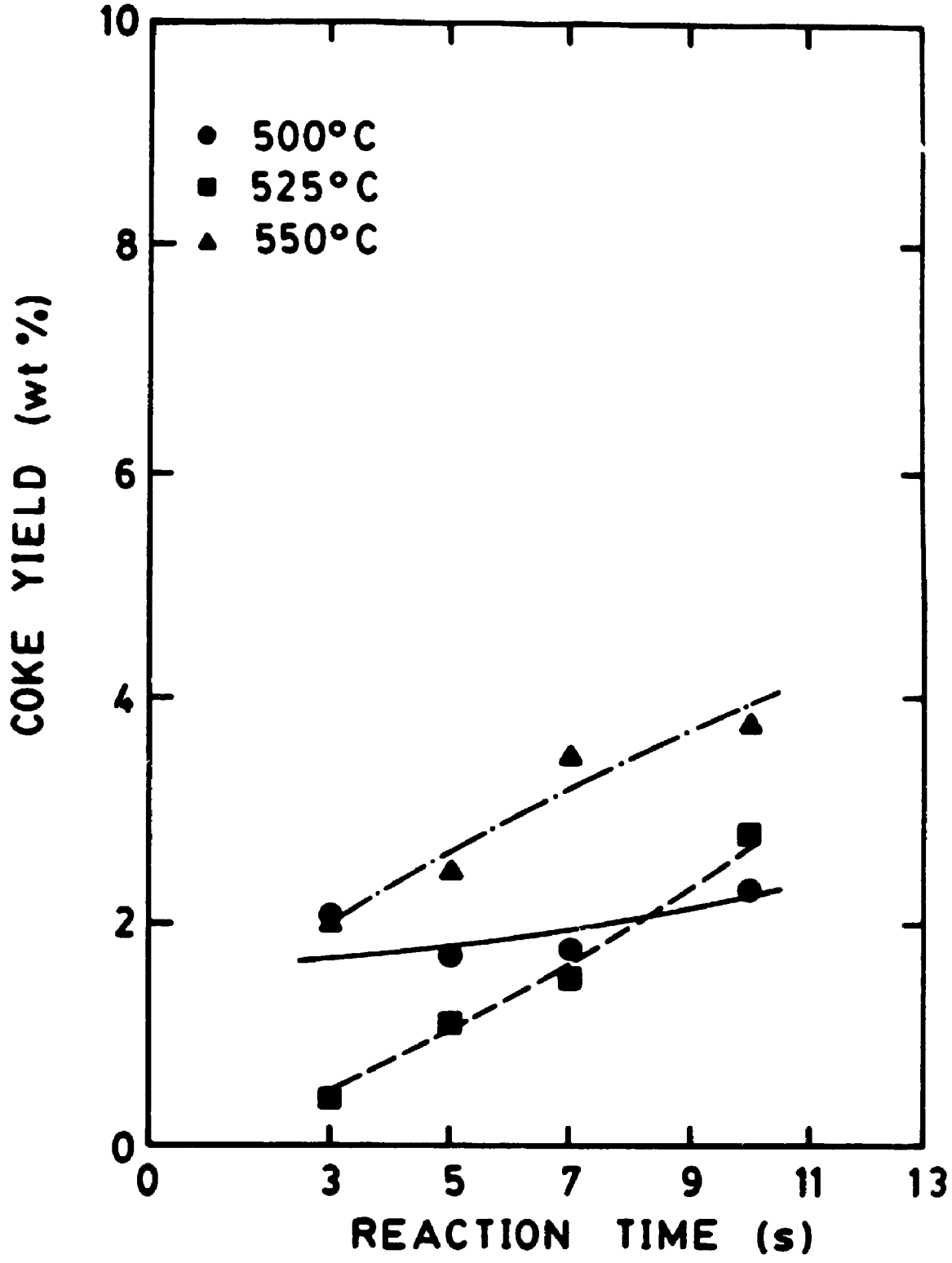

Figure 6.13 Coke yields for the cracking of feedstock A on Octacat as a function of reaction time and temperature.

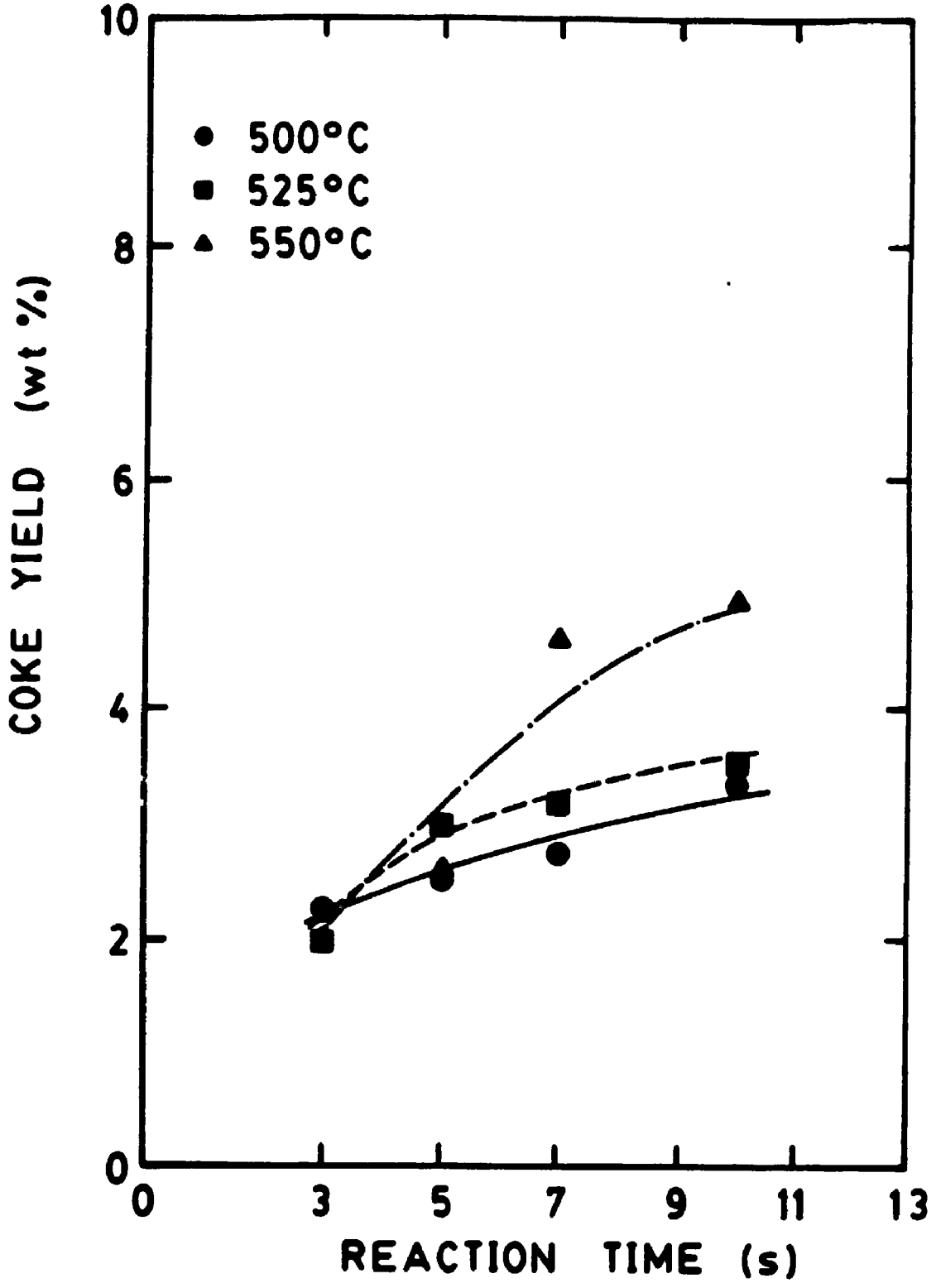

Figure 6.14 Coke yields for the cracking of feedstock A on GX-30 as a function of reaction time and temperature.

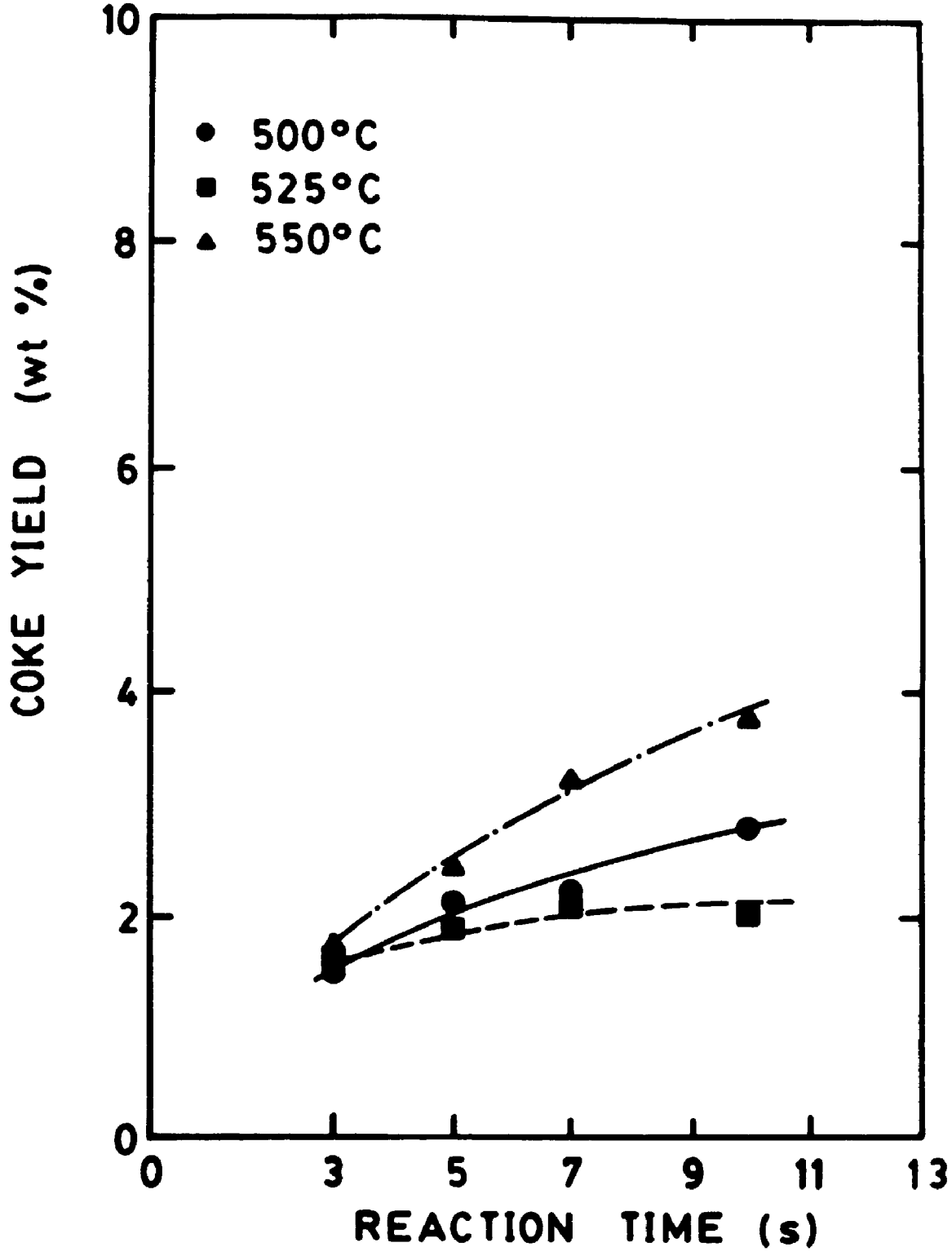

Figure 6.15 Coke yields for the cracking of feedstock B on Octacat as a function of reaction time and temperature.

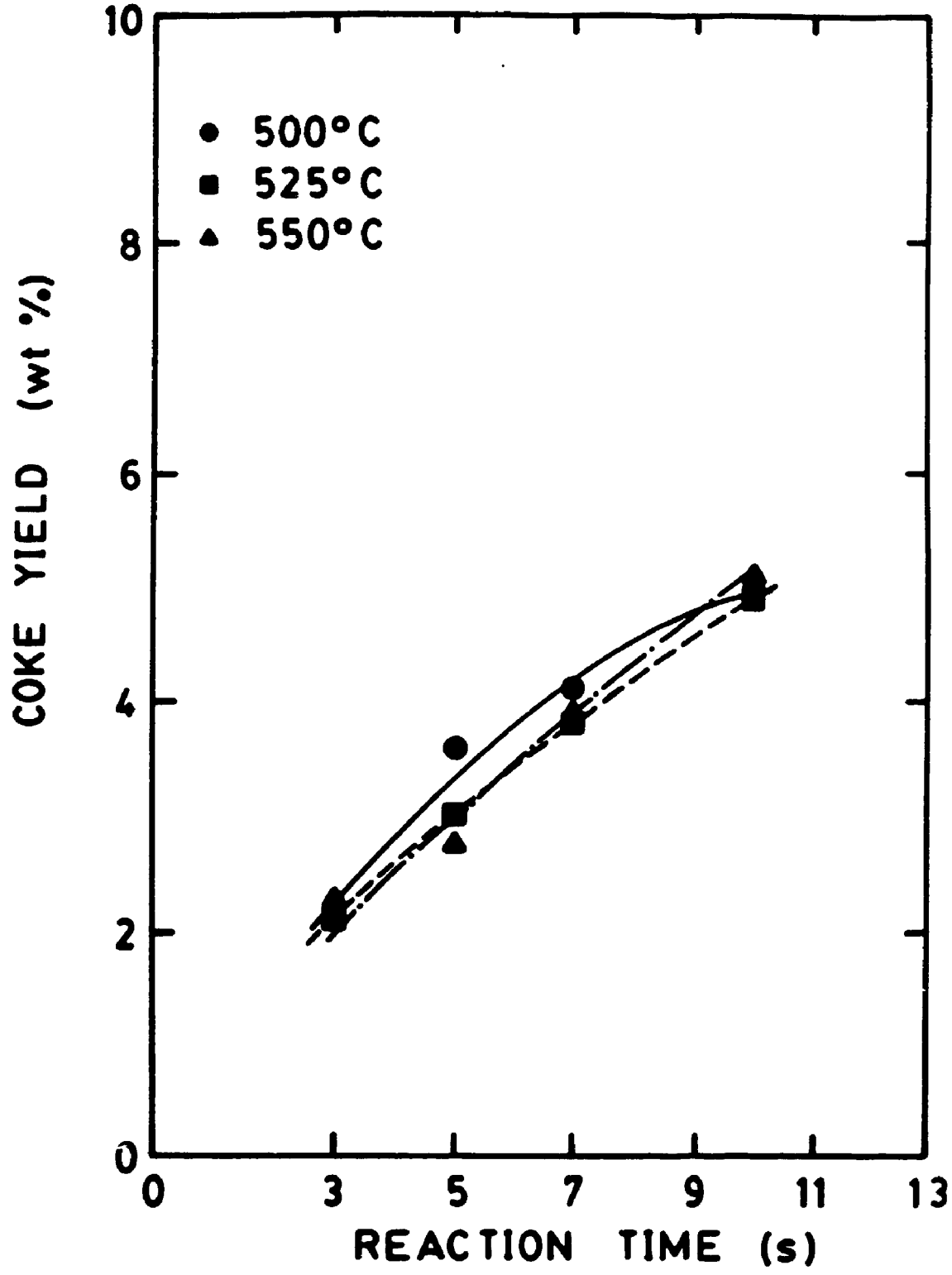

Figure 6.16 Coke yields for the cracking of feedstock B on GX-30 as a function of reaction time and temperature.

was increased so did coke yield. On the other hand, referring to Figure 6.16 for feedstock B on GX-30 the coke yields changed only slightly with temperature showing a decreasing yield at the higher temperatures. This result agrees with the general statement that coke formation generally decreases with increasing temperatures for a constant conversion (Chen and Luki, 1986: Archibald et al., 1952; Scherzer,1989). However, since in a batch mode of operation as in the case of the Riser Simulator conversion cannot be a fixed parameter, but rather increases with time (which is the case for gas oil cracking) then it is difficult to observe coke yields on a constant conversion basis. The higher coke yields at 550°C are likely due to the increased conversion levels.

It is also interesting to see that Octacat catalyst yielded less coke than GX-30 which has a larger unit cell size than Octacat. A lower unit cell size can be correlated to a lower concentration of acid sites for dealluminated zeolites (Pine et al., 1984) which in turn means a reduction in the ratio of the rate of hydrogen transfer to cracking rate. This results in a reduced rate of conversion of aromatics into condensed polycycles yielding less coke (Scherzer, 1989).

6.2.5 Gasoline GC-Research Octane Number

The calculated GC-RON values for the gasoline fractions obtained from the cracking of Feedstocks A and B with both Octacat and GX-30 catalysts are shown in Table 6.35. Some general observations can be made with regards to the effect of operating conditions on octane number. Increasing reaction time (increased conversion) resulted, on average, in an increase of GC-RON at the higher conversions although this was not a significant effect. In some cases the GC-RON decreased when reaction time was increased from 3 to 5 seconds but then subsequently increased at higher reaction times.

The effect of increased temperature resulted in increased GC-RON values for all cases as expected. For example, feedstock A cracked with Octacat showed an average GC-RON of 100.3 (average of the 4 reaction times used) at 500°C and 102.4 at 550°C resulting in a 2.1 octane increase. The increased olefinicity of the gasoline as a result of more thermal cracking at higher temperatures is a major contributor to higher octane values. This also corresponds to lowered hydrogen transfer reactions at the higher temperatures which means less conversion of olefins and naphthenes into paraffins.

The effect of feedstock on the GC-RON indicated that the more aromatic gas oil gave a slightly higher octane gasoline. This is seen by the fact that on average the GC-RON values for feedstock which is highly aromatic B are higher than for

Table 6.35 Calculated GC-RON values for Feedstocks A and B cracked with Octacat and GX-30 catalyst.

		Octacat		GX-30	
t(s)	T(°C)	Feed A	Feed B	Feed A	FeedB
3	500	100.3	99.1	100.1	99.0
5		99.9	101.5	98.8	100.1
7		100.3	101.5	99.1	100.2
10		100.8	101.7	99.2	99.9
3	525	101.8	101.6	101.0	100.0
5		100.3	102.0	101.2	101.9
7		101.7	102.2	100.3	101.8
10		101.8	102.7	100.4	101.8
3	550	101.9	102.1	101.6	101.2
5		102.3	102.4	101.5	102.0
7		102.5	103.0	101.5	102.7
10		102.8	103.1	101.8	102.9

feedstock A which is mostly paraffinic. The result is not surprising since aromatics show the highest octane rating of the hydrocarbon groups (Scherzer, 1989).

It is also interesting to see that average octane values for the gasolines obtained using Octacat catalyst are slightly higher than those using GX-30. This can be explained in terms of unit cell sizes for the two catalysts. In general, the decrease in unit cell size and corresponding increase in frame.ork silica/alumina ratio favour the formation of compounds with a high octane value (Scherzer, 1989). This is to say that a lower unit cell size results in lower total acidity hence decreasing hydrogen transfer activity and giving a higher olefinic product. Thus, Octacat which has a smaller unit cell size than GX-30 produces a higher octane gasoline at the expense of lower conversion and selectivity.

6.2.6 Analysis of Oil Lump Yields

The three lump model groups the C_{12}+ hydrocarbons into one oil lump which is defined as the unconverted feed and constitutes a wide range of hydrocarbon types. To take a closer account of the chemistry of the feedstock the eight-lump model subdivides this oil lump into six groups: light paraffins (P_l), light naphthenes (N_l), light aromatics (A_l), heavy paraffins (P_h), heavy naphthenes (N_h) and heavy aromatics (A_h). The abbreviated notation will be used throughout the text for simplicity. The light lumps are defined by a boiling

range of 220°C to 345°C representing light cycle oil (LCO) and the heavy lumps contain molecules boiling above 345°C which represents heavy cycle oil (HCO). The cut point between LCO and HCO on the chromatogram reports was taken as the n-C_{20} peak, with n-C_{20} included in the LCO fraction.

From the GC-MS analysis of the cracked products (as discussed in Chapter 5) the weight fractions of each lumped species were determined and the results for both feedstocks cracked with both catalysts are tabulated in Tables 6.5 to 6.8. showing average values based on three repeat runs for most of the experimental points. It should be mentioned that the use of the word "yield" for the gas oil lumps refers to unconverted oil and even though some LCO is formed from the cracking of HCO, it is not included in the calculation for overall conversion.

To trace the compositional changes of the unconverted gas oil fraction during cracking, plots of oil lump yield versus reaction time for the three temperatures used were made (Figures 6.17 to 6.30). For all these figures the curves represent model predictions as obtained using the 8-lump model with exponential decay and the symbols indicate experimental values. The fit of the model to the data will be discussed later when the kinetic results are presented (section 6.5). Figure 6.17 shows yields of the P_i lump for both feedstocks on Octacat. It can be seen that the amount of the light paraffins decreased with increasing time and temperature as the cracking reaction proceeded. The drop is more pronounced

Table 6.5 Summary of average individual gas oil lump yields for the cracking of Feedstock A with Octacat catalyst.

T(°C)	t_R(s)	wt%					
		P_l	N_l	A_l	P_h	N_h	A_h
500	3	15.1	8.5	7.5	18.1	12.3	4.0
	5	12.4	8.0	9.5	17.1	9.3	3.2
	7	11.1	7.1	6.8	15.7	9.0	3.0
	10	10.5	6.7	5.0	11.5	8.1	2.9
525	3	13.4	7.1	7.0	15.7	10.1	3.2
	5	12.9	5.9	7.6	13.9	8.1	2.9
	7	11.3	5.0	6.0	11.1	7.9	2.2
	10	9.9	4.6	4.5	10.0	7.3	1.2
550	3	13.7	6.2	6.6	12.8	9.1	2.3
	5	11.3	5.9	5.6	11.8	8.9	2.1
	7	10.8	5.0	5.3	9.3	7.0	1.9
	10	9.2	4.2	3.9	7.4	6.8	1.1

Table 6.6 Summary of average individual gas oil lump yields for the cracking of Feedstock A with GX-30 catalyst.

T(°C)	t_R(s)	wt%					
		P_l	N_l	A_l	P_h	N_h	A_h
500	3	15.2	7.4	7.3	15.5	8.3	4.7
	5	13.9	6.8	7.0	13.5	7.6	4.3
	7	12.5	6.6	6.4	11.5	7.4	4.2
	10	11.2	6.2	5.1	10.0	5.7	3.5
525	3	14.4	7.8	6.0	12.2	6.6	3.3
	5	13.0	6.3	5.6	8.4	4.9	3.1
	7	12.1	5.0	4.3	7.1	4.3	2.9
	10	8.8	4.8	3.9	5.0	4.0	2.4
550	3	14.1	7.1	5.8	10.9	5.3	2.8
	5	12.7	6.3	4.8	7.5	4.2	2.4
	7	11.9	5.3	5.0	5.5	3.4	1.4
	10	8.3	4.5	3.4	4.5	3.3	1.2

Table 6.7 Summary of average individual gas oil lump yields for the cracking of Feedstock B with Octacat catalyst.

T(°C)	t_R(s)	wt%					
		P_l	N_l	A_l	P_h	N_h	A_h
500	3	3.4	13.0	16.6	1.9	13.6	25.7
	5	3.0	13.4	15.3	2.0	10.5	21.7
	7	3.2	13.0	13.1	1.9	8.8	17.7
	10	2.6	12.5	12.8	1.2	7.5	13.2
525	3	3.0	12.3	15.8	1.5	11.6	21.4
	5	2.9	10.8	14.1	2.0	10.3	18.0
	7	2.4	9.1	12.9	2.0	8.2	15.5
	10	2.2	8.9	12.4	0.7	6.8	12.8
550	3	2.6	11.1	14.6	1.2	10.4	18.3
	5	3.1	9.4	12.9	1.6	7.3	13.7
	7	3.0	8.5	12.7	1.5	5.8	11.7
	10	2.5	7.9	12.0	0.9	5.4	9.9

Table 6.8 Summary of average individual gas oil lump yields for the cracking of Feedstock B with GX-30 catalyst.

T(°C)	t_R(s)	wt%					
		P_l	N_l	A_l	P_h	N_h	A_h
500	3	3.2	13.9	15.1	2.1	14.1	21.6
	5	3.2	12.2	13.9	1.8	12.1	18.8
	7	2.9	11.8	12.2	1.6	11.1	15.6
	10	2.8	10.8	11.3	1.2	6.2	12.8
525	3	3.1	13.0	13.3	1.2	12.9	18.9
	5	2.2	11.8	10.4	1.1	11.2	14.8
	7	2.0	10.3	9.0	0.9	8.8	10.9
	10	1.6	9.0	7.9	0.8	6.1	9.6
550	3	2.8	12.8	13.0	0.9	10.7	15.4
	5	1.2	10.5	10.1	0.8	8.9	11.4
	7	1.1	9.2	8.5	0.7	6.9	8.9
	10	1.0	8.8	6.5	0.7	5.3	7.8

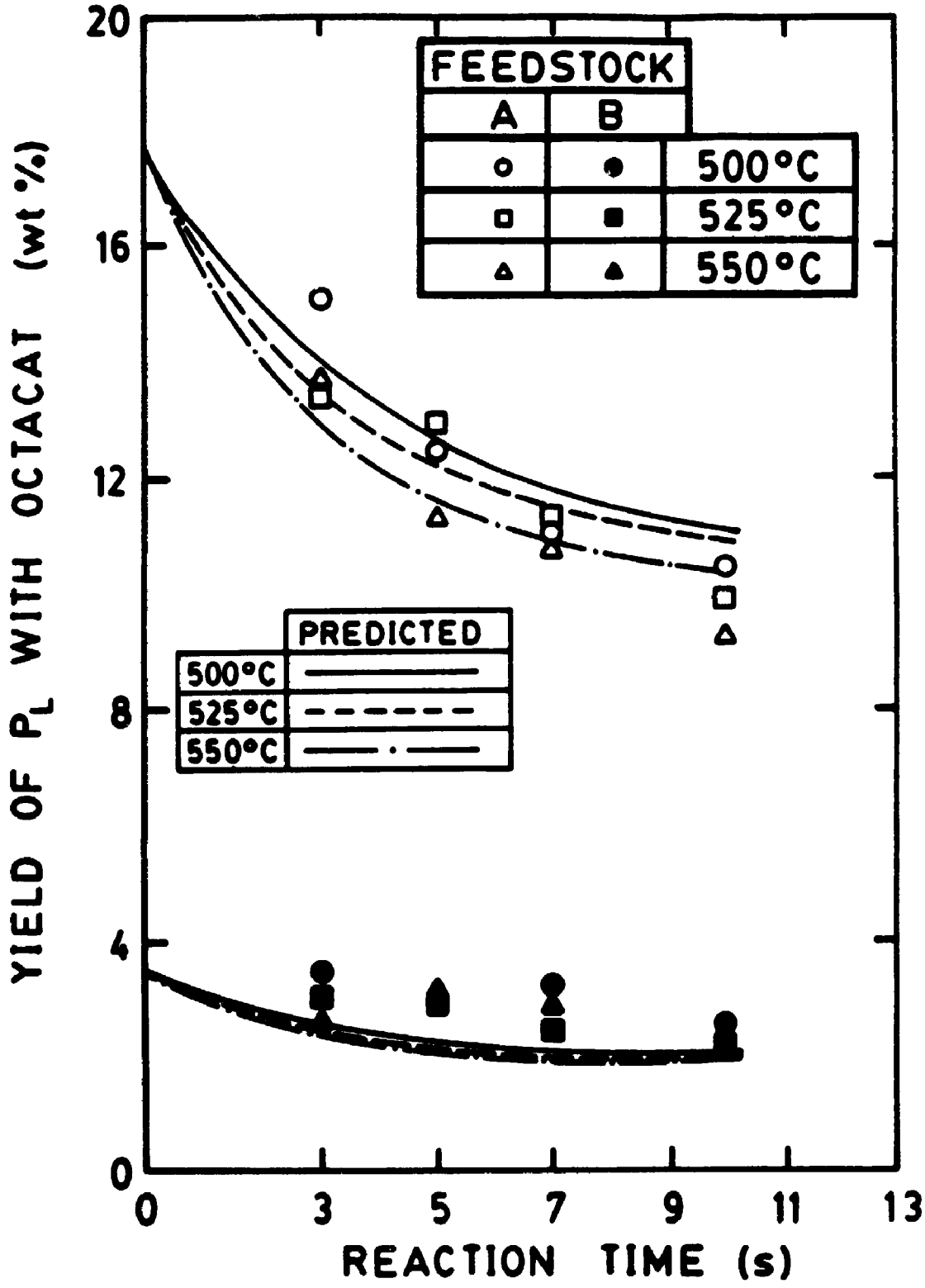

Figure 6.17 Yields of P_l for feedstocks A and B on Octacat as a function of reaction time and temperature.

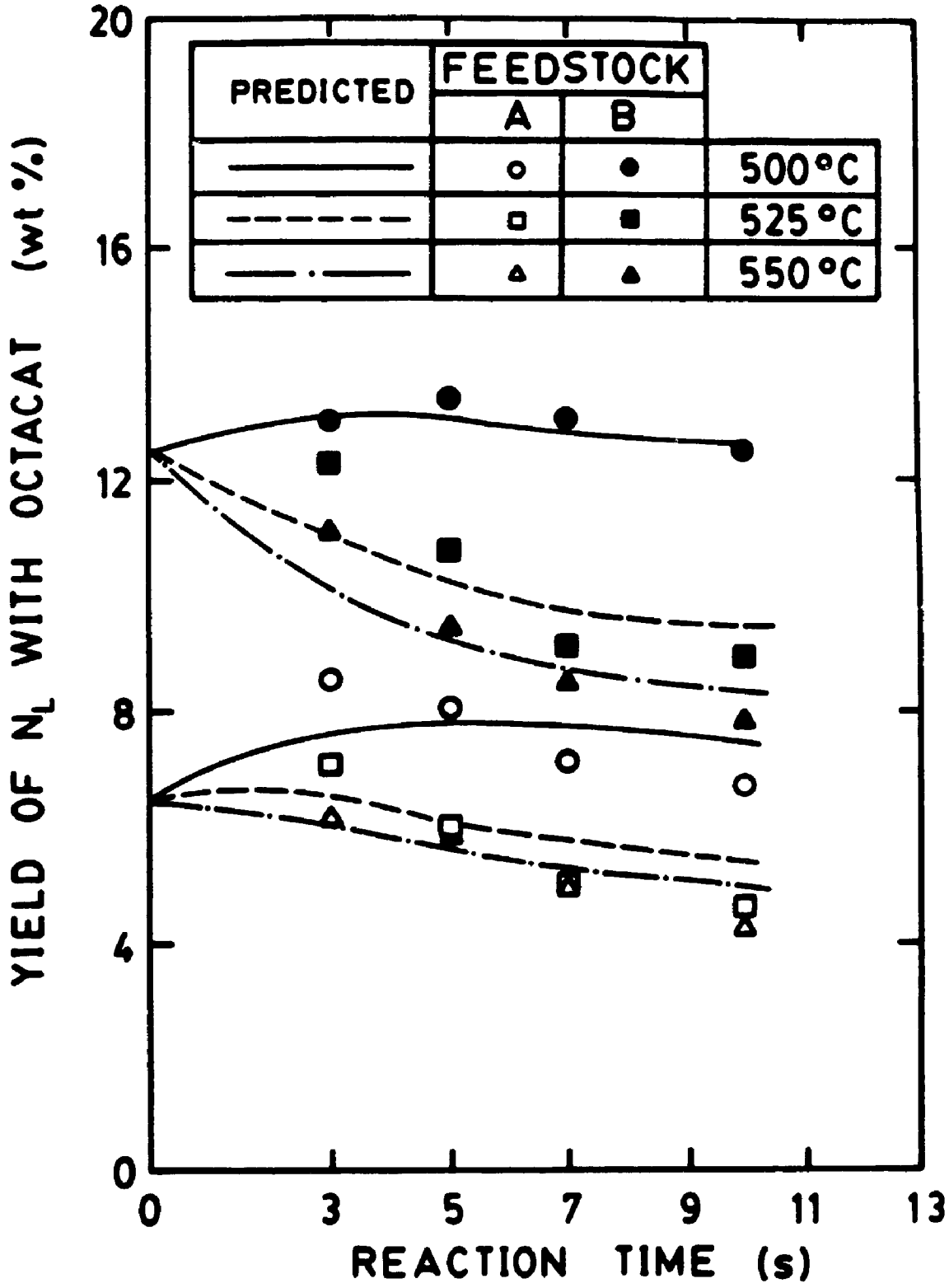

Figure 6.18 Yields of N_l for feedstocks A and B on Octacat as a function of reaction time and temperature.

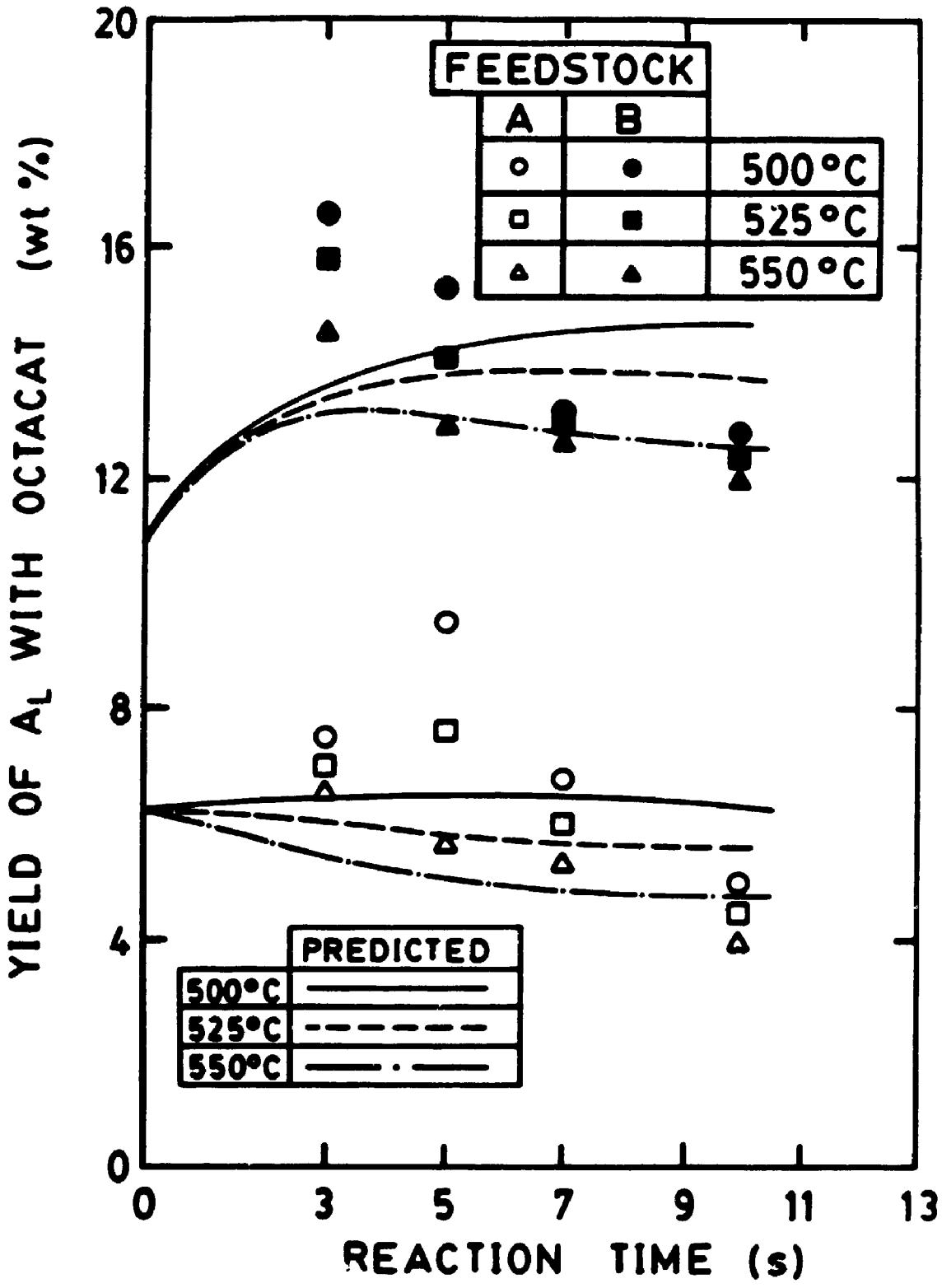

Figure 6.19 Yields of A_l for feedstocks A and B on Octacat as a function of reaction time and temperature.

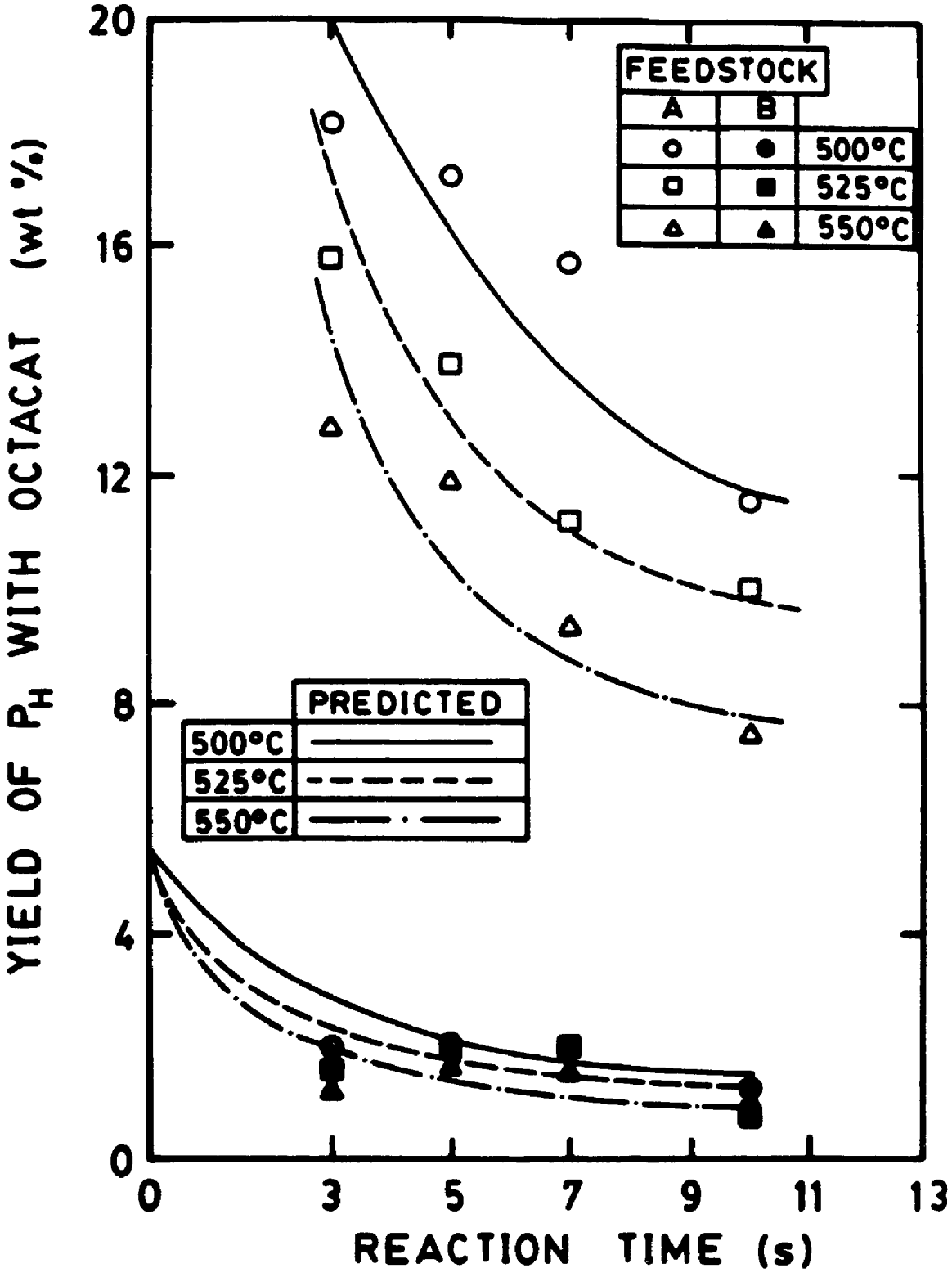

Figure 6.20 Yields of P_h for feedstocks A and B on Octacat as a function of reaction time and temperature.

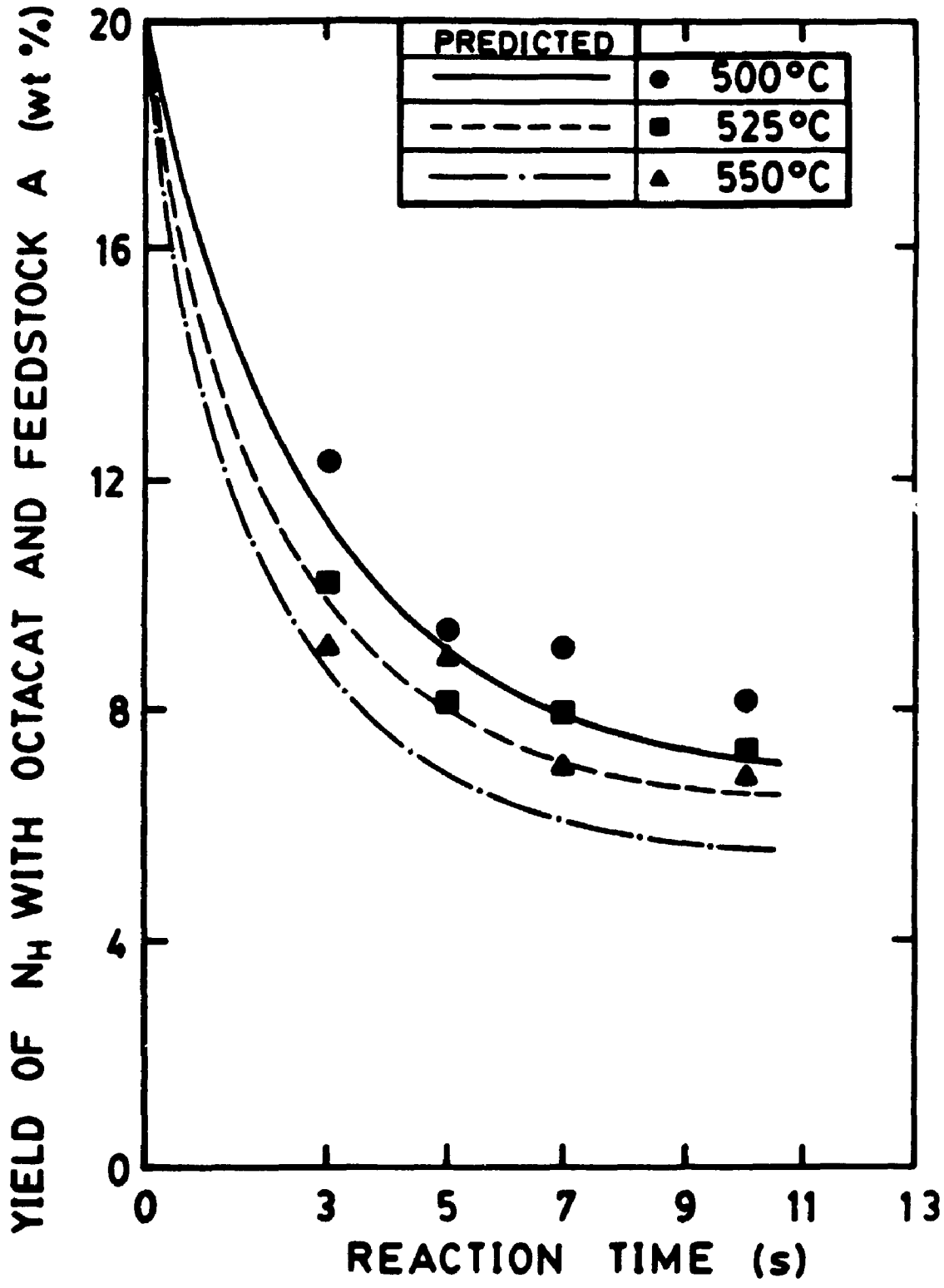

Figure 6.21 Yields of N_h for feedstock A on Octacat as a function of reaction time and temperature.

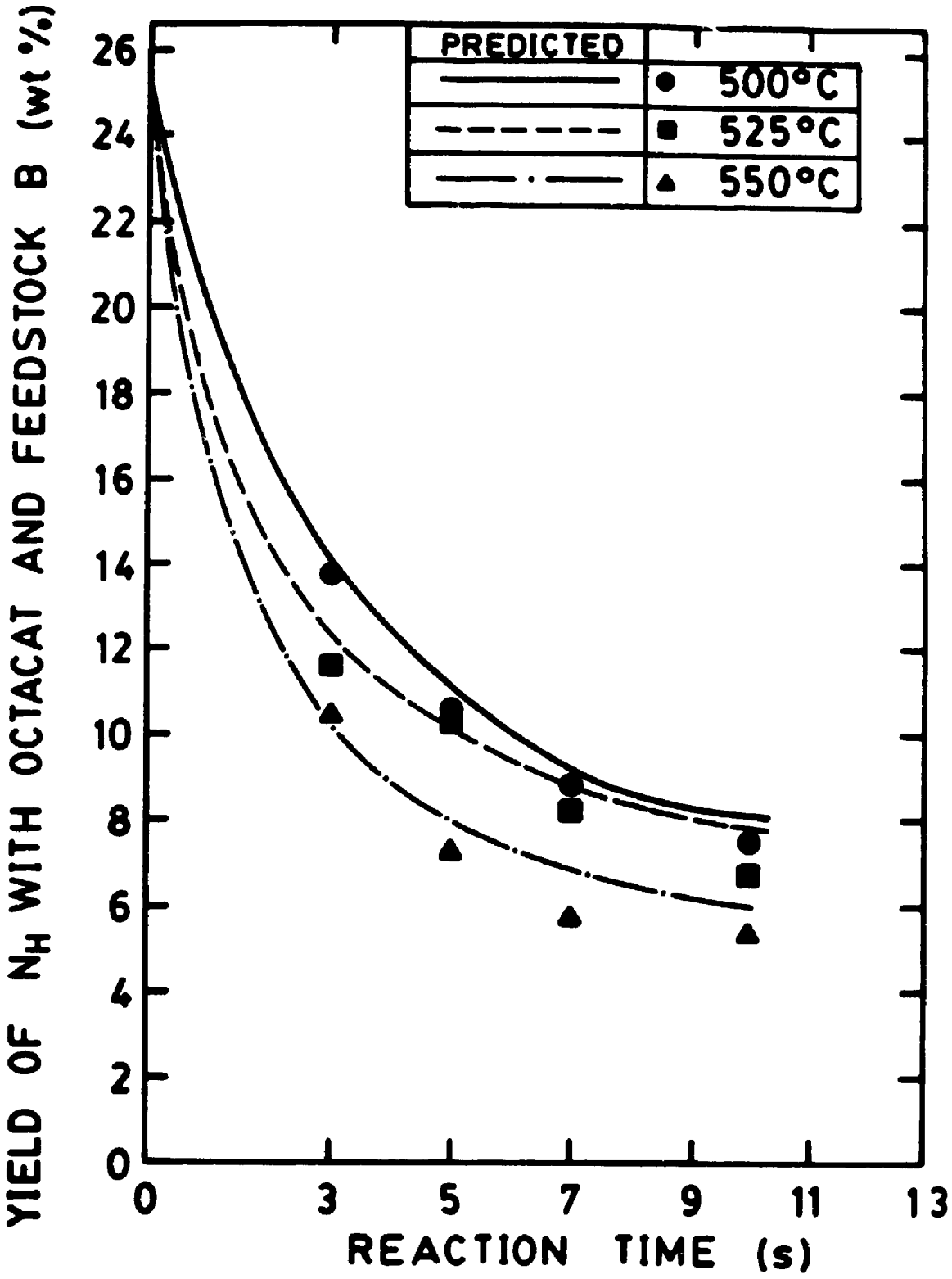

Figure 6.22 Yields of N_h for feedstock B on Octacat as a function of reaction time and temperature.

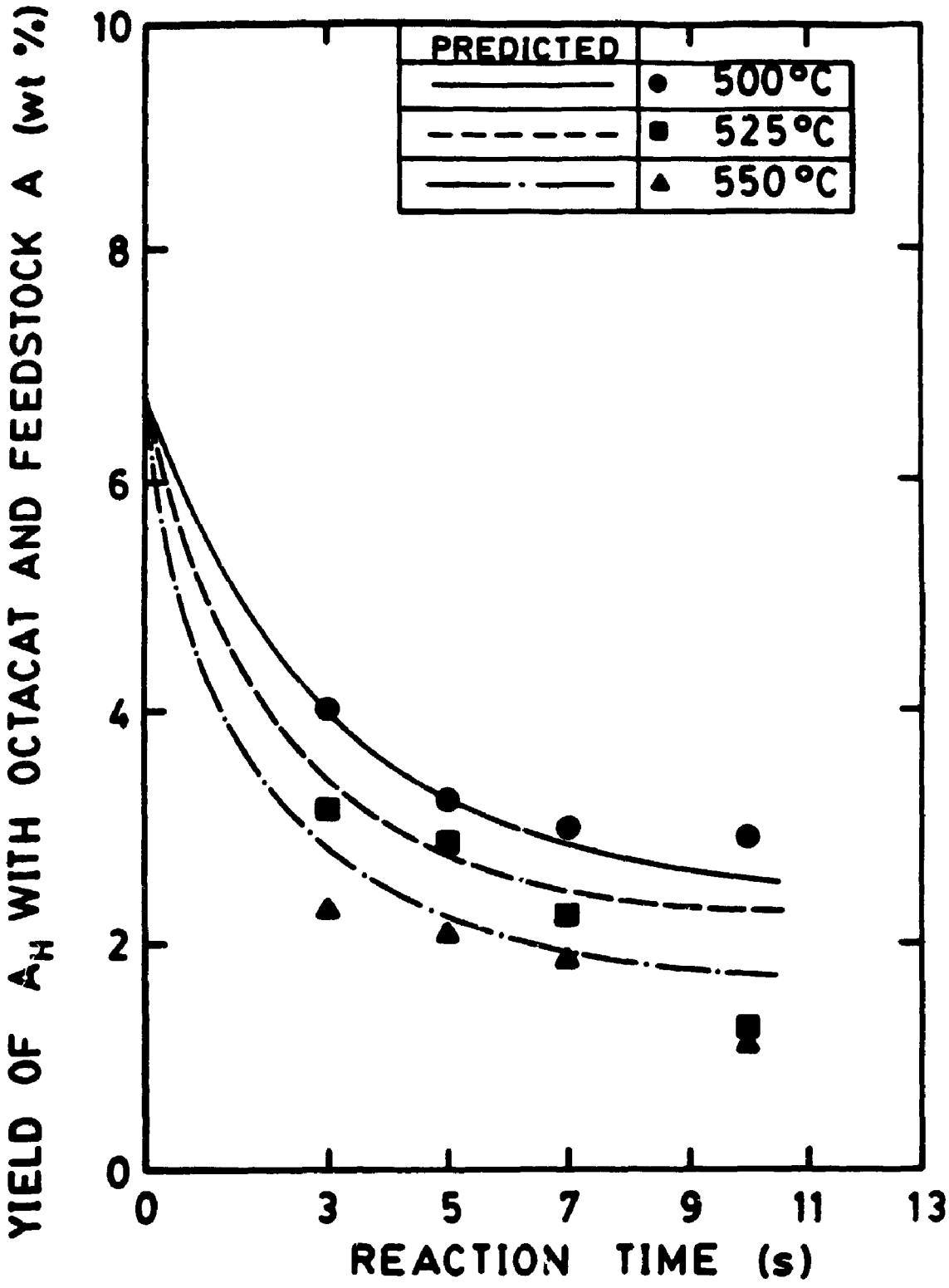

Figure 6.23 Yields of A_h for feedstock A on Octacat as a function of reaction time and temperature.

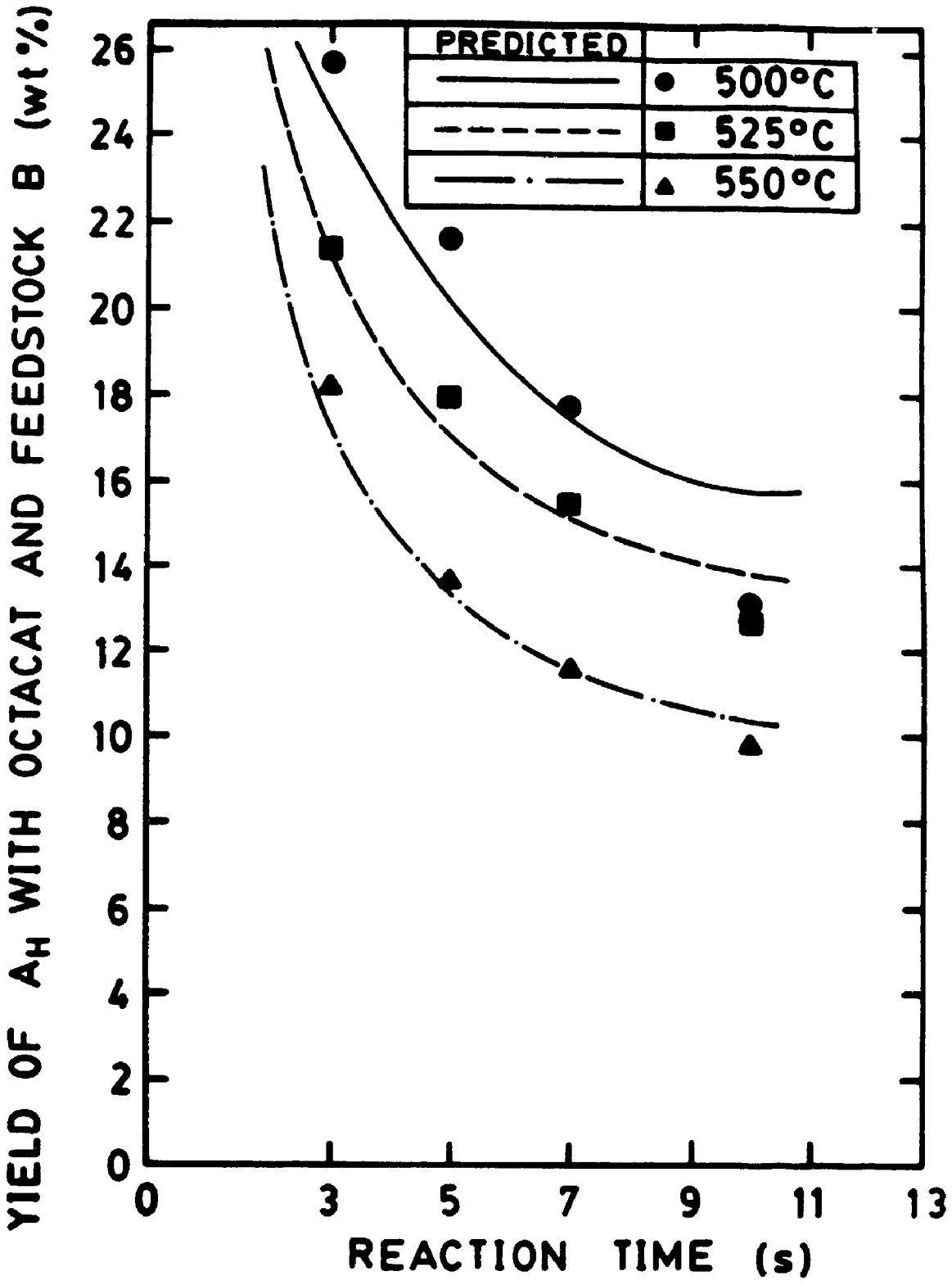

Figure 6.24 Yields of A_h for feedstock B on Octacat as a function of reaction time and temperature.

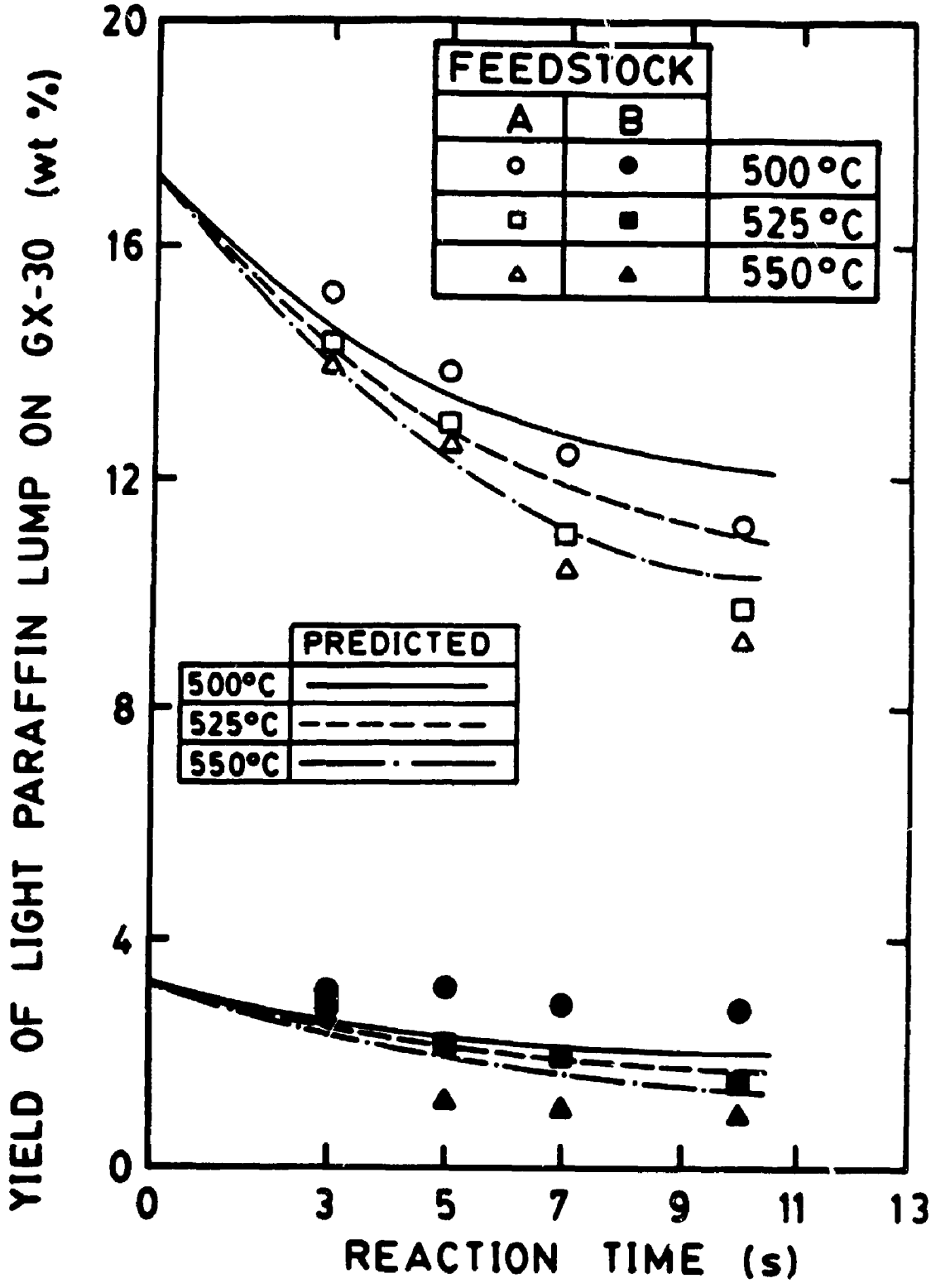

Figure 6.25 Yields of P_l for feedstocks A and B on GX-30 as a function of reaction time and temperature.

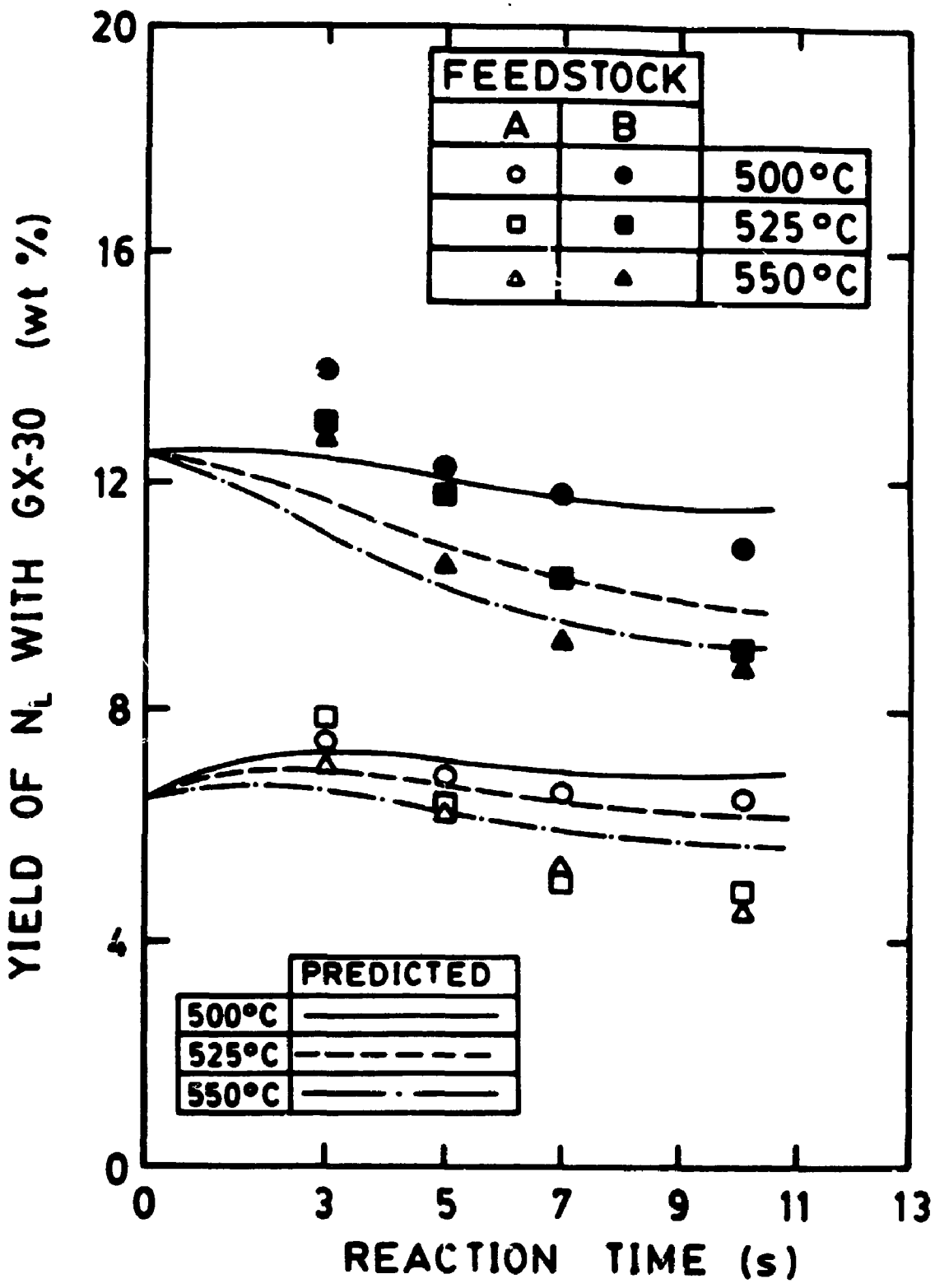

Figure 6.26 Yields of N_l for feedstocks A and B on GX-30 as a function of reaction time and temperature.

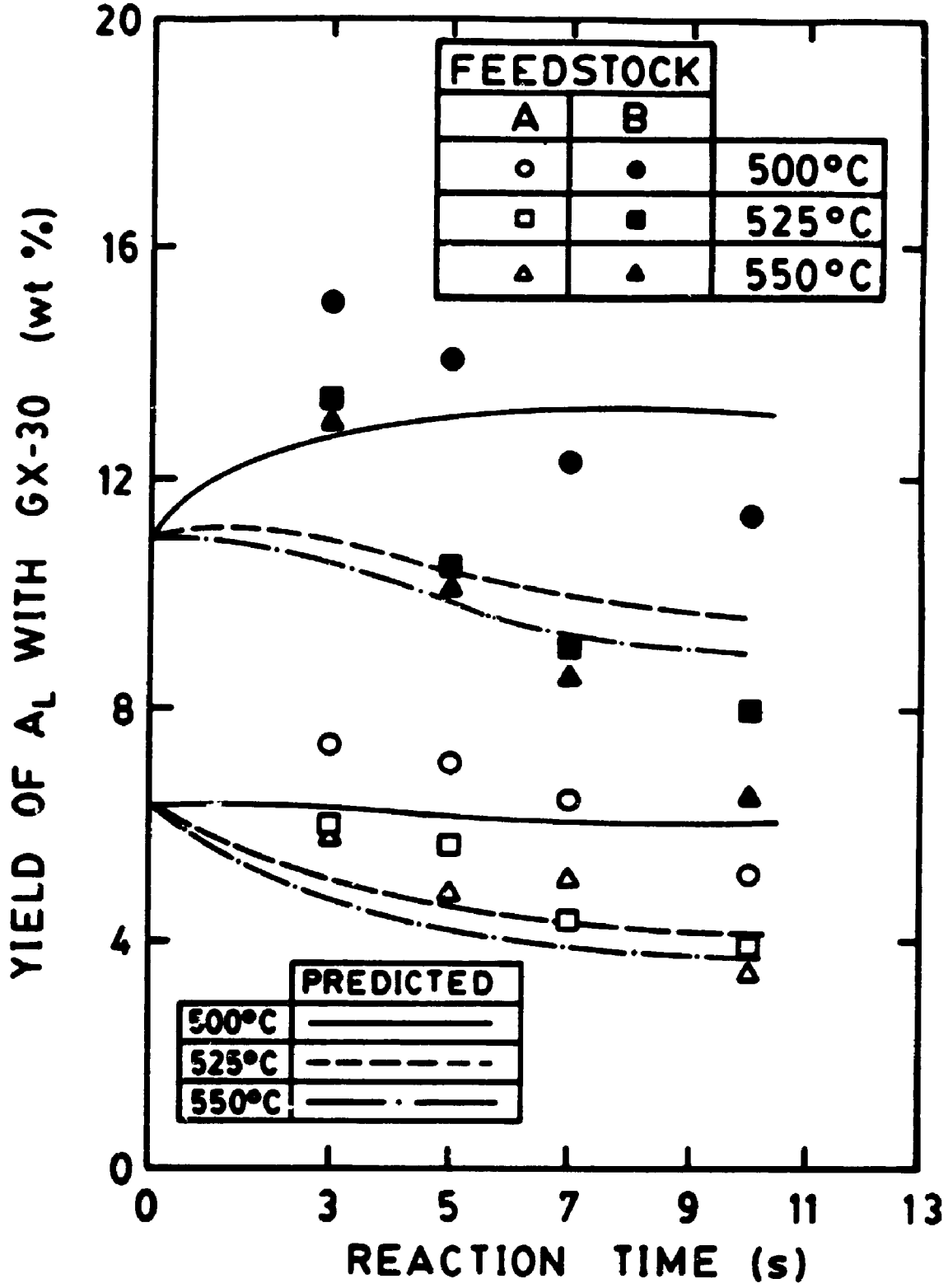

Figure 6.27 Yields of A_l for feedstocks A and B on GX-30 as a function of reaction time and temperature.

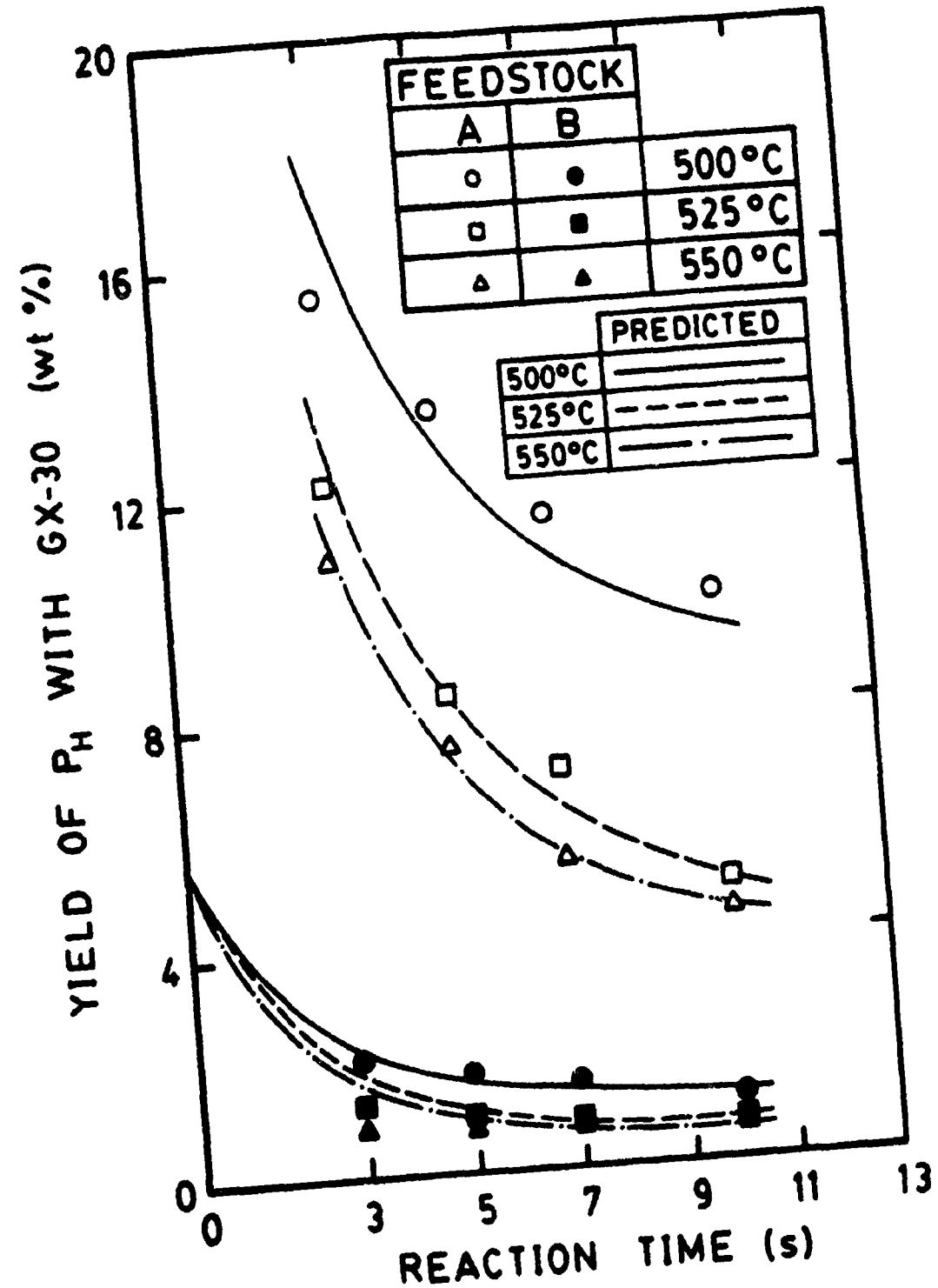

Figure 6.28 Yields of P_h for feedstocks A and B on GX-30 as a function of reaction time and temperature.

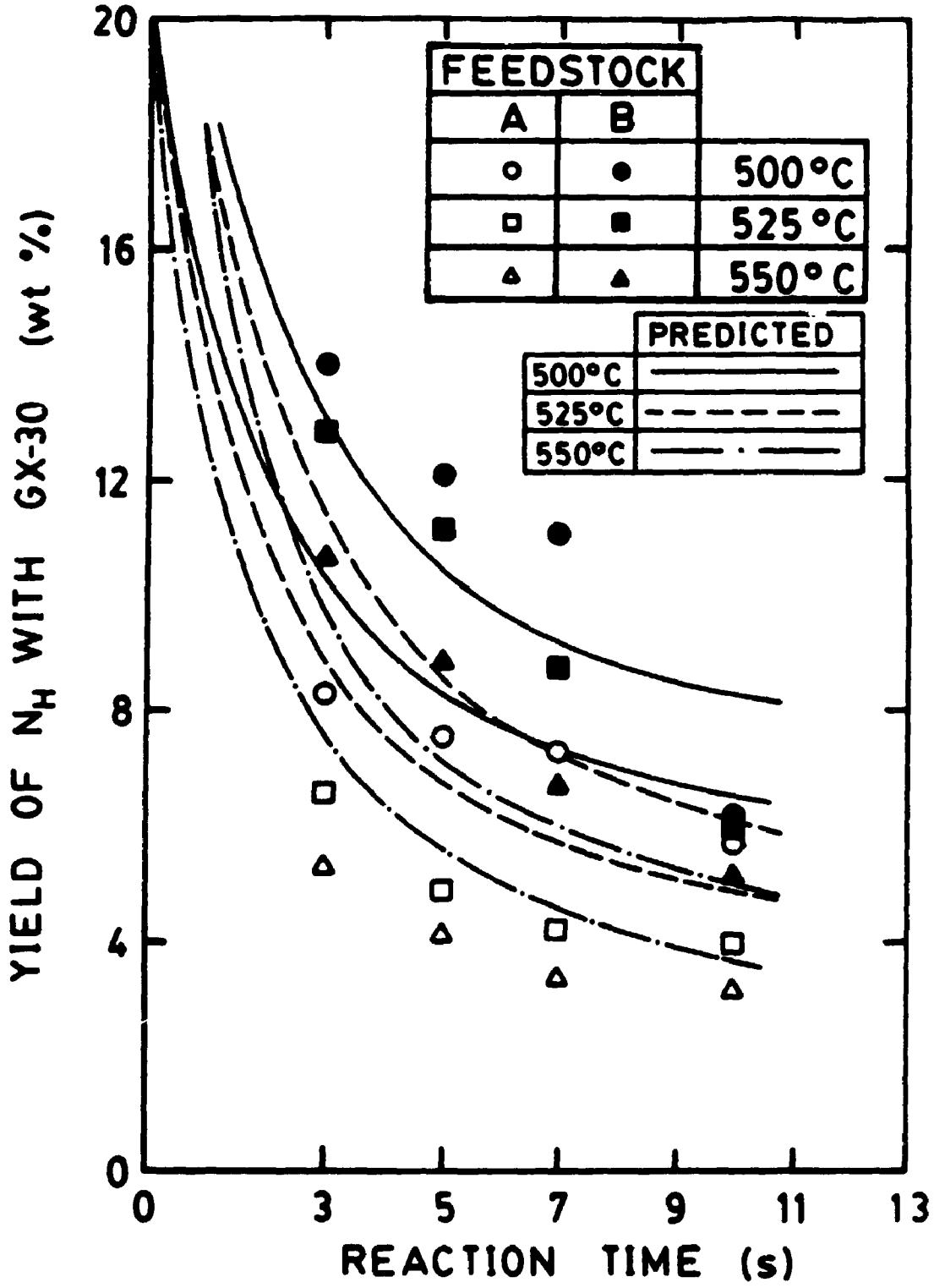

Figure 6.29 Yields of N_h for feedstocks A and B on GX-30 as a function of reaction time and temperature.

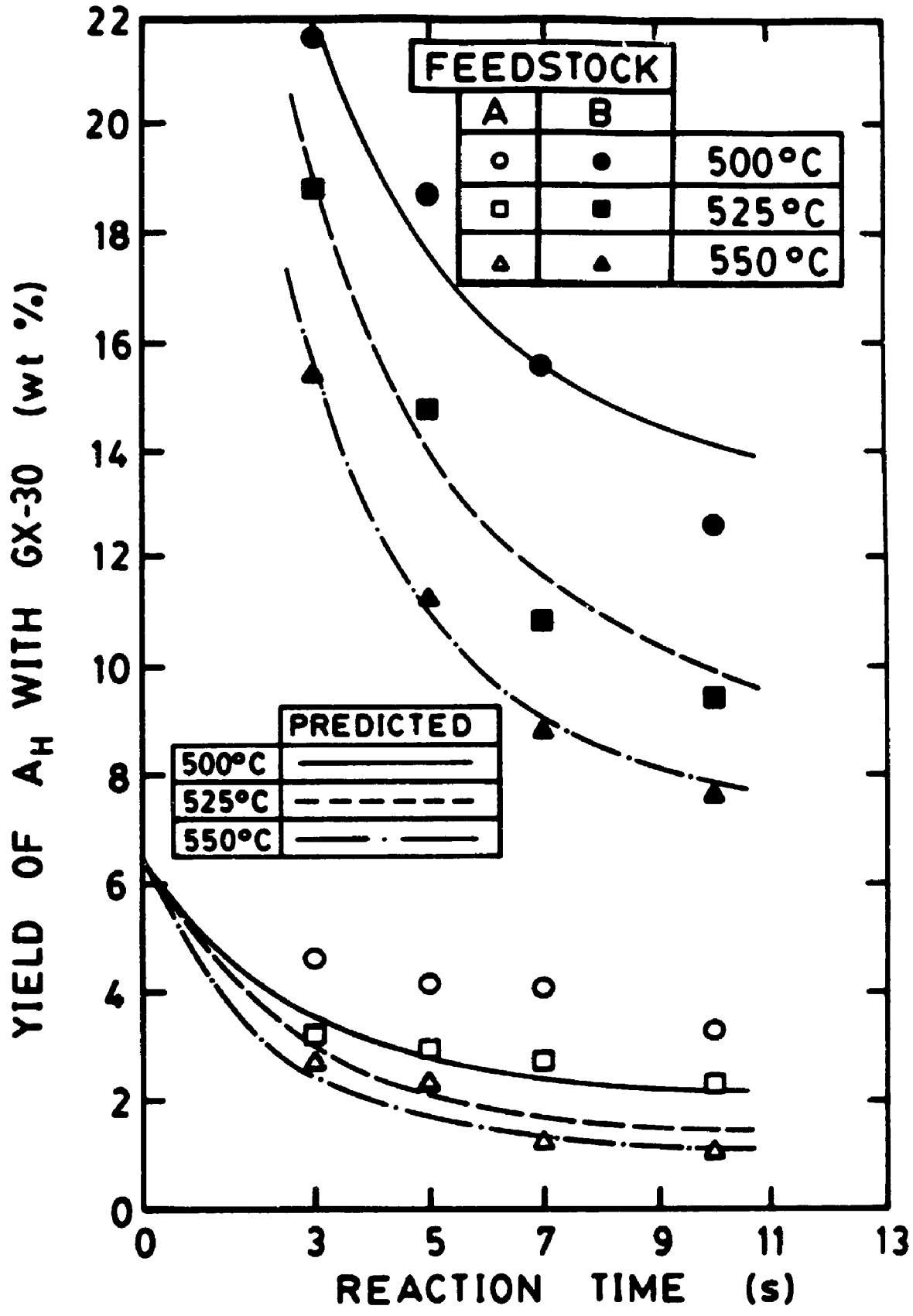

Figure 6.30 Yields of A_h for feedstocks A and B on GX-30 as a function of reaction time and temperature.

for feedstock A which has a higher concentration of light paraffins than feedstock B. It appears that with Octacat catalyst, for the reaction times considered, the net difference between rates of formation and consumption of light paraffins is high enough so that no significant initial increase of the P_l lump is observed as the model suggests and as was found elsewhere (Jacob et al., 1976). This increase in the light paraffins would presumably be observed for reaction times smaller than three seconds.

The pattern for the N_l lump yields , as illustrated in Figure 6.18, showed initial increases with a short reaction time and then decreased as the reaction proceeded. This is due to a fraction of the heavy naphthene group cracking to form compounds in the N_l group which simultaneously are being cracked to gasoline and C-lump. This is consistent with the 8-lump model which accounts for the cracking of heavy lumps into light lumps. When temperature was raised, the initial rise in N_l concentration was not as large and the subsequent decrease with reaction time was more rapid indicating greater reaction rates at the higher temperatures as expected.

The yields of the A_l lump with Octacat catalyst are shown in Figure 6.19 and exhibit similar trends with respect to the ones observed with the N_l lumps. The large initial increase in A_l yields is likely due to the cracking of alkyl aromatics in the heavy aromatic lump to give a more refractory A_l compound. For example, an A_h compound consisting of a three ringed aromatic with a side chain group could crack at the

linkage of the side group to the ring, forming a gasoline compound and a refractory A_l compound (three rings). This refractory A_l species would then not crack as rapidly as other alkyl aromatic A_l molecules resulting in a net reduction of the cracking rate of the A_l lump.

The yields of the heavy lump compounds are shown in Figures 6.20 to 6.24 for the cracking of both feedstocks on Octacat. The continuous decreasing amounts of heavy oil lumps with increasing time were expected since conversion also increases and then levels off as the catalyst becomes coked. The effect of increasing temperature, as discussed before, results in a decrease of the heavy lump yields (i.e. increased conversion). It can also be seen from the yield versus reaction time curves that the heavy lumps decreased more sharply than the light lumps indicating higher overall cracking rates for longer chain molecules.

The compositional changes of the two feedstocks cracked on GX-30 are traced in Figures 6.25 to 6.30 where again each oil lump is plotted versus reaction time for the three temperatures. The same general trends for product yields with temperature and reaction time as discussed for Octacat catalyst were also observed with GX-30.

6.3 CRACKING OF PURE HYDROCARBON MIXTURES

In addition to the two commercial feedstocks cracked in the present study, mixtures of pure hydrocarbons were prepared (as discussed in Chapter 5) to simulate the three light oil lumps (P_l, N_l, and A_l). These mixtures were cracked in the Riser Simulator to reduce the number of data points necessary with just two feedstocks to solve the equations for the 8-lump model. The conditions used were reaction times of 3, 5, 7 and 10 seconds at temperatures of 500 and 550°C using both Octacat and GX-30 catalysts.

6.3.1 Conversion

Tabulated results for the conversion and yields of the pure mixtures cracked on the two catalysts are shown in Tables 6.9 to 6.14. Plots of conversion versus reaction time and temperature for the three pure lump mixtures are shown in Figures 6.31 to 6.33. For all three pure mixtures the conversion was greater when cracked with GX-30 catalyst as compared to Octacat at 500°C. At 550°C this was also true except for the light paraffins which showed a higher conversion when cracked with Octacat than with GX-30. This suggests a higher activation energy for the pure light paraffins when cracked with Octacat. The fact that conversion in general, with the only exception of light paraffins at 550°C, is higher with GX-30 as compared to Octacat can be

Table 6.9 Summary of average yields and conversions for the cracking of the pure P_1 mixture with Octacat catalyst (c/o = 5.17).

		wt%				
T(°C)	t_R(s)	coke	Gases	Gasoline	Conversion	Sel.*
500	3	1.26	19.12	22.46	42.84	52.4%
	5	1.68	28.29	28.74	58.71	48.2%
	7	2.71	31.65	32.15	66.51	47.8%
	10	3.26	38.55	36.72	78.53	46.8%
550	3	1.32	36.65	22.15	60.12	36.8
	5	2.33	45.81	27.04	75.18	35.9
	7	2.81	51.68	28.26	82.75	34.2
	10	3.67	57.48	28.47	89.62	31.8

* Selectivity to gasoline = wt% gasoline / wt% conversion

Table 6.10 Summary of average yields and conversions for the cracking of the pure P_1 mixture with GX-30 catalyst (c/o = 5.17).

		wt%				
T(°C)	t_R(s)	coke	Gases	Gasoline	Conversion	Sel.*
500	3	0.8	27.25	24.64	52.51	46.6%
	5	1.46	32.81	28.29	62.56	45.2%
	7	3.45	34.10	31.47	69.02	45.6%
	10	4.32	36.45	33.10	73.87	44.8%
550	3	1.0	37.07	23.24	61.31	37.9%
	5	2.91	40.26	25.12	68.29	36.8%
	7	4.36	41.51	26.45	72.32	36.6%
	10	5.01	42.19	27.88	75.08	37.1%

* Selectivity to gasoline = wt% gasoline / wt% conversion

Table 6.11 Summary of average yields and conversions for the cracking of the pure N_1 mixture with Octacat catalyst (c/o = 4.5).

		wt%				
T(°C)	t_R(s)	coke	Gases	Gasoline	Conversion	Sel.*
500	3	1.67	17.09	26.97	45.73	59.0%
	5	2.12	17.95	28.73	48.80	59.0%
	7	2.22	20.78	35.34	58.34	60.6%
	10	3.40	27.30	40.95	71.65	57.1%
550	3	0.65	20.77	32.63	54.05	60.4%
	5	0.80	26.19	37.21	64.20	58.0%
	7	0.81	27.46	41.80	70.07	59.7%
	10	1.31	32.51	42.68	76.50	55.8%

* Selectivity to gasoline = wt% gasoline / wt% conversion

Table 6.12 Summary of average yields and conversions for the cracking of the pure N_1 mixture with GX-30 catalyst (c/o = 4.5).

		wt%				
T(°C)	t_R(s)	coke	Gases	Gasoline	Conversion	Sel.*
500	3	3.13	7.16	47.02	57.31	82.0%
	5	3.8	7.69	50.78	62.27	81.5%
	7	4.2	9.09	56.08	69.37	80.8%
	10	4.84	11.81	57.21	73.86	77.5%
550	3	1.60	17.32	49.33	68.25	72.3%
	5	2.11	18.81	51.59	72.51	71.1%
	7	2.17	19.45	53.35	74.97	71.2%
	10	2.29	24.43	55.34	82.06	67.4%

* Selectivity to gasoline = wt% gasoline / wt% conversion

Table 6.13 Summary of average yields and conversions for the cracking of the pure A_1 mixture with Octacat catalyst (c/o = 4.35).

		wt%				
T(°C)	t_R(s)	coke	Gases	Gasoline	Conversion	Sel.*
500	3	0.64	10.26	21.95	32.85	66.8%
	5	0.98	12.71	30.35	44.04	68.9%
	7	1.01	14.42	31.09	46.52	66.8%
	10	1.2	15.46	32.22	48.88	65.9%
550	3	0.55	12.21	25.52	38.28	66.7%
	5	0.6	13.75	33.55	47.90	70.0%
	7	1.13	14.76	35.10	50.99	68.8%
	10	1.52	16.74	33.75	52.01	64.9%

* Selectivity to gasoline = wt% gasoline / wt% conversion

Table 6.14 Summary of average yields and conversions for the cracking of the pure A_1 mixture with GX-30 catalyst (c/o = 4.35).

		wt%				
T(°C)	t_R(s)	Coke	Gases	Gasoline	Conversion	Sel.*
500	3	2.56	7.94	39.82	50.32	79.1%
	5	3.01	8.21	45.62	56.84	80.3%
	7	3.67	8.95	47.43	60.05	79.0%
	10	4.21	10.93	48.94	64.08	76.4%
550	3	2.94	12.77	43.42	59.13	73.4%
	5	3.39	12.78	46.21	62.38	74.1%
	7	4.18	13.48	48.07	65.73	73.1%
	10	4.98	15.29	48.82	69.09	70.7%

* Selectivity to gasoline = wt% gasoline / wt% conversion

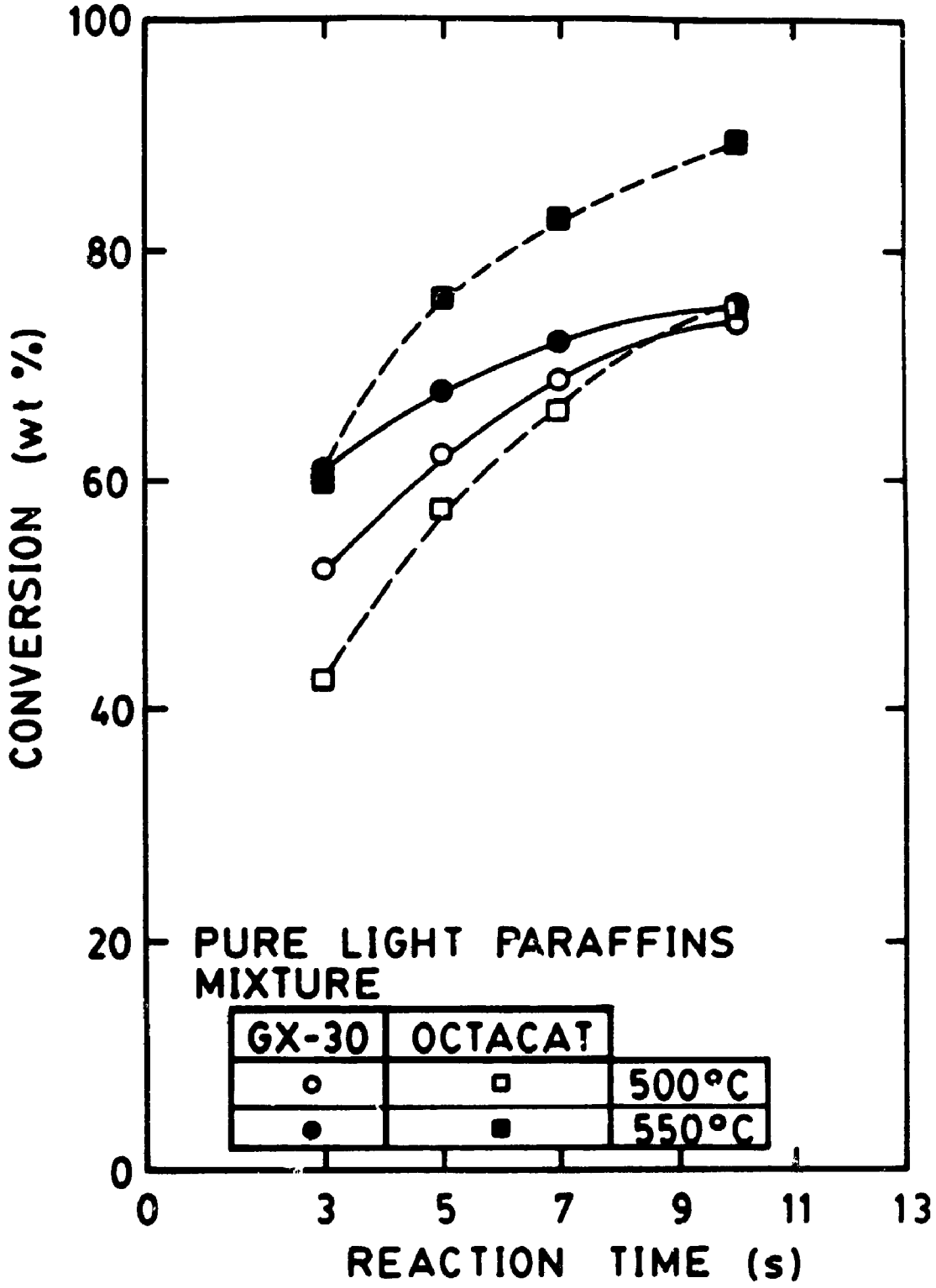

Figure 6.31 Conversions for the pure P_l mixture as a function of reaction time and temperature.

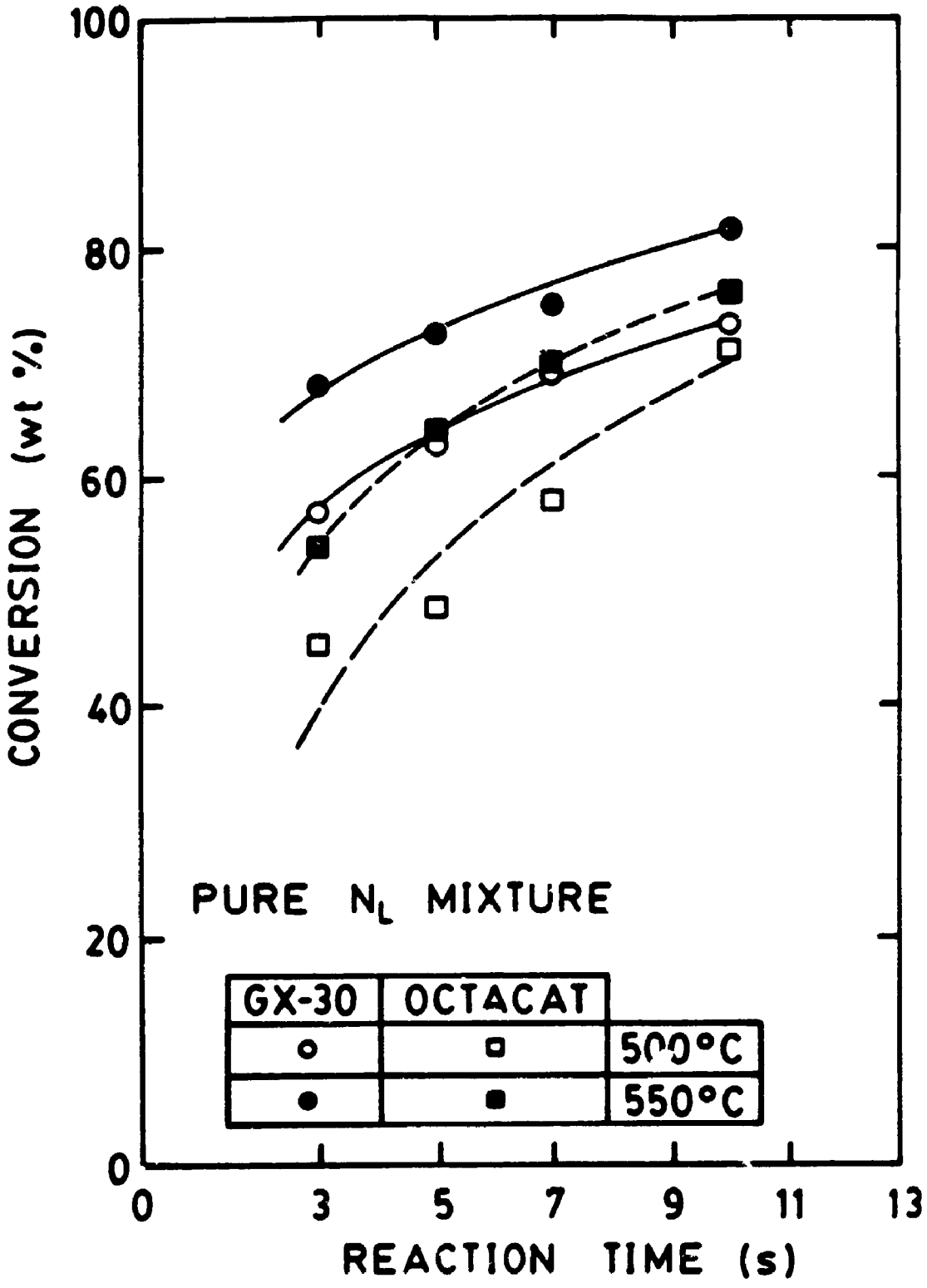

Figure 6.32 Conversions for the pure N_l mixture as a function of reaction time and temperature.

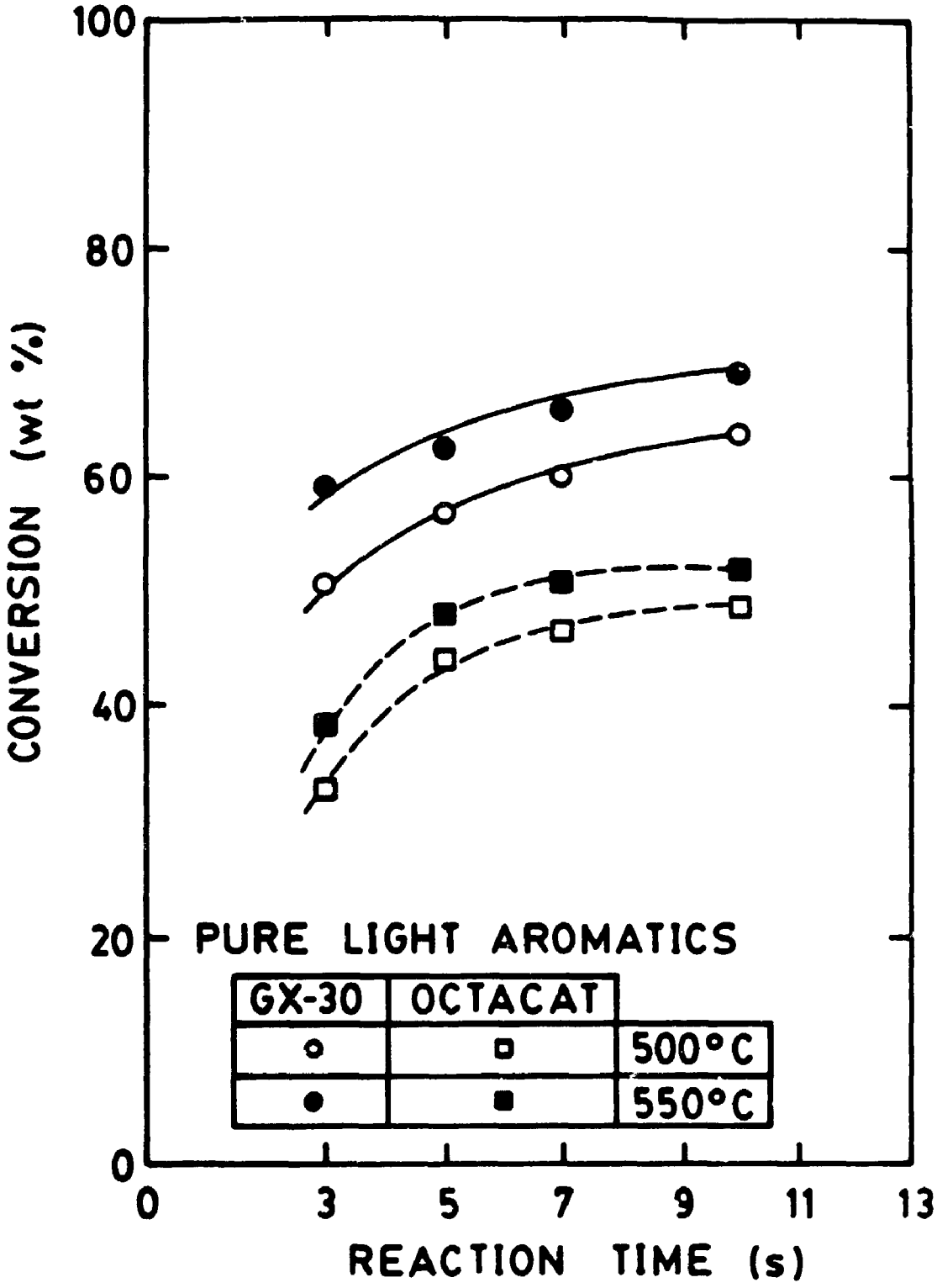

Figure 6.33 Conversions for the pure A_l mixture as a function of reaction time and temperature.

related to the unit cell size. As the unit cell size decreases (Si/Al ratio increases) the catalytic conversion or catalyst activity decreases (Scherzer, 1989). Therefore, since GX-30 has a larger unit cell size than Octacat, one would expect higher conversions for GX-30, as is the case in this study.

Comparing the different 'crackabilities' of the three pure lumps with GX-30 it is evident that the pure light naphthenes achieved higher conversions for both temperatures studied, with light paraffins next then the light aromatics. It has been reported (Decroocq, 1984) that naphthenes and alkyl aromatics crack more readily than paraffins although for paraffins and naphthenes of the same carbon number the rates are similar (Greensfelder et al., 1949). In this study the aromatic mixture contained a combination of aromatic compounds including alkyl aromatics and bare ring aromatics as discussed in Chapter 5. The bare rings are more difficult to crack thus the combined mixture of bare rings and rings with substituent groups would have a lower cracking rate than what could be expected with just pure alkyl aromatics (Greensfelder et al., 1945). This explains the result that the paraffins showed a higher conversion than the aromatics with GX-30 catalyst.

For Octacat, the pure light paraffins showed higher conversions than the pure light naphthenes or the aromatics with the aromatics being the least reactive. This observation may suggest that diffusional controls become important with Octacat catalyst where more bulky molecules, such as

naphthenes and aromatics have difficulty in moving through the fine porous networks of the catalyst.

6.3.2 Product Yields and Selectivity

The product yields for the three pure light mixtures are shown in Figures 6.34 through to 6.39 for both catalysts used. Referring to Figures 6.34 and 6.35 for the pure light paraffins, the gasoline yields decreased as the temperature was increased from 500 to 550°C for both catalysts. As well, the slope of the gasoline yield versus time curve became more flat at the higher temperature level indicating the increased overcracking of gasoline and the shift in product selectivity. This drop in gasoline selectivity with temperature is quite sharp as can be seen in Table 6.9 where the selectivity drops by an average of approximately 15% with Octacat catalyst and by 9% with GX-30 (Table 6.10).

The yields of gasoline for the light naphthenes on Octacat as indicated in Figure 6.36 showed an increase when the temperature was increased from 500°C to 550°C. As well, at the higher temperature, the gasoline yields decreased more sharply with increasing reaction time than at the lower temperature level. These same trends were observed with the pure light aromatics cracked with Octacat catalyst (Figure 6.38). However, for both the pure light naphthenes and aromacics cracked with GX-30, the gasoline yields at 550°C were slightly higher at low reaction times but then dipped

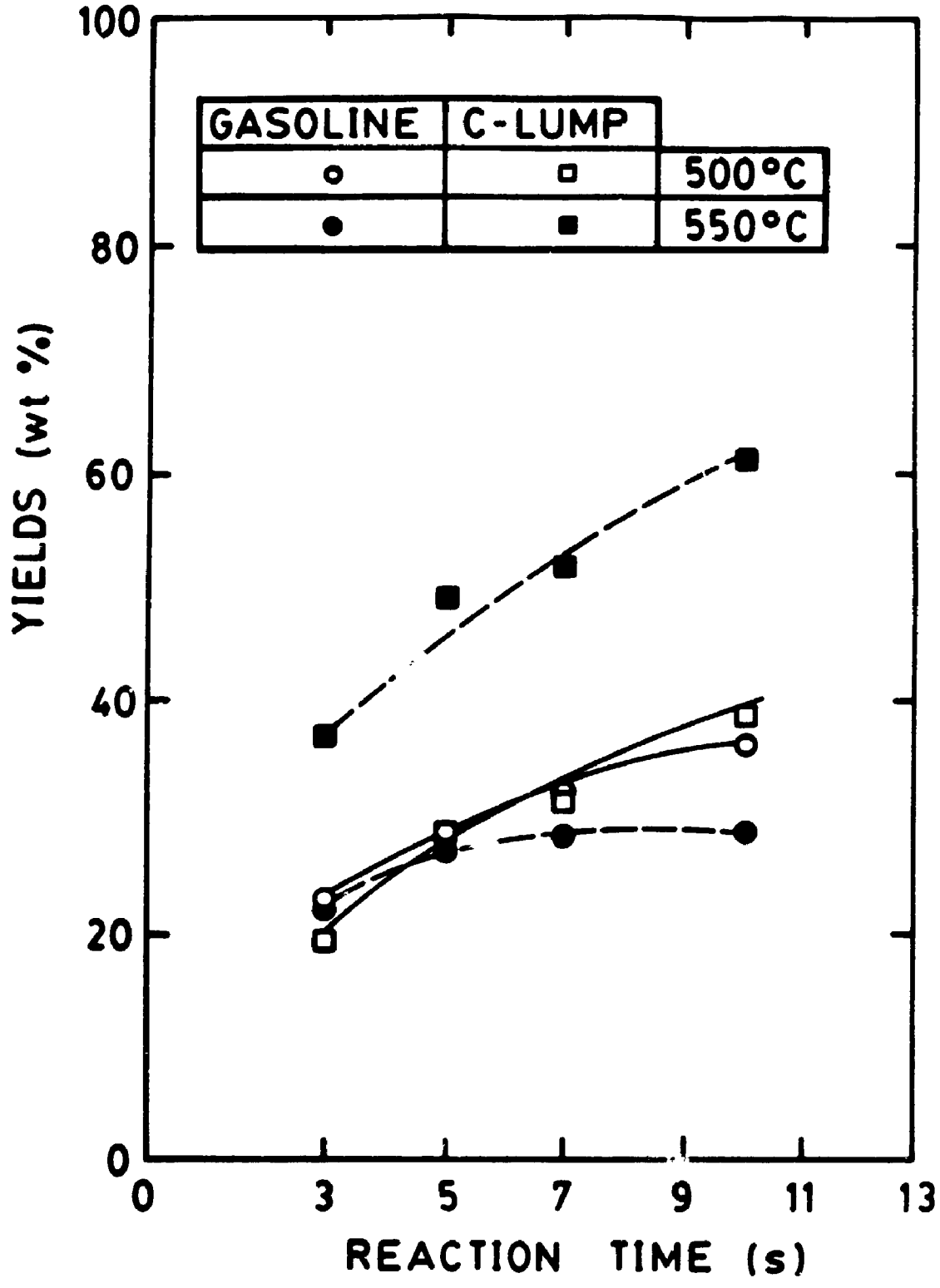

Figure 6.34 Product yields for the pure P_t mixture with Octacat as a function of reaction time and temperature.

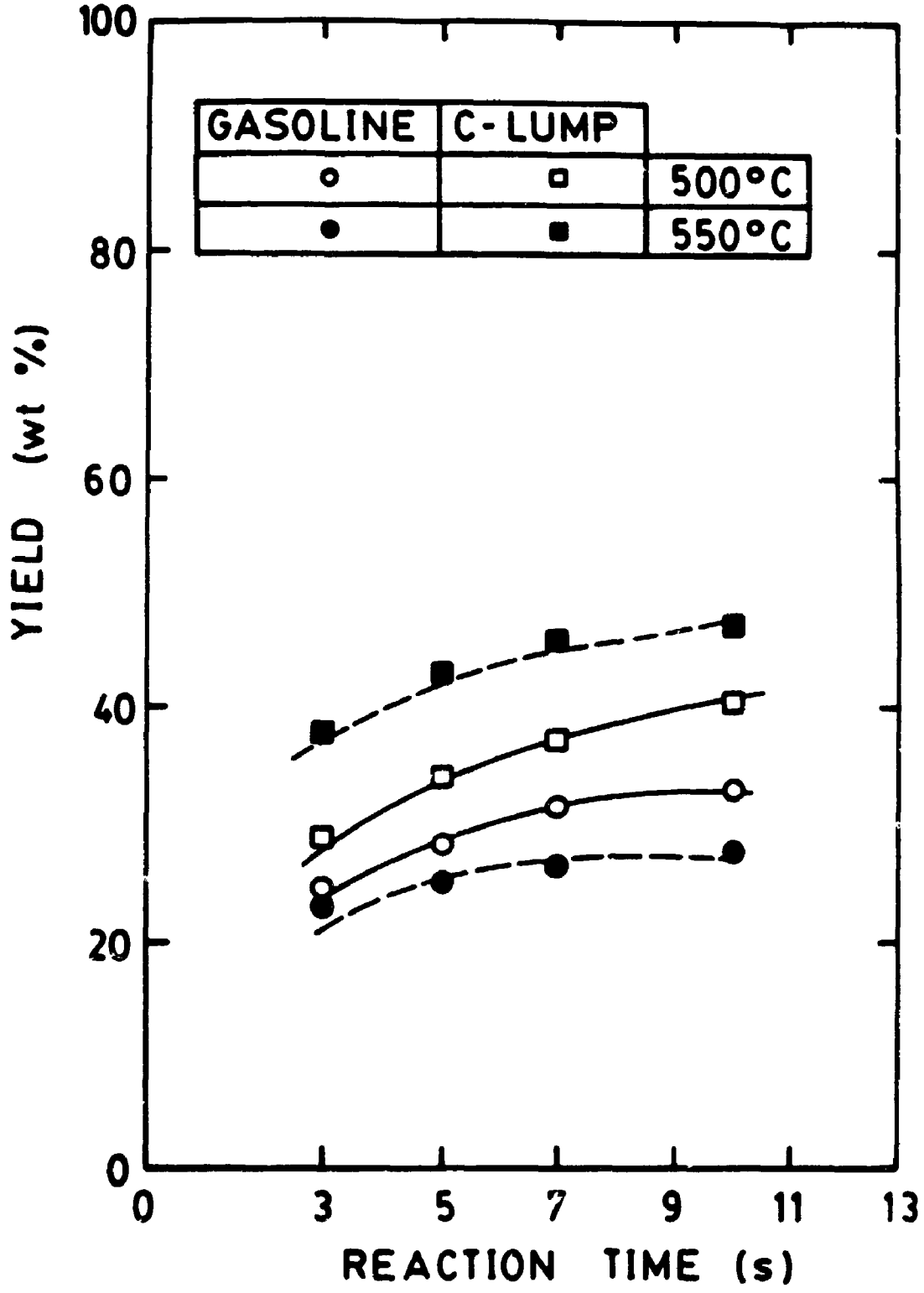

Figure 6.35 Product yields for the pure P_1 mixture with GX-30 as a function of reaction time and temperature.

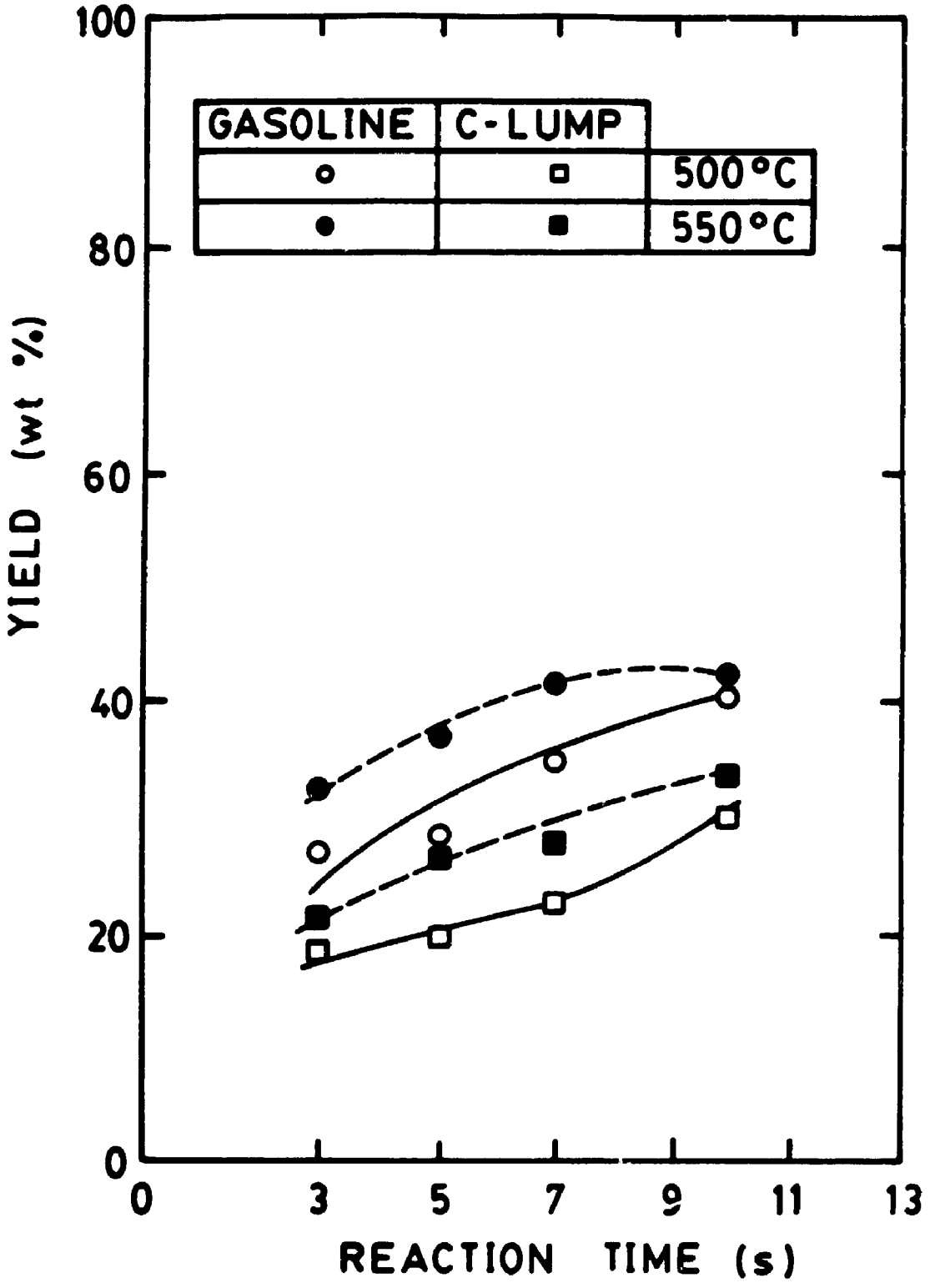

Figure 6.36 Product yields for the pure N_l mixture with Octacat as a function of reaction time and temperature.

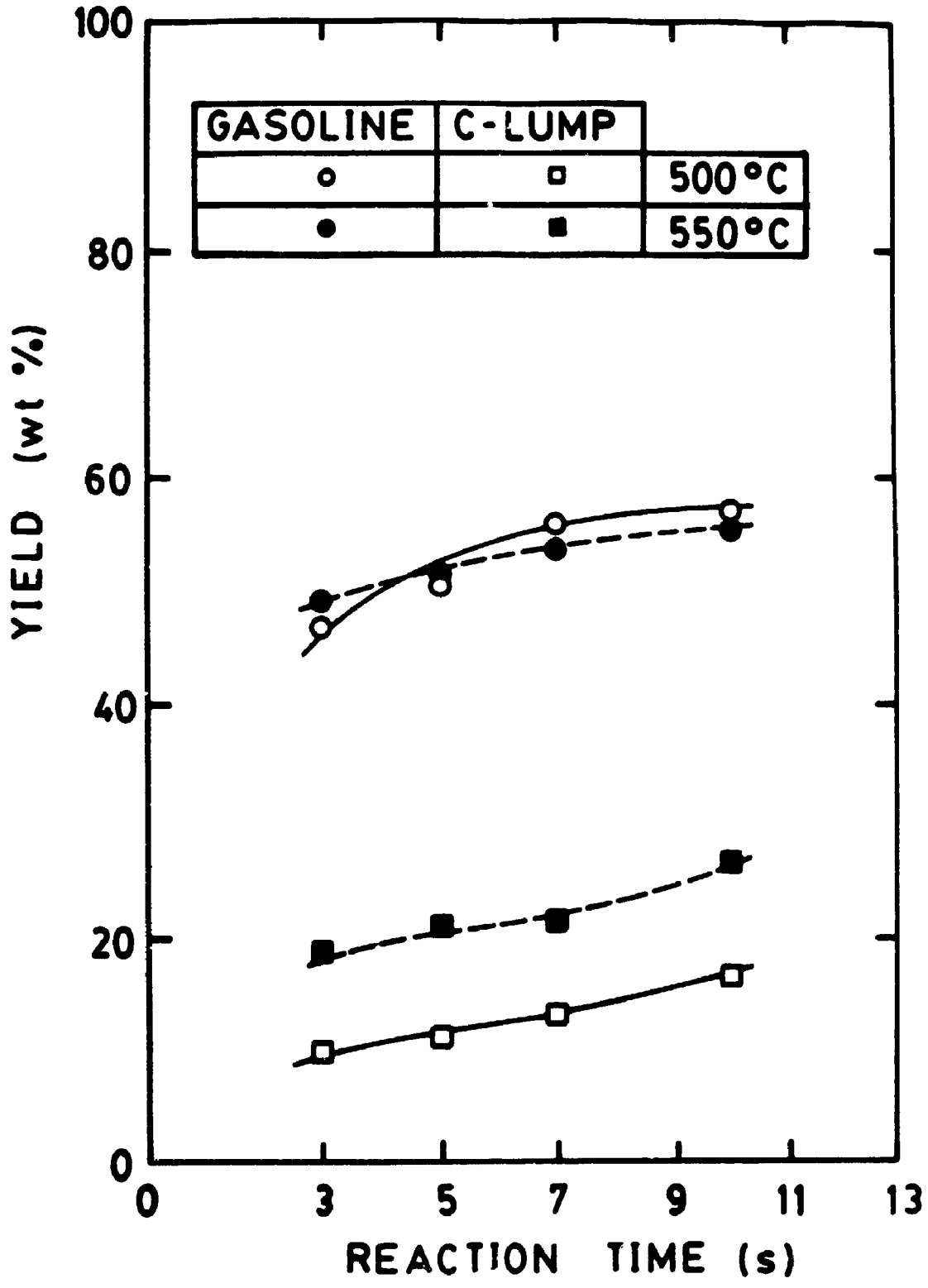

Figure 6.37 Product yields for the pure N_1 mixture with GX-30 as a function of reaction time and temperature.

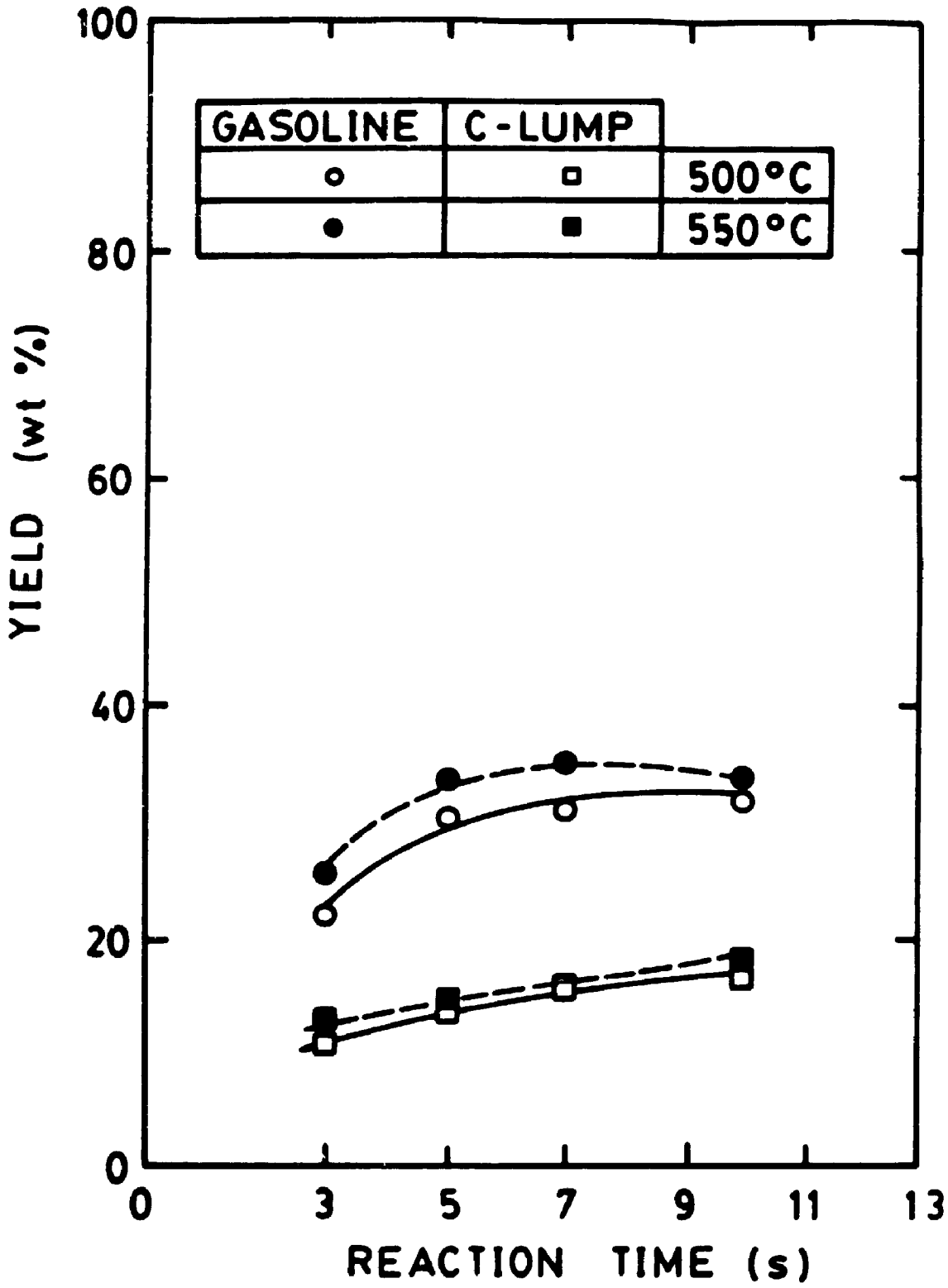

Figure 6.38 Product yields for the pure A_1 mixture with Octacat as a function of reaction time and temperature.

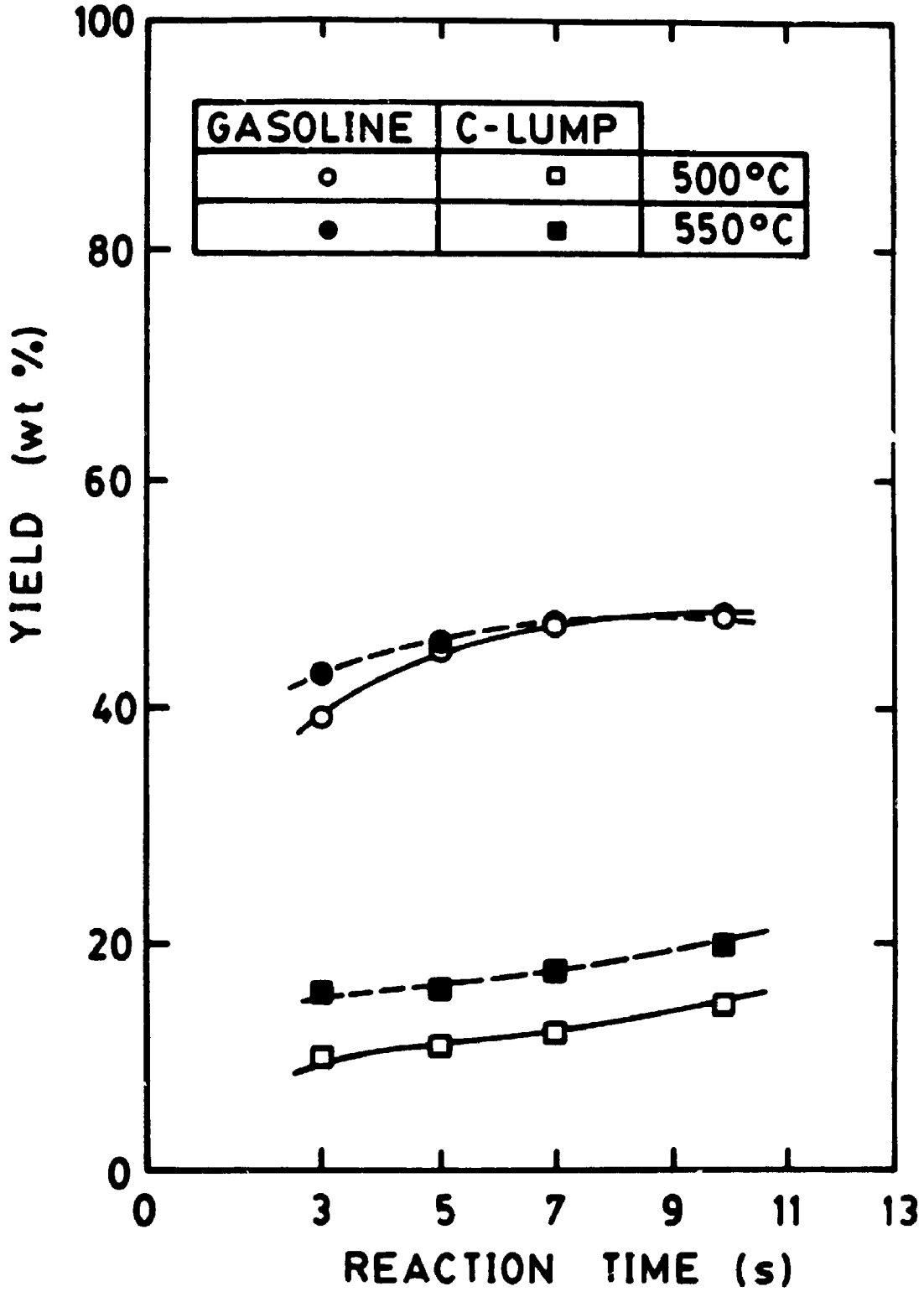

Figure 6.39 Product yields for the pure A_1 mixture with GX-30 as a function of reaction time and temperature.

below the yields obtained at 500°C for higher reaction times. This is a result of conversion being higher for the GX-30 catalyst and shows that the extent of gasoline overcracking also depends on the conversion level.

It is also interesting to observe the effect of catalyst on gasoline selectivity. The selectivity was higher for GX-30 catalyst than Octacat for the pure naphthenes and aromatics as seen in Tables 6.11 to 6.14. The light paraffins showed slightly lower selectivity with GX-30 compared to Octacat at 500°C at 550°C higher values were observed with GX-30. The fact that gasoline selectivity was poorer with Octacat is consistent with the fact that lower unit cell sized catalysts tend to promote free radical cracking relative to hydrogen transfer reactions, hence producing more light gases (Scherzer, 1989). In addition, the effect of temperature on selectivity was more pronounced with the GX-30 catalyst than with the Octacat catalyst, which is to say that selectivity dropped with an increase in temperature from 500°C to 550°C. Also, selectivity values were much higher for the pure light naphthenes and aromatic mixtures than for the pure paraffins.

Another general observation can be made regarding the effect of catalyst on coke yields for the pure light mixtures. The coke yields are tabulated in Tables 6.9 to 6.14 and it can be seen that in general coke yields are lower for the Octacat catalyst. These results are in line with those obtained with the commercial feedstocks and are attributed to the effect of unit cell size as explained previously.

6.4 KINETIC PARAMETERS FOR THE THREE LUMP MODEL

To describe the kinetics of catalytic cracking the three lump model was used in combination with three different catalyst deactivation models as discussed in Chapter 1. Summaries of the overall gas oil cracking kinetic constants (k_o or k_o') along with the decay parameters for the three decay models used are shown in Tables 6.15 to 6.18, for the four feedstock-catalyst combinations. These constants were obtained by solving the gas oil mass balance equation for the three lump model (see equation 3.5). For the case where the power law decay equation was used, the overall gas oil cracking constant was called k_o' since it has different units than k_o (equation 3.10).

Examining the kinetic values it can be seen that the k_o values are of a similar order of magnitude for the three separate decay models used. The values of k_o for the exponential decay law case were consistently lower than those values of k_o from the Froment-Bischoff (F-B) model. However, the differences between these values are not significant, which can be concluded through the 95% confidence intervals for each k_o value. For instance, referring to Table 6.15 the value of k_o (evaluated with feedstock A and Octacat catalyst at 500°C for the exponential decay case) has a value ranging from 0.845 to 1.305 $m^6/(kg_{mol}.kg_{cat}.s)$. For the F-B decay case k_o has a confidence interval between 0.924 to 1.564. This overlap means that the two values are not significantly

temperature. The dicyclohexyl and 1,5,9-cyclododecatriene were added in excess amounts to help dissolve the other two solids. In this way 10 mL each of dicyclohexyl and cyclododecatriene were added to approximately 2.5 g each of tricyclodecane and cyclododecane to make up the N_l mixture.

The classification of light aromatic compounds in the 220°C to 345°C range includes completely unsaturated ring compounds or in general any compound containing a benzene ring. This includes rings with long paraffin chains and/or cyclic alkanes attached. For single ring compounds side chains with C_6 up to C_{14} alkanes are possible as well as cyclic side groups. For two ringed compounds side chains with up to 7 carbons atoms are possible. Also present in this boiling range are 3-ringed aromatics with no side groups. Thus a representative sample from each of these possibilities was chosen resulting in six compounds as shown in Table 5.1 for the composition of the A_l oil. The mixture was made by adding 10 mL of each of the liquid compounds (phenylhexane, cyclohexyl-benzene, dimethyl naphthalene isomers and dodecylbenzene) and 10 grams of fluorene and phenanthrene.

The properties of the two commercial feedstocks used are shown in Table 5.2. Feedstock A consists mainly of paraffinic molecules and feedstock B is mainly aromatic. These two gas oils thus gave a different range of oil lump distributions which were used in calculating the kinetic constants for the 8-lump model.

Table 6.15 Overall gas oil cracking kinetic constant for the 3-lump model using 3 different decay functions (feedstock A with Octacat catalyst)

Decay:	$e^{-\alpha t}$		t^{-N}		F-B	
T(°C)	k_o	α	k_o'	N	k_o	k_d
500	1.08 ±0.2	0.12 ±.08	0.89 ±.05	0.32 ±.14	1.24 ±.32	2,818 ±1,784
525	1.65 ±0.2	0.16 ±.12	1.26 ±.08	0.40 ±.17	2.09 ±.4	4,752 ±3,147
550	2.26 ±.29	0.19 ±.09	1.60 ±.08	0.42 ±.11	3.02 ±.41	6,652 ±2,800
-----	-----		-----		-----	
E_A:	18.84		14.81		22.45	

units of k_o: $(m^6/kgmol.kg_{cat}.s)$

units of k_o': $(m^6/kgmol.kg_{cat}.s^{1-N})$

units of α: 1/s

units of k_d: $m^6/kgmol^2.s$

units of E_A: kcal/gmol

± denotes the 95% confidence interval

Table 6.16 Overall gas oil cracking kinetic constant for the 3-lump model using 3 different decay functions (feedstock A with GX-30 catalyst)

Decay:	$e^{-\alpha t}$		t^{-N}		F-B	
T(°C)	k_o	α	k_o'	N	k_o	k_d
500	1.29 ±0.3	0.08 ±.05	1.18 ±.11	0.22 ±.18	1.49 ±.48	2,268 ±2,410
525	2.18 ±0.3	0.12 ±.11	1.81 ±.17	0.29 ±.23	2.77 ±1.2	4,710 ±4,514
550	2.50 ±.31	0.12 ±.10	2.07 ±.20	0.29 ±.21	3.22 ±1.3	5,225 ±4,715
E_A:	16.76		14.37		19.61	

units of k_o: $(m^6/kgmol.kg_{cat}.s)$

units of k_o': $(m^6/kgmol.kg_{cat}.s^{1-N})$

units of α: 1/s

units of k_d: $m^6/kgmol^2.s$

units of E_A: kcal/gmol

± denotes the 95% confidence interval

Table 6.17 Overall gas oil cracking kinetic constant for the 3-lump model using 3 different decay functions (feedstock B with Octacat catalyst)

Decay:	$e^{-\alpha t}$		t^{-N}		F-B	
T(°C)	k_o	α	k_o'	N	k_o	k_d
500	0.63 ±.07	0.04 ±.03	0.60 ±.04	0.13 ±.09	0.66 ±.10	747 ±586
525	1.05 ±.18	0.11 ±.06	0.90 ±.06	0.29 ±.12	1.22 ±.27	2,306 ±1,187
550	1.50 ±.11	0.14 ±.03	1.20 ±.07	0.34 ±.12	1.85 ±.28	3,566 ±1,056
E_A:	22.05		17.58		26.07	

units of k_o: $(m^6/kgmol.kg_{cat}.s)$

units of k_o': $(m^6/kgmol.kg_{cat}.s^{1-N})$

units of α: 1/s

units of k_d: $m^6/kgmol^2.s$

units of E_A: kcal/gmol

± denotes the 95% confidence interval

Table 6.18 Overall gas oil cracking kinetic constant for the 3-lump model using 3 different decay functions (feedstock B with GX-30 catalyst)

Decay:	$e^{-\alpha t}$		t^{-N}		F-B	
T(°C)	k_o	α	k_o'	N	k_o	k_d
500	0.70 ±.10	0.03 ±.03	0.68 ±.06	0.11 ±.10	0.74 ±.14	656 ±851
525	1.01 ±.09	0.01 ±.01	1.00 ±.06	0.04 ±.03	1.03 ±.14	305 ±398
550	1.40 ±.24	0.02 ±.01	1.36 ±.16	0.04 ±.03	1.43 ±.25	434 ±899
E_A:	17.48		17.60		16.79	

units of k_o: $(m^6/kgmol.kg_{cat}.s)$

units of k_o': $(m^6/kgmol.kg_{cat}.s^{1-N})$

units of α: 1/s

units of k_d: $m^6/kgmol^2.s$

units of E_A: kcal/gmol

± denotes the 95% confidence interval

different from each other. This trend is repeated with the three other catalyst-feedstock combinations for all three temperature levels.

A further examination of the confidence intervals on the parameters (as viewed in Tables 6.15 to 6.18) shows that the F-B decay model gave the largest intervals and the power law decay model the lowest with the exponential law model having confidence intervals somewhere in between. In some cases the F-B model gave overlaps of the k_o values at one temperature level to that at a higher temperature level which would mean these two values are not significantly different from each other. This was not found with the other two models which may indicate a somewhat better confidence with the results of this study in the power law or the exponential decay.

Concerning the decay parameters for each model, no clear trend was established between the catalyst decay constant and temperature. Again, referring to Tables 6.15 to 6.18 the decay constant, α, for the exponential decay model for the most part increased with increasing temperature, except for the combination of feedstock B with GX-30 (Table 6.18). Here, α decreased from 0.034 1/s at 500°C to 0.012 1/s at 525°C then increased to 0.017 1/s at 550°C. However, it can be seen from the confidence intervals on this parameter that the values overlap each other from 500°C to 550°C meaning they are not significantly different. This implies that the decay constant, α, is a weak function of temperature and could be considered as a constant value. The effect of temperature on

α, which is defined as a kinetic constant for catalyst decay is also unclear in the literature. For example, Weekman and Nace (1970) report α values decreasing with increasing temperature levels (hence a negative activation energy for decay) whereas Paraskos et al. (1976) report an α increasing with increasing temperature (positive activation energy). These differences are likely due to the types of equipment used to obtain the data. Weekman and Nace (1970) used a fluidized dense bed reactor with relatively long catalyst times on stream while Paraskos et al. (1976) used a pilot-scale riser unit to obtain their data.

For the F-B model, the trends in the decay parameter, k_d, with temperature were similar to that for α. The 95% confidence interval on k_d is as well quite wide which dictates the result that k_d values are not significantly different at higher temperatures. The same can be said for the value of N in the power law decay model. However, this result is more plausible since N is proportional to the order of decay, n, where $n = (1 + 1/N)$ and is not a function of temperature. Thus, for example from Table 6.15 for feedstock A on Octacat, a value of $N = 0.4$ for all three temperature levels gives an order of decay of 3.5 (i.e. 3.5 active sites lost per deactivation event) and for feedstock A on GX-30, the order of decay is approximately 4.5.

Effects of type of feedstock and type of catalyst on the kinetic constants can be seen by comparing activation energies which were calculated by regression on the Arrehnius equation

for the three temperatures studied. From Tables 6.15 and Table 6.16, the values of the activation energy for feedstock A on GX-30 are lower than the ones for Octacat for all three models examined. The same is true for feedstock B on GX-30 (Tables 6.17 and 6.18) except for the power law model where the E_A values are almost identical for the two catalysts. The fact that activation energies are lower for GX-30 catalyst is not surprising considering that it has a larger unit cell size than Octacat, thus providing a higher density of acid sites (more activity). It is also noted that feedstock B which is high in aromatics shows a larger activation energy for cracking than does feedstock A.

It is further mentioned that the activation energies found in this study ranging from 16.76 to 22.05 kcal/gmol using the exponential decay model are in agreement with other values reported in the literature (Decrooq, 1984; Wollastow and Haflin, 1975; Weekman, 1979).

In Chapter 1, the use of several mathematical models used to describe the deactivation of cracking catalysts was discussed. It is now possible to see from the data obtained in the Riser Simulator, the effectiveness of the three decay models studied. In Appendix C, Tables C.1 to C.4 show tabulated results of calculated conversions from the 3-lump model for the three decay functions versus experimentally determined conversions. The kinetic parameters from Tables 6.15 to 6.18 (for the four catalyst-feedstock combinations) were used for the simulation. As well, Tables C.1 to C.4 are

split into parts a and b with part a showing the calculated versus experimental conversion and part b showing the analysis of variance (ANOVA) for each model prediction. Referring to Table C.1a for feedstock A cracked with Octacat, it can be seen that each decay model gave nearly the same fit to the data. This is further evidenced by the standard deviation values where for example at 500°C the standard deviations for the exponential law, power law and F-B model are ±1.94, ±1.44 and ±1.7 respectively. As well, the power law decay gave the lowest standard deviation values of the three, however the differences are not large. Furthermore it would not be correct to reject the other two models just based on the standard deviation values. Table C.1b shows the ANOVA for the corresponding data of Table C.1a. In this analysis the lack of fit of the data to each model was checked by using a 95% confidence interval for the F-distribution as discussed in detail in Appendix C. As can be seen, none of the decay models contradict the data which is to say statistically that there is no reason to assume any of these models is inadequate. This result of model adequacy was also obtained for the other 3 catalyst-feedstock combinations. The conclusion drawn from these findings then, is that all three decay functions used can equally represent the data for the conditions used in the present work. Thus the choice of the model to use for the catalyst deactivation could be based on other factors such as simplicity and significance (Kraemer et al., 1990). The use of the F-B model which is an approach

more fundamentally sound in describing catalyst decay does not seem justified due to its complexity and the power law function uses a combined cracking and decay kinetic constant and assumes the unrealistic limits that the catalyst decay is infinite at zero time. From this point of view it is concluded that the use of the simpler exponential decay function to describe riser cracking under short contact times is an effective model and a preferred one over the other two. However, it should be pointed out that the use of a more generalized model which accounts for variation in mechanism and observable order of catalyst decay with time (Corella et al., 1985) may be necessary for contact times greater than say 20 seconds as in the case of dense phase FCC operation.

The model predictions for the conversion of gas oil using the 3-lump model with exponential decay are shown in Figures 6.1 to 6.4 which were discussed earlier. In these figures the lines refer to model predictions (3-lump with exponential decay) and the points are experimental results. From these figures it is evident that the predicted responses fit the experimental data quite well with an average standard error of ±2.0 weight percent.

To complete the analysis of the three lump model the kinetic constants k_1 and k_2 were estimated from the gasoline equation (equation 3.7) using Marquardt's non-linear regression technique on and then k_3 was found by difference. As a comparison, both the exponential decay function and the power law function were used to represent the catalyst decay.

The results are shown in Tables 6.19 to 6.22 for each catalyst-feedstock combination. In general it can be seen that the kinetic constant for the cracking of gasoline, k_2, is small showing that for short contact times there is no significant over-cracking of gasoline. In all cases the value of k_3 was smaller than k_1 which shows that the reaction is more selective for production of gasoline than for light gases and coke.

To see the fit of the product yield data to the three lump model for both exponential decay and power law decay functions a plot of yields versus reaction time is shown in Figure 6.40 for feedstock A on GX-30. In this figure the lines represent model predictions, with the solid line indicating the use of the exponential decay function and the dashed line for the power law decay function. The symbols refer to experimental data. It is evident that both models give close to identical simulations of the data with a reasonably good fit. Again this shows the adequacy of either decay model to be used to describe the kinetics of catalytic cracking for the range of short reaction times (less than 10 seconds) covered in this study. Furthermore, 3-lump model predictions of gasoline yields using the exponential decay law for all feedstock-catalyst combinations and the three temperatures used are shown by the lines in Figures 6.5 to 6.8. In all cases a reasonable fit of the data is realized using the parameter estimates obtained in this study. Also tabulated data showing experimental versus calculated yields for both gasoline and

Table 6.19 Kinetic constants for the 3-lump model using feedstock A cracked with Octacat catalyst

Using exponential decay:

T(°C)	k_1	k_3	k_2
500	0.63	0.44	2.65×10^{-4}
525	0.93	0.72	2.20×10^{-3}
550	1.23	1.04	2.22×10^{-3}

Using power law decay:

T(°C)	k_1'	k_3'	k_2'
500	0.56	0.34	7.24×10^{-4}
525	0.76	0.50	2.33×10^{-3}
550	0.95	0.65	2.69×10^{-3}

units of k_1 and k_3: $m^6/kgmol.kg_{cat}.s$

units of k_2: $m^3/kg_{cat}.s$

units of k_1' and k_3': $m^6/kgmol.kg_{cat}.s^{1-N}$

units of k_2': $m^3/kg_{cat}.s^{1-N}$

Table 6.20 Kinetic constants for the 3-lump model using feedstock A cracked with GX-30 catalyst

Using exponential decay:

T(°C)	k_1	k_3	k_2
500	0.80	0.49	4.11×10^{-4}
525	1.22	0.96	8.52×10^{-4}
550	1.28	1.22	3.10×10^{-3}

Using power law decay:

T(°C)	k_1'	k_3'	k_2'
500	0.75	0.43	5.00×10^{-4}
525	1.06	0.75	1.23×10^{-3}
550	1.09	0.98	2.89×10^{-3}

units of k_1 and k_3: $m^6/kgmol.kg_{cat}.s$

units of k_2: $m^3/kg_{cat}.s$

units of k_1' and k_3': $m^6/kgmol.kg_{cat}.s^{1-N}$

units of k_2': $m^3/kg_{cat}.s^{1-N}$

Table 6.21 Kinetic constants for the 3-lump model using feedstock B cracked with Octacat catalyst

Using exponential decay:

T(°C)	k_1	k_3	k_2
500	0.40	0.23	1.58×10^{-3}
525	0.65	0.40	2.01×10^{-3}
550	0.95	0.56	4.98×10^{-3}

Using power law decay:

T(°C)	k_1'	k_3'	k_2'
500	0.39	0.21	1.74×10^{-3}
525	0.59	0.31	2.33×10^{-3}
550	0.79	0.41	4.60×10^{-3}

units of k_1 and k_3: $m^6/kgmol.kg_{cat}.s$

units of k_2: $m^3/kg_{cat}.s$

units of k_1' and k_3': $m^6/kgmol.kg_{cat}.s^{1-N}$

units of k_2': $m^3/kg_{cat}.s^{1-N}$

Table 6.22 Kinetic constants for the 3-lump model using feedstock B cracked with GX-30 catalyst

Using exponential decay:

T(°C)	k_1	k_3	k_2
500	0.37	0.32	6.80×10^{-5}
525	0.58	0.43	4.32×10^{-4}
550	0.97	0.61	3.32×10^{-3}

Using power law decay:

T(°C)	k_1'	k_3'	k_2'
500	0.37	0.31	1.40×10^{-4}
525	0.57	0.42	4.61×10^{-4}
550	0.84	0.52	2.98×10^{-3}

units of k_1 and k_3: $m^6/kgmol.kg_{cat}.s$

units of k_2: $m^3/kg_{cat}.s$

units of k_1' and k_3': $m^6/kgmol.kg_{cat}.s^{1-N}$

units of k_2': $m^3/kg_{cat}.s^{1-N}$

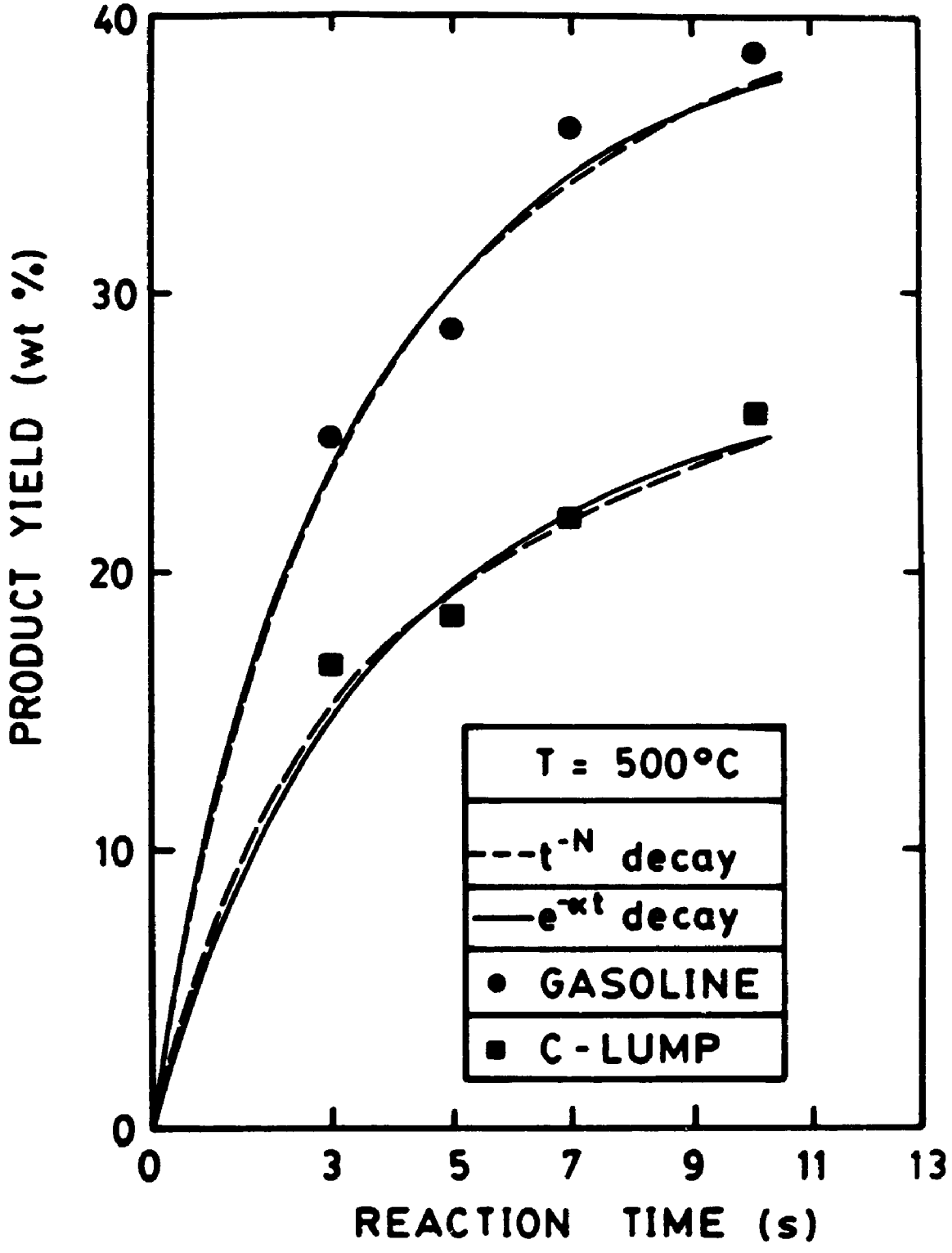

Figure 6.40 Experimental versus calculated product yields for feedstock A on GX-30 (3-lump model with exponential and power law decay).

C-lump can be found in Appendix C.

It is also interesting to compare the kinetic constants (k_1 and k_3) for two different feedstocks cracked with the same catalyst. For example, feedstock A produced larger values of k_1 and k_3 than feedstock B as seen in Tables 6.19 and 6.21. If the three lump model were to be applicable for any feedstock this would mean that these rate constants should be similar. However, they are significantly different from each other (k_1 for feed A is approximately 40% higher than for feed B) and the reason is due to the difference in chemical composition of each charge stock. This result which has been reported elsewhere (Voltz et al., 1971) and shows the need for the application of higher lumping models which account for the varying cracking rates of different species found in gas oils. In summary, the results obtained here for the three lump model with feedstocks of differing amounts of paraffins, naphthenes and aromatics are in general agreement with findings in the literature that a more sophisticated cracking scheme is required to obtain a kinetic model that could incorporate the effect of composition, making it feedstock independent. With this incentive then, an 8-lump model was also used in this work to describe the cracking reactions and will be the discussed in a subsequent section.

6.5 KINETIC PARAMETERS FOR THE PURE HYDROCARBON MIXTURES

The overall cracking constants for the pure hydrocarbon groups (P_l, N_l, and A_l) are presented in Table 6.23. Values obtained using both the exponential decay function and the power law function are presented. These constants were obtained by solving the light lump equation (equation 3.13) in the 8-lump model with Y_{ih} set to zero. This is equivalent to using the three lump model for each separate light lump oil mixture with first order kinetics.

Referring to Table 6.23 it is interesting to note that the values for the decay constant, α, follow the decreasing order aromatics, naphthenics, paraffinics on both catalysts at both temperatures which indicates the coking tendency for the different lumps. The same is true for the constant N of the power law decay function. Also, decay parameters are consistently higher in value for GX-30 catalyst than with Octacat catalyst. Further, comparing rate constants of the individual light lumps (exponential decay case) at both temperatures, it is observed that the light naphthenic compounds show the highest reactivity followed by the aromatics and then paraffins with the A_l and P_l groups being nearly the same for GX-30 catalyst. For Octacat the constants are very similar for all the lumps, with the only exception of the aromatic lump at 550°C. This comparison refers to pure cracking potential with no coke on the catalyst. However, when considering the observed rate of cracking (in combination

Table 6.23 Overall cracking kinetic constants obtained from the cracking of pure light oil mixtures.

Using Exponential Decay:

		Octacat			GX-30		
	T(°C)	α	k_{il}	E_A	α	k_{il}	E_A
P_l:	500	.09	11.9±1.9	13.2	.23	19.0±1.3	10.7
	550	.10	20.1±1.7		.37	28.9±2.2	
N_l:	500	.11	11.2±2.1	14.4	.33	23.9±1.1	10.1
	550	.22	19.9±3.0		.40	35.7±2.4	
A_l:	500	.28	11.6±.07	6.2	.37	21.3±1.8	8.8
	550	.34	14.8±1.1		.47	30.2±2.1	

[α in 1/s, k_{il} in $cm^3/g_{cat}.s$, E_A in kcal/gmol]

Using Power Law Decay:

		Octacat			GX-30		
	T(°C)	N	k_{il}'	E_A	N	k_{il}'	E_A
P_l:	500	.24	10.5±0.6	12.6	.50	12.2±0.7	3.0
	550	.25	17.3±1.5		.68	13.7±1.1	
N_l:	500	.34	9.7±0.9	7.7	.61	11.8±1.5	2.9
	550	.51	13.2±0.9		.71	13.2±2.1	
A_l:	500	.59	6.3±1.3	1.7	.69	8.8±0.8	1.9
	550	.69	6.8 ±1.1		.74	9.5±0.9	

[k_{il}' in $cm^3/g_{cat}.s^{1-N}$]

with coking of the catalyst) in the range of 3 to 10 seconds it is highest for the light paraffins, followed by the naphthenes than the aromatics.

In comparing the overall cracking kinetic constants for the pure light compounds obtained from both catalysts used, it is observed that the values are consistently larger for the GX-30 catalyst. This suggests that GX-30 has a higher concentration of acid sites than Octacat, which is also consistent with its larger unit cell size, providing a higher cracking potential. This trend is less pronounced for the values resulting from the power law decay function where k_{il} values for GX-30 are only slightly higher than those for Octacat.

To complete the description of the kinetic scheme for the pure light groups the values of the kinetic rate constants of pure lumps cracking to gasoline (k_{ilG}), pure lumps cracking to C-lump (k_{ilC}) and gasoline cracking to C-lump (k_{GC}) are shown in Table 6.24. The summation of k_{ilG} and k_{ilC} is equal to k_{il} and indicates the approximate selectivity of each pure group. Referring to Table 6.24, the pure light paraffins show the lowest selectivity to gasoline (k_{ilG}/k_{il}) which is also portrayed by the magnitude of k_{plC} which is largest for the light paraffins. The pure light naphthenes and aromatics show approximately similar selectivities. This trend was also observed by Jacob et.al. (1976) for light oil lumps in their 10-lump model. A possible explanation for this is attributed to the structure of the individual hydrocarbon types. For

Table 6.24 Summary of the individual kinetic constants obtained for the pure light oil mixtures using exponential decay.

		Octacat		
	T(°C)	k_{ilG}	k_{il}	k_{OC}
P_l:	500	6.35 ±0.7	5.6 ±0.6	1.4 ±1.8
	550	8.13 ±0.4	11.9 ±0.3	3.2 ±1.0
N_l:	500	7.10 ±3.0	4.2 ±1.9	1.6 ±4.0
	550	12.1 ±1.4	5.6 ±1.1	1.8 ±3.0
A_l:	500	8.1 ±2.0	3.5 ±0.8	1.4 ±8.0
	550	10.5 ±2.8	4.3 ±1.5	4.2 ±10.0

		GX-30		
	T(°C)	k_{ilG}	k_{il}	k_{OC}
P_l:	500	9.1 ±1.1	9.8 ±1.0	1.6 ±3.3
	550	11.5 ±2.5	17.4 ±2.0	2.8 ±8.7
N_l:	500	21.2 ±4.9	2.7 ±3.1	3.4 ±8.7
	550	29.2 ±3.1	6.5 ±2.3	6.4 ±4.7
A_l:	500	18.4 ±0.8	2.9 ±0.9	4.0 ±1.8
	550	25.4 ±3.3	4.8 ±1.1	7.4 ±6.7

* Values in $cm^3/g_{cat}.s$

example, comparing the cracking of a molecule from the pure light paraffin mixture such as n-tridecane and a molecule from the light aromatic group such as 1-hexyl benzene it can be envisioned that the straight paraffin molecule has a higher potential to crack to smaller fragments (less than 4 carbon atoms) than does 1-hexyl benzene. The paraffin molecule will crack more readily at the third carbon-carbon bond from either end of the chain as compared to the first or second C-C bond with a tendancy to crack off fragments with three or more carbon atoms (Greensfelder and Vogue, 1945). After these initial ruptures or simultaneously, additional cracking of the larger fragment continues. Thus products consist largely of C_3 to C_6 molecules. On the other hand, the 1-hexyl benzene will undergo scission mainly and most readily at the link bond between the ring and the alkyl group leaving two gasoline range molecules. It is possible that small fragments may result from cracking in the alkyl side group, but most of this will occur as secondary cracking of the new hexene molecule formed from the initial rupture from the benzene ring. A similar cracking behaviour occurs for light naphthenic compounds such as dicyclohexyl where the main reaction is cracking of the joining carbon bond between the two cyclo C_6 rings. In this way the kinetic values indicate that light paraffins produce more C-lump molecules than the other two light oil groups.

Comparisons of predicted versus observed conversions, gasoline yields and C-lump yields for the pure light mixtures

for a reaction temperature of 500°C can be seen in Figures 6.41, 6.42 and 6.43 respectively. Predicted values were obtained by using the kinetic constants of Tables 6.23 and 6.24 in the mass balance equations. Tabulated values of experimental versus observed yields are also given in Appendix C for all conditions used in the study. From Figures 6.41 to 6.43 there is reasonable agreement between experimental and calculated values showing the accuracy of the model and validity of the parameter estimates.

6.6 KINETIC PARAMETERS FOR THE 8-LUMP MODEL

An 8-lump model, as described in Chapter 3, was also evaluated based on the cracking data from the two different feedstocks and pure mixtures used in this study. The model is an extension of the 3-lump model where the feed is subdivided into six groups to help account for the chemical make-up of gas oil making it possible to use the kinetic parameters obtained for other feedstocks. The detailed outline for the determination of the kinetic rate constants associated with the 8-lump model can be found in Appendix A. In solving for the kinetic parameters both the exponential decay law and power law decay functions were used and both sets of data are presented here.

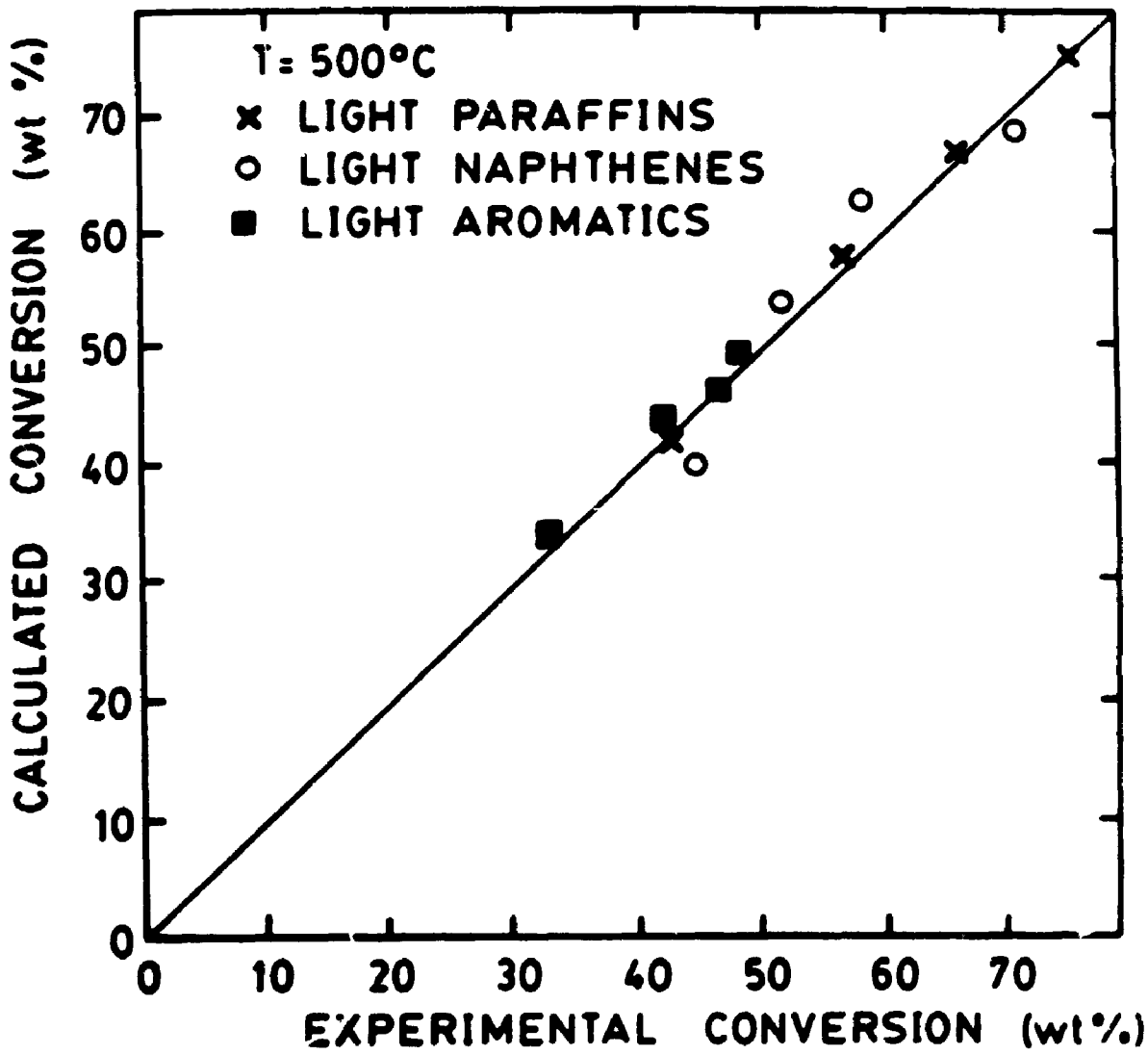

Figure 6.41 Experimental versus calculated conversions for the pure oil mixtures (Octacat, 500°C).

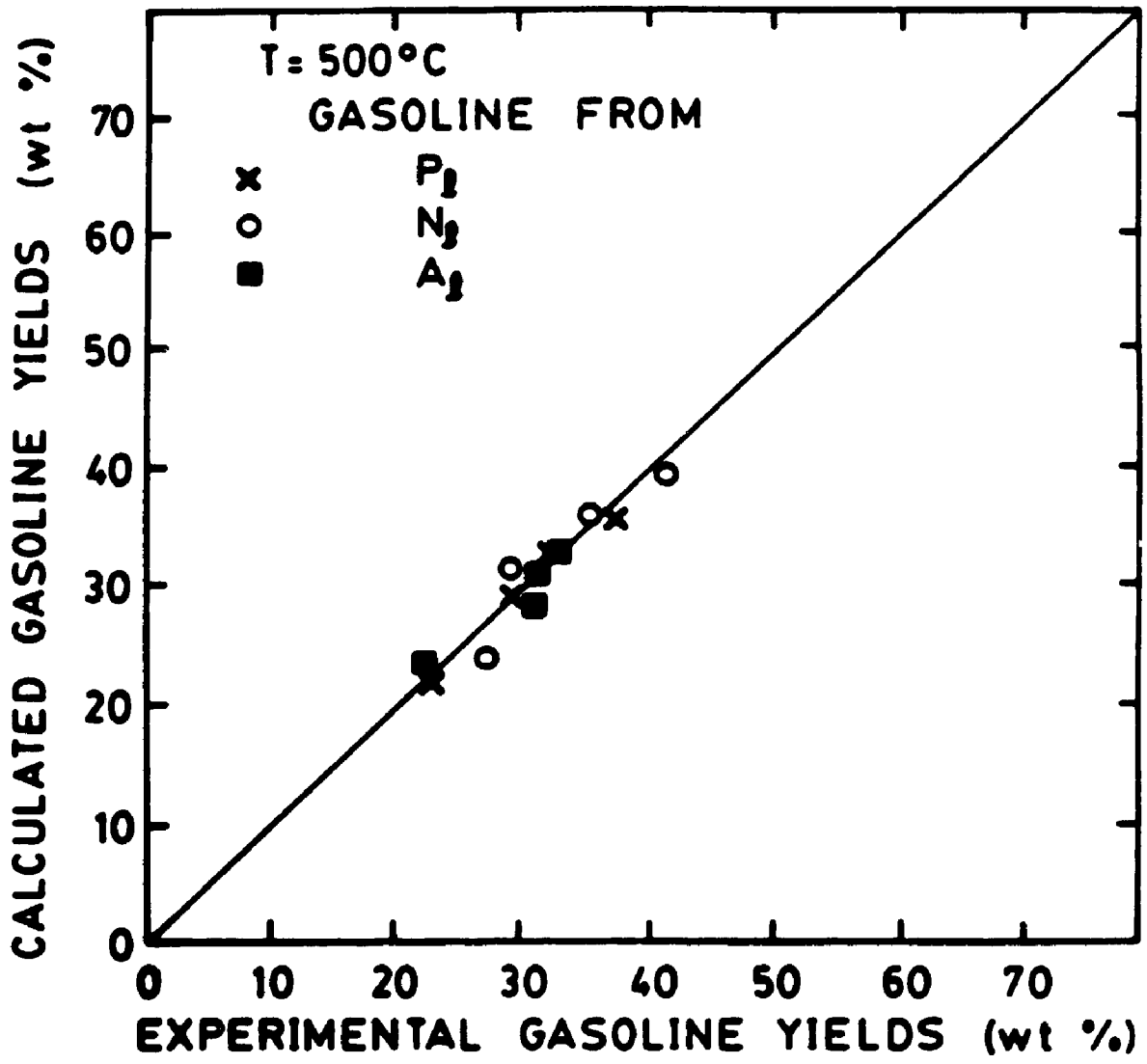

Figure 6.42 Experimental versus calculated gasoline yields for the pure oil mixtures (Octacat, 500°C).

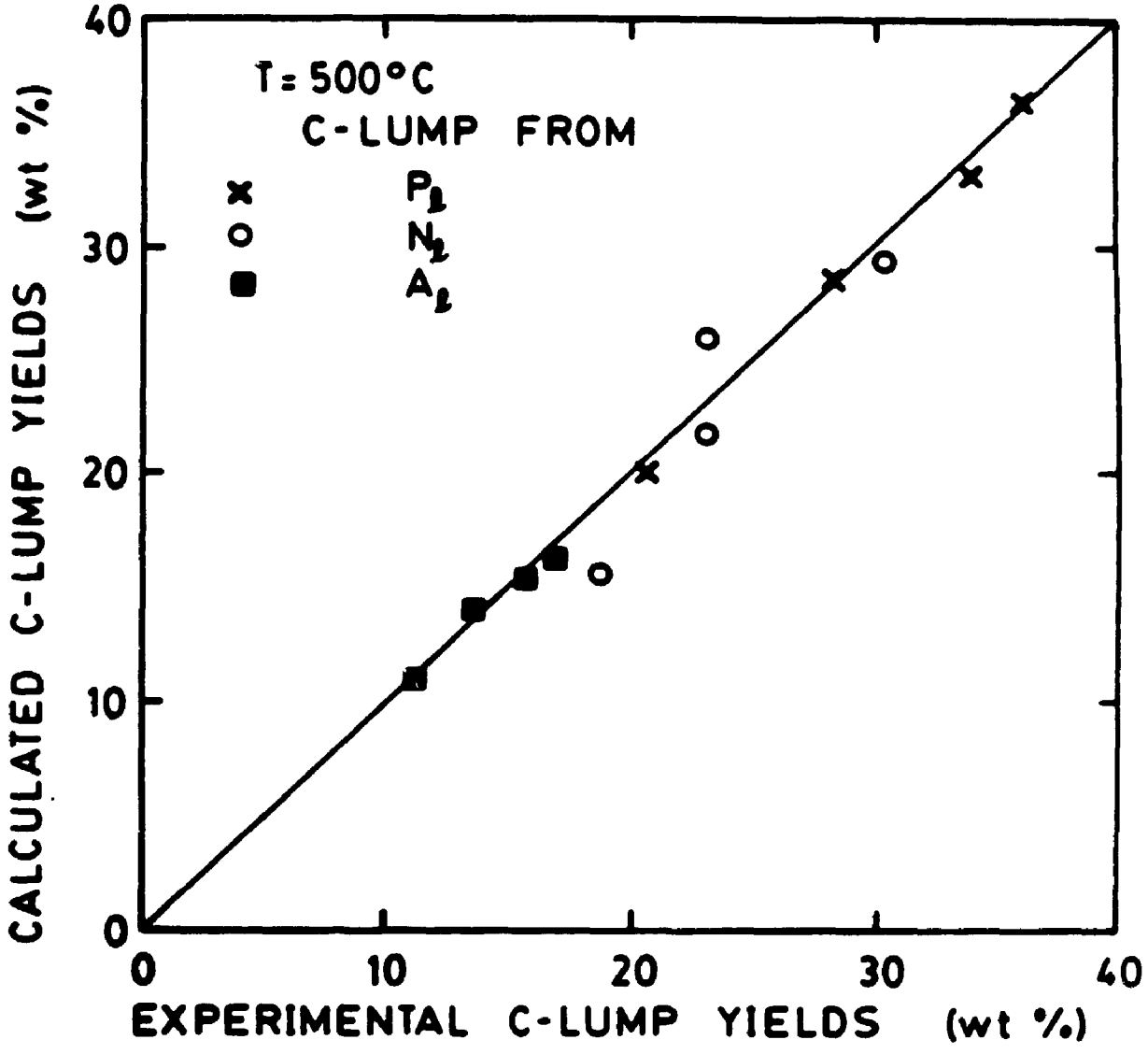

Figure 6.43 Experimental versus calculated coke yields for the pure oil mixtures (Octacat, 500°C).

6.6.1 Overall kinetic constants for the 6 oil lumps

The overall kinetic rate constants for the six oil lumps, as described in the kinetic scheme of Figure 3.9, are tabulated in Tables 6.25 to 6.28. The overall kinetic constant is a summation of the individual kinetic parameters describing the cracking of a particular lump into other lumps according to the model. Table 6.25 gives the results obtained using Octacat catalyst and exponential decay; Table 6.26 with GX-30 catalyst and exponential decay; Table 6.27 with Octacat and power law decay; and Table 6.28 with GX-30 and power law decay. Referring to Table 6.25, it is observed that the paraffins in both light and heavy fractions show the highest reactivity for all three temperature levels although the differences are not large. The heavy naphthenes and heavy aromatics have very similar cracking rates. The heavy aromatic lump shows a comparatively high reactivity since it is a combination of alkyl aromatics which exhibit high crackability and polynuclear aromatics which tend to be more refractory and favour coke formation.

Similar trends are also seen for GX-30 catalyst (Table 6.26). Again the paraffins show higher cracking rates than the naphthenes or aromatics, with the heavy naphthenes and aromatics showing nearly the same values. Apparently both the GX-30 and Octacat, which are octane enhancing catalysts, tend to crack heavy paraffins more readily than the heavy naphthenes or heavy aromatics. As well, GX-30 catalyst gives

Table 6.25 Overall cracking kinetic constants for heavy and light oil lumps of the 8-lump model with Octacat catalyst using exponential decay.

Heavy Lumps

T(°C)	Paraffins	Naphthenes	Aromatics
	k_{Ph}	k_{Nh}	k_{Ah}
500	18.56 ±2.13	15.21 ±1.6	14.24 ±1.4
525	26.31 ±1.63	20.35 ±1.7	19.90 ±1.1
550	31.88 ±2.4	24.63 ±3.7	25.80 ±0.9

Light Lumps

T(°C)	Paraffins	Naphthenes	Aromatics
	k_{Pl}	k_{Nl}	k_{Al}
500	9.49 ±2.1	5.28 ±1.9	1.28 ±0.5
525	12.43 ±0.9	11.27 ±2.1	4.88 ±1.2
550	17.64 ±1.0	16.04 ±2.4	9.55 ±2.1

note:
- units of k_i are $cm^3/g_{cat}.s$
- ± values denote 95% confidence intervals
- $k_{ih} = k_{ihil} + k_{ihG} + k_{ihC}$
- $k_{il} = k_{ilG} + k_{ilC}$

Table 6.26 Overall cracking kinetic constants for heavy and light oil lumps of the 8-lump model with GX-30 catalyst using exponential decay.

Heavy Lumps

T(°C)	Paraffins	Naphthenes	Aromatics
	k_{Ph}	k_{Nh}	k_{Ah}
500	25.10 ±1.6	18.28 ±1.1	18.18 ±1.8
525	31.58 ±1.2	20.65 ±1.1	21.47 ±1.2
550	37.58 ±1.0	26.89 ±2.4	28.21 ±0.7

Light Lumps

T(°C)	Paraffins	Naphthenes	Aromatics
	k_{Pl}	k_{Nl}	k_{Al}
500	11.60 ±0.3	6.89 ±1.1	1.97 ±0.7
525	12.81 ±0.6	10.96 ±1.4	8.84 ±2.2
550	20.93 ±1.3	12.89 ±1.0	12.4 ±2.3

note:
- units of k_i are $cm^3/g_{cat}.s$
- ± values denote 95% confidence intervals
- $k_{ih} = k_{ihil} + k_{ihG} + k_{ihC}$
- $k_{il} = k_{ilG} + k_{ilC}$

Table 6.27 Overall cracking kinetic constants for heavy and light oil lumps of the 8-lump model with Octacat catalyst using power law decay.

Heavy Lumps

T(°C)	Paraffins	Naphthenes	Aromatics
	k_{Ph}	k_{Nh}	k_{Ah}
500	11.66 ±0.9	9.57 ±1.1	8.96 ±1.0
525	14.13 ±0.6	10.90 ±0.8	10.66 ±0.3
550	16.60 ±1.1	12.79 ±1.9	13.39 ±0.4

Light Lumps

T(°C)	Paraffins	Naphthenes	Aromatics
	k_{Pl}	k_{Nl}	k_{Al}
500	4.88 ±1.7	4.02 ±0.5	3.57 ±2.0
525	6.04 ±0.8	6.82 ±1.8	4.92 ±2.8
550	6.98 ±1.2	9.33 ±1.6	6.51 ±2.2

note:
- units of k_i are $cm^3/g_{cat}.s^{1-N}$
- ± values denote 95% confidence intervals
- $k_{ih} = k_{ihil} + k_{ihG} + k_{ihC}$
- $k_{il} = k_{ilG} + k_{ilC}$

Table 6.28 Overall cracking kinetic constants for heavy and light oil lumps of the 8-lump model with GX-30 catalyst using power law decay.

Heavy Lumps			
T(°C)	Paraffins	Naphthenes	Aromatics
	k_{Ph}	k_{Nh}	k_{Ah}
500	14.34 ±0.9	10.44 ±1.6	10.38 ±0.9
525	19.52 ±0.4	12.74 ±2.5	13.24 ±0.8
550	21.24 ±0.6	15.17 ±2.4	15.93 ±0.6
Light Lumps			
T(°C)	Paraffins	Naphthenes	Aromatics
	k_{Pl}	k_{Nl}	k_{Al}
500	3.89 ±2.4	4.68 ±1.9	4.78 ±2.8
525	8.70 ±2.2	7.52 ±1.9	6.27 ±2.2
550	11.35 ±0.8	7.86 ±1.2	8.35 ±1.3

note:
- units of k_i are $cm^3/g_{cat}.s^{1-N}$
- ± values denote 95% confidence intervals
- $k_{ih} = k_{ihil} + k_{ihG} + k_{ihC}$
- $k_{il} = k_{ilG} + k_{ilC}$

higher rate constants for the six oil lumps than for Octacat which is expected since GX-30 achieved higher conversions and has a higher unit cell size (hence higher activity) than Octacat. Also, the rate constants for the cracking of the heavy oil lumps are greater than for the respective ones for the light oil fractions consistent with the fact that cracking rate increases with an increase in molecular weight.

The kinetic values obtained using the power law decay function (Tables 6.27 and 6.28) show similar trends as discussed above concerning order of reactivity among the oil lumps and catalyst effects. It is noted however that the three light oil lumps show approximately the same cracking rates. Furthermore, the 95% confidence intervals for the parameter estimates indicated by the ± values in Tables 6.25 to 6.28 are of similar magnitude showing that either decay model is appropriate for use in the model for the reaction conditions used in this study.

It is interesting to compare the overall rate constants for the cracking of light oil compounds (k_{il}) obtained from pure hydrocarbon mixtures and those obtained from the 8-lump model. For example, k_{il} for the light paraffins from the pure mixture data (for Octacat at 500°C) is 11.9 $cm^3/g_{cat}.s$ as compared to 9.5 $cm^3/g_{cat}.s$ obtained from the 8-lump model. AT 550°C the same values are 20.1 and 13.64 respectively showing relatively similar results. However, for the light naphthenes and light aromatics larger differences are observed, especially for GX-30 catalyst where for example the value of

k_{Nl} at 500°C for the pure mixture is 23.9 $cm^3/g_{cat}.s$ and the corresponding value from the 8-lump model is 6.89 $cm^3/g_{cat}.s$. The fact that the values for the light lumps obtained from pure mixture data are higher than for the values obtained from the 8-lump model indicate that interaction effects may be important. The presence of other hydrocarbon species competing for active sites could explain the differences observed as well as the fact that the partial pressures of the pure light oil lump mixtures were higher than for the light oil lumps in the commercial feedstocks. Also, in solving for k_{il} in the 8-lump model, an averaged value for the deactivation parameter based on the three different chemical species was used. For the pure mixtures it was possible to assign to each group different values for the deactivation parameter. This may help explain differences in the values of k_{il} obtained from the two methods.

The energies of activation for the six oil lumps from the 8-lump model are tabulated in Table 6.33 for both Octacat and GX-30 catalysts with exponential decay. These values were computed based on the three temperature levels used in the present study. Comparing the different species of oil groups it can be seen that the aromatics showed the highest E_A values for both light and heavy fractions. It is also noted that GX-30 catalyst gave energy of activation values and frequency factors which were lower and higher respectively than those obtained using Octacat catalyst. This means that the rate of cracking is increased to a larger extent as the temperature

Table 6.33 Activation energies for the six oil lumps from the 8-lump model (exponential decay case).

E_A (kcal/gmol)

	P_h	N_h	A_h
Octacat:	13.7	12.2	15.0
GX-30:	10.2	9.7	11.1
	P_l	N_l	A_l
Octacat:	15.7	28.2	50.9
GX-30:	14.8	15.9	46.9

is increased when using GX-30 catalyst.

A further observation pertaining to Table 6.33 is that the light oil fractions showed higher energies of activation than the corresponding heavy oil fractions. These differences are largest for the naphthene and aromatic groups and may suggest diffusional limitations for heavier, more bulkier molecules attempting to enter the small crystallite structures of the zeolite particles. The usual procedure for determining if diffusional controls are significant is to change the size of the catalyst particles for a given set of experiments for comparison of results. However with FCC catalysts this is not possible because the zeolite crystals are dispersed amongst a silica-alumina matrix and thus changing the catalyst size does not alter the zeolite crystal size. This task would involve more sophisticated techniques whereby zeolite particles of known size could be dispersed into the matrix. Such work on catalytic cracking of hydrocarbon feedstocks with zeolites having different pore diameters has recently been investigated (Biswass and Maxwell, 1990).

6.6.2 Individual kinetic constants for the 8-lump model

The complete parameter estimates obtained from the regression analysis on the 8-lump model equations are shown in Tables 6.29 to 6.32 (for cases of Octacat and GX-30 with both exponential and power law decay functions).

The ratios of the respective rate constants for gasoline

Table 6.29 Individual kinetic parameters for the 8-lump model (Octacat catalyst using exponential decay function).

Heavy Lumps

T(°C)	Paraffins	Naphthenes	Aromatics
	k_{PhPl}	k_{NhNl}	k_{AhAl}
500	1.88	4.56	2.63
525	2.77	4.79	4.50
550	2.83	6.73	6.63
	k_{PhG}	k_{NhG}	k_{AhG}
500	9.35	6.66	5.50
525	13.88	7.33	7.91
550	15.01	9.12	8.07
	k_{PhC}	k_{NhC}	k_{AhC}
500	7.32	4.00	6.11
525	9.67	8.24	7.49
550	14.04	8.78	11.09

Light Lumps

T(°C)	Paraffins	Naphthenes	Aromatics
	k_{PlG}	k_{NlG}	k_{AlG}
500	5.06	3.20	0.89
525	5.50	7.33	3.41
550	7.79	11.71	6.75
	k_{PlC}	k_{NlC}	k_{AlC}
500	4.43	2.08	0.39
525	6.69	3.94	1.47
550	9.85	4.33	2.80

	Gasoline k_{GC}	Deactivation parameter α (1/s)
500	0.92	0.23
525	2.11	0.30
550	3.60	0.32

• units of k_i are $cm^3/g_{cat}.s$

Table 6.30 Individual kinetic parameters for the 8-lump model (GX-30 catalyst using exponential decay function).

	Heavy Lumps		
T(°C)	Paraffins	Naphthenes	Aromatics
	k_{HPI}	k_{HNI}	k_{HAI}
500	4.13	5.05	2.33
525	5.70	5.99	3.35
550	10.41	7.14	4.70
	k_{HPG}	k_{HNG}	k_{HAG}
500	13.03	8.10	5.92
525	14.10	9.08	6.85
550	14.30	9.31	7.10
	k_{HPC}	k_{HNC}	k_{HAC}
500	7.92	5.13	9.93
525	11.96	5.58	11.27
550	12.87	10.44	16.41
	Light Lumps		
T(°C)	Paraffins	Naphthenes	Aromatics
	k_{PIG}	k_{NIG}	k_{AIG}
500	5.57	6.38	1.69
525	5.64	9.54	7.43
550	8.31	10.72	10.40
	k_{PIC}	k_{NIC}	k_{AIC}
500	6.03	0.51	0.28
525	7.17	1.42	1.41
550	12.62	2.17	2.04
	Gasoline k_{GC}	**Deactivation parameter** α (1/s)	
500	0.24	0.27	
525	0.64	0.24	
550	3.21	0.28	

• units of k_i are $cm^3/g_{cat}.s$

Table 6.31 Individual kinetic parameters for the 8-lump model (Octacat catalyst using the power law decay function).

Heavy Lumps

T(°C)	Paraffins	Naphthenes	Aromatics
	k_{PhPl}	k_{NhNl}	k_{AhAl}
500	0.10	3.25	2.33
525	0.53	2.61	2.91
550	0.62	3.46	3.75
	k_{PhG}	k_{NhG}	k_{AhG}
500	7.07	4.32	3.77
525	8.45	4.95	4.23
550	9.01	5.0	4.50
	k_{PhC}	k_{NhC}	k_{AhC}
500	4.49	2.0	2.86
525	5.14	3.35	3.52
550	6.94	4.53	5.23

Light Lumps

T(°C)	Paraffins	Naphthenes	Aromatics
	k_{PlG}	k_{NlG}	k_{AlG}
500	2.44	2.72	2.85
525	2.80	4.50	3.94
550	3.64	6.75	5.21
	k_{PlC}	k_{NlC}	k_{AlC}
500	2.44	1.30	0.71
525	3.24	2.32	0.98
550	3.34	2.57	1.30

	Gasoline k_{GC}	Deactivation parameter N
500	1.23	
525	2.33	0.566
550	3.65	

• units of k_i are $cm^3/g_{cat}.s^{1-N}$

Table 6.32 Individual kinetic parameters for the 8-lump model (GX-30 catalyst using the power law decay function).

Heavy Lumps

T(°C)	Paraffins	Naphthenes	Aromatics
	k_{PhPl}	k_{NhNl}	k_{AhAl}
500	0.62	2.93	1.83
525	3.04	3.99	2.16
550	4.66	3.82	2.87
	k_{PhG}	k_{NhG}	k_{AhG}
500	10.65	4.80	4.37
525	10.85	4.96	4.67
550	9.0	5.1	5.30
	k_{PhC}	k_{NhC}	k_{AhC}
500	3.07	2.7	4.18
525	5.63	3.79	6.42
550	7.58	6.25	7.76

Light Lumps

T(°C)	Paraffins	Naphthenes	Aromatics
	k_{PlG}	k_{NlG}	k_{AlG}
500	2.24	3.28	3.11
525	5.05	5.64	4.04
550	6.58	5.89	5.37
	k_{PlC}	k_{NlC}	k_{AlC}
500	1.65	1.41	1.67
525	3.65	1.88	2.23
550	4.76	1.96	2.98

	Gasoline k_{GC}	Deactivation parameter N
500	0.32	
525	0.85	0.55
550	2.94	

• units of k_i are $cm^3/g_{cat}.s^{1-N}$

formation to the corresponding ones for C-lump formation give an indication of the selectivity of the lump for gasoline formation. In Table 6.29 which gives rate constants for the case of Octacat catalyst and exponential decay the selectivity of heavy paraffins and heavy naphthenes (at 500°C) are fairly close with k_{PhG}/k_{PhC} = 1.28 and k_{NhG}/k_{NhC} = 1.66. At 550°C these values are nearly equivalent (1.07 and 1.04 respectively). The heavy aromatic lump shows lower selectivity (k_{AhG}/k_{AhC} = 0.9). In general all three lumps show declining selectivities to gasoline at the higher temperature which is to be expected considering that cracking rates increase more sharply than hydrogen transfer rates at higher temperatures.

Similar patterns of selectivity to gasoline are seen with GX-30 catalyst (Table 6.30) where the values for P_h, N_h and A_h are respectively 1.64, 1.57 and 0.60 at 500°C and 1.12, 0.89 and 0.43 at 550°C. The GX-30 catalyst gives a slightly better gasoline selectivity for paraffins and slightly less gasoline formation for naphthenes and aromatics. Furthermore, these selectivity trends also are true for the parameters obtained using the power law decay function (Tables 6.31 and 6.32).

The observed result of low selectivity for the heavy aromatics can be explained because of the presence of refractory aromatic rings which exhibit coke forming tendencies with no gasoline formation. As well, the presence of alkyl aromatics especially with C_3 and C_4 side groups exhibit high cracking rates thus forming C-lump compounds when the side group is severed from the polynuclear ring structure.

On the other hand the light aromatics show a relatively high selectivity to gasoline, as discussed previously when describing the cracking of pure mixtures. The presence of polynuclear aromatics and aromatics with C_3 and C_4 side groups is less frequent in light aromatic fractions than in heavy aromatic fractions. Explaining further, the A_l group was defined as having a boiling range from 220°C to 340°C. Thus no 3 ringed aromatics with side chains will be present but a bare 3 ringed aromatic compound is possible (i.e. phenanthrene boils at 340°C). Two ringed aromatics with up to 7 carbon atoms in a side chain are also possible to be found in the A_l lump but upon cracking at least one gasoline fragment is made giving an increased selectivity value as compared to heavy aromatics.

Another observation concerning heavy lump cracking selectivity is the result that the kinetic rate constants for the cracking of heavy lumps into light lumps (k_{ihil}) are the smallest of the three that make up the overall constant k_{ih}. This holds true for values obtained using the two catalysts and for all temperature levels as seen in Tables 6.29 and 6.30 (one exception being k_{WhWl} at 500°C which is slightly higher than k_{WhC}). This indicates that the heavy components tend to form more products in the gasoline lump and C-lump upon cracking than the formation of lighter gas oil compounds.

In terms of secondary cracking it was observed that the cracking of gasoline to C-lump (k_{GC}) was much smaller than its formation rate constants from the heavy and light oil

fractions. This result holds true for most cases as evidenced in Tables 6.29 to 6.32 except for the formation of gasoline from light aromatics for the case of Octacat catalyst with exponential decay law (Table 6.29). In general it can be said that Octacat and GX-30 catalyst used in this study showed the ability to provide larger gasoline yields while reducing secondary cracking of gasoline to light gases and coke.

The deactivation parameters for the 8-lump model for both the exponential decay function and power law function were obtained by averaging the values resulting from the regression analysis of the heavy oil lump equations for the paraffin, naphthene and aromatic lumps. For the exponential decay parameter, α, the values obtained for Octacat (0.228 s^{-1} at 500°C, Table 6.29) and GX-30 (0.274 s^{-1} at 500°C, Table 6.30) were quite similar. As well, the effect of temperature on α was not significant, a result also found using the 3-lump model. It is also observed that α values obtained using the 8-lump model are 2 to 3 times higher than those obtained using the 3-lump model (see Tables 6.15 to 6.18). For the power law decay function values for N of 0.566 for Octacat and 0.55 for GX-30 were computed which correspond to a deactivation order of approximately 2.8. This value is in reasonably good agreement but slightly lower than the order of decay found from the 3-lump model where for example feedstock A on Octacat gave N = 0.4 which results in a deactivation order of 3.5. The differences observed here for the deactivation parameters obtained using the 3-lump and 8-lump models are likely due to

the models themselves where the 3-lump model assumes second order cracking of gas oil and the 8-lump model assumes first order cracking and should be valid for any feedstock.

A limited comparison of rate constants with values found in the literature can be made. Table 6.34 shows some kinetic parameters obtained from Mobil workers (Gross et al., 1976) and values obtained in this study. Only the paraffinic and naphthenic groups are compared here since the Mobil 10-lump model further subdivides their aromatic lump into aromatics with side groups and bare aromatic rings. As well, comparing kinetic parameters from different works is not straight forward because of the varying conditions used which include type of catalyst, temperature and catalyst steaming conditions. Thus, in Table 6.34 it was only possible to compare the results from this work for the P and N lumps for Octacat and GX-30 at 500°C with the P and N lumps for a 10% REY zeolite at 482°C, the only conditions reported by Gross et al. (1976). As can be seen, the overall kinetic constant for the heavy paraffins, k_{Ph}, obtained in this work is in the range of the value reported by Gross et al. (1976). The main difference in the individual contributions for this overall constant is that k_{PhPl} is less than k_{PhC} for this work whereas k_{PhPl} is greater than k_{PhC} for the values obtained by Gross et al. (1976). Good agreement is also evident for the overall cracking of the light paraffins k_{Pl}. The data of Gross et al. (1976) however show a value of k_{PlG}/k_{PlC} higher than obtained in this work.

Table 6.34 A comparison of kinetic constants obtained in this work using the 8-lump model with data reported for a 10-lump model (Gross et al., 1976).

	10-lump	8-lump			10-lump	8-lump	
	*	**	***		*	**	***
k_{PhPl}:	5.75	1.88	4.13	k_{NhNl}:	6.25	4.56	5.05
k_{PhG}:	15.28	9.35	13.03	k_{NhG}:	23.53	6.66	8.10
k_{PhC}:	2.18	7.32	7.92	k_{NhC}:	4.13	4.00	5.13
k_{Ph}:	23.21	18.56	25.08	k_{Nh}:	33.91	15.22	18.28
k_{PlG}:	6.62	5.06	5.57	k_{NhG}:	18.37	3.20	6.38
k_{PlC}:	2.63	4.43	6.03	k_{NlC}:	2.27	2.08	0.51
k_{Pl}:	9.25	9.49	11.60	k_{Nl}:	20.64	5.28	6.89

[units of k_i are $cm^3/g_{cat}.s$]

* Values obtained at 482°C using 10% REY zeolite FCC catalyst

** Values using Octacat catalyst @ 500°C

*** Values using GX-30 catalyst @ 500°C

The agreement for the values of k_{Nh} and k_{Nl} from the two studies was not as good as for the case of the paraffins. Reported values by Gross et al. (1976) of the overall cracking constants for the heavy and light naphthenic lumps were at least twice as large as the values found in this work. Reasonable agreement can be seen for k_{NhNl}, k_{NhC} and k_{NlC} for the two sets of data. It is important to mention that the Mobil experiments were performed at catalyst residence times between 1.25 and 5.0 minutes whereas residence times in this work were 10 seconds and less which is more representative of advanced risers. This difference is a probable contributor to the difference in kinetic values between the two studies.

6.6.3 Simulation of experimental data using the 8-lump model

Using the kinetic parameter estimates for the 8-lump model with exponential decay the compositional changes in the given feedstock were simulated as the cracking reaction proceeded. Tabulated values from the 8-lump model simulation for gas oil yields, conversion and product yields for all experimental conditions are shown in Tables C.9 to C.14 of Appendix C. These values were plotted along with experimental results to see the fit of the model to the data. Referring back to Figures 6.17 to 6.30 the curves in these figures are the predicted gas oil lump yields computed from the simulation. For example, from Figure 6.20 the predicted yield of P_h (on Octacat) fits the experimental data reasonably well for all

three temperatures (average standard deviation = ±1.05 wt%). The response shows a smooth drop in heavy paraffins as reaction time increases, levelling off at the higher reaction time. Good fit of the model to the data for the heavy naphthenes and aromatics was also obtained as evidenced in Figures 6.21 to 6.24 with average errors of ±1.07 and ±0.82 wt% respectively.

The predicted yields for the light lumps on Octacat catalyst are seen in Figures 6.17 to 6.19. The model fits the data well for the light paraffins (Figure 6.17) although for Feedstock B the model gives an under prediction of light paraffins yields (average error = ±0.78 wt%). Figure 6.18 shows model predicted N_l yields on Octacat with good agreement to experimental values (error = ±0.70). At 500°C for feedstock B for example the model accurately shows the initial increase in N_l yields with a subsequent decrease at higher reaction times. The model predictions are not as good for the A_l yields (± 1.41 wt%) as seen in Figure 6.19. The large initial increase in light aromatics is not achieved by the model, but shows a more conservative increase at short reaction times and a more level profile at the higher reaction times.

Predicted responses for light lump yields with GX-30 catalyst (Figures 6.25 to 6.27) show similar results as with Octacat. The fit is less accurate for the A_l yields, especially at 500°C (Figure 6.27) where a relatively flat profile is predicted for both feedstocks. Averaged standard

deviations for the predicted responses for all three temperatures for P_l, N_l and A_l yields are respectively ±0.85, ±0.89 and ±1.41 wt%. Furthermore, the model responses for the heavy lump yields on GX-30 (Figures 6.28 to 6.30) also showed good predictions with average standard errors for the P_h, N_h and A_h yields of ±0.50, ±1.67 and ±0.77 respectively.

The 8-lump model also predicts gasoline and C-lump yields with reasonable accuracy for the two different feedstocks. Figure 6.44 shows calculated versus experimental gasoline yields for both feedstocks cracked on Octacat (exponential decay law case) with the average standard deviation being ±2.0 wt%. Similarly, Figure 6.45 shows calculated versus experimental C-lump yields for the two feeds cracked with Octacat, giving a standard error of ±2.85 wt%. As well, with GX-30 catalyst, Figures 6.46 and 6.47 show calculated versus experimental gasoline and C-lump yields respectively. Deviations are slightly higher for GX-30 with the error for gasoline yields being ±2.93 and for the C-lump yields, ±3.9 wt%.

It is interesting to note that using the power law decay function, the standard errors on predicted gasoline and C-lump yields were higher being ±2.1 and ±3.0 wt% for gasoline and C-lump yields on Octacat respectively and ±5.1 and ±5.7 wt% for gasoline and C-lump yields on GX-30 respectively.

In general the 8-lump model obtained from the two different feedstocks, along with pure mixture data and the range of experimental conditions used, gives reasonable

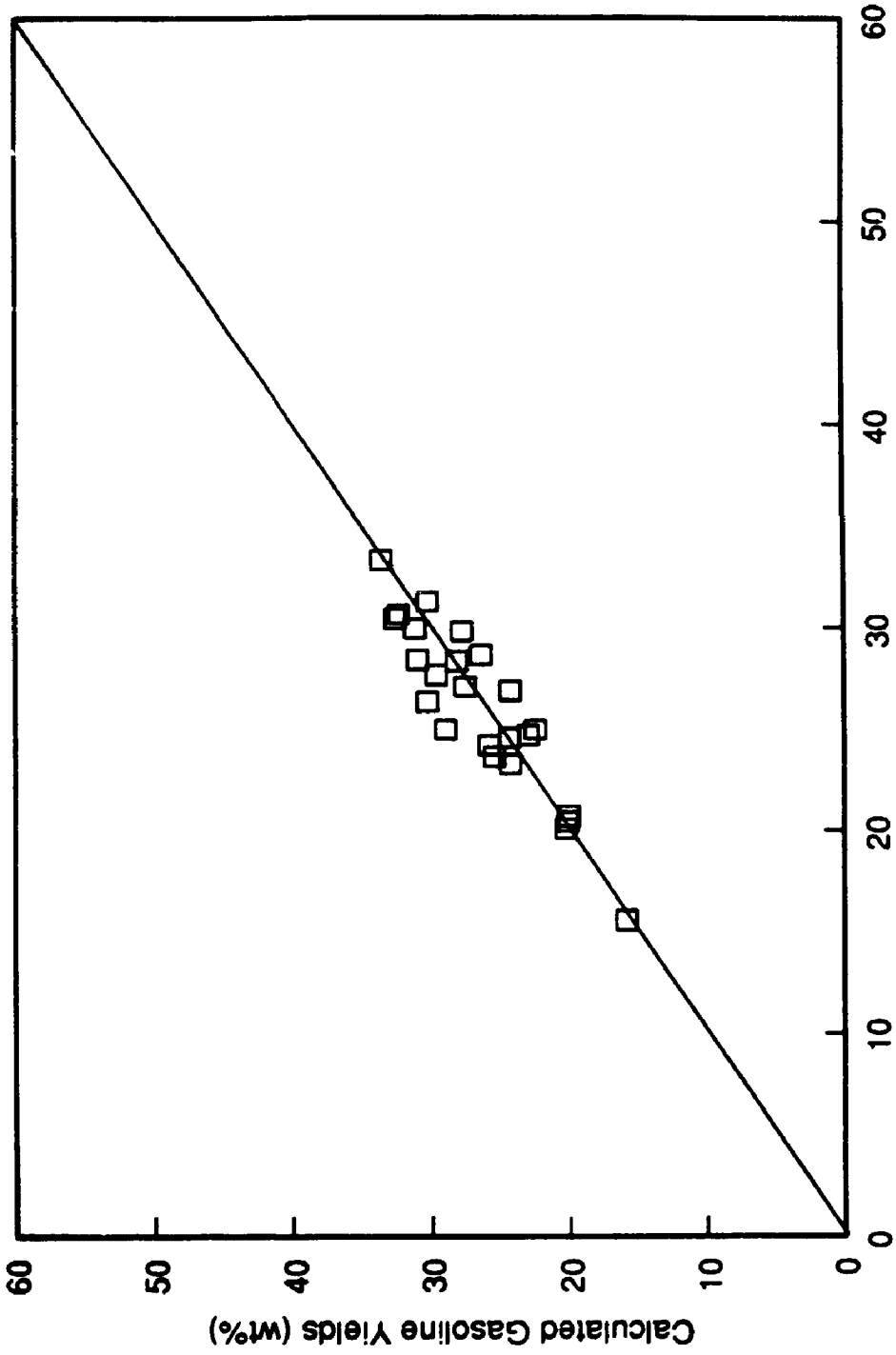

Figure 6.44 Experimental versus calculated gasoline yields from the 8-lump model (exponential decay, Octacat).

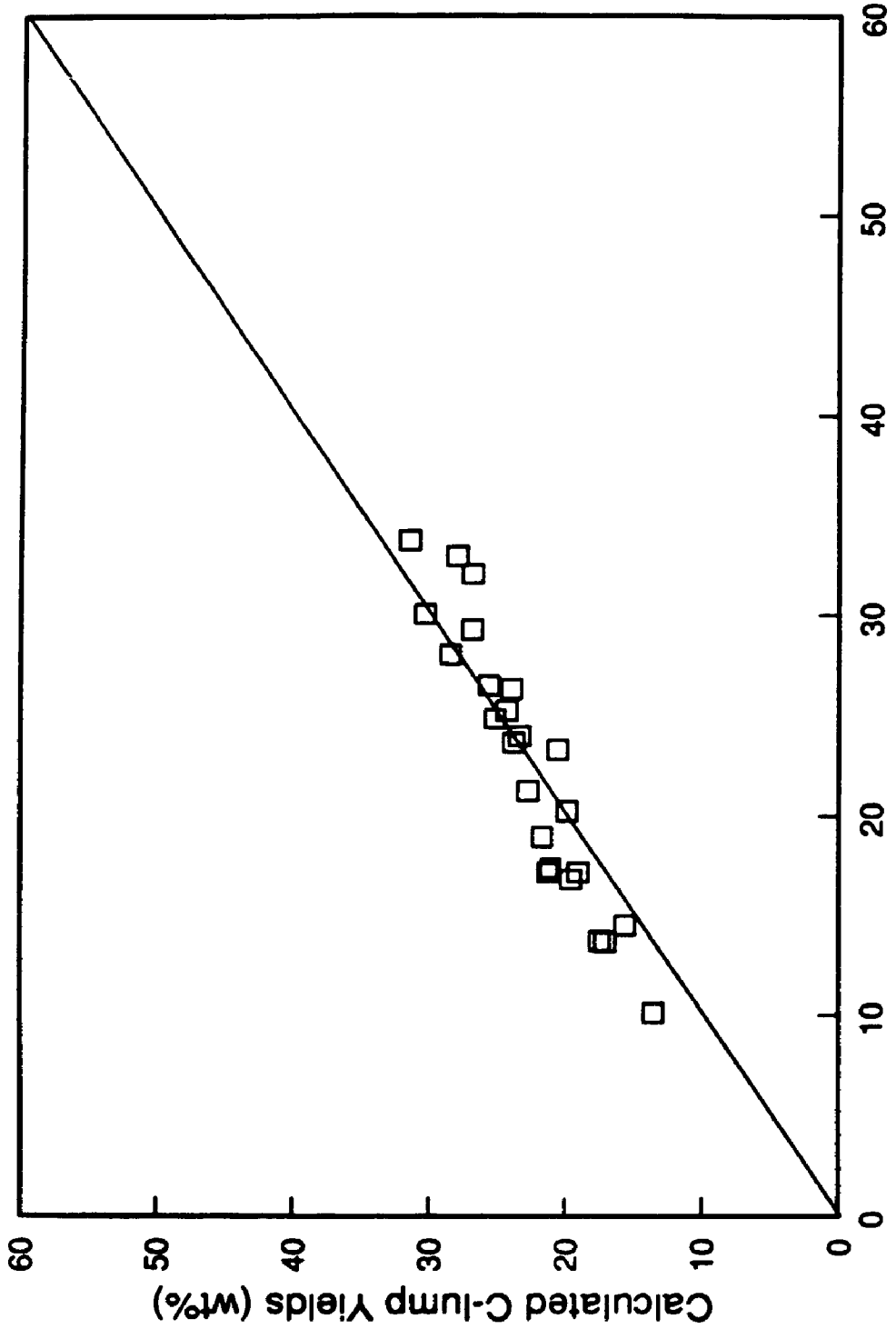

Figure 6.45 Experimental versus calculated C-lump yields from the 8-lump model (exponential decay, Octacat).

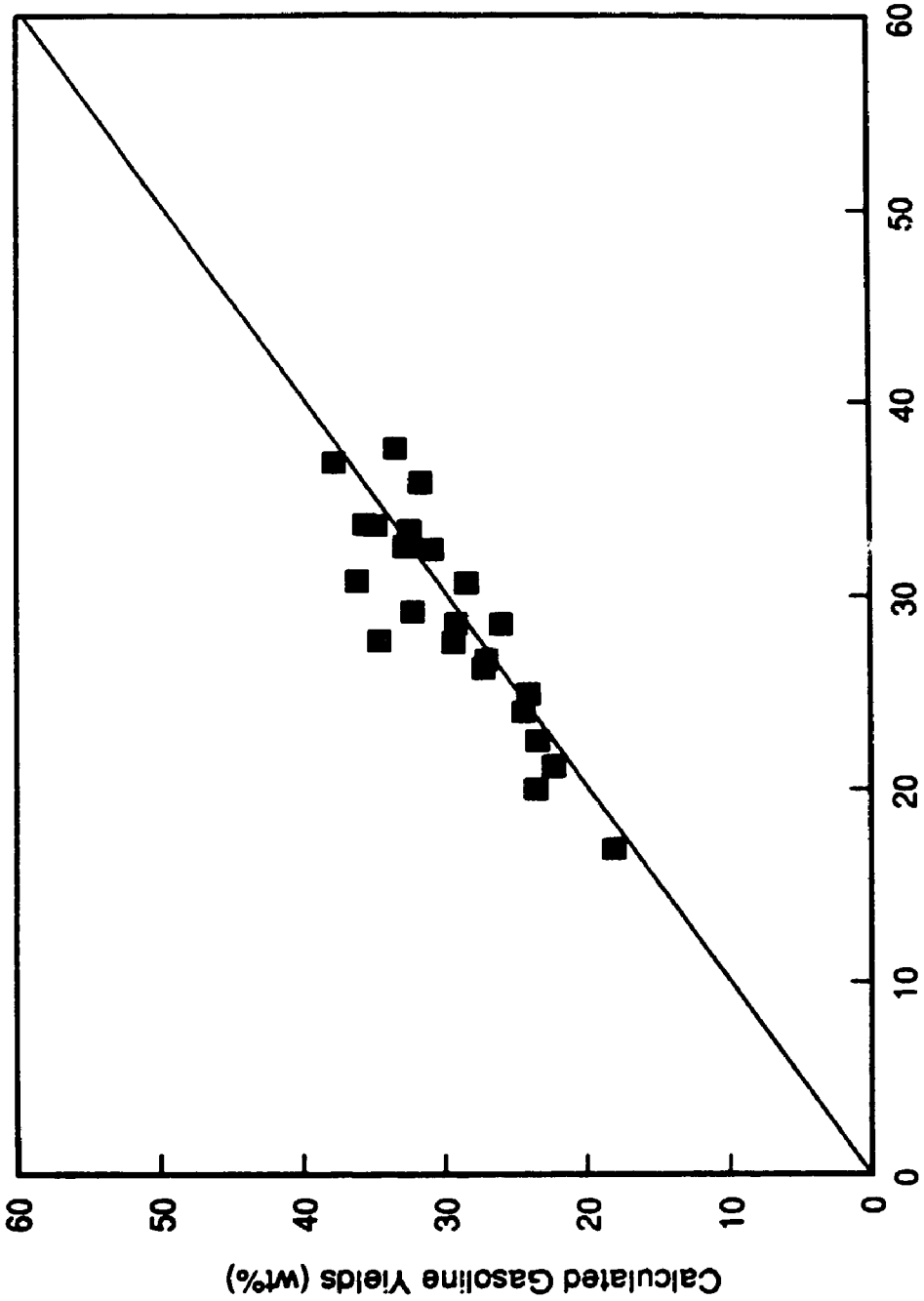

Figure 6.46 Experimental versus calculated gasoline yields from the 8-lump model (exponential decay, GX-30).

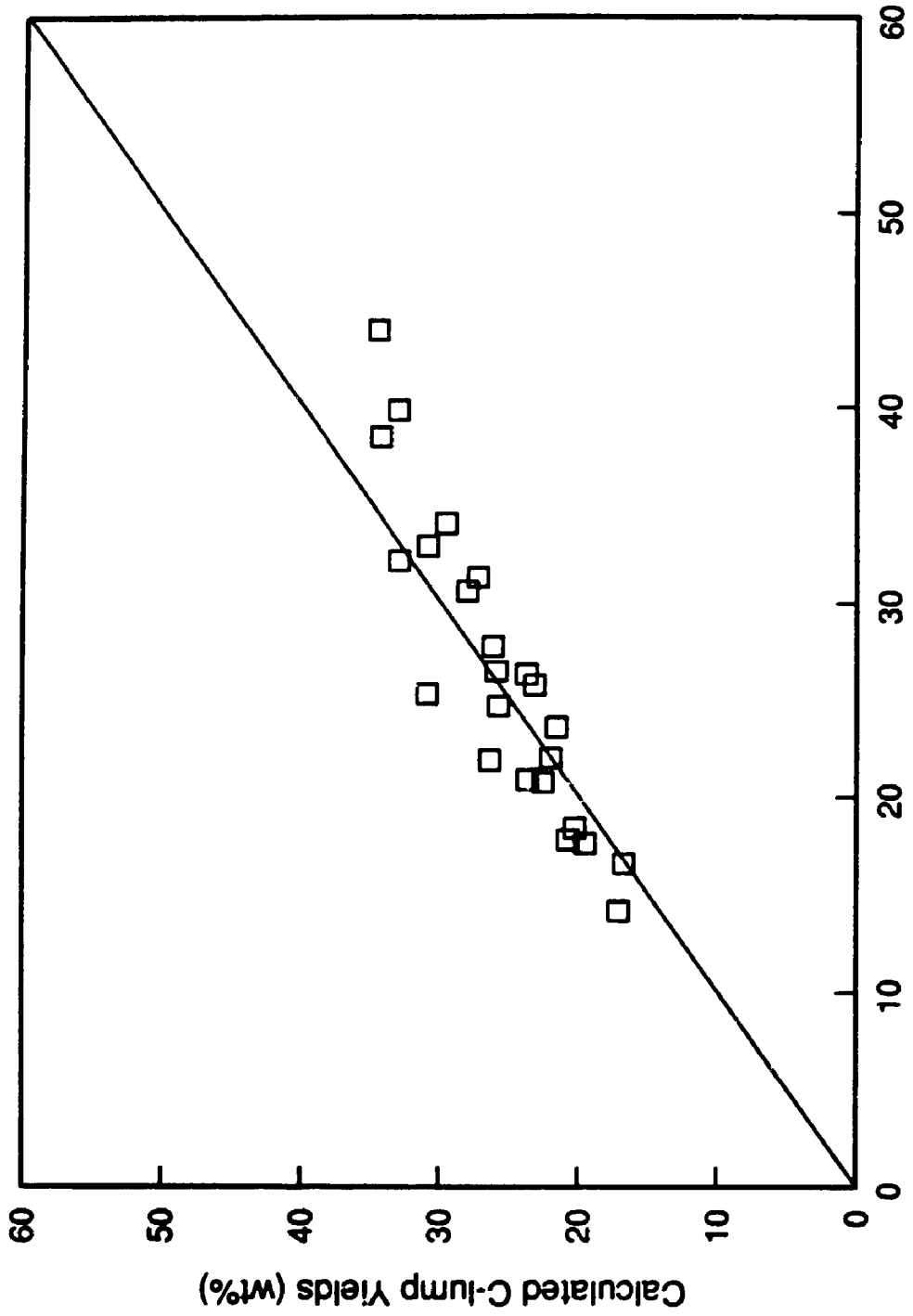

Figure 6.47 Experimental versus calculated C-lump yields from the 8-lump model (exponential decay, GX-30)

predictions for oil compositional changes during cracking as well as for the gasoline and C-lump yields.

CHAPTER 7

CONCLUSIONS AND RECOMMENDATIONS

The general results obtained during this investigation indicate that the Riser Simulator can effectively represent the catalytic cracking reactions which take place in an FCC riser reactor. The technique allows for similar conditions to be used such as temperature, catalyst to oil ratio, partial pressure of hydrocarbons, solids loading and reaction time as those used in commercial units. Moreover, the contacting of the hydrocarbons with the catalyst is more representative of riser cracking where the catalyst moves in time with the vapours, than that achieved in the MAT test.

The use of a fibre optic probe proved to be a valuable experimental method for studying the fluid-solid dynamics taking place in the reactor. The analysis showed that the gas density in the unit was the most significant variable influencing the pumping rate through the bed at constant impeller speed. By simulating, at room temperature, the density and viscosity of the gas mixture which would be present under reaction conditions it was concluded that the catalyst bed is well fluidized, providing uniform mixing between the reactants and catalyst.

The catalytic cracking of the two commercial feedstocks over the two commercial catalysts showed trends, in terms of conversions, product yields and gasoline research octane

numbers as those found in commercial FCC processes. The correlations between catalyst characteristics and product yields showed that a larger unit cell size catalyst provides a higher cracking potential due to the higher concentration of acid sites. As well, a lower unit cell size correlated well with reduced coke make and higher octane numbers for the gasoline product, though its yield was lower. These observations are in line with existing explanations of catalytic cracking chemistry on octane catalysts.

Kinetic modelling in the Riser Simulator deals with batch kinetics resulting in relatively simple equations as compared to other reaction systems. Also, there is no approximation necessary to account for volume expansion during cracking, which occurs in a flow vessel due to the increased number of moles being generated, since the reactor is a closed system. The kinetic parameters determined for the three-lump model reproduced the experimental data with a good fit. These parameters, determined using short reaction times ($\leq$ 10 seconds) fall in the range of reported values obtained in pilot scale riser units stressing the importance of evaluating cat-cracking reactions under appropriate conditions. The small value of the gasoline cracking rate constant indicated little over-cracking for short contact times. The model also verified the feed molecular type dependence of the kinetic constants suggesting the use of higher lumped models.

The three catalyst activity decay functions evaluated (exponential decay, power law decay and a Froment-Bischoff

type decay) showed that no one particular function predicted the experimental data better than the others for the range of experimental conditions used. It is concluded that for short reaction times (below 10 seconds) the simple exponential decay law may be used to effectively predict the data. It was also observed that the deactivation constant (k_d or α) was not strongly influenced by temperature.

The evaluation of the eight-lump model has provided data for cat-cracking kinetics which is lacking in the open literature. This model provides kinetic parameters which account for chemistry of the feedstock and are applicable to fast reaction times. The model fit the data with reasonable success with predictions of product yields to within ± 3 wt%. The model also provides insights to the relative cracking rates of molecular types. The paraffinic groups exhibited higher cracking rates than the naphthenic and the aromatic groups which suggests that the bulkier molecules encounter diffusional limitations in the zeolite. Also, kinetic values obtained from pure light oil mixture data were higher than values obtained from the eight-lump model indicating that interaction effects may be important.

It is concluded that the Riser Simulator is a suitable system for kinetic modelling studies of riser cracking and can also be used as a quick and reliable method for the screening of FCC catalysts. It is recommended that the latter statement be further evaluated by direct comparison with the MAT test and commercial FCC data. This comparison would have to be

made using identical operating conditions, feedstocks, catalysts and catalyst steaming conditions and would therefore require collaboration with the industrial sector.

In terms of improvements to the Riser Simulator experimental system, it is recommended that the valve sequences be automated. This would give more accuracy to the measured reaction time and with computer control would make the system less labour intensive. It may also allow the use of shorter reaction times, below 3 seconds, with improved accuracy. The use of an automatic heated injection system would also be desirable for ease of operation.

Furthermore, a method of regenerating the catalyst while on stream would reduce the time required for obtaining experimental data and would avoid repeated cycles of heating and cooling of the reactor for recovering the catalyst (hence longer seal life). Such a method could possibly be realized by pulsed injections of oxygen into the reactor with subsequent analysis of the combustion products. It is envisioned that the use of two reactors in tandem could also speed the data acquisition time when evaluating different catalysts under varying catalyst/oil ratios.

Improvements to the eight-lump model would include the use of a wider range of feedstocks, especially with higher concentrations of light naphthenes and light aromatics, to improve the predictive capabilities of the model. With the advancement of analytical techniques in GC-MS it may also be possible to split the aromatic lumps into aromatics with side

chains and bare aromatic rings, as done in the ten-lump model, to give insights about the cracking rates of these species under short reaction times. However, the use of higher lumping models means additional experimentation and hence cost and the value of this information must be weighed against simpler models where, with the appropriate experimental systems, the kinetics could be re-evaluated quickly for different feedstocks.

REFERENCES

Abbot, J. and Wojciechowski, B.W., "Catalytic reaction of n-hexenes on amorphous silica-alumina", Can. J. Chem. Eng., **63**(10), 818-825 (1985a).

Abbot, J. and Wojciechowski, B.W., "Catalytic Cracking and Skeletal Isomerization of n-Hexene on ZSM-5 Zeolite", Can. J. Chem. Eng., **63**(6), 451-461 (1985b).

Abbot, J. and Wojciechowski, B.W., "The Mechanism of Catalytic Cracking of n-Alkenes on ZSM-5 Zeolite", Can. J. Chem. Eng., **63**(6), 462-469 (1985c).

Alkemade, U., Cartlidge, S. and Thompson, J.M., "Improved alumina sol FCC catalyst meet challenges of the 1990s", Oil and Gas J., Oct. 1, 52-62 (1990).

Anderson, C.D. and Dwyer, F.G., "A new cracking catalyst for higher octane using ZSM-5", Paper presented at the 9th Actas Simp. Iberoam. Catal., 247-258 (1984).

Anderson, P.C., Sharkey, J.M. and Walsh, R.P., "Calculation of the Research Octane Number of Motor Gasolines from Gas Chromatographic Data and a New Approach to Motor Gasoline Quality Control", J. Inst. Pet., **58**, 83-94 (1972).

Andrews, J.M., "Cracking Characteristics of Catalytic Cracking Units", Ind. Eng. Chem., **51**, 507 (1959).

Appleby, W.G., Gibson, J.W. and Good, G.M., "Coke Formation in Catalytic Cracking", Ind. Eng. Chem. Proc. Des. Dev., 1, 102 (1962).

Archibald, R.C., May, N.C. and Greensfelder, B.S., "Experimental Catalytic and Thermal Cracking at High Temperature and High Space Velocity", Ind. Eng. Chem. **44**(8), 1811-1817 (1952).

ASTM, "Manual on Hydrocarbon Analysis", Committee D-2 on Petroleum Products and Lubricants, 3rd Ed., 1-5 (1977).

Avidan, A.A., Edwards, M. and Owen, H., "Innovative improvements highlight FCC's past and future", Oil & Gas J., January 8, 33-58 (1990a).

Avidan A.A., Krambeck, F.J., Owen, H. and Schipper P.H., "FCC closed-cyclone system eliminates post-riser cracking", Oil and Gas J., Mar 26, 56-62 (1990b).

Barlow, R.C., "Commercial Application of Vanadium Passivation Technology", Paper presented at the NPRA Spring Meeting (1986).

Berak, J.M. and Manik, B., "Deactivation of high silica ultrazet zeolite by steam treatment", React. Kinet. Catal. Lett., **20**, 3-4 (1982).

Berker, A. and Tulig, T.J., "Hydrodynamics of gas-solid flow in a catalytic cracker riser: Implications for reactor selectivity performance", Chem. Eng. Sci., **41**(4), 821-827 (1986).

Berty, J.M., "Reactor for Vapour-Phase Catalytic Studies", Chem. Eng. Prog., **70**(5), 78-84 (1974).

Berty, J.M., "Testing Commercial Catalysts in Recycle Reactors", Catal. Rev. Sec. Eng., **20**(1), 75-96 (1979).

Berty, J.M., "20 Years of Recycle Reactors in Reaction Engineering", Plant/Operations Prog., **3**(3), 163-168 (1984).

Best, D.A., Pachovsky, R.A., and Wojciechowski, B.W., "Diffusion effects in catalytic gas oil cracking", Can. J. Chem. Eng., 809 (1971).

Bett, J.A.S. and Hall, W.K., "Kinetic Characterization From Pulse Reactors", J. Catal., **10**, 105 (1968).

Biswas, J. and Maxwell, I.E., "Octane enhancement in fluid catalytic cracking. I. Role of ZSM-5 addition and reactor temperature", Applied Catalysis, **58**, 1-18 (1990).

Blanding, F.H., "Reaction Rates in Catalytic Cracking of Petroleum", Ind. Eng. Chem., **45**, 1186-1197 (1953).

Blazek, J.J., "Gains from FCC revival evident now", Oil and Gas Journal, Oct., 65 (1973).

Blazek, J.J., "A new era for the coke selective fluid cracking catalyst", Davison Catalagram, No. 75, 1-3 (1987).

Bryson, M.C. and Huling, G.P., "Gulf explores riser cracking", Hydrocarbon Processing, May, 85 (1972).

Bunn, D.P., Gruenke, G.F., Jones H.B., Luessenhop, D.C. and Youngblood, D.J., "Texaco's Fluid Catalytic Cracking Process", Chem. Eng. Progress, **65**(6), 88-93 (1969).

Caldwell, L., "An improved internal gas recirculation reactor for catalytic studies", Applied Catalysis, **8**, 199 (1983).

Campagna, R.J., Brady, M.F., Fort, D.L. and Wick, J.P., "Fresh FCC catalyst tests predict performance", Oil and Gas J., March 24, 85 (1986).

Campbell, D.R. and Wojciechowski, B.W., "Theoretical Patterns

of Selectivity in Aging Catalysts with Special Reference to the Catalytic Cracking of Petroleum", Can. J. Chem. Eng. 47, 413-417 (1969).

Campbell, D.R. and Wojciechowski, B.W., "Selectivity of Aging Catalyst in Static, Moving and Fluidized Bed Reactors", Can. J. Chem. Eng., 48, 4 (1970).

Campbell, D.R. and Wojciechowski, B.W., "The Catalytic Cracking of Cumene on Aging Catalysts. II. An experimental Study", J. of Catal., 23, 307 (1971).

Carberry, J.J., "Heat and Mass Diffusional Intrusions in Catalytic Reactor Behavior", Catalysis Reviews, 3(1), 61-91 (1969).

Carter, G.D. and McElhiney, G., "FCC Catalyst Selection: A modification of the ASTM microactivity test (MAT) proves useful", Hydrocarbon Processing, September, 63-64 (1989).

Chabot, J., "Fiber Optic Sensors for Studies in Multiphase Reactors", M.E.Sc. Thesis, The University of Western Ontario, London, Ontario, Canada (1989).

Chen, N.Y. and Degnan, T.F., "Industrial Catalytic Application of Zeolites", Chem. Eng. Prog., Feb., 32-41 (1988).

Chen, N.Y. and Garwood, W.E., "Industrial application of shape-selective catalysis", Cat. Rev. Sci. Eng., 28(2-3), 185 (1986).

Chen, N.Y. and Lucki, S.J., "Nonregenerative Catalytic Cracking of Gas Oil", Ind. Eng. Chem. Proc. Des. Dev., 25, 814-820 (1986).

Chen, N.Y., Mitchell, T.O., Olson, D.H. and Pelrine, B.P., "Irreversible Deactivation of Zeolite Fluid Cracking Catalyst. 1. X-Ray and Catalytic Studies of Catalyst Aged in an Automated Microcatalytic System for Gas Oil Cracking", Ind. Eng. Chem. Prod. Res. Dev., 16(3), 244-247 (1977a).

Chen, N.Y., Mitchell, T.O., Olson, D.H. and Pelrine, B.P., "Irreversible Deactivation of Zeolite Fluid Cracking Catalyst. 2. Hydrothermal Stability of Catalysts Containing NH_4Y and Rare Earth Y", Ind. Eng. Chem. Prod. Res. Dev., 16(3), 247-252 (1977b).

Chester, A.W. and Stover, W.A., "Steam Deactivation Kinetics of Zeolite Cracking Catalysts", Ind. Eng. Chem. Prod. Res. Dev., 16(4), 285-290 (1977).

Chester, A.W., Schwartz, A.B., Stover, W.A. and McWilliams,

J.P., "CO Oxidation Promoters in Catalytic Cracking", Paper presented at the Symposium on Advances in Petroleum Processing, Joint Meeting of the ACS and Chemical Society of Japan, Honolulu, April 1-6 (1979).

Collyer, R., "Fast Catalytic Cracking and Catalyst Deactivation Using the Pulse Technique", M.E.Sc. Thesis, University of Western Ontario, January (1987).

Corbett, R.A., "Refining catalyst choices expand again", Oil and Gas J., Oct. 13, 39-52 (1986).

Corbett, R.A., "New catalyst designs meet environmental challenges of the 1990s", Oil and Gas J., Oct. 1, 49-51 (1990).

Corella, J. and Menendez, M., "The Modelling of the Kinetics of Deactivation of Monofunctional Catalysts with an Acid Strength Distribution in their Non-homogeneous Surface. Application of the Deactivation of Commercial Catalysts in the FCC Process", Chem. Eng. Sci., 41(7), 1817-1826 (1986).

Corella, J., Bilbao, R., Molina, J.A. and Artigas, A., "Variation with Time of the Mechanism, Observable Order and Activation Energy of the Catalyst Deactivation by Coke in the FCC Process", Ind. Eng. Chem. Proc. Des. Dev., 24, 625-636 (1985).

Corella, J., Fernandez, A. and Vidal, J.M., "Pilot Plant for the Fluid Catalytic Cracking Process: Determination of the Kinetic Parameters of Deactivation of the Catalyst", Ind. Eng. Chem. Proc. Des. Dev., 25, 554-562 (1986).

Corma, A., Monton, J.B. and Orchillés, A.V., "Influence of the process variables on the product distribution and catalyst decay during cracking of paraffins", Applied Catalysis, 23, 255-269 (1986).

Corma, A., Fornes, V., Monton, J.B. and Orchilles, A.V., "Catalytic Cracking of Alkanes on Large Pore, High SiO_2/Al_2O_3 Zeolites in the Presence of Basic Nitrogen Compounds. Influence of Catalyst Structure and Composition in the Activity and Selectivity", Ind. Eng. Chem. Res., 26, 882-886 (1987).

Corma, A., Fornes, V., Martinez, A. and Orchilles, A.V., "Parameters in addition to the unit cell that determine the cracking activity and selectivity of dealuminated HY zeolites", ACS Symposium Series No. 368 in "Perspectives in Molecular Sieve Science", W.H. Flank and T.E. Whyte, Eds., 542-554 (1988).

Corma, A. and Orchillés, A.V., "Formation of products responsible for motor and research octane of gasolines produced by cracking. The implication of framework Si/Al ratio and operation variables", J. Catal., **115**, 551 (1989).

Corma, A. and Wojciechowski, B.W., "The Catalytic Cracking of Cumene", Catal. Rev. Sci. Eng., **24**(1), 1 (1982).

Coxson, P.G. and Bischoff, K.B., "Lumping Strategy. 1. Introductory Techniques and Applications of Cluster Analysis", Ind. Eng. Chem. Res., **26**, 1239-1248 (1987).

Culberson, S.F., Yepson, G.L. and Bartholomew, K.D., "Refiners mull no-lead options", Oil and Gas J., Mar 18, 108-114 (1985).

Dale, G.H. and McKay, D.L., "Passivate Metals in FCC feeds", Hydrocarbon Processing, **56**, Sept., 97 (1977).

Davies, J.C., "FCC units get crack catalysts", Chem. Engng. **84**(12), 77 (1977).

Davis, B.H. and Hettinger, W.P., "Heterogeneous Catalysis. Selected American Histories", ACS Symposium Series, 222 (1983).

Davison, "Davison Octacat meets the challenge", Catalagram Number 69 (1984).

Dean, W.J. and Dadyburjor, D.B., "Activity and coke depostion on a composite acid catalyst and its components", Ind. Eng. Chem. Res., **28**, 271-276 (1989).

Decroocq, D., "Catalytic Cracking of Heavy Petroleum Fractions", Chapter 4, Gulf Publishing Co., Houston, Texas (1984).

de Jong, J.I., "Hydrogen transfer in catalytic cracking", Paper F-2, presented at the Ketjen Catalyst Symposium, Scheveningen, The Netherlands (1986).

de Lasa, H.I., "Fluidized Bed Catalytic Cracking Technology", Lat. Am. J. Chem. Eng. Appl. Chem., **12**, 171-184 (1982).

de Lasa, H.I., "Riser Simulator for Catalytic Cracking Studies", Canadian Patent Application, April, (1987).

Desai, P.H. and Haseltine, R.P., "Advanced FCC catalyst formulations can be used to boost motor octane number of gasoline", Oil and Gas J., Oct. 23, 68-76 (1989).

Desay, N. and Anthony, R.G., "Interpretation of data from pulse reactor", AIChE Meeting, Hew York, N.Y., Nov. 16-20

(1987).

Dietz, W.A., "Response factors for gas chromatographic analyses", J. of G.C., Feb., 68 (1967).

Donnelly, S.P., "Addition of shape selective zeolites to catalytic cracking units", U.S. Patent 4,927,523 May 22 (1990).

Doraiswamy, L.K. and Tajbl, D.B., "Laboratory Catalytic Reactors", Cat. Rev. Sci. Eng., 10, 177 (1974).

Eberly, P.E., Kimberlie, C.N., Miller, W.H. and Drushel, H.V., "Coke Formation on Silica-Alumina Cracking Catalysts", Ind. Eng. Chem. Proc. Des. Dev., 5, 193 (1966).

Edelman, A.M., Lipuma, C.R. and Turpin, F.G., "Developments in Thermal and Catalytic Cracking Processes for Heavy Feeds", Paper presented at the 10th World Petroleum Congress, Bucharest, Romania (1979).

El-Kady, F.Y.A. and Mann, R., "Fouling and Deactivation of a FCC Catalyst I", Applied Catalysis, 3, 211 (1982a)

El-Kady, F.Y.A. and Mann, R., "Fouling and Deactivation of a FCC Catalyst II", Applied Catalysis, 3, 235 (1982b)

Elvin, F.J., "Answer to four basic questions provide key to successful resid processing in FCC units", Oil and Gas J., May 9, 102-112 (1983).

Fetting, F., Gallei, E. and Kredel, P., "Quantitative Determination of Coke Deposition on Zeolite Catalysts by Infrared Spectroscopy", Ger. Chem. Eng., 7, 32-38 (1984).

Finnerman, J.A., Murphy, J.R.and Whittington, E.L., "Heavy-Oil cracking boosts distillates", Oil and Gas Journal, Jan., 53 (1974).

Forzatti, P., Buzzi, G., Morbidelli, M. and Carra, S., "Deactivation of Catalysts. 1. Chemical and Kinetic Aspects", Int. Chem. Eng., 24(1), 60-73 (1984).

Froment, G.F. and Bischoff, K.B., "Non-steady state behaviour of fixed bed catalytic reactors due to catalyst fouling", Chem. Eng. Sci., 16, 189 (1961).

Froment, G.F. and Bischoff, K.B., "Kinetic data and product distribution from fixed bed catalytic reactors subject to catalyst fouling", Chem. Eng. Sci., 17, 105 (1962).

Froment, G.F. and Bischoff, K.B., "Chemical Reactor Analysis and Design", J. Wiley (1979).

Fu, C.M. and Schaffer, A.M., "Effect of Nitrogen Compounds on Cracking Catalysts", Ind. Eng. Chem. Prod. Res. Dev., 24, 68-75 (1985).

Fuentes, G.A., "Catalyst Deactivation and Steady State Activity: A Generalized Power Law Equation Model", Applied Catalysis, 15, 33-40 (1985).

Gates, B.C., Katzer, J.R. and Schuit, G.C., "Chemistry of Catalytic Processes", McGraw-Hill Inc., (1979).

Galtier, P.A. and Pontier, R.J., "Near Full-Scale Cold Flow Model For the R2R Catalytic Cracking Process", in Fluidizaion IV, J.R. Grace, L.W. Shemilt and M.A. Bergougnou, Eds., United Engineering Trustees, Inc., New York, 17-24 (1989).

Gelbin, D. and Fiedler, K., "Concentration Dependence of Diffusion Coefficients in Zeolites", AIChE J., 26(3), 510 (1980).

Greensfelder, B.S. and Voge H.H., "Catalytic Cracking of Pure Hydrocarbons. Cracking of Paraffins", Ind. Eng. Chem. 37(6), 514-520 (1945a).

Greensfelder, B.S. and Voge H.H., "Catalytic Cracking of Pure Hydrocarbons. Cracking of Olefins", Ind. Eng. Chem. 37(10), 983-988 (1945b).

Greensfelder, B.S. and Voge H.H., "Catalytic Cracking of Pure Hydrocarbons. Cracking of Naphthenes", Ind. Eng. Chem. 37(11), 1038-1043 (1945c).

Greensfelder, B.S., Voge, H.H. and Good, G.M., "Catalytic Cracking of Pure Hydrocarbons. Aromatics and Comparison of Hydrocarbon Classes", Ind. Eng. Chem. 37(12), 1168-1176 (1945).

Greensfelder, B.S., Voge, H.H. and Good, G.M., "Catalytic and Thermal Cracking of Pure Hydrocarbons. Mechanisms of Reaction", Ind. Eng. Chem., 41(11), 2573-2584 (1949).

Gross, B., Nace, D.M. and Voltz, S.E., "Application of a Kinetic Model for Comparison of Catalytic Cracking in a Fixed Bed Microreactor and a Fluidized Dense Bed", Ind. Eng. Chem. Proc. Des. Dev., 13, 199-203 (1974).

Gross, B., Jacob, S.M., Nace, D.M. and Voltz, S.E., "Simulation of Catalytic Cracking Process", U.S. Patent 3,960,707 June 1 (1976).

Gussov, S., Higginson, G.W. and Schwint, I.A., "New FCC catalysts score high commercially", Oil and Gas Journal, 70(25), 71 (1972).

Gustafson, W.R., "Evaluation Procedure for Cracking Catalysts", Ind. Eng. Chem. Proc. Des. Dev., 11, 507 (1972).

Hannoun, H. and Regalbuto, J.R., "The Mixing Characteristics of a Novel Microberty Catalytic Reactor", Paper presented at the AIChE Annual Meeting, Washington, D.C., Nov. 27 to Dec. 2 (1988).

Hartzell, F.D. and Chester, A.W., "CO burn promoter produces multiple FCC benefits", Oil and Gas J., 77(16), 83 (1979).

Hatcher, W.J., "Cracking Catalyst Deactivation Models", Ind. Eng. Chem. Prod. Res. Dev., 24, 10-15 (1985).

Heite, R.S., English, A.R. and Smith, G.A., "Bismuth nickel passivation effective in FCCU", Oil and Gas J., June 4, 81-87 (1990).

Hemler, C.L., Lomas, D.A. and Tajbl, D.G., "FCCU reflects technological response to resid cracking", Oil and Gas J., May 28, 79-88 (1984).

Hemler, C.L., Smith R.M. and Cabrera, C.A., "Catalytic Cracking and the Changing Refinery", Paper presented at the UOP Technology Conference, Sept.-Nov. (1985).

Hettinger, W.P., Bech, H.W., Cornelius E.B., Doolin, P.K., Kmecak, R.A. and Kovach, S.M., "Hdrothermal screening of reduced crude conversion catalysts", Symposium on Advances in Catalytic Cracking, ACS, Washington, D.C., Aug. 28 - Sep. 2, 920-933 (1983).

Houdry, E.J., "Catalytic Cracking", Bull. Ass. Fran. Tech. Petr., 117, 177 (1956).

Humes, W.H., "ARCO's Updated Cat-Cracking Pilot Unit", Chem. Eng. Prog., February, 51-54 (1983).

Humphries, A. and Wilcox, J.R., "Zeolite Components and Matrix Composition Determine FCC Catalyst Performance", Akzo Catalysts Courier, Chemical division, North America, Spring (1990).

Huskey, D., "Evaluation of a Multitubular-Cracker-Exchanger FCC Unit", M.E.Sc. Thesis, The University of Western Ontario, London, Ontario, Canada (1990).

Huss, A. and Schwartz, A.B., "Coke reduction in catalytic cracking using silicon-enriched ZSM 20", U.S. Patent 4,933,069 June 12 (1990).

Hsu, L.K.P. and Haynes, H.W., "Effective diffusivity by the

gas chromatographic technique: Analysis and application to measurements of diffusion of various hydrocarbons in zeolite NaY", AIChE J., 27(1), 81 (1981).

Jacob, S.H., Gross, B., Voltz, S.E. and Weekman V.M. "A Lumping and Reaction Scheme for Catalytic Cracking", AIChE J., 22, 701-713 (1976).

Jahnig, C.E., Martin, H.Z. and Campbell, D.L., "History of Fluidized Solids Development at Exxon", in "Fluidization", J.R. Grace and J.M. Matsen Eds., Plenum Press, New York, 3-24 (1980).

Jahnig, C.E., Martin, H.Z. and Campbell, D.L., "The development of fluid catalytic cracking", Chemtech, 106-112, February (1984).

John, T. and Wojciechowski, B.W., "Effect of reaction temperature on product distribution in the catalytic cracking of a neutral distillate", J. Catal., 37, 348 (1975a)

John, T. and Wojciechowski, B.W., "On identifying the primary and secondary products of the catalytic cracking of neutral distillates", J. Catal., 37, 240-250 (1975b)

Johnson, T.E., Murphy J.R. and Tasker, K.G., "Combined Cracking Processes Boost Fuel Yield From Low-Quality Crudes and Residua", Oil and Gas J., 83, 50-55, July 1 (1985).

Kalthod, D.G., "A Method of Obtaining Langmuir-Hinshelwood Parameters From Pulsed Microcatalytic Reactors", Chem. Eng. Comm., 39, 323 (1985).

Kraemer, D.W., "Catalytic Cracking in a Novel Riser Simulator: Design and Testing", M.E.Sc. Thesis, The University of Western Ontario, London Ont., Canada, (1987).

Kraemer, D.W.and de Lasa, H.I., "Catalytic Cracking of Hydrocarbon Feedstocks in a Novel Riser Simulator", Conference Proceedings, 37th Canadian Society of Chemical Engineering Conference, Montreal, P.Q., Canada, 35-37 (1987).

Kraemer, D.W. and de Lasa, H.I., "Catalytic Cracking of Hydrocarbons in a Riser Simulator", Ind. Eng. Chem. Res., 27(11), 2002-2008 (1988a).

Kraemer, D.W. and de Lasa, H.I., "Modelling Catalytic cracking in a Novel Riser Simulator", Paper presented at the AIChE Annual Meeting, November 27 to December 2, Washington, D.C (1988b).

Kraemer, D.W. and de Lasa, H.I., "Modelling Catalytic Cracking in a Fluidized Riser Simulator", Poster Session, International Fluidization Conference, Banff, Alberta (1989).

Kraemer, D.W., Sedran, U. and de Lasa, H.I., "Catalytic Cracking Kinetics in a Novel Riser Simulator", Chem. Eng. Sci., 45(8), 2447-2452 (1990).

Kraemer, D.W., Larocca, M. and de Lasa, H.I., "Deactivation of Cracking Catalysts in Short Contact Time Reactors: Alternative Models", Can. J. of Chem. Eng., accepted for publication (1990).

Krug, R.R. and Schmidt, P.C., "Separation of reacted hydrocarbons and catalyst in fluidized catalytic cracking", U.S. Patent 4,721,603 Jan. 26 (1988).

Kuchcinski, B.R. and Squires, R.G., "Low-Pressure Operation of the Union Carbide Gradientless Reactor", J. Catal., 41, 484-488 (1976).

Kuo, J.C.W. and Wei J., "A Lumping Analysis in Monomolecular Reaction Systems. Analysis of the Approximately Lumpable System", Ind. Eng. Chem. Fund., 8(1), 124-133 (1969).

Larocca, M., "Fast Catalytic Cracking with Nickel and Vanadium Contaminants", Ph.D. Thesis, The University of Western Ontario, London, Ontario, Canada (1988).

Lee, S.L.P., "Bubble Dynamisc in Three Phase Fluidized Beds", Ph.D. Thesis, The University of Western Ontario, London, Ontario, Canada (1986).

Letzsch, W.S., Ritter, R.E. and Vaughan, D.E.W., "Lab can evaluate zeolite FCC catalyst", Oil and Gas J., 74(4), 130 (1976).

Leuenberger, E.L. and Wilbert, L.J., "Octane catalysts raise heat of cracking, reduce coke make", Oil and Gas J., May 25, 38-44 (1987).

Leuenberger, E.L., Moorehead, E.L. and Newell, D.F., "Effects of Feedstock Type on FCC Overcracking", Paper Presented at the NPRA Annual Meeting, San Antonio, Texas, March 20-22 (1988).

Levenspiel, O., "Chemical Reaction Engineering", 2nd Edn., Wiley, New York (1972).

Ligarus, D.K. and Allen, D.T., "Structural Models for Catalytic Cracking. 1. Model Compound Reactions. 2. Reactions of Simulated Oil Mixtures", Ind. Eng. Chem. Res. 28, 665-683 (1989).

Magee, J.S., Ritter, R.E. and Rheaume, L., "A Look at FCC Catalyst Advances", Hydrocarbon Processing, Sep., 123 (1979).

Magee, J.S., Cormier, W.E. and Woltermann, G. M., "Octane catalysts contain special sieves", Oil and Gas J., May 27, 59-64 (1985).

Magee, J.S. and Blazek, J.J., "Zeolite Chemistry and Catalysis", in ACS Monograph No. 171, J.A. Rabo, ed., ACS, Washington, DC (1976).

Mahoney, J.A., "The Use of a Gradientless Reactor in Petroleum Reaction Engineering Studies", J. Catal., 32, 247-253 (1974).

Mann, R., Sharratt, H.P.N. and Thomson, G., "Deactivation of a supported zeolite catalyst: diffusion, reaction and coke deposition in stochastic pure networks", Chem. Eng. Sci., 41(4), 711 (1986).

Mann, R. and Thomson, G., "Deactivation of a supported zeolite catalyst: simulation of diffusion, reaction and coke deposition in a parallel bundle", Chem. Eng. Sci., 42, 3 (1987).

Marcilly, C., Deves, J.M. and Bourgogne, M., "Catalytic cracking catalyst and process", Eur. Pat. Appl. EP 325,502 July 26 (1989).

Marquardt, D.W., "An Algorithm for Least-Squares Estimation of Nonlinear Parameters", J. Soc. Indust. Appl. Math., 11(2), 431-441 (1963).

Maselli, J.M. and Peters, A.W., "Preparation and Properties of Fluid Cracking Catalysts for Residual Oil Conversion", Catal. Rev. Sci. Eng., 26(3), 525-554 (1984).

Matsen, J.M., Harking, J.W. and Mage, E.M., "Chromatographic Pulse Reactors", J. Phys. Chem., 69, 522 (1965).

Mauge, F. and Courcelle, J.C., "New developments in zeolite science and technology", Elsevier, Amsterdam, 28, 803 (1986).

Mauleon, J.L. and Courcelle, J.C., "FCC heat balance critical for heavy fuels", Oil and Gas J., Oct. 21, 64-70 (1985).

Mauleon, J.L. and Sigaud, J.B., "Mix temperature control enhances FCC flexibility in use of wider range of feeds", Oil and Gas J., Feb. 23, 52-55 (1987).

McCabe, W.L. and Smith, J.C., "Unit Operations of Chemical Engineering", 3rd Edn., McGraw-Hill Book Company (1976).

McElhiney, G., "FCC catalyst selectivity determined from microactivity tests", Oil and Gas J., Feb. 8, 35-38 (1988).

McKetta, J.J., "Catalytic Cracking", Encylopedia of Chemical Processing and Design, Dekker, NY, 13, 1-132 (1981).

McLaughlin, K.W. and Anthony, R.G., "The role of zeolite pore structure during deactivation by coking", AIChE J., 31, 927 (1985).

Mitchell, M.M. and Moore, H.F., "Protocol Development For Evaluation of Commercial Catalytic Cracking Catalysts", Paper Presented at the Symposium on Preparation and Characterization of Catalysts before the Division of Petroleum Chemistry, Inc., American Chemical Society Meeting, Los Angeles, September 25-30 (1988).

Montgomery, J.A., "Recycle Rates Reflect FCC Advances", Oil and Gas Journal 70(50), 81 (1972).

Montgomery, J.A., "The Evolution of the Fluid Catalytic Cracking Unit", in the Davison Chemical Guide to Catalytic Cracking, 9-14 (1980).

Montgomery, J.A., "The effect of coke-selective catalysts on fluid cat cracking", Davison Catalagram, No. 73, 3-12 (1985).

Montgomery, J.A. and Letzsch, W.S., "Microactivity test modified for better measure of cracking-catalyst activity", Oil and Gas J., Nov. 22, 60-63 (1971).

Moorehead, E.L., Margolis, M.J. and McLean, J.B., "FCC Catalyst Evaluation: A Comparative Study of Testing Philosophies", Paper Presented at the Symposium on Preparation and Characterization of Catalysts before the Division of Petroleum Chemistry, Inc., American Chemical Society Meeting, Los Angeles, September 25-30 (1988).

Moorman, J.W., "Space velocity and catalyst-to-oil ratio together provide a measure of cracking severity", Oil and Gas J., 52(44), 108 (1954).

Morely, K., "Catalytic Cracking Regeneration Studies", M.E.Sc. Thesis, The University of Western Ontario, London, Ontario, Canada (1987).

Moscou, L. and Moné, R., "Structure and catalytic properties of thermally and hydrothermally treated zeolites. Acid strength distribution on REX and REY", J. Catal., 30, 471 (1973).

Mott, R.W., "New concept measures catalyst performance", Oil

and Gas J., Jan. 26, 73-77 (1987).

Murcia, A.A., Soudek, M., Quinn G.P. and D'Souza, G.J., "Add Flexibility to FCC's", Hydrocarbon Processing, Sep., 131 (1979).

Murphy, J.R. and Soudek, M., "Modern FCC units incorporate many design advances", Oil and Gas Journal, Jan., 71 (1977).

Murphy, J.R., "The development of feed and air distribution systems in fluid catalytic cracking", paper presented at the Ketjen Catalysts Symposium, Amsterdam, The Netherlands, May 27-30 (1984).

Nace, D.M., "Catalytic cracking over crystalline aluminosilicates. I. Instantaneous rate measurements for hexadecane cracking", Ind. Eng. Chem. Proc. Des. Dev., 8(1), 24-31 (1969a).

Nace, D.M., "Catalytic cracking over crystalline aluminosilicates. II. Application of Microreactor Technique to Investigation of Structural Effects of Hydrocarbon reactants", Ind. Eng. Chem. Proc. Des. Dev., 8(1), 31-38 (1969b).

Nace, D.M., "Catalytic Cracking over Crystalline Aluminosilicates. Microreactor Study of Gas Oil Cracking", Ind. Eng. Chem. Prod. Res. Dev., 9(2), 203-209 (1970).

Nace, D.M., Voltz, S.E. and Weekman, V.W., "Application of a Kinetic Model for Catalytic Cracking. Effects of Charge Stocks", Ind. Eng. Chem. Proc. Des. Dev., 10, 530-537 (1971).

Nam, I. and Kittrell, J.R., "Use of Catalyst Coke Content in Deactivation Modelling", Ind. Eng. Chem. Proc. Des. Dev., 23, 237-242 (1984).

Newson, E., "Catalyst deactivation due to pore-plugging by reaction products", Ind. Eng. Chem. Proc. Des. Dev., 14, 1 (1975).

Nieskens, M.J., Khouw, F.H., Borley M.J. and Roebschlaeger K.W., "Shell's resid FCC technology reflects evolutionary development", Oil & Gas J., June 11, 37-44 (1990).

Occelli, M.L., "Recent Trends in Fluid Catalytic Cracking Technology", Chapter 1 in Fluid catalytic Cracking: Role in Modern Refining, ACS Symposium Series, M. Occelli (Ed), 1-16, (1988).

O'Connor, P. and Hartkamp, M.B., "A Microscale Simulation Test

for FCC Development", Paper Presented at the Symposium on Preparation and Characterization of Catalysts before the Division of Petroleum Chemistry, Inc., American Chemical Society Meeting, Los Angeles, September 25-30 (1988).

Oliveira, L.L. and Biscaia, E.C., "Catalytic Cracking Kinetic Models. Parameter Estimation and Model Evaluation", Ind. Eng. Chem. Res., **28**, 264-271 (1989).

Otterstadt, J.E., Gevert, S.B., Jaras, S.G. and Menon, P.G., "Fluid Catalytic Cracking of Heavy (Residual) Oil Fractions: A Review", Applied Catalysis, **22**, 159-179 (1986).

Ozawa, Y. and Bischoff, K.B., "Coke Formation Kinetics on Silica-Alumina Catalyst", Ind. Eng. Chem. Proc. Des. Dev., **7**, 22 (1968).

Pachovsky, R.A. and Wojciechowski, B.W., "Theoretical Interpretation of Gas Oil Conversion Data on an X-Sieve Catalyst", Can. J. Chem. Eng. **49**, 365-369 (1971).

Pachovsky, R.A. and Wojciechowski, B.W., "Effects of diffusion resistance on gasoline selectivity in Catalytic Cracking", AIChE J., **19**, 1121 (1973).

Pachovsky, R.A. and Wojciechowski, B.W., "Effects of Charge Stock Compostion of the Kinetic Parameters in Catalytic Cracking", Can. J. Chem. Eng. **53**, 308-312 (1975a).

Pachovsky, R.A. and Wojciechowski, B.W., "Temperature effects on conversion in the catalytic cracking of a dewaxed neutral distillate", J. Catal., **37**, 120 (1975b).

Pachovsky, R.A. and Wojciechowski, B.W., "Temperature effects on gasoline selectivity in the cracking of a neutral distillate", J. Catal., **37**, 358 (1975c).

Pachovsky, R.A., Best, D.A. and Wojciechowski, B.W., "Applications of the Time-on-Stream Theory of Catalyst Decay", Ind. Eng. Chem. Proc. Des. Dev., **12**(3), 254-261 (1973).

Palekar, M.G. and Rajadhyaksha, R.A., "Sorption accompanied by chemical reaction on zeolites", Catal. Rev. Sci. Eng., **28**(4), 371 (1986).

Paraskos, J.A., Shah, J.T., McKinney, J.D. and Carr, N.L., "A Kinematic Model for Catalytic Cracking in a Transfer Line Reactor", Ind. Eng. Chem. Proc. Des. Dev., **15**, 165-169 (1976).

Parker, A., Dewitz, T.S., Hinds, G.P., Gwyn, J.E., Bilgic, A.H. and Hardesty D.E., "Separation of Fluid Cracking

Catalyst Particles From Gaseous Hydrocarbons", U.S. Patent 4,455,220 Jun. 19 (1984).

Parkinson, G. and Johnson, E., "Designer Catalysts Are All the Rage", Chem. Eng., Sept., 31-46 (1989).

Pasek, E.A. and Morgan, N.C., "Vanadium passivation in a hydrocarbon catalytic cracking process", U.S. Patent 4,929,583 May 29 (1990).

Pierce, W.L., Souter, R., Kaufman, T.G. and Ryan, D.F., "Innovations in Flexicracking", Hydrocarbon Processing, May, 92 (1972).

Pierce, V.E. and Logwinuk, A.K., "Which route to more octane?", Hydrocarbon Processing, Sept., 75-79, (1985).

Piel, W.J., "Ethers will play key role in 'clean' gasoline blends", Oil and Gas J., Dec 4, 40-44 (1989).

Pine, L.A., Maher, P.J. and Wachter, W.A., "Prediction of cracking catalyst behavior by a zeolite unit cell size model", J. Catal., 85, 466-476 (1984).

Plank, C.J., Rosinski, E.J. and Hawthorne, W.P., "Acidic Crystalline Aluminosilicates", Ind. Eng. Chem. Prod. Res. Dev., 3, 165 (1964).

Plank, C.J., "The invention of zeolite cracking catalysts", Chemtech, 243-249, April (1984).

Pohlenz, J.B., "How operational varibales affect FCC", Oil and Gas J., 61(13), 124 (1963).

Prater, C.D. and Lago, R.M., "Kinetics of the Cracking of Cumene", Advances in Catalysis, VIII, 238 (1956).

Rajagopalan, K., Peters, A.W. and Edwards, G.C., "Influence of zeolite particle size on selectivity during fluid catalytic cracking", Applied Catalysis, 23, 69-80 (1986).

Reichele, A.D., "Early Days of Cat Cracking at Exxon", presented at the AIChE Fall National Meeting, San Francisco, November 5-10 (1989).

Ritter, R.E., "Coke selective cracking catalysts for the FCC", Davison Catalagram, No. 73, 14-29 (1985).

Ritter, R.E., Rheaume, L., Welsh, W.A. and Magee, J.S., "A look at new FCC catalysts for resid", Oil and Gas J., July 6, 103-110 (1981).

Ritter, R.E., Creighton, J.E., Roberie, T.B., Chin, D.S. and Wear, C.C., "Catalytic Octane from the FCC", Paper

presented at the NPRA Annual Mtg., Los Angeles, CA, March 23-25 (1986).

Rudershausen, C.G. and Watson, C.C., "Variables affecting activity of molybdena-alumina hydroforming catalyst in aromatization of cyclohexane", Chem. Eng. Sci, 3, 110 (1954).

Ruthven, D.M., "Diffusion in A, X and Y zeolites", ACS Symp. Series, 218, 345 (1983).

Sachanen, A.N., "The Chemical Constitiuents of Petroleum", Reinhold, New York, 289-303 (1945).

Santilli, D.S., "Mechanism of Hexane Cracking in ZSM-5", Applied Catalysis, 60, 137-141 (1990).

Satterfield, C.N., "Heterogeneous Catalysis in Practice", McGraw-Hill, N.Y., (1980).

Saxton, A.L. and Worley, A.C., "Modern talytic-cracking design", Oil and Gas J., 68(20), 82-99, May 18 (1970).

Scherzer, J., "Octane-Enhancing, Zeolitic FCC Catalysts: Scientific and technical aspects", Catal. Rev.-Sci. Eng., 31(3), 215-354 (1989).

Scherzer, J. and Ritter, R.E., "Ion-exchanged ultrastable Y zeolites. 3. Gas oil cracking over rare earth-exchanged ultrastable Y zeolites.", Ind. Eng. Chem. Prod. Res. Dev., 17, 219 (1978).

Shah, Y.T., Huling, G.P., Paraskos, J.A. and McKinney, J.D., "A Kinematic Model for an Adiaibatic Transfer Line Catalytic Reactor", Ind. Eng. Chem. Proc. Des. Dev., 16, 89-94 (1977).

Shaikh, A.A. and Carberry, J.J., "Model of Isothermal Transport-Line (Riser) and Moving-Bed Catalytic Reactor", Chem. Eng. Res. Des., 62(11), 387-390 (1984).

Speronello, B.K. and Reagan, W.J., "Test measures FCC catalyst deactivation by Ni and V", Oil and Gas, J., Jan 30, 139 (1984).

Squires, M., "The Story of Fluid Catalytic Cracking: The First Circulating Fluid Bed", in "Circulating Fluidized Bed Technology", P. Basu, Ed., Pergamon Press, Toronto, 1-19 (1986)

Sterte, J. and Otterstedt, J.E., "Catalytic Cracking of Heavy Oil: Use of Alumina-Montmorillonites both as catalysts and as martices for rare earth exchanged zeolite Y molecular sieve", Applied Catalysis, 38, 131-142 (1988).

Stokes, G.M., Wear, C.C., Suarez, W. and Young G.W., "Reformulated gasoline will change FCC operations and catalysts", Oil and Gas J., July 2, 58-63 (1990).

Strother, C.W., Vermillion, W.L. and Conner, A.J., "FCC getting boost from all-riser cracking", Oil and Gas Journal, May, 103 (1972).

Sunderland, P., "An assessment of laboratory reactors for heterogeneously catalyzed vapour phase reactions", Trans. Instn. Chem. Engrs., **54**, 135 (1976).

Szepe, S. and Levenspiel, O., "Catalyst Deactivation", Chemical Reaction Engineering, Proceedings of the Fourth European Sysmp., Brussels, Pergamon Press, Oxford, 265 (1971).

Takatsuka, T., Sato, S., Morimoto, Y. and Hashimoto, H., "A reaction model for fluidized-bed catalytic cracking of residual oil", Int. Chem. Eng., **27**(1), 107-116 (1987).

Tan, C.H. and Fuller, O.M., "A model fouling reaction in a zeolite catalyst", Can. J. Chem. Eng., **48**, 4 (1970).

Tauster, S.J., Ho, T.C. and Fung, S.C., "Assessment of Diffusional Inhibition via Primary and Secondary Cracking Analysis", J. Catal., **106**, 105-110 (1987).

Thomas, C.L. and Barmby, D.S., "The chemistry of catalytic cracking with molecular sieve catalysts", J. Catal., **12**, 341 (1968).

Tsai, T.C., Kung, H.Y., Yu, S.T. and Chen, C.T., "Effects of acid strength of fluid cracking catalysts on resid cracking operation", Applied Catalysis, **50**, 1-13 (1989).

Tsai, T.C., Pan, W.P., Leu, L.J. and Yu, S.T., "A Procedure for Evaluation of Commercial FCC Catalysts", Chem. Eng. Comm., **78**, 97-109 (1989).

Unzelman, G.H., "Future Role of Ethers in U.S. Gasoline", Paper Presented at the NPRA Annual Meeting, San Francisco, March 19-21 (1989).

Unzelman, G.H., "Reformulated gasolines will challenge product-quality maintenance", Oil and Gas J., Apr. 9, 43-48 (1990).

Upson, L.L., Lawson, R.J., Cormier, W.E. and Baars, F.J., "Matrix, sieve, binder developments improve FCC catalysts", Oil and Gas J., Oct. 1, 64-74 (1990).

Vaughan, D.E., "The synthesis and manufacture of zeolites", Chem. Eng. Progr., February, 25-31 (1988).

Venuto, P.B. and Habib, E.T., "Catalyst-Feedstock-Engineering Interactions in Fluid Catalytic Cracking", Catal. Rev. Sci. Eng., 18(1), 1-150 (1978).

Vermillion, W.L., "Modern FCC design: Evolution and revolution", Paper presented at the Belgium Petr. Inst. Conference., Antwerp, Belgium, Nov. 4 (1974).

Voltz, S.E., Nace, D.M. and Weekman, V.W., "Application of a Kinetic Model for Catalytic Cracking - Some Correlations of Rate Constants", Ind. Eng. Chem. Proc. Des. Dev., 10, 538-541 (1971).

Voorhies, A., "Carbon Formation in Catalytic Cracking", Ind. Eng. Chem., 37(4), 318-322 (1945).

Weekman, V.W., "A model of catalytic cracking conversion in fixed, moving and fluid-bed reactors", Ind. Eng. Chem. Proc. Des. Dev., 7, 90-95 (1968).

Weekman, V.W., "Kinetics and Dynamics of Catalytic Cracking Selectivity in Fixed Beds", Ind. Eng. Chem. Proc. Des. Dev., 8, 385-391 (1969).

Weekman, V.W., "Laboratory Reactors and Their Limitations", AIChE J., 20(5), 833-840 (1974).

Weekman, V.W., "Lumps, Models and Kinetics in Practice", AIChE J., Monograph Series, 75(11), 1-29 (1979).

Weekman, V.M. and Nace, D.M., "Kinetics of Catalytic Cracking Selectivity in Fixed, Moving and Fluid Bed Reactors", AIChE J., 16, 397-404 (1970).

Wei J., and Kuo, J.C.W., "A Lumping Analysis in Monomolecular Reaction Systems. Analysis of the Exactly Lumpable System", Ind. Eng. Chem. Fund., 8(1), 114-123 (1969).

Weiszmann, J.A., D'Auria, J.H., McWilliams, F.G. and Hibbs, F.M., "Pick your option for higher octane", Hydrocarbon Processing, June, 41-45 (1986).

Whitemore, F.C., "Mechanism for catalytic reactions", Chem.Eng. News, 26, 668 (1984).

Whittington, E.L., Murphy, J.R. and Lutz, I.H., "Striking advances show up in modern FCC design", Oil and Gas Journal, Oct., 49 (1972).

Wojciechowski, B.W., "A Theoretical Treatment of Catalyst Decay", Can. J. Chem. Eng., 46, 48-52 (1968).

Wojciechowski, B.W., "The kinetic foundation and practical application of the time on stream theory of catalyst

decay", Cat. Rev. Sci. Eng., 9(1), 79-113 (1974).

Wojciechowski, B.W. and Corma, A., "Catalytic Cracking", Dekker, New York (1986).

Wolf, E.E. and Alfani, F., "Catalysts Deactivation by Coking", Catal. Rev. Sci. Eng., 24(3), 329-371 (1982).

Wollaston, E.G., Haflin, W.J., Ford, W.D. and D'Souza, G.J., "What influences cat cracking", Hydrocarbon Processing, September, 93-100 (1975).

Wrench, R.E., Wilson, R.E., Logwinnk, A.K. and Kendrick, H.D.S., "Fifty Years of Catalytic Cracking", an M.W. Kellogg Co. publication (1986).

Yanik, S.J., Demmel, E.J., Humphries, A.P. and Campagna, R.J., "FCC catalysts containing shape-selective zeolites boost gasoline octane number and yield", Oil and Gas J., May 13, 108-117 (1985).

Yates, J.G., "Fundamentals of Fluidized Bed chemical Processes", Butlewood Monographs in Chemical Engineering, London, England, 121 (1983).

Yatsu, C.A. and Keyworth, D.A., "Modified MAT and GC help predict FCC gasoline quality", Oil and Gas J., Mar 26, 64-73 (1990).

Yen, L.C., Wrench, R.E. and Ong, A.S., "Reaction kinetic correlation equation predicts fluid catalytic cracking coke yields", Oil and Gas J., Jan. 11, 67-70 (1988).

Young, G.W. and Rajagopalan, K., "Techniques for Evaluating Heavy Oil Cracking Catalyst", Ind. Eng. Chem. Proc. Des. Dev., 24, 995-999 (1985).

Young, G.W. and Weatherbee, G.D., "FCCU Studies with an Adiabatic Circulating Pilot Unit", Paper Presented at the AIChE Annual Meeting, San Francisco, November (1989).

MODELLING CATALYTIC CRACKING IN A NOVEL RISER SIMULATOR

Volume II

Appendices

by

Daniel W. Kraemer

Faculty of Engineering Science

Submitted in partial fulfilment
of the requirements for the degree of
Doctor of Philosophy

Faculty of Graduate Studies
The University of Western Ontario
London, Ontario
December 1990

VOLUME II

Appendices

APPENDIX A

DERIVATION OF KINETIC EQUATIONS

A.1 Reactor Model

The reactor operates in a batch condition and achieves close to ideal mixing, thus the change in concentration of component i (C_i) with time (t) is equal to the reaction rate of that component (r_i):

$$\frac{dC_i(gmol/cm^3)}{dt\ (s)} = \frac{r_i(gmol/g_{cat}.s)\ m_c(g_{cat})}{V_T(cm^3)} \qquad (A1).$$

The concentration of component i can also be expressed in terms of its partial pressure (P_i) within the reactor:

$$dC_i = P_i\ /\ (RT) \qquad (A2).$$

Furthermore, since the total mass (w_T) is constant in the reactor C_i may be expressed in terms of its weight fraction (Y_i) by the following derivation:

$$N_i(gmol) = w_i(g)\ /\ M_i(g/gmol)$$
$$= Y_i(g/g_{total}) * w_T(g_{total})\ /\ M_i(g/gmol)$$

Since $C_i = N_i/V_T$ then;

$$C_i = Y_i\ w_T\ /\ (M_i\ V_T) \qquad (A3).$$

A.2 Kinetic Equations for the Three-Lump Model

The three lump model consists of a the triangular reaction scheme as discussed in Chapter 1 with gas oil (A) cracking to both gasoline (B) and light gases plus coke (C). The gasoline can also crack to the light gases plus coke lump. The cracking of the gas oil is normally assumed to be second order and the gasoline cracking is taken as first order. To completely describe the kinetics a deactivation function is included as an integral part of the rate expression to account for the loss of catalyst activity due to coke deposits. The expression for r_i can then be expressed as:

for gas oil: $r_A = - \Phi\ k_o\ C_A^2$

for gasoline: $r_B = \Phi(v_1\ k_o\ C_A^2 - k_2\ C_B)$

where $k_o = k_1 + k_3$ (units of $cm_6/(g_{cat}.s.gmol)$), v_1 is the stoichiometric coefficient (M_A/M_B) and Φ is assumed to be the same for gas oil molecules and gasoline molecules. Substituting the rate expression for gas oil into the reactor model, equation (A1), gives the following expression:

$$-dC_A/dt = \Phi\ k_o\ C_A^2\ m_c\ /V_T \qquad \text{(A4)}.$$

Converting concentrations to weight fractions by using equation (A3) gives:

$$-dY_A/dt = \Phi\ k_o\ Y_A^2\ w_T\ m_c\ /(M_A\ V_T^2) \qquad \text{(A5)}.$$

Similarly for the gasoline lump the following two equations

result:

$$dC_B/dt = \Phi \left[v_1 k_1 C_A^2 - k_2 C_B \right] m_c / V_T \qquad (A6)$$

and

$$dY_B/dt = \Phi \left[(w_T/M_A V_T) k_1 Y_A^2 - k_2 Y_B \right] m_c/V_T \qquad (A7).$$

Similar expressions could be written for the light gases plus coke lump, but are not necessary to determine the kinetic constants. This is to say that once parameter estimates are found for k_o and k_1 then k_3 may be determined by difference ($k_3 = k_o - k_1$). Depending on the form of the decay function used, equations (A5) to (A7) may have analytical solutions. However, these equations may also be solved numerically, for example using a Runge-Kutta method which was the method used in this study.

A.3 Kinetic Equations for the 8-Lump Model

The kinetic scheme for the 8-lump model was shown in Chapter 3 in Figure 3.9. The six oil lumps represent a reasonably narrow boiling range of compounds and thus the cracking order is assumed to be one. Thus the rate of cracking (or disappearance) of a lump may be expressed as:

$$r_i = - \Phi k_i C_i \qquad (A8).$$

Using equation (A8) and equation (A3) to express the kinetics in terms of weight fractions and substituting into the reactor model, equation (A1), gives the following equations for the

six oil lumps and the gasoline lump:

Heavy paraffins:

$$dY_{Ph}/dt = - \Phi\, k_{Ph}\, Y_{Ph}\, m_c / V_T \qquad (A9)$$

Heavy naphthenes:

$$dY_{Nh}/dt = - \Phi\, k_{Nh}\, Y_{Nh}\, m_c / V_T \qquad (A10)$$

Heavy aromatics:

$$dY_{Ah}/dt = - \Phi\, k_{Ah}\, Y_{Ah}\, m_c / V_T \qquad (A11)$$

Light paraffins:

$$dY_{Pl}/dt = \Phi\, [\, k_{PhPl}\, Y_{Ph} - k_{Pl}\, Y_{Pl}\,]\, m_c / V_T \qquad (A12)$$

Light naphthenes:

$$dY_{Nl}/dt = \Phi\, [\, k_{NhNl}\, Y_{Nh} - k_{Nl}\, Y_{Nl}\,]\, m_c / V_T \qquad (A13)$$

Light aromatics:

$$dY_{Al}/dt = \Phi\, [\, k_{AhAl}\, Y_{Ah} - k_{Al}\, Y_{Al}\,]\, m_c / V_T \qquad (A14)$$

Gasoline:

$$dY_G/dt = \Phi\, [\, k_{PhC}\, Y_{Ph} + k_{NhG}\, Y_{Nh} + k_{AhG}\, Y_{Ah} + k_{PlG}\, Y_{Pl} + k_{NlG}\, Y_{Nl} + k_{AlG}\, Y_{Al} - k_{GC}\, Y_G\,]\, m_c / V_T \qquad (A15).$$

It also follows that for the cracking of the pure light oil mixtures the pure light oil equations are equivalent to the heavy oil lump equations with a change in nomenclature:

Pure light oil lumps:

$$dY_{il}/dt = - \Phi\, k_{il}\, Y_{il}\, m_c / V_T \qquad (A16).$$

Similarly the gasoline equation for the cracking of the pure light oil mixtures is equivalent to the general light oil lump equations (equations A12 to A14) with a change in nomenclature:

Pure light oil lumps gasoline equation:

$$dY_G/dt = \Phi \left[k_{OG} Y_o - k_{GC} Y_G \right] m_c / V_T \qquad \text{(A17)}.$$

A.5 Catalyst Deactivation Functions

The catalyst decay can be describe in terms of its activity where the fraction of active sites is defined as the concentration of available active sites divided by the total number of active sites. Thus, the rate of loss of the fractional active sites, Φ, can be expressed as (Wojciechowski, 1974):

$$- d\Phi/dt = k_d \Phi^n \qquad \text{(A18)}.$$

In equation (A18) k_d is the rate constant of catalyst decay (units of 1/s) and n is the order of decay.

General n^{th} order catalyst decay function:

Integrating equation (A16) between the limits $\Phi = 1$, Φ and $t = 0$, t leads to the following expression for the general n^{th} order power law catalyst decay function:

$$\Phi = \left[1 + k_d t(n-1) \right]^{-1/(n-1)} \qquad \text{(A19)}.$$

This expression is valid for all cases except when n is equal to one (i.e. first order decay).

The Exponential Law:

In the case for n = 1, the integration of equation (A18) with the limits (Φ = 1 at t = 0 and Φ = Φ at t = t) results in the following expression:

$$\Phi = \exp(-k_d t) \qquad \text{(A20)}.$$

The catalyst decay function expressed as equation (A20) is commonly called the exponential law and has been used in several studies (i.e. decay is assumed to be first order).

The Power Law:

Another catalyst decay function commonly used throughout the literature and referred to as the power law function is obtained by integrating equation (A18) using the unrealistic limits of $\Phi = \infty$, Φ. This results in the following equation:

$$\Phi = [(n-1)k_d t]^{-1/(n-1)} \qquad \text{(A21)}.$$

where n is greater than 1.0.

This same result is arrived at by assuming that for long catalyst times on stream, the value of $k_d t(n-1)$ is much larger than 1. Equation (A21) is frequently written as:

$$\Phi = Dt^{-N}$$

$$\text{where} \quad D = [(n-1)k_d]^{-N} \quad \text{and} \quad N = 1/(n-1) \qquad \text{(A22)}.$$

Catalyst Decay as a Function of Coke on the Catalyst:

Froment and Bischoff (1961, 1962) argue from a fundamental point of view that the catalyst decay should be related to the mass of coke deposited on the catalyst during cracking. In this case the fraction of active sites can be expressed as:

$$\Phi = (1 - \sigma C_c/C_t)^{\perp} \qquad \text{(A23)}$$

with: C_c = sites covered by coke (gmol coke / g catalyst)
σ = proportionality factor (gmol sites/gmol coke)
C_t = total active sites (gmol sites/g catalyst).

Equation (A23) can be rearranged to give:

$$C_c = - C_t(1 - \Phi^{1/n})/\sigma \qquad \text{(A24)}.$$

Differentiating equation (A24) with respect to time gives:

$$dC_c/dt = - (C_t\Phi^{(1/n)-1})(1/n\sigma)\ (d\Phi/dt) \qquad \text{(A25)}.$$

The rate of coke formation in the Riser Simulator (dC_c/dt) can also be expressed in terms of the cracking of gas oil (assuming negligible contribution from gasoline cracking):

$$dC_c/dt = k_c\ C_A^2\ \Phi \qquad \text{(A26)}$$

where k_c is the cracking rate constant of gas oil to coke (which is a fraction of k_3 describing the cracking of gas oil to light gases plus coke from the 3-lump model). As well, equation (A4) can be rearranged to give:

$$C_A^2\Phi = (dC_A/dt)(-V_T/k_om_c) \qquad \text{(A27)}.$$

Equation (A27) can be substituted into equation (A26) for $C_A^2\Phi$ and the resulting equation set equal to equation (A25) to give the following differential equation:

$$dC_A = (k_o m_c C_t / k_c V_T n \sigma)\ \Phi^{(1/n)-1}\ d\Phi \qquad \text{(A28)}.$$

If equation (A3) is used to convert C_A to a weight fraction (Y_A) and the resulting equation is integrated between the limits $Y_A = 1$, Y_A and $\Phi = 1$, Φ then the following expression results:

$$\Phi = \{1 + [(Y_A - 1)\ w_T\ k_c\sigma\ /\ (C_t k_o\ m_c\ M_A)]\}^n \qquad \text{(A29)}.$$

Finally, calling k_d' ($= k_c\sigma/C_t$) the deactivation kinetic constant and letting n=1, then the catalyst decay function relating the deactivation to the amount of coke on the catalyst can be written as:

$$\Phi = 1 + [(Y_A - 1)\ w_T\ k_d'\ /\ (k_o\ m_c\ M_A)] \qquad \text{(A30)}.$$

Summary of Kinetic Equations With Analytical Solutions

- Oil equation for the three lump model with exponential decay ($k_d = \alpha$);

$$Y_A = [(1/Y_A^\circ) - (w_T m_c k_o / M_A V_T^2 \alpha)(e^{-\alpha t} - 1)]^{-1}$$

- Oil equation for the three lump model with power law decay;

$$Y_A = [(1/Y_A^\circ) - t^{1-N}\ w_T m_c k_o' /\ ((M_A V_T^2 (N - 1)))]^{-1}$$

- Heavy oil lump equations for the eight lump model with exponential decay ($k_d = \alpha$ and i = P, N or A);

$$Y_h = Y_h^\circ \exp\left[m_c k_h (e^{-\alpha t} - 1)/(V_T \alpha)\right]$$

• Heavy oil lump equation for the eight lump model with power law decay;

$$Y_h = Y_h^\circ \exp\left[m_c k_h\, t^{1-N}/(V_T(N-1))\right]$$

A.6 Solution Strategy for the Kinetic Models

Three Lump Model

Appendix G lists the computer programs used to obtain the kinetic parameter estimates for the 3-lump model. The non-linear least-squares estimation was performed using an algorithm given by Marquardt (1963). The values of k_o and k_d were found using programs OOPT3A.FTN, OOPT3B.FTN and OOPT3FB.FTN for the exponential decay, power law decay and Froment-Bischoff type decay functions. These programs are identical except for the subroutine FUNC which evaluates the specific equation obtained depending on the decay function used.

The programs GOPT3A.FTN, GOPT3B.FTN and GOPT3FB.FTN find estimates for k_1 and k_2 from the gasoline equation for the three different decay functions based on the k_o and k_d values obtained from OOPT3.FTN. The value of k_3 is found by the relation $k_o = k_1 + k_3$.

In the GOPT3.FTN programs a fourth-order Runge-Kutta algoritnm is used to solve the set of differential equations.

The step size was optimized by using different values until the parameter estimates did not change significantly. The accuracy of the method was checked using a set of differential equations with a known analytical solution as described by the program TEST.FTN in Appendix G and was found to be very precise for a large step size.

The program TEST3.FTN solved the 3-lump model equations using the Runge-Kutta algorithm with the parameter estimates obtained. The computed yields obtained for a given reaction time and set of kinetic constants could then be compared with experimental data to test the predictive capabilities of the model.

Eight-Lump Model

The matrix of rate constants for the 8-lump model is lower triangular due to the irreversible nature of the cracking network leading to a stepwise solution. The heavy lump equations can be solved independently from each other as well as independently from the light oil equations and the gasoline equation. Similarly, the three light oil equations can be solved, in conjunction with the known values from the corresponding heavy oil equations, independently of each other and the gasoline equation. Marquardt nonlinear regression coupled with a fourth-order Runge-Kutta algorithm was used for the computer analysis. The following solution method was used to determine the 16 kinetic constants for the 8-lump model:

1. The values of k_{ii} and either α of N were determined for

the three oil lumps (equations A9 to A11) using the program (HLOPT8.FTN). The values of the deactivation parameter (α or N) were then averaged.

2. The values of k_{ahl} and k_{il} were determined from the light oil lump equations (A12 to A14) by program LLOPT8.FTN using information from 1.

3. The ratio of k_{iG}/k_{il} (ie. selectivity to gasoline) from the pure light oil mixture data and the value of k_2 (= k_{GC}) from the 3-lump model were used in the gasoline equation (equation A15). Program GLOPT8.FTN was then used to estimate the parameters k_{ahG}.

4. The remaining parameters, k_{ahC} and k_{iiC} were found by difference using the relations $k_{ah} = k_{ahl} + k_{ahG} + k_{ahC}$ and $k_{il} = k_{iiG} + k_{iiC}$.

It should be mentioned that determination of the pure light oil mixture kinetic parameters was performed using the program HLOPT8.FTN since the equations used in this program apply for a single lump (i.e. equations A12 to A14 with Y_{ah} set equal to zero). This allowed evaluation of k_{il} (= k_{iiG} + k_{iiC}) and the deactivation parameter. The values of k_{iiG} and k_{GC} for the pure light oil mixtures were then solved using the LLOPT8.FTN programs since these equations are equivalent to the gasoline equation for the pure light oil mixtures (equation A17) with a change in nomenclature.

The parameter estimates obtained from the regression analysis on the 8-lump model equations were entered into program TEST8L.FTN which solved the 7 differential equations (A9 to A15) simultaneously using the 4th order Runge-Kutta algorithm. This simulation allowed generation of conversion and yield data for any reaction time which was compared with experimental data to see the predictive capabilities of the model.

APPENDIX B

DERIVATION OF MASS BALANCE EQUATIONS

Mass of Hydrocarbons Purged:

At the end of the reaction period, the vapours from the reactor are rapidly purged into the vacuum-purge system. Since the vacuum-purge system is a closed vessel this process results in a pressure equilibrium between the reactor and total purge volume. Knowing the pressure in the vacuum-purge unit before and after this equilibration allows calculation of the total number of moles purged:

$$N_{purged} = (P_{vf} - P_{vi})V_v \;/\; RT_v \qquad (B1).$$

The total mass purged can be calculated by multiplying the total moles purged by the average molecular weight of the vapours:

$$m_p = M_{avg}(P_{vf} - P_{vi})V_v \;/\; RT_v \qquad (B2).$$

The purged vapours consist of hydrocarbons and argon from the reactor, thus M_{avg} may be expressed as:

$$M_{avg} = n_{HC}\, M_{HC} + n_{Ar}\, M_{Ar} \qquad (B3).$$

The sum of the mole fractions $n_{HC} + n_{Ar}$ is equal to one. As well, since the purged gases are those coming from the reactor which operates as a closed system during cracking, then the ratio of grams of hydrocarbons to grams of argon (w_o/w_{Ar}) is constant. The mass of hydrocarbons is denoted as w_o which is equal to the mass of oil injected minus the amount of coke formed at the end of the reaction period. In other words, the

mass fraction of hydrocarbons (X_{HC}) in the reactor (and hence purged gases) is a constant:

$$X_{HC} = w_o / (w_o + w_{Ar}) = w_o/w_T \qquad (B4).$$

The mass of argon, w_{Ar}, is defined by the initial reactor conditions:

$$w_{Ar} = P_{Ri} V_R M_{Ar} / (R T_R) \qquad (B5).$$

Substituting equation (B5) into equation (B4) for w_{Ar} and letting $\Psi = P_{Ri} V_R / (R T_R w_o)$ leads to the following expression:

$$X_{HC} = 1/(1 + \Psi M_{Ar}) \qquad (B6).$$

Multiplying X_{HC} by the total mass of gases purged, m_p, as given by equation (B2) gives the mass of hydrocarbons purged:

$$m_{HC,p} = X_{HC} M_{avg}(P_{vf} - P_{vi}) V_v / RT_v \qquad (B7).$$

An expression for M_{avg} can also be derived by rearranging the expression for the mole fraction of hydrocarbons, n_{HC}:

$$n_{HC} = w_o M_{HC}/(w_o M_{HC} + w_{Ar} M_{Ar}) = 1/[1 + (w_{Ar} M_{HC}/w_o M_{Ar})] \qquad (B8).$$

Substituting equation (B5) for w_{Ar} in equation (B8) and using the expression for Ψ gives an equation for the mole fraction of hydrocarbons similar to equation (B6):

$$n_{HC} = 1/(1 + \Psi M_{HC}) \qquad (B9).$$

When equation (B9) is substituted into equation (B3) and

remembering that $n_{HC} = 1 - n_{Ar}$, then the following equation results:

$$M_{avg} = M_{HC}(1 + \Psi M_{Ar})/(1 + \Psi M_{HC}) \qquad \text{(B10)}.$$

Finally, making the substitution for X_{HC} as given by equation (B6) and for M_{avg} as given by equation (B10) into equation (B7) gives the following equation for the mass of hydrocarbons purged:

$$m_{HC,p} = [M_{HC} / (1 + \Psi M_{HC})] [(P_{Vf} - P_{Vi}) V_V / (RT_V)] \qquad \text{(B11)}.$$

Mass of Hydrocarbons Remaining in the Reactor:

The final pressure in the reactor is equivalent to the final vacuum system pressure since the two vessels attain pressure equilibrium. This allows calculation of the total number of moles left in the reactor, $N_{remaining}$:

$$N_{remaining} = P_{Vf} V_R / (R T_R) \qquad \text{(B12)}.$$

The mass of hydrocarbons remaining in the reactor can be found by multiplying equation (B12) by the average molecular weight (M_{avg}) and the mass fraction of hydrocarbons (X_{HC}) from the expressions already derived above. The resulting equation for the mass of hydrocarbons remaining in the reactor is thus:

$$m_{HC,r} = [M_{HC} / (1 + \Psi M_{HC})] [P_{Vf} V_R / (R T_R)] \qquad \text{(B13)}.$$

The summation of equations (B11) and (B13) then gives the total mass of hydrocarbons in the system ($m_{HC} = m_{HC,p} + m_{HC,r}$):

$$m_{HC} = [M_{HC}/(1 + \Psi M_{HC})][(P_{Vf} - P_{Vi})V_V/(RT_V) + P_{Vf}V_R/(RT_R)] \quad (B14).$$

The value of m_{HC}, obtained from the measured variables, can then be compared to the known mass of oil injected to the reactor minus the coke formed for each run.

One of the problems with using equation (B14) is that the molecular weight of hydrocarbons must be estimated from the GC analysis. This is not always reliable because of the large number of peaks and splitter discrimination which misses some of the oil fraction. Thus, another useful relationship can be developed for the average molecular weight of the vapours at the end of the reaction period. M_{avg} can be expressed as the mass of fluid divided by the total moles of fluid as given by the pressure at the end of the reaction period pressure (P_{Re}):

$$M_{avg} = m_T \; R \; T_R \; / \; (P_{Re} \; V_R) \quad (B15).$$

The total mass of fluid, w_T, is equal to $(w_o + w_{Af})$. The value of P_{Re} can be calculated from the measured variables using the equilibrium relationship (moles purged from the reactor equals the moles purged into the vacuum chamber):

$$(P_{Vf} - P_{Vi})V_V/RT_V = (P_{Re} - P_{Rf})V_R/RT_R \quad (B16).$$

Knowing that the final reactor pressure (P_{Re}) is equal to the final vacuum pressure (P_{Vf}) then the following expression results for P_{Re}:

$$P_{Re} = (P_{Vf} - P_{Vi})V_VT_R/(V_RT_V) + P_{Vf} \quad (B17).$$

Thus, substituting for P_{Re} and w_{Ar} in equation (B15) and rearranging gives an expression for the average molecular weight of the reaction fluid as follows:

$$M_{avg} = RT_R T_V w_T \; / \; [(P_{Vf} - P_{Vi})V_V T_R + P_{Vf} V_R T_V] \qquad \text{(B18)}.$$

This value can be used to compare with the measured molecular weight obtained from the GC analysis on the sampled vapours. It should be noted that equation (B18) when used to evaluate the mass of hydrocarbons purged (equation (B11)) and the mass of hydrocarbons remaining in the reactor (equation (B13)) the resulting sum is equal to w_o which gives a redundant mass balance. In this way, an independent value for the molecular weight, as assessed by GC methods must be used.

Alternatively, the mass of hydrocarbons remaining in the reactor can be measured from the sample loop injection to the GC. The total area measured by the integrator from this sample can be calibrated using a standard gas (eg. propane). Thus, a certain area from the integrator will correspond to certain mass, known from the calibration injection. Knowing that the partial pressure of hydrocarbons in the sample loop is the same as those remaining in the reactor then $m_{HC,r}$ can be found using the ratio of sample loop and reactor volumes:

$$m_{HC,r} = m_{HC,l} \; (V_l T_R / V_R T_l) \qquad \text{(B19)}.$$

In equation (B19) $m_{HC,l}$ is the mass of hydrocarbons in the loop, V_l is the sample loop volume and T_l is the sample loop temperature. To find $m_{HC,l}$ the ratio of total areas from

reported by the integrator for the calibration and sample loop injections can be used:

$$m_{HC,l} = a_l \, m_{cal} \, / \, a_{cal} \qquad (B20)$$

where a_l and a_{cal} are total area counts for the loop injection and calibration injection respectively and m_{cal} is the mass of the calibration gas used. Substituting equation (B20) into (B19) results in:

$$m_{HC,r} = a_l \, m_{cal} \, V_R \, T_l \, / \, (a_{cal} \, V_l \, T_R) \qquad (B21).$$

Letting the average molecular weight of the fluid in the reactor be given by equation (B18) and substituting this into equation (B7) and combining with equation (B21) gives the final mass balance equation:

$$m_{HC} = w_o/\{1 + P_f V_R T_V/((P_{Vf} - P_{Vi}) V_V T_R)\} + a_l m_{cal} V_R T_l/(a_{cal} V_l T_R) \qquad (B22).$$

A computer program (MASSBAL.FTN in appendix G) was written for the calculation of the mass balance, and calibration of the GC area was done using gas injections of known amounts of propane.

APPENDIX C

PREDICTED RESULTS FROM THE KINETIC MODELS WITH STATISTICAL ANALYSIS

This appendix presents tabulated data from experimental values and calculated values from the various kinetic models used. As well, analysis of variance (ANOVA) data is presented for the data obtained using the 3-lump model. The nomenclature for the ANOVA tables is as follows:

SS = sum of squares

df = degrees of freedom

MS = mean sum of squares (= SS/df)

PE = pure error

LOF = lack of fit

RES = residuals

SS of the residuals was calculated by taking the summation of the square of the difference between calculated and experimental values. The degrees of freedom is the number of observations minus the number of parameters. The SS for the pure error is obtained by summing the squares of the difference between calculated values and the average experimental values for each repeat group. The degrees of freedom for the PE is equal to the number of data points in repeat groups minus the number of repeat groups. The SS for the lack of fit was calculated by the difference between the SS due to residuals and the SS due to PE.

The value MS(LOF/PE) was calculated by dividing the MS for the LOF by the MS for the PE. The standard F-distribution was used to establish if there was lack of fit with a 95% confidence interval. If MS(LOF/PE) is less than the value of $F_{.95}(df_{LOF}/df_{pe})$ then there is no lack of fit.

Table C.1a Calculated versus experimental conversions for the 3-lump model using three different decay functions (feedstock A cracked on Octacat).

		conversion (wt%)			
		calculated			experimental
T(°C)	t(s)	$e^{-\alpha t}$	t^{-N}	F-B	
500	3	33.07	33.71	33.35	34.59
	5	42.36	41.83	42.13	40.44
	7	48.00	47.46	47.75	47.30
	10	53.06	53.50	53.31	55.26
	s.d.:	± 1.94	± 1.44	± 1.70	
525	3	41.83	42.75	42.27	43.48
	5	50.89	50.37	50.64	48.60
	7	55.86	55.41	55.64	56.47
	10	59.93	60.62	60.37	62.56
	s.d.:	± 2.29	± 1.71	± 1.98	
550	3	48.60	48.98	48.79	49.41
	5	57.12	56.31	56.67	54.38
	7	61.44	61.01	61.22	60.78
	10	64.78	65.78	65.42	67.19
	s.d.:	± 1.76	± 1.28	± 1.47	

s.d. = standard deviation from experimental data

Table C.1b ANOVA for the conversion data of feedstock A cracked with Octacat catalyst.

T = 500°C Decay:	$e^{-\alpha t}$			t^{-N}			F-B		
	SS	df	MS	SS	df	MS	SS	df	MS
PE	3.98	3	1.33	3.98	3	1.33	3.98	3	1.33
LOF	22.3	3	7.43	10.5	3	3.51	16.3	3	5.44
RES	26.3	6		14.5	6		20.3	6	
MS(LOF/PE):	5.59			2.64			4.09		
T = 525°C									
PE	3.70	3	1.23	3.70	3	1.23	3.70	3	1.23
LOF	33.3	3	11.1	16.7	3	5.28	23.9	3	7.99
RES	36.9	6		20.4	6		27.6	6	
MS(LOF/PE):	8.90			4.54			6.50		
T = 525°C									
PE	5.11	4	1.28	5.11	4	1.28	5.11	4	1.28
LOF	16.6	2	8.30	6.43	2	3.22	10.1	2	5.06
RES	21.7	6		11.5	6		15.2	6	
MS(LOF/PE):	6.50			2.51			3.95		

$F_{.95}(3,3) = 9.28$

$F_{.95}(2,4) = 6.94$

■ Since MS(LOF/PE) < $F_{.95}(n,m)$ then the model does not contradict the data.

Table C.2a Calculated versus experimental conversions for the 3-lump model using three different decay functions (feedstock A cracked on GX-30).

		conversion (wt%)			
		calculated			experimental
T(°C)	t(s)	$e^{-\alpha t}$	t^{-N}	F-B	
500	3	38.77	39.46	39.17	41.54
	5	49.49	49.21	49.34	47.01
	7	56.06	55.71	55.85	57.90
	10	62.14	62.39	62.32	63.42
	s.d.:	± 2.05	± 1.77	± 1.88	
525	3	50.12	50.52	50.40	50.27
	5	59.95	59.42	59.59	59.08
	7	65.30	64.99	65.06	64.40
	10	69.78	70.48	70.27	71.02
	s.d.:	± 2.43	± 2.33	± 2.35	
550	3	53.53	53.82	53.74	54.05
	5	63.21	62.64	62.81	62.13
	7	68.38	68.05	68.14	67.54
	10	72.66	73.30	73.17	74.78
	s.d.:	± 2.40	± 2.24	± 2.27	

s.d. = standard deviation from experimental data

Table C.2b ANOVA for the conversion data of feedstock A cracked with GX-30 catalyst.

T = 500°C Decay:	$e^{-\alpha t}$			t^{-N}			F-B		
	SS	df	MS	SS	df	MS	SS	df	MS
PE	7.34	4	1.84	7.34	4	1.84	7.34	4	1.84
LOF	22.1	2	11.0	14.5	2	7.27	17.5	2	8.74
RES	29.4	6		21.9	6		24.8	6	
MS(LOF/PE):	6.00			3.95			4.75		
T = 525°C									
PE	37.3	4	9.33	37.3	4	9.33	37.3	4	9.33
LOF	4.07	2	2.04	0.65	2	0.33	1.27	2	0.64
RES	41.4	6		37.9	6		38.6	6	
MS(LOF/PE):	0.22			0.04			0.07		
T = 525°C									
PE	31.9	4	7.98	31.9	4	7.98	31.9	4	7.98
LOF	8.40	2	4.20	3.16	2	1.58	4.20	2	2.10
RES	40.3	6		35.1	6		36.1	6	
MS(LOF/PE):	0.53			0.20			0.26		

$F_{.95}(3,3) = 9.28$

$F_{.95}(2,4) = 6.94$

■ Since MS(LOF/PE) < $F_{.95}(n,m)$ then the model does not contradict the data.

Table C.3a Calculated versus experimental conversions for the 3-lump model using three different decay functions (feedstock B cracked on Octacat).

		conversion (wt%)			
		calculated			experimental
T(°C)	t(s)	$e^{-\alpha t}$	t^{-N}	F-B	
500	3	25.85	26.14	25.99	25.75
	5	35.77	35.58	35.70	34.11
	7	42.78	42.55	42.66	42.14
	10	50.10	50.26	50.17	50.17
	s.d.:	± 0.98	± 0.94	± 0.96	
525	3	34.62	35.23	34.94	34.43
	5	44.35	43.88	44.14	41.92
	7	50.30	49.81	50.30	49.89
	10	55.70	56.11	55.91	56.19
	s.d.:	± 1.49	± 1.31	± 1.38	
550	3	42.08	42.57	42.39	41.87
	5	51.62	50.97	51.27	51.93
	7	56.98	56.50	56.67	56.95
	10	61.51	62.19	61.85	61.42
	s.d.:	± 0.22	± 0.86	± 0.57	

s.d. = standard deviation from experimental data

Table C.3b ANOVA for the conversion data of feedstock B cracked with Octacat catalyst.

T = 500°C Decay:	$e^{-\alpha t}$			t^{-N}			F-B		
	SS	df	MS	SS	df	MS	SS	df	MS
PE	4.95	4	1.24	4.95	4	1.24	4.95	4	1.24
LOF	1.83	2	0.92	1.22	2	0.61	1.50	2	0.75
RES	6.78	6		6.17	6		6.45	6	
MS(LOF/PE):	0.74			0.49			0.60		
T = 525°C									
PE	6.05	4	1.51	6.05	4	1.51	6.05	4	1.51
LOF	9.44	2	4.72	5.98	2	2.99	7.37	2	3.69
RES	15.5	6		12.0	6		13.4	6	
MS(LOF/PE):	3.13			1.98			2.44		
T = 525°C									
PE	5.21	4	1.30	5.21	4	1.30	5.21	4	1.30
LOF	9.20	2	4.60	16.9	2	8.45	10.7	2	5.35
RES	14.4	6		22.1	6		15.9	6	
MS(LOF/PE):	3.53			6.48			4.11		

$F_{.95}(3,3) = 9.28$

$F_{.95}(2,4) = 6.94$

■ Since MS(LOF/PE) < $F_{.95}(n,m)$ then the model does not contradict the data.

Table C.4a Calculated versus experimental conversions for the 3-lump model using three different decay functions (feedstock B cracked on GX-30).

		conversion (wt%)			
		calculated			experimental
T(°C)	t(s)	$e^{-\alpha t}$	t^{-N}	F-B	
500	3	28.17	28.56	28.37	30.05
	5	38.73	38.64	38.70	38.01
	7	46.14	45.94	46.03	44.76
	10	53.83	53.86	53.84	54.88
	s.d.:	± 1.24	± 1.12	± 1.18	
525	3	36.93	37.05	37.01	37.63
	5	49.08	49.03	49.05	48.49
	7	57.14	57.08	57.09	58.10
	10	65.16	65.21	65.20	65.04
	s.d.:	± 0.81	± 0.79	± 0.80	
550	3	44.53	44.51	44.52	44.40
	5	56.81	56.72	56.74	57.01
	7	64.43	64.42	64.41	64.63
	10	71.62	71.83	71.80	71.17
	s.d.:	± 1.92	± 1.93	± 1.93	

s.d. = standard deviation from experimental data

Table C.4b ANOVA for the conversion data of feedstock B cracked with GX-30 catalyst.

T = 500°C Decay:	$e^{-\alpha t}$			t^{-N}			F-B		
	SS	df	MS	SS	df	MS	SS	df	MS
PE	5.50	4	1.38	5.50	4	1.38	5.50	4	1.38
LOF	5.35	2	2.68	3.30	2	1.65	4.26	2	2.13
RES	10.9	6		8.80	6		9.76	6	
MS(LOF/PE):	1.95			1.20			1.54		
T = 525°C									
PE	2.52	4	0.63	2.52	4	0.63	2.52	4	0.63
LOF	2.05	2	1.02	1.86	2	0.93	1.93	2	0.97
RES	4.57	6		4.38	6		4.45	6	
MS(LOF/PE):	1.63			1.48			1.53		
T = 525°C									
PE	15.7	4	3.92	15.7	4	3.92	15.7	4	3.92
LOF	10.1	2	5.05	10.4	2	5.19	10.3	2	5.17
RES	25.8	6		26.1	6		26.0	6	
MS(LOF/PE):	1.29			1.32			1.32		

$F_{.95}(3,3) = 9.28$

$F_{.95}(2,4) = 6.94$

■ Since MS(LOF/PE) < $F_{.95}(n,m)$ then the model does not contradict the data.

Table C.5 Calculated versus experimental gasoline yields from the 3-lump model for feedstocks A and B with Octacat.

T(°C)	t(s)	$e^{-\alpha t}$ Y_G cal	t^{-N} Y_G cal	Y_G exp
Feedstock A				
500	3	19.31	19.50	20.08
	5	24.64	24.41	23.59
	7	27.84	27.69	28.35
	10	30.67	31.03	31.29
		± 1.82	± 1.73	
525	3	22.35	22.45	23.24
	5	26.45	26.26	24.93
	7	28.44	28.42	29.97
	10	29.87	30.23	30.46
		± 1.49	± 1.37	
550	3	24.94	24.99	24.16
	5	28.57	28.39	26.32
	7	30.18	30.15	30.69
	10	31.27	31.44	33.39
		± 0.81	± 0.77	
Feedstock B				
500	3	15.31	15.48	15.62
	5	20.65	20.62	20.42
	7	24.08	24.03	24.94
	10	27.20	27.24	26.88
		± 0.95	± 0.95	
525	3	19.94	20.17	20.69
	5	24.88	24.73	24.52
	7	27.57	27.45	28.64
	10	29.71	29.79	29.84
		± 0.72	± 0.78	
550	3	22.98	22.97	24.67
	5	26.44	26.31	27.08
	7	27.73	27.77	27.64
	10	28.31	28.40	28.42
		± 1.14	± 1.13	

Table C.6 Calculated versus experimental gasoline yields from the 3-lump model for feedstocks A and B with GX-30.

Decay:		$e^{-\alpha t}$	t^{-N}	
T(°C)	t(s)	Y_G cal	Y_G cal	Y_G exp
Feedstock A				
500	3	23.85	24.02	24.92
	5	30.22	30.04	28.58
	7	34.02	33.90	35.90
	10	37.40	37.66	37.64
		± 1.63	± 1.52	
525	3	27.43	27.59	26.69
	5	32.37	32.25	32.61
	7	34.88	34.83	33.75
	10	36.81	36.95	36.92
		± 0.86	± 0.88	
550	3	25.18	25.14	26.27
	5	28.30	28.23	29.20
	7	29.41	29.47	27.69
	10	29.83	29.90	30.81
		± 1.15	± 1.15	
Feedstock B				
500	3	15.04	15.21	16.88
	5	20.66	20.64	21.18
	7	24.57	24.53	23.99
	10	28.62	28.70	28.54
		± 0.85	± 0.83	
525	3	20.91	20.96	19.98
	5	27.53	27.51	27.59
	7	31.72	31.70	33.41
	10	35.62	35.63	33.69
		± 1.58	± 1.60	
550	3	25.36	24.93	22.51
	5	29.61	29.72	30.70
	7	31.27	31.45	32.44
	10	31.93	31.43	32.70
		± 1.74	± 1.67	

Table C.7 Calculated versus experimental C-lump yields from the 3-lump model for feedstocks A and B with Octacat.

Decay:		$e^{-\alpha t}$	t^{-N}	
T(°C)	t(s)	Y_C cal	Y_C cal	Y_C exp
Feedstock A				
500	3	13.76	14.21	14.51
	5	17.72	17.42	16.85
	7	20.16	19.77	18.95
	10	22.39	22.47	23.97
		± 1.33	± 1.06	
525	3	19.48	20.30	20.24
	5	24.44	24.11	23.67
	7	27.42	26.99	26.50
	10	30.06	30.39	32.10
		± 1.44	± 1.06	
550	3	23.66	23.94	25.25
	5	28.55	27.92	28.06
	7	31.26	30.86	30.09
	10	33.51	34.34	33.80
		± 1.19	± 0.91	
Feedstock B				
500	3	10.54	10.66	10.13
	5	15.12	14.96	13.69
	7	18.70	18.52	17.20
	10	22.90	23.02	23.29
		± 1.24	± 1.11	
525	3	14.68	15.06	13.74
	5	19.47	19.15	17.40
	7	22.73	22.36	21.25
	10	25.99	26.32	26.35
		± 1.58	± 1.42	
550	3	19.10	19.60	17.20
	5	25.18	24.66	24.85
	7	29.25	28.73	29.31
	10	33.20	33.79	33.00
		± 1.12	± 1.50	

Table C.8 Calculated versus experimental C-lump yields from the 3-lump model for feedstocks A and B with GX-30.

Decay:		$e^{-\alpha t}$	t^{-N}	
T(°C)	t(s)	Y_C cal	Y_C cal	Y_C exp
Feedstock A				
500	3	14.92	15.44	16.62
	5	19.27	19.17	18.43
	7	22.04	21.81	22.00
	10	24.74	24.73	25.78
		± 1.25	± 1.01	
525	3	22.69	22.93	23.58
	5	27.58	27.17	26.47
	7	30.42	30.16	30.65
	10	32.97	33.53	34.10
		± 1.06	± 0.70	
550	3	28.35	28.68	27.78
	5	34.91	34.41	32.93
	7	38.97	38.58	39.85
	10	42.83	43.40	43.97
		± 1.45	± 1.28	
Feedstock B				
500	3	13.13	13.35	14.17
	5	18.07	18.00	17.83
	7	21.57	21.41	20.77
	10	25.21	25.16	26.34
		± 1.01	± 0.91	
525	3	16.02	16.09	17.65
	5	21.55	21.52	20.90
	7	25.42	25.38	24.69
	10	29.54	29.58	31.35
		± 1.52	± 1.46	
550	3	19.17	19.58	21.89
	5	27.20	27.00	25.31
	7	33.16	32.97	32.19
	10	39.69	40.40	38.47
		± 2.11	± 2.04	

Table C.9 Calculated versus experimental conversions for the 8-lump model (feedstocks A and B on Octacat).

Decay:		$e^{-\alpha t}$	t^{-N}	
T(°C)	t(s)	$conv_{cal}$	$conv_{cal}$	$conv_{exp}$
Feedstock A				
500	3	35.92	32.94	34.59
	5	44.99	40.39	40.44
	7	49.88	45.59	47.30
	10	53.62	51.26	55.26
		± 3.47	± 3.84	
525	3	44.13	38.80	43.48
	5	52.71	47.07	48.60
	7	56.73	52.72	56.47
	10	59.38	58.76	62.56
		± 3.16	± 3.97	
550	3	50.07	43.38	49.41
	5	58.73	52.06	54.38
	7	62.60	57.85	60.78
	10	65.04	63.91	67.19
		± 2.38	± 4.39	
Feedstock B				
500	3	29.43	26.39	25.75
	5	37.22	32.81	34.11
	7	41.51	37.43	42.14
	10	44.82	42.61	50.17
		± 3.46	± 3.84	
525	3	37.50	32.35	34.43
	5	45.37	39.86	41.92
	7	49.14	45.17	49.89
	10	51.66	51.01	56.19
		± 3.16	± 3.97	
550	3	44.26	38.18	41.87
	5	52.64	46.52	51.93
	7	56.49	52.28	56.95
	10	58.95	58.47	61.42
		± 2.38	± 4.39	

Table C.10 Calculated versus experimental conversions for the 8-lump model (feedstocks A and B on GX-30).

Decay:		$e^{-\alpha t}$	t^{-N}	
T(°C)	t(s)	$conv_{cal}$	$conv_{cal}$	$conv_{exp}$
Feedstock A				
500	3	40.75	36.30	41.54
	5	49.35	44.18	47.01
	7	53.57	49.58	57.90
	10	56.50	55.36	63.42
		± 3.72	± 3.32	
525	3	48.56	44.30	50.27
	5	58.59	53.17	59.08
	7	63.61	59.06	64.40
	10	67.24	65.21	71.02
		± 3.29	± 5.12	
550	3	53.32	48.23	54.05
	5	63.06	57.55	62.13
	7	67.59	63.66	67.54
	10	70.61	69.91	74.78
		± 3.01	± 4.74	
Feedstock B				
500	3	35.17	31.35	30.05
	5	43.00	38.78	38.01
	7	46.91	44.01	44.76
	10	49.65	49.85	54.88
		± 3.72	± 3.32	
525	3	43.06	38.64	37.63
	5	52.99	47.17	48.49
	7	58.13	53.04	58.10
	10	61.93	59.33	65.04
		± 3.29	± 5.12	
550	3	49.79	44.02	44.40
	5	59.28	53.10	57.01
	7	63.76	59.19	64.63
	10	66.78	65.56	71.17
		± 3.01	± 4.74	

Table C.11 Calculated versus experimental gasoline yields from the 8-lump model for feedstocks A and B with Octacat.

Decay:		$e^{-\alpha t}$	t^{-N}	
T(°C)	t(s)	Y_G cal	Y_G cal	Y_G exp
Feedstock A				
500	3	20.27	20.30	20.08
	5	25.39	24.89	23.59
	7	28.15	28.09	28.35
	10	30.26	31.59	31.29
		± 1.59	± 0.81	
525	3	24.26	23.36	23.24
	5	28.94	28.31	24.93
	7	31.13	31.69	29.97
	10	32.57	35.28	30.46
		± 2.17	± 2.46	
550	3	25.79	24.53	24.16
	5	30.28	29.47	26.32
	7	32.30	32.78	30.69
	10	33.57	36.24	33.39
		± 2.22	± 2.95	
Feedstock B				
500	3	15.88	16.60	15.62
	5	20.12	20.68	20.42
	7	22.45	23.63	24.94
	10	24.26	26.95	26.88
		± 1.59	± 0.81	
525	3	20.01	19.44	20.69
	5	24.29	24.02	24.52
	7	26.35	27.28	28.64
	10	27.74	30.88	29.84
		± 2.17	± 2.46	
550	3	22.95	21.34	24.67
	5	27.49	26.17	27.08
	7	29.61	29.54	27.64
	10	30.98	33.21	28.42
		± 2.22	± 2.95	

Table C.12 Calculated versus experimental gasoline yields from the 8-lump model for feedstocks A and B with GX-30.

T(°C)	t(s)	Decay: $e^{-\alpha t}$ Y_G cal	Decay: t^{-N} Y_G cal	Y_G exp
Feedstock A				
500	3	24.06	25.37	24.92
	5	29.15	30.77	28.58
	7	31.65	34.44	35.90
	10	33.39	38.33	37.64
		± 3.26	± 1.63	
525	3	27.02	27.52	26.69
	5	32.73	33.00	32.61
	7	35.61	36.65	33.75
	10	37.71	40.44	36.92
		± 1.76	± 2.54	
550	3	27.20	26.44	26.27
	5	32.21	31.67	29.20
	7	34.55	35.12	27.69
	10	36.12	38.69	30.81
		± 3.78	± 4.59	
Feedstock B				
500	3	18.10	17.96	16.88
	5	22.30	22.18	21.18
	7	24.44	25.16	23.99
	10	25.96	28.43	28.54
		± 3.26	± 1.63	
525	3	23.57	20.74	19.98
	5	29.36	25.44	27.59
	7	32.44	28.71	33.41
	10	34.75	32.25	33.69
		± 1.76	± 2.54	
550	3	23.45	22.49	22.51
	5	28.40	27.39	30.70
	7	30.81	30.74	32.44
	10	32.48	34.33	32.70
		± 3.78	± 4.59	

Table C.13 Calculated versus experimental C-lump yields from the 8-lump model for feedstocks A and B with Octacat.

Decay:		$e^{-\alpha t}$	t^{-N}	
T(°C)	t(s)	Y_C cal	Y_C cal	Y_C exp
Feedstock A				
500	3	15.64	12.64	14.51
	5	19.60	15.50	16.85
	7	21.73	17.50	18.95
	10	23.56	19.67	23.97
		± 2.70	± 3.75	
525	3	19.87	15.45	20.24
	5	23.77	18.76	23.67
	7	25.60	21.04	26.50
	10	26.81	23.47	32.10
		± 3.04	± 5.41	
550	3	24.29	18.85	25.25
	5	28.45	22.58	28.06
	7	30.30	25.07	30.09
	10	31.47	27.67	33.80
		± 2.80	± 6.07	
Feedstock B				
500	3	13.55	9.79	10.13
	5	17.11	12.13	13.69
	7	19.06	13.80	17.20
	10	20.56	15.66	23.29
		± 2.70	± 3.75	
525	3	17.49	12.91	13.74
	5	21.08	15.84	17.40
	7	22.79	17.89	21.25
	10	23.93	20.13	26.35
		± 3.04	± 5.41	
550	3	21.31	16.84	17.20
	5	25.15	20.35	24.85
	7	26.88	22.73	29.31
	10	27.97	25.25	33.00
		± 2.80	± 6.07	

Table C.14 Calculated versus experimental C-lump yields from the 8-lump model for feedstocks A and B with GX-30.

T(°C)	t(s)	Decay: $e^{-\alpha t}$ Y_C cal	Decay: t^{-N} Y_C cal	Y_C exp
Feedstock A				
500	3	16.69	10.93	16.62
	5	20.20	13.41	18.43
	7	21.93	15.14	22.00
	10	23.11	17.03	25.78
		± 3.57	± 3.61	
525	3	21.54	16.79	23.58
	5	25.87	20.17	26.47
	7	28.00	22.42	30.65
	10	29.52	24.77	34.10
		± 2.71	± 5.74	
550	3	26.12	21.79	27.78
	5	30.85	25.88	32.93
	7	33.03	28.54	39.85
	10	34.48	31.22	43.97
		± 5.39	± 7.80	
Feedstock B				
500	3	17.07	13.39	14.17
	5	20.70	16.60	17.83
	7	22.47	18.89	20.77
	10	23.69	21.42	26.34
		± 3.57	± 3.61	
525	3	19.50	17.90	17.65
	5	23.63	21.73	20.90
	7	25.69	24.33	24.69
	10	27.18	27.08	31.35
		± 2.71	± 5.74	
550	3	26.34	21.53	21.89
	5	30.88	25.71	25.31
	7	32.95	28.44	32.19
	10	34.30	31.23	38.47
		± 5.39	± 7.80	

APPENDIX D

CALCULATIONS AND DATA FOR TESTING OF THE REACTOR SYSTEM

D.1 ERROR IMPARTED ON THE KINETIC CONSTANT FROM ASSUMING ISOTHERMAL CONDITIONS

This section is included to show the validity of assuming isothermal conditions in the reactor. In reality, small temperature drops were observed during cracking, however the error or percent deviation on the calculated kinetic constant is small as shown below.

The Arrehnius equation relates the effect of temperature on the kinetic constant:

$$k = A_o \exp\ (-E_A/RT) \qquad (D1).$$

If a small temperature change is observed during the reaction then an equation for the ratio of kinetic constants at the assumed temperature (k_a @ T_a) and deviated temperature (k_b @ T_b) can be expressed as:

$$k_a/k_b = \exp(-E_A/RT_a)/\exp(-E_A/RT_b) \qquad (D2).$$

Rearranging equation (D2) gives:

$$k_a/k_b = \exp[E_A(T_a - T_b)/RT_aT_b] \qquad (D3).$$

The error on the kinetic constant can be expressed as a percentage deviation:

$$\text{Error} = 100(k_a - k_b)/k_a = 100(1 - k_b/k_a) \qquad \text{(D4)}.$$

Thus for a maximum temperature drop of 5°C when operating at 500°C, the ratio of k_a/k_b can be calculated from equation (D3) with E_A = 18,000 cal/gmol, R = 1.987 cal/K/gmol, T_a = 773°C and T_b = 768°C giving a value of 1.08. Substituting this value into equation (D4) gives:

$$\text{Error} = 100\ (1 - 1/1.08) = 7.3\%.$$

For an average temperature drop of 2°C the ratio of k_a/k_b is:

$$k_a/k_b = \exp\ [18{,}000*2\ /\ (1.987*773*771)] = 1.03$$

and thus the deviation is only 3%.

D.2 SPECTRUMS OBTAINED FROM THE FIBER OPTIC PROBE MEASUREMENTS

Table D1: List of experimental conditions corresponding to each spectrum (@ 25°C).

Spectrum No.	Gas	P(atm)	RPM	Catalyst
cold model				
1	nitrogen	1	5000	Octacat
2	"	"	6300	"
3	"	"	6930	"
4	"	"	7560	"
5	"	"	7875	"
6	"	"	8820	"
7	"	"	10080	"
8	helium	"	7875	"
9	argon	"	6300	"
10	argon	"	7875	"
11	methane	"	7875	"
12	air	"	7875	coked Oct.
13	nitrogen	"	7875	none
Hot model				
14	nitrogen	1	5250	Octacat
15	"	"	6300	"
16	"	"	6825	"
17	"	"	7350	"
18	"	"	7875	"
19	"	"	8500	"
20	"	2	7875	"
21	"	3	7875	"
22	argon	1	7875	"
23	argon	2.5	7875	"
24	methane	1	7875	"
25	helium	1	7875	"
26	"	2.7	"	"
27	nitrogen	1	"	none
28*	N_2/air	1-2	"	Octacat

* N_2 and air initially at 1 atm, then injected 50 mL of air

Table D2: Average Signal Frequency and Intensity Values (± denotes standard deviation based on repeat values)

Spectrum No.	Avg. Frequency (peaks/s)	Avg. Intensity (mV)
1	0	29.8 ±3.2
2	0.8 ±0.6	43.7 ±4.0
3	7.5 ±2.1	59.4 ±5.3
4	28.8 ±2.7	95.3 ±4.9
5	32.3 ±3.5	99.8 ±6.2
6	42.9 ±4.1	162.4 ±11.2
7	49.7 ±3.8	213.0 ±12.1
14	0	25.7 ±2.2
15	0	38.5 ±4.1
16	8.9 ±2.1	57.1 ±3.6
17	28.7 ±4.4	92.6 ±9.8
18	38.5 ±5.0	118.7 ±8.7
19	41.5 ±3.6	140.2 ±9.2
23	47.7 ±2.4	183.0 ±10.4
24	5.0 ±1.8	51.0 ±8.5
20	-	168.0 ±11.3
22	-	118.1 ±9.9
25	-	0
26	-	27.0 ±5.5

SPECTRUM 1

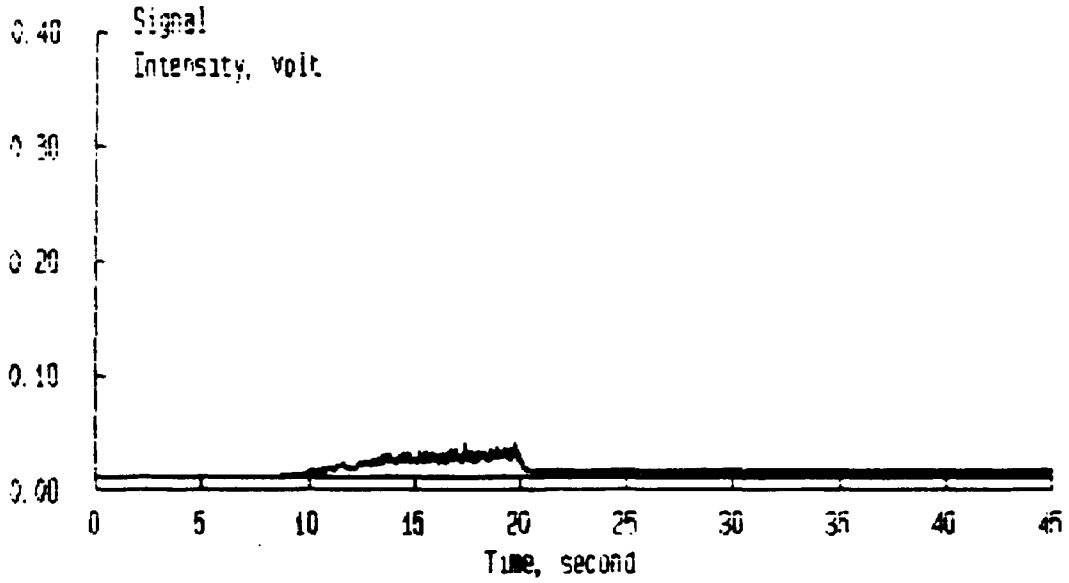
Signal
Intensity, volt
0.40
0.30
0.20
0.10
0.00
0
5
10
15
20
25
30
35
40
45
Time, second

SPECTRUM 2

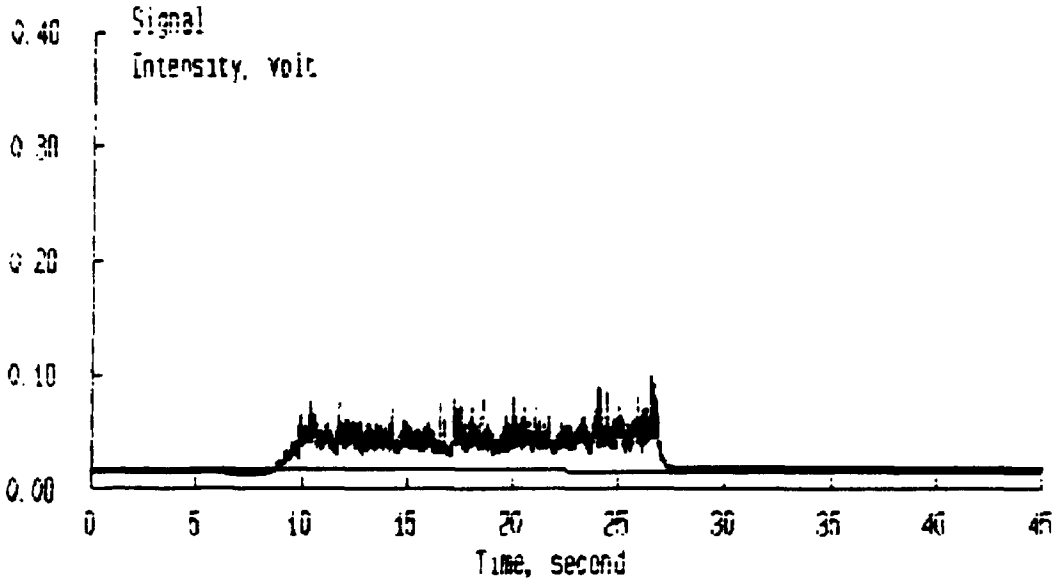
Signal
Intensity, Volt
0.40
0.30
0.20
0.10
0.00
0
5
10
15
20
25
30
35
40
45
Time, second

SPECTRUM 3

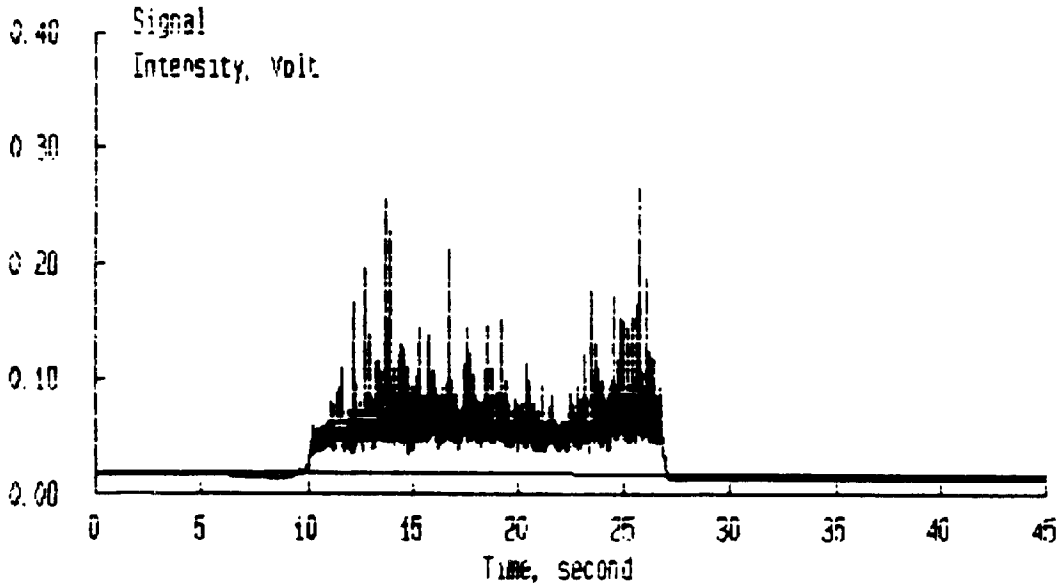
Signal
Intensity, Volt
0.40
0.30
0.20
0.10
0.00
0
5
10
15
20
25
30
35
40
45
Time, second

SPECTRUM 4

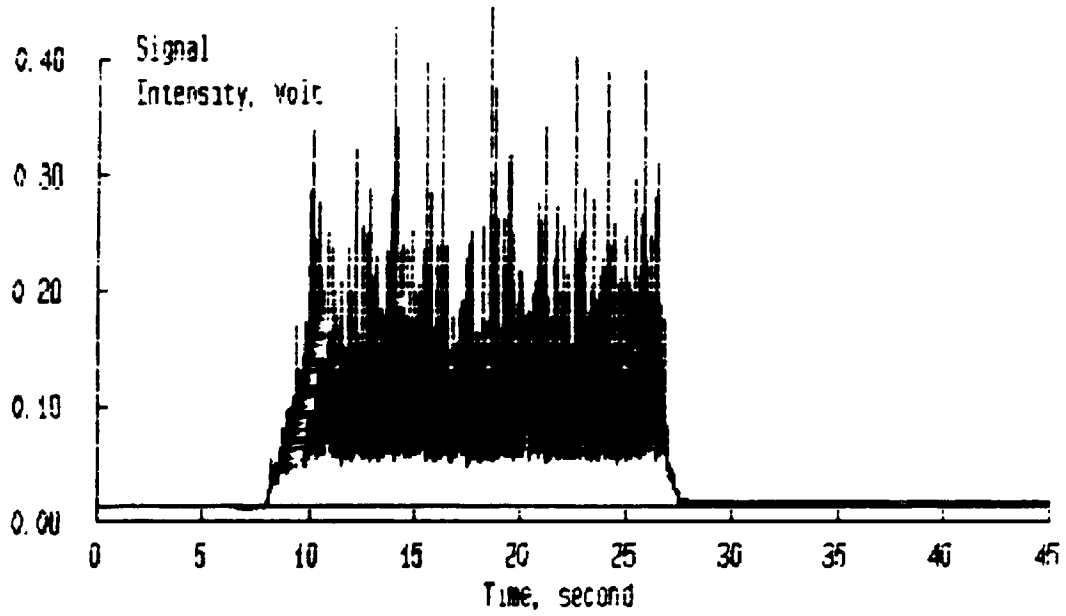
Signal
Intensity, Volt
0.40
0.30
0.20
0.10
0.00
0
5
10
15
20
25
30
35
40
45
Time, second

SPECTRUM 5

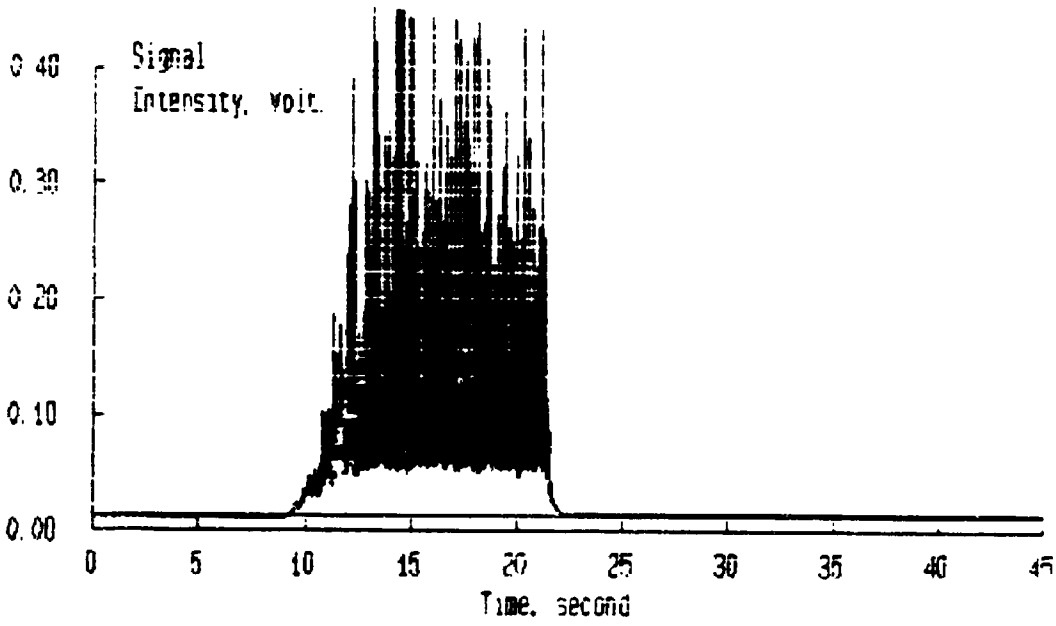
Signal
Intensity, volt.
0.40
0.30
0.20
0.10
0.00
0
5
10
15
20
25
30
35
40
45
Time, second

SPECTRUM 6

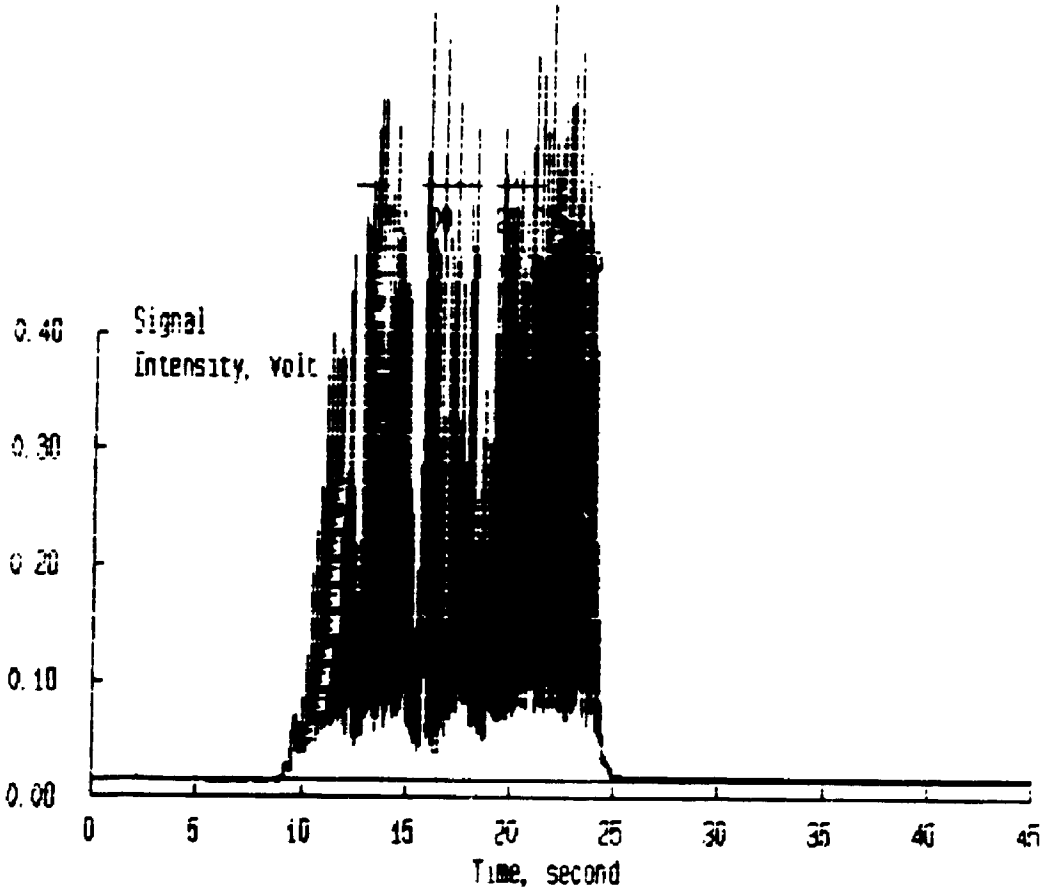
Signal
Intensity, Volt
0.40
0.30
0.20
0.10
0.00
0
5
10
15
20
25
30
35
40
45
Time, second

SPECTRUM 7

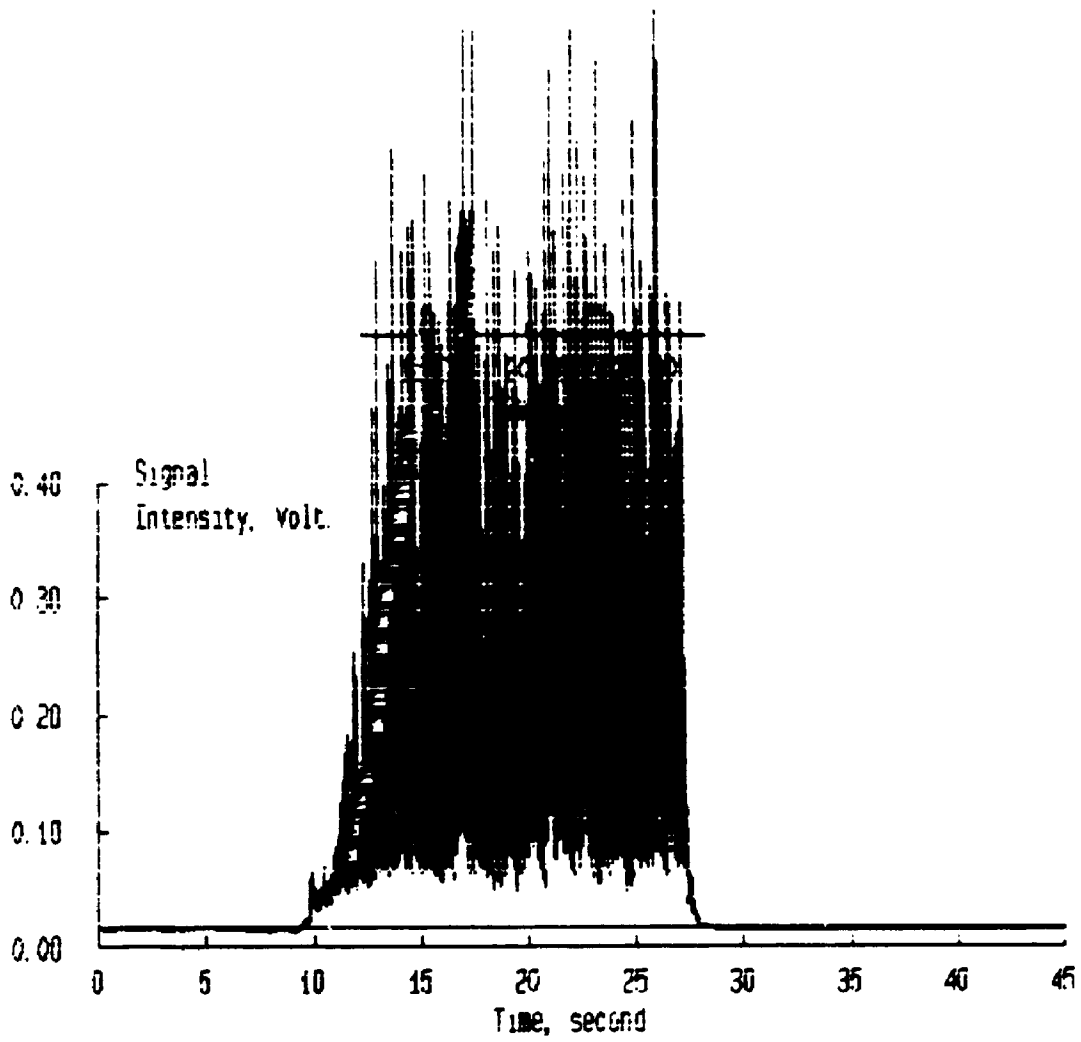
Signal
Intensity, Volt.
0.40
0.30
0.20
0.10
0.00
0
5
10
15
20
25
30
35
40
45
Time, second

SPECTRUM 8

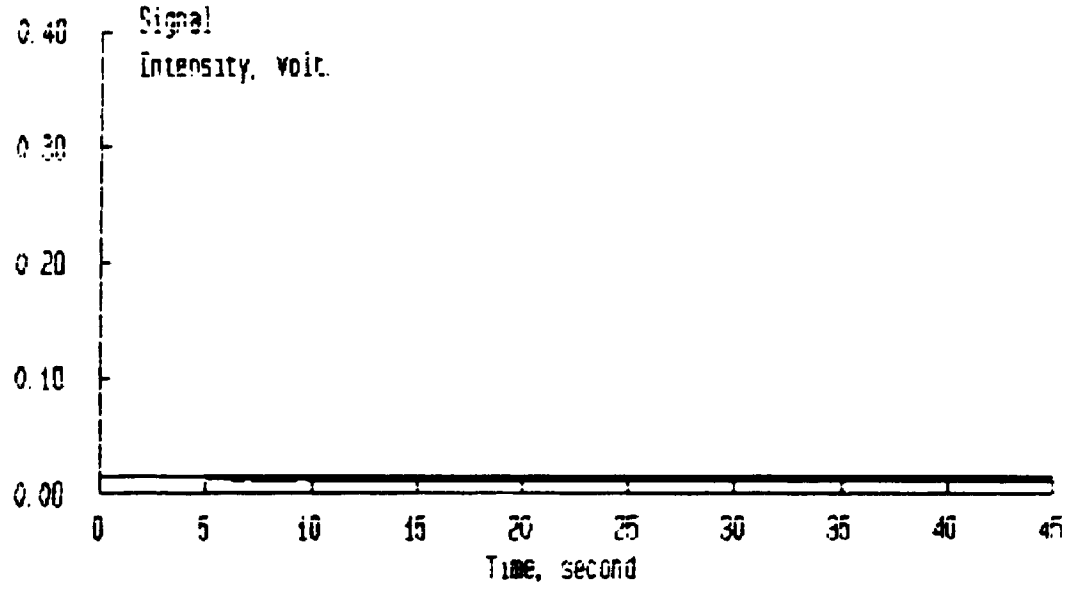
Signal
Intensity, Volt.
0.40
0.30
0.20
0.10
0.00
0
5
10
15
20
25
30
35
40
45
Time, second

SPECTRUM 9

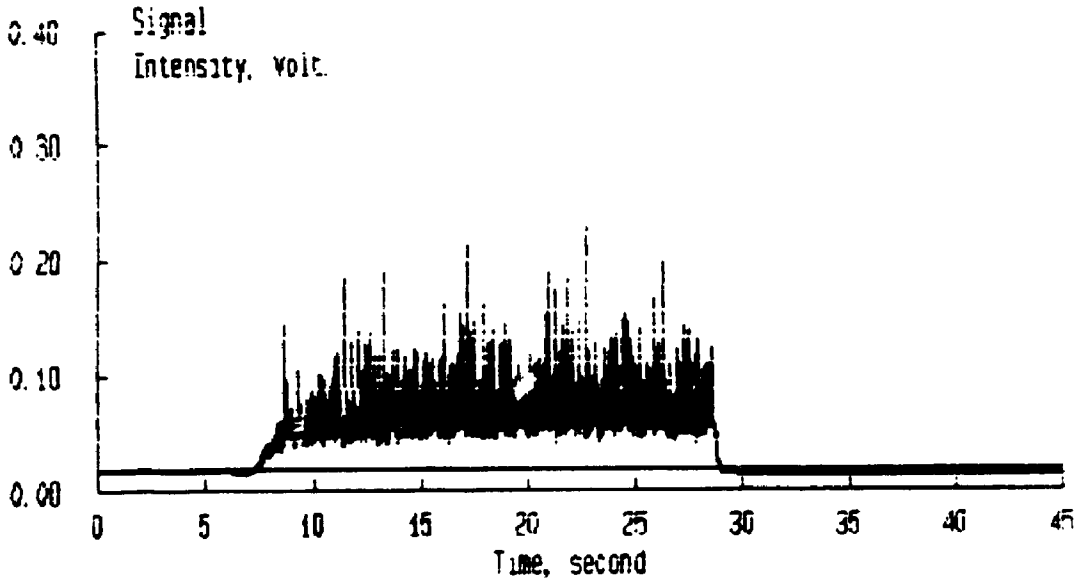
Signal
Intensity, volt.
0.40
0.30
0.20
0.10
0.00
0
5
10
15
20
25
30
35
40
45
Time, second

SPECTRUM 10

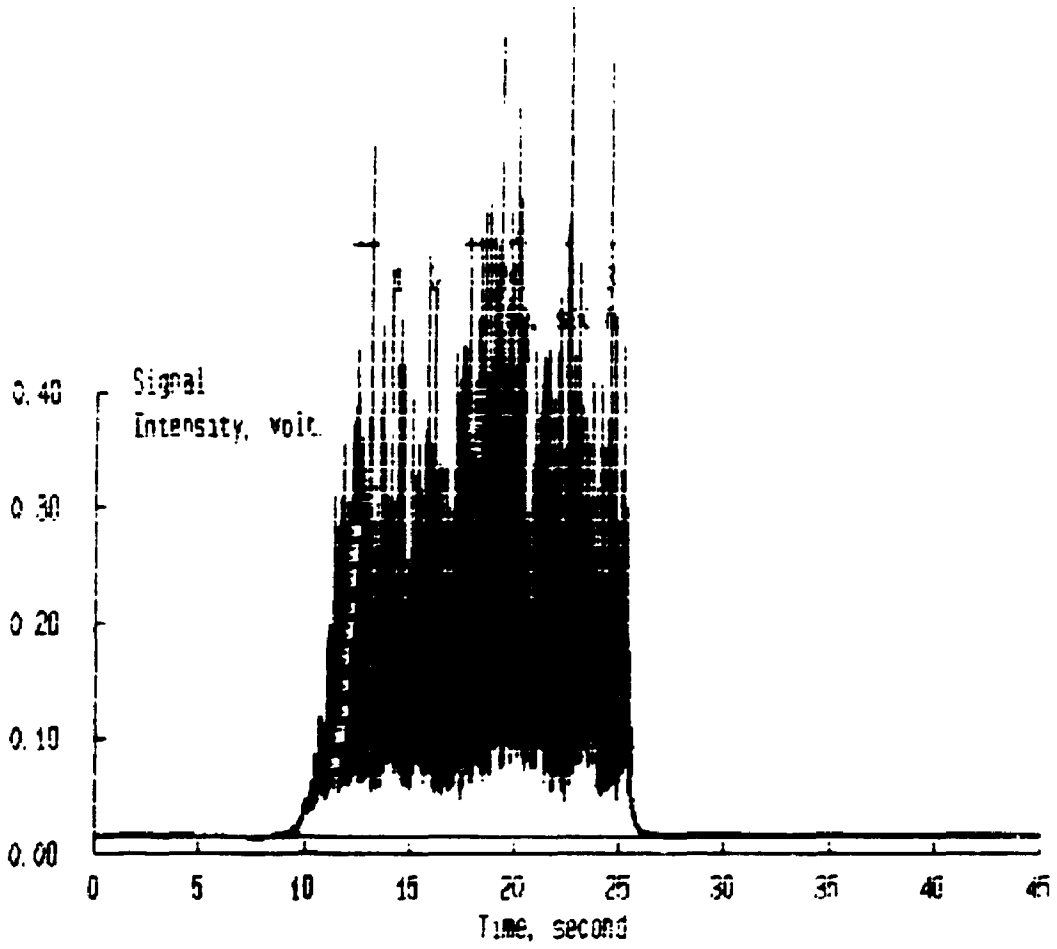
Signal
Intensity, volt
0.40
0.30
0.20
0.10
0.00
0
5
10
15
20
25
30
35
40
45
Time, second

SPECTRUM 11

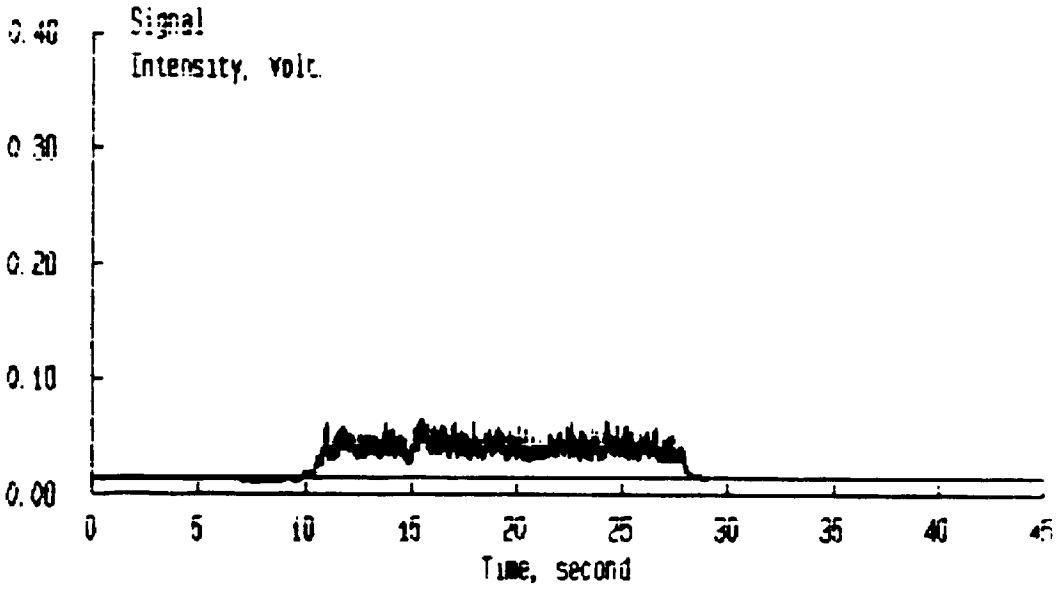
Signal
Intensity, Volt
0.40
0.30
0.20
0.10
0.00
0
5
10
15
20
25
30
35
40
45
Time, second

SPECTRUM 12

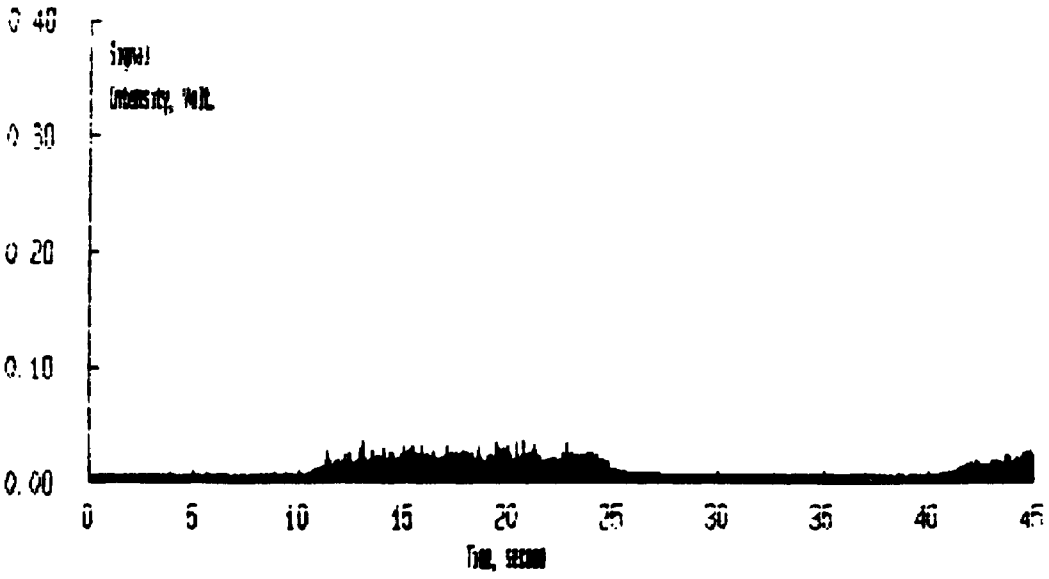

SPECTRUM 13

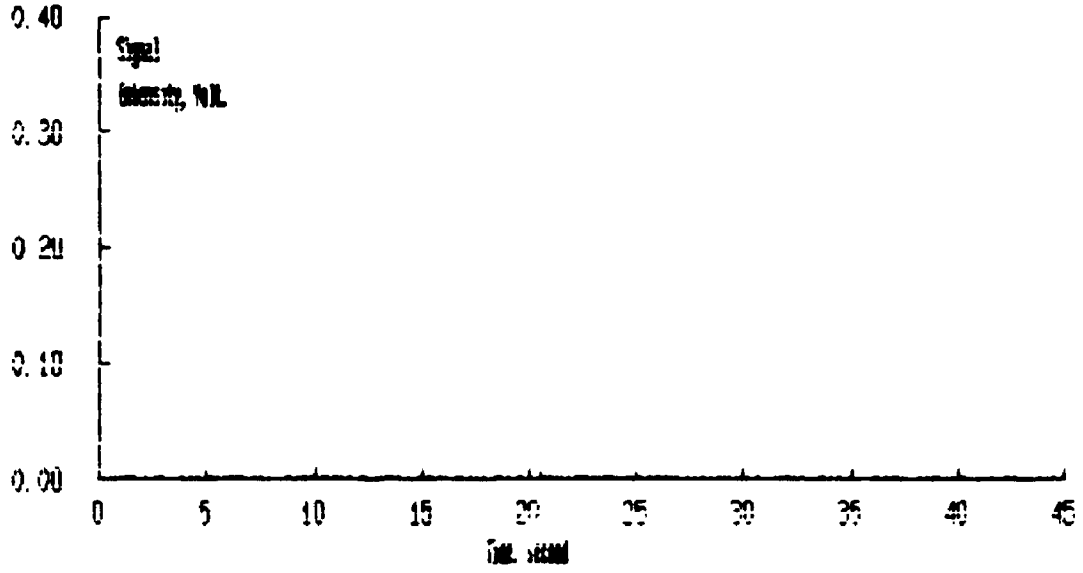

SPECTRUM 14

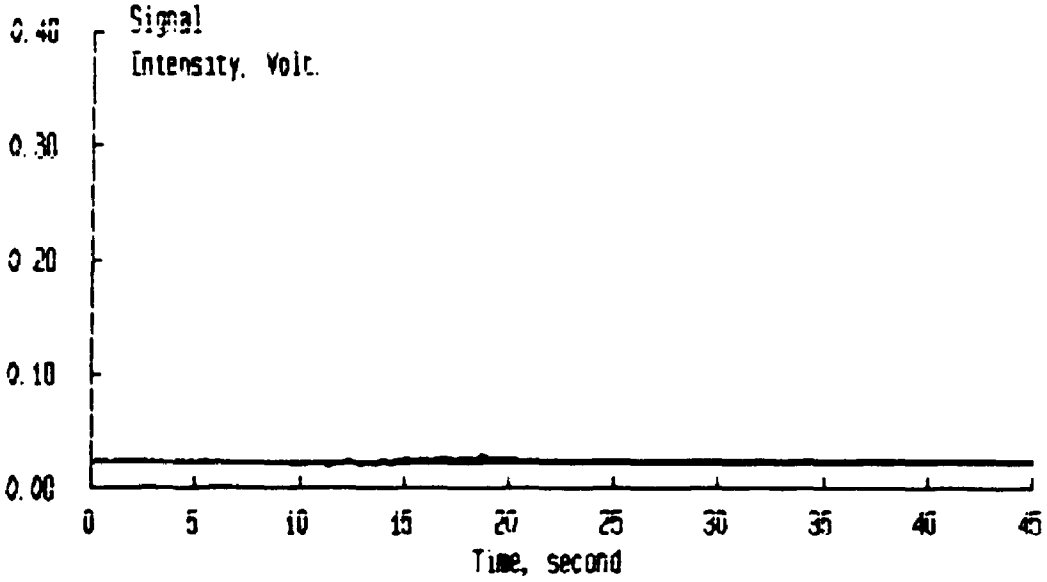
Signal
Intensity, Volt.
0.40
0.30
0.20
0.10
0.00
0
5
10
15
20
25
30
35
40
45
Time, second

SPECTRUM 15

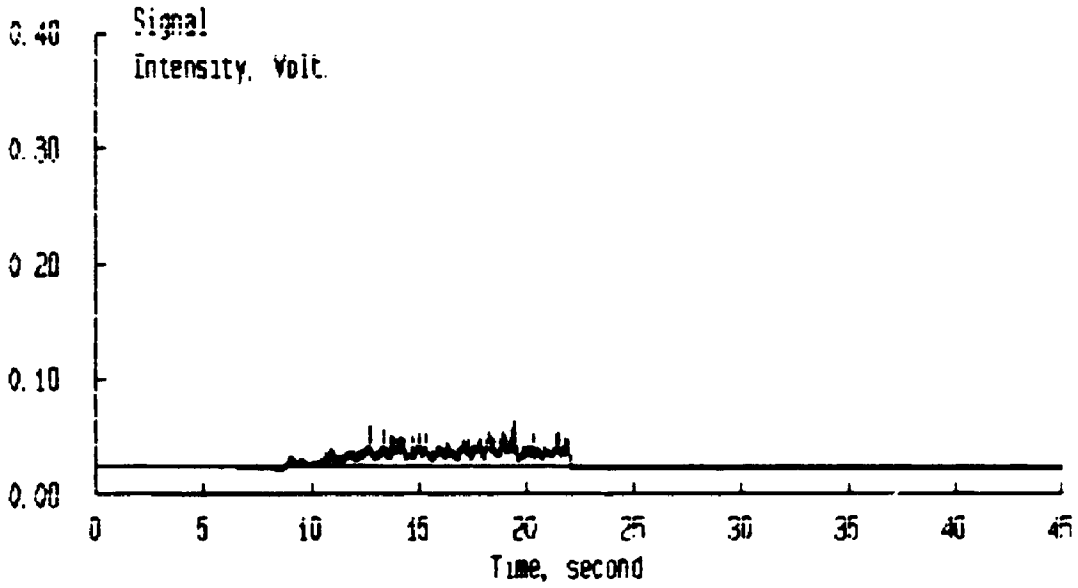
Signal
Intensity, Volt.
0.40
0.30
0.20
0.10
0.00
0
5
10
15
20
25
30
35
40
45
Time, second

SPECTRUM 16

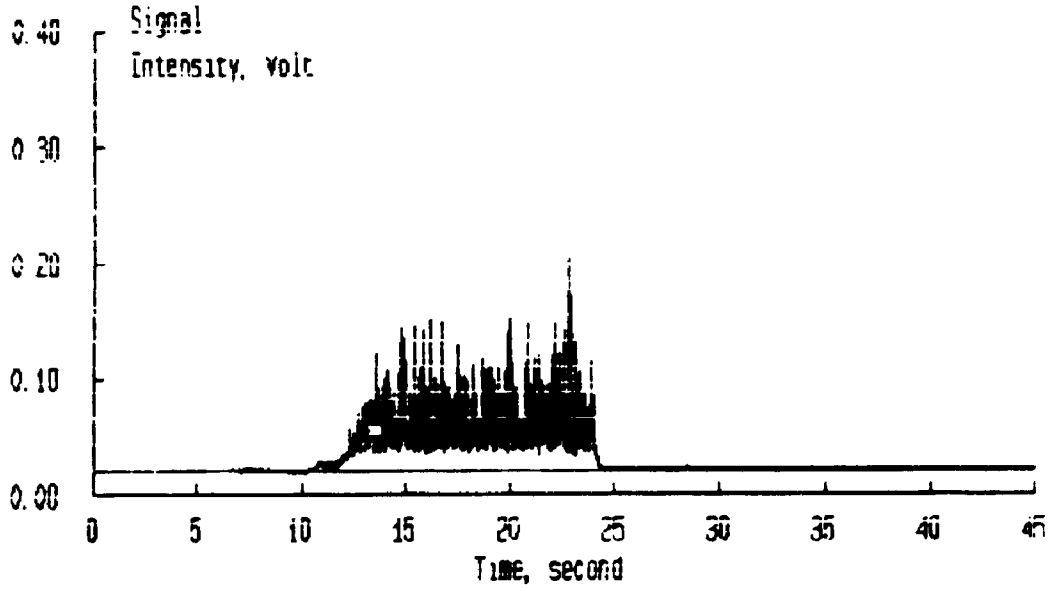
Signal
Intensity, Volt
0.40
0.30
0.20
0.10
0.00
0
5
10
15
20
25
30
35
40
45
Time, second

SPECTRUM 17

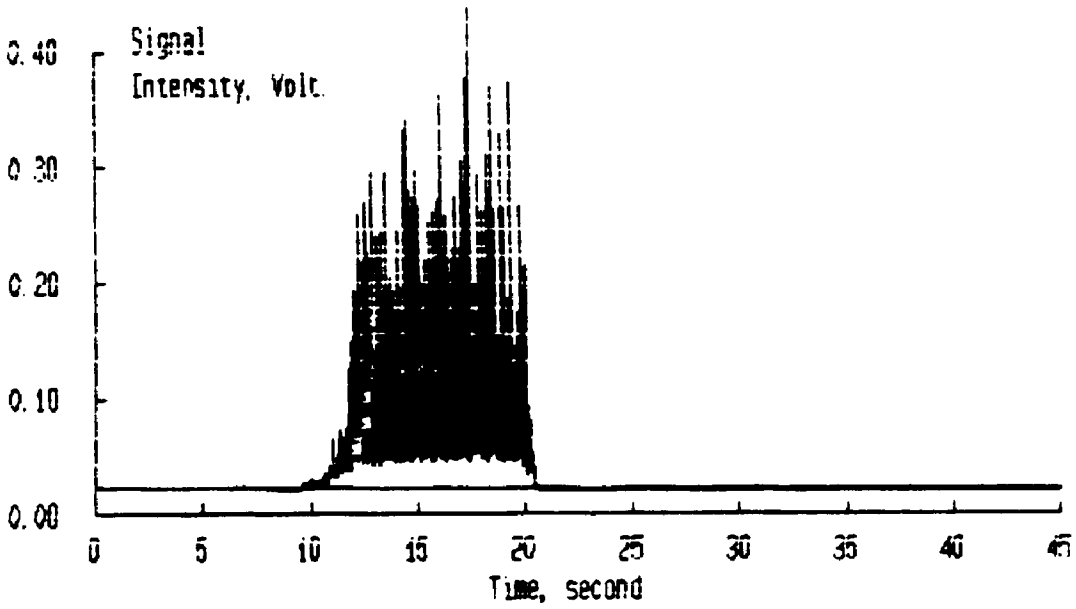
Signal
Intensity, Volt.
0.40
0.30
0.20
0.10
0.00
0
5
10
15
20
25
30
35
40
45
Time, second

SPECTRUM 18

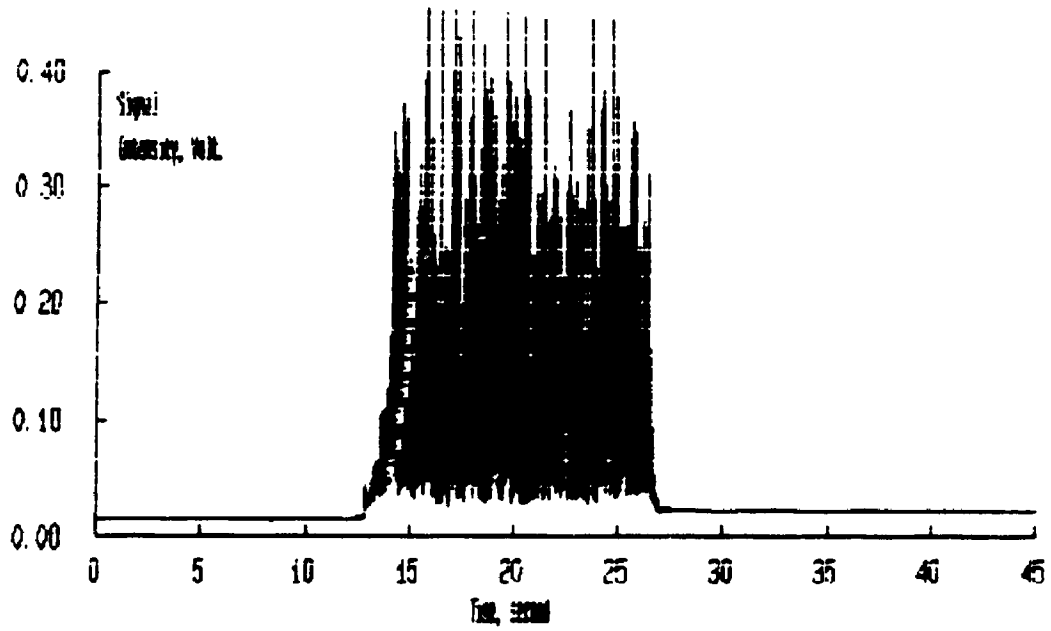

SPECTRUM 19

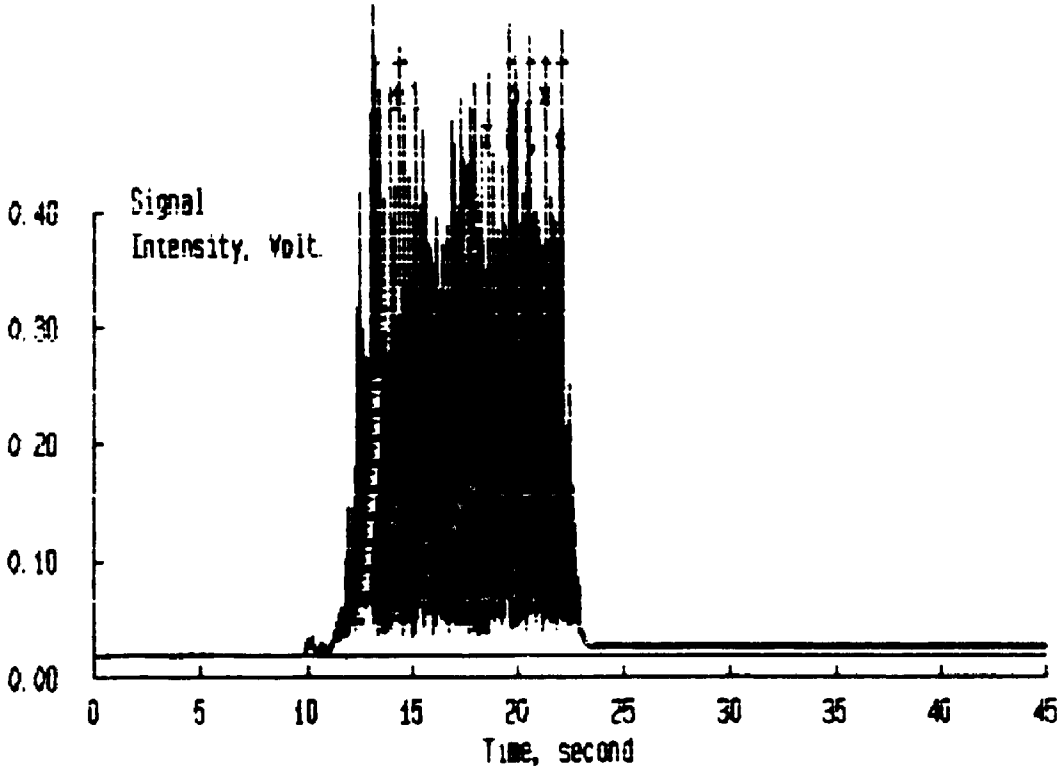
Signal
Intensity, Volt
0.40
0.30
0.20
0.10
0.00
0
5
10
15
20
25
30
35
40
45
Time, second

SPECTRUM 20

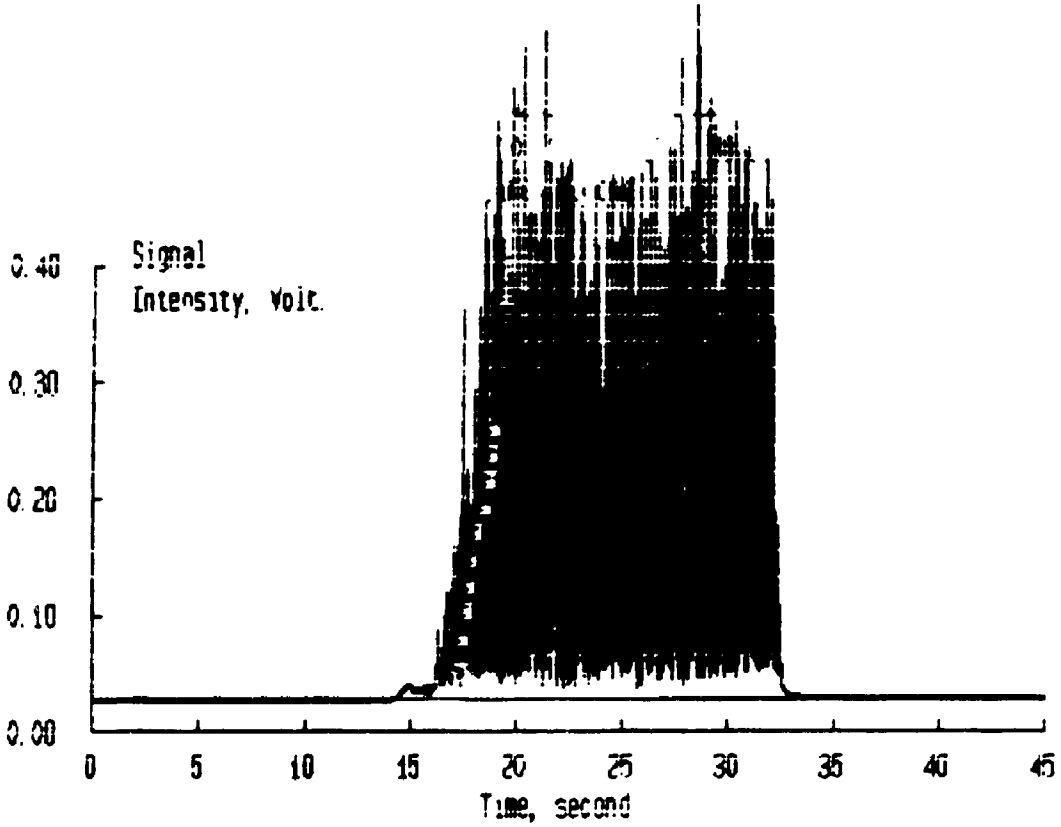
Signal
Intensity, Volt.
0.40
0.30
0.20
0.10
0.00
0
5
10
15
20
25
30
35
40
45
Time, second

SPECTRUM 21

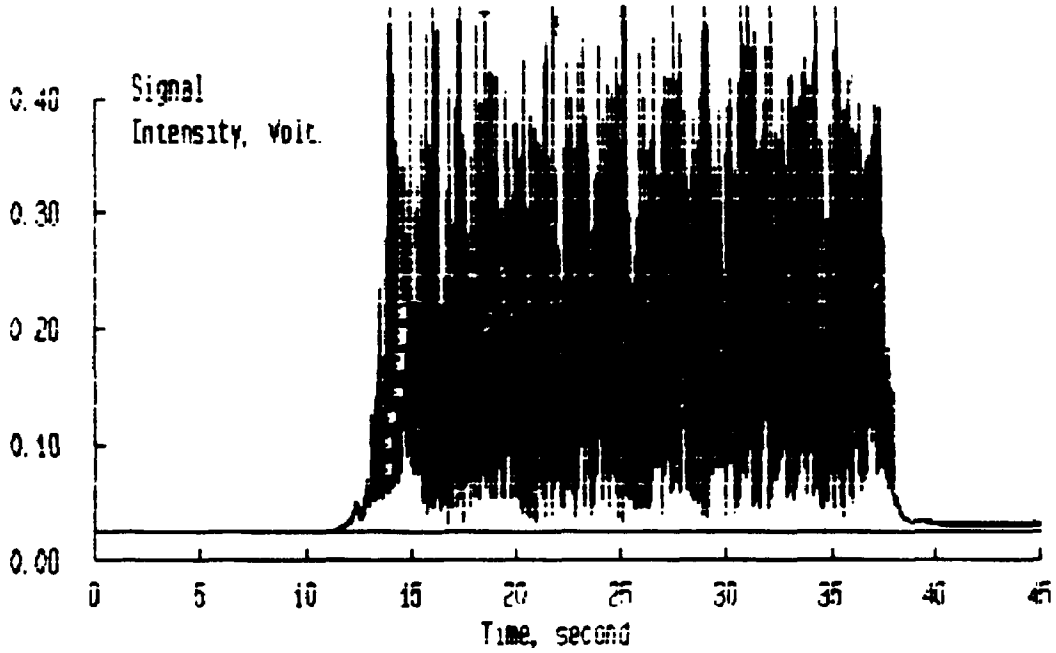
Signal
Intensity, Volt.
0.40
0.30
0.20
0.10
0.00
0
5
10
15
20
25
30
35
40
45
Time, second

SPECTRUM 22

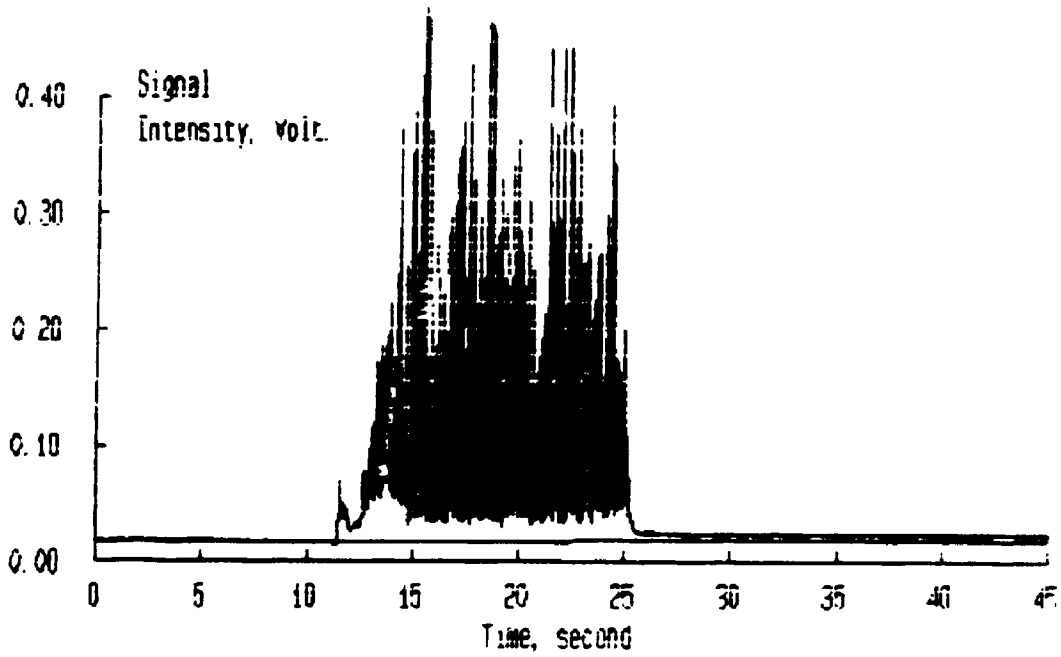
Signal
Intensity, Volt.
0.40
0.30
0.20
0.10
0.00
0
5
10
15
20
25
30
35
40
Time, second

SPECTRUM 23

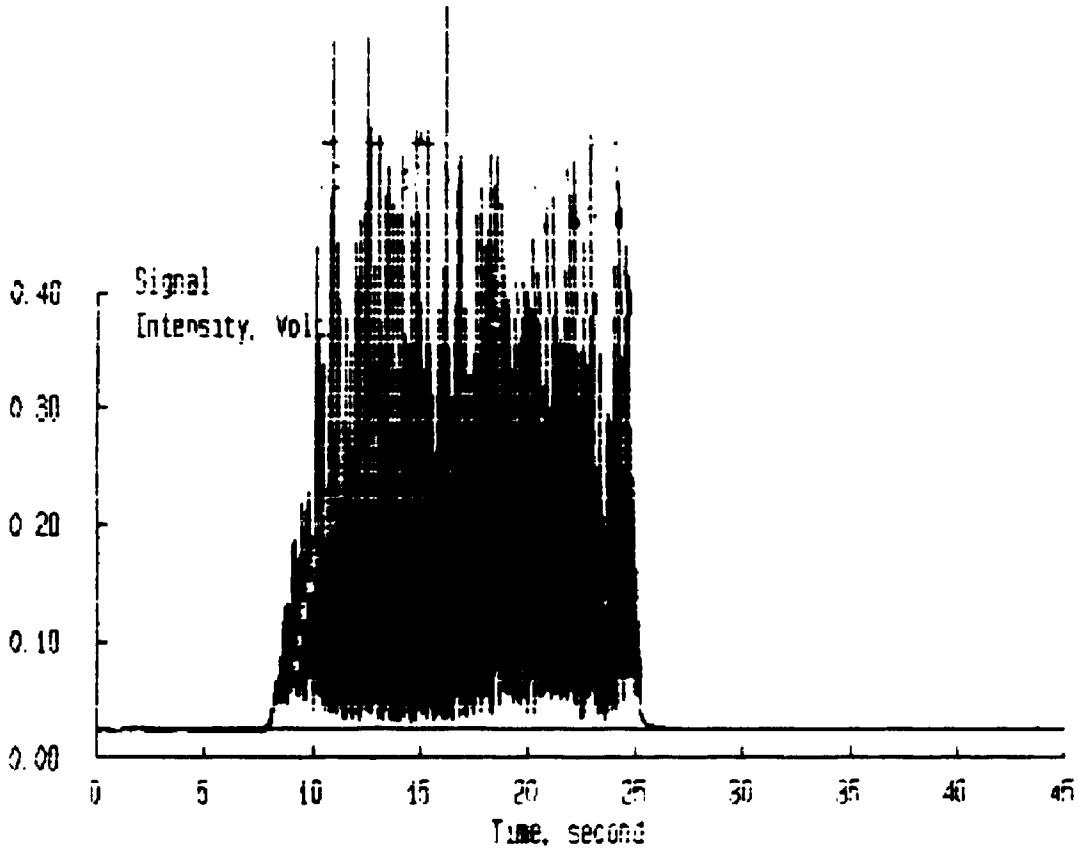
Signal
Intensity, Volt
0.40
0.30
0.20
0.10
0.00
0
5
10
15
20
25
30
35
40
45
Time, second

SPECTRUM 24

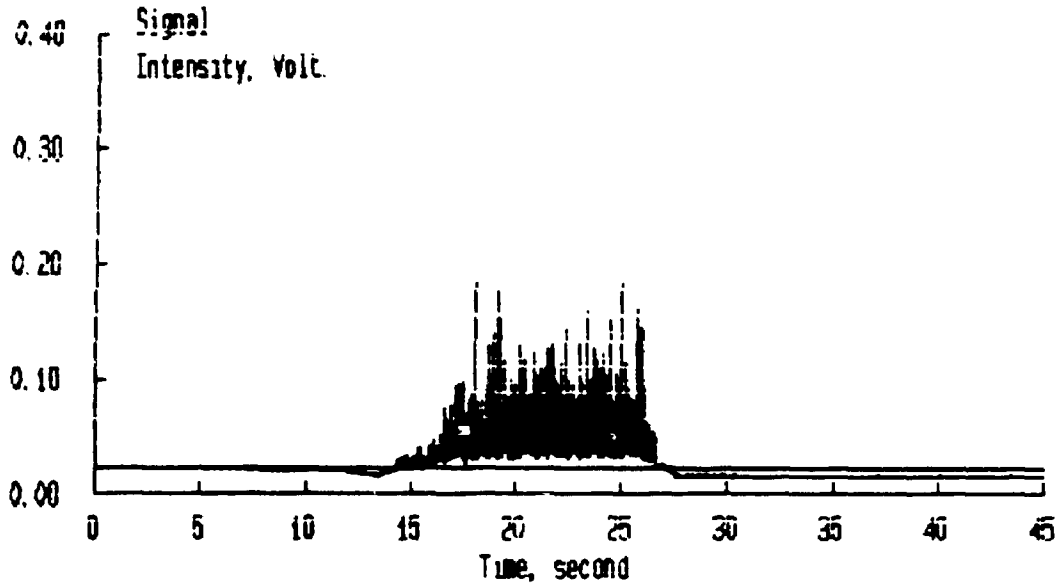
Signal
Intensity, Volt.
0.40
0.30
0.20
0.10
0.00
0
5
10
15
20
25
30
35
40
45
Time, second

SPECTRUM 25

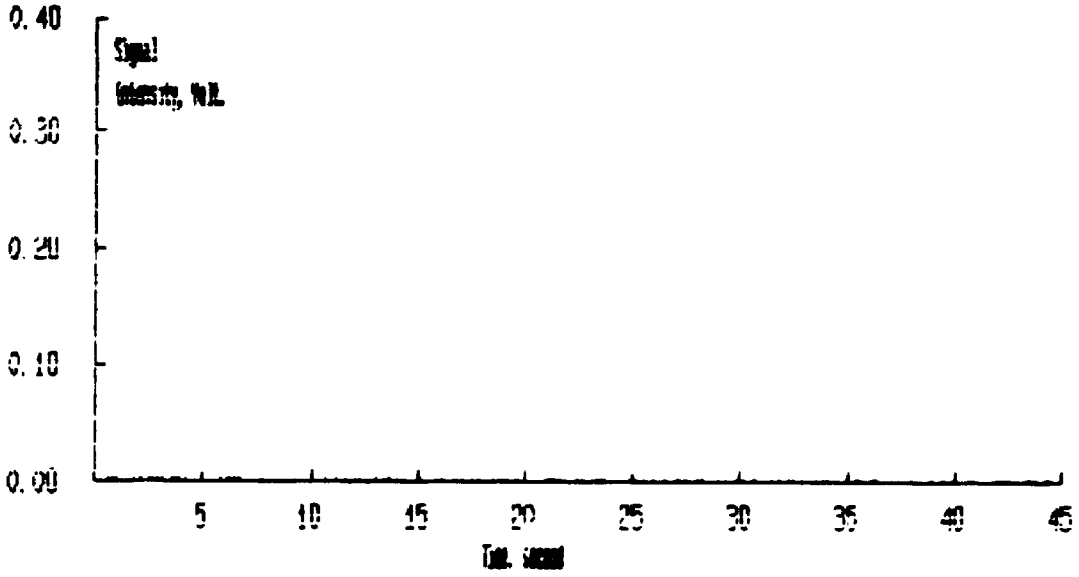

SPECTRUM 26

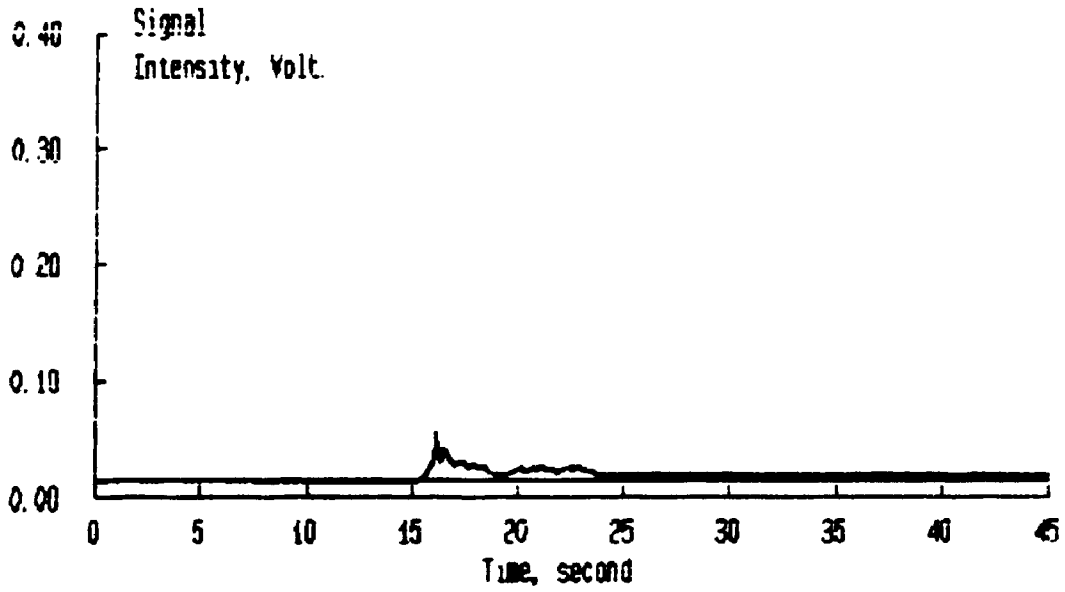
Signal
Intensity, Volt.
0.40
0.30
0.20
0.10
0.00
0
5
10
15
20
25
30
35
40
45
Time, second

SPECTRUM 27

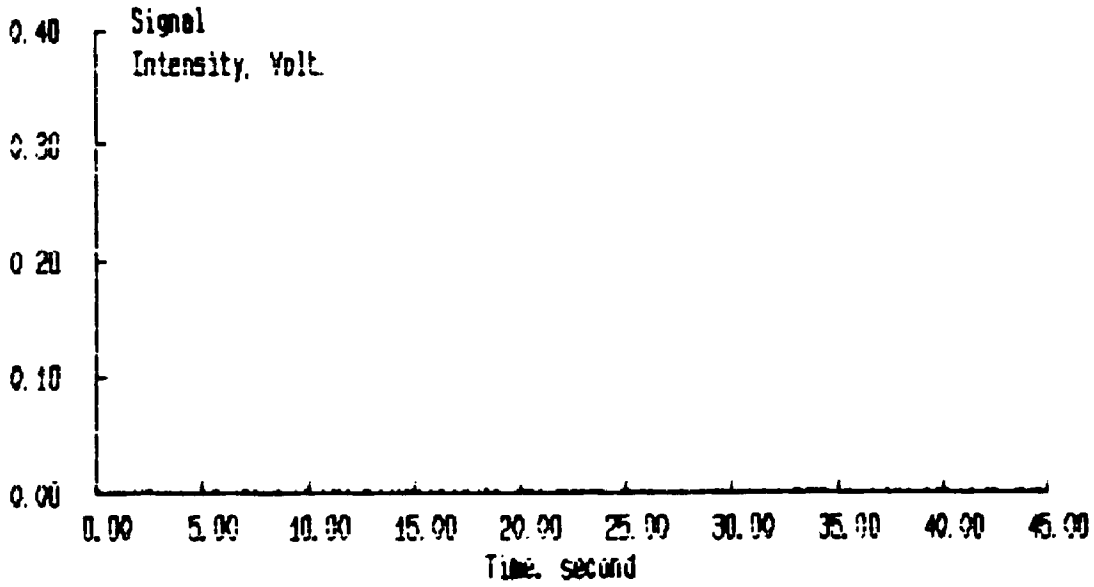
Signal
Intensity, Volt
0.40
0.30
0.20
0.10
0.00
0.00
5.00
10.00
15.00
20.00
25.00
30.00
35.00
40.00
45.00
Time, second

SPECTRUM 28

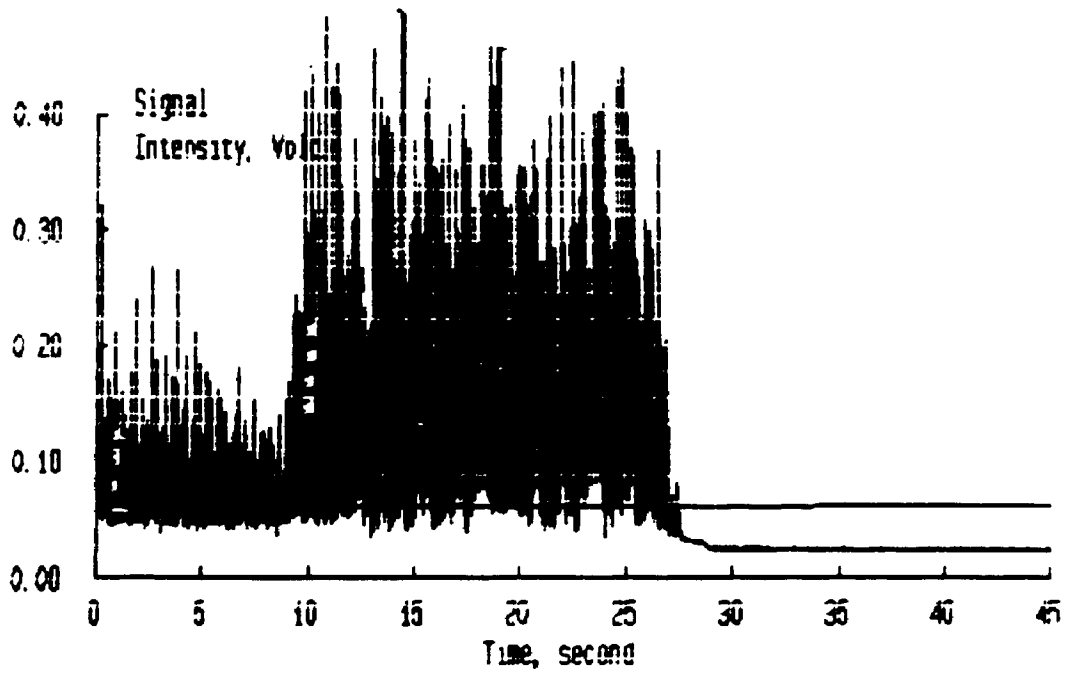
Signal
Intensity, Volts
0.40
0.30
0.20
0.10
0.00
0
5
10
15
20
25
30
35
40
45
Time, seconds

D.3 EQUATIONS USED AND SAMPLE CALCULATIONS FOR SIMULATING DENSITY AND VISCOSITY OF THE REACTION MIXTURE

Since it was not possible to use the fibre optic probe under actual reaction conditions, the measurements were made at room temperature under conditions that simulated the reaction fluid density and viscosity. These two parameters which in general change with temperature, pressure and composition, influence the gas re-circulation rate in the reactor with density having the most significant effect.

D.3.1 Calculation of fluid density under reaction conditions:

The density of the reaction mixture can be calculated by knowing the total gaseous mass in the reactor and the total internal gas volume. Since the reactor operates as a closed system, then the vapour density remains constant (assuming coke deposit has minor effect on total mass) since total mass and volume are also fixed. The maximum gas density in the reactor will occur at the lowest temperature used which was 500°C. Thus the density can be calculated from the known injected mass of oil into the reactor and the known initial mass of argon. The inert gas (argon) is always present initially in the reactor at 1 atm and the given temperature. Therefore the density of the vapour mixture, f_{mix}, can be calculated as follows:

$$f_{mix} = W_T \; / \; V_R \qquad \text{(D5)}$$

where the total mass, w_T is given by:

$$w_T = (1\ atm)V_R M_{Ar}/RT + w_o \qquad (D6).$$

DATA: Feedstock A injected to reactor at 500°C:

w_o = 0.16 g (from known syringe reading and oil density)
V_R = 45 mL
T = 773 K
R = 82.05 atm.mL/gmol.K
M_{Ar} = 40 g/gmol

Thus, $w_T = 1*45*40/(82.05*773) + 0.16 = 0.188$ (g)

and $f_{mix} = 0.188/45 = 4.18 \times 10^{-3}$ (g/mL).

D.3.2 Calculation of reaction mixture viscosity:

The viscosity of a gas mixture, μ_{mix}, can be calculated by the following equation:

$$\mu_{mix} = \Sigma\ y_i\mu_i M_i^{1/2} \ /\ \Sigma\ y_i M_i^{1/2} \qquad (D7)$$

where y_i is the mole fraction, μ_i is the viscosity and M_i is the molecular weight of component i. The initial mixture consists of the inert gas (argon) and the oil. As the cracking reactions take place the composition changes with the generation of light gases and gasoline molecules. The viscosity of both these mixtures will be assessed.

1) Initial gas viscosity (@ 500°C):

Data: (McCabe and Smith, 1976)
μ_{Ar} = 0.045 cp
M_{Ar} = 40 g/gmol
μ_{oil} = ~0.01 cp
M_{oil} = 350 g/gmol
y_{Ar} = 0.60

$y_{oil} = 0.40$

Thus from equation (D7): $\mu_{mix} = 0.0218$ cp

2) Final gas viscosity (end of reaction period, @ 500°C):

Data: Assume 75 wt% conversion with 50% gasoline and 25% light gases.

Light gases: y = 0.413, μ = 0.018 cp, M = 35 g/gmol
Gasoline: y = 0.289, μ = 0.016 cp, M = 100 g/gmol
Oil: y = 0.041, μ = 0.01 cp, M = 350 g/gmol
Argon: y = 0.256, μ= 0.045 cp, M = 40 g/gmol

Substituting into equation (D7) gives μ_{mix} = 0.022 cp.

Thus the change in fluid viscosity from the time of injection to the time of purge is not significant.

D.3.3 Simulation of the reaction mixture at room temperature:

The viscosity of argon at 20°C is 0.0224 cp (McCabe and Smith, 1976) which corresponds well to the reaction mixture viscosity at 500°C. To simulate the density of the reaction mixture at 500°C (4.1×10^{-3} g/mL) the pressure of argon in the reactor at 20°C can be found by:

$$P = f_{mix}RT/M_{Ar} \qquad \text{(D8)}.$$

Substituting in the appropriate values gives a pressure of 2.5 atm. Thus, filling the reactor to 2.5 atm of argon gas at 20°C will produce a similar viscosity and density as the reaction mixture at 500°C.

D.3.4 Simulation of the fluid density before oil injection:

Just before oil is injected to the reactor, the impeller is rotating at 8000 RPM with 1 atm of argon present at 500°C. Under these conditions the density is 6.31×10^{-4} g/mL. From the ideal gas law the molecular weight of a gas to simulate this density at room conditions (25°C, 1 atm) can be calculated:

$$M = \rho RT/P = 6.31 \times 10^{-4} * 82.05 * 298/1 = 15.4 \text{ g/gmol.}$$

Methane was available in the laboratory and has a molecular weight of 16 and was thus used in the fibre optic probe experiments. Alternatively, a lighter gas such as helium could be used but the pressure would have to be higher than 1 atm.

D.4 ESTIMATION OF THE VOLUMETRIC RE-CIRCULATION RATE

The impeller motion induces a swirling flow of gas as observed in the cold experiments (Plexiglas unit). The gas flow patterns are similar to a cyclone flow. Measuring pressure drop does not necessarily give the appropriate velocity through the bed, only the linear velocity. The actual velocity has tangential and axial components. The volumetric flow rate can be estimated by calculating the overall velocity vector and using the area of the spiral tunnel through which the flow travels.

Assumptions:

1. From visual observations, particles at the surface of the bed are transported up, therefore assume the vertical velocity component is that of the terminal velocity of the particle.

2. Assume 3 complete spirals through the bed chamber and that the circumference of the spiral is πd, where d is the diameter of the inner catalyst chamber.

3. The area of the 'tunnel' is h/3 times d/2 where h is the height of the catalyst chamber.

Calculations:

For a single spherical particle in gravity settling the terminal velocity is given by (McCabe and Smith, 1976):

$$u_t = [2g(f_p - f_f)m/(A_p f_p C_D f_f)]^{1/2} \qquad (D9).$$

To evaluate the drag coefficient, C_D, the criterion of McCabe and Smith will be used. It is therefore necessary to evaluate a function F given by:

$$F = D_p \left[g f_f (f_p - f_f) / \mu^2 \right]^{1/3} \qquad \text{(D10)}$$

whereby if F is in a certain range, then a specific equation for u_t may be used accounting for C_D.

Data:

$D_p = 60 \times 10^{-6}$ m
$g = 9.81$ m/s$_2$
$f_p = 1900$ kg/m^3
$f_f = 4.1$ kg/m^3 (reaction mixture @ 500°C)
$\mu = 2.2 \times 10^{-5}$ kg/m.s

Substituting the appropriate data into equation (D10) gives a value for F of 3.7. This value corresponds to the range of F values for the intermediate law (McCabe and Smith, 1976):

$$u_t = 0.153 \; g^{0.71} \; D_p^{1.14} \; (f_p - f_f)^{0.71} \; / \; (f_f^{0.29} \; \mu_f^{0.43}) \qquad \text{(D11)}.$$

Substituting in the appropriate data gives a terminal velocity of 16.9 cm/s. The magnitude of the velocity vector (v) related to its vertical component (u_t) is given by $\sin \beta = u_t / v$ The angle ß can be calculated by the assumption of three spirals through the bed and the circumference of the spiral equal to that of the bed chamber:

$$\sin \beta = (h/3) \; / \; \pi d \qquad \text{(D11)}.$$

The height of the catalyst chamber, h, is 1.6 cm and the diameter, d, is 1.35 cm. This gives a value of ß equal to 7.2° according to equation (D11). Thus the magnitude of the velocity vector that passes through the bed is:

$v = u_t/\sin\beta = 16.9 / \sin(7.2) = 134.3$ cm/s.

The area of the 'tunnel' is $(h/3)*(d/2) = (1.6/3)*(1.35/2) = 0.36$ cm^2. Thus the volumetric flow rate (Q) through the bed is:

$Q = 0.36 * 134.3 = 48$ cm^3/s.

APPENDIX E

PRODUCT DISTRIBUTION AND MASS BALANCE TABLES

This appendix presents the detailed product distributions for the experimental cracking runs performed in the Riser Simulator unit. Also, for each experimental condition, the mass balances are shown in tables E.6 to E.10. The run number nomenclature is denoted by two letters and a number. The first letter corresponds to the feedstock, the second to the catalyst used and the number refers to the experimental conditions. For example, run A-O-1 refers to the cracking of feedstock A on Octacat at condition 1 (3 seconds, 500°C). The experimental conditions corresponding to each run are shown in tables E.1 to E.5. All runs were done using 0.8 grams of catalyst.

TYPICAL DATA SHEET USED FOR EACH RUN:

RUN #:

CONDITIONS: REACTOR TEMP. =
REACTION TIME =
INJECTION VOLUME =
WEIGHT OF CATALYST =
REACTOR GAS VOLUME =

SYSTEM TEMPERATURES (°C)

T1= T2=

T3= T4=

T5= TVB=

T6= T7=

T8=

PRESSURE (in. Hg vac)

P vac. initial =

P vac. final =

GC CONDITIONS

carrier flow = mL/min
det. temp. =
inj. temp. =

Range =
Attn =
Thrsh =

Temperature Program:

	Init. T (°C)	Init. time (min)	Rate (° C/min)	Final T (°C)	Final time (min)
1					
2					
3					

PROPANE CALIBRATION : loop size = mL, T(room) =
range =
attn = TA =
thrsh =

INTEGRATOR REPORT :

GASES = GASOLINE = OIL =

CONV = ; TA =

Table E.1 Run identification and corresponding operating conditions for the cracking runs of feed A.

Run i.d.	Feed	Catalyst	t_R(s)	T(°C)	c/o
A-O-1	A	Octacat	3	500	5.0
A-O-2			5		
A-O-3			7		
A-O-4			10		
A-O-5			3	525	
A-O-6			5		
A-O-7			7		
A-O-8			10		
A-O-9			3	550	
A-O-10			5		
A-O-11			7		
A-O-12			10		
A-G-1	A	GX-30	3	500	5.0
A-G-2			5		
A-G-3			7		
A-G-4			10		
A-G-5			3	525	
A-G-6			5		
A-G-7			7		
A-G-8			10		
A-G-9			3	550	
A-G-10			5		
A-G-11			7		
A-G-12			10		

Table E.2 Run identification and corresponding operating conditions for the cracking runs of feed B.

Run i.d.	Feed	Catalyst	t_R(s)	T(°C)	c/o
B-O-1	B	Octacat	3	500	4.85
B-O-2			5		
B-O-3			7		
B-O-4			10		
B-O-5			3	525	
B-O-6			5		
B-O-7			7		
B-O-8			10		
B-O-9			3	550	
B-O-10			5		
B-O-11			7		
B-O-12			10		
B-G-1	B	GX-30	3	500	4.85
B-G-2			5		
B-G-3			7		
B-G-4			10		
B-G-5			3	525	
B-G-6			5		
B-G-7			7		
B-G-8			10		
B-G-9			3	550	
B-G-10			5		
B-G-11			7		
B-G-12			10		

Table E.3 Run identification and corresponding operating conditions for the cracking runs of feed P_1.

Run i.d.	Feed	Catalyst	t_R(s)	T(°C)	c/o
P_1-O-1	P_1	Octacat	3	500	5.17
P_1-O-2			5		
P_1-O-3			7		
P_1-O-4			10		
P_1-O-5			3	550	
P_1-O-6			5		
P_1-O-7			7		
P_1-O-8			10		
P_1-G-1	P_1	GX-30	3	500	5.17
P_1-G-2			5		
P_1-G-3			7		
P_1-G-4			10		
P_1-G-5			3	550	
P_1-G-6			5		
P_1-G-7			7		
P_1-G-8			10		

Table E.4 Run identification and corresponding operating conditions for the cracking runs of feed N_1.

Run i.d.	Feed	Catalyst	t_R(s)	T(°C)	c/o
N_1-O-1	N_1	Octacat	3	500	4.5
N_1-O-2			5		
N_1-O-3			7		
N_1-O-4			10		
N_1-O-5			3	550	
N_1-O-6			5		
N_1-O-7			7		
N_1-O-8			10		
N_1-G-1	N_1	GX-30	3	500	4.5
N_1-G-2			5		
N_1-G-3			7		
N_1-G-4			10		
N_1-G-5			3	550	
N_1-G-6			5		
N_1-G-7			7		
N_1-G-8			10		

Table E.5 Run identification and corresponding operating conditions for the cracking runs of feed A_1.

Run i.d.	Feed	Catalyst	t_R(s)	T(°C)	c/o
A_1-O-1	A_1	Octacat	3	500	4.35
A_1-O-2			5		
A_1-O-3			7		
A_1-O-4			10		
A_1-O-5			3	550	
A_1-O-6			5		
A_1-O-7			7		
A_1-O-8			10		
A_1-G-1	A_1	GX-30	3	500	4.35
A_1-G-2			5		
A_1-G-3			7		
A_1-G-4			10		
A_1-G-5			3	550	
A_1-G-6			5		
A_1-G-7			7		
A_1-G-8			10		

Table E.6 Mass Balances for Feedstock A

RUN i.d.	P_{vi} (atm)	P_f (atm)	T_v (°C)	% purged (wt%)	m_{sal} (g)	m_{inj} (g)
A-O-1	0.106	0.248	373	92	0.156	0.160
A-O-2	0.104	0.248	368	93	0.150	0.160
A-O-3	0.131	0.273	364	94	0.147	0.160
A-O-4	0.123	0.298	368	91	0.152	0.160
A-O-5	0.131	0.265	367	95	0.149	0.160
A-O-6	0.123	0.248	374	96	0.148	0.160
A-O-7	0.131	0.281	382	95	0.150	0.160
A-O-8	0.128	0.307	365	91	0.149	0.160
A-O-9	0.131	0.298	376	92	0.157	0.160
A-O-10	0.123	0.290	350	95	0.153	0.160
A-O-11	0.104	0.281	370	95	0.152	0.160
A-O-12	0.123	0.328	366	92	0.146	0.160
A-G-1	0.131	0.265	343	93	0.152	0.160
A-G-2	0.114	0.255	355	94	0.152	0.160
A-G-3	0.106	0.261	354	93	0.155	0.160
A-G-4	0.106	0.298	378	92	0.145	0.160
A-G-5	0.106	0.265	358	94	0.154	0.160
A-G-6	0.123	0.290	380	95	0.151	0.160
A-G-7	0.123	0.298	385	95	0.152	0.160
A-G-8	0.104	0.307	380	91	0.146	0.160
A-G-9	0.131	0.298	357	95	0.153	0.160
A-G-10	0.131	0.308	385	96	0.150	0.160
A-G-11	0.106	0.292	361	95	0.154	0.160
A-G-12	0.104	0.332	380	92	0.150	0.160

Table E.7 Mass Balances for Feedstock B

RUN i.d.	P_{vi} (atm)	P_f (atm)	T_v (°C)	% purged (wt%)	m_{cal} (g)	m_{inj} (g)
B-O-1	0.131	0.273	365	93	0.154	0.165
B-O-2	0.123	0.281	368	91	0.156	0.165
B-O-3	0.111	0.281	368	91	0.158	0.165
B-O-4	0.098	0.281	366	91	0.157	0.165
B-O-5	0.106	0.256	370	92	0.162	0.165
B-O-6	0.106	0.290	370	92	0.150	0.165
B-O-7	0.114	0.298	372	91	0.156	0.165
B-O-8	0.106	0.312	366	92	0.149	0.165
B-O-9	0.114	0.281	370	92	0.152	0.165
B-O-10	0.114	0.298	365	94	0.158	0.165
B-O-11	0.114	0.315	365	93	0.154	0.165
B-O-12	0.123	0.332	372	92	0.159	0.165
B-G-1	0.440	0.566	360	83	0.154	0.165
B-G-2	0.440	0.559	360	84	0.151	0.165
B-G-3	0.340	0.465	350	88	0.153	0.165
B-G-4	0.106	0.315	380	91	0.160	0.165
B-G-5	0.390	0.507	350	83	0.158	0.165
B-G-6	0.415	0.541	351	87	0.150	0.165
B-G-7	0.131	0.298	358	92	0.162	0.165
B-G-8	0.104	0.323	381	90	0.157	0.165
B-G-9	0.382	0.549	354	86	0.161	0.165
B-G-10	0.131	0.265	348	95	0.156	0.165
B-G-11	0.131	0.298	344	93	0.160	0.165
B-G-12	0.114	0.348	386	95	0.159	0.165

Table E.8 Mass Balances for Feedstock P_L

RUN i.d.	P_{vi} (atm)	P_f (atm)	T_v (°C)	% purged (wt%)	m_{cal} (g)	m_{inj} (g)
P_l-O-1	0.123	0.295	355	91	0.139	0.155
P_l-O-2	0.449	0.616	349	84	0.147	0.155
P_l-O-3	0.123	0.302	350	91	0.150	0.155
P_l-O-4	0.449	0.632	344	90	0.141	0.155
P_l-O-5	0.123	0.332	365	94	0.144	0.155
P_l-O-6	0.398	0.616	341	95	0.141	0.155
P_l-O-7	0.123	0.312	350	90	0.150	0.155
P_l-O-8	0.415	0.649	339	92	0.146	0.155
P_l-G-1	0.424	0.582	309	85	0.147	0.155
P_l-G-2	0.424	0.594	310	85	0.149	0.155
P_l-G-3	0.373	0.557	328	88	0.154	0.155
P_l-G-4	0.373	0.568	330	89	0.150	0.155
P_l-G-5	0.457	0.649	319	83	0.148	0.155
P_l-G-6	0.457	0.653	321	82	0.148	0.155
P_l-G-7	0.372	0.589	327	86	0.145	0.155
P_l-G-8	0.372	0.601	330	90	0.149	0.155

Table E.9 Mass Balances for Feedstock N_l

RUN i.d.	P_{vi} (atm)	P_f (atm)	T_v (°C)	% purged (wt%)	m_{cal} (g)	m_{inj} (g)
N_l-O-1	0.131	0.325	368	95	0.166	0.178
N_l-O-2	0.452	0.641	349	90	0.168	0.178
N_l-O-3	0.131	0.357	371	95	0.166	0.178
N_l-O-4	0.373	0.572	335	91	0.169	0.178
N_l-O-5	0.131	0.357	368	97	0.168	0.178
N_l-O-6	0.390	0.591	332	91	0.170	0.178
N_l-O-7	0.131	0.290	372	96	0.168	0.178
N_l-O-8	0.357	0.576	338	91	0.169	0.178
N_l-G-1	0.465	0.641	303	86	0.171	0.178
N_l-G-2	0.131	0.318	376	90	0.176	0.178
N_l-G-3	0.365	0.549	320	88	0.167	0.178
N_l-G-4	0.114	0.340	373	91	0.173	0.178
N_l-G-5	0.459	0.657	314	85	0.176	0.178
N_l-G-6	0.123	0.373	375	93	0.169	0.178
N_l-G-7	0.365	0.569	316	91	0.173	0.178
N_l-G-8	0.114	0.373	377	92	0.176	0.178

Table E.10 Mass Balances for Feedstock A_1

RUN i.d.	P_{vi} (atm)	P_f (atm)	T_v (°C)	% purged (wt%)	m_{cal} (g)	m_{inj} (g)
A_1-O-1	0.123	0.323	372	96	0.173	0.184
A_1-O-2	0.373	0.995	335	90	0.170	0.184
A_1-O-3	0.123	0.365	370	92	0.173	0.184
A_1-O-4	0.348	0.524	342	91	0.180	0.184
A_1-O-5	0.123	0.332	370	92	0.178	0.184
A_1-O-6	0.432	0.626	337	89	0.175	0.184
A_1-O-7	0.123	0.348	371	91	0.170	0.184
A_1-O-8	0.415	0.616	346	90	0.179	0.184
A_1-G-1	0.405	0.572	321	87	0.175	0.184
A_1-G-2	0.131	0.357	371	90	0.175	0.184
A_1-G-3	0.365	0.532	320	90	0.183	0.184
A_1-G-4	0.123	0.340	375	91	0.169	0.184
A_1-G-5	0.439	0.624	316	91	0.183	0.184
A_1-G-6	0.114	0.340	373	92	0.175	0.184
A_1-G-7	0.382	0.566	326	90	0.182	0.184
A_1-G-8	0.114	0.365	375	92	0.180	0.184

PRODUCT DISTRIBUTION FOR RUN I.D.: A-O-1

NO.	COMPOUND(S)	wt%
1	Methane	1.43
2	Ethylene	2.36
3	Ethane	1.12
4	Propylene	3.26
5	Propane	.57
6	i-Butane	.56
7	i-Butylene	1.85
8	1-Butene	.55
9	n-Butane	.10
10	t,2-Butene	.39
11	c,2-Butene	.29
12	3-Methyl-1-butene	.12
13	i-Pentane	.68
14	C5 olefins	.85
15	n-Pentane	.07
16	C5 olefins, naphthenes; C6 olefins, i-para.	1.75
17	2- and 3-methylpentane, C6 isoparaffins	.49
18	C6 olefins	.72
19	n-Hexane	.05
20	C6 olefins, naph.; C7 olef., i-para, naph.	1.00
21	Benzene	.93
22	C6 naphthene; C7 olefins, i-para., naph.	.36
23	2- and 3-methylhexane, C7 i-paraffins	.35
24	C7 olefins, naph., i-para.; C8 i-para.	.59
25	n-Heptane	.14
26	C7 olefins, naphthenes; C8 i-paraffins	.64
27	toluene	1.36
28	C8 isoparaffins	.27
29	2- and 3-methylheptane; C8 i-paraffins	.49
30	C7 and C8 naphthenes; C9 i-paraffins	.03
31	n-Octane	.03
32	C9 olefins; C8, C9 naph., C9 i-para.	.30
33	Ethylbenzene	.37
34	C9 naphthenes and i-paraffins	.04
35	p-Xylene and m-Xylene	.93
36	C9 i-paraffins and naphthenes	.50
37	o-Xylene	.39
38	n-Nonane, C9 naphthenes	.43
39	C9 aromatics; C10 i-para. and naphthenes	1.84
40	n-Decane	2.77
41	n-C10; C9, C10 arom.; C10, C11 i-para., naph.	1.61
42	Light paraffins	15.06
43	Light naphthenes	8.51
44	Light aromatics	7.50
45	Heavy paraffins	13.07
46	Heavy naphthenes	12.28
47	Heavy aromatics	3.99
48	Coke	2.03

PRODUCT DISTRIBUTION FOR RUN I.D.: A-O-2

NO.	COMPOUND(S)	wt%
1	Methane	1.40
2	Ethylene	2.12
3	Ethane	1.08
4	Propylene	4.00
5	Propane	.71
6	i-Butane	1.52
7	i-Butylene	2.30
8	1-Butene	.51
9	n-Butane	.33
10	t,2-Butene	.70
11	c,2-Butene	.51
12	3-Methyl-1-butene	.13
13	i-Pentane	1.62
14	C5 olefins	.88
15	n-Pentane	.14
16	C5 olefins, naphthenes; C6 olefins, i-para.	2.02
17	2- and 3-methylpentane, C6 isoparaffins	1.13
18	C6 olefins	.66
19	n-Hexane	.10
20	C6 olefins, naph.; C7 olef., i-para, naph.	1.25
21	Benzene	.53
22	C6 naphthene; C7 olefins, i-para., naph.	.33
23	2- and 3-methylhexane, C7 i-paraffins	.63
24	C7 olefins, naph., i-para.; C8 i-para.	.64
25	n-Heptane	.17
26	C7 olefins, naphthenes; C8 i-paraffins	.86
27	toluene	1.29
28	C8 isoparaffins	.41
29	2- and 3-methylheptane; C8 i-paraffins	.58
30	C7 and C8 naphthenes; C9 i-paraffins	.04
31	n-Octane	.05
32	C9 olefins; C8, C9 naph., C9 i-para.	.67
33	Ethylbenzene	.36
34	C9 naphthenes and i-paraffins	0.00
35	p-Xylene and m-Xylene	1.34
36	C9 i-paraffins and naphthenes	.26
37	o-Xylene	.53
38	n-Nonane, C9 naphthenes	.38
39	C9 aromatics; C10 i-para. and naphthenes	2.33
40	n-Decane	3.29
41	n-C10; C9, C10 arom.; C10, C11 i-para., naph.	.99
42	Light paraffins	12.40
43	Light naphthenes	8.00
44	Light aromatics	9.51
45	Heavy paraffins	17.12
46	Heavy naphthenes	9.31
47	Heavy aromatics	3.22
48	Coke	1.68

PRODUCT DISTRIBUTION FOR RUN I.D.: A-O-3

NO.	COMPOUND(S)	wt%
1	Methane	2.11
2	Ethylene	3.11
3	Ethane	1.02
4	Propylene	4.70
5	Propane	.55
6	i-Butane	1.14
7	i-Butylene	2.50
8	1-Butene	.88
9	n-Butane	.23
10	t,2-Butene	.56
11	c,2-Butene	.42
12	3-Methyl-1-butene	.16
13	i-Pentane	2.06
14	C5 olefins	.96
15	n-Pentane	.16
16	C5 olefins, naphthenes; C6 olefins, i-para.	3.26
17	2- and 3-methylpentane, C6 isoparaffins	1.36
18	C6 olefins	.39
19	n-Hexane	.11
20	C6 olefins, naph.; C7 olef., i-para, naph.	1.58
21	Benzene	1.50
22	C6 naphthene; C7 olefins, i-para., naph.	.14
23	2- and 3-methylhexane, C7 i-paraffins	.62
24	C7 olefins, naph., i-para.; C8 i-para.	.37
25	n-Heptane	.12
26	C7 olefins, naphthenes; C8 i-paraffins	.54
27	toluene	2.42
28	C8 isoparaffins	.19
29	2- and 3-methylheptane; C8 i-paraffins	.34
30	C7 and C8 naphthenes; C9 i-paraffins	0.00
31	n-Octane	.04
32	C9 olefins; C8, C9 naph., C9 i-para.	.36
33	Ethylbenzene	.41
34	C9 naphthenes and i-paraffins	0.00
35	p-Xylene and m-Xylene	2.16
36	C9 i-paraffins and naphthenes	.36
37	o-Xylene	.80
38	n-Nonane, C9 naphthenes	.21
39	C9 aromatics; C10 i-para. and naphthenes	3.15
40	n-Decane	3.86
41	n-C10; C9, C10 arom.; C10, C11 i-para., naph.	.74
42	Light paraffins	11.08
43	Light naphthenes	7.10
44	Light aromatics	6.76
45	Heavy paraffins	15.68
46	Heavy naphthenes	9.05
47	Heavy aromatics	3.03
48	Coke	1.73

PRODUCT DISTRIBUTION FOR RUN I.D.: A-O-4

NO.	COMPOUND(S)	wt%
1	Methane	4.70
2	Ethylene	4.84
3	Ethane	.32
4	Propylene	6.94
5	Propane	.03
6	i-Butane	.63
7	i-Butylene	2.49
8	1-Butene	.90
9	n-Butane	.10
10	t,2-Butene	.40
11	c,2-Butene	.31
12	3-Methyl-1-butene	.22
13	i-Pentane	.56
14	C5 olefins	1.30
15	n-Pentane	.12
16	C5 olefins, naphthenes; C6 olefins, i-para.	2.81
17	2- and 3-methylpentane, C6 isoparaffins	.37
18	C6 olefins	1.33
19	n-Hexane	.01
20	C6 olefins, naph.; C7 olef., i-para, naph.	1.35
21	Benzene	3.28
22	C6 naphthene; C7 olefins, i-para., naph.	.61
23	2- and 3-methylhexane, C7 i-paraffins	.48
24	C7 olefins, naph., i-para.; C8 i-para.	.84
25	n-Heptane	.03
26	C7 olefins, naphthenes; C8 i-paraffins	.89
27	toluene	3.13
28	C8 isoparaffins	.15
29	2- and 3-methylheptane; C8 i-paraffins	.50
30	C7 and C8 naphthenes; C9 i-paraffins	.47
31	n-Octane	.04
32	C9 olefins; C8, C9 naph., C9 i-para.	.60
33	Ethylbenzene	.27
34	C9 naphthenes and i-paraffins	.08
35	p-Xylene and m-Xylene	1.77
36	C9 i-paraffins and naphthenes	.03
37	o-Xylene	.52
38	n-Nonane, C9 naphthenes	1.17
39	C9 aromatics; C10 i-para. and naphthenes	3.07
40	n-C10; C9, C10 arom.; C10, C11 i-para., naph.	3.34
41	C12 hydrocarbons	1.98
42	Light paraffins	10.48
43	Light naphthenes	6.69
44	Light aromatics	5.02
45	Heavy paraffins	11.52
46	Heavy naphthenes	8.10
47	Heavy aromatics	2.93
48	Coke	2.30

PRODUCT DISTRIBUTION FOR RUN I.D.: A-O-5

NO.	COMPOUND(S)	wt%
1	Methane	2.30
2	Ethylene	3.84
3	Ethane	2.75
4	Propylene	4.34
5	Propane	1.36
6	i-Butane	.44
7	i-Butylene	2.35
8	1-Butene	1.45
9	n-Butane	.38
10	t,2-Butene	.38
11	c,2-Butene	.29
12	3-Methyl-1-butene	.17
13	i-Pentane	.42
14	C5 olefins	1.18
15	n-Pentane	.09
16	C5 olefins, naphthenes; C6 olefins, i-para.	2.61
17	2- and 3-methylpentane, C6 isoparaffins	.28
18	C6 olefins	1.16
19	n-Hexane	.03
20	C6 olefins, naph.; C7 olef., i-para, naph.	1.02
21	Benzene	1.60
22	C6 naphthene; C7 olefins, i-para., naph.	.41
23	2- and 3-methylhexane, C7 i-paraffins	.38
24	C7 olefins, naph., i-para.; C8 i-para.	.74
25	n-Heptane	.03
26	C7 olefins, naphthenes; C8 i-paraffins	.74
27	toluene	2.08
28	C8 isoparaffins	.13
29	2- and 3-methylheptane; C8 i-paraffins	.88
30	C7 and C8 naphthenes; C9 i-paraffins	.04
31	n-Octane	.01
32	C9 olefins; C8, C9 naph., C9 i-para.	.39
33	Ethylbenzene	.38
34	C9 naphthenes and i-paraffins	.07
35	p-Xylene and m-Xylene	1.14
36	C9 i-paraffins and naphthenes	.36
37	o-Xylene	.48
38	n-Nonane, C9 naphthenes	.52
39	C9 aromatics; C10 i-para. and naphthenes	2.02
40	n-C10; C9, C10 arom.; C10, C11 i-para., naph.	2.39
41	C12 hydrocarbons	1.49
42	Light paraffins	13.41
43	Light naphthenes	7.05
44	Light aromatics	7.04
45	Heavy paraffins	15.71
46	Heavy naphthenes	10.14
47	Heavy aromatics	3.17
48	Coke	.37

PRODUCT DISTRIBUTION FOR RUN I.D.: A-O-6

NO.	COMPOUND(S)	wt%
1	Methane	2.22
2	Ethylene	3.59
3	Ethane	1.26
4	Propylene	6.06
5	Propane	1.10
6	i-Butane	2.40
7	i-Butylene	3.11
8	1-Butene	.93
9	n-Butane	.47
10	t,2-Butene	.82
11	c,2-Butene	.62
12	3-Methyl-1-butene	.14
13	i-Pentane	2.02
14	C5 olefins	.45
15	n-Pentane	.46
16	C5 olefins, naphthenes; C6 olefins, i-para.	2.53
17	2- and 3-methylpentane, C6 isoparaffins	1.05
18	C6 olefins	.58
19	n-Hexane	.10
20	C6 olefins, naph.; C7 olef., i-para, naph.	1.22
21	Benzene	.81
22	C6 naphthene; C7 olefins, i-para., naph.	.37
23	2- and 3-methylhexane, C7 i-paraffins	.38
24	C7 olefins, naph., i-para.; C8 i-para.	.45
25	n-Heptane	.10
26	C7 olefins, naphthenes; C8 i-paraffins	.47
27	toluene	2.22
28	C8 isoparaffins	.10
29	2- and 3-methylheptane; C8 i-paraffins	.22
30	C7 and C8 naphthenes; C9 i-paraffins	.24
31	n-Octane	.01
32	C9 olefins; C8, C9 naph., C9 i-para.	.50
33	Ethylbenzene	.46
34	C9 naphthenes and i-paraffins	0.00
35	p-Xylene and m-Xylene	2.19
36	C9 i-paraffins and naphthenes	.15
37	o-Xylene	.79
38	n-Nonane, C9 naphthenes	.26
39	C9 aromatics; C10 i-para. and naphthenes	2.70
40	n-C10; C9, C10 arom.; C10, C11 i-para., naph.	2.61
41	C12 hydrocarbons	1.33
42	Light paraffins	12.93
43	Light naphthenes	5.96
44	Light aromatics	7.58
45	Heavy paraffins	13.90
46	Heavy naphthenes	8.14
47	Heavy aromatics	2.89
48	Coke	1.09

PRODUCT DISTRIBUTION FOR RUN I.D.: A-O-7

NO.	COMPOUND(S)	wt%
1	Methane	4.07
2	Ethylene	5.48
3	Ethane	2.96
4	Propylene	5.67
5	Propane	1.30
6	i-Butane	.52
7	i-Butylene	2.59
8	1-Butene	1.46
9	n-Butane	.28
10	t,2-Butene	.39
11	c,2-Butene	.29
12	3-Methyl-1-butene	.17
13	i-Pentane	.66
14	C5 olefins	1.12
15	n-Pentane	.12
16	C5 olefins, naphthenes; C6 olefins, i-para.	2.92
17	2- and 3-methylpentane, C6 isoparaffins	.40
18	C6 olefins	1.04
19	n-Hexane	.05
20	C6 olefins, naph.; C7 olef., i-para, naph.	1.21
21	Benzene	3.49
22	C6 naphthene; C7 olefins, i-para., naph.	.49
23	2- and 3-methylhexane, C7 i-paraffins	.40
24	C7 olefins, naph., i-para.; C8 i-para.	.71
25	n-Heptane	.11
26	C7 olefins, naphthenes; C8 i-paraffins	.66
27	toluene	3.41
28	C8 isoparaffins	.13
29	2- and 3-methylheptane; C8 i-paraffins	.41
30	C7 and C8 naphthenes; C9 i-paraffins	.39
31	n-Octane	.03
32	C9 olefins; C8, C9 naph., C9 i-para.	.37
33	Ethylbenzene	.46
34	C9 naphthenes and i-paraffins	.06
35	p-Xylene and m-Xylene	1.88
36	C9 i-paraffins and naphthenes	.02
37	o-Xylene	.58
38	n-Nonane, C9 naphthenes	1.13
39	C9 aromatics; C10 i-para. and naphthenes	2.94
40	n-C10; C9, C10 arom.; C10, C11 i-para., naph.	3.10
41	C12 hydrocarbons	1.54
42	Light paraffins	11.33
43	Light naphthenes	4.97
44	Light aromatics	6.04
45	Heavy paraffins	11.10
46	Heavy naphthenes	7.86
47	Heavy aromatics	2.23
48	Coke	1.49

PRODUCT DISTRIBUTION FOR RUN I.D.: A-O-8

NO.	COMPOUND(S)	wt%
1	Methane	3.79
2	Ethylene	5.68
3	Ethane	3.91
4	Propylene	7.44
5	Propane	0.00
6	i-Butane	.92
7	i-Butylene	3.71
8	1-Butene	2.29
9	n-Butane	.64
10	t,2-Butene	.48
11	c,2-Butene	.44
12	3-Methyl-1-butene	.23
13	i-Pentane	.80
14	C5 olefins	1.39
15	n-Pentane	.14
16	C5 olefins, naphthenes; C6 olefins, i-para.	3.22
17	2- and 3-methylpentane, C6 isoparaffins	.53
18	C6 olefins	1.20
19	n-Hexane	.01
20	C6 olefins, naph.; C7 olef., i-para, naph.	1.59
21	Benzene	2.07
22	C6 naphthene; C7 olefins, i-para., naph.	.56
23	2- and 3-methylhexane, C7 i-paraffins	.45
24	C7 olefins, naph., i-para.; C8 i-para.	.80
25	n-Heptane	.03
26	C7 olefins, naphthenes; C8 i-paraffins	1.00
27	toluene	2.62
28	C8 isoparaffins	.52
29	2- and 3-methylheptane; C8 i-paraffins	.59
30	C7 and C8 naphthenes; C9 i-paraffins	.45
31	n-Octane	.07
32	C9 olefins; C8, C9 naph., C9 i-para.	.50
33	Ethylbenzene	.50
34	C9 naphthenes and i-paraffins	.09
35	p-Xylene and m-Xylene	1.68
36	C9 i-paraffins and naphthenes	.14
37	o-Xylene	.48
38	n-Nonane, C9 naphthenes	1.18
39	C9 aromatics; C10 i-para. and naphthenes	3.03
40	n-C10; C9, C10 arom.; C10, C11 i-para., naph.	3.03
41	C12 hydrocarbons	1.57
42	Light paraffins	9.87
43	Light naphthenes	4.62
44	Light aromatics	4.48
45	Heavy paraffins	9.96
46	Heavy naphthenes	7.27
47	Heavy aromatics	1.24
48	Coke	2.80

PRODUCT DISTRIBUTION FOR RUN I.D.: A-O-9

NO.	COMPOUND(S)	wt%
1	Methane	2.89
2	Ethylene	4.26
3	Ethane	3.24
4	Propylene	5.08
5	Propane	1.53
6	i-Butane	.57
7	i-Butylene	2.84
8	1-Butene	1.56
9	n-Butane	.46
10	t,2-Butene	.46
11	c,2-Butene	.34
12	3-Methyl-1-butene	.18
13	i-Pentane	.46
14	C5 olefins	1.22
15	n-Pentane	.07
16	C5 olefins, naphthenes; C6 olefins, i-para.	2.48
17	2- and 3-methylpentane, C6 isoparaffins	.30
18	C6 olefins	1.19
19	n-Hexane	.01
20	C6 olefins, naph.; C7 olef., i-para, naph.	1.17
21	Benzene	1.39
22	C6 naphthene; C7 olefins, i-para., naph.	.57
23	2- and 3-methylhexane, C7 i-paraffins	.23
24	C7 olefins, naph., i-para.; C8 i-para.	.81
25	n-Heptane	.04
26	C7 olefins, naphthenes; C8 i-paraffins	.91
27	toluene	1.95
28	C8 isoparaffins	.35
29	2- and 3-methylheptane; C8 i-paraffins	.93
30	C7 and C8 naphthenes; C9 i-paraffins	.05
31	n-Octane	.03
32	C9 olefins; C8, C9 naph., C9 i-para.	.43
33	Ethylbenzene	.42
34	C9 naphthenes and i-paraffins	.09
35	p-Xylene and m-Xylene	1.18
36	C9 i-paraffins and naphthenes	.42
37	o-Xylene	.51
38	n-Nonane, C9 naphthenes	.54
39	C9 aromatics; C10 i-para. and naphthenes	2.26
40	n C10; C9, C10 arom.; C10, C11 i-para., naph.	2.82
41	C12 hydrocarbons	1.14
42	Light paraffins	13.68
43	Light naphthenes	6.15
44	Light aromatics	6.57
45	Heavy paraffins	12.77
46	Heavy naphthenes	9.12
47	Heavy aromatics	2.30
48	Coke	2.00

PRODUCT DISTRIBUTION FOR RUN I.D.: A-O-10

NO.	COMPOUND(S)	wt%
1	Methane	4.86
2	Ethylene	5.61
3	Ethane	3.29
4	Propylene	5.48
5	Propane	1.43
6	i-Butane	.49
7	i-Butylene	2.29
8	1-Butene	1.26
9	n-Butane	.34
10	t,2-Butene	.33
11	c,2-Butene	.25
12	3-Methyl-1-butene	.15
13	i-Pentane	.45
14	C5 olefins	.62
15	n-Pentane	.27
16	C5 olefins, naphthenes; C6 olefins, i-para.	2.00
17	2- and 3-methylpentane, C6 isoparaffins	.19
18	C6 olefins	1.03
19	n-Hexane	.03
20	C6 olefins, naph.; C7 olef., i-para, naph.	.83
21	Benzene	3.42
22	C6 naphthene; C7 olefins, i-para., naph.	.14
23	2- and 3-methylhexane, C7 i-paraffins	.34
24	C7 olefins, naph., i-para.; C8 i-para.	.67
25	n-Heptane	.02
26	C7 olefins, naphthenes; C8 i-paraffins	.65
27	toluene	3.69
28	C8 isoparaffins	.08
29	2- and 3-methylheptane; C8 i-paraffins	.37
30	C7 and C8 naphthenes; C9 i-paraffins	.39
31	n-Octane	.03
32	C9 olefins; C8, C9 naph., C9 i-para.	.42
33	Ethylbenzene	.27
34	C9 naphthenes and i-paraffins	.06
35	p-Xylene and m-Xylene	1.85
36	C9 i-paraffins and naphthenes	.53
37	o-Xylene	.74
38	n-Nonane, C9 naphthenes	.42
39	C9 aromatics; C10 i-para. and naphthenes	2.63
40	n-C10; C9, C10 arom.; C10, C11 i-para., naph.	2.42
41	C12 hydrocarbons	1.61
42	Light paraffins	11.29
43	Light naphthenes	5.87
44	Light aromatics	5.64
45	Heavy paraffins	11.84
46	Heavy naphthenes	8.88
47	Heavy aromatics	2.10
48	Coke	2.43

PRODUCT DISTRIBUTION FOR RUN I.D.: A-O-11

NO.	COMPOUND(S)	wt%
1	Methane	3.07
2	Ethylene	4.23
3	Ethane	2.11
4	Propylene	6.93
5	Propane	1.39
6	i-Butane	1.83
7	i-Butylene	3.76
8	1-Butene	.97
9	n-Butane	.50
10	t,2-Butene	1.03
11	c,2-Butene	.77
12	3-Methyl-1-butene	.19
13	i-Pentane	1.71
14	C5 olefins	1.23
15	n-Pentane	.20
16	C5 olefins, naphthenes; C6 olefins, i-para.	3.13
17	2- and 3-methylpentane, C6 isoparaffins	1.05
18	C6 olefins	.82
19	n-Hexane	.14
20	C6 olefins, naph.; C7 olef., i-para, naph.	1.76
21	Benzene	1.07
22	C6 naphthene; C7 olefins, i-para., naph.	.43
23	2- and 3-methylhexane, C7 i-paraffins	.51
24	C7 olefins, naph., i-para.; C8 i-para.	.68
25	n-Heptane	.06
26	C7 olefins, naphthenes; C8 i-paraffins	1.14
27	toluene	2.36
28	C8 isoparaffins	.44
29	2- and 3-methylheptane; C8 i-paraffins	.67
30	C7 and C8 naphthenes; C9 i-paraffins	.17
31	n-Octane	.04
32	C9 olefins; C8, C9 naph., C9 i-para.	.71
33	Ethylbenzene	.54
34	C9 naphthenes and i-paraffins	.05
35	p-Xylene and m-Xylene	2.08
36	C9 i-paraffins and naphthenes	.38
37	o-Xylene	.83
38	n-Nonane, C9 naphthenes	.51
39	C9 aromatics; C10 i-para. and naphthenes	3.03
40	n-C10; C9, C10 arom.; C10, C11 i-para., naph.	3.82
41	C12 hydrocarbons	.96
42	Light paraffins	10.77
43	Light naphthenes	4.98
44	Light aromatics	5.31
45	Heavy paraffins	9.29
46	Heavy naphthenes	7.01
47	Heavy aromatics	1.86
48	Coke	3.50

PRODUCT DISTRIBUTION FOR RUN I.D.: A-O-12

NO.	COMPOUND(S)	wt%
1	Methane	4.10
2	Ethylene	5.52
3	Ethane	3.71
4	Propylene	6.20
5	Propane	1.86
6	i-Butane	.79
7	i-Butylene	3.52
8	1-Butene	2.44
9	n-Butane	.92
10	t,2-Butene	.52
11	c,2-Butene	.41
12	3-Methyl-1-butene	.26
13	i-Pentane	.64
14	C5 olefins	1.52
15	n-Pentane	.16
16	C5 olefins, naphthenes; C6 olefins, i-para.	3.76
17	2- and 3-methylpentane, C6 isoparaffins	.42
18	C6 olefins	1.39
19	n-Hexane	.01
20	C6 olefins, naph.; C7 olef., i-para, naph.	1.66
21	Benzene	2.17
22	C6 naphthene; C7 olefins, i-para., naph.	.62
23	2- and 3-methylhexane, C7 i-paraffins	.47
24	C7 olefins, naph., i-para.; C8 i-para.	.89
25	n-Heptane	.04
26	C7 olefins, naphthenes; C8 i-paraffins	1.12
27	toluene	2.79
28	C8 isoparaffins	.56
29	2- and 3-methylheptane; C8 i-paraffins	.65
30	C7 and C8 naphthenes; C9 i-paraffins	.50
31	n-Octane	.09
32	C9 olefins; C8, C9 naph., C9 i-para.	.64
33	Ethylbenzene	.57
34	C9 naphthenes and i-paraffins	.11
35	p-Xylene and m-Xylene	1.76
36	C9 i-paraffins and naphthenes	.18
37	o-Xylene	.53
38	n-Nonane, C9 naphthenes	1.32
39	C9 aromatics; C10 i-para. and naphthenes	3.38
40	n-Decane	3.48
41	n-C10; C9, C10 arom.; C10, C11 i-para., naph.	1.72
42	Light paraffins	9.23
43	Light naphthenes	4.22
44	Light aromatics	3.94
45	Heavy paraffins	7.44
46	Heavy naphthenes	6.84
47	Heavy aromatics	1.14
48	Coke	3.80

PRODUCT DISTRIBUTION FOR RUN I.D.: A-G-1

NO.	COMPOUND(S)	wt%
1	Methane	1.40
2	Ethylene	2.12
3	Ethane	1.13
4	Propylene	3.38
5	Propane	.91
6	i-Butane	1.87
7	i-Butylene	1.77
8	1-Butene	.44
9	n-Butane	.49
10	t,2-Butene	.49
11	c,2-Butene	.35
12	3-Methyl-1-butene	.11
13	i-Pentane	2.05
14	C5 olefins	.78
15	n-Pentane	.20
16	C5 olefins, naphthenes; C6 olefins, i-para.	1.68
17	2- and 3-methylpentane, C6 isoparaffins	1.89
18	C6 olefins	.17
19	n-Hexane	.14
20	C6 olefins, naph.; C7 olef., i-para, naph.	.88
21	Benzene	.58
22	C6 naphthene; C7 olefins, i-para., naph.	.73
23	2- and 3-methylhexane, C7 i-paraffins	.44
24	C7 olefins, naph., i-para.; C8 i-para.	.67
25	n-Heptane	.03
26	C7 olefins, naphthenes; C8 i-paraffins	.65
27	toluene	1.78
28	C8 isoparaffins	.52
29	2- and 3-methylheptane; C8 i-paraffins	.65
30	C7 and C8 naphthenes; C9 i-paraffins	.30
31	n-Octane	.09
32	C9 olefins; C8, C9 naph., C9 i-para.	.22
33	Ethylbenzene	.43
34	C9 naphthenes and i-paraffins	.03
35	p-Xylene and m-Xylene	1.95
36	C9 i-paraffins and naphthenes	.30
37	o-Xylene	.75
38	n-Nonane, C9 naphthenes	.41
39	C9 aromatics; C10 i-para. and naphthenes	3.08
40	n-Decane	2.42
41	n-C10; C9, C10 arom.; C10, C11 i-para., naph.	1.00
42	Light paraffins	15.24
43	Light naphthenes	7.13
44	Light aromatics	7.30
45	Heavy paraffins	15.46
46	Heavy naphthenes	8.23
47	Heavy aromatics	4.71
48	Coke	2.26

PRODUCT DISTRIBUTION FOR RUN I.D.: A-G-2

NO.	COMPOUND(S)	wt%
1	Methane	1.85
2	Ethylene	2.62
3	Ethane	1.21
4	Propylene	4.01
5	Propane	.87
6	i-Butane	1.61
7	i-Butylene	1.98
8	1-Butene	.55
9	n-Butane	.41
10	t,2-Butene	.47
11	c,2-Butene	.35
12	3-Methyl-1-butene	.13
13	i-Pentane	2.28
14	C5 olefins	.81
15	n-Pentane	.22
16	C5 olefins, naphthenes; C6 olefins, i-para.	2.16
17	2- and 3-methylpentane, C6 isoparaffins	1.30
18	C6 olefins	.53
19	n-Hexane	.14
20	C6 olefins, naph.; C7 olef., i-para, naph.	1.29
21	Benzene	1.10
22	C6 naphthene; C7 olefins, i-para., naph.	.31
23	2- and 3-methylhexane, C7 i-paraffins	.62
24	C7 olefins, naph., i-para.; C8 i-para.	.55
25	n-Heptane	.17
26	C7 olefins, naphthenes; C8 i-paraffins	.70
27	toluene	2.66
28	C8 isoparaffins	.29
29	2- and 3-methylheptane; C8 i-paraffins	.53
30	C7 and C8 naphthenes; C9 i-paraffins	.03
31	n-Octane	.06
32	C9 olefins; C8, C9 naph., C9 i-para.	.27
33	Ethylbenzene	.49
34	C9 naphthenes and i-paraffins	.03
35	p-Xylene and m-Xylene	2.53
36	C9 i-paraffins and naphthenes	.31
37	o-Xylene	.97
38	n-Nonane, C9 naphthenes	.29
39	C9 aromatics; C10 i-para. and naphthenes	3.18
40	n-Decane	3.76
41	n-C10; C9, C10 arom.; C10, C11 i-para., naph.	.87
42	Light paraffins	13.90
43	Light naphthenes	6.81
44	Light aromatics	7.01
45	Heavy paraffins	13.37
46	Heavy naphthenes	7.59
47	Heavy aromatics	4.31
48	Coke	2.50

PRODUCT DISTRIBUTION FOR RUN I.D.: A-G-3

NO.	COMPOUND(S)	wt%
1	Methane	2.50
2	Ethylene	3.04
3	Ethane	1.49
4	Propylene	4.75
5	Propane	1.09
6	i-Butane	1.95
7	i-Butylene	2.34
8	1-Butene	.61
9	n-Butane	.53
10	t,2-Butene	.57
11	c,2-Butene	.41
12	3-Methyl-1-butene	.14
13	i-Pentane	3.10
14	C5 olefins	.92
15	n-Pentane	.30
16	C5 olefins, naphthenes; C6 olefins, i-para.	2.63
17	2- and 3-methylpentane, C6 isoparaffins	1.75
18	C6 olefins	.51
19	n-Hexane	.18
20	C6 olefins, naph.; C7 olef., i-para, naph.	1.51
21	Benzene	1.40
22	C6 naphthene; C7 olefins, i-para., naph.	.35
23	2- and 3-methylhexane, C7 i-paraffins	.81
24	C7 olefins, naph., i-para.; C8 i-para.	.52
25	n-Heptane	.19
26	C7 olefins, naphthenes; C8 i-paraffins	.74
27	toluene	3.59
28	C8 isoparaffins	.31
29	2- and 3-methylheptane; C8 i-paraffins	.58
30	C7 and C8 naphthenes; C9 i-paraffins	.04
31	n-Octane	.07
32	C9 olefins; C8, C9 naph., C9 i-para.	.30
33	Ethylbenzene	.66
34	C9 naphthenes and i-paraffins	.04
35	p-Xylene and m-Xylene	3.48
36	C9 i-paraffins and naphthenes	.45
37	o-Xylene	1.36
38	n-Nonane, C9 naphthenes	.33
39	C9 aromatics; C10 i-para. and naphthenes	3.95
40	n-Decane	3.52
41	n-C10; C9, C10 arom.; C10, C11 i-para., naph.	2.16
42	Light paraffins	12.45
43	Light naphthenes	6.57
44	Light aromatics	6.36
45	Heavy paraffins	11.47
46	Heavy naphthenes	7.36
47	Heavy aromatics	4.25
48	Coke	2.72

PRODUCT DISTRIBUTION FOR RUN I.D.: A-G-4

NO.	COMPOUND(S)	wt%
1	Methane	2.99
2	Ethylene	4.75
3	Ethane	1.07
4	Propylene	5.79
5	Propane	.15
6	i-Butane	2.02
7	i-Butylene	3.04
8	1-Butene	1.09
9	n-Butane	.44
10	t,2-Butene	.64
11	c,2-Butene	.48
12	3-Methyl-1-butene	.23
13	i-Pentane	1.93
14	C5 olefins	1.45
15	n-Pentane	.31
16	C5 olefins, naphthenes; C6 olefins, i-para.	3.46
17	2- and 3-methylpentane, C6 i-paraffins	1.22
18	C6 olefins	1.28
19	n-Hexane	.12
20	C6 olefins, naph.; C7 olef., i-para, naph.	1.70
21	Benzene	1.86
22	C6 naphthene; C7 olefins, i-para., naph.	.82
23	2- and 3-methylhexane, C7 i-paraffins	.82
24	C7 olefins, naph., i-para.; C8 i-para.	1.07
25	n-Heptane	.24
26	C7 olefins, naphthenes; C8 i-paraffins	1.03
27	toluene	2.90
28	C8 isoparaffins	.23
29	2- and 3-methylheptane; C8 i-paraffins	.61
30	C7 and C8 naphthenes; C9 i-paraffins	.52
31	n-Octane	.04
32	C9 olefins; C8, C9 naph., C9 i-para.	.55
33	Ethylbenzene	.66
34	C9 naphthenes and i-paraffins	.11
35	p-Xylene and m-Xylene	2.49
36	C9 i-paraffins and naphthenes	.66
37	o-Xylene	1.04
38	n-Nonane, C9 naphthenes	.69
39	C9 aromatics; C10 i-para. and naphthenes	4.02
40	n-C10; C9, C10 arom.; C10, C11 i-para., naph.	3.47
41	C12 hydrocarbons	2.10
42	Light paraffins	11.24
43	Light naphthenes	6.15
44	Light aromatics	5.12
45	Heavy paraffins	9.99
46	Heavy naphthenes	5.74
47	Heavy aromatics	3.46
48	Coke	3.30

PRODUCT DISTRIBUTION FOR RUN I.D.: A-G-5

NO.	COMPOUND(S)	wt%
1	Methane	2.88
2	Ethylene	3.64
3	Ethane	1.84
4	Propylene	5.34
5	Propane	1.26
6	i-Butane	1.76
7	i-Butylene	2.64
8	1-Butene	.73
9	n-Butane	.48
10	t,2-Butene	.63
11	c,2-Butene	.45
12	3-Methyl-1-butene	.13
13	i-Pentane	1.75
14	C5 olefins	.89
15	n-Pentane	.21
16	C5 olefins, naphthenes; C6 olefins, i-para.	2.20
17	2- and 3-methylpentane, C6 isoparaffins	.99
18	C6 olefins	.70
19	n-Hexane	.12
20	C6 olefins, naph.; C7 olef., i-para, naph.	1.24
21	Benzene	1.08
22	C6 naphthene; C7 olefins, i-para., naph.	.37
23	2- and 3-methylhexane, C7 i-paraffins	.45
24	C7 olefins, naph., i-para.; C8 i-para.	.53
25	n-Heptane	.03
26	C7 olefins, naphthenes; C8 i-paraffins	.87
27	toluene	2.64
28	C8 isoparaffins	.26
29	2- and 3-methylheptane; C8 i-paraffins	.67
30	C7 and C8 naphthenes; C9 i-paraffins	.04
31	n-Octane	.06
32	C9 olefins; C8, C9 naph., C9 i-para.	.37
33	Ethylbenzene	.50
34	C9 naphthenes and i-paraffins	.04
35	p-Xylene and m-Xylene	2.20
36	C9 i-paraffins and naphthenes	.33
37	o-Xylene	.88
38	n-Nonane, C9 naphthenes	.34
39	C9 aromatics; C10 i-para. and naphthenes	2.61
40	n-C10; C9, C10 arom.; C10, C11 i-para., naph.	2.54
41	C12 hydrocarbons	1.61
42	Light paraffins	14.38
43	Light naphthenes	7.82
44	Light aromatics	6.00
45	Heavy paraffins	12.19
46	Heavy naphthenes	6.61
47	Heavy aromatics	3.27
48	Coke	1.93

PRODUCT DISTRIBUTION FOR RUN I.D.: A-G-6

NO.	COMPOUND(S)	wt%
1	Methane	3.25
2	Ethylene	3.10
3	Ethane	1.69
4	Propylene	5.09
5	Propane	1.94
6	i-Butane	3.55
7	i-Butylene	2.25
8	1-Butene	.48
9	n-Butane	.98
10	t,2-Butene	.69
11	c,2-Butene	.52
12	3-Methyl-1-butene	.12
13	i-Pentane	3.56
14	C5 olefins	.78
15	n-Pentane	.41
16	C5 olefins, naphthenes; C6 olefins, i-para.	2.04
17	2- and 3-methylpentane, C6 isoparaffins	1.64
18	C6 olefins	.57
19	n-Hexane	.22
20	C6 olefins, naph.; C7 olef., i-para, naph.	1.18
21	Benzene	1.09
22	C6 naphthene; C7 olefins, i-para., naph.	.22
23	2- and 3-methylhexane, C7 i-paraffins	.60
24	C7 olefins, naph., i-para.; C8 i-para.	.46
25	n-Heptane	.03
26	C7 olefins, naphthenes; C8 i-paraffins	.64
27	toluene	4.30
28	C8 isoparaffins	.13
29	2- and 3-methylheptane; C8 i-paraffins	.47
30	C7 and C8 naphthenes; C9 i-paraffins	.02
31	n-Octane	.06
32	C9 olefins; C8, C9 naph., C9 i-para.	.19
33	Ethylbenzene	.69
34	C9 naphthenes and i-paraffins	.02
35	p-Xylene and m-Xylene	3.71
36	C9 i-paraffins and naphthenes	.22
37	o-Xylene	1.38
38	n-Nonane, C9 naphthenes	.24
39	C9 aromatics; C10 i-para. and naphthenes	3.24
40	n-C10; C9, C10 arom.; C10, C11 i-para., naph.	2.42
41	C12 hydrocarbons	1.96
42	Light paraffins	12.96
43	Light naphthenes	6.30
44	Light aromatics	5.59
45	Heavy paraffins	8.43
46	Heavy naphthenes	4.90
47	Heavy aromatics	3.09
48	Coke	2.94

PRODUCT DISTRIBUTION FOR RUN I.D.: A-G-7

NO.	COMPOUND(S)	wt%
1	Methane	3.66
2	Ethylene	4.55
3	Ethane	2.39
4	Propylene	6.43
5	Propane	1.90
6	i-Butane	2.16
7	i-Butylene	3.31
8	1-Butene	1.17
9	n-Butane	.75
10	t,2-Butene	.69
11	c,2-Butene	.50
12	3-Methyl-1-butene	.18
13	i-Pentane	2.04
14	C5 olefins	1.16
15	n-Pentane	.28
16	C5 olefins, naphthenes; C6 olefins, i-para.	2.63
17	2- and 3-methylpentane, C6 isoparaffins	1.11
18	C6 olefins	1.13
19	n-Hexane	.15
20	C6 olefins, naph.; C7 olef., i-para, naph.	1.40
21	Benzene	1.47
22	C6 naphthene; C7 olefins, i-para., naph.	.55
23	2- and 3-methylhexane, C7 i-paraffins	.57
24	C7 olefins, naph., i-para.; C8 i-para.	.82
25	n-Heptane	.22
26	C7 olefins, naphthenes; C8 i-paraffins	.84
27	toluene	3.19
28	C8 isoparaffins	.22
29	2- and 3-methylheptane; C8 i-paraffins	.89
30	C7 and C8 naphthenes; C9 i-paraffins	.04
31	n-Octane	.08
32	C9 olefins; C8, C9 naph., C9 i-para.	.41
33	Ethylbenzene	.64
34	C9 naphthenes and i-paraffins	.06
35	p-Xylene and m-Xylene	2.65
36	C9 i-paraffins and naphthenes	.50
37	o-Xylene	1.07
38	n-Nonane, C9 naphthenes	.64
39	C9 aromatics; C10 i-para. and naphthenes	3.62
40	n-C10; C9, C10 arom.; C10, C11 i-para., naph.	3.06
41	C12 hydrocarbons	2.15
42	Light paraffins	12.08
43	Light naphthenes	5.02
44	Light aromatics	4.32
45	Heavy paraffins	7.06
46	Heavy naphthenes	4.26
47	Heavy aromatics	2.86
48	Coke	3.14

PRODUCT DISTRIBUTION FOR RUN I.D.: A-G-8

NO.	COMPOUND(S)	wt%
1	Methane	4.30
2	Ethylene	5.54
3	Ethane	4.74
4	Propylene	5.17
5	Propane	2.74
6	i-Butane	.98
7	i-Butylene	3.21
8	1-Butene	2.29
9	n-Butane	.96
10	t,2-Butene	.39
11	c,2-Butene	.31
12	3-Methyl-1-butene	.27
13	i-Pentane	.79
14	C5 olefins	1.61
15	n-Pentane	.23
16	C5 olefins, naphthenes; C6 olefins, i-para.	3.60
17	2- and 3-methylpentane, C6 isoparaffins	.47
18	C6 olefins	1.55
19	n-Hexane	.05
20	C6 olefins, naph.; C7 olef., i-para, naph.	1.57
21	Benzene	2.35
22	C6 naphthene; C7 olefins, i-para., naph.	.72
23	2- and 3-methylhexane, C7 i-paraffins	.54
24	C7 olefins, naph., i-para.; C8 i-para.	1.21
25	n-Heptane	.19
26	C7 olefins, naphthenes; C8 i-paraffins	1.21
27	toluene	3.40
28	C8 isoparaffins	.35
29	2- and 3-methylheptane; C8 i-paraffins	.79
30	C7 and C8 naphthenes; C9 i-paraffins	.66
31	n-Octane	.14
32	C9 olefins; C8, C9 naph., C9 i-para.	.98
33	Ethylbenzene	.38
34	C9 naphthenes and i-paraffins	.14
35	p-Xylene and m-Xylene	2.10
36	C9 i-paraffins and naphthenes	.76
37	o-Xylene	.88
38	n-Nonane, C9 naphthenes	.89
39	C9 aromatics; C10 i-para. and naphthenes	3.56
40	n-C10; C9, C10 arom.; C10, C11 i-para., naph.	3.37
41	C12 hydrocarbons	2.16
42	Light paraffins	8.82
43	Light naphthenes	4.85
44	Light aromatics	3.89
45	Heavy paraffins	4.96
46	Heavy naphthenes	4.02
47	Heavy aromatics	2.44
48	Coke	3.50

PRODUCT DISTRIBUTION FOR RUN I.D.: A-G-9

NO.	COMPOUND(S)	wt%
1	Methane	3.83
2	Ethylene	4.17
3	Ethane	2.21
4	Propylene	5.93
5	Propane	1.83
6	i-Butane	2.41
7	i-Butylene	2.82
8	1-Butene	.77
9	n-Butane	.72
10	t,2-Butene	.67
11	c,2-Butene	.50
12	3-Methyl-1-butene	.13
13	i-Pentane	1.73
14	C5 olefins	.87
15	n-Pentane	.25
16	C5 olefins, naphthenes; C6 olefins, i-para.	2.04
17	2- and 3-methylpentane, C6 isoparaffins	.76
18	C6 olefins	.75
19	n-Hexane	.13
20	C6 olefins, naph.; C7 olef., i-para, naph.	1.09
21	Benzene	1.17
22	C6 naphthene; C7 olefins, i-para., naph.	.38
23	2- and 3-methylhexane, C7 i-paraffins	.32
24	C7 olefins, naph., i-para.; C8 i-para.	.51
25	n-Heptane	.14
26	C7 olefins, naphthenes; C8 i-paraffins	.63
27	toluene	3.22
28	C8 isoparaffins	.25
29	2- and 3-methylheptane; C8 i-paraffins	.58
30	C7 and C8 naphthenes; C9 i-paraffins	.04
31	n-Octane	.05
32	C9 olefins; C8, C9 naph., C9 i-para.	.35
33	Ethylbenzene	.53
34	C9 naphthenes and i-paraffins	.05
35	p-Xylene and m-Xylene	2.29
36	C9 i-paraffins and naphthenes	.32
37	o-Xylene	.90
38	n-Nonane, C9 naphthenes	.42
39	C9 aromatics; C10 i-para. and naphthenes	2.41
40	n-C10; C9, C10 arom.; C10, C11 i-para., naph.	2.16
41	C12 hydrocarbons	1.79
42	Light paraffins	14.08
43	Light naphthenes	7.06
44	Light aromatics	5.81
45	Heavy paraffins	10.89
46	Heavy naphthenes	5.31
47	Heavy aromatics	2.80
48	Coke	1.92

PRODUCT DISTRIBUTION FOR RUN I.D.: A-G-10

NO.	COMPOUND(S)	wt%
1	Methane	4.36
2	Ethylene	5.08
3	Ethane	2.64
4	Propylene	7.28
5	Propane	1.92
6	i-Butane	2.31
7	i-Butylene	3.60
8	1-Butene	.97
9	n-Butane	.78
10	t,2-Butene	.81
11	c,2-Butene	.59
12	3-Methyl-1-butene	.15
13	i-Pentane	1.95
14	C5 olefins	.93
15	n-Pentane	.28
16	C5 olefins, naphthenes; C6 olefins, i-para.	2.41
17	2- and 3-methylpentane, C6 isoparaffins	1.04
18	C6 olefins	.67
19	n-Hexane	.15
20	C6 olefins, naph.; C7 olef., i-para, naph.	1.25
21	Benzene	1.54
22	C6 naphthene; C7 olefins, i-para., naph.	.35
23	2- and 3-methylhexane, C7 i-paraffins	.46
24	C7 olefins, naph., i-para.; C8 i-para.	.48
25	n-Heptane	.15
26	C7 olefins, naphthenes; C8 i-paraffins	.62
27	toluene	3.43
[illegible]	C8 isoparaffins	.16
29	2- and 3-methylheptane; C8 i-paraffins	.28
30	C7 and C8 naphthenes; C9 i-paraffins	.28
31	n-Octane	.05
32	C9 olefins; C8, C9 naph., C9 i-para.	.28
33	Ethylbenzene	.54
34	C9 naphthenes and i-paraffins	.04
35	p-Xylene and m-Xylene	2.57
36	C9 i-paraffins and naphthenes	.39
37	o-Xylene	1.02
38	n-Nonane, C9 naphthenes	.31
39	C9 aromatics; C10 i-para. and naphthenes	2.85
40	n-C10; C9, C10 arom.; C10, C11 i-para., naph.	2.64
41	C12 hydrocarbons	1.95
42	Light paraffins	12.66
43	Light naphthenes	6.26
44	Light aromatics	4.79
45	Heavy paraffins	.54
46	Heavy naphthenes	4.18
47	Heavy aromatics	2.44
48	Coke	2.58

PRODUCT DISTRIBUTION FOR RUN I.D.: A-G-11

NO.	COMPOUND(S)	wt%
1	Methane	5.84
2	Ethylene	6.03
3	Ethane	3.20
4	Propylene	8.19
5	Propane	2.23
6	i-Butane	2.32
7	i-Butylene	3.95
8	1-Butene	1.19
9	n-Butane	.82
10	t,2-Butene	.85
11	c,2-Butene	.63
12	3-Methyl-1-butene	.12
13	i-Pentane	1.61
14	C5 olefins	.80
15	n-Pentane	.24
16	C5 olefins, naphthenes; C6 olefins, i-para.	2.33
17	2- and 3-methylpentane, C6 isoparaffins	.77
18	C6 olefins	.61
19	n-Hexane	.13
20	C6 olefins, naph.; C7 olef., i-para, naph.	1.12
21	Benzene	1.74
22	C6 naphthene; C7 olefins, i-para., naph.	.25
23	2- and 3-methylhexane, C7 i-paraffins	.32
24	C7 olefins, naph., i-para.; C8 i-para.	.42
25	n-Heptane	.14
26	C7 olefins, naphthenes; C8 i-paraffins	.51
27	toluene	3.76
28	C8 isoparaffins	.12
29	2- and 3-methylheptane; C8 i-paraffins	.45
30	C7 and C8 naphthenes; C9 i-paraffins	.02
31	n-Octane	.04
32	C9 olefins; C8, C9 naph., C9 i-para.	.31
33	Ethylbenzene	.53
34	C9 naphthenes and i-paraffins	.03
35	p-Xylene and m-Xylene	2.58
36	C9 i-paraffins and naphthenes	.32
37	o-Xylene	1.00
38	n-Nonane, C9 naphthenes	.25
39	C9 aromatics; C10 i-para. and naphthenes	2.59
40	n-C10; C9, C10 arom.; C10, C11 i-para., naph.	2.60
41	C12 hydrocarbons	1.97
42	Light paraffins	11.89
43	Light naphthenes	5.25
44	Light aromatics	4.99
45	Heavy paraffins	5.51
46	Heavy naphthenes	3.44
47	Heavy aromatics	1.37
48	Coke	4.61

PRODUCT DISTRIBUTION FOR RUN I.D.: A-G-12

NO.	COMPOUND(S)	wt%
1	Methane	5.88
2	Ethylene	6.87
3	Ethane	3.00
4	Propylene	7.78
5	Propane	4.63
6	i-Butane	1.75
7	i-Butylene	4.08
8	1-Butene	2.79
9	n-Butane	1.26
10	t,2-Butene	.56
11	c,2-Butene	.45
12	3-Methyl-1-butene	.21
13	i-Pentane	.92
14	C5 olefins	1.28
15	n-Pentane	.22
16	C5 olefins, naphthenes; C6 olefins, i-para.	3.15
17	2- and 3-methylpentane, C6 isoparaffins	.50
18	C6 olefins	1.22
19	n-Hexane	.01
20	C6 olefins, naph.; C7 olef., i-para, naph.	1.31
21	Benzene	2.01
22	C6 naphthene; C7 olefins, i-para., naph.	.53
23	2- and 3-methylhexane, C7 i-paraffins	.45
24	C7 olefins, naph., i-para.; C8 i-para.	.92
25	n-Heptane	.15
26	C7 olefins, naphthenes; C8 i-paraffins	.91
27	toluene	3.33
28	C8 isoparaffins	.48
29	2- and 3-methylheptane; C8 i-paraffins	.57
30	C7 and C8 naphthenes; C9 i-paraffins	.45
31	n-Octane	.06
32	C9 olefins; C8, C9 naph., C9 i-para.	.45
33	Ethylbenzene	.57
34	C9 naphthenes and i-paraffins	.09
35	p-Xylene and m-Xylene	1.97
36	C9 i-paraffins and naphthenes	.55
37	o-Xylene	.82
38	n-Nonane, C9 naphthenes	.56
39	C9 aromatics; C10 i-para. and naphthenes	2.69
40	n-Decane	2.53
41	n-C10; C9, C10 arom.; C10, C11 i-para., naph.	1.91
42	Light paraffins	8.26
43	Light naphthenes	4.52
44	Light aromatics	3.43
45	Heavy paraffins	4.48
46	Heavy naphthenes	3.28
47	Heavy aromatics	1.25
48	Coke	4.92

PRODUCT DISTRIBUTION FOR RUN I.D.: B-O-1

NO.	COMPOUND(S)	wt%
1	Methane	1.32
2	Ethylene	1.72
3	Ethane	1.09
4	Propylene	1.86
5	Propane	.49
6	i-Butane	.25
7	i-Butylene	.97
8	1-Butene	.51
9	n-Butane	.16
10	t,2-Butene	.16
11	c,2-Butene	.13
12	3-Methyl-1-butene	.09
13	i-Pentane	.40
14	C5 olefins	.54
15	n-Pentane	.05
16	C5 olefins, naphthenes; C6 olefins, i-para.	1.47
17	2- and 3-methylpentane, C6 isoparaffins	.26
18	C6 olefins	.41
19	n-Hexane	.02
20	C6 olefins, naph.; C7 olef., i-para, naph.	.69
21	Benzene	1.11
22	C6 naphthene; C7 olefins, i-para., naph.	.23
23	2- and 3-methylhexane, C7 i-paraffins	.22
24	C7 olefins, naph., i-para.; C8 i-para.	.39
25	n-Heptane	.07
26	C7 olefins, naphthenes; C8 i-paraffins	.44
27	toluene	1.44
28	C8 isoparaffins	.08
29	2- and 3-methylheptane; C8 i-paraffins	.38
30	C7 and C8 naphthenes; C9 i-paraffins	0.00
31	n-Octane	.04
32	C9 olefins; C8, C9 naph., C9 i-para.	.33
33	Ethylbenzene	.27
34	C9 naphthenes and i-paraffins	.04
35	p-Xylene and m-Xylene	.98
36	C9 i-paraffins and naphthenes	.03
37	o-Xylene	.26
38	n-Nonane, C9 naphthenes	.63
39	C9 aromatics; C10 i-para. and naphthenes	1.69
40	n-Decane	2.10
41	n-C10; C9, C10 arom.; C10, C11 i-para., naph.	.96
42	Light paraffins	3.36
43	Light naphthenes	12.98
44	Light aromatics	16.63
45	Heavy paraffins	1.89
46	Heavy naphthenes	13.65
47	Heavy aromatics	25.74
48	Coke	1.47

PRODUCT DISTRIBUTION FOR RUN I.D.: B-O-2

NO.	COMPOUND(S)	wt%
1	Methane	2.06
2	Ethylene	2.45
3	Ethane	.52
4	Propylene	3.19
5	Propane	0.00
6	i-Butane	.62
7	i-Butylene	1.54
8	1-Butene	.50
9	n-Butane	.11
10	t,2-Butene	.32
11	c,2-Butene	.24
12	3-Methyl-1-butene	.07
13	i-Pentane	.82
14	C5 olefins	.46
15	n-Pentane	.07
16	C5 olefins, naphthenes; C6 olefins, i-para.	1.66
17	2- and 3-methylpentane, C6 isoparaffins	.47
18	C6 olefins	.32
19	n-Hexane	.04
20	C6 olefins, naph.; C7 olef., i-para, naph.	.76
21	Benzene	1.64
22	C6 naphthene; C7 olefins, i-para., naph.	.27
23	2- and 3-methylhexane, C7 i-paraffins	.26
24	C7 olefins, naph., i-para.; C8 i-para.	.32
25	n-Heptane	.07
26	C7 olefins, naphthenes; C8 i-paraffins	.41
27	toluene	2.37
28	C8 isoparaffins	.07
29	2- and 3-methylheptane; C8 i-paraffins	.16
30	C7 and C8 naphthenes; C9 i-paraffins	.14
31	n-Octane	.02
32	C9 olefins; C8, C9 naph., C9 i-para.	.14
33	Ethylbenzene	.37
34	C9 naphthenes and i-paraffins	0.00
35	p-Xylene and m-Xylene	1.71
36	C9 i-paraffins and naphthenes	.41
37	o-Xylene	.70
38	n-Nonane, C9 naphthenes	.16
39	C9 aromatics; C10 i-para. and naphthenes	2.40
40	n-Decane	2.68
41	n-C10; C9, C10 arom.; C10, C11 i-para., naph.	1.45
42	Light paraffins	2.98
43	Light naphthenes	13.36
44	Light aromatics	15.29
45	Heavy paraffins	2.04
46	Heavy naphthenes	10.52
47	Heavy aromatics	21.70
48	Coke	2.13

PRODUCT DISTRIBUTION FOR RUN I.D.: B-O-3

NO.	COMPOUND(S)	wt%
1	Methane	2.59
2	Ethylene	2.99
3	Ethane	.72
4	Propylene	4.07
5	Propane	0.00
6	i-Butane	.89
7	i-Butylene	2.02
8	1-Butene	.71
9	n-Butane	.17
10	t,2-Butene	.45
11	c,2-Butene	.35
12	3-Methyl-1-butene	.11
13	i-Pentane	1.27
14	C5 olefins	.63
15	n-Pentane	.10
16	C5 olefins, naphthenes; C6 olefins, i-para.	2.22
17	2- and 3-methylpentane, C6 isoparaffins	.80
18	C6 olefins	.35
19	n-Hexane	.07
20	C6 olefins, naph.; C7 olef., i-para, naph.	1.21
21	Benzene	1.62
22	C6 naphthene; C7 olefins, i-para., naph.	.13
23	2- and 3-methylhexane, C7 i-paraffins	.36
24	C7 olefins, naph., i-para.; C8 i-para.	.57
25	n-Heptane	.11
26	C7 olefins, naphthenes; C8 i-paraffins	.58
27	toluene	2.43
28	C8 isoparaffins	.11
29	2- and 3-methylheptane; C8 i-paraffins	.25
30	C7 and C8 naphthenes; C9 i-paraffins	.19
31	n-Octane	.04
32	C9 olefins; C8, C9 naph., C9 i-para.	.13
33	Ethylbenzene	.45
34	C9 naphthenes and i-paraffins	0.00
35	p-Xylene and m-Xylene	1.91
36	C9 i-paraffins and naphthenes	.09
37	o-Xylene	.31
38	n-Nonane, C9 naphthenes	.91
39	C9 aromatics; C10 i-para. and naphthenes	2.91
40	n-Decane	3.44
41	n-C10; C9, C10 arom.; C10, C11 i-para., naph.	1.66
42	Light paraffins	3.16
43	Light naphthenes	13.04
44	Light aromatics	13.14
45	Heavy paraffins	1.95
46	Heavy naphthenes	8.84
47	Heavy aromatics	17.73
48	Coke	2.24

PRODUCT DISTRIBUTION FOR RUN I.D.: B-O-4

NO.	COMPOUND(S)	wt%
1	Methane	4.01
2	Ethylene	4.15
3	Ethane	1.08
4	Propylene	5.55
5	Propane	0.00
6	i-Butane	1.14
7	i-Butylene	2.60
8	1-Butene	.86
9	n-Butane	.21
10	t,2-Butene	.52
11	c,2-Butene	.39
12	3-Methyl-1-butene	.06
13	i-Pentane	1.36
14	C5 olefins	.44
15	n-Pentane	.10
16	C5 olefins, naphthenes; C6 olefins, i-para.	2.15
17	2- and 3-methylpentane, C6 isoparaffins	.74
18	C6 olefins	.21
19	n-Hexane	.05
20	C6 olefins, naph.; C7 olef., i-para, naph.	.98
21	Benzene	2.30
22	C6 naphthene; C7 olefins, i-para., naph.	.10
23	2- and 3-methylhexane, C7 i-paraffins	.35
24	C7 olefins, naph., i-para.; C8 i-para.	.31
25	n-Heptane	.07
26	C7 olefins, naphthenes; C8 i-paraffins	.40
27	toluene	3.45
28	C8 isoparaffins	.08
29	2- and 3-methylheptane; C8 i-paraffins	.18
30	C7 and C8 naphthenes; C9 i-paraffins	.15
31	n-Octane	.02
32	C9 olefins; C8, C9 naph., C9 i-para.	.07
33	Ethylbenzene	.45
34	C9 naphthenes and i-paraffins	0.00
35	p-Xylene and m-Xylene	2.64
36	C9 i-paraffins and naphthenes	.45
37	o-Xylene	1.02
38	n-Nonane, C9 naphthenes	.18
39	C9 aromatics; C10 i-para. and naphthenes	3.34
40	n-Decane	3.53
41	n-C10; C9, C10 arom.; C10, C11 i-para., naph.	1.69
42	Light paraffins	2.55
43	Light naphthenes	12.53
44	Light aromatics	12.82
45	Heavy paraffins	1.24
46	Heavy naphthenes	7.54
47	Heavy aromatics	13.15
48	Coke	2.80

PRODUCT DISTRIBUTION FOR RUN I.D.: B-O-5

NO.	COMPOUND(S)	wt%
1	Methane	2.41
2	Ethylene	2.77
3	Ethane	.54
4	Propylene	3.24
5	Propane	.01
6	i-Butane	.40
7	i-Butylene	1.59
8	1-Butene	.55
9	n-Butane	.02
10	t,2-Butene	.31
11	c,2-Butene	.24
12	3-Methyl-1-butene	.12
13	i-Pentane	.40
14	C5 olefins	.70
15	n-Pentane	.07
16	C5 olefins, naphthenes; C6 olefins, i-para.	1.89
17	2- and 3-methylpentane, C6 isoparaffins	.17
18	C6 olefins	.65
19	n-Hexane	.03
20	C6 olefins, naph.; C7 olef., i-para, naph.	.84
21	Benzene	1.77
22	C6 naphthene; C7 olefins, i-para., naph.	.33
23	2- and 3-methylhexane, C7 i-paraffins	.29
24	C7 olefins, naph., i-para.; C8 i-para.	.50
25	n-Heptane	.09
26	C7 olefins, naphthenes; C8 i-paraffins	.53
27	toluene	2.24
28	C8 isoparaffins	.10
29	2- and 3-methylheptane; C8 i-paraffins	.28
30	C7 and C8 naphthenes; C9 i-paraffins	.23
31	n-Octane	.05
32	C9 olefins; C8, C9 naph , C9 i-para.	.32
33	Ethylbenzene	.36
34	C9 naphthenes and i-paraffins	.06
35	p-Xylene and m-Xylene	1.43
36	C9 i-paraffins and naphthenes	.42
37	o-Xylene	.61
38	n-Nonane, C9 naphthenes	.28
39	C9 aromatics; C10 i-para. and naphthenes	2.08
40	n-Decane	2.45
41	n-C10; C9, C10 arom.; C10, C11 i-para., naph.	1.39
42	Light paraffins	2.97
43	Light naphthenes	12.25
44	Light aromatics	15.81
45	Heavy paraffins	1.51
46	Heavy naphthenes	11.61
47	Heavy aromatics	21.42
48	Coke	1.65

PRODUCT DISTRIBUTION FOR RUN I.D.: B-O-6

NO.	COMPOUND(S)	wt%
1	Methane	4.32
2	Ethylene	4.07
3	Ethane	0.00
4	Propylene	3.93
5	Propane	0.00
6	i-Butane	.36
7	i-Butylene	1.75
8	1-Butene	.60
9	n-Butane	.02
10	t,2-Butene	.26
11	c,2-Butene	.20
12	3-Methyl-1-butene	.11
13	i-Pentane	.31
14	C5 olefins	.66
15	n-Pentane	.07
16	C5 olefins, naphthenes; C6 olefins, i-para.	1.87
17	2- and 3-methylpentane, C6 isoparaffins	.18
18	C6 olefins	.60
19	n-Hexane	.04
20	C6 olefins, naph.; C7 olef., i-para, naph.	.85
21	Benzene	3.04
22	C6 naphthene; C7 olefins, i-para., naph.	.40
23	2- and 3-methylhexane, C7 i-paraffins	.28
24	C7 olefins, naph., i-para.; C8 i-para.	.49
25	n-Heptane	.07
26	C7 olefins, naphthenes; C8 i-paraffins	.51
27	toluene	3.19
28	C8 isoparaffins	.09
29	2- and 3-methylheptane; C8 i-paraffins	.28
30	C7 and C8 naphthenes; C9 i-paraffins	.23
31	n-Octane	.05
32	C9 olefins; C8, C9 naph., C9 i-para.	.31
33	Ethylbenzene	.36
34	C9 naphthenes and i-paraffins	.06
35	p-Xylene and m-Xylene	1.88
36	C9 i-paraffins and naphthenes	.64
37	o-Xylene	.76
38	n-Nonane, C9 naphthenes	.29
39	C9 aromatics; C10 i-para. and naphthenes	2.44
40	n-Decane	2.67
41	n-C10; C9, C10 arom.; C10, C11 i-para., naph.	1.79
42	Light paraffins	2.87
43	Light naphthenes	10.78
44	Light aromatics	14.11
45	Heavy paraffins	1.96
46	Heavy naphthenes	10.34
47	Heavy aromatics	18.02
48	Coke	1.90

PRODUCT DISTRIBUTION FOR RUN I.D.: B-O-7

NO.	COMPOUND(S)	wt%
1	Methane	3.74
2	Ethylene	4.10
3	Ethane	.57
4	Propylene	5.18
5	Propane	.02
6	i-Butane	.99
7	i-Butylene	2.64
8	1-Butene	.87
9	n-Butane	.10
10	t,2-Butene	.54
11	c,2-Butene	.41
12	3-Methyl-1-butene	.16
13	i-Pentane	.87
14	C5 olefins	.99
15	n-Pentane	.12
16	C5 olefins, naphthenes; C6 olefins, i-para.	2.66
17	2- and 3-methylpentane, C6 isoparaffins	.53
18	C6 olefins	.73
19	n-Hexane	.04
20	C6 olefins, naph.; C7 olef., i-para, naph.	1.31
21	Benzene	1.99
22	C6 naphthene; C7 olefins, i-para., naph.	.46
23	2- and 3-methylhexane, C7 i-paraffins	.41
24	C7 olefins, naph., i-para.; C8 i-para.	.72
25	n-Heptane	.03
26	C7 olefins, naphthenes; C8 i-paraffins	.84
27	toluene	2.89
28	C8 isoparaffins	.14
29	2- and 3-methylheptane; C8 i-paraffins	.36
30	C7 and C8 naphthenes; C9 i-paraffins	.28
31	n-Octane	.03
32	C9 olefins; C8, C9 naph., C9 i-para.	.32
33	Ethylbenzene	.50
34	C9 naphthenes and i-paraffins	0.00
35	p-Xylene and m-Xylene	2.14
36	C9 i-paraffins and naphthenes	.43
37	o-Xylene	.84
38	n-Nonane, C9 naphthenes	.30
39	C9 aromatics; C10 i-para. and naphthenes	3.20
40	n-Decane	3.50
41	n-C10; C9, C10 arom.; C10, C11 i-para., naph.	1.83
42	Light paraffins	2.38
43	Light naphthenes	9.10
44	Light aromatics	12.91
45	Heavy paraffins	1.99
46	Heavy naphthenes	8.22
47	Heavy aromatics	15.51
48	Coke	2.09

PRODUCT DISTRIBUTION FOR RUN I.D.: B-O-8

NO.	COMPOUND(S)	wt%
1	Methane	6.00
2	Ethylene	5.29
3	Ethane	.96
4	Propylene	6.19
5	Propane	0.00
6	i-Butane	1.04
7	i-Butylene	2.84
8	1-Butene	.93
9	n-Butane	.18
10	t,2-Butene	.51
11	c,2-Butene	.39
12	3-Methyl-1-butene	.11
13	i-Pentane	.97
14	C5 olefins	.64
15	n-Pentane	.11
16	C5 olefins, naphthenes; C6 olefins, i-para.	1.81
17	2- and 3-methylpentane, C6 isoparaffins	.49
18	C6 olefins	.55
19	n-Hexane	.05
20	C6 olefins, naph.; C7 olef., i-para, naph.	.86
21	Benzene	3.43
22	C6 naphthene; C7 olefins, i-para., naph.	.10
23	2- and 3-methylhexane, C7 i-paraffins	.33
24	C7 olefins, naph., i-para.; C8 i-para.	.58
25	n-Heptane	.09
26	C7 olefins, naphthenes; C8 i-paraffins	.49
27	toluene	4.46
28	C8 isoparaffins	.07
29	2- and 3-methylheptane; C8 i-paraffins	.25
30	C7 and C8 naphthenes; C9 i-paraffins	.24
31	n-Octane	.05
32	C9 olefins; C8, C9 naph., C9 i-para.	.19
33	Ethylbenzene	.49
34	C9 naphthenes and i-paraffins	0.00
35	p-Xylene and m-Xylene	2.85
36	C9 i-paraffins and naphthenes	.58
37	o-Xylene	1.14
38	n-Nonane, C9 naphthenes	.23
39	C9 aromatics; C10 i-para. and naphthenes	3.50
40	n-Decane	3.01
41	n-C10; C9, C10 arom.; C10, C11 i-para., naph.	2.17
42	Light paraffins	2.17
43	Light naphthenes	8.96
44	Light aromatics	12.41
45	Heavy paraffins	.72
46	Heavy naphthenes	6.77
47	Heavy aromatics	12.78
48	Coke	2.03

PRODUCT DISTRIBUTION FOR RUN I.D.: B-O-9

NO.	COMPOUND(S)	wt%
1	Methane	3.76
2	Ethylene	3.74
3	Ethane	.52
4	Propylene	3.83
5	Propane	0.00
6	i-Butane	.43
7	i-Butylene	1.85
8	1-Butene	.70
9	n-Butane	0.00
10	t,2-Butene	.34
11	c,2-Butene	.27
12	3-Methyl-1-butene	.16
13	i-Pentane	.30
14	C5 olefins	.94
15	n-Pentane	.08
16	C5 olefins, naphthenes; C6 olefins, i-para.	2.17
17	2- and 3-methylpentane, C6 isoparaffins	.18
18	C6 olefins	.81
19	n-Hexane	.06
20	C6 olefins, naph.; C7 olef., i-para, naph.	1.09
21	Benzene	2.24
22	C6 naphthene; C7 olefins, i-para., naph.	.42
23	2- and 3-methylhexane, C7 i-paraffins	.31
24	C7 olefins, naph., i-para.; C8 i-para.	.49
25	n-Heptane	.03
26	C7 olefins, naphthenes; C8 i-paraffins	.74
27	toluene	2.78
28	C8 isoparaffins	.12
29	2- and 3-methylheptane; C8 i-paraffins	.35
30	C7 and C8 naphthenes; C9 i-paraffins	.30
31	n-Octane	.07
32	C9 olefins; C8, C9 naph., C9 i-para.	.42
33	Ethylbenzene	.45
34	C9 naphthenes and i-paraffins	.08
35	p-Xylene and m-Xylene	1.62
36	C9 i-paraffins and naphthenes	.56
37	o-Xylene	.70
38	n-Nonane, C9 naphthenes	.37
39	C9 aromatics; C10 i-para. and naphthenes	2.49
40	n-Decane	2.67
41	n-C10; C9, C10 arom.; C10, C11 i-para., naph.	1.68
42	Light paraffins	2.55
43	Light naphthenes	11.10
44	Light aromatics	14.60
45	Heavy paraffins	1.17
46	Heavy naphthenes	10.40
47	Heavy aromatics	18.31
48	Coke	1.76

PRODUCT DISTRIBUTION FOR RUN I.D.: B-O-10

NO.	COMPOUND(S)	wt%
1	Methane	4.33
2	Ethylene	4.81
3	Ethane	1.60
4	Propylene	5.99
5	Propane	.07
6	i-Butane	1.00
7	i-Butylene	2.48
8	1-Butene	.93
9	n-Butane	.17
10	t,2-Butene	.58
11	c,2-Butene	.48
12	3-Methyl-1-butene	.14
13	i-Pentane	.77
14	C5 olefins	.86
15	n-Pentane	.11
16	C5 olefins, naphthenes; C6 olefins, i-para.	2.48
17	2- and 3-methylpentane, C6 isoparaffins	.42
18	C6 olefins	.63
19	n-Hexane	.05
20	C6 olefins, naph.; C7 olef., i-para, naph.	1.14
21	Benzene	2.04
22	C6 naphthene; C7 olefins, i-para., naph.	.36
23	2- and 3-methylhexane, C7 i-paraffins	.35
24	C7 olefins, naph., i-para.; C8 i-para.	.59
25	n-Heptane	.12
26	C7 olefins, naphthenes; C8 i-paraffins	.66
27	toluene	3.02
28	C8 isoparaffins	.11
29	2- and 3-methylheptane; C8 i-paraffins	.30
30	C7 and C8 naphthenes; C9 i-paraffins	.24
31	n-Octane	.03
32	C9 olefins; C8, C9 naph., C9 i-para.	.29
33	Ethylbenzene	.51
34	C9 naphthenes and i-paraffins	0.00
35	p-Xylene and m-Xylene	2.07
36	C9 i-paraffins and naphthenes	.50
37	o-Xylene	.89
38	n-Nonane, C9 naphthenes	.30
39	C9 aromatics; C10 i-para. and naphthenes	2.93
40	n-Decane	3.41
41	n-C10; C9, C10 arom.; C10, C11 i-para., naph.	1.79
42	Light paraffins	3.15
43	Light naphthenes	9.41
44	Light aromatics	12.92
45	Heavy paraffins	1.59
46	Heavy naphthenes	7.26
47	Heavy aromatics	13.74
48	Coke	2.42

PRODUCT DISTRIBUTION FOR RUN I.D.: B-O-11

NO.	COMPOUND(S)	wt%
1	Methane	5.02
2	Ethylene	5.27
3	Ethane	3.33
4	Propylene	5.23
5	Propane	1.45
6	i-Butane	.71
7	i-Butylene	2.60
8	1-Butene	1.35
9	n-Butane	.45
10	t,2-Butene	.37
11	c,2-Butene	.29
12	3-Methyl-1-butene	.14
13	i-Pentane	.54
14	C5 olefins	.76
15	n-Pentane	.10
16	C5 olefins, naphthenes; C6 olefins, i-para.	2.19
17	2- and 3-methylpentane, C6 isoparaffins	.27
18	C6 olefins	.68
19	n-Hexane	.03
20	C6 olefins, naph.; C7 olef., i-para, naph.	1.01
21	Benzene	2.69
22	C6 naphthene; C7 olefins, i-para., naph.	.46
23	2- and 3-methylhexane, C7 i-paraffins	.32
24	C7 olefins, naph., i-para.; C8 i-para.	.50
25	n-Heptane	.08
26	C7 olefins, naphthenes; C8 i-paraffins	.59
27	toluene	3.57
28	C8 isoparaffins	.09
29	2- and 3-methylheptane; C8 i-paraffins	.60
30	C7 and C8 naphthenes; C9 i-paraffins	.10
31	n-Octane	.02
32	C9 olefins; C8, C9 naph., C9 i-para.	.36
33	Ethylbenzene	.46
34	C9 naphthenes and i-paraffins	0.00
35	p-Xylene and m-Xylene	2.35
36	C9 i-paraffins and naphthenes	.54
37	o-Xylene	.90
38	n-Nonane, C9 naphthenes	.25
39	C9 aromatics; C10 i-para. and naphthenes	2.87
40	n-Decane	3.18
41	n-C10; C9, C10 arom.; C10, C11 i-para., naph.	1.98
42	Light paraffins	2.97
43	Light naphthenes	8.47
44	Light aromatics	12.67
45	Heavy paraffins	1.49
46	Heavy naphthenes	5.75
47	Heavy aromatics	11.70
48	Coke	3.25

PRODUCT DISTRIBUTION FOR RUN I.D.: B-O-12

NO.	COMPOUND(S)	wt%
1	Methane	3.50
2	Ethylene	5.79
3	Ethane	4.10
4	Propylene	6.29
5	Propane	1.95
6	i-Butane	.65
7	i-Butylene	3.36
8	1-Butene	2.00
9	n-Butane	.55
10	t,2-Butene	.56
11	c,2-Butene	.44
12	3-Methyl-1-butene	.18
13	i-Pentane	.48
14	C5 olefins	1.11
15	n-Pentane	.08
16	C5 olefins, naphthenes; C6 olefins, i-para.	2.66
17	2- and 3-methylpentane, C6 isoparaffins	.31
18	C6 olefins	.91
19	n-Hexane	.02
20	C6 olefins, naph.; C7 olef., i-para, naph.	1.37
21	Benzene	2.04
22	C6 naphthene; C7 olefins, i-para., naph.	.42
23	2- and 3-methylhexane, C7 i-paraffins	.34
24	C7 olefins, naph., i-para.; C8 i-para.	.61
25	n-Heptane	.04
26	C7 olefins, naphthenes; C8 i-paraffins	.88
27	toluene	2.73
28	C8 isoparaffins	.38
29	2- and 3-methylheptane; C8 i-paraffins	.46
30	C7 and C8 naphthenes; C9 i-paraffins	.32
31	n-Octane	.06
32	C9 olefins; C8, C9 naph., C9 i-para.	.43
33	Ethylbenzene	.53
34	C9 naphthenes and i-paraffins	.07
35	p-Xylene and m-Xylene	1.62
36	C9 i-paraffins and naphthenes	.69
37	o-Xylene	.72
38	n-Nonane, C9 naphthenes	.40
39	C9 aromatics; C10 i-para. and naphthenes	2.77
40	n-Decane	3.43
41	n-C10; C9, C10 arom.; C10, C11 i-para., naph.	2.40
42	Light paraffins	2.49
43	Light naphthenes	7.90
44	Light aromatics	11.99
45	Heavy paraffins	.91
46	Heavy naphthenes	5.39
47	Heavy aromatics	9.90
48	Coke	3.81

PRODUCT DISTRIBUTION FOR RUN I.D.: B-G-1

NO.	COMPOUND(S)	wt%
1	Methane	1.65
2	Ethylene	1.86
3	Ethane	1.21
4	Propylene	2.68
5	Propane	.62
6	i-Butane	.59
7	i-Butylene	1.37
8	1-Butene	.29
9	n-Butane	.16
10	t,2-Butene	.34
11	c,2-Butene	.25
12	3-Methyl-1-butene	.09
13	i-Pentane	.81
14	C5 olefins	.52
15	n-Pentane	.08
16	C5 olefins, naphthenes; C6 olefins, i-para.	1.50
17	2- and 3-methylpentane, C6 isoparaffins	.50
18	C6 olefins	.28
19	n-Hexane	.05
20	C6 olefins, naph.; C7 olef., i-para, naph.	.93
21	Benzene	.97
22	C6 naphthene; C7 olefins, i-para., naph.	.41
23	2- and 3-methylhexane, C7 i-paraffins	.39
24	C7 olefins, naph., i-para.; C8 i-para.	.17
25	n-Heptane	.03
26	C7 olefins, naphthenes; C8 i-paraffins	.46
27	toluene	1.71
28	C8 isoparaffins	.30
29	2- and 3-methylheptane; C8 i-paraffins	.28
30	C7 and C8 naphthenes; C9 i-paraffins	.19
31	n-Octane	.15
32	C9 olefins; C8, C9 naph., C9 i-para.	.06
33	Ethylbenzene	.33
34	C9 naphthenes and i-paraffins	0.00
35	p-Xylene and m-Xylene	1.26
36	C9 i-paraffins and naphthenes	.22
37	o-Xylene	.53
38	n-Nonane, C9 naphthenes	.12
39	C9 aromatics; C10 i-para. and naphthenes	2.11
40	n-Decane	1.54
41	n-C10; C9, C10 ar m.; C10, C11 i-para., naph.	.88
42	Light paraffins	3.16
43	Light naphthenes	13.91
44	Light aromatics	15.13
45	Heavy paraffins	2.07
46	Heavy naphthenes	14.06
47	Heavy aromatics	21.64
48	Coke	2.15

PRODUCT DISTRIBUTION FOR RUN I.D.: B-G-2

NO.	COMPOUND(S)	wt%
1	Methane	1.84
2	Ethylene	2.07
3	Ethane	1.47
4	Propylene	3.04
5	Propane	.93
6	i-Butane	.97
7	i-Butylene	1.60
8	1-Butene	.37
9	n-Butane	.29
10	t,2-Butene	.39
11	c,2-Butene	.29
12	3-Methyl-1-butene	.09
13	i-Pentane	1.28
14	C5 olefins	.56
15	n-Pentane	.13
16	C5 olefins, naphthenes; C6 olefins, i-para.	1.60
17	2- and 3-methylpentane, C6 isoparaffins	.79
18	C6 olefins	.33
19	n-Hexane	.08
20	C6 olefins, naph.; C7 olef., i-para, naph.	1.05
21	Benzene	1.01
22	C6 naphthene; C7 olefins, i-para., naph.	.52
23	2- and 3-methylhexane, C7 i-paraffins	.54
24	C7 olefins, naph., i-para.; C8 i-para.	.20
25	n-Heptane	.04
26	C7 olefins, naphthenes; C8 i-paraffins	.57
27	toluene	1.99
28	C8 isoparaffins	.37
29	2- and 3-methylheptane; C8 i-paraffins	.36
30	C7 and C8 naphthenes; C9 i-paraffins	.28
31	n-Octane	.06
32	C9 olefins; C8, C9 naph., C9 i-para.	.09
33	Ethylbenzene	.41
34	C9 naphthenes and i-paraffins	0.00
35	p-Xylene and m-Xylene	1.65
36	C9 i-paraffins and naphthenes	.30
37	o-Xylene	.68
38	n-Nonane, C9 naphthenes	.17
39	C9 aromatics; C10 i-para. and naphthenes	2.80
40	n-Decane	2.01
41	n-C10; C9, C10 arom.; C10, C11 i-para., naph.	1.23
42	Light paraffins	3.24
43	Light naphthenes	12.20
44	Light aromatics	13.89
45	Heavy paraffins	1.80
46	Heavy naphthenes	12.11
47	Heavy aromatics	18.75
48	Coke	3.58

PRODUCT DISTRIBUTION FOR RUN I.D.: B-G-3

NO.	COMPOUND(S)	wt%
1	Methane	2.01
2	Ethylene	2.44
3	Ethane	1.57
4	Propylene	3.73
5	Propane	1.24
6	i-Butane	1.91
7	i-Butylene	1.87
8	1-Butene	.42
9	n-Butane	.58
10	t,2-Butene	.51
11	c,2-Butene	.38
12	3-Methyl-1-butene	.09
13	i-Pentane	1.92
14	C5 olefins	.54
15	n-Pentane	.18
16	C5 olefins, naphthenes; C6 olefins, i-para.	1.49
17	2- and 3-methylpentane, C6 isoparaffins	1.13
18	C6 olefins	.34
19	n-Hexane	.11
20	C6 olefins, naph.; C7 olef., i-para, naph.	1.14
21	Benzene	.80
22	C6 naphthene; C7 olefins, i-para., naph.	.62
23	2- and 3-methylhexane, C7 i-paraffins	.70
24	C7 olefins, naph., i-para.; C8 i-para.	.23
25	n-Heptane	.04
26	C7 olefins, naphthenes; C8 i-paraffins	.64
27	toluene	2.16
28	C8 isoparaffins	.39
29	2- and 3-methylheptane; C8 i-paraffins	.46
30	C7 and C8 naphthenes; C9 i-paraffins	.19
31	n-Octane	.19
32	C9 olefins; C8, C9 naph., C9 i-para.	.08
33	Ethylbenzene	.48
34	C9 naphthenes and i-paraffins	0.00
35	p-Xylene and m-Xylene	2.04
36	C9 i-paraffins and naphthenes	.26
37	o-Xylene	.82
38	n-Nonane, C9 naphthenes	.17
39	C9 aromatics; C10 i-para. and naphthenes	3.22
40	n-Decane	2.74
41	n-C10; C9, C10 arom.; C10, C11 i-para., naph.	.81
42	Light paraffins	2.93
43	Light naphthenes	11.80
44	Light aromatics	12.21
45	Heavy paraffins	1.58
46	Heavy naphthenes	11.08
47	Heavy aromatics	15.64
48	Coke	4.12

PRODUCT DISTRIBUTION FOR RUN I.D.: B-G-4

NO.	COMPOUND(S)	wt%
1	Methane	3.48
2	Ethylene	4.42
3	Ethane	2.19
4	Propylene	4.73
5	Propane	1.26
6	i-Butane	.93
7	i-Butylene	2.23
8	1-Butene	1.06
9	n-Butane	.39
10	t,2-Butene	.37
11	c,2-Butene	.29
12	3-Methyl-1-butene	.11
13	i-Pentane	1.14
14	C5 olefins	.41
15	n-Pentane	.31
16	C5 olefins, naphthenes; C6 olefins, i-para.	2.26
17	2- and 3-methylpentane, C6 isoparaffins	.79
18	C6 olefins	.50
19	n-Hexane	.07
20	C6 olefins, naph.; C7 olef., i-para, naph.	1.20
21	Benzene	2.46
22	C6 naphthene; C7 olefins, i-para., naph.	.20
23	2- and 3-methylhexane, C7 i-paraffins	.39
24	C7 olefins, naph., i-para.; C8 i-para.	.63
25	n-Heptane	.11
26	C7 olefins, naphthenes; C8 i-paraffins	.64
27	toluene	3.31
28	C8 isoparaffins	.12
29	2- and 3-methylheptane; C8 i-paraffins	.30
30	C7 and C8 naphthenes; C9 i-paraffins	.21
31	n-Octane	.03
32	C9 olefins; C8, C9 naph., C9 i-para.	.09
33	Ethylbenzene	.55
34	C9 naphthenes and i-paraffins	0.00
35	p-Xylene and m-Xylene	2.43
36	C9 i-paraffins and naphthenes	.67
37	o-Xylene	.99
38	n-Nonane, C9 naphthenes	.21
39	C9 aromatics; C10 i-para. and naphthenes	3.23
40	n-C10; C9, C10 arom.; C10, C11 i-para., naph.	3.37
41	C12 hydrocarbons	1.79
42	Light paraffins	2.88
43	Light naphthenes	10.84
44	Light aromatics	11.28
45	Heavy paraffins	1.15
46	Heavy naphthenes	6.23
47	Heavy aromatics	12.74
48	Coke	4.98

PRODUCT DISTRIBUTION FOR RUN I.D.: B-G-5

NO.	COMPOUND(S)	wt%
1	Methane	2.22
2	Ethylene	3.07
3	Ethane	2.05
4	Propylene	3.76
5	Propane	.91
6	i-Butane	.20
7	i-Butylene	2.04
8	1-Butene	.53
9	n-Butane	.11
10	t,2-Butene	.40
11	c,2-Butene	.27
12	3-Methyl-1-butene	.15
13	i-Pentane	.16
14	C5 olefins	.95
15	n-Pentane	.30
16	C5 olefins, naphthenes; C6 olefins, i-para.	1.63
17	2- and 3-methylpentane, C6 isoparaffins	.79
18	C6 olefins	.07
19	n-Hexane	.18
20	C6 olefins, naph.; C7 olef., i-para, naph.	.96
21	Benzene	.79
22	C6 naphthene; C7 olefins, i-para., naph.	.45
23	2- and 3-methylhexane, C7 i-paraffins	.64
24	C7 olefins, naph., i-para.; C8 i-para.	.40
25	n-Heptane	.11
26	C7 olefins, naphthenes; C8 i-paraffins	.60
27	toluene	1.14
28	C8 isoparaffins	.63
29	2- and 3-methylheptane; C8 i-paraffins	.47
30	C7 and C8 naphthenes; C9 i-paraffins	.87
31	n-Octane	.04
32	C9 olefins; C8, C9 naph., C9 i-para.	.48
33	Ethylbenzene	.05
34	C9 naphthenes and i-paraffins	0.00
35	p-Xylene and m-Xylene	.72
36	C9 i-paraffins and naphthenes	.37
37	o-Xylene	.36
38	n-Nonane, C9 naphthenes	.57
39	C9 aromatics; C10 i-para. and naphthenes	2.52
40	n-C10; C9, C10 arom.; C10, C11 i-para., naph.	2.23
41	C12 hydrocarbons	1.35
42	Light paraffins	3.06
43	Light naphthenes	13.04
44	Light aromatics	13.34
45	Heavy paraffins	1.21
46	Heavy naphthenes	12.87
47	Heavy aromatics	18.85
48	Coke	2.10

PRODUCT DISTRIBUTION FOR RUN I.D.: B-G-6

NO.	COMPOUND(S)	wt%
1	Methane	2.55
2	Ethylene	2.70
3	Ethane	1.79
4	Propylene	4.11
5	Propane	1.26
6	i-Butane	1.55
7	i-Butylene	2.10
8	1-Butene	.42
9	n-Butane	.48
10	t,2-Butene	.54
11	c,2-Butene	.38
12	3-Methyl-1-butene	.11
13	i-Pentane	1.73
14	C5 olefins	.89
15	n-Pentane	.27
16	C5 olefins, naphthenes; C6 olefins, i-para.	2.26
17	2- and 3-methylpentane, C6 isoparaffins	.74
18	C6 olefins	0.00
19	n-Hexane	.11
20	C6 olefins, naph.; C7 olef., i-para, naph.	1.29
21	Benzene	1.31
22	C6 naphthene; C7 olefins, i-para., naph.	.55
23	2- and 3-methylhexane, C7 i-paraffins	.55
24	C7 olefins, naph., i-para.; C8 i-para.	.30
25	n-Heptane	.14
26	C7 olefins, naphthenes; C8 i-paraffins	.48
27	toluene	3.13
28	C8 isoparaffins	.37
29	2- and 3-methylheptane; C8 i-paraffins	.41
30	C7 and C8 naphthenes; C9 i-paraffins	.20
31	n-Octane	.28
32	C9 olefins; C8, C9 naph., C9 i-para.	.32
33	Ethylbenzene	.58
34	C9 naphthenes and i-paraffins	0.00
35	p-Xylene and m-Xylene	2.50
36	C9 i-paraffins and naphthenes	.30
37	o-Xylene	1.00
38	n-Nonane, C9 naphthenes	.18
39	C9 aromatics; C10 i-para. and naphthenes	3.65
40	n-C10; C9, C10 arom.; C10, C11 i-para., naph.	2.88
41	C12 hydrocarbons	1.08
42	Light paraffins	2.18
43	Light naphthenes	11.81
44	Light aromatics	10.42
45	Heavy paraffins	1.09
46	Heavy naphthenes	11.20
47	Heavy aromatics	14.81
48	Coke	3.01

PRODUCT DISTRIBUTION FOR RUN I.D.: B-G-7

NO.	COMPOUND(S)	wt%
1	Methane	2.72
2	Ethylene	2.99
3	Ethane	1.78
4	Propylene	4.63
5	Propane	1.61
6	i-Butane	2.50
7	i-Butylene	2.20
8	1-Butene	.52
9	n-Butane	.86
10	t,2-Butene	.63
11	c,2-Butene	.46
12	3-Methyl-1-butene	.11
13	i-Pentane	2.52
14	C5 olefins	.97
15	n-Pentane	.31
16	C5 olefins, naphthenes; C6 olefins, i-para.	1.62
17	2- and 3-methylpentane, C6 isoparaffins	1.85
18	C6 olefins	.20
19	n-Hexane	.14
20	C6 olefins, naph.; C7 olef., i-para, naph.	1.19
21	Benzene	1.13
22	C6 naphthene; C7 olefins, i-para., naph.	.70
23	2- and 3-methylhexane, C7 i-paraffins	.76
24	C7 olefins, naph., i-para.; C8 i-para.	.36
25	n-Heptane	.18
26	C7 olefins, naphthenes; C8 i-paraffins	.50
27	toluene	3.53
28	C8 isoparaffins	.49
29	2- and 3-methylheptane; C8 i-paraffins	.50
30	C7 and C8 naphthenes; C9 i-paraffins	.28
31	n-Octane	.88
32	C9 olefins; C8, C9 naph., C9 i-para.	.13
33	Ethylbenzene	.71
34	C9 naphthenes and i-paraffins	.01
35	p-Xylene and m-Xylene	3.16
36	C9 i-paraffins and naphthenes	.35
37	o-Xylene	1.25
38	n-Nonane, C9 naphthenes	.24
39	C9 aromatics; C10 i-para. and naphthenes	4.62
40	n-C10; C9, C10 arom.; C10, C11 i-para., naph.	3.29
41	C12 hydrocarbons	1.44
42	Light paraffins	2.02
43	Light naphthenes	10.30
44	Light aromatics	8.99
45	Heavy paraffins	.85
46	Heavy naphthenes	8.82
47	Heavy aromatics	10.92
48	Coke	3.80

PRODUCT DISTRIBUTION FOR RUN I.D.: B-G-8

NO.	COMPOUND(S)	wt%
1	Methane	3.72
2	Ethylene	4.42
3	Ethane	3.16
4	Propylene	4.98
5	Propane	2.37
6	i-Butane	1.99
7	i-Butylene	2.74
8	1-Butene	1.29
9	n-Butane	.90
10	t,2-Butene	.50
11	c,2-Butene	.36
12	3-Methyl-1-butene	.16
13	i-Pentane	1.85
14	C5 olefins	.61
15	n-Pentane	.41
16	C5 olefins, naphthenes; C6 olefins, i-para.	2.79
17	2- and 3-methylpentane, C6 isoparaffins	1.04
18	C6 olefins	.79
19	n-Hexane	.15
20	C6 olefins, naph.; C7 olef., i-para, naph.	1.60
21	Benzene	1.52
22	C6 naphthene; C7 olefins, i-para., naph.	.44
23	2- and 3-methylhexane, C7 i-paraffins	.47
24	C7 olefins, naph., i-para.; C8 i-para.	.82
25	n-Heptane	.17
26	C7 olefins, naphthenes; C8 i-paraffins	.83
27	toluene	3.53
28	C8 isoparaffins	.16
29	2- and 3-methylheptane; C8 i-paraffins	.40
30	C7 and C8 naphthenes; C9 i-paraffins	.32
31	n-Octane	.06
32	C9 olefins; C8, C9 naph., C9 i-para.	.47
33	Ethylbenzene	.75
34	C9 naphthenes and i-paraffins	0.00
35	p-Xylene and m-Xylene	2.94
36	C9 i-paraffins and naphthenes	.61
37	o-Xylene	1.23
38	n-Nonane, C9 naphthenes	.35
39	C9 aromatics; C10 i-para. and naphthenes	3.67
40	n-C10; C9, C10 arom.; C10, C11 i-para., naph.	3.31
41	C12 hydrocarbons	2.23
42	Light paraffins	1.57
43	Light naphthenes	9.03
44	Light aromatics	7.95
45	Heavy paraffins	.75
46	Heavy naphthenes	6.08
47	Heavy aromatics	9.58
48	Coke	4.91

PRODUCT DISTRIBUTION FOR RUN I.D.: B-G-9

NO.	COMPOUND(S)	wt%
1	Methane	2.95
2	Ethylene	3.00
3	Ethane	2.21
4	Propylene	4.11
5	Propane	1.65
6	i-Butane	1.65
7	i-Butylene	2.07
8	1-Butene	.52
9	n-Butane	.58
10	t,2-Butene	.51
11	c,2-Butene	.37
12	3-Methyl-1-butene	.11
13	i-Pentane	1.30
14	C5 olefins	.86
15	n-Pentane	.26
16	C5 olefins, naphthenes; C6 olefins, i-para.	1.44
17	2- and 3-methylpentane, C6 isoparaffins	.62
18	C6 olefins	.46
19	n-Hexane	.10
20	C6 olefins, naph.; C7 olef., i-para, naph.	1.08
21	Benzene	1.13
22	C6 naphthene; C7 olefins, i-para., naph.	.49
23	2- and 3-methylhexane, C7 i-paraffins	.45
24	C7 olefins, naph., i-para.; C8 i-para.	.26
25	n-Heptane	.04
26	C7 olefins, naphthenes; C8 i-paraffins	.50
27	toluene	2.89
28	C8 isoparaffins	.31
29	2- and 3-methylheptane; C8 i-paraffins	.32
30	C7 and C8 naphthenes; C9 i-paraffins	.27
31	n-Octane	.19
32	C9 olefins; C8, C9 naph., C9 i-para.	.07
33	Ethylbenzene	.50
34	C9 naphthenes and i-paraffins	0.00
35	p-Xylene and m-Xylene	2.06
36	C9 i-paraffins and naphthenes	.24
37	o-Xylene	.81
38	n-Nonane, C9 naphthenes	.19
39	C9 aromatics; C10 i-para. and naphthenes	2.71
40	n-C10; C9, C10 arom.; C10, C11 i-para., naph.	2.11
41	C12 hydrocarbons	.75
42	Light paraffins	2.80
43	Light naphthenes	12.75
44	Light aromatics	12.98
45	Heavy paraffins	.93
46	Heavy naphthenes	10.70
47	Heavy aromatics	15.44
48	Coke	2.27

PRODUCT DISTRIBUTION FOR RUN I.D.: B-G-10

NO.	COMPOUND(S)	wt%
1	Methane	3.54
2	Ethylene	4.12
3	Ethane	2.37
4	Propylene	5.51
5	Propane	1.38
6	i-Butane	1.45
7	i-Butylene	2.73
8	1-Butene	.86
9	n-Butane	.50
10	t,2-Butene	.65
11	c,2-Butene	.47
12	3-Methyl-1-butene	.16
13	i-Pentane	1.26
14	C5 olefins	.94
15	n-Pentane	.18
16	C5 olefins, naphthenes; C6 olefins, i-para.	2.46
17	2- and 3-methylpentane, C6 isoparaffins	.63
18	C6 olefins	.66
19	n-Hexane	.10
20	C6 olefins, naph.; C7 olef., i-para, naph.	1.56
21	Benzene	1.38
22	C6 naphthene; C7 olefins, i-para., naph.	.64
23	2- and 3-methylhexane, C7 i-paraffins	.62
24	C7 olefins, naph., i-para.; C8 i-para.	.44
25	n-Heptane	.14
26	C7 olefins, naphthenes; C8 i-paraffins	.63
27	toluene	3.26
28	C8 isoparaffins	.54
29	2- and 3-methylheptane; C8 i-paraffins	.45
30	C7 and C8 naphthenes; C9 i-paraffins	.43
31	n-Octane	.19
32	C9 olefins; C8, C9 naph., C9 i-para.	.11
33	Ethylbenzene	.61
34	C9 naphthenes and i-paraffins	.02
35	p-Xylene and m-Xylene	2.37
36	C9 i-paraffins and naphthenes	.37
37	o-Xylene	.99
38	n-Nonane, C9 naphthenes	.33
39	C9 aromatics; C10 i-para. and naphthenes	4.25
40	n-C10; C9, C10 arom.; C10, C11 i-para., naph.	3.48
41	C12 hydrocarbons	1.51
42	Light paraffins	1.23
43	Light naphthenes	10.50
44	Light aromatics	10.12
45	Heavy paraffins	.85
46	Heavy naphthenes	8.94
47	Heavy aromatics	11.35
48	Coke	2.74

PRODUCT DISTRIBUTION FOR RUN I.D.: B-G-11

NO.	COMPOUND(S)	wt%
1	Methane	4.54
2	Ethylene	3.99
3	Ethane	2.72
4	Propylene	6.15
5	Propane	2.13
6	i-Butane	2.84
7	i-Butylene	2.91
8	1-Butene	.54
9	n-Butane	.96
10	t,2-Butene	.89
11	c,2-Butene	.64
12	3-Methyl-1-butene	.12
13	i-Pentane	2.21
14	C5 olefins	1.12
15	n-Pentane	.26
16	C5 olefins, naphthenes; C6 olefins, i-para.	1.80
17	2- and 3-methylpentane, C6 isoparaffins	1.17
18	C6 olefins	.47
19	n-Hexane	.17
20	C6 olefins, naph.; C7 olef., i-para, naph.	1.37
21	Benzene	1.32
22	C6 naphthene; C7 olefins, i-para., naph.	.69
23	2- and 3-methylhexane, C7 i-paraffins	.68
24	C7 olefins, naph., i-para.; C8 i-para.	.41
25	n-Heptane	.16
26	C7 olefins, naphthenes; C8 i-paraffins	.49
27	toluene	3.87
28	C8 isoparaffins	.49
29	2- and 3-methylheptane; C8 i-paraffins	.46
30	C7 and C8 naphthenes; C9 i-paraffins	.41
31	n-Octane	.10
32	C9 olefins; C8, C9 naph., C9 i-para.	.11
33	Ethylbenzene	.80
34	C9 naphthenes and i-paraffins	0.00
35	p-Xylene and m-Xylene	3.14
36	C9 i-paraffins and naphthenes	.28
37	o-Xylene	1.24
38	n-Nonane, C9 naphthenes	.20
39	C9 aromatics; C10 i-para. and naphthenes	4.04
40	n-C10; C9, C10 arom.; C10, C11 i-para., naph.	3.07
41	C12 hydrocarbons	1.79
42	Light paraffins	1.15
43	Light naphthenes	9.22
44	Light aromatics	8.50
45	Heavy paraffins	.74
46	Heavy naphthenes	6.85
47	Heavy aromatics	8.91
48	Coke	3.88

PRODUCT DISTRIBUTION FOR RUN I.D.: B-G-12

NO.	COMPOUND(S)	wt%
1	Methane	6.85
2	Ethylene	6.70
3	Ethane	3.08
4	Propylene	6.76
5	Propane	2.20
6	i-Butane	1.56
7	i-Butylene	3.03
8	1-Butene	1.59
9	n-Butane	.78
10	t,2-Butene	.48
11	c,2-Butene	.36
12	3-Methyl-1-butene	.11
13	i-Pentane	1.19
14	C5 olefins	.39
15	n-Pentane	.32
16	C5 olefins, naphthenes; C6 olefins, i-para.	2.57
17	2- and 3-methylpentane, C6 isoparaffins	.56
18	C6 olefins	.55
19	n-Hexane	.07
20	C6 olefins, naph.; C7 olef., i-para, naph.	1.14
21	Benzene	2.97
22	C6 naphthene; C7 olefins, i-para., naph.	.18
23	2- and 3-methylhexane, C7 i-paraffins	.26
24	C7 olefins, naph., i-para.; C8 i-para.	.53
25	n-Heptane	.11
26	C7 olefins, naphthenes; C8 i-paraffins	.59
27	toluene	4.95
28	C8 isoparaffins	.09
29	2- and 3-methylheptane; C8 i-paraffins	.26
30	C7 and C8 naphthenes; C9 i-paraffins	.20
31	n-Octane	.02
32	C9 olefins; C8, C9 naph., C9 i-para.	.25
33	Ethylbenzene	.68
34	C9 naphthenes and i-paraffins	0.00
35	p-Xylene and m-Xylene	3.15
36	C9 i-paraffins and naphthenes	.70
37	o-Xylene	1.24
38	n-Nonane, C9 naphthenes	.21
39	C9 aromatics; C10 i-para. and naphthenes	3.29
40	n-Decane	3.34
41	n-C10; C9, C10 arom.; C10, C11 i-para., naph.	2.76
42	Light paraffins	1.05
43	Light naphthenes	8.84
44	Light aromatics	6.46
45	Heavy paraffins	.70
46	Heavy naphthenes	5.28
47	Heavy aromatics	7.81
48	Coke	5.10

PRODUCT DISTRIBUTION FOR RUN I.D.: P_1-O-1

NO.	COMPOUND(S)	wt%
1	Methane	2.15
2	Ethylene	3.71
3	Ethane	.81
4	Propylene	4.89
5	Propane	.01
6	i-Butane	.91
7	i-Butylene	5.17
8	1-Butene	.64
9	n-Butane	.19
10	t,2-Butene	.37
11	c,2-Butene	.26
12	3-Methyl-1-butene	.15
13	i-Pentane	1.48
14	C5 olefins	1.08
15	n-Pentane	.99
16	C5 olefins, naphthenes; C6 olefins, i-para.	4.43
17	2- and 3-methylpentane, C6 isoparaffins	.83
18	C6 olefins	.90
19	n-Hexane	.16
20	C6 olefins, naph.; C7 olef., i-para, naph.	1.69
21	Benzene	2.37
22	C6 naphthene; C7 olefins, i-para., naph.	.19
23	2- and 3-methylhexane, C7 i-paraffins	.37
24	C7 olefins, naph., i-para.; C8 i-para.	.73
25	n-Heptane	.06
26	C7 olefins, naphthenes; C8 i-paraffins	.29
27	toluene	1.95
28	C8 isoparaffins	.04
29	2- and 3-methylheptane; C8 i-paraffins	.03
30	C7 and C8 naphthenes; C9 i-paraffins	.34
31	n-Octane	.03
32	C9 olefins; C8, C9 naph., C9 i-para.	.11
33	Ethylbenzene	.16
34	C9 naphthenes and i-paraffins	0.00
35	p-Xylene and m-Xylene	.87
36	C9 i-paraffins and naphthenes	.12
37	o-Xylene	.32
38	n-Nonane, C9 naphthenes	.29
39	C9 aromatics; C10 i-para. and naphthenes	1.06
40	n-C10; C9, C10 arom.; C10, C11 i-para., naph.	1.16
41	C12 hydrocarbons	.27
42	Light paraffins	57.16
43	Coke	1.26

PRODUCT DISTRIBUTION FOR RUN I.D.: P_1-O-2

NO.	COMPOUND(S)	wt%
1	Methane	.89
2	Ethylene	1.10
3	Ethane	.68
4	Propylene	5.91
5	Propane	1.90
6	i-Butane	7.35
7	i-Butylene	5.66
8	1-Butene	.11
9	n-Butane	1.65
10	t,2-Butene	1.79
11	c,2-Butene	1.25
12	3-Methyl-1-butene	.19
13	i-Pentane	5.70
14	C5 olefins	1.50
15	n-Pentane	.99
16	C5 olefins, naphthenes; C6 olefins, i-para.	4.09
17	2- and 3-methylpentane, C6 isoparaffins	2.89
18	C6 olefins	.18
19	n-Hexane	.50
20	C6 olefins, naph.; C7 olef., i-para, naph.	2.50
21	Benzene	.19
22	C6 naphthene; C7 olefins, i-para., naph.	.16
23	2- and 3-methylhexane, C7 i-paraffins	.98
24	C7 olefins, naph., i-para.; C8 i-para.	.65
25	n-Heptane	.01
26	C7 olefins, naphthenes; C8 i-paraffins	1.09
27	toluene	.52
28	C8 isoparaffins	.34
29	2- and 3-methylheptane; C8 i-paraffins	.55
30	C7 and C8 naphthenes; C9 i-paraffins	.08
31	n-Octane	.17
32	C9 olefins; C8, C9 naph., C9 i-para.	.13
33	Ethylbenzene	.08
34	C9 naphthenes and i-paraffins	0.00
35	p-Xylene and m-Xylene	.92
36	C9 i-paraffins and naphthenes	.15
37	o-Xylene	.31
38	n-Nonane, C9 naphthenes	.45
39	C9 aromatics; C10 i-para. and naphthenes	1.74
40	n-C10; C9, C10 arom.; C10, C11 i-para., naph.	1.31
41	C12 hydrocarbons	.37
42	Light paraffins	41.29
43	Coke	1.68

PRODUCT DISTRIBUTION FOR RUN I.D.: P_1-O-3

NO.	COMPOUND(S)	wt%
1	Methane	.89
2	Ethylene	1.11
3	Ethane	.58
4	Propylene	6.68
5	Propane	2.33
6	i-Butane	8.51
7	i-Butylene	6.04
8	1-Butene	.08
9	n-Butane	1.92
10	t,2-Butene	2.08
11	c,2-Butene	1.42
12	3-Methyl-1-butene	.20
13	i-Pentane	6.44
14	C5 olefins	1.61
15	n-Pentane	1.08
16	C5 olefins, naphthenes; C6 olefins, i-para.	4.51
17	2- and 3-methylpentane, C6 isoparaffins	3.31
18	C6 olefins	.19
19	n-Hexane	.47
20	C6 olefins, naph.; C7 olef., i-para, naph.	2.82
21	Benzene	.16
22	C6 naphthene; C7 olefins, i-para., naph.	.20
23	2- and 3-methylhexane, C7 i-paraffins	1.22
24	C7 olefins, naph., i-para.; C8 i-para.	1.32
25	n-Heptane	.16
26	C7 olefins, naphthenes; C8 i-paraffins	.65
27	toluene	.55
28	C8 isoparaffins	.06
29	2- and 3-methylheptane; C8 i-paraffins	.42
30	C7 and C8 naphthenes; C9 i-paraffins	.37
31	n-Octane	.17
32	C9 olefins; C8, C9 naph., C9 i-para.	.16
33	Ethylbenzene	.09
34	C9 naphthenes and i-paraffins	0.00
35	p-Xylene and m-Xylene	1.07
36	C9 i-paraffins and naphthenes	.17
37	o-Xylene	.37
38	n-Nonane, C9 naphthenes	.46
39	C9 aromatics; C10 i-para. and naphthenes	2.13
40	n-C10; C9, C10 arom.; C10, C11 i-para., naph.	1.33
41	C12 hydrocarbons	.42
42	Light paraffins	33.49
43	Coke	2.71

PRODUCT DISTRIBUTION FOR RUN I.D.: P_1-O-4

NO.	COMPOUND(S)	wt%
1	Methane	3.06
2	Ethylene	3.53
3	Ethane	1.46
4	Propylene	8.58
5	Propane	1.81
6	i-Butane	6.45
7	i-Butylene	9.41
8	1-Butene	.76
9	n-Butane	1.16
10	t,2-Butene	1.40
11	c,2-Butene	.92
12	3-Methyl-1-butene	.25
13	i-Pentane	6.42
14	C5 olefins	2.16
15	n-Pentane	.93
16	C5 olefins, naphthenes; C6 olefins, i-para.	5.28
17	2- and 3-methylpentane, C6 isoparaffins	2.91
18	C6 olefins	.17
19	n-Hexane	.81
20	C6 olefins, naph.; C7 olef., i-para, naph.	2.55
21	Benzene	.98
22	C6 naphthene; C7 olefins, i-para., naph.	.23
23	2- and 3-methylhexane, C7 i-paraffins	1.05
24	C7 olefins, naph., i-para.; C8 i-para.	1.14
25	n-Heptane	.02
26	C7 olefins, naphthenes; C8 i-paraffins	.90
27	toluene	1.71
28	C8 isoparaffins	.31
29	2- and 3-methylheptane; C8 i-paraffins	.57
30	C7 and C8 naphthenes; C9 i-paraffins	.02
31	n-Octane	.12
32	C9 olefins; C8, C9 naph., C9 i-para.	.17
33	Ethylbenzene	.17
34	C9 naphthenes and i-paraffins	0.00
35	p-Xylene and m-Xylene	1.81
36	C9 i-paraffins and naphthenes	.18
37	o-Xylene	.62
38	n-Nonane, C9 naphthenes	.43
39	C9 aromatics; C10 i-para. and naphthenes	2.50
40	n-C10; C9, C10 arom.; C10, C11 i-para., naph.	1.94
41	C12 hydrocarbons	.36
42	Light paraffins	21.47
43	Coke	3.26

PRODUCT DISTRIBUTION FOR RUN I.D.: P_i-O-5

NO.	COMPOUND(S)	wt%
1	Methane	4.59
2	Ethylene	7.22
3	Ethane	1.79
4	Propylene	9.66
5	Propane	.21
6	i-Butane	1.87
7	i-Butylene	8.40
8	1-Butene	1.17
9	n-Butane	.38
10	t,2-Butene	.81
11	c,2-Butene	.55
12	3-Methyl-1-butene	.12
13	i-Pentane	1.29
14	C5 olefins	.78
15	n-Pentane	.80
16	C5 olefins, naphthenes; C6 olefins, i-para.	4.23
17	2- and 3-methylpentane, C6 isoparaffins	.53
18	C6 olefins	.62
19	n-Hexane	.12
20	C6 olefins, naph.; C7 olef., i-para, naph.	1.54
21	Benzene	2.95
22	C6 naphthene; C7 olefins, i-para., naph.	.20
23	2- and 3-methylhexane, C7 i-paraffins	.22
24	C7 olefins, naph., i-para.; C8 i-para.	.49
25	n-Heptane	.06
26	C7 olefins, naphthenes; C8 i-paraffins	.33
27	toluene	2.59
28	C8 isoparaffins	.06
29	2- and 3-methylheptane; C8 i-paraffins	.01
30	C7 and C8 naphthenes; C9 i-paraffins	.24
31	n-Octane	.03
32	C9 olefins; C8, C9 naph., C9 i-para.	.11
33	Ethylbenzene	.19
34	C9 naphthenes and i-paraffins	0.00
35	p-Xylene and m-Xylene	1.10
36	C9 i-paraffins and naphthenes	.20
37	o-Xylene	.40
38	n-Nonane, C9 naphthenes	.21
39	C9 aromatics; C10 i-para. and naphthenes	1.18
40	n-C10; C9, C10 arom.; C10, C11 i-para., naph.	1.36
41	C12 hydrocarbons	.19
42	Light paraffins	39.88
43	Coke	1.32

PRODUCT DISTRIBUTION FOR RUN I.D.: P_1-O-6

NO.	COMPOUND(S)	wt%
1	Methane	6.34
2	Ethylene	3.60
3	Ethane	3.25
4	Propylene	8.84
5	Propane	2.95
6	i-Butane	7.21
7	i-Butylene	9.25
8	1-Butene	.53
9	n-Butane	1.43
10	t,2-Butene	1.50
11	c,2-Butene	.92
12	3-Methyl-1-butene	.14
13	i-Pentane	4.09
14	C5 olefins	1.09
15	n-Pentane	.85
16	C5 olefins, naphthenes; C6 olefins, i-para.	3.11
17	2- and 3-methylpentane, C6 isoparaffins	1.42
18	C6 olefins	0.00
19	n-Hexane	.40
20	C6 olefins, naph.; C7 olef., i-para, naph.	1.47
21	Benzene	3.[illegible]9
22	C6 naphthene; C7 olefins, i-para., naph.	.07
23	2- and 3-methylhexane, C7 i-paraffins	.39
24	C7 olefins, naph., i-para.; C8 i-para.	.32
25	n-Heptane	.21
26	C7 olefins, naphthenes; C8 i-paraffins	.[illegible]
27	toluene	3.[illegible]
28	C8 isoparaffins	.[illegible]
29	2- and 3-methylheptane; C8 i-paraffins	.21
30	C7 and C8 naphthenes; C9 i-paraffins	.01
31	n-Octane	.12
32	C9 olefins; C8, C9 naph., C9 i-para.	.18
33	Ethylbenzene	.22
34	C9 naphthenes and i-paraffins	0.00
35	p-Xylene and m-Xylene	1.80
36	C9 i-paraffins and naphthenes	.08
37	o-Xylene	.72
38	n-Nonane, C9 naphthenes	.21
39	C9 aromatics; C10 i-para. and naphthenes	1.58
40	n-C10; C9, C10 arom.; C10, C11 i-para., naph.	1.51
41	C12 hydrocarbons	.08
42	Light paraffins	24.82
43	Coke	2.33

PRODUCT DISTRIBUTION FOR RUN I.D.: P_1-O-7

NO.	COMPOUND(S)	wt%
1	Methane	1.78
2	Ethylene	2.52
3	Ethane	1.36
4	Propylene	10.81
5	Propane	3.28
6	i-Butane	12.21
7	i-Butylene	11.45
8	1-Butene	.32
9	n-Butane	2.78
10	t,2-Butene	3.06
11	c,2-Butene	2.10
12	3-Methyl-1-butene	.17
13	i-Pentane	5.11
14	C5 olefins	1.54
15	n-Pentane	.89
16	C5 olefins, naphthenes; C6 olefins, i-para.	3.89
17	2- and 3-methylpentane, C6 isoparaffins	2.61
18	C6 olefins	.15
19	n-Hexane	.71
20	C6 olefins, naph.; C7 olef., i-para, naph.	2.40
21	Benzene	.25
22	C6 naphthene; C7 olefins, i-para., naph.	.17
23	2- and 3-methylhexane, C7 i-paraffins	.89
24	C7 olefins, naph., i-para.; C8 i-para.	.80
25	n-Heptane	.01
26	C7 olefins, naphthenes; C8 i-paraffins	1.11
27	toluene	.51
28	C8 isoparaffins	.31
29	2- and 3-methylheptane; C8 i-paraffins	.60
30	C7 and C8 naphthenes; C9 i-paraffins	.08
31	n-Octane	.16
32	C9 olefins; C8, C9 naph., C9 i-para.	.15
33	Ethylbenzene	.07
34	C9 naphthenes and i-paraffins	0.00
35	p-Xylene and m-Xylene	.85
36	C9 i-paraffins and naphthenes	.16
37	o-Xylene	.29
38	n-Nonane, C9 naphthenes	.45
39	C9 aromatics; C10 i-para. and naphthenes	1.90
40	n-C10; C9, C10 arom.; C10, C11 i-para., naph.	1.56
41	C12 hydrocarbons	.47
42	Light paraffins	17.25
43	Coke	2.81

PRODUCT DISTRIBUTION FOR RUN I.D.: P_1-O-8

NO.	COMPOUND(S)	wt%
1	Methane	6.19
2	Ethylene	6.64
3	Ethane	3.81
4	Propylene	13.47
5	Propane	2.97
6	i-Butane	6.43
7	i-Butylene	11.82
8	1-Butene	1.16
9	n-Butane	1.42
10	t,2-Butene	2.11
11	c,2-Butene	1.45
12	3-Methyl-1-butene	.19
13	i-Pentane	3.43
14	C5 olefins	1.67
15	n-Pentane	.66
16	C5 olefins, naphthenes; C6 olefins, i-para.	4.52
17	2- and 3-methylpentane, C6 isoparaffins	1.54
18	C6 olefins	.74
19	n-Hexane	.36
20	C6 olefins, naph.; C7 olef., i-para, naph.	1.79
21	Benzene	1.47
22	C6 naphthene; C7 olefins, i-para., naph.	.57
23	2- and 3-methylhexane, C7 i-paraffins	.55
24	C7 olefins, naph., i-para.; C8 i-para.	.74
25	n-Heptane	.03
26	C7 olefins, naphthenes; C8 i-paraffins	.42
27	toluene	2.09
28	C8 isoparaffins	.11
29	2- and 3-methylheptane; C8 i-paraffins	.16
30	C7 and C8 naphthenes; C9 i-paraffins	.47
31	n-Octane	.04
32	C9 olefins; C8, C9 naph., C9 i-para.	.08
33	Ethylbenzene	.20
34	C9 naphthenes and i-paraffins	0.00
35	p-Xylene and m-Xylene	1.62
36	C9 i-paraffins and naphthenes	.14
37	o-Xylene	.58
38	n-Nonane, C9 naphthenes	.25
39	C9 aromatics; C10 i-para. and naphthenes	2.10
40	n-C10; C9, C10 arom.; C10, C11 i-para., naph.	1.68
41	C12 hydrocarbons	.31
42	Light paraffins	10.38
43	Coke	3.67

PRODUCT DISTRIBUTION FOR RUN I.D.: P_1-G-1

NO.	COMPOUND(S)	wt%
1	Methane	.70
2	Ethylene	1.05
3	Ethane	.60
4	Propylene	4.31
5	Propane	1.94
6	i-Butane	10.29
7	i-Butylene	4.25
8	1-Butene	.13
9	n-Butane	1.95
10	t,2-Butene	1.19
11	c,2-Butene	.84
12	3-Methyl-1-butene	.08
13	i-Pentane	5.76
14	C5 olefins	.86
15	n-Pentane	.92
16	C5 olefins, naphthenes; C6 olefins, i-para.	2.31
17	2- and 3-methylpentane, C6 isoparaffins	2.99
18	C6 olefins	.52
19	n-Hexane	.57
20	C6 olefins, naph.; C7 olef., i-para, naph.	1.14
21	Benzene	.18
22	C6 naphthene; C7 olefins, i-para., naph.	.10
23	2- and 3-methylhexane, C7 i-paraffins	1.23
24	C7 olefins, naph., i-para.; C8 i-para.	.87
25	n-Heptane	.07
26	C7 olefins, naphthenes; C8 i-paraffins	.46
27	toluene	.46
28	C8 isoparaffins	.07
29	2- and 3-methylheptane; C8 i-paraffins	.45
30	C7 and C8 naphthenes; C9 i-paraffins	.34
31	n-Octane	.15
32	C9 olefins; C8, C9 naph., C9 i-para.	.12
33	Ethylbenzene	.07
34	C9 naphthenes and i-paraffins	0.00
35	p-Xylene and m-Xylene	.89
36	C9 i-paraffins and naphthenes	.17
37	o-Xylene	.30
38	n-Nonane, C9 naphthenes	.34
39	C9 aromatics; C10 i-para. and naphthenes	1.54
40	n-C10; C9, C10 arom.; C10, C11 i-para., naph.	1.10
41	C12 hydrocarbons	.39
42	Light paraffins	47.49
43	Coke	.80

PRODUCT DISTRIBUTION FOR RUN I.D.: P_1-G-2

NO.	COMPOUND(S)	wt%
1	Methane	.84
2	Ethylene	1.33
3	Ethane	.73
4	Propylene	5.84
5	Propane	1.85
6	i-Butane	10.73
7	i-Butylene	6.53
8	1-Butene	.18
9	n-Butane	1.85
10	t,2-Butene	1.74
11	c,2-Butene	1.20
12	3-Methyl-1-butene	.13
13	i-Pentane	5.31
14	C5 olefins	1.31
15	n-Pentane	.97
16	C5 olefins, naphthenes; C6 olefins, i-para.	3.37
17	2- and 3-methylpentane, C6 isoparaffins	2.80
18	C6 olefins	.74
19	n-Hexane	.66
20	C6 olefins, naph.; C7 olef., i-para, naph.	1.74
21	Benzene	.23
22	C6 naphthene; C7 olefins, i-para., naph.	.17
23	2- and 3-methylhexane, C7 i-paraffins	1.21
24	C7 olefins, naph., i-para.; C8 i-para.	1.22
25	n-Heptane	.12
26	C7 olefins, naphthenes; C8 i-paraffins	.65
27	toluene	.48
28	C8 isoparaffins	.11
29	2- and 3-methylheptane; C8 i-paraffins	.50
30	C7 and C8 naphthenes; C9 i-paraffins	.50
31	n-Octane	.20
32	C9 olefins; C8, C9 naph., C9 i-para.	.22
33	Ethylbenzene	.07
34	C9 naphthenes and i-paraffins	0.00
35	p-Xylene and m-Xylene	.89
36	C9 i-paraffins and naphthenes	.22
37	o-Xylene	.31
38	n-Nonane, C9 naphthenes	.49
39	C9 aromatics; C10 i-para. and naphthenes	1.84
40	n-C10; C9, C10 arom.; C10, C11 i-para., naph.	1.33
41	C12 hydrocarbons	.48
42	Light paraffins	37.44
43	Coke	1.46

PRODUCT DISTRIBUTION FOR RUN I.D.: P_t-G-3

NO.	COMPOUND(S)	wt%
1	Methane	.75
2	Ethylene	.88
3	Ethane	.58
4	Propylene	5.04
5	Propane	2.54
6	i-Butane	14.25
7	i-Butylene	4.67
8	1-Butene	.10
9	n-Butane	2.66
10	t,2-Butene	1.54
11	c,2-Butene	1.09
12	3-Methyl-1-butene	.11
13	i-Pentane	7.96
14	C5 olefins	.87
15	n-Pentane	1.26
16	C5 olefins, naphthenes; C6 olefins, i-para.	2.94
17	2- and 3-methylpentane, C6 isoparaffins	4.25
18	C6 olefins	.35
19	n-Hexane	.80
20	C6 olefins, naph.; C7 olef., i-para, naph.	1.41
21	Benzene	.17
22	C6 naphthene; C7 olefins, i-para., naph.	.11
23	2- and 3-methylhexane, C7 i-paraffins	1.81
24	C7 olefins, naph., i-para.; C8 i-para.	.94
25	n-Heptane	.10
26	C7 olefins, naphthenes; C8 i-paraffins	.53
27	toluene	.63
28	C8 isoparaffins	.11
29	2- and 3-methylheptane; C8 i-paraffins	.67
30	C7 and C8 naphthenes; C9 i-paraffins	.23
31	n-Octane	.21
32	C9 olefins; C8, C9 naph., C9 i-para.	.14
33	Ethylbenzene	.11
34	C9 naphthenes and i-paraffins	0.00
35	p-Xylene and m-Xylene	1.26
36	C9 i-paraffins and naphthenes	.27
37	o-Xylene	.43
38	n-Nonane, C9 naphthenes	.25
39	C9 aromatics; C10 i-para. and naphthenes	1.96
40	n-C10; C9, C10 arom.; C10, C11 i-para., naph.	1.32
41	C12 hydrocarbons	.29
42	Light paraffins	30.98
43	Coke	3.45

PRODUCT DISTRIBUTION FOR RUN I.D.: P_1-G-4

NO.	COMPOUND(S)	wt%
1	Methane	3.48
2	Ethylene	2.63
3	Ethane	2.27
4	Propylene	5.77
5	Propane	2.56
6	i-Butane	8.52
7	i-Butylene	6.90
8	1-Butene	.32
9	n-Butane	1.88
10	t,2-Butene	1.31
11	c,2-Butene	.81
12	3-Methyl-1-butene	.15
13	i-Pentane	5.60
14	C5 olefins	1.73
15	n-Pentane	1.23
16	C5 olefins, naphthenes; C6 olefins, i-para.	3.39
17	2- and 3-methylpentane, C6 isoparaffins	2.41
18	C6 olefins	1.42
19	n-Hexane	.67
20	C6 olefins, naph.; C7 olef., i-para, naph.	1.76
21	Benzene	1.32
22	C6 naphthene; C7 olefins, i-para., naph.	.12
23	2- and 3-methylhexane, C7 i-paraffins	.84
24	C7 olefins, naph., i-para.; C8 i-para.	1.61
25	n-Heptane	.07
26	C7 olefins, naphthenes; C8 i-paraffins	.67
27	toluene	1.09
28	C8 isoparaffins	.06
29	2- and 3-methylheptane; C8 i-paraffins	.28
30	C7 and C8 naphthenes; C9 i-paraffins	.81
31	n-Octane	.16
32	C9 olefins; C8, C9 naph., C9 i-para.	.28
33	Ethylbenzene	.13
34	C9 naphthenes and i-paraffins	0.00
35	p-Xylene and m-Xylene	1.02
36	C9 i-paraffins and naphthenes	.12
37	o-Xylene	.40
38	n-Nonane, C9 naphthenes	.84
39	C9 aromatics; C10 i-para. and naphthenes	2.28
40	n-C10; C9, C10 arom.; C10, C11 i-para., naph.	1.88
41	C12 hydrocarbons	.77
42	Light paraffins	26.13
43	Coke	4.32

PRODUCT DISTRIBUTION FOR RUN I.D.: P_1-G-5

NO.	COMPOUND(S)	wt%
1	Methane	2.26
2	Ethylene	3.16
3	Ethane	1.79
4	Propylene	6.92
5	Propane	2.94
6	i-Butane	8.86
7	i-Butylene	6.56
8	1-Butene	.30
9	n-Butane	2.07
10	t,2-Butene	1.33
11	c,2-Butene	.89
12	3-Methyl-1-butene	.11
13	i-Pentane	4.25
14	C5 olefins	1.30
15	n-Pentane	.82
16	C5 olefins, naphthenes; C6 olefins, i-para.	2.28
17	2- and 3-methylpentane, C6 isoparaffins	1.63
18	C6 olefins	1.07
19	n-Hexane	.41
20	C6 olefins, naph.; C7 olef., i-para, naph.	1.19
21	Benzene	.42
22	C6 naphthene; C7 olefins, i-para., naph.	.12
23	2- and 3-methylhexane, C7 i-paraffins	.52
24	C7 olefins, naph., i-para.; C8 i-para.	1.09
25	n-Heptane	.06
26	C7 olefins, naphthenes; C8 i-paraffins	.42
27	toluene	.82
28	C8 isoparaffins	.04
29	2- and 3-methylheptane; C8 i-paraffins	.18
30	C7 and C8 naphthenes; C9 i-paraffins	.66
31	n-Octane	.09
32	C9 olefins; C8, C9 naph., C9 i-para.	.12
33	Ethylbenzene	.10
34	C9 naphthenes and i-paraffins	0.00
35	p-Xylene and m-Xylene	.93
36	C9 i-paraffins and naphthenes	.08
37	o-Xylene	.32
38	n-Nonane, C9 naphthenes	.64
39	C9 aromatics; C10 i-para. and naphthenes	1.63
40	n-C10; C9, C10 arom.; C10, C11 i-para., naph.	1.27
41	C12 hydrocarbons	.68
42	Light paraffins	38.69
43	Coke	1.00

PRODUCT DISTRIBUTION FOR RUN I.D.: P_1-G-6

NO.	COMPOUND(S)	wt%
1	Methane	.98
2	Ethylene	1.15
3	Ethane	.77
4	Propylene	6.23
5	Propane	2.55
6	i-Butane	15.55
7	i-Butylene	6.81
8	1-Butene	.20
9	n-Butane	2.68
10	t,2-Butene	1.97
11	c,2-Butene	1.37
12	3-Methyl-1-butene	.10
13	i-Pentane	5.49
14	C5 olefins	.86
15	n-Pentane	.98
16	C5 olefins, naphthenes; C6 olefins, i-para.	2.73
17	2- and 3-methylpentane, C6 isoparaffins	3.01
18	C6 olefins	.38
19	n-Hexane	.65
20	C6 olefins, naph.; C7 olef., i-para, naph.	1.38
21	Benzene	.18
22	C6 naphthene; C7 olefins, i-para., naph.	.14
23	2- and 3-methylhexane, C7 i-paraffins	1.37
24	C7 olefins, naph., i-para.; C8 i-para.	.88
25	n-Heptane	.10
26	C7 olefins, naphthenes; C8 i-paraffins	.53
27	toluene	.45
28	C8 isoparaffins	.10
29	2- and 3-methylheptane; C8 i-paraffins	.56
30	C7 and C8 naphthenes; C9 i-paraffins	.25
31	n-Octane	.19
32	C9 olefins; C8, C9 naph., C9 i-para.	.18
33	Ethylbenzene	.07
34	C9 naphthenes and i-paraffins	0.00
35	p-Xylene and m-Xylene	.84
36	C9 i-paraffins and naphthenes	.24
37	o-Xylene	.30
38	n-Nonane, C9 naphthenes	.26
39	C9 aromatics; C10 i-para. and naphthenes	1.53
40	n-C10; C9, C10 arom.; C10, C11 i-para., naph.	1.06
41	C12 hydrocarbons	.29
42	Light paraffins	31.71
43	Coke	2.91

PRODUCT DISTRIBUTION FOR RUN I.D.: P_1-G-7

NO.	COMPOUND(S)	wt%
1	Methane	2.58
2	Ethylene	2.69
3	Ethane	1.85
4	Propylene	7.17
5	Propane	3.81
6	i-Butane	11.66
7	i-Butylene	6.01
8	1-Butene	.25
9	n-Butane	2.81
10	t,2-Butene	1.59
11	c,2-Butene	1.09
12	3-Methyl-1-butene	.12
13	i-Pentane	6.11
14	C5 olefins	1.03
15	n-Pentane	1.17
16	C5 olefins, naphthenes; C6 olefins, i-para.	2.67
17	2- and 3-methylpentane, C6 isoparaffins	2.53
18	C6 olefins	.58
19	n-Hexane	.60
20	C6 olefins, naph.; C7 olef., i-para, naph.	1.24
21	Benzene	.43
22	C6 naphthene; C7 olefins, i-para., naph.	.12
23	2- and 3-methylhexane, C7 i-paraffins	.77
24	C7 olefins, naph., i-para.; C8 i-para.	.84
25	n-Heptane	.05
26	C7 olefins, naphthenes; C8 i-paraffins	.38
27	toluene	1.15
28	C8 isoparaffins	.04
29	2- and 3-methylheptane; C8 i-paraffins	.24
30	C7 and C8 naphthenes; C9 i-paraffins	.32
31	n-Octane	.12
32	C9 olefins; C8, C9 naph., C9 i-para.	.18
33	Ethylbenzene	.13
34	C9 naphthenes and i-paraffins	0.00
35	p-Xylene and m-Xylene	1.36
36	C9 i-paraffins and naphthenes	.09
37	o-Xylene	.49
38	n-Nonane, C9 naphthenes	.34
39	C9 aromatics; C10 i-para. and naphthenes	1.72
40	n-C10; C9, C10 arom.; C10, C11 i-para., naph.	1.31
41	C12 hydrocarbons	.32
42	Light paraffins	27.68
43	Coke	4.36

PRODUCT DISTRIBUTION FOR RUN I.D.: P_1-G-8

NO.	COMPOUND(S)	wt%
1	Methane	4.13
2	Ethylene	2.71
3	Ethane	2.63
4	Propylene	6.42
5	Propane	3.31
6	i-Butane	10.60
7	i-Butylene	7.37
8	1-Butene	.29
9	n-Butane	2.33
10	t,2-Butene	1.46
11	c,2-Butene	.93
12	3-Methyl-1-butene	.11
13	i-Pentane	5.01
14	C5 olefins	1.22
15	n-Pentane	1.01
16	C5 olefins, naphthenes; C6 olefins, i-para.	2.69
17	2- and 3-methylpentane, C6 isoparaffins	2.15
18	C6 olefins	.90
19	n-Hexane	.53
20	C6 olefins, naph.; C7 olef., i-para, naph.	1.39
21	Benzene	1.23
22	C6 naphthene; C7 olefins, i-para., naph.	.14
23	2- and 3-methylhexane, C7 i-paraffins	.73
24	C7 olefins, naph., i-para.; C8 i-para.	1.07
25	n-Heptane	.05
26	C7 olefins, naphthenes; C8 i-paraffins	.50
27	toluene	1.02
28	C8 isoparaffins	.05
29	2- and 3-methylheptane; C8 i-paraffins	.24
30	C7 and C8 naphthenes; C9 i-paraffins	.51
31	n-Octane	.12
32	C9 olefins; C8, C9 naph., C9 i-para.	.26
33	Ethylbenzene	.17
34	C9 naphthenes and i-paraffins	0.00
35	p-Xylene and m-Xylene	.95
36	C9 i-paraffins and naphthenes	.18
37	o-Xylene	.38
38	n-Nonane, C9 naphthenes	.51
39	C9 aromatics; C10 i-para. and naphthenes	1.61
40	n-C10; C9, C10 arom.; C10, C11 i-para., naph.	1.79
41	C12 hydrocarbons	1.33
42	Light paraffins	24.92
43	Coke	5.01

PRODUCT DISTRIBUTION FOR RUN I.D.: N_i-O-1

NO.	COMPOUND(S)	wt%
1	Methane	1.65
2	Ethylene	3.64
3	Ethane	.95
4	Propylene	3.90
5	Propane	.77
6	i-Butane	1.64
7	i-Butylene	1.67
8	1-Butene	1.63
9	n-Butane	.40
10	t,2-Butene	.48
11	c,2-Butene	.36
12	3-Methyl-1-butene	.04
13	i-Pentane	1.37
14	C5 olefins	.31
15	n-Pentane	.10
16	C5 olefins, naphthenes; C6 olefins, i-para.	1.89
17	2- and 3-methylpentane, C6 isoparaffins	.65
18	C6 olefins	.17
19	n-Hexane	.04
20	C6 olefins, naph.; C7 olef., i-para, naph.	2.83
21	Benzene	2.73
22	C6 naphthene; C7 olefins, i-para., naph.	.45
23	2- and 3-methylhexane, C7 i-paraffins	1.23
24	C7 olefins, naph., i-para.; C8 i-para.	.22
25	n-Heptane	.03
26	C7 olefins, naphthenes; C8 i-paraffins	.80
27	toluene	2.54
28	C8 isoparaffins	.04
29	2- and 3-methylheptane; C8 i-paraffins	.16
30	C7 and C8 naphthenes; C9 i-paraffins	.28
31	n-Octane	.01
32	C9 olefins; C8, C9 naph., C9 i-para.	.19
33	Ethylbenzene	.90
34	C9 naphthenes and i-paraffins	0.00
35	p-Xylene and m-Xylene	1.63
36	C9 i-paraffins and naphthenes	.49
37	o-Xylene	.70
38	n-Nonane, C9 naphthenes	.07
39	C9 aromatics; C10 i-para. and naphthenes	2.12
40	n-C10; C9, C10 arom.; C10, C11 i-para., naph.	2.08
41	C12 hydrocarbons	2.89
42	Light naphthenes	54.27
43	Coke	1.67

PRODUCT DISTRIBUTION FOR RUN I.D.: N_1-O-2

NO.	COMPOUND(S)	wt%
1	Methane	2.03
2	Ethylene	3.44
3	Ethane	1.36
4	Propylene	4.26
5	Propane	.85
6	i-Butane	1.42
7	i-Butylene	2.33
8	1-Butene	.97
9	n-Butane	.40
10	t,2-Butene	.52
11	c,2-Butene	.39
12	3-Methyl-1-butene	.04
13	i-Pentane	1.29
14	C5 olefins	.38
15	n-Pentane	.11
16	C5 olefins, naphthenes; C6 olefins, i-para.	2.37
17	2- and 3-methylpentane, C6 isoparaffins	.63
18	C6 olefins	.26
19	n-Hexane	.05
20	C6 olefins, naph.; C7 olef., i-para, naph.	2.83
21	Benzene	2.46
22	C6 naphthene; C7 olefins, i-para., naph.	.50
23	2- and 3-methylhexane, C7 i-paraffins	1.02
24	C7 olefins, naph., i-para.; C8 i-para.	.34
25	n-Heptane	.02
26	C7 olefins, naphthenes; C8 i-paraffins	.87
27	toluene	2.50
28	C8 isoparaffins	.10
29	2- and 3-methylheptane; C8 i-paraffins	.23
30	C7 and C8 naphthenes; C9 i-paraffins	.36
31	n-Octane	.02
32	C9 olefins; C8, C9 naph., C9 i-para.	.19
33	Ethylbenzene	.83
34	C9 naphthenes and i-paraffins	0.00
35	p-Xylene and m-Xylene	1.55
36	C9 i-paraffins and naphthenes	.41
37	o-Xylene	.61
38	n-Nonane, C9 naphthenes	.13
39	C9 aromatics; C10 i-para. and naphthenes	2.17
40	n-C10; C9, C10 arom.; C10, C11 i-para., naph.	2.43
41	C12 hydrocarbons	4.04
42	Light naphthenes	51.20
43	Coke	2.12

PRODUCT DISTRIBUTION FOR RUN I.D.: N_1-O-3

NO.	COMPOUND(S)	wt%
1	Methane	3.34
2	Ethylene	5.30
3	Ethane	1.52
4	Propylene	5.34
5	Propane	.83
6	i-Butane	1.34
7	i-Butylene	1.93
8	1-Butene	0.00
9	n-Butane	.30
10	t,2-Butene	.48
11	c,2-Butene	.38
12	3-Methyl-1-butene	.03
13	i-Pentane	1.39
14	C5 olefins	.22
15	n-Pentane	.10
16	C5 olefins, naphthenes; C6 olefins, i-para.	2.36
17	2- and 3-methylpentane, C6 isoparaffins	.59
18	C6 olefins	.05
19	n-Hexane	.04
20	C6 olefins, naph.; C7 olef., i-para, naph.	2.36
21	Benzene	5.86
22	C6 naphthene; C7 olefins, i-para., naph.	.31
23	2- and 3-methylhexane, C7 i-paraffins	.57
24	C7 olefins, naph., i-para.; C8 i-para.	.13
25	n-Heptane	.01
26	C7 olefins, naphthenes; C8 i-paraffins	.53
27	toluene	5.01
28	C8 isoparaffins	.01
29	2- and 3-methylheptane; C8 i-paraffins	.09
30	C7 and C8 naphthenes; C9 i-paraffins	.15
31	n-Octane	.04
32	C9 olefins; C8, C9 naph., C9 i-para.	.15
33	Ethylbenzene	1.00
34	C9 naphthenes and i-paraffins	0.00
35	p-Xylene and m-Xylene	2.66
36	C9 i-paraffins and naphthenes	1.15
37	o-Xylene	1.03
38	n-Nonane, C9 naphthenes	.01
39	C9 aromatics; C10 i-para. and naphthenes	2.97
40	n-C10; C9, C10 arom.; C10, C11 i-para., naph.	2.26
41	C12 hydrocarbons	4.26
42	Light naphthenes	41.66
43	Coke	2.22

PRODUCT DISTRIBUTION FOR RUN I.D.: N_1-O-4

NO.	COMPOUND(S)	wt%
1	Methane	2.90
2	Ethylene	4.91
3	Ethane	1.96
4	Propylene	6.25
5	Propane	1.63
6	i-Butane	2.77
7	i-Butylene	3.15
8	1-Butene	1.49
9	n-Butane	.83
10	t,2-Butene	.82
11	c,2-Butene	.61
12	3-Methyl-1-butene	.04
13	i-Pentane	2.25
14	C5 olefins	.44
15	n-Pentane	.18
16	C5 olefins, naphthenes; C6 olefins, i-para.	3.22
17	2- and 3-methylpentane, C6 isoparaffins	1.04
18	C6 olefins	.28
19	n-Hexane	.08
20	C6 olefins, naph.; C7 olef., i-para, naph.	4.64
21	Benzene	3.26
22	C6 naphthene; C7 olefins, i-para., naph.	.75
23	2- and 3-methylhexane, C7 i-paraffins	1.64
24	C7 olefins, naph., i-para.; C8 i-para.	.47
25	n-Heptane	.03
26	C7 olefins, naphthenes; C8 i-paraffins	1.37
27	toluene	3.67
28	C8 isoparaffins	.14
29	2- and 3-methylheptane; C8 i-paraffins	.35
30	C7 and C8 naphthenes; C9 i-paraffins	.47
31	n-Octane	.02
32	C9 olefins; C8, C9 naph., C9 i-para.	.22
33	Ethylbenzene	1.36
34	C9 naphthenes and i-paraffins	0.00
35	p-Xylene and m-Xylene	2.48
36	C9 i-paraffins and naphthenes	.57
37	o-Xylene	.97
38	n-Nonane, C9 naphthenes	.15
39	C9 aromatics; C10 i-para. and naphthenes	3.37
40	n-C10; C9, C10 arom.; C10, C11 i-para., naph.	3.61
41	C12 hydrocarbons	3.87
42	Light naphthenes	28.35
43	Coke	3.40

PRODUCT DISTRIBUTION FOR RUN I.D.: N_1-O-5

NO.	COMPOUND(S)	wt%
1	Methane	2.19
2	Ethylene	4.10
3	Ethane	1.25
4	Propylene	5.01
5	Propane	1.18
6	i-Butane	2.04
7	i-Butylene	1.83
8	1-Butene	1.55
9	n-Butane	.57
10	t,2-Butene	.60
11	c,2-Butene	.46
12	3-Methyl-1-butene	.04
13	i-Pentane	1.50
14	C5 olefins	.34
15	n-Pentane	.14
16	C5 olefins, naphthenes; C6 olefins, i-para.	2.71
17	2- and 3-methylpentane, C6 isoparaffins	.56
18	C6 olefins	.14
19	n-Hexane	.06
20	C6 olefins, naph.; C7 olef., i-para, naph.	2.76
21	Benzene	3.86
22	C6 naphthene; C7 olefins, i-para., naph.	.45
23	2- and 3-methylhexane, C7 i-paraffins	1.00
24	C7 olefins, naph., i-para.; C8 i-para.	.14
25	n-Heptane	.02
26	C7 olefins, naphthenes; C8 i-paraffins	.47
27	toluene	4.43
28	C8 isoparaffins	.03
29	2- and 3-methylheptane; C8 i-paraffins	.08
30	C7 and C8 naphthenes; C9 i-paraffins	.08
31	n-Octane	.02
32	C9 olefins; C8, C9 naph., C9 i-para.	.15
33	Ethylbenzene	1.60
34	C9 naphthenes and i-paraffins	0.00
35	p-Xylene and m-Xylene	2.49
36	C9 i-paraffins and naphthenes	.54
37	o-Xylene	.98
38	n-Nonane, C9 naphthenes	.04
39	C9 aromatics; C10 i-para. and naphthenes	2.65
40	n-C10; C9, C10 arom.; C10, C11 i-para., naph.	2.25
41	C12 hydrocarbons	3.08
42	Light naphthenes	45.95
43	Coke	.65

PRODUCT DISTRIBUTION FOR RUN I.D.: N_1-O-6

NO.	COMPOUND(S)	wt%
1	Methane	2.54
2	Ethylene	4.61
3	Ethane	1.87
4	Propylene	5.90
5	Propane	2.12
6	i-Butane	3.21
7	i-Butylene	2.05
8	1-Butene	1.34
9	n-Butane	1.02
10	t,2-Butene	.87
11	c,2-Butene	.65
12	3-Methyl-1-butene	.03
13	i-Pentane	2.03
14	C5 olefins	.29
15	n-Pentane	.20
16	C5 olefins, naphthenes; C6 olefins, i-para.	2.85
17	2- and 3-methylpentane, C6 isoparaffins	.81
18	C6 olefins	.12
19	n-Hexane	.08
20	C6 olefins, naph.; C7 olef., i-para, naph.	3.46
21	Benzene	3.37
22	C6 naphthene; C7 olefins, i-para., naph.	.64
23	2- and 3-methylhexane, C7 i-paraffins	1.29
24	C7 olefins, naph., i-para.; C8 i-para.	.20
25	n-Heptane	.03
26	C7 olefins, naphthenes; C8 i-paraffins	.77
27	toluene	4.46
28	C8 isoparaffins	.05
29	2- and 3-methylheptane; C8 i-paraffins	.18
30	C7 and C8 naphthenes; C9 i-paraffins	.19
31	n-Octane	.01
32	C9 olefins; C8, C9 naph., C9 i-para.	.16
33	Ethylbenzene	1.85
34	C9 naphthenes and i-paraffins	0.00
35	p-Xylene and m-Xylene	2.73
36	C9 i-paraffins and naphthenes	.49
37	o-Xylene	1.04
38	n-Nonane, C9 naphthenes	.05
39	C9 aromatics; C10 i-para. and naphthenes	3.28
40	n-C10; C9, C10 arom.; C10, C11 i-para., naph.	3.18
41	C12 hydrocarbons	3.38
42	Light naphthenes	35.80
43	Coke	.80

PRODUCT DISTRIBUTION FOR RUN I.D.: N_1-O-7

NO.	COMPOUND(S)	wt%
1	Methane	4.60
2	Ethylene	6.44
3	Ethane	2.17
4	Propylene	6.44
5	Propane	1.25
6	i-Butane	1.51
7	i-Butylene	2.21
8	1-Butene	1.42
9	n-Butane	.40
10	t,2-Butene	.57
11	c,2-Butene	.45
12	3-Methyl-1-butene	.03
13	i-Pentane	1.31
14	C5 olefins	.20
15	n-Pentane	.12
16	C5 olefins, naphthenes; C6 olefins, i-para.	2.73
17	2- and 3-methylpentane, C6 isoparaffins	.45
18	C6 olefins	.04
19	n-Hexane	.04
20	C6 olefins, naph.; C7 olef., i-para, naph.	1.92
21	Benzene	8.40
22	C6 naphthene; C7 olefins, i-para., naph.	.29
23	2- and 3-methylhexane, C7 i-paraffins	.39
24	C7 olefins, naph., i-para.; C8 i-para.	.06
25	n-Heptane	0.00
26	C7 olefins, naphthenes; C8 i-paraffins	.19
27	toluene	7.56
28	C8 isoparaffins	0.00
29	2- and 3-methylheptane; C8 i-paraffins	.02
30	C7 and C8 naphthenes; C9 i-paraffins	0.00
31	n-Octane	.06
32	C9 olefins; C8, C9 naph., C9 i-para.	.12
33	Ethylbenzene	1.46
34	C9 naphthenes and i-paraffins	0.00
35	p-Xylene and m-Xylene	3.34
36	C9 i-paraffins and naphthenes	1.54
37	o-Xylene	1.28
38	n-Nonane, C9 naphthenes	.01
39	C9 aromatics; C10 i-para. and naphthenes	3.27
40	n-C10; C9, C10 arom.; C10, C11 i-para., naph.	2.24
41	C12 hydrocarbons	4.69
42	Light naphthenes	29.93
43	Coke	.81

PRODUCT DISTRIBUTION FOR RUN I.D.: N_1-O-8

NO.	COMPOUND(S)	wt%
1	Methane	3.01
2	Ethylene	4.95
3	Ethane	2.13
4	Propylene	6.74
5	Propane	3.53
6	i-Butane	5.45
7	i-Butylene	2.29
8	1-Butene	1.06
9	n-Butane	1.83
10	t,2-Butene	.88
11	c,2-Butene	.66
12	3-Methyl-1-butene	.02
13	i-Pentane	3.09
14	C5 olefins	.23
15	n-Pentane	.31
16	C5 olefins, naphthenes; C6 olefins, i-para.	2.63
17	2- and 3-methylpentane, C6 isoparaffins	1.20
18	C6 olefins	.06
19	n-Hexane	.13
20	C6 olefins, naph.; C7 olef., i-para, naph.	4 21
21	Benzene	3.44
22	C6 naphthene; C7 olefins, i-para., naph.	.66
23	2- and 3-methylhexane, C7 i-paraffins	1.01
24	C7 olefins, naph., i-para.; C8 i-para.	.25
25	n-Heptane	.03
26	C7 olefins, naphthenes; C8 i-paraffins	.77
27	toluene	5.74
28	C8 isoparaffins	.06
29	2- and 3-methylheptane; C8 i-paraffins	.14
30	C7 and C8 naphthenes; C9 i-paraffins	.14
31	n-Octane	.02
32	C9 olefins; C8, C9 naph., C9 i-para.	.07
33	Ethylbenzene	2.39
34	C9 naphthenes and i-paraffins	0.00
35	p-Xylene and m-Xylene	3.79
36	C9 i-paraffins and naphthenes	.47
37	o-Xylene	1.35
38	n-Nonane, C9 naphthenes	.01
39	C9 aromatics; C10 i-para. and naphthenes	3.97
40	n-C10; C9, C10 arom.; C10, C11 i-para., naph.	3.13
41	C12 hydrocarbons	3.37
42	Light naphthenes	23.50
43	Coke	1.31

PRODUCT DISTRIBUTION FOR RUN I.D.: N_1-G-1

NO.	COMPOUND(S)	wt%
1	Methane	.06
2	Ethylene	.58
3	Ethane	.25
4	Propylene	1.25
5	Propane	.98
6	i-Butane	2.16
7	i-Butylene	.35
8	1-Butene	.22
9	n-Butane	.81
10	t,2-Butene	.28
11	c,2-Butene	.21
12	3-Methyl-1-butene	.01
13	i-Pentane	3.00
14	C5 olefins	.10
15	n-Pentane	.32
16	C5 olefins, naphthenes; C6 olefins, i-para.	1.90
17	2- and 3-methylpentane, C6 isoparaffins	1.52
18	C6 olefins	.04
19	n-Hexane	.15
20	C6 olefins, naph.; C7 olef., i-para, naph.	6.77
21	Benzene	1.14
22	C6 naphthene; C7 olefins, i-para., naph.	.95
23	2- and 3-methylhexane, C7 i-paraffins	1.64
24	C7 olefins, naph., i-para.; C8 i-para.	.49
25	n-Heptane	.03
26	C7 olefins, naphthenes; C8 i-paraffins	2.22
27	toluene	2.32
28	C8 isoparaffins	.11
29	2- and 3-methylheptane; C8 i-paraffins	.57
30	C7 and C8 naphthenes; C9 i-paraffins	.69
31	n-Octane	.02
32	C9 olefins; C8, C9 naph., C9 i-para.	.47
33	Ethylbenzene	1.13
34	C9 naphthenes and i-paraffins	0.00
35	p-Xylene and m-Xylene	2.15
36	C9 i-paraffins and naphthenes	.25
37	o-Xylene	.83
38	n-Nonane, C9 naphthenes	.11
39	C9 aromatics; C10 i-para. and naphthenes	2.11
40	n-C10; C9, C10 arom.; C10, C11 i-para., naph.	4.19
41	C12 hydrocarbons	11.82
42	Light naphthenes	42.69
43	Coke	3.13

PRODUCT DISTRIBUTION FOR RUN I.D.: N_1-G-2

NO.	COMPOUND(S)	wt%
1	Methane	.88
2	Ethylene	1.64
3	Ethane	.51
4	Propylene	1.77
5	Propane	.46
6	i-Butane	.67
7	i-Butylene	.65
8	1-Butene	.53
9	n-Butane	.26
10	t,2-Butene	.18
11	c,2-Butene	.14
12	3-Methyl-1-butene	.06
13	i-Pentane	2.41
14	C5 olefins	.43
15	n-Pentane	.24
16	C5 olefins, naphthenes; C6 olefins, i-para.	3.73
17	2- and 3-methylpentane, C6 isoparaffins	1.10
18	C6 olefins	.28
19	n-Hexane	.12
20	C6 olefins, naph.; C7 olef., i-para, naph.	4.39
21	Benzene	6.34
22	C6 naphthene; C7 olefins, i-para., naph.	.67
23	2- and 3-methylhexane, C7 i-paraffins	1.32
24	C7 olefins, naph., i-para.; C8 i-para.	.07
25	n-Heptane	.02
26	C7 olefins, naphthenes; C8 i-paraffins	.93
27	toluene	6.79
28	C8 isoparaffins	.04
29	2- and 3-methylheptane; C8 i-paraffins	.14
30	C7 and C8 naphthenes; C9 i-paraffins	.22
31	n-Octane	.04
32	C9 olefins; C8, C9 naph., C9 i-para.	.19
33	Ethylbenzene	1.82
34	C9 naphthenes and i-paraffins	0.00
35	p-Xylene and m-Xylene	3.90
36	C9 i-paraffins and naphthenes	1.91
37	o-Xylene	1.46
38	n-Nonane, C9 naphthenes	.07
39	C9 aromatics; C10 i-para. and naphthenes	3.96
40	n-C10; C9, C10 arom.; C10, C11 i-para., naph.	3.11
41	C12 hydrocarbons	5.03
42	Light naphthenes	37.73
43	Coke	3.80

PRODUCT DISTRIBUTION FOR RUN I.D.: N_1-G-3

NO.	COMPOUND(S)	wt%
1	Methane	.16
2	Ethylene	.65
3	Ethane	.26
4	Propylene	1.47
5	Propane	1.33
6	i-Butane	2.93
7	i-Butylene	.39
8	1-Butene	.10
9	n-Butane	1.18
10	t,2-Butene	.36
11	c,2-Butene	.26
12	3-Methyl-1-butene	.01
13	i-Pentane	4.11
14	C5 olefins	.10
15	n-Pentane	.46
16	C5 olefins, naphthenes; C6 olefins, i-para.	2.42
17	2- and 3-methylpentane, C6 isoparaffins	2.16
18	C6 olefins	.02
19	n-Hexane	.20
20	C6 olefins, naph.; C7 olef., i-para, naph.	9.52
21	Benzene	1.25
22	C6 naphthene; C7 olefins, i-para., naph.	1.32
23	2- and 3-methylhexane, C7 i-paraffins	2.22
24	C7 olefins, naph., i-para.; C8 i-para.	.70
25	n-Heptane	.04
26	C7 olefins, naphthenes; C8 i-paraffins	3.12
27	toluene	2.76
28	C8 isoparaffins	.13
29	2- and 3-methylheptane; C8 i-paraffins	.84
30	C7 and C8 naphthenes; C9 i-paraffins	.96
31	n-Octane	.02
32	C9 olefins; C8, C9 naph., C9 i-para.	.68
33	Ethylbenzene	1.46
34	C9 naphthenes and i-paraffins	.02
35	p-Xylene and m-Xylene	2.78
36	C9 i-paraffins and naphthenes	.31
37	o-Xylene	1.05
38	n-Nonane, C9 naphthenes	.13
39	C9 aromatics; C10 i-para. and naphthenes	4.07
40	n-C10; C9, C10 arom.; C10, C11 i-para., naph.	4.46
41	C12 hydrocarbons	8.74
42	Light naphthenes	30.63
43	Coke	4.20

PRODUCT DISTRIBUTION FOR RUN I.D.: N_1-G-4

NO.	COMPOUND(S)	wt%
1	Methane	1.04
2	Ethylene	1.99
3	Ethane	.68
4	Propylene	2.57
5	Propane	.97
6	i-Butane	1.66
7	i-Butylene	.88
8	1-Butene	.83
9	n-Butane	.65
10	t,2-Butene	.31
11	c,2-Butene	.24
12	3-Methyl-1-butene	.05
13	i-Pentane	3.42
14	C5 olefins	.38
15	n-Pentane	.36
16	C5 olefins, naphthenes; C6 olefins, i-para.	3.73
17	2- and 3-methylpentane, C6 isoparaffins	1.60
18	C6 olefins	.17
19	n-Hexane	.15
20	C6 olefins, naph.; C7 olef., i-para, naph.	6.78
21	Benzene	3.99
22	C6 naphthene; C7 olefins, i-para., naph.	1.01
23	2- and 3-methylhexane, C7 i-paraffins	2.18
24	C7 olefins, naph., i-para.; C8 i-para.	.06
25	n-Heptane	.03
26	C7 olefins, naphthenes; C8 i-paraffins	1.70
27	toluene	6.37
28	C8 isoparaffins	.10
29	2- and 3-methylheptane; C8 i-paraffins	.28
30	C7 and C8 naphthenes; C9 i-paraffins	.35
31	n-Octane	.02
32	C9 olefins; C8, C9 naph., C9 i-para.	.28
33	Ethylbenzene	2.18
34	C9 naphthenes and i-paraffins	0.00
35	p-Xylene and m-Xylene	4.54
36	C9 i-paraffins and naphthenes	.83
37	o-Xylene	1.70
38	n-Nonane, C9 naphthenes	.09
39	C9 aromatics; C10 i-para. and naphthenes	4.81
40	n-C10; C9, C10 arom.; C10, C11 i-para., naph.	4.14
41	C12 hydrocarbons	5.90
42	Light naphthenes	26.14
43	Coke	4.84

PRODUCT DISTRIBUTION FOR RUN I.D.: N_1-G-5

NO.	COMPOUND(S)	wt%
1	Methane	1.35
2	Ethylene	2.18
3	Ethane	.86
4	Propylene	3.04
5	Propane	1.95
6	i-Butane	3.55
7	i-Butylene	1.01
8	1-Butene	.86
9	n-Butane	1.51
10	t,2-Butene	.57
11	c,2-Butene	.43
12	3-Methyl-1-butene	.03
13	i-Pentane	3.49
14	C5 olefins	.31
15	n-Pentane	.45
16	C5 olefins, naphthenes; C6 olefins, i-para.	3.12
17	2- and 3-methylpentane, C6 isoparaffins	1.49
18	C6 olefins	.16
19	n-Hexane	.19
20	C6 olefins, naph.; C7 olef., i-para, naph.	5.35
21	Benzene	3.56
22	C6 naphthene; C7 olefins, i-para., naph.	.81
23	2- and 3-methylhexane, C7 i-paraffins	1.92
24	C7 olefins, naph., i-para.; C8 i-para.	.08
25	n-Heptane	.01
26	C7 olefins, naphthenes; C8 i-paraffins	1.09
27	toluene	6.12
28	C8 isoparaffins	.10
29	2- and 3-methylheptane; C8 i-paraffins	.17
30	C7 and C8 naphthenes; C9 i-paraffins	.22
31	n-Octane	.01
32	C9 olefins; C8, C9 naph., C9 i-para.	.28
33	Ethylbenzene	2.46
34	C9 naphthenes and i-paraffins	0.00
35	p-Xylene and m-Xylene	3.85
36	C9 i-paraffins and naphthenes	.34
37	o-Xylene	1.46
38	n-Nonane, C9 naphthenes	.06
39	C9 aromatics; C10 i-para. and naphthenes	3.37
40	n-C10; C9, C10 arom.; C10, C11 i-para., naph.	2.87
41	C12 hydrocarbons	5.97
42	Light naphthenes	31.75
43	Coke	1.60

PRODUCT DISTRIBUTION FOR RUN I.D.: N_1-G-6

NO.	COMPOUND(S)	wt%
1	Methane	2.84
2	Ethylene	3.96
3	Ethane	1.63
4	Propylene	4.08
5	Propane	1.43
6	i-Butane	1.36
7	i-Butylene	1.39
8	1-Butene	.92
9	n-Butane	.56
10	t,2-Butene	.36
11	c,2-Butene	.27
12	3-Methyl-1-butene	.03
13	i-Pentane	1.97
14	C5 olefins	.33
15	n-Pentane	.25
16	C5 olefins, naphthenes; C6 olefins, i-para.	3.39
17	2- and 3-methylpentane, C6 isoparaffins	.68
18	C6 olefins	.10
19	n-Hexane	.09
20	C6 olefins, naph.; C7 olef., i-para, naph.	2.48
21	Benzene	9.72
22	C6 naphthene; C7 olefins, i-para., naph.	.38
23	2- and 3-methylhexane, C7 i-paraffins	.59
24	C7 olefins, naph., i-para.; C8 i-para.	.03
25	n-Heptane	.01
26	C7 olefins, naphthenes; C8 i-paraffins	.33
27	toluene	10.20
28	C8 isoparaffins	.01
29	2- and 3-methylheptane; C8 i-paraffins	.02
30	C7 and C8 naphthenes; C9 i-paraffins	.06
31	n-Octane	.06
32	C9 olefins; C8, C9 naph., C9 i-para.	.10
33	Ethylbenzene	1.92
34	C9 naphthenes and i-paraffins	0.00
35	p-Xylene and m-Xylene	4.14
36	C9 i-paraffins and naphthenes	2.05
37	o-Xylene	1.53
38	n-Nonane, C9 naphthenes	.02
39	C9 aromatics; C10 i-para. and naphthenes	3.43
40	n-C10; C9, C10 arom.; C10, C11 i-para., naph.	2.28
41	C12 hydrocarbons	5.35
42	Light naphthenes	27.49
43	Coke	2.11

PRODUCT DISTRIBUTION FOR RUN I.D.: N_1-G-7

NO.	COMPOUND(S)	wt%
1	Methane	1.27
2	Ethylene	2.10
3	Ethane	.94
4	Propylene	3.07
5	Propane	2.81
6	i-Butane	4.65
7	i-Butylene	.91
8	1-Butene	.51
9	n-Butane	2.15
10	t,2-Butene	.60
11	c,2-Butene	.44
12	3-Methyl-1-butene	.02
13	i-Pentane	4.80
14	C5 olefins	.23
15	n-Pentane	.60
16	C5 olefins, naphthenes; C6 olefins, i-para.	3.04
17	2- and 3-methylpentane, C6 isoparaffins	2.06
18	C6 olefin	0.00
19	n-Hexane	.26
20	C6 olefins, naph.; C7 olef., i-para, naph.	6.80
21	Benzene	3.15
22	C6 naphthene; C7 olefins, i-para., naph.	.96
23	2- and 3-methylhexane, C7 i-paraffins	1.85
24	C7 olefins, naph., i-para.; C8 i-para.	.07
25	n-Heptane	.04
26	C7 olefins, naphthenes; C8 i-paraffins	1.25
27	toluene	6.54
28	C8 isoparaffins	.08
29	2- and 3-methylheptane; C8 i-paraffins	.21
30	C7 and C8 naphthenes; C9 i-paraffins	.18
31	n-Octane	0.00
32	C9 olefins; C8, C9 naph., C9 i-para.	.23
33	Ethylbenzene	2.95
34	C9 naphthenes and i-paraffins	0.00
35	p-Xylene and m-Xylene	4.61
36	C9 i-paraffins and naphthenes	.21
37	o-Xylene	1.69
38	n-Nonane, C9 naphthenes	.03
39	C9 aromatics; C10 i-para. and naphthenes	3.84
40	n-C10; C9, C10 arom.; C10, C11 i-para., naph.	2.75
41	C12 hydrocarbons	4.91
42	Light naphthenes	25.03
43	Coke	2.17

PRODUCT DISTRIBUTION FOR RUN I.D.: N_1-G-8

NO.	COMPOUND(S)	wt%
1	Methane	3.23
2	Ethylene	5.19
3	Ethane	1.78
4	Propylene	4.74
5	Propane	2.04
6	i-Butane	2.32
7	i-Butylene	1.56
8	1-Butene	1.76
9	n-Butane	1.05
10	t,2-Butene	.43
11	c,2-Butene	.33
12	3-Methyl-1-butene	.04
13	i-Pentane	3.03
14	C5 olefins	.24
15	n-Pentane	.41
16	C5 olefins, naphthenes; C6 olefins, i-para.	2.68
17	2- and 3-methylpentane, C6 isoparaffins	1.11
18	C6 olefins	.07
19	n-Hexane	.14
20	C6 olefins, naph.; C7 olef., i-para, naph.	3.55
21	Benzene	10.33
22	C6 naphthene; C7 olefins, i-para., naph.	.52
23	2- and 3-methylhexane, C7 i-paraffins	.99
24	C7 olefins, naph., i-para.; C8 i-para.	0.00
25	n-Heptane	.04
26	C7 olefins, naphthenes; C8 i-paraffins	.39
27	toluene	10.56
28	C8 isoparaffins	0.00
29	2- and 3-methylheptane; C8 i-paraffins	.04
30	C7 and C8 naphthenes; C9 i-paraffins	0.00
31	n-Octane	.07
32	C9 olefins; C8, C9 naph., C9 i-para.	.08
33	Ethylbenzene	2.33
34	C9 naphthenes and i-paraffins	0.00
35	p-Xylene and m-Xylene	4.35
36	C9 i-paraffins and naphthenes	1.75
37	o-Xylene	1.78
38	n-Nonane, C9 naphthenes	.03
39	C9 aromatics; C10 i-para. and naphthenes	3.87
40	n-C10; C9, C10 arom.; C10, C11 i-para., naph.	1.76
41	C12 hydrocarbons	5.17
42	Light naphthenes	17.94
43	Coke	2.29

PRODUCT DISTRIBUTION FOR RUN I.D.: A_1-O-1

NO.	COMPOUND(S)	wt%
1	Methane	1.30
2	Ethylene	2.80
3	Ethane	.86
4	Propylene	2.48
5	Propane	.24
6	i-Butane	.36
7	i-Butylene	1.13
8	1-Butene	.53
9	n-Butane	.05
10	t,2-Butene	.28
11	c,2-Butene	.22
12	3-Methyl-1-butene	.03
13	i-Pentane	.41
14	C5 olefins	.29
15	n-Pentane	.03
16	C5 olefins, naphthenes; C6 olefins, i-para.	.99
17	2- and 3-methylpentane, C6 isoparaffins	.36
18	C6 olefins	.09
19	n-Hexane	.03
20	C6 olefins, naph.; C7 olef., i-para, naph.	1.28
21	Benzene	8.93
22	C6 naphthene; C7 olefins, i-para., naph.	.07
23	2- and 3-methylhexane, C7 i-paraffins	.24
24	C7 olefins, naph., i-para.; C8 i-para.	.07
25	n-Heptane	.03
26	C7 olefins, naphthenes; C8 i-paraffins	.06
27	toluene	1.81
28	C8 isoparaffins	0.00
29	2- and 3-methylheptane; C8 i-paraffins	.05
30	C7 and C8 naphthenes; C9 i-paraffins	.02
31	n-Octane	.01
32	C9 olefins; C8, C9 naph., C9 i-para.	0.00
33	Ethylbenzene	.69
34	C9 naphthenes and i-paraffins	0.00
35	p-Xylene and m-Xylene	.30
36	C9 i-paraffins and naphthenes	0.00
37	o-Xylene	2.32
38	n-Nonane, C9 naphthenes	.19
39	C9 aromatics; C10 i-para. and naphthenes	.95
40	n-C10; C9, C10 arom.; C10, C11 i-para., naph.	1.13
41	C12 hydrocarbons	1.57
42	Light aromatics	67.15
43	Coke	.64

PRODUCT DISTRIBUTION FOR RUN I.D.: A_1-O-2

NO.	COMPOUND(S)	wt%
1	Methane	1.53
2	Ethylene	3.14
3	Ethane	1.54
4	Propylene	2.82
5	Propane	.36
6	i-Butane	.39
7	i-Butylene	1.52
8	1-Butene	.55
9	n-Butane	.11
10	t,2-Butene	.44
11	c,2-Butene	.32
12	3-Methyl-1-butene	.03
13	i-Pentane	.40
14	C5 olefins	.63
15	n-Pentane	.17
16	C5 olefins, naphthenes; C6 olefins, i-para.	1.27
17	2- and 3-methylpentane, C6 isoparaffins	.37
18	C6 olefins	.25
19	n-Hexane	.05
20	C6 olefins, naph.; C7 olef., i-para, naph.	2.05
21	Benzene	11.35
22	C6 naphthene; C7 olefins, i-para., naph.	.29
23	2- and 3-methylhexane, C7 i-paraffins	.34
24	C7 olefins, naph., i-para.; C8 i-para.	.17
25	n-Heptane	.02
26	C7 olefins, naphthenes; C8 i-paraffins	.22
27	toluene	2.07
28	C8 isoparaffins	.03
29	2- and 3-methylheptane; C8 i-paraffins	.07
30	C7 and C8 naphthenes; C9 i-paraffins	.12
31	n-Octane	.01
32	C9 olefins; C8, C9 naph., C9 i-para.	.01
33	Ethylbenzene	1.19
34	C9 naphthenes and i-paraffins	0.00
35	p-Xylene and m-Xylene	.26
36	C9 i-paraffins and naphthenes	.01
37	o-Xylene	3.58
38	n-Nonane, C9 naphthenes	.16
39	C9 aromatics; C10 i-para. and naphthenes	1.48
40	n-C10; C9, C10 arom.; C10, C11 i-para., naph.	2.38
41	C12 hydrocarbons	1.35
42	Light aromatics	55.96
43	Coke	.98

PRODUCT DISTRIBUTION FOR RUN I.D.: A_1-O-3

NO.	COMPOUND(S)	wt%
1	Methane	2.23
2	Ethylene	4.41
3	Ethane	1.41
4	Propylene	3.46
5	Propane	0.00
6	i-Butane	.17
7	i-Butylene	1.31
8	1-Butene	.82
9	n-Butane	.10
10	t,2-Butene	.28
11	c,2-Butene	.23
12	3-Methyl-1-butene	.03
13	i-Pentane	.22
14	C5 olefins	.24
15	n-Pentane	.03
16	C5 olefins, naphthenes; C6 olefins, i-para.	1.16
17	2- and 3-methylpentane, C6 isoparaffins	.19
18	C6 olefins	.04
19	n-Hexane	.03
20	C6 olefins, naph.; C7 olef., i-para, naph.	.80
21	Benzene	12.18
22	C6 naphthene; C7 olefins, i-para., naph.	.04
23	2- and 3-methylhexane, C7 i-paraffins	.15
24	C7 olefins, naph., i-para.; C8 i-para.	.02
25	n-Heptane	.01
26	C7 olefins, naphthenes; C8 i-paraffins	.02
27	toluene	3.88
28	C8 isoparaffins	0.00
29	2- and 3-methylheptane; C8 i-paraffins	.03
30	C7 and C8 naphthenes; C9 i-paraffins	0.00
31	n-Octane	0.00
32	C9 olefins; C8, C9 naph., C9 i-para.	.17
33	Ethylbenzene	1.18
34	C9 naphthenes and i-paraffins	0.00
35	p-Xylene and m-Xylene	.45
36	C9 i-paraffins and naphthenes	0.00
37	o-Xylene	4.22
38	n-Nonane, C9 naphthenes	.42
39	C9 aromatics; C10 i-para. and naphthenes	1.18
40	n-C10; C9, C10 arom.; C10, C11 i-para., naph.	1.68
41	C12 hydrocarbons	2.75
42	Light aromatics	53.48
43	Coke	1.01

PRODUCT DISTRIBUTION FOR RUN I.D.: A_1-O-4

NO.	COMPOUND(S)	wt%
1	Methane	2.24
2	Ethylene	3.98
3	Ethane	1.83
4	Propylene	3.48
5	Propane	.41
6	i-Butane	.33
7	i-Butylene	1.66
8	1-Butene	.65
9	n-Butane	.10
10	t,2-Butene	.45
11	c,2-Butene	.34
12	3-Methyl-1-butene	.03
13	i-Pentane	.36
14	C5 olefins	.51
15	n-Pentane	.25
16	C5 olefins, naphthenes; C6 olefins, i-para.	1.30
17	2- and 3-methylpentane, C6 isoparaffins	.31
18	C6 olefins	.14
19	n-Hexane	.04
20	C6 olefins, naph.; C7 olef., i-para, naph.	1.53
21	Benzene	12.39
22	C6 naphthene; C7 olefins, i-para., naph.	.23
23	2- and 3-methylhexane, C7 i-paraffins	.20
24	C7 olefins, naph., i-para.; C8 i-para.	.08
25	n-Heptane	.02
26	C7 olefins, naphthenes; C8 i-paraffins	.08
27	toluene	3.05
28	C8 isoparaffins	.01
29	2- and 3-methylheptane; C8 i-paraffins	.05
30	C7 and C8 naphthenes; C9 i-paraffins	.03
31	n-Octane	.01
32	C9 olefins; C8, C9 naph., C9 i-para.	0.00
33	Ethylbenzene	1.38
34	C9 naphthenes and i-paraffins	0.00
35	p-Xylene and m-Xylene	.33
36	C9 i-paraffins and naphthenes	0.00
37	o-Xylene	4.17
38	n-Nonane, C9 naphthenes	.17
39	C9 aromatics; C10 i-para. and naphthenes	1.43
40	n-C10; C9, C10 arom.; C10, C11 i-para., naph.	2.32
41	C12 hydrocarbons	1.82
42	Light aromatics	51.12
43	Coke	1.20

PRODUCT DISTRIBUTION FOR RUN I.D.: A_1-O-5

NO.	COMPOUND(S)	wt%
1	Methane	1.65
2	Ethylene	3.51
3	Ethane	1.14
4	Propylene	2.83
5	Propane	.31
6	i-Butane	.34
7	i-Butylene	1.20
8	1-Butene	.61
9	n-Butane	.12
10	t,2-Butene	.29
11	c,2-Butene	.22
12	3-Methyl-1-butene	.02
13	i-Pentane	.37
14	C5 olefins	.31
15	n-Pentane	.04
16	C5 olefins, naphthenes; C6 olefins, i-para.	1.01
17	2- and 3-methylpentane, C6 isoparaffins	.29
18	C6 olefins	.11
19	n-Hexane	.03
20	C6 olefins, naph.; C7 olef., i-para, naph.	1.14
21	Benzene	9.70
22	C6 naphthene; C7 olefins, i-para., naph.	.11
23	2- and 3-methylhexane, C7 i-paraffins	.13
24	C7 olefins, naph., i-para.; C8 i-para.	.05
25	n-Heptane	.01
26	C7 olefins, naphthenes; C8 i-paraffins	.02
27	toluene	2.29
28	C8 isoparaffins	0.00
29	2- and 3-methylheptane; C8 i-paraffins	.02
30	C7 and C8 naphthenes; C9 i-paraffins	.02
31	n-Octane	0.00
32	C9 olefins; C8, C9 naph., C9 i-para.	.06
33	Ethylbenzene	1.02
34	C9 naphthenes and i-paraffins	0.00
35	p-Xylene and m-Xylene	.29
36	C9 i-paraffins and naphthenes	0.00
37	o-Xylene	3.48
38	n-Nonane, C9 naphthenes	.21
39	C9 aromatics; C10 i-para. and naphthenes	1.07
40	n-C10; C9, C10 arom.; C10, C11 i-para., naph.	1.66
41	C12 hydrocarbons	2.05
42	Light aromatics	61.72
43	Coke	.55

PRODUCT DISTRIBUTION FOR RUN I.D.: A_1-O-6

NO.	COMPOUND(S)	wt%
1	Methane	1.58
2	Ethylene	2.58
3	Ethane	1.38
4	Propylene	3.27
5	Propane	.57
6	i-Butane	.87
7	i-Butylene	1.74
8	1-Butene	.43
9	n-Butane	.26
10	t,2-Butene	.61
11	c,2-Butene	.46
12	3-Methyl-1-butene	.04
13	i-Pentane	.74
14	C5 olefins	.63
15	n-Pentane	.14
16	C5 olefins, naphthenes; C6 olefins, i-para.	1.36
17	2- and 3-methylpentane, C6 isoparaffins	.61
18	C6 olefins	.24
19	n-hexane	.09
20	C6 olefins, naph.; C7 olef., i-para, naph.	2.46
21	Benzene	14.25
22	C6 naphthene; C7 olefins, i-para., naph.	.30
23	2- and 3-methylhexane, C7 i-paraffins	.33
24	C7 olefins, naph., i-para.; C8 i-para.	.16
25	n-Heptane	.02
26	C7 olefins, naphthenes; C8 i-paraffins	.20
27	toluene	2.04
28	C8 isoparaffins	.01
29	2- and 3-methylheptane; C8 i-paraffins	.05
30	C7 and C8 naphthenes; C9 i-paraffins	.10
31	n-Octane	0.00
32	C9 olefins; C8, C9 naph., C9 i-para.	.03
33	Ethylbenzene	1.53
34	C9 naphthenes and i-paraffins	0.00
35	p-Xylene and m-Xylene	.43
36	C9 i-paraffins and naphthenes	0.00
37	o-Xylene	2.23
38	n-Nonane, C9 naphthenes	.22
39	C9 aromatics; C10 i-para. and naphthenes	1.34
40	n-C10; C9, C10 arom.; C10, C11 i-para., naph.	2.14
41	C12 hydrocarbons	1.87
42	Light aromatics	52.10
43	Coke	.60

PRODUCT DISTRIBUTION FOR RUN I.D.: A_1-O-7

NO.	COMPOUND(S)	wt%
1	Methane	2.08
2	Ethylene	3.82
3	Ethane	1.39
4	Propylene	3.39
5	Propane	.41
6	i-Butane	.46
7	i-Butylene	1.63
8	1-Butene	.68
9	n-Butane	.17
10	t,2-Butene	.41
11	c,2-Butene	.32
12	3-Methyl-1-butene	.03
13	i-Pentane	.50
14	C5 olefins	.44
15	n-Pentane	.07
16	C5 olefins, naphthenes; C6 olefins, i-para.	1.51
17	2- and 3-methylpentane, C6 isoparaffins	.42
18	C6 olefins	.14
19	n-Hexane	.05
20	C6 olefins, naph.; C7 olef., i-para, naph.	1.85
21	Benzene	15.05
22	C6 naphthene; C7 olefins, i-para., naph.	.11
23	2- and 3-methylhexane, C7 i-paraffins	.24
24	C7 olefins, naph., i-para.; C8 i-para.	.08
25	n-Heptane	.02
26	C7 olefins, naphthenes; C8 i-paraffins	.07
27	toluene	2.90
28	C8 isoparaffins	0.00
29	2- and 3-methylheptane; C8 i-paraffins	.03
30	C7 and C8 naphthenes; C9 i-paraffins	.02
31	n-Octane	.01
32	C9 olefins; C8, C9 naph., C9 i-para.	.08
33	Ethylbenzene	1.39
34	C9 naphthenes and i-paraffins	0.00
35	p-Xylene and m-Xylene	.38
36	C9 i-paraffins and naphthenes	0.00
37	o-Xylene	3.73
38	n-Nonane, C9 naphthenes	.28
39	C9 aromatics; C10 i-para. and naphthenes	1.44
40	n-C10; C9, C10 arom.; C10, C11 i-para., naph.	1.75
41	C12 hydrocarbons	2.50
42	Light aromatics	49.01
43	Coke	1.13

PRODUCT DISTRIBUTION FOR RUN I.D.: A_1-O-8

NO.	COMPOUND(S)	wt%
1	Methane	2.10
2	Ethylene	3.02
3	Ethane	1.67
4	Propylene	3.95
5	Propane	.72
6	i-Butane	1.04
7	i-Butylene	2.12
8	1-Butene	.53
9	n-Butane	.31
10	t,2-Butene	.72
11	c,2-Butene	.55
12	3-Methyl-1-butene	.05
13	i-Pentane	.75
14	C5 olefins	.58
15	n-Pentane	.16
16	C5 olefins, naphthenes; C6 olefins, i-para.	1.38
17	2- and 3-methylpentane, C6 isoparaffins	.60
18	C6 olefins	.17
19	n-Hexane	.09
20	C6 olefins, naph.; C7 olef., i-para, naph.	2.35
21	Benzene	15.17
22	C6 naphthene; C7 olefins, i-para., naph.	.29
23	2- and 3-methylhexane, C7 i-paraffins	.30
24	C7 olefins, naph., i-para.; C8 i-para.	.12
25	n-Heptane	.03
26	C7 olefins, naphthenes; C8 i-paraffins	.12
27	toluene	2.26
28	C8 isoparaffins	0.00
29	2- and 3-methylheptane; C8 i-paraffins	.06
30	C7 and C8 naphthenes; C9 i-paraffins	.06
31	n-Octane	.02
32	C9 olefins; C8, C9 naph., C9 i-para.	0.00
33	Ethylbenzene	1.59
34	C9 naphthenes and i-paraffins	0.00
35	p-Xylene and m-Xylene	.48
36	C9 i-paraffins and naphthenes	0.00
37	o-Xylene	1.85
38	n-Nonane, C9 naphthenes	.22
39	C9 aromatics; C10 i-para. and naphthenes	1.22
40	n-C10; C9, C10 arom.; C10, C11 i-para., naph.	1.76
41	C12 hydrocarbons	2.07
42	Light aromatics	47.99
43	Coke	1.52

PRODUCT DISTRIBUTION FOR RUN I.D.: A_1-G-1

NO.	COMPOUND(S)	wt%
1	Methane	.46
2	Ethylene	.67
3	Ethane	.37
4	Propylene	1.84
5	Propane	.58
6	i-Butane	1.94
7	i-Butylene	.66
8	1-Butene	.02
9	n-Butane	.53
10	t,2-Butene	.50
11	c,2-Butene	.38
12	3-Methyl-1-butene	.01
13	i-Pentane	2.11
14	C5 olefins	.26
15	n-Pentane	.18
16	C5 olefins, naphthenes; C6 olefins, i-para.	.97
17	2- and 3-methylpentane, C6 isoparaffins	1.71
18	C6 olefins	.01
19	n-Hexane	.17
20	C6 olefins, naph.; C7 olef., i-para, naph.	4.62
21	Benzene	17.71
22	C6 naphthene; C7 olefins, i-para., naph.	.31
23	2- and 3-methylhexane, C7 i-paraffins	.94
24	C7 olefins, naph., i-para.; C8 i-para.	.37
25	n-Heptane	.01
26	C7 olefins, naphthenes; C8 i-paraffins	.31
27	toluene	1.56
28	C8 isoparaffins	.03
29	2- and 3-methylheptane; C8 i-paraffins	.22
30	C7 and C8 naphthenes; C9 i-paraffins	.05
31	n-Octane	.04
32	C9 olefins; C8, C9 naph., C9 i-para.	.04
33	Ethylbenzene	.86
34	C9 naphthenes and i-paraffins	0.00
35	p-Xylene and m-Xylene	.71
36	C9 i-paraffins and naphthenes	.28
37	o-Xylene	.28
38	n-Nonane, C9 naphthenes	.01
39	C9 aromatics; C10 i-para. and naphthenes	1.25
40	n-C10; C9, C10 arom.; C10, C11 i-para., naph.	1.68
41	C12 hydrocarbons	3.13
42	Light aromatics	49.68
43	Coke	2.56

PRODUCT DISTRIBUTION FOR RUN I.D.: A_1-G-2

NO.	COMPOUND(S)	wt%
1	Methane	1.27
2	Ethylene	2.25
3	Ethane	.90
4	Propylene	2.10
5	Propane	.30
6	i-Butane	.30
7	i-Butylene	.71
8	1-Butene	0.00
9	n-Butane	.08
10	t,2-Butene	.17
11	c,2-Butene	.13
12	3-Methyl-1-butene	.03
13	i-Pentane	1.01
14	C5 olefins	.37
15	n-Pentane	.10
16	C5 olefins, naphthenes; C6 olefins, i-para.	1.74
17	2- and 3-methylpentane, C6 isoparaffins	.67
18	C6 olefins	.12
19	n-Hexane	.07
20	C6 olefins, naph.; C7 olef., i-para, naph.	1.85
21	Benzene	14.02
22	C6 naphthene; C7 olefins, i-para., naph.	.14
23	2- and 3-methylhexane, C7 i-paraffins	.36
24	C7 olefins, naph., i-para.; C8 i-para.	.12
25	n-Heptane	.03
26	C7 olefins, naphthenes; C8 i-paraffins	.11
27	toluene	5.35
28	C8 isoparaffins	0.00
29	2- and 3-methylheptane; C8 i-paraffins	.07
30	C7 and C8 naphthenes; C9 i-paraffins	.04
31	n-Octane	.01
32	C9 olefins; C8, C9 naph., C9 i-para.	.07
33	Ethylbenzene	1.67
34	C9 naphthenes and i-paraffins	0.00
35	p-Xylene and m-Xylene	1.19
36	C9 i-paraffins and naphthenes	4.88
37	o-Xylene	.58
38	n-Nonane, C9 naphthenes	.07
39	C9 aromatics; C10 i-para. and naphthenes	2.19
40	n-C10; C9, C10 arom.; C10, C11 i-para., naph.	3.15
41	C12 hydrocarbons	5.62
42	Light aromatics	43.16
43	Coke	3.01

PRODUCT DISTRIBUTION FOR RUN I.D.: A_1-G-3

NO.	COMPOUND(S)	wt%
1	Methane	.32
2	Ethylene	.53
3	Ethane	.28
4	Propylene	2.15
5	Propane	.56
6	i-Butane	2.42
7	i-Butylene	.84
8	1-Butene	0.00
9	n-Butane	.63
10	t,2-Butene	.70
11	c,2-Butene	.53
12	3-Methyl-1-butene	.03
13	i-Pentane	2.51
14	C5 olefins	.23
15	n-Pentane	.21
16	C5 olefins, naphthenes; C6 olefins, i-para.	1.19
17	2- and 3-methylpentane, C6 isoparaffins	2.13
18	C6 olefins	.01
19	n-Hexane	.19
20	C6 olefins, naph.; C7 olef., i-para, naph.	5.96
21	Benzene	21.90
22	C6 naphthene; C7 olefins, i-para., naph.	.37
23	2- and 3-methylhexane, C7 i-paraffins	1.22
24	C7 olefins, naph., i-para.; C8 i-para.	.40
25	n-Heptane	.01
26	C7 olefins, naphthenes; C8 i-paraffins	.40
27	toluene	1.45
28	C8 isoparaffins	.04
29	2- and 3-methylheptane; C8 i-paraffins	.30
30	C7 and C8 naphthenes; C9 i-paraffins	.05
31	n-Octane	.05
32	C9 olefins; C8, C9 naph., C9 i-para.	.09
33	Ethylbenzene	.89
34	C9 naphthenes and i-paraffins	0.00
35	p-Xylene and m-Xylene	.67
36	C9 i-paraffins and naphthenes	.19
37	o-Xylene	.27
38	n-Nonane, C9 naphthenes	.01
39	C9 aromatics; C10 i-para. and naphthenes	1.43
40	n-C10; C9, C10 arom.; C10, C11 i-para., naph.	2.07
41	C12 hydrocarbons	3.14
42	Light aromatics	39.95
43	Coke	3.67

PRODUCT DISTRIBUTION FOR RUN I.D.: A_1-G-4

NO.	COMPOUND(S)	wt%
1	Methane	1.37
2	Ethylene	2.33
3	Ethane	1.00
4	Propylene	2.43
5	Propane	.64
6	i-Butane	1.13
7	i-Butylene	.84
8	1-Butene	.41
9	n-Butane	.35
10	t,2-Butene	.25
11	c,2-Butene	.20
12	3-Methyl-1-butene	.03
13	i-Pentane	2.05
14	C5 olefins	.26
15	n-Pentane	.19
16	C5 olefins, naphthenes; C6 olefins, i-para.	1.03
17	2- and 3-methylpentane, C6 isoparaffins	1.51
18	C6 olefins	.08
19	n-Hexane	.14
20	C6 olefins, naph.; C7 olef., i-para, naph.	3.60
21	Benzene	20.43
22	C6 naphthene; C7 olefins, i-para., naph.	.23
23	2- and 3-methylhexane, C7 i-paraffins	.68
24	C7 olefins, naph., i-para.; C8 i-para.	.18
25	n-Heptane	.05
26	C7 olefins, naphthenes; C8 i-paraffins	.17
27	toluene	3.22
28	C8 isoparaffins	0.00
29	2- and 3-methylheptane; C8 i-paraffins	.18
30	C7 and C8 naphthenes; C9 i-paraffins	.03
31	n-Octane	.03
32	C9 olefins; C8, C9 naph., C9 i-para.	.03
33	Ethylbenzene	.92
34	C9 naphthenes and i-paraffins	0.00
35	p-Xylene and m-Xylene	.97
36	C9 i-paraffins and naphthenes	2.45
37	o-Xylene	.46
38	n-Nonane, C9 naphthenes	.04
39	C9 aromatics; C10 i-para. and naphthenes	1.53
40	n-C10; C9, C10 arom.; C10, C11 i-para., naph.	1.62
41	C12 hydrocarbons	6.83
42	Light aromatics	35.92
43	Coke	4.21

```
      CONV = 100.0 - YO
      IF (NANS.EQ.1) GO TO 44
      GO TO 82
   44 YLCO = 0.0
   45 READ(10,FMT=LABEL) TIME,AREA
      YLCO = YLCO + AREA
      IF(TIME.GE.ELO) GO TO 83
      GO TO 45
   83 CONTINUE
      YHCO = YO - YLCO
   82 CLOSE(10)
      WRITE(1,60) YLG
      WRITE(1,61) YG
      IF (NANS.EQ.1) GO TO 800
      GO TO 801
  800 WRITE(1,72) YLCO
      WRITE(1,73) YHCO
  801 WRITE(1,62) YO
      WRITE(1,63) CONV
      WRITE(1,*) 'DO YOU WANT TO PRINT RESULTS? (1=YES, 2=NO)'
      READ(1,*) NANSW
      IF (NANSW.EQ.2) GO TO 605
      WRITE(6,51) NAME
   51 FORMAT(1X, 'PRODUCT YIELDS FOR RUN #: ',A15,/)
      WRITE(6,60) YLG
   60 FORMAT(5X,' GASES= ',F5.2,'%',/)
      WRITE(6,61) YG
   61 FORMAT(5X,' GASOLINE= ',F5.2,'%',/)
      IF (NANS.EQ.1) GO TO 900
      GO TO 901
  900 WRITE(6,72) YLCO
   72 FORMAT(5X,' LIGHT OIL= ',F5.2,'%',/)
      WRITE(6,73) YHCO
   73 FORMAT(5X,' HEAVY OIL= ',F5.2,'%',/)
  901 WRITE(6,62) YO
   62 FORMAT(5X,' OIL= ',F5.2,'%',/)
      WRITE(6,63) CONV
   63 FORMAT(5X,' CONV= ',F5.2,'%',/)
  605 CONTINUE
  600 FORMAT(3X,F6.2,24X,F7.3)
  500 Format(3x,F6.2,28X,F7.3)
      End
```

PRODUCT DISTRIBUTION FOR RUN I.D.: A_1-G-6

NO.	COMPOUND(S)	wt%
1	Methane	2.39
2	Ethylene	2.54
3	Ethane	1.28
4	Propylene	2.44
5	Propane	.94
6	i-Butane	1.17
7	i-Butylene	.87
8	1-Butene	.26
9	n-Butane	.43
10	t,2-Butene	.26
11	c,2-Butene	.20
12	3-Methyl-1-butene	.03
13	i-Pentane	1.64
14	C5 olefins	.38
15	n-Pentane	.22
16	C5 olefins, naphthenes; C6 olefins, i-para.	1.05
17	2- and 3-methylpentane, C6 isoparaffins	.97
18	C6 olefins	.19
19	n-Hexane	.15
20	C6 olefins, naph.; C7 olef , i-para, naph.	1.96
21	Benzene	18.57
22	C6 naphthene; C7 olefins, i-para., naph.	.15
23	2- and 3-methylhexane, C7 i-paraffins	.31
24	C7 olefins, naph., i-para.; C8 i-para.	.11
25	n-Heptane	.04
26	C7 olefins, naphthenes; C8 i-paraffins	.04
27	toluene	4.16
28	C8 isoparaffins	0.00
29	2- and 3-methylheptane; C8 i-paraffins	.04
30	C7 and C8 naphthenes; C9 i-paraffins	.04
31	n-Octane	.01
32	C9 olefins; C8, C9 naph., C9 i-para.	.10
33	Ethylbenzene	1.46
34	C9 naphthenes and i-paraffins	0.00
35	p-Xylene and m-Xylene	1.05
36	C9 i-paraffins and naphthenes	2.67
37	o-Xylene	.48
38	n-Nonane, C9 naphthenes	.05
39	C9 aromatics; C10 i-para. and naphthenes	1.40
40	n-C10; C9, C10 arom.; C10, C11 i-para., naph.	1.60
41	C12 hydrocarbons	7.34
42	Light aromatics	37.62
43	Coke	3.39

PRODUCT DISTRIBUTION FOR RUN I.D.: A_1-G-7

NO.	COMPOUND(S)	wt%
1	Methane	1.35
2	Ethylene	1.40
3	Ethane	.98
4	Propylene	2.82
5	Propane	1.09
6	i-Butane	2.60
7	i-Butylene	1.08
8	1-Butene	.08
9	n-Butane	.90
10	t,2-Butene	.67
11	c,2-Butene	.51
12	3-Methyl-1-butene	.03
13	i-Pentane	2.51
14	C5 olefins	.32
15	n-Pentane	.30
16	C5 olefins, naphthenes; C6 olefins, i-para.	1.23
17	2- and 3-methylpentane, C6 isoparaffins	1.89
18	C6 olefins	0.00
19	n-Hexane	.25
20	C6 olefins, naph.; C7 olef., i-para, naph.	3.97
21	Benzene	21.[illegible]
22	C6 naphthene; C7 olefins, i-para., naph.	.[illegible]
23	2- and 3-methylhexane, C7 i-paraffins	.74
24	C7 olefins, naph., i-para.; C8 i-para.	.23
25	n-Heptane	.09
26	C7 olefins, naphthenes; C8 i-paraffins	.18
27	toluene	2.86
28	C8 isoparaffins	.01
29	2- and 3-methylheptane; C8 i-paraffins	.14
30	C7 and C8 naphthenes; C9 i-paraffins	.04
31	n-Octane	.03
32	C9 olefins; C8, C9 naph., C9 i-para.	.09
33	Ethylbenzene	1.49
34	C9 naphthenes and i-paraffins	0.00
35	p-Xylene and m-Xylene	.98
36	C9 i-paraffins and naphthenes	.03
37	o-Xylene	.68
38	n-Nonane, C9 naphthenes	.40
39	C9 aromatics; C10 i-para. and naphthenes	1.46
40	n-C10; C9, C10 arom.; C10, C11 i-para., naph.	1.52
41	C12 hydrocarbons	5.07
42	Light aromatics	34.27
43	Coke	4.18

PRODUCT DISTRIBUTION FOR RUN I.D.: A_1-G-8

NO.	COMPOUND(S)	wt%
1	Methane	2.99
2	Ethylene	3.09
3	Ethane	1.57
4	Propylene	2.95
5	Propane	1.08
6	i-Butane	1.21
7	i-Butylene	1.04
8	1-Butene	.42
9	n-Butane	.48
10	t,2-Butene	.26
11	c,2-Butene	.19
12	3-Methyl-1-butene	.01
13	i-Pentane	1.58
14	C5 olefins	.22
15	n-Pentane	.22
16	C5 olefins, naphthenes; C6 olefins, i-para.	.99
17	2- and 3-methylpentane, C6 isoparaffins	.90
18	C6 olefins	.06
19	n-Hexane	.13
20	C6 olefins, naph.; C7 olef., i-para, naph.	1.55
21	Benzene	20.79
22	C6 naphthene; C7 olefins, i-para., naph.	.10
23	2- and 3-methylhexane, C7 i-paraffins	.23
24	C7 olefins, naph., i-para.; C8 i-para.	.06
25	n-Heptane	.03
26	C7 olefins, naphthenes; C8 i-paraffins	.03
27	toluene	4.81
28	C8 isoparaffins	0.00
29	2- and 3-methylheptane; C8 i-paraffins	.04
30	C7 and C8 naphthenes; C9 i-paraffins	.01
31	n-Octane	0.00
32	C9 olefins; C8, C9 naph., C9 i-para.	.09
33	Ethylbenzene	1.36
34	C9 naphthenes and i-paraffins	0.00
35	p-Xylene and m-Xylene	1.10
36	C9 i-paraffins and naphthenes	3.03
37	o-Xylene	.51
38	n-Nonane, C9 naphthenes	.03
39	C9 aromatics; C10 i-para. and naphthenes	1.35
40	n-C10; C9, C10 arom.; C10, C11 i-para., naph.	1.22
41	C12 hydrocarbons	8.38
42	Light aromatics	30.91
43	Coke	4.98

APPENDIX F

MEASUREMENT OF VOLUMES

F.1 MEASUREMENT OF THE REACTOR VOLUME

To find the reactor volume measured volumes of nitrogen gas were injected into the reactor (catalyst loaded in basket) with the 4-port valve in the closed position. The calculated volume then represents the total gas volume in the reactor which includes the volume in the transfer lines from the reactor to the 4PV (<0.2 mL). A gas tight syringe was used to inject a known volume of nitrogen into the reactor and a pressure gauge with readings to 0.25 psig was used to measure the reactor pressure. The following equation was used to calcuate the reactor volume (V_R):

$$V_R = 14.7\ V_{inj} / P_R$$

where P_R is the measured reactor pressure after injection with unit of psig. The following table summarizes the calibration:

V_{inj} (mL)	P_R (psig)	V_R (mL)
10	3.2	45.94
20	6.5	45.23
30	10.0	44.10
50	16.5	44.55
	avg:	44.95 ±0.80 mL

Thus the reactor volume is 45 mL.

F.2 CALIBRATION OF THE VACUUM SYSTEM VOLUME

The vacuum system volume refers to the total system volume except for the reactor with the 4PV closed. The vacuum volume includes the volume associated with the line from V1 to the 4PV, lines 4, 5 and 6, the vacuum chamber and the line leading to V2 (see Figure 3.8 in chapter 3). To find this volume, the reactor was filled with nitrogen gas to a certain pressure which was recorded, then the 4PV was closed. Next, the vacuum system was set to vacuum pressure, which was also recorded. Then the 4PV was opened and the two vessels were allowed to reach equilibrium pressure, which was also recorded. All experiments were done at room temperature. The vacuum system volume (V_V) is calculated by the equilibrium mass balance which sets the moles leaving the reactor equal to the moles entering the vacuum system according to the pressure differences:

$$V_V = V_R * (P_{Ri} - P_f)/(P_{Vi} - P_f)$$

where P_{Ri} is the initial reactor pressure (atm), P_{Vi} is the initial vacuum pressure (atm) and P_f is the final pressure (atm). The following table summarizes the measurements:

note: 1 atm = 1.0 - (25.4/760)*1 in.Hg vac.

and V_R = 45 mL

P_{Ni} (psig)	P_{Vi} (in.Hg vac)	P_f (in.Hg vac)	V_v (mL)
25	17.0	12.0	565.83
25	17.0	12.2	591.30
25	17.0	12.0	591.30
20	16.75	12.7	593.44
20	16.75	12.5	563.37
20	16.75	12.5	563.37
10	16.5	13.75	558.38
10	16.5	13.8	569.55
10	16.5	13.85	581.15
		avg:	575.30 ± 14.0

Thus the vacuum system volume was taken as 575 mL.

APPENDIX G

COMPUTER PROGRAMS

```
      PROGRAM SUM
C
C  THIS PROGRAM SUMS AREAS FROM A RAW GC REPORT FOR THE CASE
   OF CRACKING OF A HEAVY OIL (ie. program calculates heavy
   and light fractions for the unconverted oil)
C
      CHARACTER IN*81, NAME*20
      REAL TIME, AREA
      INTEGER LABEL
C
C  Selection of the Integrator
C
      write(1,*) 'Indicate on which integrator the report was
produced:'
      write(1,*) ' Enter   for 3392A : 1 ;   for 3393A : 2 '
      read (1,*) INT
      if ( INT.eq.1 ) then
         Assign 500 to LABEL
         IS = 2
      else
      Assign 600 to LABEL
         IS = 1
      endif
      Call FPARM(NAME)
      Open(10,File=NAME)
      DO 1 I=1,4
      READ(10,'(A81)') IN
    1 CONTINUE
      YLG = 0.0
      YG = 0.0
      WRITE(1,*) 'ENTER LAST LIGHT PEAK RETENTION TIME'
      READ(1,*) ELG
      WRITE(1,*) 'ENTER LAST GASOLINE PEAK RETENTION TIME'
      READ(1,*) EG
      WRITE(1,*)  'DO  YOU  NEED  TO  ASSESS  LIGHT/HEAVY  OIL
YIELDS'
      WRITE(1,*) '1=YES, 2=NO'
      READ(1,*) NANS
      IF (NANS.EQ.1) GO TO 2
      GO TO 3
    2 WRITE(1,*) 'ENTER LAST LIGHT OIL PEAK RETENTION TIME'
    READ(1,*) ELO
    3 CONTINUE
    5 READ(10,FMT=LABEL) TIME, AREA
      YLG =YLG + AREA
      IF (TIME.GE.ELG) GO TO 30
      GO TO 5
   30 CONTINUE
   40 READ (10,FMT=LABEL) TIME, AREA
      YG = YG + AREA
      IF (TIME.GE.EG) GO TO 35
      GO TO 40
   35 CONTINUE
      YO = 100.0 - (YG + YLG)
```

```
      CONV = 100.0 - YO
      IF (NANS.EQ.1) GO TO 44
      GO TO 82
   44 YLCO = 0.0
   45 READ(10,FMT=LABEL) TIME,AREA
      YLCO = YLCO + AREA
      IF(TIME.GE.ELO) GO TO 83
      GO TO 45
   83 CONTINUE
      YHCO = YO - YLCO
   82 CLOSE(10)
      WRITE(1,60) YLG
      WRITE(1,61) YG
      IF (NANS.EQ.1) GO TO 800
      GO TO 801
  800 WRITE(1,72) YLCO
      WRITE(1,73) YHCO
  801 WRITE(1,62) YO
      WRITE(1,63) CONV
      WRITE(1,*) 'DO YOU WANT TO PRINT RESULTS? (1=YES, 2=NO)'
      READ(1,*) NANSW
      IF (NANSW.EQ.2) GO TO 605
      WRITE(6,51) NAME
   51 FORMAT(1X, 'PRODUCT YIELDS FOR RUN #: ',A15,/)
      WRITE(6,60) YLG
   60 FORMAT(5X,' GASES= ',F5.2,'%',/)
      WRITE(6,61) YG
   61 FORMAT(5X,' GASOLINE= ',F5.2,'%',/)
      IF (NANS.EQ.1) GO TO 900
      GO TO 901
  900 WRITE(6,72) YLCO
   72 FORMAT(5X,' LIGHT OIL= ',F5.2,'%',/)
      WRITE(6,73) YHCO
   73 FORMAT(5X,' HEAVY OIL= ',F5.2,'%',/)
  901 WRITE(6,62) YO
   62 FORMAT(5X,' OIL= ',F5.2,'%',/)
      WRITE(6,63) CONV
   63 FORMAT(5X,' CONV= ',F5.2,'%',/)
  605 CONTINUE
  600 FORMAT(3X,F6.2,24X,F7.3)
  500 Format(3x,F6.2,28X,F7.3)
      End
```

```
      PROGRAM CLEAN
c
     This program is an editor that will allow the user to
edit peaks on a GC report by comparing the report to another
that has already been edited.  A menu is produced that shows
retention times and areas for the edited(clean) file and the
raw(dirty) file.  The updated revision file is also displayed.
The user selects an option and then the table is updated.  The
user scrolls through the entire file until the entire file has
been edited.  The final report is stored in a file whose name
must be specified in the runstring.
c
c RUNSTRING: CLEAN (reference file name) (raw file name)
(cleaned name)
c      e.g.    CLEAN          PL.REF            PLGX30_1A.RAW
PLGX30.1A
C
C NOTE: THE REFERENCE REPORT MUST HAVE THE SAME FORMAT AS THE
RAW GC REPORT
C (The cleaned report has a new format).
c
c      Match=line number pointer
c      TimeX,AreaX=Retention times and peak areas
c      Mark=length of reference file[top to last peak]
c      Counter=length of dirty file[top to last peak]
C*************************************************************
c
c  Declare and initialize variables
c
      Character In1(10)*40,In2(10)*40,Cut*13,Ans*3,In*81
      Character Name1*20,Name2*20,NAME3*20
      Real Time1(200),Area1(200)
      Real Time2(300),Area2(300),PArea2(300)
      Real Time3(300),Area3(300)
      Integer Count,I,L,N,Match,Mark,Num,IS, Label
      Data Time1/200*0./
      Data Time2/300*0./
      Data Time3/300*0./
      Count=0
      Match=1
      Mark=0
c
c  Selection of the Integrator
c
      write(1,*) 'Indicate on which integrator the report was
produced:'
      write(1,*) ' Enter   for 3392A : 1 ;   for 3393A : 2 '
      read (1,*) INT
      if ( INT.eq.1 ) then
         Assign 500 to Label
         IS = 2
      else
         Assign 600 to Label
         IS = 1
```

```
      endif
c
c  Open files
c
      Call FPARM(NAME1,NAME2,NAME3)
      Open(10,File=NAME1)
      Open(20,File=NAME2)
      Open(30,FILE=NAME3)
      WRITE(30,100) NAME3
  100 FORMAT(1X,' CLEANED GC REPORT FOR RUN: ',A20)
c
c  Find the length of the reference file, which is the number
of lines from
c  the top of the report to the last peak, and reset the file
to the first
c  peak.
c
    3 Read(10,'(A42)') In
         Mark=Mark+1
         Cut=In(IS:10+IS)
         If(Cut.ne.' TOTAL AREA') Goto 3
         Rewind 10
c
      Do 5 I=1,4
         Read(10,'(A81)') In
    5 Continue
c
      Do 10 I=1,Mark-5
         Read(10,FMT=Label) Time1(I), Area1(I)
   10 Continue
c
c  Find the length of the dirty file and reset to the first
peak
c
   15 Read(20,'(A42)') In
         Count=Count+1
         Cut=In(IS:10+IS)
         If(Cut.ne.' TOTAL AREA') Goto 15
         Rewind 20
c
      Do 20 I=1,4
         Read(20,'(A81)') In
   20 Continue
      Do 25 I=1,Count-5
         Read(20,FMT=Label) Time2(I), Area2(I), PArea2(I)
         Time3(I)=Time2(I)
         Area3(I)=Area2(I)
   25 Continue
c
c  Produce the table showing times,areas, and options of the
screen
c
   30 Write(1,502)
      Write(1,504)
```

```
c
      Do 35 I=Match, Match+10
        Write(1,505) I,Time1(I),Time2(I),Time3(I),Area1(I)
     *,Area2(I),Area3(I)
         If(Count-5.eq.I) then
              Do 37 J=I+1, Match+10
                 Write(1,508) J,Time1(J),Area1(J)
   37        Continue
             Match=J-11
             Goto 39
         Endif
   35 Continue
      Match=I-11
c
   39 Write(1,*) 'POINTER IS SET AT PEAK #', Match
      Write(1,*)  'SELECT  A  NUMBER  FOR  THE  CORRESPONDING
OPTION'
      Write(1,*) 'Save top peak as it is displayed<1>'
      Write(1,*) 'Eliminate peak<2>'
      Write(1,*) 'Insert a blank line<3>'
      Write(1,*) 'Add peaks together<4>'
      Write(1,*) 'Save a number of peaks<5>'
      Read(1,*) Choice
      If(Choice.eq.1) then
         Goto 200
      Elseif(Choice.eq.2) then
         Goto 201
      Elseif(Choice.eq.3) then
         Goto 202
      Elseif(Choice.eq.4) then
         Goto 203
      Elseif(Choice.eq.5) then
         Goto 204
      Else
         Write(1,*) 'WHAT?????!!!!!! YOU MUST SELECT 1-5 SO
TRY AGAIN!'
         Goto 30
      Endif
c
c  This option will save the peak which is indicated by the
pointer in the final file REPORT.  The point is incremented by
1 and the updated table is displayed to the user.
c
  200 Write(30,501) Match, Time2(Match), Area2(Match),
PArea2(Match)
      Match=Match+1
      If(Match.eq.Mark-4) then
         Goto 999
      Endif
      Goto 30
c
c  This option will eliminate the peak in the dirty file at
which the pointer is set.  The pointer is not incremented and
no peak is stored in the final file.  The updated table is
```

```
then displayed.
c
  201 Count=Count-1
      Do 40 K=Match,Count
         Time2(K)=Time2(K+1)
         Area2(K)=Area2(K+1)
         PArea2(K)=PArea2(K+1)
   40 Continue
      Time2(Count+1)=0.
      Area2(Count+1)=0.
      PArea2(Count+1)=0.
      If(Match.eq.Mark-4) then
         Goto 999
      Endif
      Goto 30
c
c  This option inserts a blank line where the pointer is set.
The area is saved in the report file as zero while the
retention time saved is from the reference file.
c
  202 Count=Count+1
      Do 45 K=Count, Match+1, -1
         Time2(K)=Time2(K-1)
         Area2(K)=Area2(K-1)
         PArea2(K)=PArea2(K-1)
   45 Continue
      Time2(Match)=Time2(Match)
      Area2(Match)=0.
      PArea2(Match)=0.
      Write(30,501)   Match,   Time2(Match),   Area2(Match),
PArea2(Match)
      Match=Match+1
      If(Match.eq.Mark-4) then
         Goto 999
      Endif
      Goto 30
c
c  This option adds peaks together.  The summed area is saved
in the report file, while average of the retention times is
saved.
c
  203 Write(1,*) 'How many peaks to add?'
      Read(1,*) N
      Do 46 L=1,N-1
         Time2(Match)=Time2(Match+L)+Time2(Match)
         Area2(Match)=Area2(Match+L)+Area2(Match)
         PArea2(Match)=PArea2(Match+L)+PArea2(Match)
   46 Continue
      Time2(Match)=Time2(Match)/N
      Count=Count-N+1
      Do 47 L=Match+1, Match+N-1
         Time2(L)=0.
         Area2(L)=0.
         PArea2(L)=0.
```

```
   47 Continue
      Do 48 L=Match, Count-6
         Time2(L+1)=Time2(L+N)
         Area2(L+1)=Area2(L+N)
         PArea2(L+1)=PArea2(L+N)
   48 Continue
      Do 55 L=0,N-1
         Time2(Count-4+L)=0.
         Area2(Count-4+L)=0.
         PArea2(Count-4+L)=0.
   55 Continue
      Write(30,501)   Match,   Time2(Match),   Area2(Match),
PArea2(Match)
      Match=Match+1
      If(Match.eq.Mark-4) then
         Goto 999
      Endif
      Goto 30
c
c  This option will save a specified number of peaks as they
are displayed into the report file.  The pointer is updated by
the correct amount, and the new table is displayed.
c
  204 Write(1,*) 'How many peaks do you want saved?'
      Read(1,*) Num
      Do 52 I=Match, Match+Num-1
            Write(30,501) I, Time2(I),Area2(I),PArea2(I)
            If(I.eq.Mark-5' then
               Goto 999
            Endif
   52 Continue
      Match=Match+Num
      Goto 30
c
  999 Write(1,*) 'You have reached the end of the file...'
      Write(1,*) 'To view the final edited file type LI ',
NAME3
c
c  Format Statements and termination of program
      Stop
  600 Format(3X,F6.2,1X,F10.0,13x,F7.3)
  500 Format(3x,F6.2,1x,F10.0,17x,F7.3)
  501 Format(I3,2x,F7.2,2x,I10,2x,F7.3)
  502 Format('         CLEAN FILE = FILE 1',5X,
     *'REVISED FILE = FILE 2'5x,'DIRTY FILE = FILE 3')
  504 Format(/,'Peak    Time 1   Time2   Time3'
     *14x,'Area1       Area2       Area3',/)
                                5                 0                5
Format(1x,I3,2x,F7.3,2x,F7.3,2x,F7.3,7x I10,2x,I10,2x,I10)
  506 Format(I3,3x,F7.3,3x,F7.3,3x,I10,3x,I10)
  507 Format(/,'Peak     Time2   Time3    Area2   Area3',/)
  508 Format(1x,I3,2x,F7.3,25x,I10)
      End
```

```
      PROGRAM MASSBAL
C*****************************************************************
THIS PROGRAM CALCULATES THE MASS BALANCE FOR A CRACKING
RUN DONE IN THE RISER SIMULATOR.  THE TOTAL MASS OF HYDRO-
CARBONS IN THE SYSTEM IS ASSESSED.   THIS INCLUDES
CALCULATING THE HCs REMAINING IN THE REACTOR AFTER PURGING
AND COMBINING IT WITH THE TOTAL MASS PURGED FROM THE REACTOR.
THE TOTAL AREA FROM THE SAMPLED INJECTION TO THE GC AND THE
PRESSURE CHANGE IN THE VACUUM SYSTEM ARE USED TO PERFORM THIS
CALCULATION.  ALSO THE PROGRAM CALCULATES THEORITICAL VALUES
AND CALCULATES THE AVG. MW OF THE HCs BASED ON THE MEASURED
PRESSURES.  TO RUN THE PROGRAM A DATA FILE MUST BE CREATED
ENTERING THE VARIABLES AS LISTED BELOW IN THE FIRST READ
STATEMENT.
C   RUNSTRING:  MASSBAL 'FILENAME'  eg.  PLOCT1AMB.DAT
 C*****************************************************************
      CHARACTER NAME*20
      REAL MWLG,MWG,MWO,MWAVG,MCAL,MWAVGT
      CALL FPARM(NAME)
      OPEN(10,FILE=NAME)
      READ(10,*) DEN, TR, T1, T2, TV, PVI, PVF, TAL, TAC, VCL,
      MWLG, MWG, MWO, YLG, YG,YC
C
C          DEFINITION OF VARIABLES:
C   DEN = DENSITY OF THE OIL (g/ml)
C   TR = REACTION TEMPERATURE (C)
C   T1 = T1 READING FROM THERMOCOUPLE (C)
C   T2 = T2 READING FROM THERMOCOUPLE (C)
C   TV = T3 READING (VACUUM BOX) (C)
C   PVI = INITIAL VACUUM PRESSURE (in. Hg vac)
C   PVF = FINAL VACUUM PRESSURE (in. Hg vac)
C   TAL = TOTAL AREA READING FROM SAMPLED HC  INJ.
C   TAC = TOTAL AREA READING OF PROPANE CAL. INJ.
C   VCL = VOLUME OF CALIBRATION LOOP USED
C   MWLG = MOL. WT. OF LIGHT GASES
C   MWG = MOL. WT. OF GASOLINE (approx = 110)
C   MWO = MOL. WT. OF THE OIL (assume = original value)
C   YLG = WT. PERCENT GC YIELD OF LIGHT GASES
C   YG  = WT. PERCENT GC YIELD OF GASOLINE
C   YC  = WT. PERCENT YIELD OF COKE
      VR = 49.0
      VL = 2.0
      VV = 575.0
      VOIL = 0.2
      R = 82.05
      PRI = 1.0
C    EXPLANATION OF CONSTANTS:
C
C  VR = REACTOR VOLUME (mL)
C  VL = VOLUME OF SAMPLE LOOP (mL)
C  VV = VOLUME OF VACUUM SYSTEM (mL)
C  VOIL = VOLUME OF INJECTED OIL (mL)
C  R = GAS CONSTANT  (atm.ml/gmol/K)
C  PRI = INITIAL REACTOR PRESSURE BEFORE INJECTION (1 ATM)
```

```
C
C    CONVERT TEMPERATURES TO KELVIN
C
       TR = 273.15 + TR
       T1 = 273.15 + T1
       T2 = 273.15 + T2
       TV = 273.15 + TV
       TL = (T1 + T2)/2
C
C    CONVERT VACUUM PRESSURES TO ATMOSPHERES
C
       PVI = 1.0 - PVI*25.4/760.0
       PVF = 1.0 - PVF*25.4/760.0
C
C    CALCULATE MASS OF PROPANE CALIBRATION
C
       MCAL = 1.0*VCL*44.0 / (R * 293.15)
C
C    CALCULATE YIELD OF OIL
C
       YO = 100.0 - ( YLG + YG )
C
C    CALCULATE AVERAGE MOL. WT. OF HYDROCARBONS
C
       MWAVG = 100.0 / ( YLG/MWLG + YG/MWG + YO/MWO )
C
C    CALCULATE TOTAL MASS OF HYDROCARBONS (GRAMS)
C
       A = PRI*VR / (R*TR*VOIL*DEN*(1 - YC/100.0))
       DUM1 = MWAVG / ( 1 + A*MWAVG )
       DUM2 = (PVF - PVI)*VV/(R*TV)
C DUM4 IS THE MASS OF HC PURGED
       DUM4 = DUM1*DUM2
C DUM3 IS THE MASS OF HC REMAINING IN THE REACTOR
       DUM3 = (TAL*MCAL*VR*TL)/(TAC*VL*TR)
C TMHC IS THE TOTAL CALCULATED MASS OF HC IN THE SYSTEM
       TMHC = DUM1*DUM2 + DUM3
C
C    CALCULATE THE THEORITICAL MASS OF HC REMAINING IN REACTOR
C
       XMHCR = PVF*VR*MWAVG/(1 + A*MWAVG)/(R*TR)
C
C    CALCULATE INITIAL INJECTED MASS OF HC AND SUBTRACT COKE
C
       TMHCI = DEN * VOIL
       THC = TMHCI*(1.0 - YC/100.0)
C
C    CALCULATE PERCENT DIFFERENCE
C
       PDIFF = 100.0 * (THC - TMHC)/THC
C
C   CALCULATE PERCENT BY WEIGHT OF HC's PURGED:
C
C      PPURGE = 100.0*DUM1*DUM2/THC
```

```
C       PPURGE = 100.0*(THC - DUM3)/THC
        PPURGE = 100.0*(THC - XMHCR)/THC
C
C   CORRECT THE YIELDS BY FINDING THE MW AVG. FROM MEASURED
C     PARAMETERS
C
        DUMA = (PVF-PVI)*VV*TR/(VR*TV) + PVF - 1.0
        MWAVGT = R*TR*THC/(DUMA*VR)
        B = YLG/YG
        DUMB = B/MWLG + 1.0/MWG - (B+1.0)/MWO
        CYG = 100.0*(1.0/MWAVGT - 1.0/MWO)/DUMB
        CYLG = B*CYG
        CCONV = CYLG + CYG
        CYO = 100.0 - CCONV
        CLOSE(10)
        WRITE (1,1) TMHC
     1  FORMAT(1X,'CALCULATED TOTAL HC (g) = ',F9.8,//)
        WRITE(1,21) THC
    21  FORMAT(1X,'ACTUAL TOTAL HC (g) = ',F9.8,//)
        WRITE(1,2) PDIFF
     2  FORMAT(1X, 'PERCENT DIFFERENCE = ',F6.2,'%',//)
        WRITE(1,83) PPURGE
    83  FORMAT(1X, 'PERCENT OF HCs PURGED =',F6.2,'wt%',//)
        WRITE(1,84) MWAVG
    84  FORMAT(1X, 'AVERAGE MW OF HCs =',F6.2,//)
        WRITE(1,110) CYLG
   110  FORMAT(/,5X, 'CORRECTED LIGHT GASES YIELD =',F5.2,/)
        WRITE(1,111) CYG
   111  FORMAT(5X, 'CORRECTED GASOLINE YIELD =',F5.2,/)
        WRITE(1,112) CYO
   112  FORMAT(5X, 'CORRECTED OIL YIELD =',F5.2,/)
        WRITE(1,113) CCONV
   113  FORMAT(5X, 'CORRECTED CONVERSION =',F5.2,/)
        WRITE(1,114) MWAVGT
   114  FORMAT(5X, 'MEASURED AVG. MW OF HCs =',F6.2,/,1H1)
        WRITE(1,*) ' DO YOU WANT A HARD COPY (1=YES, 2=NO)'
        READ(1,*) NANS
        IF (NANS.EQ.1) GO TO 10
        GO TO 100
    10  WRITE(6,9) NAME
     9  FORMAT(1X, ' MASS BALANCE RESULTS FOR RUN: ', A8,/)
        WRITE(6,31) DUM3
    31  FORMAT(5X, ' MASS OF HC REMAINING IN REACTOR (g) =
',F7.5,/)
        WRITE(6,32) XMHCR
    32  FORMAT(5X, ' THEORITICAL MASS OF HC REMAINING (g) =
',F7.5,/)
        WRITE(6,41) DUM4
    41  FORMAT(5X, ' MASS OF HC PURGED (g) = ',F7.5,/)
        WRITE(6,11) TMHC
    11  FORMAT(5X, ' CALCULATED TOTAL HC (g) = ',F7.5,/)
        WRITE(6,13) THC
    13  FORMAT(5X, ' ACTUAL TOTAL HC (g) = ',F7.5,/)
        WRITE(6,12) PDIFF
```

```
 12 FORMAT(5X, ' PERCENT DIFFERENCE = ',F6.2,'%',/)
    WRITE(6,93) PPURGE
 93 FORMAT(5X, ' PERCENT OF HCs PURGED =',F6.2,'wt%',/)
    WRITE(6,94) MWAVG
 94 FORMAT(5X, ' AVERAGE MW OF HCs =',F6.2,//)
    WRITE(6,110) CYLG
    WRITE(6,111) CYG
    WRITE(6,112) CYO
    WRITE(6,113) CCONV
    WRITE(6,114) MWAVGT
100 CONTINUE
    END
```

```
      PROGRAM RONMWG
C-----------------------------------------------------------
THIS PROGRAM CALCULATES THE GC RESEARCH OCTANE NUMBER OF THE
GASOLINE FRACTION (C5-C12) BASED ON THE METHOD BY ANDERSON
et.al. AS WELL THE MOL. WEIGHT OF THE GASOLINE IS ASSESSED.
THIS PROGRAM REQUIRES A CLEANED GC REPORT FROM THE PROGRAM
"CLEAN" WHICH USES THE "OIL.REF" REFERENCE FILE (41 GROUPS IN
TOTAL).
C-----------------------------------------------------------
C  RUNSTRING:  RONMWG  (CLEANED FILE NAME)
C       e.g.    RONMWG   ELGX30_1A.GAZ
C
      CHARACTER IN*81,NAME*20
                          D   I   M   E   N   S   I   O   N
TIME(200),A(200),RON(200),WRON(200),ARON(200),BR(30),
     $XMW(100),WP(100),XMOLES(200),WPL(10)
      CALL FPARM(NAME)
      OPEN(10,FILE=NAME)
C
C  READ THE VALUES FOR THE AREA OF EACH GROUP FROM THE CLEANED
REPORT
C
      READ(10,'(A81)') IN
      DO 1 I=1,41
      READ(10,2) TIME(I),A(I)
    2 FORMAT(5X,F7.2,2X,I10)
    1 CONTINUE
      CLOSE (10)
C
C  CALCULATE THE TOTAL AREA OF THE GASOLINE RANGE
C
      ARON(1) =A(10)+A(11)+A(12)
      ATOTAL = ARON(1)
      DO 3 I=2,28
      ARON(I) = A(I+11)
      ATOTAL = ATOTAL + ARON(I)
    3 CONTINUE
      ARON(29) = A(40) + A(41)
      ATOTAL = ATOTAL + ARON(29)
C
C  CALCULATE THE WEIGHT FRACTION OF EACH GASOLINE GROUP
C
      DO 4 I=1,29
      WRON(I) = ARON(I)/ATOTAL
    4 CONTINUE
      BR(1) = 144.3
      BR(2) = 84.0
      BR(3) = 198.2
      BR(4) = 67.9
      BR(5) = 95.2
      BR(6) = 86.6
      BR(7) = 95.9
      BR(8) = 20.9
      BR(9) = 94.9
```

```
      BR(10) = 105.2
      BR(11) = 113.6
      BR(12) = 80.0
      BR(13) = 97.8
      BR(14) = -47.8
      BR(15) = 62.3
      BR(16) = 113.9
      BR(17) = 115.1
      BR(18) = 81.7
      BR(19) = 109.7
      BR(20) = 10.5
      BR(21) = 96.1
      BR(22) = 122.6
      BR(23) = 45.4
      BR(24) = 102.0
      BR(25) = 73.3
      BR(26) = 123.6
      BR(27) = 35.0
      BR(28) = 112.0
      BR(29) = 85.6
C
C   CALCULATE THE GC-RON VALUE FOR THE GASOLINE RANGE
C
      RONAVG = 0.0
      DO 5 I=1,29
      RON(I) = WRON(I)*BR(I)
      RONAVG = RONAVG + RON(I)
    5 CONTINUE
C
C   CALCULATE THE MW OF THE GASOLINE
C
      XMW(12) = 70.0
      XMW(13) = 72.0
      XMW(14) = 70.0
      XMW(15) = 72.0
      XMW(16) = 73.0
      XMW(17) = 86.0
      XMW(18) = 84.0
      XMW(19) = 86.0
      XMW(20) = 84.0
      XMW(21) = 78.0
      XMW(22) = 88.4
      XMW(23) = 100.0
      XMW(24) = 103.0
      XMW(25) = 100.0
      XMW(26) = 105.0
      XMW(27) = 92.0
      XMW(28) = 114.0
      XMW(29) = 114.0
      XMW(30) = 113.0
      XMW(31) = 114.0
      XMW(32) = 123.0
      XMW(33) = 106.0
      XMW(34) = 125.0
```

```
      XMW(35) = 106.0
      XMW(36) = 125.0
      XMW(37) = 106.0
      XMW(38) = 127.0
      XMW(39) = 133.0
      XMW(40) = 140.0
      XMW(41) = 170.0
      AT = ATOTAL - A(10) - A(11)
      XMOLEST = 0.0
      DO 6 I=12,41
      WP(I) = 100.0*A(I)/AT
      XMOLES(I) = WP(I)/XMW(I)
      XMOLEST = XMOLEST + XMOLES(I)
    6 CONTINUE
      XMWAVG = 100.0/XMOLEST
C
C  WRITE VALUES TO THE SCREEN
C
      WRITE(1,10) RONAVG
   10 FORMAT(1X, ' THE GC RON FOR THE GASOLINE I = ',F6.2,/)
      WRITE(1,11) XMWAVG
   11 FORMAT(1X, ' THE MW OF THE GASOLINE IS= ',F6.2,/)
C
C WRITE VALUES TO THE PRINTER
C
      WRITE(1,*) 'DO YOU WANT TO PRINT RESULTS (1=YES, 2=NO)'
      READ(1,*) N
      IF (N.EQ.1) GO TO 99
      GO TO 100
   99 WRITE(6,19) NAME
   19 FORMAT(//,1X, 'RON AND MW RESULTS FOR PUN: ',A20)
      WRITE(6,*) '----------------------------------------'
      WRITE(6,*)
      WRITE(6,10) RONAVG
      WRITE(6,11) XMWAVG
      WRITE(6,*) ' #          wt. frac.          br'
      DO I=1,29
      WRITE(6,25) I,WRON(I),BR(I)
   25 FORMAT(1X,I2,8X,f6.5,13x,f6.2)
      ENDDO
      WRITE(6,26) ATOTAL
   26 FORMAT(/,1X, 'TOTAL AREA FOR RON =',I9,/,1H1)
  100 CONTINUE
      END
```

```
      PROGRAM OOPT3A
C*************************************************************
   THIS PROGRAM USES MARQUARDT REGRESSION TO FIND KINETIC
CONSTANTS ASSOCIATED WITH THE EXPONENTIAL LAW OF DECAY FOR
CATALYTIC CRACKING.  THE MODEL USED IS THE THREE LUMP MODEL
AND THE EQUATION SOLVED IS THE OIL YIELD EQUATION. THE
CONSTANTS TO BE OPTIMIZED ARE ALPHA AND KO.
C*************************************************************
      DIMENSION A(20,20),AC(20,20),BMIN(10),BMAX(10),X(20)
      DIMENSION XMC(20),WO(20),XMW(20),YI(20),YO(20)
      REAL
 P(80),COV(20,20),COR(20,20),VAR(20),ERR(20),ERR2(20)
      REAL Z(25), Y(25), BY(20),BV(20),B(20)
      INTEGER IPVT(20)
      EMA COV
      CHARACTER*50 FILE1*25,FILE2*25
      EXTERNAL FUNC,WMAB,WSWP,WSMY,WPIV
      COMMON /TRES/ ERR,COR,VAR
      WRITE(1,*) 'ENTER THE TEMPERATURE( *C)'
      READ(1,*) TR
      WRITE(1,*) ' ENTER THE NUMBER OF DATA POINTS'
      READ(1,*) NN
      KK=2
C
      call fparm(FILE1,FILE2)
      OPEN(10,FILE=FILE1)
      READ(10,*) (X(I),XMC(I),WO(I),XMW(I),YI(I), I=1,NN)
      CLOSE(10)
      WRITE(1,*) 'ENTER AN INITIAL VALUE FOR ALPHA'
      READ (1,*) B(1)
      WRITE (1,*) 'ENTER AN INITIAL VALUE FOR KO'
      READ (1,*) B(2)
      BMIN(1)=0.0001
      BMAX(1)=2.0
      BMIN(2)=0.1
      BMAX(2)=10.0
C***CONVERT TO PARTIAL PRESSURES***
      TR1 = TR + 273.15
      DO I=1,NN
      Y(I) = YI(I)*WO(I)*82.05*TR1/(XMW(I)*45.0)
      YO(I) = WO(I)*82.05*TR1/(XMW(I)*45.0)
      ENDDO
C
      FNU = 0.0
      FLA = 0.0
      TAU = 0.0
      EPS = 0.0
      PHMIN = 0.0
      I = 0
      KD = KK
      FV = 0.0
      DO J = 1, KK
          BV(J) = 1
      END DO
```

```
      ICON = KK
      ITER = 0
      NO = 1
      WRITE (NO,15)
15    FORMAT ( 10X,27HBSOLVE REGRESSION ALGORITHM)
C
200   CALL BSOLVE (KK, B, NN, Z, Y, PH, FNU, FLA, TAU, EPS,
PHMIN,I,ICON,FV,DV,BV,  BMIN,  BMAX,  P,FUNC,  DERIV,KD,A,AC,
GAMM,XMC,WO,X,XMW,COV,YO,TR1)
C
      ITER = ITER + 1
      WRITE (NO,1) ICON, PH, ITER
1     FORMAT (9X,6HICON = , I3, 4X, 5HPH = , E15.8, 4X,
     $16HIteration No. = , I3)
      WRITE(1,2) B(1),B(2)
    2 FORMAT(1X, 'ALPHA=',F7.5,5X,'K0=',F7.5)
      IF (ICON) 10, 300, 200
10    IF (ICON+1) 20, 60, 200
20    IF (ICON+2) 30, 70, 200
30    IF (ICON+3) 40, 80, 200
40    IF (ICON+4) 50, 90, 200
50    GO TO 95
60    WRITE (NO,4)
4     FORMAT (///, 9X, 32HNo Function Improvement Possible )
      GO TO 300
70    WRITE (NO,5)
5     FORMAT (//,9X, 28HMore Unknowns than Functions)
      GO TO 300
80    WRITE (NO, 6)
6     FORMAT (//,9X, 2HTotal Variables are Zero)
      GO TO 300
90    WRITE (NO,7)
7        FORMAT  (//,9X,79HCorrections  Satisfy  Convergence
Requirements but Lamda Factor (FLA) still Large)
      GO TO 300
95    WRITE (NO,8)
8     FORMAT (//,9X, 20HThis is not Possible)
      GO TO 300
 300  WRITE(1,313) B(1),B(2)
  313 FORMAT(1X,'ALPHA =',F7.5,' (1/s)',3X,'K0=',F7.5,
     $' (m**6/Kgmol.Kgcat.s)')
      OPEN (20, FILE=FILE2)
      WRITE(20,381) FILE2
 381  FORMAT(1X, 'REGRESSION RESULTS FOR RUN: ',A16,/)
      WRITE (20,312) B(1),B(2)
 312  FORMAT(1X,'ALPHA=B(1) =',F7.5, '(1/s)', 5X, 'K0=B(2)=',
F7.5, ' (m**6/Kgmol.Kgcat.s)',/)
C*************************************************************
C  STATISTICS CALCULATIONS
C*************************************************************
C
      STAT1 = 0.0
      STAT2 = 0.0
      DO  I=1,NN
```

```
      STAT1 = STAT1 + Y(I)
      STAT2 = STAT2 + Z(I)
      ENDDO
      YAV = STAT1 / NN
      DO I = 1,NN
C***percent difference**********************
        ERR(I) = 100.*(Z(I) - Y(I))/ Z(I)
c***residuals*********************************
        ERR2(I) = Y(I) - Z(I)
c***sum of squares of regression***********
        STAT3 = STAT3 + (Z(I) - YAV)**2
c***sum of squares total corrected*********
        STAT4 = STAT4 + (Y(I) - YAV)**2
c***sum of squares of the residuals*********
        STAT5 = STAT5 + (Y(I) - Z(I))**2
      ENDDO
c***correlation coefficient or coeff.of regression******
      R2 = STAT3/STAT4
      STAT6 = STAT3/KK
      STAT7 = STAT5/(NN - KK)
C     STAT8 = STAT6/STA17
C*************************************************************
      WRITE(20,499)
  499  FORMAT(1X,'t(s)',5X,'YO  cal  (wt%)',5X,'YOexp',  5X,
'Residuals', 5X,'% dev.')
      DO 315 I=1,NN
      Z(I) = 100.0*Z(I)*XMW(I)*45.0/(WO(I)*82.05*TR1)
      YI(I) = 100.0*YI(I)
      ERR2(I) = 100.0 * ERR2(I)
      WRITE (20,314) X(I),Z(I),YI(I),ERR2(I),ERR(I)
 314  FORMAT(1X,I2,8X,F5.3,10X,F5.3,7X,f6.4,8x,f5.3)
 315  CONTINUE
      write(20,*)
      WRITE(20,*) 'ANALYSIS OF VARIANCE:'
      write(20,*)
      write(20,409) STAT3,STAT4,STAT5
  409 FORMAT(1X,'SS reg.= ',F8.6,4X,'SS tot. corr.=',F8.6,4X,
     $'SS resid.=',F8.6,/)
      WRITE(20,469) KK,NN
  469 FORMAT(1X,'No. of parameters = ',I2,5X,'No. of runs =
',I2,/)
      WRITE(20,419) R2
  419 FORMAT(1X,'Coefficient of regression = ',F5.4,/)
C
C*************************************************************
C  INVERSION OF MATRIX COV= TRANSF(JACOBIAN)*JACOBIAN
C*************************************************************
C
       CALL INVRT(COV,MSIZE,KK,IPVT,IERR)
       DO I=1,KK
       VAR(I) = COV(I,I) * STAT5 / (NN-KK)
       ENDDO
C
      DO I=1,KK
```

```
          DO J=1,KK
          COR(I,J) = COV(I,J)*STAT5/(NN-KK) /
 SQRT(VAR(I)*VAR(J))
          ENDDO
        ENDDO
C*****************************************************************
        WRITE(20,449)
  449   FORMAT(1X,3'*','CORRELATION   MATRIX   OF   PARAMETER
ESTIMATES', 3'*',/)
        DO I=1,KK
        WRITE(20,459) (COR(I,J), J=1,KK)
  459 FORMAT(1X,20(F5.4,2X))
        ENDDO
        WRITE(20,448)
  448   FORMAT(/,1X,3'*','COVARIANCE   MATRIX   FOR   PARAMETER
ESTIMATES', 3'*',/)
        DO I=1,KK
        WRITE(20,458) (COV(I,J), J=1,KK)
  458 FORMAT(1X,20(F8.5,2X))
        ENDDO
        WRITE(20,429)
  429  FORMAT(/,1X,3'*','VARIANCES OF PARAMETER ESTIMATES',
3'*',/)
        DO I=1,KK
        WRITE(20,439) I,VAR(I)
  439 FORMAT(1X,'VAR (',1X,I2,1X,') = ',F10.8)
        ENDDO
        CLOSE(20)
1000    STOP
        END
C*****************************************************************
         SUBROUTINE FUNC ( KK,B,NN,Z,FV,XMC,WO,X,XMW,YO,TR1)
C*****************************************************************
        DIMENSION  (25),XMC(20),WO(20),X(20),XMW(20),YO(20)
        DIMENSION B(25),DUM1(20),DUM2(20)
        VT = 45.0*45.0
        DO 10 J=1,NN
C       DUM1(J) = XMC(J)*WO(J)*B(2)*1.0E+06 / (B(1)*XMW(J)*VT)
C       DUM2(J) = 1.0 - DUM1(J)*(EXP( -B(1)*X(J) ) - 1.0)
C       Z(J) = 1.0 / DUM2(J)
        DUM = B(2)*XMC(J)*(EXP(-B(1)*X(J) ) -1.0)/(B(1)*45.0)
        Z(J) = 1.0/( 1.0/YO(J) - 1.0E+06*DUM/(82.05*TR1) )
   10 CONTINUE
        RETURN
        END
C*****************************************************************
C
C
C
C
C
C
C
C
```

```
      SUBROUTINE BSOLVE ( KK, B, NN, Z, Y, PH, FNU, FLA, TAU,
     $EPS, PHMIN, I, ICON, FV, DV, BV,  BMIN,BMAX,P, FUNC,
     $DERIV, KD, A, AC, GAMM, XMC, WHPO, WHNO, WHAO, WLPO,
     $WLNO, WLAO, X, XKPH, XKNH, XKAH, XKPHPL, XKNHNL, XKAHAL,
     $XKPL, XKNL, XKAL, XKPLG,XKNLG,XKALG,XKGC,XA,COV)
      DIMENSION A(10,10),AC(10,10),BMIN(10),BMAX(10)
      DIMENSION  Z(25), Y(25), BV(10),B(10),X(25)
      DIMENSION P(50),FV(10),DV(10),COV(20,20)
      DIMENSION XMC(25),WHPO(25),WHNO(25),WHAO(25)
      DIMENSION WLPO(25),WLNO(25),WLAO(25)
      EMA COV
C
      K = KK
      N= NN
      KP1 = K + 1
      KP2 = KP1 + 1
      KBI1 = K * N
      KBI2 = KBI1 + K
      KZI = KBI2 + K
      IF ( FNU .LE. 0. ) FNU = 10.0
      IF ( FLA .LE. 0. ) FLA = 0.01
      IF ( TAU .LE. 0. ) TAU = 0.001
      IF ( EPS .LE. 0. ) EPS = 0.00002
      IF ( PHMIN .LE. 0. ) PHMIN = 0.
120   KE = 0
130   DO 160 I1 = 1, K
160   IF ( BV(I1) .NE. 0. ) KE = KE + 1
      IF ( KE .GT. 0 ) GO TO 170
162   ICON = - 3
163   GO TO 2120
170   IF ( N .GE. KE ) GO TO 500
180   ICON = -2
190   GO TO 2120
500   I1 = 1
530   IF ( I .GT. 0 ) GO TO 1530
550   DO 560 J1 = 1, K
          J2 = KBI1 + J1
          P(J2) = B(J1)
          J3 = KBI2 + J1
560       P(J3) = ABS ( B(J1) ) + 1.0E-02
      GO TO 1030
590   IF ( PHMIN .GT. PH .AND. I .GT. 1 ) GO TO 625
      DO 620 J1 = 1, K
          N1 = ( J1 - 1 ) * N
          IF ( BV(J1) ) 601, 620, 605
601     CALL DERIV (K, B, N, Z, P(N1+1), FV, DV, J1, JTEST )
          IF ( JTEST .NE. (-1) ) GO TO 620
          BV(J1) = 1.0
605       DO 606 J2 = 1, K
              J3 = KBI1 + J2
606       P(J3) = B(J2)
          J3 = KBI1 + J1
          J4 = KBI2 + J1
          DEN = 0.001 * AMAX1 ( P(J4), ABS(P(J3)))
```

PRODUCT DISTRIBUTION FOR RUN I.D.: A-G-12

NO.	COMPOUND(S)	wt%
1	Methane	5.88
2	Ethylene	6.87
3	Ethane	3.00
4	Propylene	7.78
5	Propane	4.63
6	i-Butane	1.75
7	i-Butylene	4.08
8	1-Butene	2.79
9	n-Butane	1.26
10	t,2-Butene	.56
11	c,2-Butene	.45
12	3-Methyl-1-butene	.21
13	i-Pentane	.92
14	C5 olefins	1.28
15	n-Pentane	.22
16	C5 olefins, naphthenes; C6 olefins, i-para.	3.15
17	2- and 3-methylpentane, C6 isoparaffins	.50
18	C6 olefins	1.22
19	n-Hexane	.01
20	C6 olefins, naph.; C7 olef., i-para, naph.	1.31
21	Benzene	2.01
22	C6 naphthene; C7 olefins, i-para., naph.	.53
23	2- and 3-methylhexane, C7 i-paraffins	.45
24	C7 olefins, naph., i-para.; C8 i-para.	.92
25	n-Heptane	.15
26	C7 olefins, naphthenes; C8 i-paraffins	.91
27	toluene	3.33
28	C8 isoparaffins	.48
29	2- and 3-methylheptane; C8 i-paraffins	.57
30	C7 and C8 naphthenes; C9 i-paraffins	.45
31	n-Octane	.06
32	C9 olefins; C8, C9 naph., C9 i-para.	.45
33	Ethylbenzene	.57
34	C9 naphthenes and i-paraffins	.09
35	p-Xylene and m-Xylene	1.97
36	C9 i-paraffins and naphthenes	.55
37	o-Xylene	.82
38	n-Nonane, C9 naphthenes	.56
39	C9 aromatics; C10 i-para. and naphthenes	2.69
40	n-Decane	2.53
41	n-C10; C9, C10 arom.; C10, C11 i-para., naph.	1.91
42	Light paraffins	8.26
43	Light naphthenes	4.52
44	Light aromatics	3.43
45	Heavy paraffins	4.48
46	Heavy naphthenes	3.28
47	Heavy aromatics	1.25
48	Coke	4.92

```
          IF ( P(J3) + DEN .LE. BMAX(J1) ) GO TO 55
          P(J3) = P(J3) - DEN
          DEN = - DEN
          GO TO 56
55        P(J3) = P(J3) + DEN
56     CALL FUNC (K, P(KBI1+1), N, P(N1+1), FV, XMC, WHPO,
      $WHNO, WHAO, WLPO, WLNO, WLAO, X, XKPH, XKNH, XKAH,
      $XKPHPL,XKNHNL,XKAHAL,XKPL,XKNL,XKAL, XKPLG, XKNLG,
      $XKALG, XKGC, XA)
          DO 610 J2 = 1, N
              JB = J2 + N1
610           P(JB) = ( P(JB) - Z(J2) ) / DEN
620    CONTINUE
C
C      SET UP CORRECTION EQUATIONS
C
625    DO 725 J1 = 1, K
          N1 = ( J1 - 1 ) * N
          A(J1,KP1) = 0.
          IF ( BV(J1) ) 630, 692, 630
630       DO 640 J2 = 1, N
          N2 = N1 + J2
640       A(J1,KP1) = A(J1,KP1) + P(N2) * (Y(J2) - Z(J2))
650       DO 681 J2 = 1, K
660           A(J1,J2) = 0.
665           N2 = ( J2 - 1 ) * N
670           DO 680 J3 = 1, N
672               N3 = N1 + J3
674               N4 = N2 + J3
680       A(J1,J2) = A(J1,J2) + P(N3) * P(N4)
681       COV(J1,J2) = A(J1,J2)
          IF (A(J1,J1).GT.1E-20) GO TO 725
          IF ( A(J1,J1) .GT. 1.E-20 ) GO TO 725
692       DO 694 J2 = 1, KP1
694           A(J1,J2) = 0.
695       A(J1,J1) = 1.0
725    CONTINUE
       GN = 0.
       DO 729 J1 = 1, K
729       GN = GN + A(J1,KP1) ** 2
C
C      SCALE CORRECTION EQUATIONS
C
       DO 726 J1 = 1, K
726       A(J1,KP2) = SQRT (A(J1,J1))
       DO 727 J1 = 1, K
          A(J1,KP1) = A(J1,KP1) / A(J1,KP2)
          DO 727 J2 = 1, K
727       A(J1,J2) = A(J1,J2)/ (A(J1 KP2)*A(J2,KP2))
730    FL = FLA / FNU
       GO TO 810
800    FL = FNU * FL
810    DO 840 J1 = 1, K
820       DO 830 J2 = 1, KP1
```

```
830           AC(J1,J2) = A(J1,J2)
840         AC(J1,J1) = AC(J1,J1) + FL
C
C      SOLVE CORRECTION EQUATIONS
C
       DO 930 L1 = 1, K
           L2 = L1 + 1
           DO 910 L3 = L2, KP1
910            AC(L1,L3) = AC(L1,L3) / AC (L1,L1)
           DO 930 L3 = 1,K
           IF (L1-L3) 920, 930, 920
920        DO 925 L4 = L2, KP1
925        AC(L3,L4) = AC(L3,L4) - AC(L1,L4) * AC(L3,L1)
930    CONTINUE
C
       DN = 0.
       DG = 0.
       DO 1028 J1 = 1, K
           AC(J1,KP2) = AC(J1,KP1) / A(J1,KP2)
           J2 = KBI1 + J1
     P(J2) = AMAX1(BMIN(J1),AMIN1(BMAX(J1),B(J1)+AC(J1,KP2)))
           DG = DG + AC(J1,KP2) * A(J1,KP1) * A(J1,KP2)
           DN = DN + AC(J1,KP2) * AC(J1,KP2)
1028       AC(J1,KP2) = P(J2) - B(J1)
       COSG = DG / SQRT (DN*DG)
       JGAM = 0
       IF (COSG) 1100, 1110, 1110
1100   JGAM = 2
       COSG = - COSG
1110   CONTINUE
       COSG = AMIN1 (COSG, 1.0)
       GAMM = ARCOS(COSG) * 180. / (3.14159265)
       IF ( JGAM .GT. 0 ) GAMM = 180. - GAMM
1030   CALL FUNC (K, P(KBI1+1), N, P(KZI+1), FV, XMC, WHPO,
      $WHNO, WHAO, WLPO, WLNO, WLAO, X, XKPH, XKNH, XKAH,
      $XKPHPL, XKNHNL, XKAHAL, XKPL, XKNL, XKAL, XKPLG, XKNLG,
      $XKALG, XKGC, XA)
1500   PHI = 0.
       DO 1520 J1 = 1, N
           J2 = KZI + J1
1520       PHI = PHI +  (P(J2)-Y(J1))**2
       IF (PHI .LT. 1.E-5 ) GO TO 3000
       IF ( I .GT. 0 ) GO TO 1540
1521   ICON = K
       GO TO 2110
1540   IF ( PHI .GE. PH ) GO TO 1530
C
C      EPSILON TEST
C
1200   ICON = 0
       DO 1220 J1 = 1, K
           J2 = KBI1 + J1
1220       IF(ABS(AC(J1,KP2))/(TAU+ABS(P(J2))) .GT. EPS) ICON
= ICON + 1
```

```
      IF ( ICON .EQ. 0 ) GO TO 1400
C
C     GAMMA LAMBDA TEST
C
      IF ( FL .GT. 1.0 .AND. GAMM .GT. 90.0 ) ICON = -1
      GO TO 2105
C
C     GAMMA EPSILON TEST
C
1400  IF ( FL .GT. 1.0 .AND. GAMM .LE. 45.0 ) ICON = -4
      GO TO 2105
C
1530  IF ( I1 - 2 ) 1531, 1531, 2310
1531  I1 = I1 +1
      GO TO (530,590,800), I1
2310  IF ( FL .LT. 1.0E+8 ) GO TO 800
1320  ICON = - 1
C
2105  FLA = FL
      DO 2091 J2 = 1, K
          J3 = KBI1 + J2
2091      B(J2) = P(J3)
2110  DO 2050 J2 = 1, N
          J3 = KZI + J2
2050      Z(J2) = P(J3)
      PH = PHI
      I = I + 1
2120  RETURN
3000  ICON = 0
      GO TO 2105
C
      END
C
C
**********************************************************************
C
      FUNCTION ARCOS(Z)
C
      X = Z
      KEY = 0
      IF ( X .LT. (-1.) ) X= -1.
      IF ( X .GT. 1. ) X = 1.
      IF ( X .GE. (-1.) .AND. X .LT. 0. ) KEY = 1
      IF ( X .LT. 0. ) X = ABS (X)
      IF ( X .EQ. 0. ) GO TO 10
      ARCOS = ATAN (SQRT(1.-X*X) / X )
      IF ( KEY .EQ. 1 ) ARCOS = 3.14159265 - ARCOS
      GO TO 999
10    ARCOS = 1.5707963
999   RETURN
      END
```

```
      PROGRAM GOPT3A
C*************************************************************
  THIS PROGRAM USES MARQUARDT REGRESSION COMBINED WITH A 4TH
ORDER RUNGE-KUTTA ALGORITHM TO FIND THE KINETIC CONSTANTS K1
AND K2 IN THE GASOLINE EQUATION FOR THE 3-LUMP MODEL USING
EXPONENTIAL DECAY.  THE VALUES OF N AND KO OBTAINED FROM
PROGRAM "OOPT3A.FTN" MUST BE USED IN THE OIL AND GASOLINE
DIFFERENTIAL EQUATIONS OF THE SUBROUTINE PROGRAM "FUNC" IN
THIS PROGRAM (enter thru data file)
 note: units of K0 must be (1/goil.gcat.s)
C*************************************************************
      DIMENSION A(10,10),AC(10,10),BMIN(10),BMAX(10),X(10)
      DIMENSION XMC(10),WO(10)
      REAL
 P(50),COV(20,20),COR(20,20),VAR(20),ERR(20),ERR2(20)
      REAL Z(25), Y(25), BY(16),BV(10),B(10)
      CHARACTER*50 FILE1*25,FILE2*25
      COMMON /DATA/ XK0 , XA
      INTEGER IPVT(20)
      EMA COV
      EXTERNAL FUNC
      COMMON /TRES/ ERR,COR,VAR
      WRITE(1,*) 'ENTER THE NUMBER OF DATA POINTS'
      READ(1,*) NN
      KK=2
C
      call fparm(FILE1,FILE2)
      OPEN(10,FILE=FILE1)
      READ(10,*) XK0,XA
      READ(10,*) (X(I),XMC(I),WO(I),Y(I), I=1,NN)
      CLOSE(10)
      write(1,*) 'initial VALUE FOR K1'
      read (1,*) b(1)
      write (1,*) 'initial VALUE FOR K2'
      read (1,*) b(2)
      bmin(1)=0.0
      bmax(1)=10.0
      bmin(2)=0.0
      bmax(2)=10.0
C
      FNU = 0.0
      FLA = 0.0
      TAU = 0.0
      EPS = 0.0
      PHMIN = 0.0
      I = 0
      KD = KK
      FV = 0.0
      DO J = 1, KK
          BV(J) = 1
      END DO
      ICON = KK
      ITER = 0
      NO = 1
```

```
      WRITE (NO,15)
15    FORMAT ( 10X,27HBSOLVE REGRESSION ALGORITHM)
C
200   CALL BSOLVE (KK, B, NN, Z, Y, PH, FNU, FLA, TAU, EPS,
PHMIN,I,ICON,FV,DV,BV,
     $BMIN,BMAX,P,FUNC,DERIV,KD,A,AC,GAMM,XMC,WO,X,COV)
C
      ITER = ITER + 1
      WRITE (NO,1) ICON, PH, ITER
1     FORMAT (9X,6HICON = , I3, 4X, 5HPH = , E15.8, 4X,
     $16HIteration No. = , I3)
      WRITE(1,2) B(1),B(2)
    2 FORMAT(1X, 'K1=',F5.3,5X,'K2=',F9.7)
      IF (ICON) 10, 300, 200
10    IF (ICON+1) 20, 60, 200
20    IF (ICON+2) 30, 70, 200
30    IF (ICON+3) 40, 80, 200
40    IF (ICON+4) 50, 90, 200
50    GO TO 95
60    WRITE (NO,4)
4     FORMAT (//, 9X, 32HNo Function Improvement Possible )
      GO TO 300
70    WRITE (NO,5)
5     FORMAT (//,9X, 28HMore Unknowns than Functions)
      GO TO 300
80    WRITE (NO, 6)
6     FORMAT (//,9X, 2HTotal Variables are Zero)
      GO TO 300
90    WRITE (NO,7)
7         FORMAT  (//,9X,79HCorrections  Satisfy  Convergence
Requirements but Lamda Factor (FLA) still Large)
      GO TO 300
95    WRITE (NO,8)
8     FORMAT (//,9X, 20HThis is not Possible)
      GO TO 300
 300  WRITE(1,313) B(1),B(2)
  313 FORMAT(1X,'K1=',F5.3,5X,'K2=',F9.7)
      OPEN (20, FILE=FILE2)
      WRITE (20,381) FILE2
 381  FORMAT(1X, 'REGRESSION RESULTS FOR DATA: ',A16,/)
      WRITE(20,410) XK0,XA
 410  FORMAT(1X,'USING: K0 = ',F6.4,' (1/goil.gcat.s)',1X,'and
alpha ='
     $,F5.4,' (1/s)',/)
      XK3 = XK0 - B(1)
      WRITE (20,312) B(1),XK3,B(2),PH
 312   FORMAT(1X,'K1=B(I)= ',F6.4,5X,'K3= ',F6.4,5X,'K2=B(2)
',F9.7,5X,
     $'Phi=',F6.5)
      WRITE(20,*) '- units of K1 and K3 are  (1/goil.gcat.s)'
      WRITE(20,*) '- units of K2 are (1/gcat.s)'
      WRITE(20,*)
C*************************************************************
C  STATISTICS CALCULATIONS
```

```
C*****************************************************************
C
      STAT1 = 0.0
      STAT2 = 0.0
      DO  I=1,NN
      STAT1 = STAT1 + Y(I)
      STAT2 = STAT2 + Z(I)
      ENDDO
      YAV = STAT1 / NN
      DO I = 1,NN
C***percent difference**********************
        ERR(I) = 100.*(Z(I) - Y(I))/ Z(I)
c***residuals*********************************
        ERR2(I) = Y(I) - Z(I)
c***sum of squares of regression**********
        STAT3 = STAT3 + (Z(I) - YAV)**2
c***sum of squares total corrected*********
        STAT4 = STAT4 + (Y(I) - YAV)**2
c***sum of squares of the residuals*********
        STAT5 = STAT5 + (Y(I) - Z(I))**2
      ENDDO
c***correlation coefficient or coeff.of regression******
      R2 = STAT3/STAT4
      STAT6 = STAT3/KK
      STAT7 = STAT5/(NN - KK)
C     STAT8 = STAT6/STAT7
C*****************************************************************
      WRITE(20,499)
  499  FORMAT(1X,'t(s)',5X,'YG cal (wt%)',5X,'YG exp', 5X,
'Residuals',
     $5X,'% dev.')
      DO 315 I=1,NN
      Z(I) = 100.0*Z(I)
      Y(I) = 100.0*Y(I)
      ERR2(I) = 100.0 * ERR2(I)
      WRITE (20,314) X(I),Z(I),Y(I),ERR2(I),ERR(I)
 314  FORMAT(1X,I2,10X,F5.3,10X,F5.3,6X,f6.4,8x,f5.3)
 315  CONTINUE
      write(20,*)
      WRITE(20,*) 'ANALYSIS OF VARIANCE:'
      write(20,*)
      write(20,409) STAT3,STAT4,STAT5
  409 FORMAT(1X,'SSreg.=',E11.9,3X,'SStot. corr.=',E11.9,3X,
     $'SSresid.=',E11.9,/)
      WRITE(20,469) KK,NN
  469 FORMAT(1X,'No. of parameters = ',I2,5X,'No. of runs =
',I2,/)
      WRITE(20,419) R2
  419 FORMAT(1X,'Coefficient of regression = ',F5.4,/)
C
C*****************************************************************
C  INVERSION OF MATRIX COV= TRANSF(JACOBIAN)*JACOBIAN
C*****************************************************************
C
```

```
       CALL INVRT(COV,MSIZE,KK,IPVT,IERR)
       DO I=1,KK
       VAR(I) = COV(I,I) * STAT5 / (NN-KK)
       ENDDO
      DO I=1,KK
         DO J=1,KK
         COR(I,J) = COV(I,J)*STAT5/(NN-KK) /
 SQRT(VAR(I)*VAR(J))
         ENDDO
      ENDDO
C*****************************************************************
      WRITE(20,449)
  449 FORMAT(1X,3'*','CORRELATION MATRIX OF PARAMETER
 ESTIMATES',
     $3'*',/)
      DO I=1,KK
      WRITE(20,459) (COR(I,J), J=1,KK)
  459 FORMAT(1X,20(F5.4,2X))
      ENDDO
      WRITE(20,448)
  448 FORMAT(/,1X,3'*','COVARIANCE MATRIX FOR PARAMETER
 ESTIMATES',
     $3'*',/)
      DO I=1,KK
      WRITE(20,458) (COV(I,J), J=1,KK)
  458 FORMAT(1X,20(F8.2,2X))
      ENDDO
      WRITE(20,429)
  429 FORMAT(/,1X,3'*','VARIANCES OF PARAMETER
 ESTIMATES',3'*',/)
      DO I=1,KK
      WRITE(20,439) I,VAR(I)
  439 FORMAT(1X,'VAR (',1X,I2,1X,') = ',F10.8)
      ENDDO
      CLOSE(20)
1000  STOP
      END
C
C*****************************************************************
      SUBROUTINE FUNC ( KK,B,NN,Z,FV,XMC,WO,X)
C*****************************************************************
      INTEGER RUNGE
      DIMENSION DW(3),W(3),Z(25),XMC(10),WO(10),X(10)
      DIMENSION B(25)
      COMMON /DATA/ XK0 , XA
      DO 101 JJ=1,NN
      W(1)=0.0
      H=0.10
      ICOUNT=0.0
      T=0.0
      NSTEPS=X(JJ)/H
    5 K=RUNGE(1,W,DW,T,H)
      IF (K.NE.1) GO TO 10
      DEAC = EXP(-XA*T)
```

```
      DUM1 = XMC(JJ)*WO(JJ)*XK0/XA
      W1 = 1.0/( 1.0 - DUM1*(DEAC - 1.0))
      DW(1)=XMC(JJ)*(WO(JJ)*B(1)*W1**2 - B(2)*W(1) )*DEAC
      GO TO 5
   10 ICOUNT=ICOUNT+1
      IF (ICOUNT.EQ.NSTEPS) GO TO 100
      GO TO 5
  100 CONTINUE
      Z(JJ)=W(1)
  101 CONTINUE
      RETURN
      END
C
      FUNCTION RUNGE(N,Y,F,T,H)
      INTEGER RUNGE
      DIMENSION PHII(50), SAVEY(50), Y(N), F(N)
      DATA M/0/
      M=M+1
      GO TO (1,2,3,4,5),M
C     ...PASS 1...
    1 RUNGE = 1
      RETURN
C     ...PASS 2...
    2 DO 22 J=1,N
      SAVEY(J)=Y(J)
      PHII(J)=F(J)
   22 Y(J)=SAVEY(J) + 0.5*H*F(J)
      T=T+0.5*H
      RUNGE=1
      RETURN
C     ...PASS 3...
    3 DO 33 J=1,N
      PHII(J) =PHII(J)+2.0*F(J)
   33 Y(J)=SAVEY(J) +0.5*H*F(J)
      RUNGE=1
      RETURN
C     ...PASS 4...
    4 DO 44 J=1,N
      PHII(J)=PHII(J) +2.0*F(J)
   44 Y(J)=SAVEY(J)+H*F(J)
      T=T+0.5*H
      RUNGE=1
      RETURN
C     ...PASS 5...
    5 DO 55 J=1,N
   55 Y(J)=SAVEY(J)+(PHII(J) + F(J))*H/6.0
      M=0
      RUNGE=0
      RETURN
C
      END
C*****************************************************************
      SUBROUTINE BSOLVE.........
```

```
      PROGRAM TEST3A
C-----------------------------------------------------------
THIS PROGRAM CALCULATES THE YIELDS FOR THE THREE LUMP MODEL
WITH THE "EXPONENTIAL" DECAY FUNCTION USING K VALUES FROM THE
REGRESSIN PROGRAM.  THE APPROPRIATE CONSTANTS (K0,K1,K2,K3 AND
ALPHA) MUST BE ENTERED.
C-----------------------------------------------------------
      IMPLICIT REAL*8(A-H, O-Z)
      INTEGER RUNGE,N
      DIMENSION DY(3), Y(3), Z(25),X(10),XMC(10),WO(10)
                          D   I   M   E   N   S   I   O   N
YO(10),YG(10),YC(10),ODEV(10),GDEV(10),CDEV(10)
      CHARACTER*50 FILE1*16, FILE2*16
      WRITE(1,*) 'ENTER THE NUMBER OF DATA POINTS'
      READ(1,*) N
      CALL FPARM(FILE1,FILE2)
      OPEN(10,FILE=FILE1)
      READ(10,*) (X(I),XMC(I),WO(I),YO(I),YG(I),YC(I), I=1,N)
      CLOSE(10)
      WRITE(1,*) 'SPECIFY THE TEMPERATURE USED'
      READ(1,*) TEMP
      WRITE(1,*) 'ENTER K0,K1,K2,K3 AND ALPHA'
      READ(1,*) XK0,XK1,XK2,XK3,XA
      DO 6 J=1,N
      Y(1) = 1.0
      Y(2) = 0.0
      Y(3) = 0.0
      H=0.005
      T=H
      ICOUNT = 0.0
      NSTEPS = X(J)/H
C     ....CALL THE RUNGE FUNCTION.....
    5 K = RUNGE(3,Y,DY,T,H)
C     ....WHEN K=1 COMPUTE DERIVATIVE VALUES....
      IF (K.NE.1) GO TO 10
      DY(1) = -XMC(J)*WO(J)*XK0*Y(1)**2*EXP(-XA*T)
      DY(2)    =    XMC(J)*(WO(J)*XK1*Y(1)**2    -    XK2*Y(2)
)*EXP(-XA*T)
      DY(3)    =    XMC(J)*(WO(J)*XK3*Y(1)**2    +    XK2*Y(2)
)*EXP(-XA*T)
      GO TO 5
   10 ICOUNT = ICOUNT + 1
      IF (ICOUNT.EQ.NSTEPS) GO TO 100
      GO TO 5
  100 CONTINUE
      Z(J) = Y(1)
      Z(J+N) = Y(2)
      Z(J+2*N) = Y(3)
    6 CONTINUE
C.....CALCULATE THE DEVIATIONS.............
      SODEV = 0.0
      SGDEV = 0.0
      SCDEV = 0.0
      DO 20 I=1,N
```

```
      ODEV(I) = Z(I) - YO(I)
      GDEV(I) = Z(I+N) - YG(I)
      CDEV(I) = Z(I+2*N) - YC(I)
      SODEV = SODEV + ABS(ODEV(I))
      SGDEV = SGDEV + ABS(GDEV(I))
      SCDEV = SCDEV + ABS(GDEV(I))
   20 CONTINUE
      AODEV = SODEV/N
      AGDEV = SGDEV/N
      ACDEV = SCDEV/N
      OPEN(20,FILE=FILE2)
      WRITE(20,*) ' CALCULATED YIELDS FOR THE 3-LUMP MODEL '
      WRITE(20,*) ' USING THE EXPONENTIAL DECAY FUNCTION'
      WRITE(20,*) '-----------------------------------------'
      WRITE(20,9) TEMP
    9 FORMAT(/, 'TEMPERATURE =',F5.1,'C',/)
      WRITE(20,12) XK0,XK1,XK2,XK3,XA
   12 FORMAT (1X, 'K0=', F5.3, 5X, 'K1=', F5.3, 5X, 'K2=',
F5.3, 5X, 'K3=', F5.3, 5X,'ALPHA=',F5.4,/)
      WRITE(20,13)
   13 FORMAT(1X,3X,'YO(cal)',7X,'YO(exp)',7X,'DEV')
      DO 11 I=1,N
      WRITE(20,8) Z(I),YO(I),ODEV(I)
    8 FORMAT(1X,4X,F4.3,10X,F4.3,10X,F5.3)
   11 CONTINUE
      WRITE(20,14) AODEV
   14 FORMAT(1X,'AVERAGE DEVIATION = ',F7.6,/)
      WRITE(20,15)
   15 FORMAT(1X,3X,'YG(cal)',7X,'YG(exp)',7X,'DEV')
      DO 16 I=1,N
      WRITE(20,17) Z(I+N),YG(I),GDEV(I)
   17 FORMAT(1X,4X,F4.3,10X,F4.3,10X,F5.3)
   16 CONTINUE
      WRITE(20,18) AGDEV
   18 FORMAT(1X,'AVERAGE DEVIATION =', F7.6,/)
      WRITE(20,19)
   19 FORMAT(1X,3X,'YC(cal)',7X,'YC(exp)',7X,'DEV')
      DO 21 I=1,N
      WRITE(20,22) Z(I+2*N),YC(I),CDEV(I)
   22 FORMAT(1X,4X,F4.3,10X,F4.3,10X,F5.3)
   21 CONTINUE
      WRITE(20,23) ACDEV
   23 FORMAT(1X,'AVERAGE DEVIATION =',F7.6,/)
      CLOSE(20)
      END
C
C
      FUNCTION RUNGE(N,Y,F,X,H)
C
      IMPLICIT REAL*8(A-H, O-Z)
      REAL*8 Y,F,X,H
      INTEGER RUNGE
      DIMENSION PHI(50), SAVEY(50), Y(N), F(N)
      DATA M/0/
```

```
C
      M=M+1
      GO TO (1,2,3,4,5),M
C     ...PASS 1...
    1 RUNGE = 1
      RETURN
C     ...PASS 2...
    2 DO 22 J=1,N
      SAVEY(J)=Y(J)
      PHI(J) = F(J)
   22 Y(J) = SAVEY(J) + 0.5*H*F(J)
      X= X +0.5*H
      RUNGE = 1
      RETURN
C     ...PASS 3...
    3 DO 33 J = 1,N
      PHI(J) = PHI(J) +2.0*F(J)
   33 Y(J) = SAVEY(J) +0.5*H*F(J)
      RUNGE = 1
      RETURN
C     ...PASS 4...
    4 DO 44 J = 1,N
      PHI(J) = PHI(J) + 2.0*F(J)
   44 Y(J) = SAVEY(J) + H*F(J)
      X = X + 0.5*H
      RUNGE = 1
      RETURN
C     ...PASS 5...
    5 DO 55 J = 1,N
   55 Y(J) = SAVEY(J) + (PHI(J) + F(J))*H/6.0
      M=0
      RUNGE = 0
      RETURN
      END
```

```
      PROGRAM HLOPT8A
C*****************************************************************
  THIS PROGRAM USES MARQUARDT REGRESSION TO SOLVE THE HEAVY
OIL EQUATION FOR THE 8-LUMP MODEL.  THE KINETIC CONSTANTS
SOLVED FOR ARE KiH AND ALPHA (from exponetial decay function).

C*****************************************************************
C
      DIMENSION A(10,10),AC(10,10),BMIN(10),BMAX(10),X(10)
      DIMENSION XMC(25),WHO(25),CORR(20),WT(20)
      REAL P(50),WO(10),YI(10),COV(20,20),COR(20,20),VAR(20)
      REAL Z(25), Y(25), BY(16),BV(10),B(10),ERR(20),ERR2(20)
      CHARACTER*50 FILE1*30,FILE2*30
      INTEGER IPVT(20)
      EMA COV
      COMMON /TRES/ ERR,COR,VAR
      EXTERNAL FUNC
      WRITE(1,*) 'ENTER THE TEMPERATURE (in celcius)'
      READ(1,*) TR
      WRITE(1,*) 'ENTER THE NUMBER OF DATA POINTS'
      READ(1,*) NN
      KK=2
c
      call fparm(FILE1,FILE2)
      OPEN(10,FILE=FILE1)
      READ(10,*) (X(I),XMC(I),WHO(I),YI(I),WO(I), I=1,NN)
C
C**WHO(I) is the initial wt. fracion of heavy lump I in the
oil
      CLOSE(10)
C***CORRECT WT. FRACTIONS *******
      TR1= TR + 273.15
      DO I=1,NN
      WT(I) = WO(I) + 21.9378/TR
      CORR(I) = WO(I)/WT(I)
      Y(I) = YI(I) * CORR(I)
      WHO(I) = WHO(I) * CORR(I)
      ENDDO
      write(1,*) 'initial VALUE FOR KIH'
      read (1,*) b(1)
      write (1,*) 'initial VALUE FOR ALPHA'
      read (1,*) b(2)
      bmin(1)=0.1
      bmax(1)=500.0
      bmin(2)=0.0001
      bmax(2)=10.0
C
      FNU = 0.0
      FLA = 0.0
      TAU = 0.0
      EPS = 0.0
      PHMIN = 0.0
      I = 0
      KD = KK
```

```
      FV = 0.0
      DO J = 1, KK
          BV(J) = 1
      END DO
      ICON = KK
      ITER = 0
      NO = 1
      WRITE (NO,15)
15    FORMAT ( 10X,27HBSOLVE  EGRESSION  LGORITHM)
200   CALL BSOLVE (KK, B, M, Z, Y, PH, FNU, FLA, TAU, EPS,
PHMIN, I, ICON,FV,DV,BV,
     $BMIN,BMAX,P,FUNC,DERIV,KD,A,AC,GAMM,X,XMC,WHO,COV)
C
      ITER = ITER + 1
      WRITE (NO,1) ICON, PH, ITER
1     FORMAT (9X,6HICON = , I3, 4X, 5HPH = , E15.8, 4X,
     $16HIteration No. = , I3)
      WRITE(1,2) B(1),B(2)
    2 FORMAT(1X, 'KiH = ',F7.4,5X,'ALPHA = ',F7.5)
      IF (ICON) 10, 300, 200
10    IF (ICON+1) 20, 60, 200
20    IF (ICON+2) 30, 70, 200
30    IF (ICON+3) 40, 80, 200
40    IF (ICON+4) 50, 90, 200
50    GO TO 95
60    WRITE (NO,4)
4     FORMAT (//, 9X, 32HNo Function Improvement Possible )
      GO TO 300
70    WRITE (NO,5)
5     FORMAT (//,9X, 28HMore Unknowns than Functions)
      GO TO 300
80    WRITE (NO, 6)
6     FORMAT (//,9X, 2HTotal Variables are Zero)
      GO TO 300
90    WRITE (NO,7)
7         FORMAT  (//,9X,79HCorrections  Satisfy  Convergence
Requirements but
     $Lamda Factor (FLA) still Large)
      GO TO 300
95    WRITE (NO,8)
8     FORMAT (//,9X, 20HThis is not Possible)
      GO TO 300
 300  WRITE(1,313) B(1),B(2)
  313 FORMAT(1X,'KiH = ',F7.5,5X,'ALPHA = ',F7.5)
      OPEN (20, FILE=FILE2)
      WRITE(20,381) FILE2
  381 FORMAT(1X, 'REGRESSION RESULTS FOR DATA: ',A20,/)
      WRITE(20,520) TR
  520 FORMAT(1X, 'TEMPERATURE =',I3,' *C',/)
      WRITE (20,312) B(1),B(2),PH
 312    FORMAT(1X,'KiH=  ',F7.5,5X,'ALPHA=',  F7.5,  '(1/s)',
5X,'PHI= ',
     $F8.6,/)
      WRITE(20,*) '- units of KiH are cm**3/gcat.s'
```

```
      write(20,*)
C*************************************************************
C  STATISTICS CALCULATIONS
C*************************************************************
C
      STAT1 = 0.0
      STAT2 = 0.0
      DO  I=1,NN
      STAT1 = STAT1 + Y(I)
      STAT2 = STAT2 + Z(I)
      ENDDO
      YAV = STAT1 / NN
      DO I = 1,NN
C***percent difference**********************
         ERR(I) = 100.*(Z(I) - Y(I))/ Z(I)
c***residuals*********************************
         ERR2(I) = Y(I) - Z(I)
c***sum of squares of regression***********
         STAT3 = STAT3 + (Z(I) - YAV)**2
c***sum of squares total corrected*********
         STAT4 = STAT4 + (Y(I) - YAV)**2
c***sum of squares of the residuals*********
         STAT5 = STAT5 + (Y(I) - Z(I))**2
      ENDDO
c***correlation coefficient or coeff.of regression******
      R2 = STAT3/STAT4
      STAT6 = STAT3/KK
      STAT7 = STAT5/(NN - KK)
C     STAT8 = STAT6/STAT7
C*************************************************************
      WRITE(20,499)
  499 FORMAT(1X,'t(s)',5X,'YiH cal (wt%)',5X,'YiH exp', 5X,
'Residuals',
     $5X,'% dev.')
      DO 315 I=1,NN
      Z(I) = 100.0*Z(I)/CORR(I)
      YI(I) = 100.0*YI(I)
      ERR2(I) = 100.0 * ERR2(I)
      WRITE (20,314) X(I),Z(I),YI(I),ERR2(I),ERR(I)
 314  FORMAT(1X,I2,8X,F5.3,12X,F5.3,8X,f6.4,8x,f5.3)
 315  CONTINUE
      write(20,*)
      WRITE(20,*) 'ANALYSIS OF VARIANCE:'
      write(20,*)
      write(20,409) STAT3,STAT4,STAT5
  409 FORMAT(1X,'SS reg.= ',F8.6,4X,'SS tot. corr.=',F8.6,4X,
     $'SS resid.=',F8.6,/)
      WRITE(20,469) KK,NN
  469 FORMAT(1X,'No. of parameters = ',I2,5X,'No. of runs =
',I2,/)
      WRITE(20,419) R2
  419 FORMAT(1X,'Coefficient of regression = ',F5.4,/)
C
C*************************************************************
```

```
C  INVERSION OF MATRIX COV= TRANSF(JACOBIAN)*JACOBIAN
C*************************************************************
C
       CALL INVRT(COV,MSIZE,KK,IPVT,IERR)
       DO I=1,KK
       VAR(I) = COV(I,I) * STAT5 / (NN-KK)
       ENDDO
C
      DO I=1,KK
         DO J=1,KK
           COR(I,J)    =    COV(I,J)*STAT5/(NN-KK)    /
SQRT(VAR(I)*VAR(J))
         ENDDO
       ENDDO
       WRITE(20,449)
  449   FORMAT(1X,3'*','CORRELATION   MATRIX   OF   PARAMETER
ESTIMATES', 3'*',/)
       DO I=1,KK
       WRITE(20,459) (COR(I,J), J=1,KK)
  459 FORMAT(1X,20(E12.10,2X))
       ENDDO
       WRITE(20,529)
  529   FORMAT(/,1X,3'*','COVARIANCE   MATRIX   FOR   PARAMETER
ESTIMATES', 3'*',/)
       DO I=1,KK
       WRITE(20,553) (COV(I,J), J=1,KK)
  553 FORMAT(1X,20(E12.10,2X))
       ENDDO
       WRITE(20,429)
  429  FORMAT(/,1X,3'*','VARIANCES OF PARAMETER ESTIMATES',
3'*',/)
       DO I=1,KK
       WRITE(20,439) I,VAR(I)
  439 FORMAT(1X,'VAR (',1X,I2,1X,') = ',F10.8)
       ENDDO
       CLOSE(20)
1000   STOP
       END
C*************************************************************
       SUBROUTINE FUNC ( KK,B,NN,Z,FV,X,XMC,WHO)
C*************************************************************
      DIMENSION Z(25),XMC(25),X(25),WHO(25)
       DIMENSION B(25)
       DO 10 J=1,NN
       DUM = EXP ( -1.0*B(2)*X(J) ) - 1.0
       Z(J)=WHO(J)*EXP( XMC(J)*B(1)*DUM / (45.0*B(2)))
    10 CONTINUE
       RETURN
       END
C
C*************************************************************
       SUBROUTINE BSOLVE.....
```

```
      PROGRAM LLOPT8A
C*****************************************************************
  This program uses Marquardt regression to solve the light
oil lump equations for KiHiL and KiL.  Exponential decay is
used and KiH and alpha must be entered (use the data file).
C*****************************************************************
      DIMENSION A(30,30),AC(30,30),BMIN(30),BMAX(30),X(30)
      DIMENSION XMC(50),WHO(50),WLO(50)
      REAL P(100),WO(50),CORR(30),WT(50),YI(50)
      REAL Z(50), Y(50), BY(50),BV(50),B(50)
      REAL COV(30,30),COR(30,30),VAR(30),ERR(30),ERR2(30)
      INTEGER IPVT(30)
      CHARACTER*50 FILE1*30,FILE2*30
      EMA COV
      COMMON /TRES/ ERR,COR,VAR
      EXTERNAL FUNC
      WRITE(1,*) 'ENTER THE TEMPERATURE USED (IN *C)'
      READ(1,*) TR
      WRITE(1,*) 'ENTER THE NUMBER OF DATA POINTS'
      READ(1,*) NN
      KK=2
C
      call fparm(FILE1,FILE2)
      OPEN(10,FILE=FILE1)
      READ(10,*) XKH,XA
      READ(10,*)    (X(I),XMC(I),WHO(I),WLO(I),YI(I),WO(I),
I=1,NN)
      CLOSE(10)
C
C****Correct the GC weight fractions to account for inert
gas******
C****Reactor volume = 45.0 mL and R = 82.05 cm**3.atm/gmol.K
C
      TR1 = TR + 273.15
      DO I=1,NN
      WT(I) = WO(I) + 21.9378/TR
      CORR(I) = WO(I)/WT(I)
      Y(I) = YI(I) * CORR(I)
      WHO(I) = WHO(I) * CORR(I)
      WLO(I) = WLO(I) * CORR(I)
      ENDDO
      write(1,*) 'initial VALUE FOR KiHiL'
      read (1,*) b(1)
      write (1,*) 'initial VALUE FOR KiL'
      read (1,*) b(2)
      bmin(1)= 0.1
      bmax(1)= XKH
      bmin(2)=1.0
      bmax(2)=40.0
C
      FNU = 0.0
      FLA = 0.0
      TAU = 0.0
      EPS = 0.0
```

```
      PHMIN = 0.0
      I = 0
      KD = KK
      FV = 0.0
      DO J = 1, KK
          BV(J) = 1
      END DO
      ICON = KK
      ITER = 0
      NO = 1
      WRITE (NO,15)
15    FORMAT ( 10X,27HBSOLVE REGRESSION ALGORITHM)
200   CALL BSOLVE (KK, B, NN, Z, Y, PH, FNU, FLA, TAU, EPS,
      PHMIN, I,ICON,FV,DV,BV, BMIN, BMAX, P, FUNC, DERIV, KD,
A, AC, GAMM, X, XMC, WHO, WLO, XKH,XA,COV)
C
      ITER = ITER + 1
      WRITE (NO,1) ICON, PH, ITER
1     FORMAT (9X,6HICON = , I3, 4X, 5HPH = , E15.8, 4X,
     $16HIteration No. = , I3)
      WRITE(1,2) B(1),B(2)
    2 FORMAT(1X, 'KiHiL = ',F7.4,5X,'KiL = ',F7.5)
      IF (ICON) 10, 300, 200
10    IF (ICON+1) 20, 60, 200
20    IF (ICON+2) 30, 70, 200
30    IF (ICON+3) 40, 80, 200
40    IF (ICON+4) 50, 90, 200
50    GO TO 95
60    WRITE (NO,4)
4     FORMAT (//, 9X, 32HNo Function Improvement Possible )
      GO TO 300
70    WRITE (NO,5)
5     FORMAT (//,9X, 28HMore Unknowns than Functions)
      GO TO 300
80    WRITE (NO, 6)
6     FORMAT (//,9X, 2HTotal Variables are Zero)
      GO TO 300
90    WRITE (NO,7)
7     FORMAT (//,9X,79HCorrections Satisfy Convergence
 Requirements but Lamda Factor (FLA) still Large)
      GO TO 300
95    WRITE (NO,8)
8     FORMAT (//,9X, 20HThis is not Possible)
      GO TO 300
 300  WRITE(1,313) B(1),B(2)
  313 FORMAT(1X,'KiHiL=',F7.4,5X,'KiL=',F7.4)
      OPEN (20, FILE=FILE2)
      WRITE(20,381) FILE2
 381  FORMAT(1X, 'REGRESSION RESULTS FOR DATA: ',A20,/)
      WRITE(20,520) TR
 520  FORMAT(1X, 'TEMPERATURE =',I3,' *C',/)
      WRITE(20,382) XKH,XA
 382  FORMAT(1X, 'USING: KiH=',F6.3,2X,'and ALPHA=',F6.4,/)
      WRITE (20,312) B(1),B(2),PH
```

```
 312  FORMAT(1X,'KiHiL=B(1)= ',F7.4,5X,'KiL= ',F7.4,5X,'PHI=
',E12.9,/)
      WRITE(20,*) '- units of K are  cm**3/gcat.s'
      WRITE(20,*)
C*************************************************************
C  STATISTICS CALCULATIONS
C*************************************************************
C
      STAT1 = 0.0
      STAT2 = 0.0
      DO  I=1,NN
      STAT1 = STAT1 + Y(I)
      STAT2 = STAT2 + Z(I)
      ENDDO
      YAV = STAT1 / NN
      DO I = 1,NN
C***percent difference**********************
         ERR(I) = 100.*(Z(I) - Y(I))/ Z(I)
c***residuals*********************************
         ERR2(I) = Y(I) - Z(I)
c***sum of squares of regression***********
         STAT3 = STAT3 + (Z(I) - YAV)**2
c***sum of squares total corrected*********
         STAT4 = STAT4 + (Y(I) - YAV)**2
c***sum of squares of the residuals*********
         STAT5 = STAT5 + (Y(I) - Z(I))**2
      ENDDO
c***correlation coefficient or coeff.of regression******
      R2 = STAT3/STAT4
      STAT6 = STAT3/KK
      STAT7 = STAT5/(NN - KK)
C     STAT8 = STAT6/STAT7
C*************************************************************
      WRITE(20,499)
  499 FORMAT(1X,'t(s)',5X,'YiL cal (wt%)',5X,'YiL exp', 5X,
'Residuals',
     $5X,'% dev.')
      DO 315 I=1,NN
      Z(I) = 100.0*Z(I)/CORR(I)
      YI(I) = 100.0*YI(I)
      ERR2(I) = 100.0 * ERR2(I)
      WRITE (20,314) X(I),Z(I),YI(I),ERR2(I),ERR(I)
 314  FORMAT(1X,I2,8X,F5.3,12X,F5.3,8X,f6.4,8x,f5.3)
 315  CONTINUE
      write(20,*)
      WRITE(20,*) 'ANALYSIS OF VARIANCE:'
      write(20,*)
      write(20,409) STAT3,STAT4,STAT5
  409 FORMAT(1X,'SS reg.= ',F8.6,4X,'SS tot. corr.=',F8.6,4X,
     $'SS resid.=',F8.6,/)
      WRITE(20,469) KK,NN
  469 FORMAT(1X,'No. of parameters = ',I2,5X,'No. of runs =
',I2,/)
      WRITE(20,419) R2
```

```
  419 FORMAT(1X,'Coefficient of regression = ',F5.4,/)
C*************************************************************
C  INVERSION OF MATRIX COV= TRANSF(JACOBIAN)*JACOBIAN
C*************************************************************
       CALL INVRT(COV,MSIZE,KK,IPVT,IERR)
       DO I=1,KK
       VAR(I) = COV(I,I) * STAT5 / (NN-KK)
       ENDDO
C
      DO I=1,KK
         DO J=1,KK
         COR(I,J) = COV(I,J)*STAT5/(NN-KK) /
 SQRT(VAR(I)*VAR(J))
         ENDDO
      ENDDO
C*************************************************************
      WRITE(20,449)
  449   FORMAT(1X,3'*','CORRELATION   MATRIX   OF   PARAMETER
ESTIMATES', 3'*',/)
      DO I=1,KK
      WRITE(20,459) (COR(I,J), J=1,KK)
  459 FORMAT(1X,20(F5.4,2X))
      ENDDO
      WRITE(20,529)
  529 FORMAT(/,1X,3'*','COVARIANCE MATRIX FOR PARAMETER
 ESTIMATES', 3'*',/)
      DO I=1,KK
      WRITE(20,553) (COV(I,J), J=1,KK)
  553 FORMAT(1X,20(F8.2,2X))
      ENDDO
      WRITE(20,429)
  429  FORMAT(/,1X,3'*','VARIANCES  OF  PARAMETER  ESTIMATES',
3'*',/)
      DO I=1,KK
      WRITE(20,439) I,VAR(I)
  439 FORMAT(1X,'VAR (',1X,I2,1X,') = ',F10.8)
      ENDDO
      CLOSE(20)
1000  STOP
      END
C
C*************************************************************
      SUBROUTINE FUNC (KK,B,NN,Z,FV,X,XMC,WHO,WLO,XKH,XA)
C*************************************************************
      INTEGER RUNGE
      DIMENSION DW(2),W(2),Z(50),WHO(50),WLO(50),XMC(50),X(50)
      DIMENSION B(30)
      DO 101 J=1,NN
      W(1)=WLO(J)
      H=0.1
      ICOUNT=0.0
      T=0.0
      NSTEPS=X(J)/H
    5 K=RUNGE(1,W,DW,T,H)
```

```
      IF (K.NE.1) GO TO 10
      DUM = EXP(-XA*T)
      WH = WHO(J)*EXP( XMC(J)*XKH*(DUM - 1.0)/45.0/XA )
      DW(1)= XMC(J)*DUM*(B(1)*WH - B(2)*W(1))/45.0
      GO TO 5
   10 ICOUNT=ICOUNT+1
      IF (ICOUNT.EQ.NSTEPS) GO TO 100
      GO TO 5
  100 CONTINUE
      Z(J)=W(1)
  101 CONTINUE
      RETURN
      END
C-------------------------------------------------
      FUNCTION RUNGE(N,Y,F,T,H)
      INTEGER RUNGE
      DIMENSION PHII(50), SAVEY(50), Y(N), F(N)
      DATA M/0/
      M=M+1
      GO TO (1,2,3,4,5),M
C     ...PASS 1...
    1 RUNGE = 1
      RETURN
C     ...PASS 2...
    2 DO 22 J=1,N
      SAVEY(J)=Y(J)
      PHII(J)=F(J)
   22 Y(J)=SAVEY(J) + 0.5*H*F(J)
      T=T+0.5*H
      RUNGE=1
      RETURN
C     ...PASS 3...
    3 DO 33 J=1,N
      PHII(J) =PHII(J)+2.0*F(J)
   33 Y(J)=SAVEY(J) +0.5*H*F(J)
      RUNGE=1
      RETURN
C     ...PASS 4...
    4 DO 44 J=1,N
      PHII(J)=PHII(J) +2.0*F(J)
   44 Y(J)=SAVEY(J)+H*F(J)
      T=T+0.5*H
      RUNGE=1
      RETURN
C     ...PASS 5...
    5 DO 55 J=1,N
   55 Y(J)=SAVEY(J)+(PHII(J) + F(J))*H/6.0
      M=0
      RUNGE=0
      RETURN
      END
C*************************************************************
      SUBROUTINE BSOLVE.........
```

```
      PROGRAM GLOPT8A
C*****************************************************************
THIS PROGRAM USES MARQUARDT REGRESSION TO SOLVE FOR KPHG,
KNHG, AND KAHG (ie. the cracking of heavy lumps into gasoline)
FOR THE 8 LUMP MODEL GASOLINE EQUATION.  ALL OTHER KINETIC
VALUES MUST BE ENTERED BY A DATA FILE.  IT IS ASSUMED THAT THE
CRACKING CONSTANTS OF LIGHT LUMPS TO GASOLINE ARE KNOWN.
C*****************************************************************
      DIMENSION A(10,10),AC(10,10),BMIN(10),BMAX(10),X(10)
      DIMENSION XMC(25),WHPO(25),WHNO(25),WHAO(25)
      DIMENSION WLPO(25),WLNO(25),WLAO(25)
      REAL P(50),WO(10),CORR(10),WT(10),YI(25)
      REAL Z(25), Y(25), BY(16),BV(10),B(10)
      REAL COV(20,20),COR(20,20),VAR(20),ERR(20),ERR2(20)
      INTEGER IPVT(20)
      EMA COV
      COMMON /TRES/ ERR,COR,VAR
      CHARACTER*50 FILE1*30,FILE2*30

      EXTERNAL FUNC
      WRITE(1,*) 'ENTER THE TEMPERATURE (in *C)'
      READ(1,*) TR
      WRITE(1,*) 'ENTER THE NUMBER OF DATA POINTS'
      READ(1,*) NN
      KK=3
C
      CALL FPARM(FILE1,FILE2)
      OPEN(10,FILE=FILE1)
      READ(10,*) XA, XKPH, XKNH, XKAH, XKPHPL, XKNHNL, XKAHAL,
     $XKPL, XKNL, XKAL,XKPLG,XKNLG,XKALG,XKGC
      DO I=1,NN
      READ(10,*)
X(I),XMC(I),WHPO(I),WHNO(I),WHAO(I),WLPO(I),WLNO(I),
     $WLAO(I),YI(I),WO(I)
      ENDDO
      CLOSE(10)
C
C** CORRECT YIELDS TO WT. FRACTIONS IN THE REACTOR (i.e.
include argon)
C
      TR1 = TR + 273.15
      DO I=1,NN
      WT(I) = WO(I) + 21.9378/TR1
      CORR(I) = WO(I)/WT(I)
      Y(I) = YI(I) * CORR(I)
      WHPO(I) = WHPO(I) * CORR(I)
      WHNO(I) = WHNO(I) * CORR(I)
      WHAO(I) = WHAO(I) * CORR(I)
      WLPO(I) = WLPO(I) * CORR(I)
      WLNO(I) = WLNO(I) * CORR(I)
      WLAO(I) = WLAO(I) * CORR(I)
      ENDDO
      WRITE(1,*) 'initial VALUE FOR KPHG, KNHG, KAHG'
      READ (1,*) B(1),B(2),B(3)
```

```
      BMIN(1)=0.10
      BMIN(2)=0.10
      BMIN(3)=0.10
      BMAX(1)= XKPH - XKPHPL
      BMAX(2)= XKNH - XKNHNL
      BMAX(3)= XKAH - XKAHAL
C
      FNU = 0.0
      FLA = 0.0
      TAU = 0.0
      EPS = 0.0
      PHMIN = 0.0
      I = 0
      KD = KK
      FV = 0.0
      DO J = 1, KK
          BV(J) = 1
      END DO
      ICON = KK
      ITER = 0
      NO = 1
      WRITE (NO,15)
15    FORMAT ( 10X,27HBSOLVE REGRESSION ALGORITHM)
C
200   CALL BSOLVE (KK, B, NN, Z, Y, PH, FNU, FLA, TAU, EPS,
     PHMIN, I, ICON, FV, DV, BV, BMIN, BMAX, P, FUNC, DERIV,
     KD, A, AC, GAMM, XMC, WHPO, WHNO, WHAO, WLPO,WLNO,
    $WLAO, X, XKPH, XKNH, XKAH, XKPHPL, XKNHNL, XKAHAL, XKPL,
     XKNL, XKAL,XKPLG,
    $XKNLG,XKALG,XKGC,XA,COV)
      ITER = ITER + 1
      WRITE (NO,1) ICON, PH, ITER
1     FORMAT (9X,6HICON = , I3, 4X, 5HPH = , E15.8, 4X,
     $16HIteration No. = , I3)
      WRITE(1,2) B(1),B(2),B(3)
   2    FORMAT(1X,  'KPHG  =',F7.4,5X,'KNHG  =',F7.4,5X,'KAHG
=',F7.4)
      IF (ICON) 10, 300, 200
10    IF (ICON+1) 20, 60, 200
20    IF (ICON+2) 30, 70, 200
30    IF (ICON+3) 40, 80, 200
40    IF (ICON+4) 50, 90, 200
50    GO TO 95
60    WRITE (NO,4)
4     FORMAT (//, 9X, 32HNo Function Improvement Possible )
      GO TO 300
70    WRITE (NO,5)
5     FORMAT (//,9X, 28HMore Unknowns than Functions)
      GO TO 300
80    WRITE (NO, 6)
6     FORMAT (//,9X, 2HTotal Variables are Zero)
      GO TO 300
90    WRITE (NO,7)
7         FORMAT  (//,9X,79HCorrections  Satisfy  Convergence
```

```
Requirements but
     $Lamda Factor (FLA) still Large)
      GO TO 300
95    WRITE (NO,8)
8     FORMAT (//,9X, 20HThis is not Possible)
      GO TO 300
 300  WRITE(1,313) B(1),B(2),B(3)
 313  FORMAT  (1X,  'KPHG=',  F5.3,  5X,  'KNHG=',  F5.3,  5X,
'KAHG=', F5.3,/)
      OPEN (20, FILE=FILE2)
      WRITE(20,381) FILE2
  381 FORMAT(1X, 'REGRESSION RESULTS FOR DATA: ',A20,/)
      WRITE(20,444) TR
  444 FORMAT(1X,'TEMPERATURE =',I3,' *C',/)
      WRITE(20,312) B(1),B(2),B(3)
 312 FORMAT (1X, 'KPHG=B1=', F6.3, 5X, 'KNHG=B2=', F6.3, 5X,
 'KAHG=B3=', F6.3,/)
      XKPHC = XKPH - XKPHPL - B(1)
      XKNHC = XKNH - XKNHNL - B(2)
      XKAHC = XKAH - XKAHAL - B(3)
      WRITE(20,520) XKPHC,XKNHC,XKAHC
  520   FORMAT(1X,'KPHC   =',F6.3,5X,'KNHC   =',F6.3,5X,'KAHC
=',F6.3,/)
C*************************************************************
C  STATISTICS CALCULATIONS
C*************************************************************
C
      STAT1 = 0.0
      STAT2 = 0.0
      DO  I=1,NN
      STAT1 = STAT1 + Y(I)
      STAT2 = STAT2 + Z(I)
      ENDDO
      YAV = STAT1 / NN
      DO I = 1,NN
C***percent difference**********************
         ERR(I) = 100.*(Z(I) - Y(I))/ Z(I)
c***residuals*********************************
         ERR2(I) = Y(I) - Z(I)
c***sum of squares of regression***********
         STAT3 = STAT3 + (Z(I) - YAV)**2
c***sum of squares total corrected*********
         STAT4 = STAT4 + (Y(I) - YAV)**2
c***sum of squares of the residuals*********
         STAT5 = STAT5 + (Y(I) - Z(I))**2
      ENDDO
c***correlation coefficient or coeff.of regression******
      R2 = STAT3/STAT4
      STAT6 = STAT3/KK
      STAT7 = STAT5/(NN - KK)
C     STAT8 = STAT6/STAT7
C*************************************************************
      WRITE(20,499)
  499 FORMAT(1X,'t(s)',5X,'YG cal (wt%)',5X,'YGexp', 5X,
```

```
 'Residuals', 5X,'% dev.')
      DO 315 I=1,NN
      Z(I) = 100.0*Z(I)/CORR(I)
      YI(I) = 100.0*YI(I)
      ERR2(I) = 100.0 * ERR2(I)
      WRITE (20,314) X(I),Z(I),YI(I),ERR2(I),ERR(I)
 314  FORMAT(1X,I2,8X,F5.3,10X,F5.3,8X,f6.4,8x,f5.3)
 315  CONTINUE
      write(20,*)
      WRITE(20,*) 'ANALYSIS OF VARIANCE:'
      write(20,*)
      write(20,409) STAT3,STAT4,STAT5
  409 FORMAT(1X,'SS reg.= ',F8.6,4X,'SS tot. corr.=',F8.6,4X,
     $'SS resid.=',F8.6,/)
      WRITE(20,469) KK,NN
  469 FORMAT(1X,'No. of parameters = ',I2,5X,'No. of runs =
',I2,/)
      WRITE(20,419) R2
  419 FORMAT(1X,'Coefficient of regression = ',F5.4,/)
C
C*****************************************************************
C  INVERSION OF MATRIX COV= TRANSF(JACOBIAN)*JACOBIAN
C*****************************************************************
C
       CALL INVRT(COV,MSIZE,KK,IPVT,IERR)
       DO I=1,KK
       VAR(I) = COV(I,I) * STAT5 / (NN-KK)
       ENDDO
C
      DO I=1,KK
        DO J=1,KK
        COR(I,J) = COV(I,J)*STAT5/(NN-KK) / SQRT (VAR(I) *
VAR(J))
         ENDDO
      ENDDO
C*****************************************************************
      WRITE(20,449)
  449   FORMAT(1X,3'*','CORRELATION MATRIX OF PARAMETER
ESTIMATES',
     $3'*',/)
      DO I=1,KK
      WRITE(20,459) (COR(I,J), J=1,KK)
  459 FORMAT(1X,20(E9.8,3X))
      ENDDO
      WRITE(20,529)
  529  FORMAT(/,1X,3'*','COVARIANCE MATRIX FOR PARAMETER
ESTIMATES',
     $3'*',/)
      DO I=1,KK
      WRITE(20,553) (COV(I,J), J=1,KK)
  553 FORMAT(1X,20(E9.8,3X))
      ENDDO
      WRITE(20,429)
  429   FORMAT(/,1X,3'*','VARIANCES OF PARAMETER
```

```
ESTIMATES',3'*',/)
      DO I=1,KK
      WRITE(20,439) I,VAR(I)
  439 FORMAT(1X,'VAR (',1X,I2,1X,') = ',F10.8)
      ENDDO
      WRITE(20,*)
      WRITE(20,*) 'The following constants were used:'
      WRITE(20,521) XKPH, XKNH, XKAH
  521   FORMAT(/,1X,'KPH   =',F6.3,5X,'KNH   =',F6.3,5X,'KAH
=',F6.3)
      WRITE(20,522) XKPHPL,XKNHNL,XKAHAL
  522  FORMAT(1X,'KPHPL  =',F6.3,3X,'KNHNL  =',F6.3,3X,'KAHAL
=',F6.3)
      WRITE(20,523) XKPL, XKNL,XKAL
  523 FORMAT(1X,'KPL =',F6.3,5X,'KNL =',F6.3,5X,'KAL =',F6.3)
      WRITE(20,392) XKPLG,XKNLG,XKALG
      XKPLC = XKPL - XKPLG
      XKNLC = XKNL - XKNLG
      XKALC = XKAL - XKALG
      WRITE(20,524) XKPLC, XKNLC, XKALC
  524   FORMAT(1X,'KPLC   =',F6.3,5X,'KNLC   =',F6.3,5X,'KALC
=',F6.3)
  392   FORMAT(1X,'KPLG   =',F6.3,5X,'KNLG   =',F6.3,5X,'KALG
=',F6.3)
      WRITE(20,525) XKGC, XA
  525 FORMAT(1X,'KGC =',F6.3,5X,'ALPHA =',F5.4)
      CLOSE(20)
1000  STOP
      END
C
C*****************************************************************
      SUBROUTINE FUNC (KK,B,NN,Z,FV,XMC,WHPO,WHNO,WHAO,WLPO,

$WLNO,WLAO,X,XKPH,XKNH,XKAH,XKPHPL,XKNHNL,XKAHAL,XKPL,XKNL,
     $XKAL,XKPLG,XKNLG,XKALG,XKGC,XA)
C*****************************************************************
C
      INTEGER RUNGE
      DIMENSION DW(7), W(7), Z(25), WHPO(25), WLPO(25),
     $XMC(25), X(25)
      DIMENSION B(25), WHNO(25), WLNO(25),WHAO(25),WLAO(25)
      DO 101 J=1,NN
      W(1)=WHPO(J)
      W(2)=WHNO(J)
      W(3)=WHAO(J)
      W(4)=WLPO(J)
      W(5)=WLNO(J)
      W(6)=WLAO(J)
      W(7)=0.0
      H=0.1
      ICOUNT=0.0
      T=0.0
      NSTEPS=X(J)/H
    5 K=RUNGE(7,W,DW,T,H)
```

```
      IF (K.NE.1) GO TO 10
      DEAC = EXP(-XA*T)
      DW(1) = -XKPH*XMC(J)*W(1)*DEAC/45.0
      DW(2) = -XKNH*XMC(J)*W(2)*DEAC/45.0
      DW(3) = -XKAH*XMC(J)*W(3)*DEAC/45.0
      DW(4) = XMC(J)*DEAC*( XKPHPL*W(1) - XKPL*W(4) )/45.0
      DW(5) = XMC(J)*DEAC*( XKNHNL*W(2) - XKNL*W(5) )/45.0
      DW(6) = XMC(J)*DEAC*( XKAHAL*W(3) - XKA_*W(6) )/45.0
      DW(7) = XMC(J)*DEAC*( B(1)*W(1) + B(2)*W(2) + B(3)*W(3)
+
     $XKPLG*W(4) + XKNLG*W(5) + XKALG*W(6) - XKGC*W(7) )/45.0
      GO TO 5
   10 ICOUNT=ICOUNT+1
      IF (ICOUNT.GE.NSTEPS) GO TO 100
      GO TO 5
  100 CONTINUE
      Z(J)=W(7)
  101 CONTINUE
      RETURN
      END
C
C
      FUNCTION RUNGE(N,Y,F,T,H)
      INTEGER RUNGE
      DIMENSION PHII(50), SAVEY(50), Y(N), F(N)
      DATA M/0/
      M=M+1
      GO TO (1,2,3,4,5),M
C     ...PASS 1...
    1 RUNGE = 1
      RETURN
C     ...PASS 2...
    2 DO 22 J=1,N
      SAVEY(J)=Y(J)
      PHII(J)=F(J)
   22 Y(J)=SAVEY(J) + 0.5*H*F(J)
      T=T+0.5*H
      RUNGE=1
      RETURN
C     ...PASS 3...
    3 DO 33 J=1,N
      PHII(J) =PHII(J)+2.0*F(J)
   33 Y(J)=SAVEY(J) +0.5*H*F(J)
      RUNGE=1
      RETURN
C     ...PASS 4...
    4 DO 44 J=1,N
      PHII(J)=PHII(J) +2.0*F(J)
   44 Y(J)=SAVEY(J)+H*F(J)
      T=T+0.5*H
      RUNGE=1
      RETURN
C     ...PASS 5...
    5 DO 55 J=1,N
```

```
   55 Y(J)=SAVEY(J)+(PHII(J) + F(J))*H/6.0
      M=0
      RUNGE=0
      RETURN
C
      END
C*************************************************************
     SUBROUTINE BSOLVE ..........
```

```
      PROGRAM TEST8LA
C*****************************************************************
THIS PROGRAM CALCULATES THE YIELDS OF HEAVY AND LIGHT OIL
LUMPS AND GASOLINE YIELDS FOR THE 8-LUMP MODEL.  THE KINETIC
CONSTANTS FOR THE MODEL MUST BE SPECIFIED (USE A DATA FILE).
THERE ARE 7 EQUATIONS WHICH ARE SOLVED SIMULTANEOUSLY USING A
RUNGE KUTTA ALGORITHM.  EXPONETIAL DECAY LAW IS USED.
C*****************************************************************
      INTEGER RUNGE
      DIMENSION XMC(25),X(25),YLCO(10),YHCO(10),CONV(10)
      DIMENSION W(10),DW(10),YLG(10),YPL(10),YNL(10),YAL(10)
     DIMENSION YPH(10),YNH(10),YAH(10),YG(10)
      DIMENSION YLCOE(10),YHCOE(10),CONVE(10),YLGE(10)
      REAL Z1(10),Z2(10),Z3(10),Z4(10),Z5(10),Z6(10),Z7(10)
      REAL WHPO(20), WHNO(20), WHAO(20), WLPO(20), WLNO(20),
WLAO(20)
      CHARACTER*50 FILE1*20,FILE2*20
C     WRITE(1,*) 'ENTER THE TEMPERATURE (in *C)'
      READ(1,*) TR
      WRITE(1,*) 'ENTER THE NUMBER OF REACTION TIMES'
      READ(1,*) NN
C
      CALL FPARM(FILE1,FILE2)
      OPEN(10,FILE=FILE1)
      READ(10,*) XA, XKPH, XKNH, XKAH, XKPHPL, XKNHNL, XKAHAL,
XKPL, XKNL, XKAL, XKPLG, XKNLG, XKALG, XKGC, XKPHG, XKNHG,
XKAHG
      READ(10,*) (X(I),XMC(I),WHPO(I),WHNO(I),WHAO(I),
     $WLPO(I),WLNO(I),WLAO(I), I=1,NN)
                          R   E   A   D   (   1   0   ,   *   )
(YPL(I),YNL(I),YAL(I),YPH(I),YNH(I),YAH(I),YG(I), I=
     $1,NN)
      CLOSE(10)
      DO 101 J=1,NN
      W(1)=WHPO(J)
      W(2)=WHNO(J)
      W(3)=WHAO(J)
      W(4)=WLPO(J)
      W(5)=WLNO(J)
      W(6)=WLAO(J)
      W(7)=0.0
      H=0.10
      ICOUNT=0.0
      T=0.0
      NSTEPS=X(J)/H
    5 K=RUNGE(7,W,DW,T,H)
      IF (K.NE.1) GO TO 10
      IF (NSTEPS.EQ.0) GO TO 10
      DEAC = EXP(-XA*T)
      DW(1) = -XKPH*XMC(J)*W(1)*DEAC/45.0
      DW(2) = -XKNH*XMC(J)*W(2)*DEAC/45.0
      DW(3) = -XKAH*XMC(J)*W(3)*DEAC/45.0
      DW(4) = XMC(J)*DEAC*( XKPHPL*W(1) - XKPL*W(4) )/45.0
      DW(5) = XMC(J)*DEAC*( XKNHNL*W(2) - XKNL*W(5) )/45.0
```

```
      DW(6) = XMC(J)*DEAC*( XKAHAL*W(3) - XKAL*W(6) )/45.0
      DW(7)   =   XMC(J)*DEAC*(XKPHG*W(1)   +   XKNHG*W(2)   +
XKAHG*W(3) +
     $XKPLG*W(4) + XKNLG*W(5) + XKALG*W(6) - XKGC*W(7) )/45.0
      GO TO 5
   10 ICOUNT=ICOUNT+1
      IF (ICOUNT.GE.NSTEPS) GO TO 100
      GO TO 5
  100 CONTINUE
      Z1(J)=100.0*W(1)
      Z2(J)=100.0*W(2)
      Z3(J)=100.0*W(3)
      Z4(J)=100.0*W(4)
      Z5(J)=100.0*W(5)
      Z6(J)=100.0*W(6)
      Z7(J)=100.0*W(7)
      YHCO(J) = Z1(J) + Z2(J) + Z3(J)
      YHCOE(J) = YPH(J) + YNH(J) + YAH(J)
      YLCO(J) = Z4(J) + Z5(J) + Z6(J)
      YLCOE(J) = YPL(J) + YNL(J) + YAL(J)
      CONV(J) = 100.0 - YHCO(J) - YLCO(J)
      CONVE(J) = 100.0 - YHCOE(J) - YLCOE(J)
      YLG(J) = CONV(J) - Z7(J)
      YLGE(J) = CONVE(J) - YG(J)
C
C*******CALCULATE STATISTICS*******************************
C
      STAT1 = 0.0
      STAT2 = 0.0
      STAT3 = 0.0
      STAT4 = 0.0
      STAT5 = 0.0
      STAT6 = 0.0
      STAT7 = 0.0
      STCONV = 0.0
      STHCO = 0.0
      STLCO = 0.0
      STLG  = 0.0
      DO I=1,NN
      STAT1 = STAT1 + ( Z1(I) - YPH(I) )**2
      STAT2 = STAT2 + ( Z2(I) - YNH(I) )**2
      STAT3 = STAT3 + ( Z3(I) - YAH(I) )**2
      STAT4 = STAT4 + ( Z4(I) - YPL(I) )**2
      STAT5 = STAT5 + ( Z5(I) - YNL(I) )**2
      STAT6 = STAT6 + ( Z6(I) - YAL(I) )**2
      STAT7 = STAT7 + ( Z7(I) -  YG(I) )**2
      STCONV = STCONV + ( CONV(I) - CONVE(I) )**2
      STHCO = STHCO + ( YHCO(I) - YHCOE(I) )**2
      STLCO = STLCO + ( YLCO(I) - YLCOE(I) )**2
      STLG = STLG + ( YLG(I) - YLGE(I) )**2
      ENDDO
      N = NN - 1
      SD1 = ( STAT1/N )**0.5
      SD2 = ( STAT2/N )**0.5
```

```
      SD3 = ( STAT3/N )**0.5
      SD4 = ( STAT4/N )**0.5
      SD5 = ( STAT5/N )**0.5
      SD6 = ( STAT6/N )**0.5
      SD7 = ( STAT7/N )**0.5
      SDCONV = ( STCONV/N )**0.5
      SDHCO = ( STHCO/N )**0.5
      SDLCO = ( STLCO/N )**0.5
      SDLG = ( STLG/N )**0.5
  101 CONTINUE
      OPEN(20,FILE=FILE2)
      WRITE(20,300) FILE2
  300 FORMAT(1X,'YIELDS FOR THE 8-LUMP MODEL:',1X,A20)
C     WRITE(20,529) TR
C 529 FORMAT(1X,'TEMPERATURE =',I3,' *C',/)
      WRITE(20,*) 'The following kinetic values were used:'
    WRITE(20,301) XKPH,XKNH,XKAH
  301  FORMAT(1X,'  KPH  =  ',F6.3,5X,'KNH  =  ',F6.3,5X,'KAH  =
',F6.3)
      WRITE(20,303) XKPHPL,XKNHNL,XKAHAL
      WRITE(20,304) XKPHG,XKNHG,XKAHG
      XKPHC = XKPH - XKPHPL - XKPHG
      XKNHC = XKNH - XKNHNL - XKNHG
      XKAHC = XKAH - XKAHAL - XKAHG
      WRITE(20,501) XKPHC,XKNHC,XKAHC
  501  FORMAT(1X,'  KPHC  =',F6.3,5X,'KNHC  =',F6.3,5X,'KAHC
=',F6.3)
      WRITE(20,302) XKPL,XKNL,XKAL
  302  FORMAT(1X,'  KPL  =  ',F6.3,5X,'KNL  =  ',F6.3,5X,'KAL  =
',F6.3)
       3  0  3        F  O  R  M  A  T  (  1  X  ,  '
KPHPL=',F6.3,5X,'KNHNL=',F6.3,5X,'KAHAL=',F6.3)
   304    FORMAT(1X,'    KPHG    =',F6.3,5X,'KNHG
=',F6.3,5X,'KAHG=',F6.3)
      WRITE(20,305) XKPLG,XKNLG,XKALG
  305    FORMAT(1X,'    KPLG=',F6.3,5X,'    KNLG=',F6.3,5X,'
KALG=',F6.3)
      XKPLC = XKPL - XKPLG
      XKNLC = XKNL - XKNLG
      XKALC = XKAL - XKALG
      WRITE(20,502) XKPLC,XKNLC,XKALC
  502  FORMAT(1X,'  KPLC  =',F6.3,5X,'KNLC  =',F6.3,5X,'KALC
=',F6.3)
      WRITE(20,310) XKGC,XA
  310 FORMAT(1X,' KGC = ',F6.4,5X, 'ALPHA = ',F6.4)
c     WRITE(20,893) XMC(1)
c 893 FORMAT(1X, 'mass of catalyst = ',F5.3)
      WRITE(20,312)
  312 FORMAT('HEAVY OIL YIELDS (wt%):')
      DO 400 J=1,NN
      WRITE(20,200) X(J),Z1(J),Z2(J),Z3(J)
  200 FORMAT(1X,'t=',F4.1,5X,'YPH=',F6.3,5X,'YNH=',F6.3,5X,
     $'YAH=',F6.3)
  400 CONTINUE
```

```
      WRITE(20,834) SD1,SD2,SD3
  834     FORMAT(12X,'s.d.=',f6.3,4x,'s.d.=',f6.3,4x,'s.d.=
',f6.3)
      WRITE(20,306)
  306 FORMAT(/,'LIGHT OIL YIELDS (wt%):')
      DO 500 J=1,NN
      WRITE(20,307) X(J),Z4(J),Z5(J),Z6(J)
  307 FORMAT(1X,'t=',F4.1,5X,'YPL=',F6.3,5X,'YNL=',F6.3,5X,
     $'YAL=',F6.3)
  500 CONTINUE
      WRITE(20,836) SD4,SD5,SD6
  836  FORMAT(12X,'s.d.=  ',f6.3,3x,'s.d.=  ',f6.3,3x,'s.d.=
',f6.3)
      WRITE(20,308)
  308 FORMAT(/,'GASOLINE YIELDS AND C-LUMP YIELDS (wt%):')
      DO 600 J=1,NN
      WRITE(20,309) X(J),YLG(J),Z7(J)
  309  FORMAT(1X, 't=',F4.1,5X,'C-LUMP= ',F6.3,5X,'GASOLINE=
',F6.3)
  600 CONTINUE
      WRITE(20,838) SDLG,SD7
  838 FORMAT(12X,'s.d.= ',f6.3,7X,^F's.d.= ',f6.3)
      WRITE(20,350)
  350 FORMAT(/,'OVERALL OIL YIELDS AND CONVERSION (wt%):')
      DO 360 J=1,NN
      WRITE(20,351) X(J),YLCO(J),YHCO(J),CONV(J)
  351 FORMAT(1X, 't=',F4.1,5X,'LCO= ',F6.3    ,'HCO= ',F6.3,5X,
     $'CONV= ',F6.3)
  360 CONTINUE
      WRITE(20,893) SDLCO,SDHCO,SDCONV
  893 FORMAT(12X,'s.d.=',f6.3,5x,'s.d.=',f6.3,5x,'s.d.=',f6.3)
      CLOSE(20)
      END
C
C
      FUNCTION RUNGE(N,Y,F,T,H)
      INTEGER RUNGE
      DIMENSION PHII(50), SAVEY(50), Y(N), F(N)
      DATA M/0/
      M=M+1
      GO TO (1,2,3,4,5),M
C     ...PASS 1...
    1 RUNGE = 1
      RETURN
C     ...PASS 2...
    2 DO 22 J=1,N
      SAVEY(J)=Y(J)
      PHII(J)=F(J)
   22 Y(J)=SAVEY(J) + 0.5*H*F(J)
      T=T+0.5*H
      RUNGE=1
      RETURN
C     ...PASS 3...
    3 DO 33 J=1,N
```

```
      PHII(J) =PHII(J)+2.0*F(J)
   33 Y(J)=SAVEY(J) +0.5*H*F(J)
      RUNGE=1
      RETURN
C     ...PASS 4...
    4 DO 44 J=1,N
      PHII(J)=PHII(J) +2.0*F(J)
   44 Y(J)=SAVEY(J)+H*F(J)
      T=T+0.5*H
      RUNGE=1
      RETURN
C     ...PASS 5...
    5 DO 55 J=1,N
   55 Y(J)=SAVEY(J)+(PHII(J) + F(J))*H/6.0
      M=0
      RUNGE=0
      RETURN
      END
```

```
      PROGRAM TEST1
C*****************************************************************
C     THIS PROGRAM TESTS THE RUNGE KUTTA ALGORITHM TO BE USED
C     FOR THE SOLUTION OF THE GASOLINE EQUATION. THE EQUATIONS
C      USED IN THIS PROGRAM ARE FOR A CONSECUTIVE REACTION
C      SCHEME OF A TO B TO C. THESE EQUATIONS CAN BE SOLVED
C      ANALYTICALLY AND ARE THUS USED TO VERIFY THE RUNGE
C      ALGORITHM AND TO SET AN APPROPRIATE STEP SIZE, H.
C*****************************************************************
      IMPLICIT REAL*8(A-H, O-Z)
      INTEGER RUNGE
      DIMENSION DY(3), Y(3)
      WRITE(1,*) 'ENTER K1,K2,TR,AND H'
      READ(1,*) XK1,XK2,TR,H
      T = H
      Y(1) = 1.0
      Y(2) = 0.0
      Y(3) = 0.0
      ICOUNT = 0.0
      NSTEPS = TR/H
C     ....CALL THE RUNGE FUNCTION.....
    5 K = RUNGE(3,Y,DY,T,H)
C     ....WHEN K=1 COMPUTE DERIVATIVE VALUES....
      IF (K.NE.1) GO TO 10
      DY(1) = -XK1*Y(1)
      DY(2) = XK1*Y(1) - XK2*Y(2)
      DY(3) = XK2*Y(2)
      GO TO 5
   10 ICOUNT = ICOUNT + 1
      IF (ICOUNT.EQ.NSTEPS) GO TO 11
      GO TO 5
   11 WRITE(1,12) Y(1),Y(2),Y(3),H
   12    FORMAT(1X,    'Y(1)=',F7.7,5X,    'Y(2)=',F7.7,5X,
'Y(3)=',F7.7,5X,
     $'H=',F7.7)
      END
C
C
      FUNCTION RUNGE(N,Y,F,X,H)
C
THE FUNCTION RUNGE EMPLOYS THE FOURTH-ORDER RUNGE-KUTTA METHOD
WITH KUTTA'S COEFFICIENTS TO INTEGRATE A SYSTEM OF N SIMULTAN-
EOUS   FIRST   ORDER   ORDINARY   DIFFERENTIAL   EQUATIONS
F(J)=DY(J)/DX.  EACH F(J) MUST BE COMPUTED FOUR TIMES PER
INTEGRATION STEP BY THE CALLING PROGRAM.  THE FUNCTION MUST BE
CALLED FIVE TIMES PER STEP SO THAT THE INDEPENDENT VARIABLE
VALUE (X) AND THE SOLUTION VALUES (Y(J)) CNA BE UPDATED USING
THE RUNGE-KUTTA ALGORITHM.
C
      IMPLICIT REAL*8(A-H, O-Z)
      REAL*8 Y,F,X,H
      INTEGER RUNGE
      DIMENSION PHI(50), SAVEY(50), Y(N), F(N)
      DATA M/0/
```

```
C
      M=M+1
      GO TO (1,2,3,4,5),M
C     ...PASS 1...
    1 RUNGE = 1
      RETURN
      ...PASS 2...
    2 DO 22 J=1,N
      SAVEY(J)=Y(J)
      PHI(J) = F(J)
   22 Y(J) = SAVEY(J) + 0.5*H*F(J)
      X= X +0.5*H
      RUNGE = 1
      RETURN
C     ...PASS 3...
    3 DO 33 J = 1,N
      PHI(J) = PHI(J) +2.0*F(J)
   33 Y(J) = SAVEY(J) +0.5*H*F(J)
      RUNGE = 1
      RETURN
C     ...PASS 4...
    4 DO 44 J = 1,N
      PHI(J) = PHI(J) + 2.0*F(J)
   44 Y(J) = SAVEY(J) + H*F(J)
      X = X + 0.5*H
      RUNGE = 1
      RETURN
     ...PASS 5...
    5 DO 55 J = 1,N
   55 Y(J) = SAVEY(J) + (PHI(J) + F(J))*H/6.0
      M=0
      RUNGE = 0
      RETURN
      END
```